R-08-110

Water-rock interaction modelling and uncertainties of mixing modelling

Site descriptive modelling
SDM-Site Laxemar

María J Gimeno, Luis F Auqué, Javier B Gómez and Patricia Acero, University of Zaragoza, Spain

January 2009

SKB

Water-rock interaction modelling and uncertainties of mixing modelling

Site descriptive modelling
SDM-Site Laxemar

María J Gimeno, Luis F Auqué, Javier B Gómez and
Patricia Acero, University of Zaragoza, Spain

January 2009

Preface

The overall objectives of hydrogeochemical description for Laxemar are to establish a detailed understanding of the hydrogeochemical conditions at the site and to develop models that fulfil the needs identified by the safety assessment groups during the site investigation phase. Issues of concern to safety assessment are radionuclide transport and technical barrier behaviour, both of which are dependent on the chemistry of groundwater and pore water and their evolution with time.

The work has involved the development of descriptive and mathematical models for groundwaters in relation to rock domains, fracture domains and deformation zones. Past climate changes are the major driving force for hydrogeochemical changes and therefore of fundamental importance for understanding the palaeohydrogeological, palaeohydrogeochemical and present evolution of groundwater in the crystalline bedrock of the Fennoscandian Shield.

Understanding current undisturbed hydrochemical conditions at the proposed repository site is important when predicting future changes in groundwater chemistry. The causes of copper corrosion and/or bentonite degradation are of particular interest as they may jeopardise the long-term integrity of the planned SKB repository system. Thus, the following variables are considered for the hydrogeochemical site descriptive modelling: pH, Eh, sulphur species, iron, manganese, carbonate, phosphate, nitrogen species, total dissolved solids (TDS), isotopes, colloids, fulvic and humic acids and microorganisms. In addition, dissolved gases (e.g. carbon dioxide, methane and hydrogen) are of interest because of their likely participation in microbial reactions.

In this series of reports, the final hydrogeochemical evaluation work of the site investigation at the Laxemar site, is presented. The work was conducted by SKB's hydrogeochemical project group, ChemNet, which consists of independent consultants and university researchers with expertise in geochemistry, hydrochemistry, hydrogeochemistry, microbiology, geomicrobiology, analytical chemistry etc. The resulting site descriptive model version, mainly based on available primary data from the extended data freeze L2.3 at Laxemar (November 30 2007). The data interpretation was carried out during November 2007 to September 2008. Several groups within ChemNet were involved and the evaluation was conducted independently using different approaches ranging from expert knowledge to geochemical and mathematical modelling including transport modelling. During regular ChemNet meetings the results have been presented and discussed.

The original works by the ChemNet modellers are presented in four level III reports containing complementary information for the bedrock hydrogeochemistry Laxemar Site Descriptive Model (SDM-Site Laxemar, R-08-93) level II report.
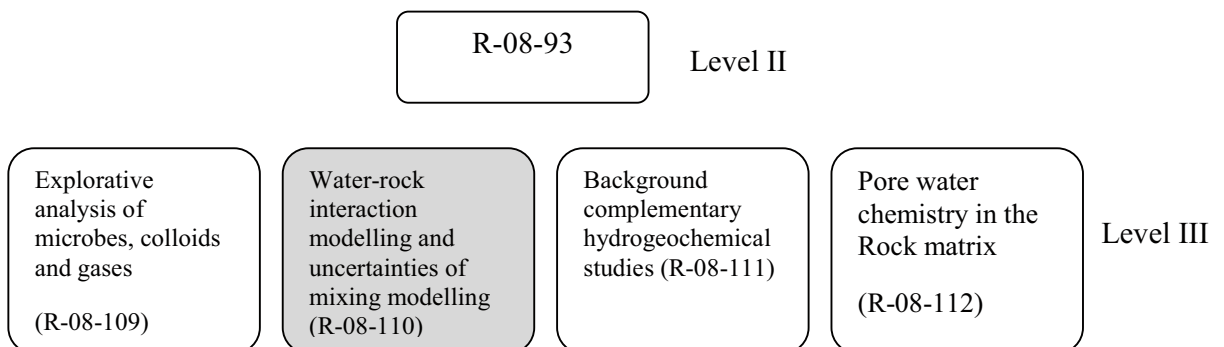
There is also a fifth level III report: Fracture mineralogy of the Laxemar area by Sandström *et al.* R-08-99.

This report presents the modelling work performed by the UZ (University of Zaragoza) group as part of the work plan for Laxemar-Simpevarp 2.2 and 2.3.

The main processes determining the global geochemical evolution of the Laxemar-Simpevarp groundwaters system are mixing and reaction processes. Mixing has taken place between different types of waters (end members) over time, making the discrimination of the main influences not always straightforward. Several lines of evidence suggest the input of dilute waters (cold or warm), at different stages, into a bedrock with pre-existing very saline groundwaters. Subsequently, marine water entered the system over the Littorina period (when the topography and the distance to the coast allowed it) and mixed with pre-existent groundwaters of variable salinity. In the Laxemar subarea mainland, the Littorina input occurred only locally and it has mostly been flushed out by the subsequent input of warm meteoric waters with a distinctive modern isotopic signature.

In addition to mixing processes and superimposed to their effects, different chemical reactions have taken place in the system due to the interaction between waters, minerals and/or microbial activity (e.g. aluminosilicate and carbonate dissolution/precipitation, cation exchange, gypsum dissolution, main redox reactions, etc).

In this context, some elements such as chloride or $\delta^{18}O$ behave conservatively (only dependant on mixing) while others are affected by chemical reactions to differing degrees, especially the redox-sensitive elements. Therefore, the general conclusions on the geochemical behaviour of two sets of elements (conservative and non-conservative, including redox) are summarised below.

Contents

1   Introduction

This report presents the modelling work performed by the UZ (University of Zaragoza) group as part of the work plan for Laxemar-Simpevarp 2.2 and 2.3. It has been organised in sections corresponding to the different INSITE issues in which the UZ group is involved. Issues corresponding to predictive modelling or based on the SR-Can results have been included as appendices. The sections included in this report are the following:

1. Introduction.

2. Final set of data for the "shallow" and "deep" groundwater systems.

3. **Geochemical modelling of the systems.** This general issue is subdivided into two main chapters corresponding to the **non-redox** (Chapter 3) and the **redox systems** (Chapter 4). Both chapters present the final picture of the system as envisaged using all available data by the time of the last data freeze together with the results obtained from modelling with different geochemical techniques. The sections are divided into the different compositional systems: chloride, environmental isotopes (^{18}O and ^{2}H), sodium, magnesium, potassium, carbonates, sulphates, silica and fluoride. In all the cases, the near surface and the deep groundwater systems are studied separately. Due to the important effects of the redox systems, the results obtained from the redox modelling are presented in a separate chapter. It provides a general overview of the redox processes controlling some of the important parameters in the system. It summarises the work done in the earlier modelling phases, updating the results with the new data from 2.2 and 2.3 data freezes. Several issues are dealt with here:
   – Issue A-1: Modelling of the existence of a relatively shallow "process zone" capable of buffering the meteoric water with respect to redox and cation exchange.
   – Issue B-1: Description of models based on reactions and other alternative models.
   – Issue E-1: Spatial variability of hydrochemical data.
   – Issue F-3: Geochemical and isotopic data used to interpret the groundwater evolution over time.
   – Issue G-1: Modelling of redox and pH-buffering and water-rock reactions at repository depth.

4. **Overall conceptual model for groundwater evolution.** In this chapter a summary of the main conclusions from the previous sections together with a conceptual model is presented.

5. **References**

   Appendix A. **Eh and pH selection.** This appendix reports the selection of Eh and pH values performed by the UZ group. A comparison with the values proposed in the Sicada database is also reported if p-reports are available.

   Appendix B. **Sensitivity analysis** to the different approaches used for the activity coefficient calculations in the saline groundwaters of the Laxemar subarea. This appendix presents the thorough analysis performed on the sensitivity of the calculated results to the different modelling approaches to saline waters.

   Appendix C. **Review of some thermodynamic data** and changes in the WATEQ4F database for the geochemical modelling performed in this work.

   Appendix D. **Solubility, particle size and specific surface area.** Some calculations related to the mineral solubility variations (for silica phases and Fe(III)-oxyhydroxides) due to the particle size effects are presented in this Appendix.

   Appendix E. **Groundwater composition at repository depth.** This appendix summarises some of the SR-Can modelling results and deals with several issues from the working plan:
   – Issue A-2: present repository conditions redox and alkalinity buffering capacity including discussion on the effects from potassium, sulphide and iron(II) on buffer and the canister.
   – Issue D-1: 3D variability of redox, pH and other SKB suitability criteria and buffer capacity at repository depth under current conditions.

Appendix F. **End members' composition.** This appendix is a summary of the work presented for Forsmark 2.2–2.3 (Gimeno *et al.* 2008) on the chemical composition of the end members, emphasising in this case the main conclusions and differences found in the Laxemar-Simpevarp area. Different INSITE issues are covered in this Appendix:

– Issue B-2: Alternative end-member selection and uncertainties in end members.
– Issue F-1: Glacial vs. Littorina in the bedrock, establish Littorina (and Deep Saline in the Laxemar-Simpevarp) compositions.
– Issue F-3: Geochemical and isotopic data used to interpret the groundwater evolution over time.

Appendix G. **Redox uncertainties.** This appendix describes the main uncertainties related to the redox data and modelling and to the integration of hydrogeochemical, mineralogical and microbiological data. Some recommendations are also indicated for future studies.

2 Final set of data for the "shallow" and "deep" groundwater systems

The dataset for this new Site Descriptive Modelling phase in the Laxemar-Simpevarp area was supplied by Sicada as Laxemar 2.2 and 2.3 data freezes and includes the old Laxemar 2.1 data freeze samples. Therefore, it includes all the relevant data from the Simpevarp peninsula and Laxemar subarea together with the available information from Äspö island (before the tunnel construction) and Ävrö island.

Table 2-1 summarises the type and number of samples included in the dataset for the Laxemar-Simpevarp area, separated by the data freeze in which they were delivered. The additional information compiled since the last SDM phase corresponds to the samples with data updated in Laxemar 2.2 data freeze (July the 11th, 2005), and all the remaining samples and updates since then.

The whole set of water data has been evaluated by Smellie and Tullborg (2009) and, after an exhaustive analysis of the data quality, an assignment to different categories has been made. This categorization has been fundamental to the selection of the samples used here for modelling purposes.

As a general rule, only the samples included in categories 1 to 4 have been used in this work. Only when a specific analysis on the evolution of a sample over time required it, the whole time series has been used. The need for pH (and sometimes Eh) field measurements has to great extent reduced the available set of samples for speciation-solubility calculations.

Altogether, there are 1,034 groundwater samples (deep and near-surface groundwaters), 302 of them with categories 1, 2, 3 and 4, and 1,437 surface water samples, 923 of them considered category 3 and 4 (as is explained in Smellie and Tullborg 2009). The number of samples indicated here does not include those samples with incomplete chemical data for major ions which were not included in the compiled table.

Table 2-1. Number and type of samples included in the final dataset for the Laxemar-Simpevarp area. The different rows indicate the number of samples delivered in each data freeze (2.1, 2.2 and 2.3) or updated between one data freeze and the next one. Numbers indicate (separated by a slash) the total number of samples and the number of these samples with category 1, 2, 3, or 4. Perc. Bhs: percussion boreholes; Cored Bhs: cored boreholes; NSGW: near-surface groundwaters; Precip: precipitation.

Data freeze	Subarea	Perc. Bhs.	Cored Bhs	Tube sampling	NSGW	Sea Water	Lake Water	Stream Water	Precip.
2.1	Äspö	14/5	137/21						
	Ävrö		61/3						
	Laxemar	15/5	122/12	35/2	45/39				
	Simpevarp	10/2	15/3	10/0	53/38	54/31	230/186	553/335	
2.1–2.2	Ävrö	9/4	4/0						
	Laxemar	5/3	39/7	64/0	4/4				
	Simpevarp		11/5	20/0	37/22	289/124	17/15	38/32	2/2
2.2.	Ävrö		3/0						
	Laxemar	14/6	49/4	46/5					
	Simpevarp		10/2		68/60	67/29	34/34	64/63	3/3
2.2–2.3	Laxemar	3/3	26/6	17/2					
	Simpevarp		2/2		8/6	4/2	2/2	6/6	3/3
2.3	Laxemar	1/1	46/9	4/0					
	Simpevarp				27/21	24/11	13/13	33/31	1/1
Total		71/29	525/74	196/9	242/190	438/197	296/250	694/467	9/9

However, an additional explorative analysis has been carried out in order to see the effect or consequences of using a sample subset instead of the whole set of samples. Figure 2-1 shows some of the plots that will be used later on, but including also the samples from category 5 and the samples corresponding to time series. As can be deduced from Figure 2-1, the presence or absence of these additional samples does not change the general picture drawn only with the ones from categories 1, 2, 3 and 4. Thus, they will not be considered in the following sections.
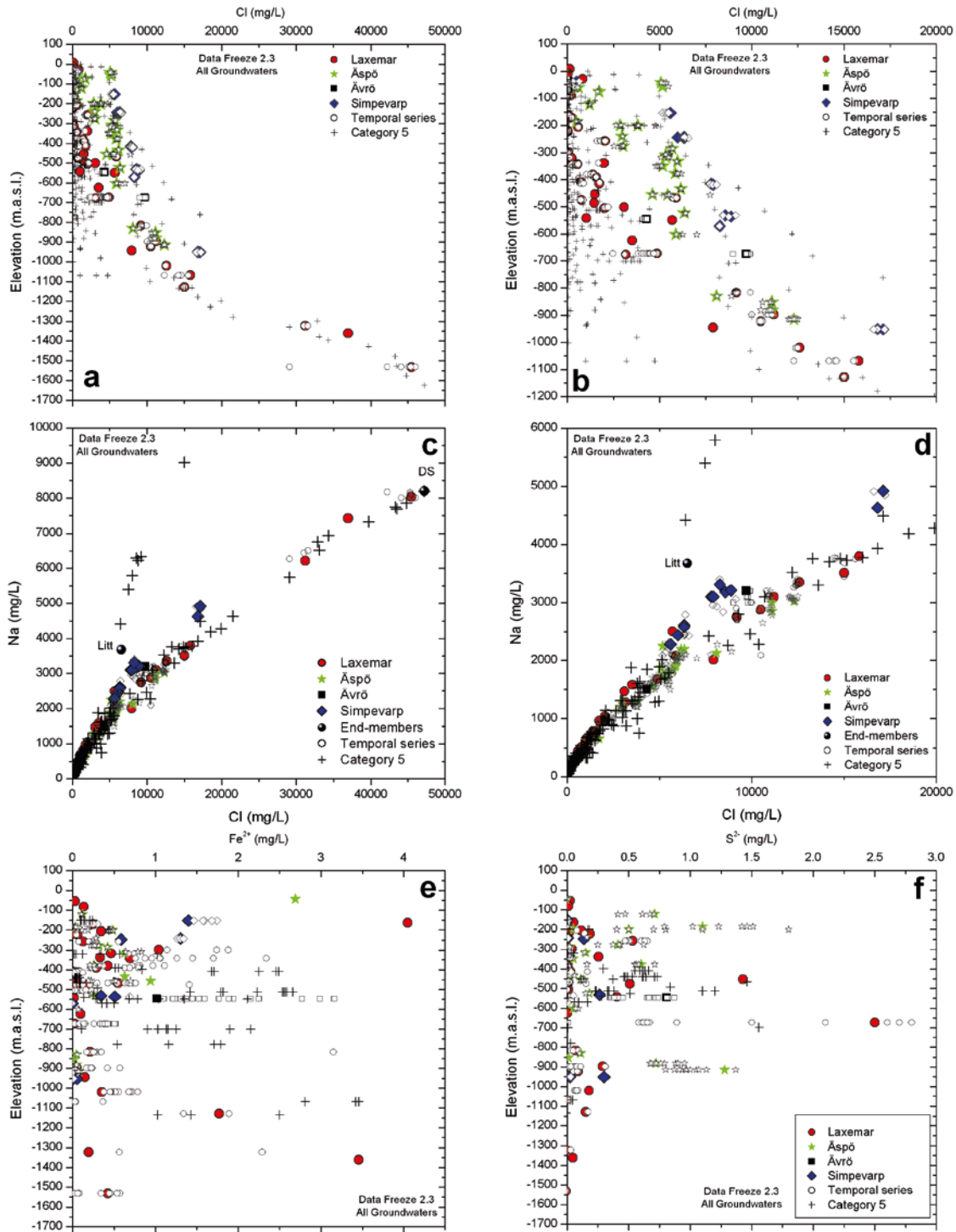
Figure 2-1. Examples of the trends shown by the samples of different categories. Plots (b) and (d) are the same as (a) and (c) respectively but with the scale enlarged.

Sample analyses for chloride and sodium corresponding to time series (open symbols in Figure 2-1) are generally coincident with the results obtained for the representative sample from each section (Figure 2-1ab). This indicates that, for major ions, the differences found in the different samples taken from the same depths are negligible. In the case of ferrous iron and sulphide concentrations, samples from the time series (and the monitoring program) usually show a range of variation that could be expected for these elements owing to their high sensitivity to the sampling procedure.

Samples categorised as 5 include tube samples and samples with large drilling water content. The effect on the plots is, in many cases, to fill in the gaps created by the subset of selected samples. In a few cases some samples follow a completely different trend (Na vs. Cl), or in the case of chloride distribution with depth, indicate more dilute waters at deeper locations.

Analysed data include the same parameters chosen in the previous stage. When available, field measurements from Chemmac logs are used in this report for pH, Eh, temperature and conductivity values. In the rest of cases, laboratory determinations have been included in the table but not used for modelling purposes.

3 Non-redox geochemical systems

This section presents the results of the explorative analysis and modelling work performed with all the available data by the time of the extended 2.3 data freeze. A summary of the main conclusions on the chemical elements distribution, their main controls and the results of geochemical modelling is also presented.

Several issues suggested by the INSITE group (INdependent Site Investigation Tracking & Evaluation) are dealt with here:

- Issue A-1: Modelling of the existence of a relatively shallow "process zone" capable of buffering the meteoric water with respect to redox and cation exchange.
- Issue B-1: Description of models based on reactions and other alternative models.
- Issue E-1: Spatial variability of hydrochemical data.

The chapter is subdivided into several sections for different elements: first, a detailed description of chloride, $\delta^{18}O$ and δ^2H (section 3.1) and of sodium, magnesium and potassium contents (section 3.2) is presented, since these elements have been crucial to differentiate water types (see section 2). Then, in the subsequent sections (3.3 to 3.6), different compositional systems (carbonates, sulphates, silica and fluoride, respectively) are thoroughly described and discussed. In all the cases, an important effort has been made to understand the recharge and discharge systems represented by the near-surface and shallow groundwaters.

The hydrochemical characters of near-surface groundwaters are important for evaluating geochemical processes during recharge (Issue A-1, above). These characters and their evolution are controlled by weathering reactions in the overburden, a system usually constituted by several hydrogeological compartments such as different types of soils, overlying sediments, buried-weathered bedrock and fractured bedrock outcrops. Weathering reactions in this complex system may also promote, inhibit or change the recharge pathways through changes in the rock porosity and permeability. Therefore, special attention has been paid to the study of these reactions and to the associated uncertainties.

Hydrogeochemical modelling has been performed with the PHREEQC code (Parkhurst and Appelo 1999) and using the WATEQ4F thermodynamic database, with the modifications reported in Appendix C. Modelling has focussed on speciation-solubility and reaction-path (and mixing) calculations related to sodium, potassium and magnesium, as well as to the carbonate, sulphate, silica and fluoride systems. These calculations were used to (a) investigate the processes that control water composition and the main hydrochemical trends, (b) test the hypotheses emerging from all the previous study, and (c) perform uncertainty analysis.

Following the same approach used in earlier stages for geochemical groundwater modelling (Simpevarp 1.1 and 1.2, SKB 2004ab, and Laxemar 1.2 and 2.1, SKB 2006ab), the evaluation of this new dataset started with the explorative analysis of different groundwater variables. The studies of fracture fillings, microbes and gases of the bedrock have also been considered in this work since they provide important information for the site description.

For the visualisation and interpretation of primary data, major ion concentrations have been plotted against depth or salinity. Three of the most important hydrochemical signatures have been selected to describe the groundwaters (Cl, Mg and $\delta^{18}O$) based on conceptual understanding of the Laxemar-Simpevarp area. Water types have been defined based on these three parameters (see section 2).

Two sets of plots are used here to visualise groundwater compositions. The first set shows all the groundwater samples from the regional scale area of the Laxemar-Simpevarp area, including the representative near-surface groundwaters and the shallow and deep groundwaters of categories 1 to 3. The second set shows only the groundwater samples from the Laxemar subarea including waters categorized as 1 to 4 (and distinguished with different symbols). Moreover, in this second set of plots, an additional symbol is used (squares and crossed squares) to indicate the samples taken from hydraulic domain C (see Laaksoharju 2008), and the depth and chloride scales are reduced to 1,200 m depth and 20,000 mg/L Cl. Moreover, near-surface groundwaters are generally described separately to better understand the processes affecting the recharge part of the system.

3.1 Conservative elements: Cl and δ¹⁸O

These parameters have been used for the definition of water types. Chloride concentration has been used as a salinity indicator. It shows the transition from the more dilute groundwaters at shallow depths to the highly saline waters at the deepest parts. Moreover, since chloride is usually conservative in groundwaters, its evolution is suitable for comparison when studying the hydrochemical evolution trends of other elements, ranging from conservative to non-conservative. Also, chloride acts as a tracer of the main irreversible process operating in this system, i.e. mixing (SKB 2004ab, 2006ab).

$\delta^{18}O$ and δ^2H are also conservative components that can be used to trace mixing processes, to differentiate recharge waters corresponding to cold or warm climates and to separate the groundwaters affected by glacial influence from the rest.

3.1.1 Chloride

The updated dataset closely follows the trends described in earlier reports (SKB 2004ab, 2006ab). As a general rule, chloride concentrations increase with depth (Figure 3-1a) but some specific points can be highlighted: a) the dilute nature of recharge meteoric waters (< 500 mg/L Cl) down to depths of around 500 m in the Laxemar subarea, followed by a marked and steady rise in salinity which in KLX02 reaches 47g/L Cl at the maximum sampled depth (1,630 m[1]); b) in comparison, the dilute recharge meteoric waters in the Äspö and Simpevarp subareas are restricted to the shallowest 100 meters; and c) at the Simpevarp subarea there is a similar but steeper increase in salinity to around 8,000–9,000 mg/L Cl at 600 m and to 17,000 mg/L Cl down to 1,000 m depth; e) the greater salinity between 100–600 m at the more coastal Äspö and Simpevarp sites is explained by discharge hydraulic conditions.

This variation in the transition depths between different water types for different subareas has also been described for other sites from the Fennoscandian shield. In Forsmark and Olkiluoto (the Finnish counterpart to Forsmark in terms of palaeoevolution), a similar transition from dilute groundwaters (<1,000 mg/L Cl) to brackish groundwaters (2,000 < Cl < 10,000 mg/L) occurs at depths ranging from 50–200 m (Figure 3-2). However, whereas the transition from brackish to more saline waters appears to occur at depths greater than 650 m in Forsmark (Figure 3-2a), in Olkiluoto the same transition takes place at around 400 m depth (Figure 3-2b).
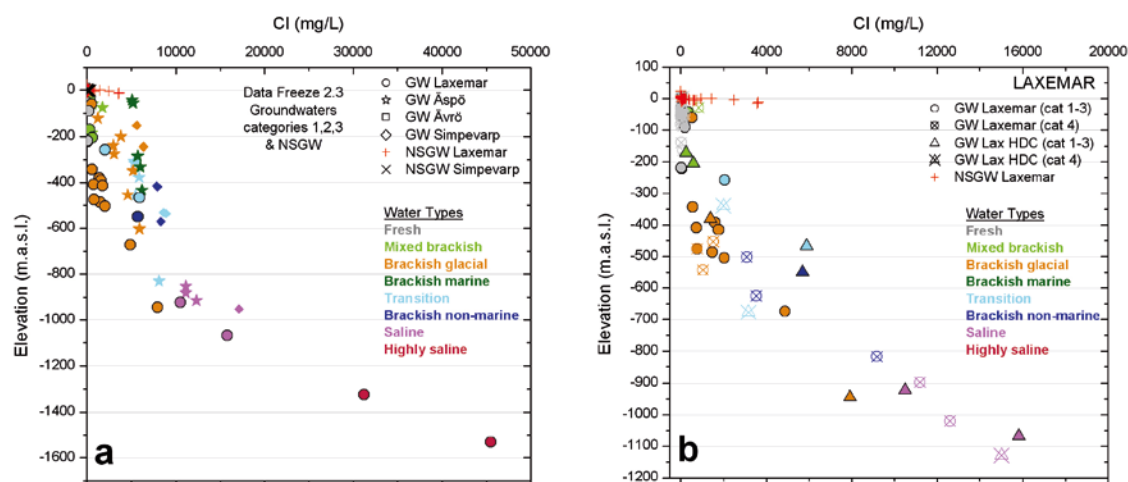
Figure 3-1. *Distribution of chloride with depth in the groundwaters from the Laxemar-Simpevarp area (a) and for the Laxemar subarea alone (b). The scale along the axes has been increased in the Laxemar subarea plot (b) to better visualise the shallow to intermediate depths.*

---

[1] That sample is not shown in the plots as it corresponds to category 5. The deepest and more saline shown sample corresponds to sample #2731, at 1,530 m depth and 45,000 mg/L Cl.
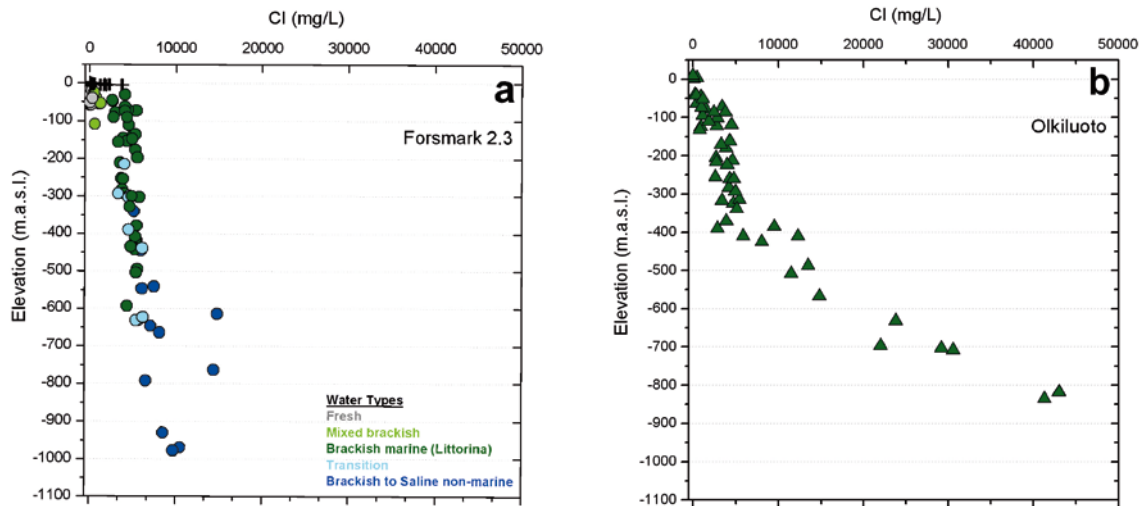
Figure 3-2. *Depth variation of chloride at Forsmark (a) and Olkiluoto (b). Forsmark groundwaters are colour-coded following the same criteria reported in Laaksoharju et al. (2008) which is the same as the one used for Laxemar-Simpevarp groundwaters. For Forsmark, the two largest chloride contents (at about 600 and 800 m depth and corresponding to boreholes KFM07A and 09A, outside the target area) seem to be due to anthropogenic upconing effects created during drilling and pumping operations. Therefore, they seem to represent a deeper origin than indicated in the plot (certainly in excess of 1,000 m).*

3.1.2 δ^{18}O and δ^{2}H

Figures 3-3a and b show the variation of δ^{18}O with depth. There is a wide range of values down to 550 m, ranging from the heaviest values in the brackish-marine type (especially at Äspö island), as in Forsmark (Figure 3-4a), to intermediate values (similar to the modern recharge) for fresh, mixed, transition and brackish-non marine types and, then, to lighter values for the brackish waters with an important Glacial component.

From 600 m down, δ^{18}O values tend to increase towards the values of the Deep Saline end member. Such enrichment has also been observed in Olkiluoto (Figure 3-4b) from 500 m down (note that the δ^{18}O value in the more saline samples from the Laxemar-Simpevarp area and from Olkiluoto is very similar; Figure 3-4bc) and in deep brines of the Canadian Shield (e.g. Frape and Fritz 1987).

The infiltration of Littorina waters having a heavy isotopic signature (estimated as –4.7‰ SMOW; Pitkänen *et al.* 1999) is the responsible for the trend in δ^{18}O values observed down to 500 m depth in the Laxemar-Simpevarp area (Figure 3-3a). The infiltration depth reaches 600 m at Forsmark and 300 m at Olkiluoto (Figure 3-4ab). Therefore, Littorina influence appears to be restricted to brackish groundwaters with chloride contents ranging from 3,000 to 5,000 mg/L at the Laxemar-Simpevarp area, Forsmark and Olkiluoto.

The same overall trend is also observed for the Laxemar subarea (Figure 3-3b) but without the presence of the brackish-marine waters at shallow depths. The samples from the Hydraulic Domain C always display the heaviest values (at all depths). Here the cold climate signature seems to have penetrated down to 1,000 m (δ^{18}O values around −14‰), as in Äspö (Figure 3-3a) and Forsmark (Figure 3-4a).

With respect to chloride (Figures 3-3cd), except for some near-surface groundwaters with very large δ^{18}O values, all the samples fall in the area delimited by the isotopic composition of the end members Deep Saline, Glacial, Littorina and Altered Meteoric (AM in panel c). The subdivision of water types is also clearly shown here. As regards the Laxemar subarea waters (Figure 3-3d), samples from the Hydraulic Domain C (between 300 and 700 m) are clearly different from the rest, which seem to be less affected by recent meteoric inputs and more affected by the signature of colder waters.

Figure 3-3. *Evolution of δ¹⁸O vs. depth (a, b) and vs. chloride concentration (c, d) at the Laxemar-Simpevarp area (a, c) and at the Laxemar subarea alone (b, d). The scales along the δ¹⁸O (plot b) and chloride (plot d) axes have been increased in the Laxemar subarea plots (i.e. absence of highly saline groundwaters) to better visualise the shallow to intermediate depths. The influence areas of modern recharge, glacial and marine waters are shown as hatched in Figure a; see text for discussion. The position of the end members is also shown in Figures c and d.*

Laxemar-Simpevarp groundwaters with a clear Glacial signature seem to be associated with brackish groundwaters with Cl < 4,000 mg/L (Figure 3-4c). As already stated, the few samples with heavy isotopic signatures clearly show Littorina influence, as in waters with Cl≈3,000–5,000 mg/L at Forsmark and Olkiluoto. For greater salinities, the decrease of cold recharge and Littorina influences is clearly observed at the Laxemar-Simpevarp area and Olkiluoto.

Figure 3-5a plots δ¹⁸O against deuterium, comparing the isotopic composition of the Laxemar-Simpevarp area waters with the Global Meteoric Water Line (GMWL). Brackish-marine, glacial and highly saline waters display different isotopic compositions. However, the fresh, mixed, transition, brackish-non marine and saline isotopic compositions are within the same range. The deviation of Baltic Sea waters from the GMWL isotopic composition is typical of evaporation effects which, to a lesser extent, have influenced some of the near surface waters and the brackish-marine groundwaters from Äspö. The depletion in δ¹⁸O observed in the highly saline groundwaters (and also in the Olkiluoto samples) as a deviation above the GMWL (Figure 3-5) is usually explained by very intensive water/rock interactions under near-stagnant conditions (Frape and Fritz 1987, Clark and Fritz 1997).
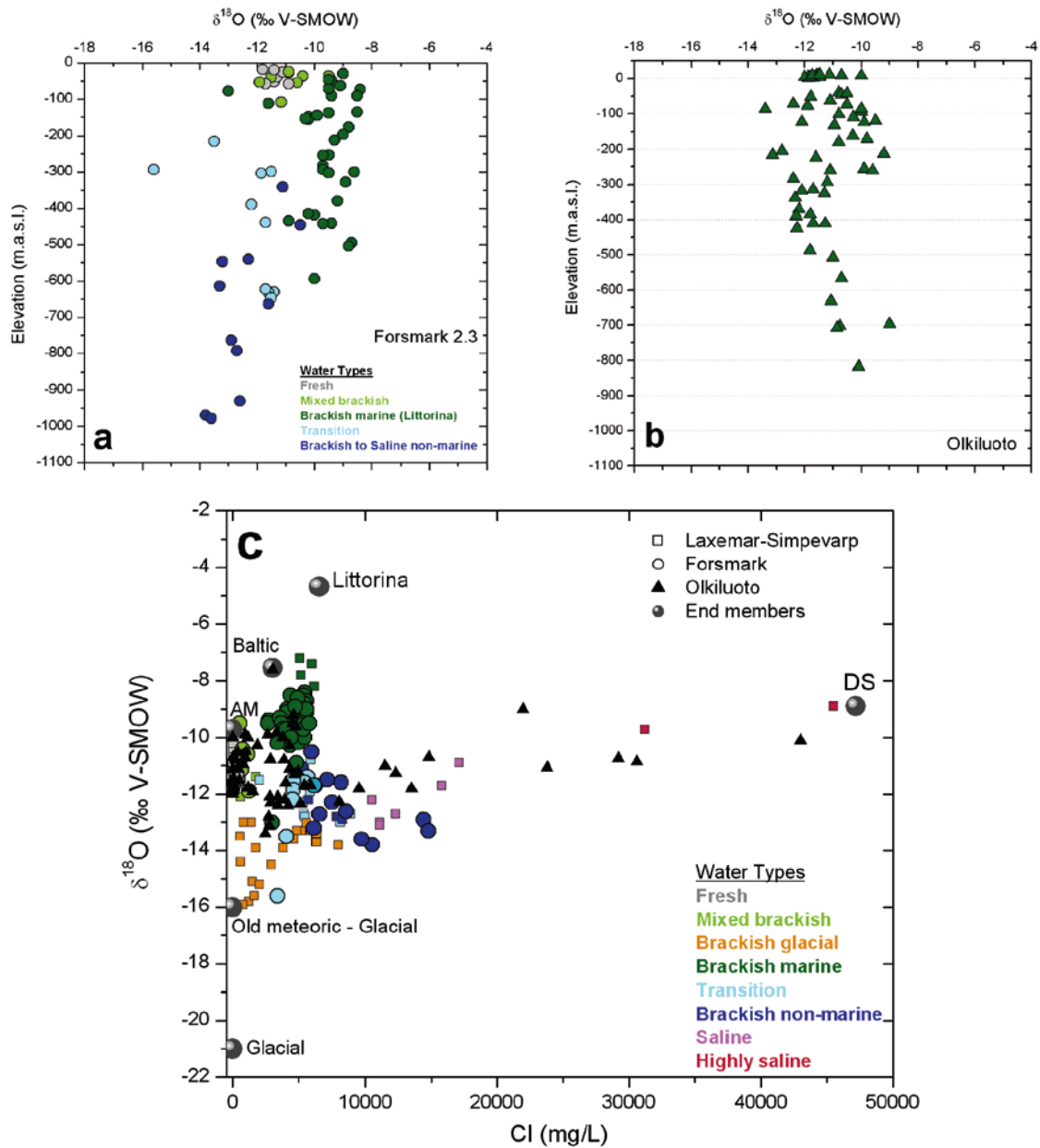
Figure 3-4. *Evolution of δ¹⁸O vs. depth at Forsmark (a) and Olkiluoto (b), and vs. chloride concentrations (c) at both sites compared with the Laxemar-Simpevarp area. The position of the end members is also shown in Figure c (DS: deep saline).*

A more detailed discussion on the meaning of these deviations in the systems represented in Figure 3-5 can be found in Gimeno *et al. (*2008).

3.2   Sodium, magnesium and potassium

The behaviour of these elements in crystalline systems is usually conditioned by reactions with aluminosilicate phases (dissolution-precipitation, cation exchange, etc). Calcium could have also been studied together with them. However, since the behaviour of this element is also associated with the carbonate system, this will be developed in section 3.3.
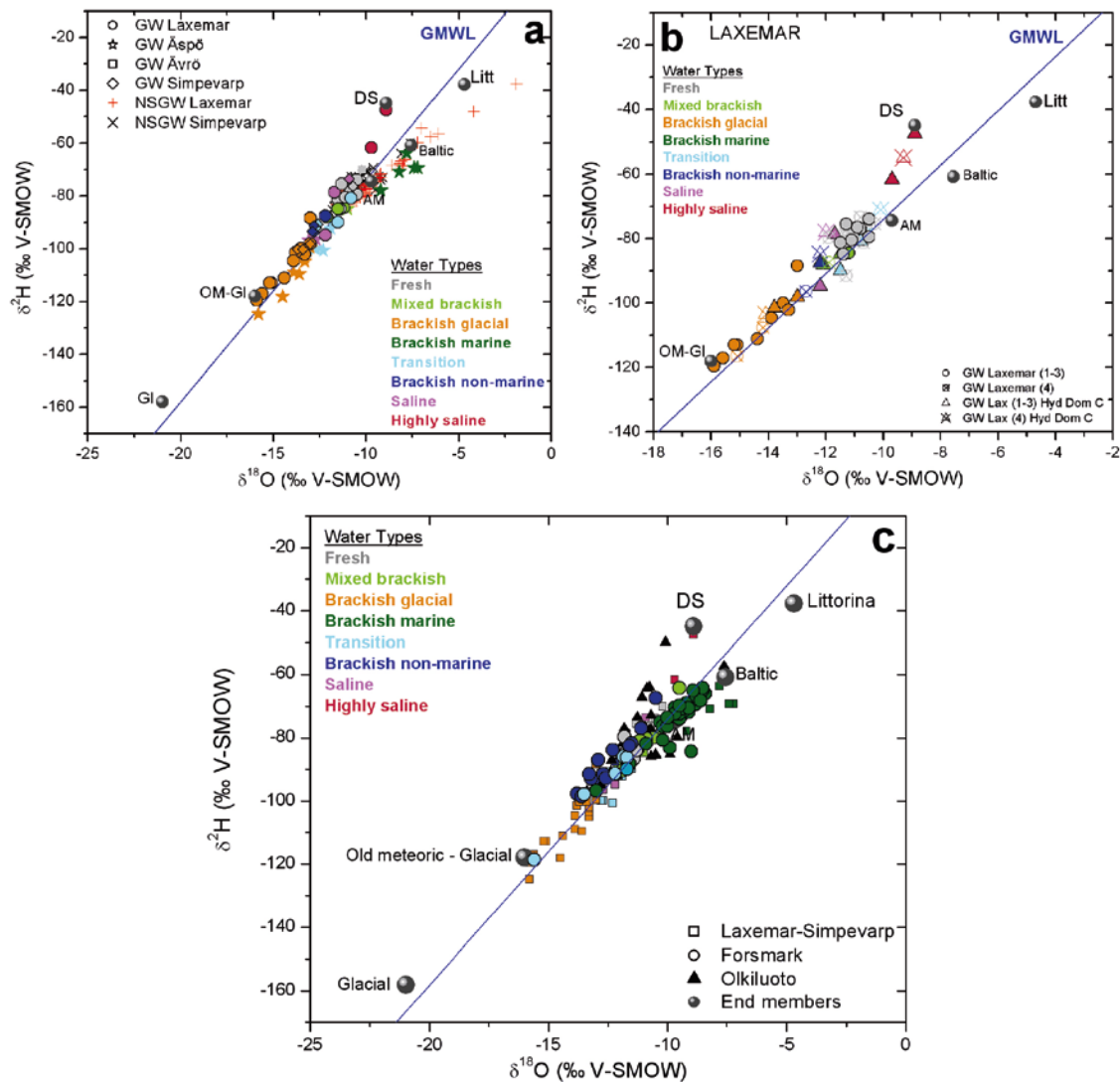
Figure 3-5. *Plot of δ¹⁸O vs. δ²H for the Laxemar-Simpevarp area (a) the Laxemar subarea (b) and Laxemar-Simpevarp together with Forsmark and Olkiluoto groundwaters (c). (GMWL = Global Meteoric Water Line). The scales along the δ¹⁸O and δ²H axes have been increased in the Laxemar subarea plot (b) to better visualise the samples and their water types. The position of the end members is also shown (Gl: glacial; OM-Gl: old meteoric-glacial; DS: deep saline; AM: altered meteoric; Litt: littorina).*

3.2.1 Hydrogeochemical data. General trends

Sodium distribution shows a wide range of concentrations at shallow depths (Figure 3-6a) reaching values of 1,900–2,230 mg/L in some soil pipes influenced by marine signatures and discharging deep groundwaters (see below). The depth distribution shows similarities with chloride (Figure 3-1). However, the subdivision of the Laxemar-Simpevarp groundwaters into those with low sodium (Laxemar subarea) and those with high sodium (Simpevarp subarea) at the same depth is more apparent. Sodium concentrations in the Äspö groundwaters are intermediate between them but closer to Laxemar (subarea) compositions corresponding to Hydraulic Domain C (Figure 3-6b).

Sodium and chloride contents are linearly correlated (Figure 3-6cd) and two slightly different slopes can be observed: the first one roughly following the seawater dilution line, which could be interpreted as mixing with a marine end member, and the second interpreted as resulting from mixing with a saline non-marine end member. Most of the aforementioned near-surface groundwaters with the largest sodium contents are included in the first group.

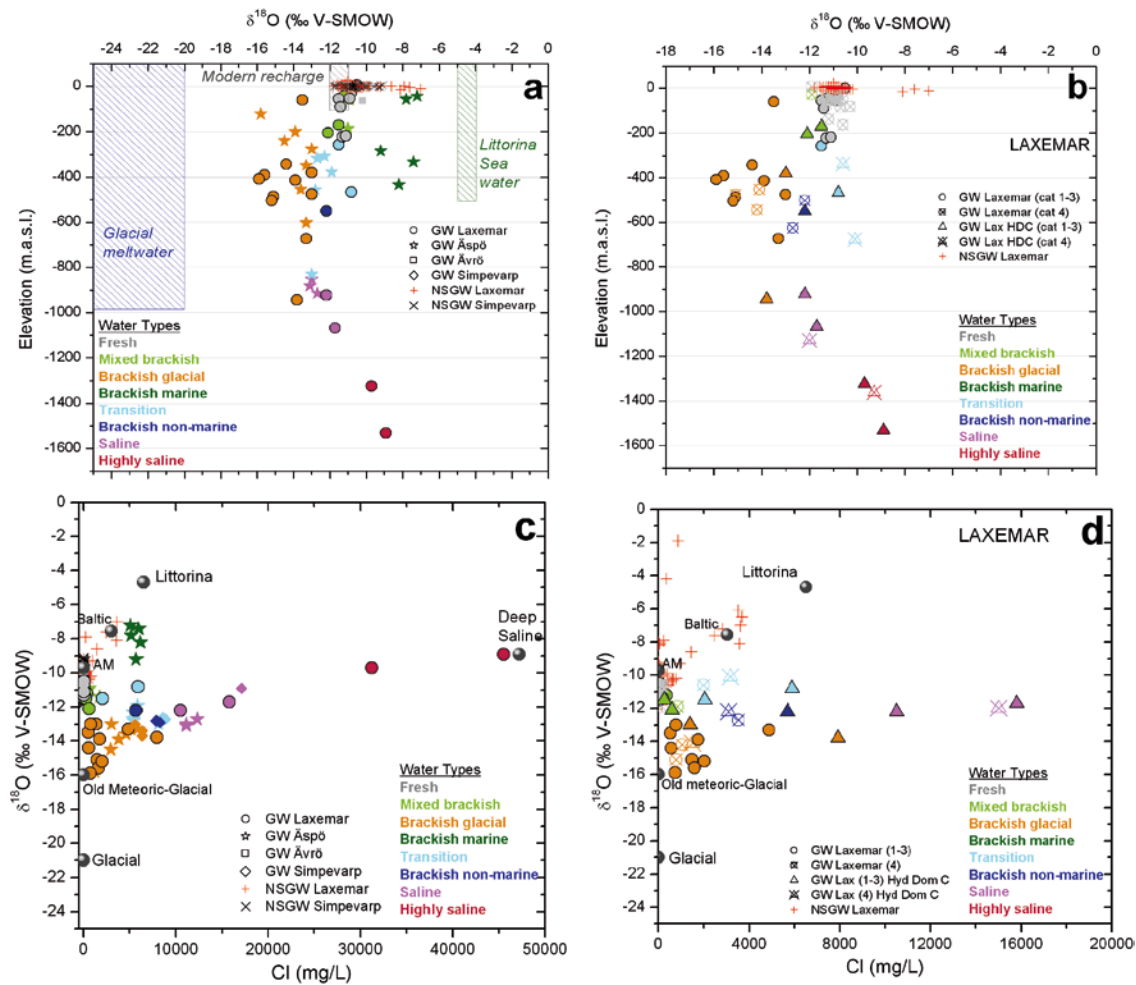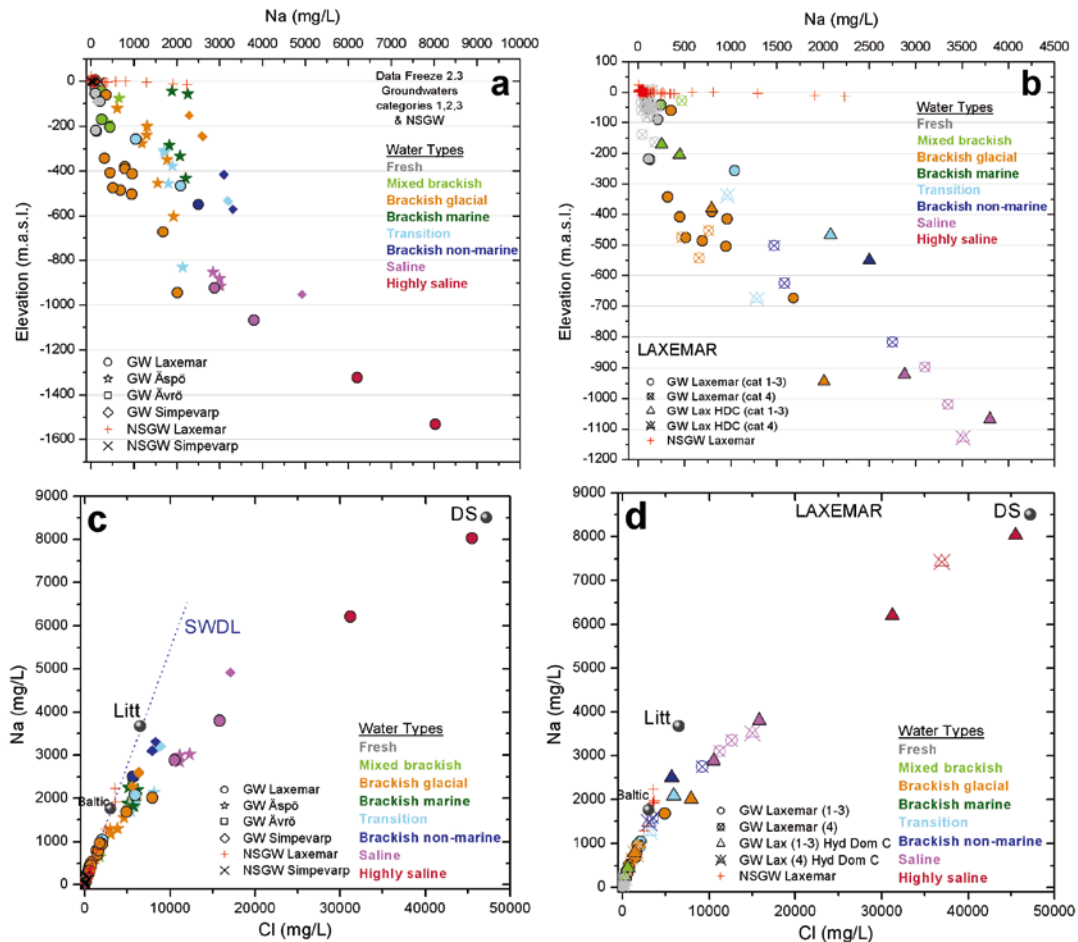**Figure 3-6.** *Evolution of sodium concentrations vs. depth (a, b) and vs. chloride content (c, d) at the Laxemar-Simpevarp area (a, c) and at the Laxemar subarea (b, d). SWDL: Sea Water Dilution Line. The scales along sodium and depth axes in the Laxemar subarea plot (b) have been increased to better visualise the shallow to intermediate depths.*

Sodium displays a near-conservative behaviour in those Laxemar (subarea) samples with high chloride contents (Cl > 10,000 mg/L) as is the case of Olkiluoto (Figure 3-7a). However, samples with Cl < 10,000 mg/L are affected by water-rock interaction, especially in dilute groundwaters down to 500 m depth at the Laxemar subarea (although at the scale of Figure 3-6cd, it cannot be appreciated because they are close to the coordinates origin).

A Littorina effect on the sodium contents of the groundwaters is less evident than in Forsmark (Figure 3-7b), where an important increase in sodium concentrations is observed for waters with chloride concentrations around 5,000 mg/L (Gimeno *et al.* 2008).

Magnesium has a wide range of concentrations at shallow depths and mainly in the near-surface groundwaters (Figure 3-8a), reaching values as high as 350 mg/L. This indicates a clear marine signature (modern Baltic and old Littorina; Figure 3-8c). Then, it decreases progressively with depth to values around 2 mg/L at 1,000 m depth, remaining constant thereafter down to the deepest and more saline groundwaters. As this element has also been used for the definition of the water types (marine indicator), in spite of its apparent reactivity, its concentration is clearly suitable for differentiating groundwaters affected by marine influence (with the highest magnesium contents) from the rest. As discussed below, this could be extended to potassium in some cases.

Figure 3-8a shows that this marine influence is different in each subarea. In general, magnesium values in the Laxemar subarea (Figure 3-8b) are close to or less than 10 mg/L irrespective of depth.
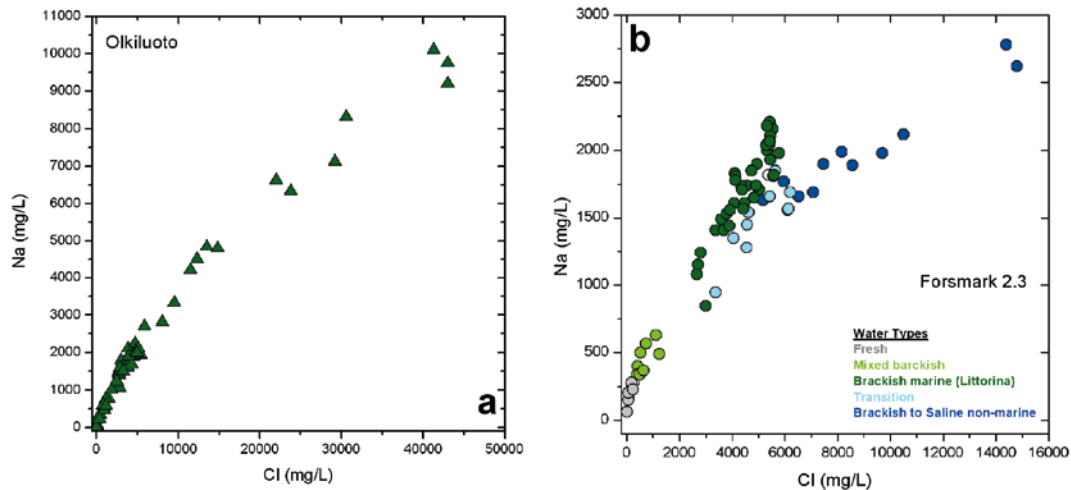
Figure 3-7. *Evolution of sodium concentrations vs. chloride content at Olkiluoto (a) and Forsmark (b). Note that the scales are different.*

However, there are some boreholes and some near-surface groundwaters with comparatively higher magnesium contents (from 20 to 60 mg/L), indicating a marine influence (e.g. boreholes KLX01, 10 and 15 and HLX38; Figure 3-8b, d). The large values found in KLX01 groundwaters have been attributed to Baltic Sea influence, since it is located close to a sea inlet, whereas for the rest of the boreholes, this influence is more likely related to remnants of Littorina waters. Äspö groundwaters have highly variable magnesium concentrations, with the highest values occurring at around 100 m depth and remaining still very high down to 500 m depth (Figure 3-8a). Simpevarp groundwaters have magnesium values intermediate between the other two subareas and also affected by discharge paths and/or by the proximity of the Baltic Sea.

The plot of magnesium *vs.* chloride (Figure 3-8c) shows that groundwaters with the highest magnesium concentrations belong to a narrow range of brackish compositions (~ 3,000–7,000 mg/L Cl). The brackish groundwaters with chloride about 5,000 mg/L and restricted to maximum depths of ~500 m (not shown in the plots) are considered to contain a significant component of Littorina Sea water, although this is less prevalent than at Forsmark or Olkiluoto (Figure 3-9) and mainly limited to Äspö, to some discharge points at Simpevarp, and to some remnants in the Laxemar subareas. The decrease of magnesium with salinity (chloride) increase suggests the influence of a magnesium-depleted saline component.

Apart from the marine influence, the large scatter of chloride concentrations in the 1,000–10,000 mg/L range suggests that reactions involving chlorites and smectites and also cation exchange could be controlling the dissolved magnesium content (see section 3.2.4 and Molinero *et al.* 2008b).

As explained for sodium and magnesium, some near surface and shallow groundwater samples from Äspö display high **potassium** concentrations, as a result of mixing with a marine component, whereas the rest have low potassium contents (Figure 3-10a). Potassium contents in groundwaters increase very slightly with depth but with values always below the seawater dilution line. This behaviour is common to the four subareas, showing a global concentration trend towards the Deep Saline end member (DS) concentrations. This may reflect the influence of mixing with a saline (non marine) component in saline groundwaters from Laxemar, as happens at Olkiluoto (Pitkänen *et al.* 2004 and Figure 3-11b). The plot of potassium *vs.* chloride concentrations (Figure 3-10b) shows that the highest potassium contents are found in the shallow groundwaters from Äspö and are restricted to groundwaters with chloride contents around 5,000 mg/L and with a significant Littorina contribution. The same character, although much clearer, can be observed at Forsmark and Olkiluoto (Figure 3-11).

Additional water-rock interactions (reaction with aluminosilicates, or cation-exchange) seem to be controlling the behaviour of this element, as suggested by the scattering of potassium concentrations in brackish waters with Cl < 10,000 mg/L (see section 3.2.4).
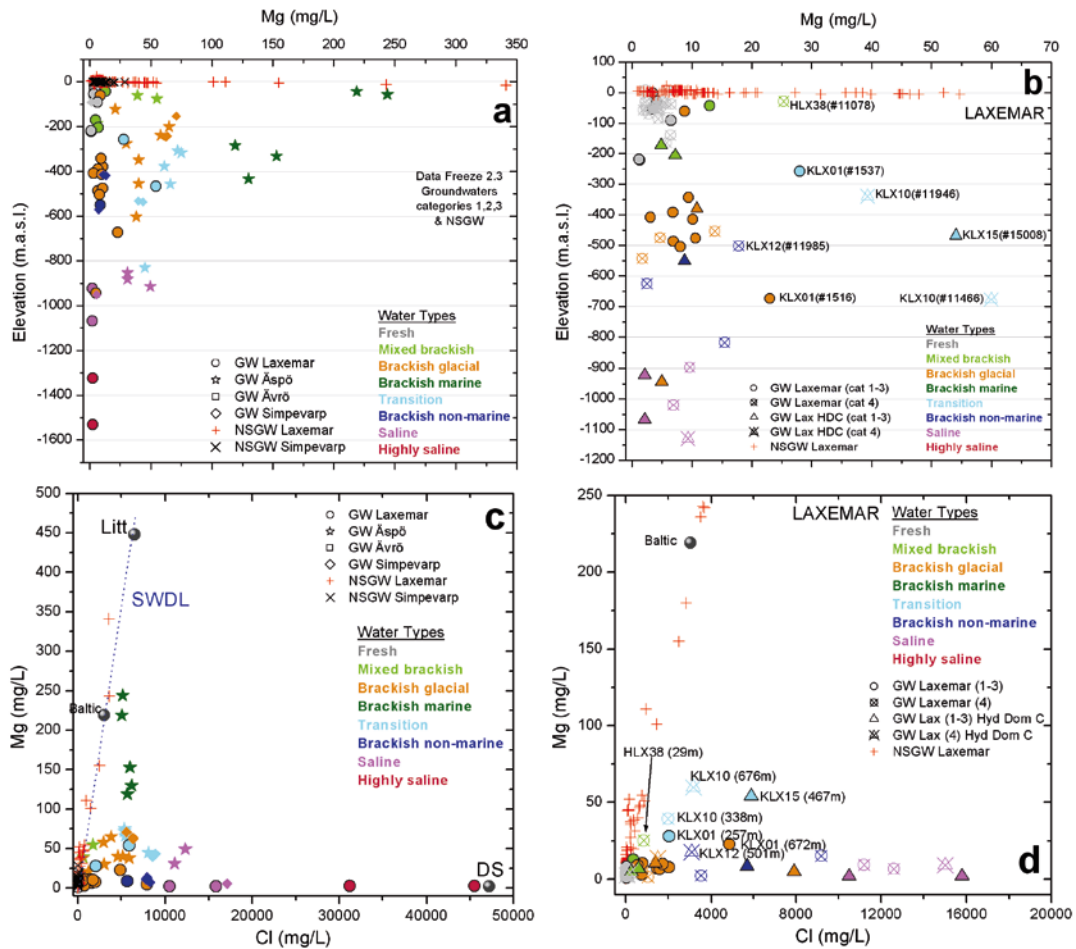
Figure 3-8. *Evolution of magnesium with depth (a, b) and chloride (c, d) in the Laxemar-Simpevarp area (a, c) and in the Laxemar subarea. SWDL: Sea Water Dilution Line. The scales along magnesium and depth, in plot b, and along chloride, in plot d, axes have been increased (depth restricted to –1,200 m and chloride to 20,000 mg/L, i.e. absence of highly saline groundwaters) in the Laxemar subarea plots (b and d) to better visualise the shallow to intermediate depths.*
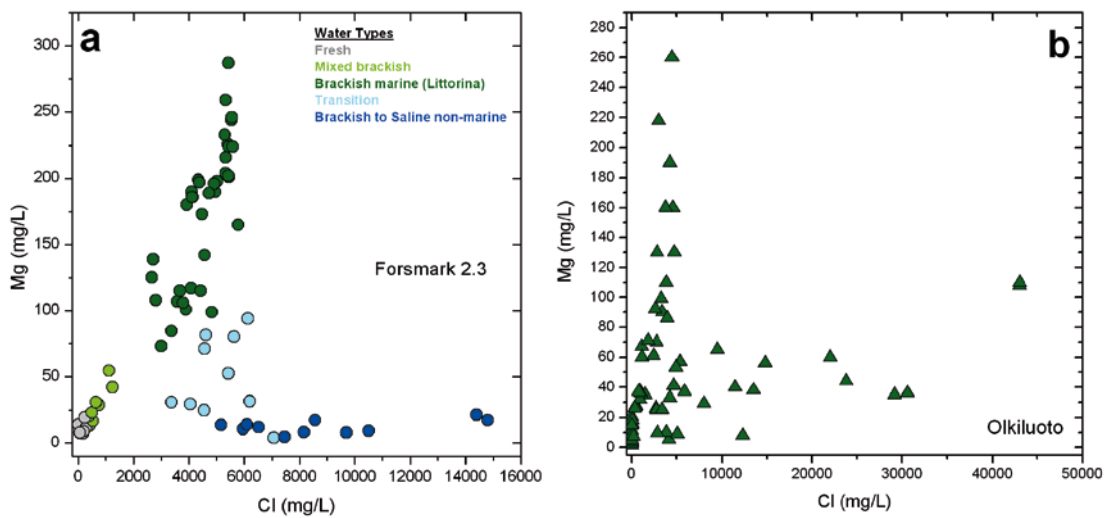
Figure 3-9. *Evolution of magnesium concentrations vs. chloride in Forsmark area (a) and in Olkiluoto (b). Note that the scales are different.*
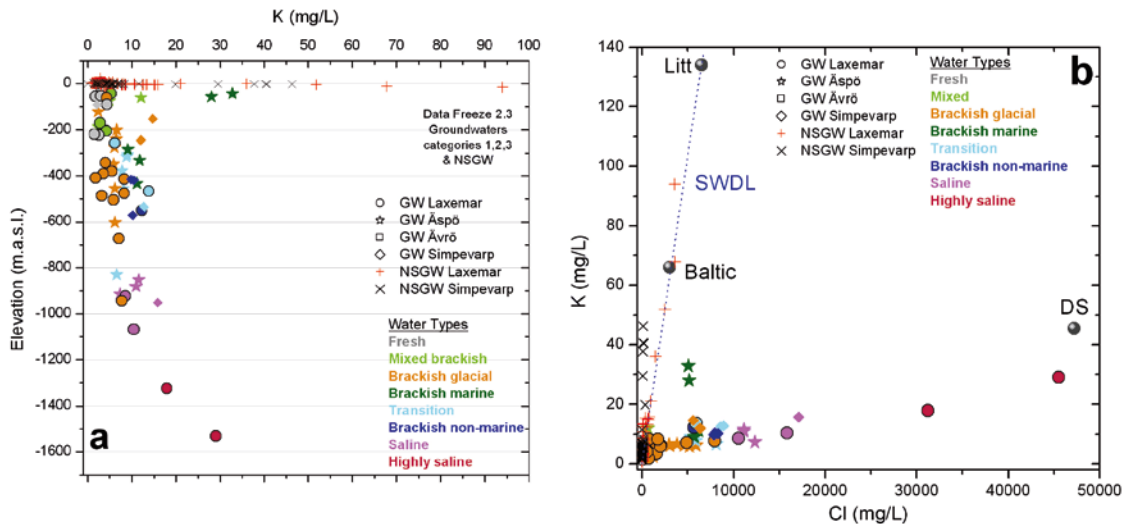
Figure 3-10. *Evolution of potassium concentrations vs. depth (a) and vs. chloride (b) in the Laxemar-Simpevarp area. SWDL: Sea Water Dilution Line.*
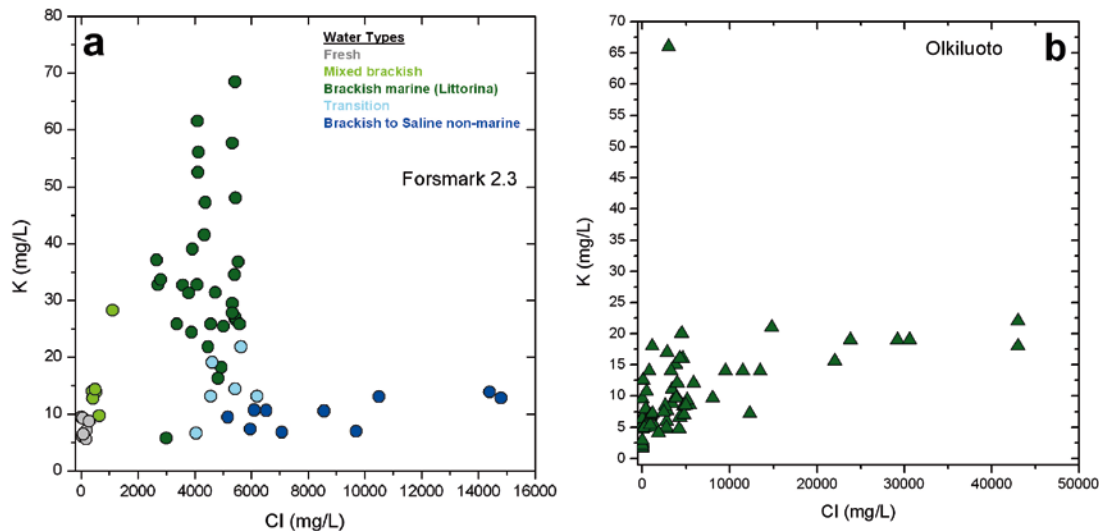
Figure 3-11. *Evolution of potassium concentrations vs. depth (a) and vs. chloride (b) in the Laxemar-Simpevarp area. Note that the scales are different.*

3.2.2 Mineralogical data

Overburden

The Laxemar-Simpevarp surface is dominated by areas of bare bedrock with thin soils and the rest is covered by till deposits and soils. This is a distinctive feature with respect to other Swedish sites (Lundin *et al.* 2005). In Forsmark, for example, there are few bedrock outcrops (less than 10%) and till deposits and soils dominate the surface; and the Olkiluoto Island is covered mostly with Quaternary soils, with only about 4% of the land area being characterised by bedrock outcrops (Posiva 2005). The mineralogy of the bedrock is, therefore, of special importance to the understanding of water-rock interaction processes at Laxemar-Simpevarp and to evaluate the buffering capacity of the shallow zone.

The Simpevarp subarea is dominated by Ävrö granite (a term that comprises rocks from quartz-monzodiorite to granite), quartz-monzodiorite and fine-grained dioritoid. The Laxemar subarea is also dominated by Ävrö granite and quartz-monzodiorite, which dominates in the southern and south-western part of this subarea and its surroundings. Some other minor rock types occur in both subareas but as smaller outcrops (Drake *et al.* 2006 and references therein).

These granitic rocks consist of plagioclase (almost 50%), K-feldspar and quartz, and lower and variable amounts of biotite, chlorite, epidote, hornblende and opaques. The calcite content of these rocks is low, being generally below 0.3%.

Mineralogical analysis of the till deposits and soils obtained in the Site Characterization Program are very scarce (only seven analyses of tills and clays; Sohlenius *et al.* 2006) and restricted to the Laxemar subarea. This situation represents a serious limitation when analyzing the type and intensity of the weathering reactions and, thus, information from other sources has been included.

The mineralogical analyses performed by Sohlenius *et al.* (2006) in the Laxemar subarea indicate that major minerals in the till matrix deposits (< 2 mm fraction) are quartz, plagioclase (oligoclase), and K-feldspar (microcline) with hornblende, illite, vermiculite, chlorite and kaolinite also present and, in some samples, significant amounts of calcite. In the clay fraction (< 2 μm), illite and chlorite are the predominant minerals, with smaller amounts of vermiculite, interstratified illite/vermiculite and kaolinite. The presence of quartz and feldspars is also documented in the clay fraction in almost all performed analyses.

Some quantitative mineralogical analysis have been performed for the < 2 mm fraction (Sohlenius *et al.* 2006) and they indicate that quartz and potassium feldspar appear in similar proportions (around 25%), with slightly higher amounts of plagioclase (around 35%) and much lower proportions of hornblende (2%), illite, chlorite and vermiculite (around 5%).

These mineralogical data, although scarce, are roughly comparable to those found in other "similar" sites (e.g. Forsmark and Olkilouto[2]) and are in agreement with the information mined in more general sources (e.g. Figure 3-12); therefore, some confidence can be given to their representativity.

From a kinetic point of view, plagioclase and mafic minerals (e.g. biotite and hornblende) may react significantly faster than quartz and K-feldspar in crystalline weathering environments (Goldich 1938, Lasaga 1984, White and Brantley 1995, White *et al.* 1998, 2001). Therefore, they may constitute the dominant sodium, potassium and magnesium sources for the near-surface groundwaters in the Laxemar-Simpevarp area.
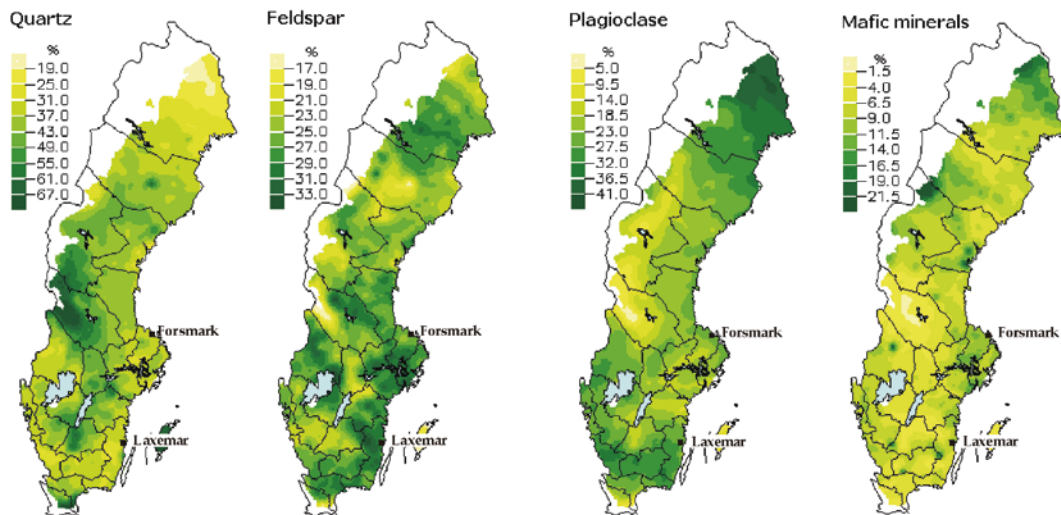
Figure 3-12. *Normative mineralogy in the Swedish soils. In the Laxemar subarea, quartz is between 25–35%, K- feldspar and plagioclase between 25–30% and mafic minerals between 4 and 6%. From MarkInfo database (created in the Department of Forest Soils, Swedish University of Agricultural Sciences, Uppsala; http://www-markinfo.slu.se/eng/index.html). For details see also Melkenud et al. (1992).*

---

[2] The mineralogical information on Quaternary deposits and soils from the Forsmark area is even scarcer than in Laxemar-Simpevarp. The only available mineralogical analyses have been presented in Sohlenius and Rudmark (2003). These authors indicate that the sandy and clayey tills in the area contain almost 40% of quartz with relatively high contents of hornblende and calcite present in all samples. Illite and, in minor amounts, chlorite are the most common clay minerals. At Olkiluoto, the mineralogical composition of soil samples is very homogeneous. In order of abundance, quartz, plagioclase, K-feldspar, mica, chlorite and hornblende are typical for the < 2 mm fraction, and correspondingly mica and chlorite for the fine fraction, i.e. < 2 μm (Posiva 2005).

In fact, some of the main chemical characters of the waters (e.g. Na/Ca ratios) in granitic environments are thought to be controlled by the incongruent dissolution of plagioclase whenever it has the largest modal abundance, as is the case in the Laxemar-Simpevarp area (Banks and Frengstad 2006 and references therein). This issue is further discussed in Section 3.3 (the carbonate system).

Typical secondary alteration products of weathering reactions in granitic environments such as kaolinite, illite and vermiculite have been identified. Kaolinite is usually the first and most common alteration product from aluminosilicate (e.g. plagioclase) incongruent dissolution (Garrels 1967, Garrels and Mackenzie 1967, Drever 1997, Langmuir 1997) although its formation does not affect the released cation contents.

However, the formation of illitic clays from the weathering of micas and feldspars, and of vermiculite and other clay minerals like chlorite or illite from the degradation of biotite and hornblende (Weaver 1989, White *et al.* 1996, Langmuir 1997, Sohlenius *et al.* 2006) may actively participate in the control of potassium (illite) and magnesium (vermiculite) contents. Therefore, although both elements are clearly mobilized during weathering (see section 3.2.3) they have partly been immobilised by the formation of clay minerals.

Fracture filling mineralogy

Different aluminosilicates with sodium, potassium and magnesium are present as fracture filling minerals in the Laxemar-Simpevarp area (Drake *et al.* 2006) and, therefore, they may participate in the control of their contents in the groundwaters.

Chlorite represents, together with calcite, the most abundant mineral in all the fracture fillings examined at the Laxemar and Simpevarp subareas, both in sealed and in open fractures. It is found at all depths including the first 100 m (although in lower amounts between 0 and 20 m depth). A minimum estimate of the chlorite content in a chlorite-bearing open fracture is a 0.1 mm thick coating covering 5% of the fracture surface. Thus, the minimum amount of this mineral would be around 0.015 kg per square meter of fracture (Drake *et al.* 2006).

The main Na-bearing mineral is albite, present as a main component in the bedrock although it is rather uncommon as a fracture mineral. Adularia (K-feldspar) occurs much more frequently than albite, especially in open fractures (7%[3]) and crushed zones (10%) from the Laxemar subarea, where it is found from 100 to 1,000 m depth and it is especially abundant in the 900–1,000 m depth interval. In the Simpevarp subarea, the detected amounts are much lower although they may be highly underestimated (Drake *et al.* 2006).

From the identified aluminosilicates, clay minerals are especially important since they are the most probable products of silicate alteration by groundwaters and represent the main substrate for surface processes (e.g. cation exchange reactions). At present, there are no available cation exchange capacity (CEC) data for the fracture filling minerals and, therefore, the possibility of this process occurring in the system can only be assessed from abundance data.

The identified clay minerals (different from chlorites) mainly include mixed-layer clays (smectite/illite, chlorite/smectite, chlorite/vermiculite) that frequently occur in the most superficial part of fracture fillings (Drake and Tullborg 2005). The relative abundance of clay minerals in sealed fractures is only around 3% whereas in open fractures they are much more abundant, particularly in the Laxemar subarea (38% vs. 4% in the Simpevarp subarea, Drake *et al.* 2006). Moreover, in fractures with an aperture larger than 1 mm, clay minerals are even more common than in open fractures with smaller aperture both in Simpevarp (18%) and Laxemar (again with higher proportions, 58%) subareas.

Crushed zones (incohesive fault breccia), usually representing zones with an elevated hydraulic conductivity (and, apparently, with indications of preferential infiltration paths of oxidising waters; Drake *et al.* 2006), were mapped separately during the drill core mapping. The fracture mineralogy of these crushed zones shows, again, high relative proportions of clay minerals, mainly in the Laxemar subarea (59% *vs.* 9% in the Simpevarp subarea).

---

[3] The percentage value represents in how many of the fractures a specific mineral has been identified, following the data reported by Drake *et al.* (2006).

Clay minerals in the Laxemar subarea occur at all the studied sections (down to 1,000 m depth) whereas in the Simpevarp subarea are concentrated in the upper 300 m, although they occur at greater depths in the crushed zones.

All these observations could suggest that the high proportions of clay minerals may be related to preferential groundwater recharge or active circulation paths, especially in the Laxemar subarea. However, this hypothesis must be verified, as other explanations are possible.

Therefore, different water-rock interaction processes affecting these mineral phases (incongruent dissolution of feldspars with formation of secondary clays, clay mineral transformations, etc; e.g. Langmuir 1997 and references therein) may participate in the control of dissolved sodium, potassium and magnesium (and calcium; see section 3.3.4 in the carbonate system). Moreover, the large amounts of clay minerals, especially in the Laxemar subarea, support the existence of suitable substrates for effective cation exchange in this system.

However, the identified phyllosilicates (smectites, vermiculite, illite and chlorite) have very different cation exchange capacities in standard conditions (Langmuir 1997, Appelo and Postma 2005): while smectite and vermiculite have large capacities, chlorite and illite have capacities noticeably smaller. Therefore, it is very important to obtain experimental data on the exchange capacities of the fracture fillings and estimations of the exchanger surface area to water ratio in the fractures.

3.2.3   Processes. Thermodynamic approach

Near-surface groundwaters

Dissolved sodium, potassium and magnesium contents in the surface (streams, lakes, etc) and near surface groundwater systems at Laxemar-Simpevarp are in the range usually measured in the Swedish context (Tröjbom and Söderbäck 2006b, Tröjbom *et al.* 2008).

As stated above, the set of near-surface groundwaters at Laxemar-Simpevarp include fresh and saline waters (chloride up to 5,000 mg/L). Some of these more saline near-surface groundwaters with higher Na (1,900 to 2,230 mg/L; Figure 3-6), magnesium (151 to 354 mg/L; Figure 3-8) and potassium (50 to 94 mg/L; Figure 3-10) are associated with soil pipes located in till below lake and sea sediments and they may represent waters strongly influenced by marine signatures (e.g. SSM000238 and SSM000239) and discharging deep groundwaters related to the main fracture zones in the area (SSM000241 and SSM000242; Tröjbom *et al.* 2008).

Moreover, road salts (NaCl, $CaCl_2$ and $MgCl_2$) are spread in the Laxemar-Simpevarp area and they can affect the concentrations of some major ions in the surface and near-surface groundwaters (Tröjbom *et al.* 2008). Therefore, to avoid this kind of contributions and effects, only near-surface groundwaters with chloride lower than 200 mg/L (fresh waters) will be considered here (as it will be done in other sections) to properly represent the weathering and recharge environment.

The highest sodium, magnesium and potassium concentrations found in these fresh near-surface groundwaters at this area (around 200–250 mg/L, 45–55 mg/L and 30–50 mg/L, respectively; Figure 3-13) correspond to samples in two soil pipes at the Island of Ävrö (SSM000018 and SSM000023; Simpevarp subarea) and one at the Laxemar subarea (SSM000034) close to the Baltic coast. The meaning of these outliers has been explained by Tröjbom *et al.* (2008) and they probably correspond to ongoing flushing of Littorina remnants and discharge of deep saline groundwaters mixed with meteoric recharge.

If these outliers are not considered, the concentrations of these elements are lower than in the fresh near-surface groundwaters at Forsmark (with maximum values of 200–250 mg/L Na, 50–55 mg/L Mg and 30–40 mg/L K) but noticeably higher than the range in the overburden at Palmottu or Olkiluoto (Blomqvist *et al.* 2000, Pitkänen *et al.* 2004).

Plotted with respect to the chloride contents (Figure 3-13), some fresh near-surface groundwaters seem to indicate a certain marine influence. However, most samples have sodium, magnesium and potassium concentrations above the Sea Water Dilution Line (SWDL; Figure 3-13) and are not related to the 1:1 Na/Cl or 1:2 Mg/Cl ratios associated with the possible effects of road salts. Therefore, the source of these elements in the fresh near-surface groundwaters is not dependent (in general) on marine or anthropogenic contributions, but related to weathering processes in the overburden.

Figure 3-13. *Sodium (a), magnesium (b) and potassium (c) concentrations vs. chloride in the fresh near-surface groundwaters from Laxemar-Simpevarp area. SWDL: Sea Water Dilution Line.*

Typical weathering reactions in the subsurface systems are mainly driven by biogenic CO_2 input in the overburden. Decay of organic matter (e.g. plant debris) and root respiration can be simplified to:

$$CH_2O + O_2 \rightarrow CO_2 + H_2O \tag{3-2-1}$$

This reaction drives the rest of the weathering processes as it provides a continuous source of CO_2 in the pedogenic environment. This input of CO_2 promotes the pH decrease and CO_2 partial pressure increase in waters. Then, CO_2 ($H_2CO_3^0$) is consumed in the weathering reactions of silicate minerals such as, for example, the alteration of albite or biotite to kaolinite:

$$2NaAlSi_3O_8 + 2H_2CO_3^0 + 9H_2O \rightarrow 2Na^+ + Al_2Si_2O_5(OH)_4 + 2HCO_3^- + 4H_4SiO_4^0 \tag{3-2-2}$$

$$2KMg_{1.5}Fe_{1.5}AlSi_3O_{10}(OH)_2 + 8CO_2 + 0.75O_2 + 16.5H_2O \rightarrow$$
$$\rightarrow 2K^+ + 3Mg^{2+} + Al_2SI_2O_5(OH)_4 + 8HCO_3^- + 3Fe(OH)_3 \tag{3-2-3}$$

Both reactions release base cations and HCO_3^- (Kehew 2001, Appelo and Postma 2005). The intensity of the weathering reactions during infiltration of the surface waters in the overburden is mainly conditioned by the evolution in open or close conditions with respect to CO_2. If the consumed CO_2 in weathering reactions is replenished by the input of biogenic CO_2 (reaction 3-2-1; open system conditions with respect to CO_2), weathering reactions will be enhanced, increasing the concentration of cations and HCO_3^- more than under closed system conditions. As the biogenic CO_2 production varies throughout the year (higher intensity in summer and lower in winter), the intensity of weathering is also conditioned by these temporal effects.

The global effect of reactions (3-2-1) to (3-2-3) is better appreciated when plotting the evolution of these elements with respect to alkalinity (Figure 3-14). Dissolved sodium, magnesium and potassium increase with alkalinity. However, as expected, these positive correlations are not perfect. Different factors are responsible for this dispersion:

a) These elements can have different mineral sources, depending on their local abundance in the overburden. However, once they are released to solution from the primary minerals (mainly plagioclase and mafic minerals such as biotite and hornblende; see above), they can be partially incorporated into secondary clays. Therefore, the net effect on their concentration increase (and the relation with the alkalinity production) depends also on the type of secondary mineral phases present.

b) These elements could be affected by other retention processes. For example, magnesium and potassium are important plant nutrients, while sodium is not usually taken up by plants.

c) Finally, although potassium has a lower affinity for cation exchange sites, magnesium and sodium (as well as calcium) can be much more actively involved in this process thus modifying their contents in the near-surface groundwaters.

In spite of all these effects, Na, Mg, and K clearly increase their contents with the weathering intensity (represented by the alkalinity production) and the incongruent dissolution of aluminosilicates seems to be the most important process in their control (see also section 3.2.2).
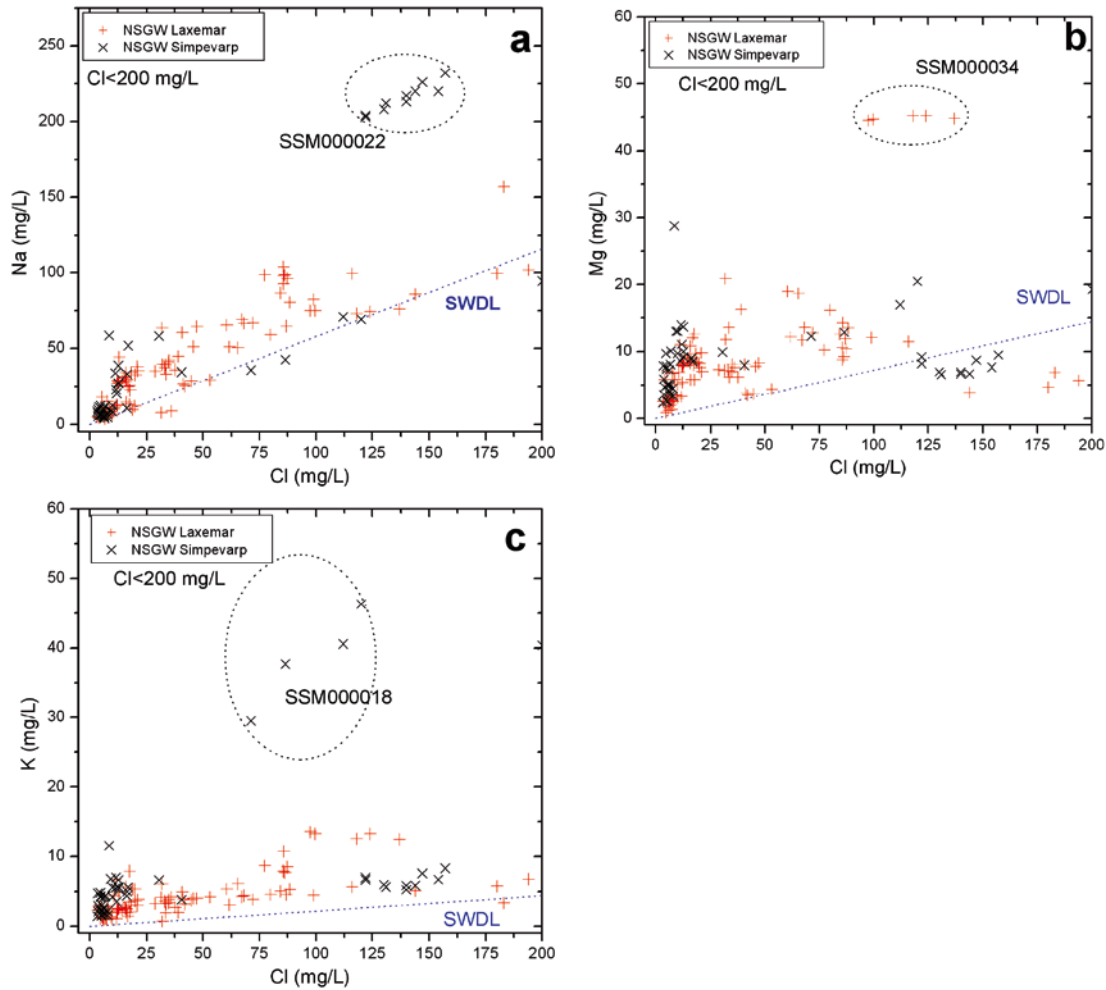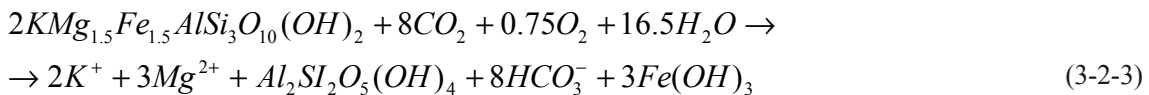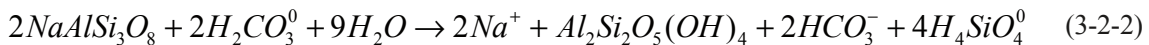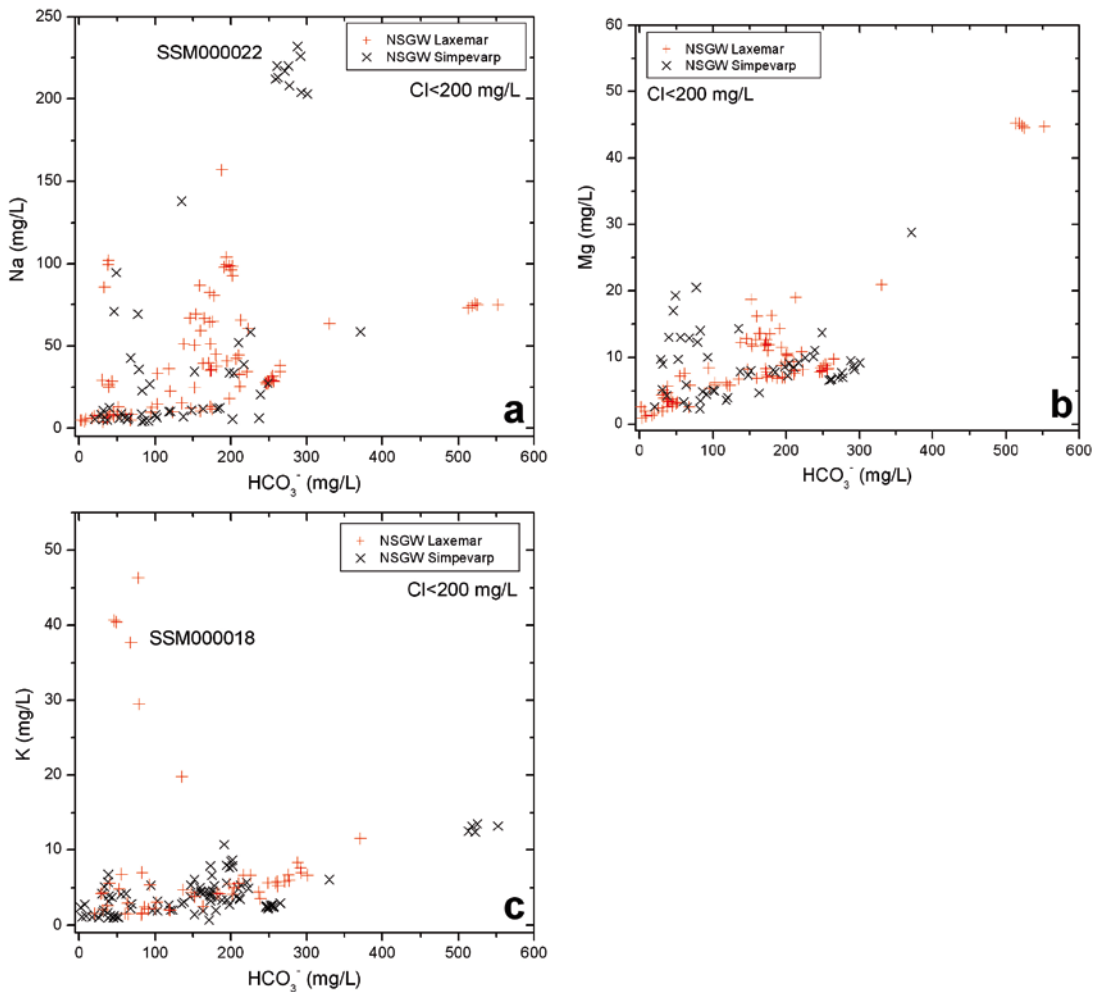

Figure 3-14. *Sodium (a), magnesium (b) and potassium (c) concentrations vs. alkalinity in the fresh near-surface groundwaters from the Laxemar-Simpevarp area.*

Cations released from primary minerals may be partially incorporated into secondary clays. Then, the net effect on their concentrations depends on the type of secondary mineral phase. An assessment of the alteration products likely to be participating in the control of dissolved sodium, potassium and magnesium is not straightforward. However, mineral stability diagrams can be used as a first and useful approach (Langmuir 1997).

Results for $\log(a_{Na+}/a_{H+})$ *vs.* $\log(a_{H4SiO4})$, $\log(a_{K+}/a_{H+})$ *vs.* $\log(a_{H4SiO4})$ and $\log(a_{Mg2+}/(a_{H+})^2)$ *vs.* $\log(a_{H4SiO4})$ diagrams, including the stability fields of some key aluminosilicate minerals, are shown in Figure 3-15.

Most of the fresh near-surface groundwaters (only samples with field pH data are considered here) fall in the kaolinite stability field (Figure 3-15a), supporting the stability of this mineral phase. Some others plot near the limit between Na-smectite (Na-beidellite) and kaolinite (Figure 3-15b) and between Mg-smectite (Mg-beidellite) and kaolinite (Figure 3-15c), suggesting a concomitant participation of smectites in the control of dissolved sodium in some groundwaters.

These observations agree with the general geochemical evolution of weathering in granitic systems (Garrels 1967, Garrels and Mackenzie 1967, Drever 1997, Langmuir 1997) in which kaolinite is usually the first and most common alteration product of the incongruent dissolution of aluminosilicates. Only in more hydrochemically evolved waters smectites (beidellites) are identified as the alteration product. Note that dilute groundwaters (Cl < 200 mg/L) from cored-boreholes (150 to 500 m depth) also plot near the limit between kaolinite and smectites, in agreement with the more evolved character of these groundwaters.

Kaolinite has frequently been identified in the overburden but smectites have not been found. This fact can be related to sampling: mineralogical data available at present are still scarce and, apparently, the distribution of smectites in the overburden seems to be much more limited.

The $\log(a_{K+}/a_{H+})$ *vs.* $\log(a_{H4SiO4})$ diagram (Figure 3-15b) provides results that are compatible with the previous ones. Most of the near-surface groundwaters fall in the kaolinite stability field. Others, however, reach the necessarily high dissolved potassium contents (and moderate silica concentrations; Langmuir 1997) to plot in the illite stability field. This supports the stability and active participation of illite in the control of dissolved potassium, in agreement with available mineralogical data.

In any case, as the activity diagrams including clay minerals are a necessary simplification of reality, other processes and/or clay minerals can participate in the control of dissolved sodium, potassium and magnesium in the near-surface groundwaters. The mineralogical analyses of till samples from Simpevarp indicate a significant amount of vermiculite as a result of clay mineral alteration by chemical weathering (Sohlenius *et al.* 2006). Therefore, weathering-induced transformations from illite or chlorite (both present in the overburden) to vermiculite can also participate in the control of dissolved potassium and magnesium.

Shallow and deep groundwaters

From the available mineralogical data in fracture fillings, several aluminosilicates could participate in the control of dissolved sodium, potassium and magnesium. Some of them, like albite or adularia, have thermodynamic data relatively well constrained whereas the most abundant (chlorite and mixed-layer clays like smectite/illite, chlorite/smectite or chlorite/vermiculite) have a wide structural and chemical complexity and they are thermodynamically ill-defined (e.g. Nordstrom *et al.* 1990, Trotignon *et al.* 1999). Therefore, as for the near-surface groundwaters, some degree of simplification is needed.

Apart from the diagrams already used for the near-surface groundwaters, the stability diagrams for adularia, albite, kaolinite and chlorite (Gimeno *et al.* 2004b, 2005) have also been applied. They have been constructed using the thermodynamic data proposed by Grimaud *et al.* (1990) for the Stripa groundwaters (at 15°C).
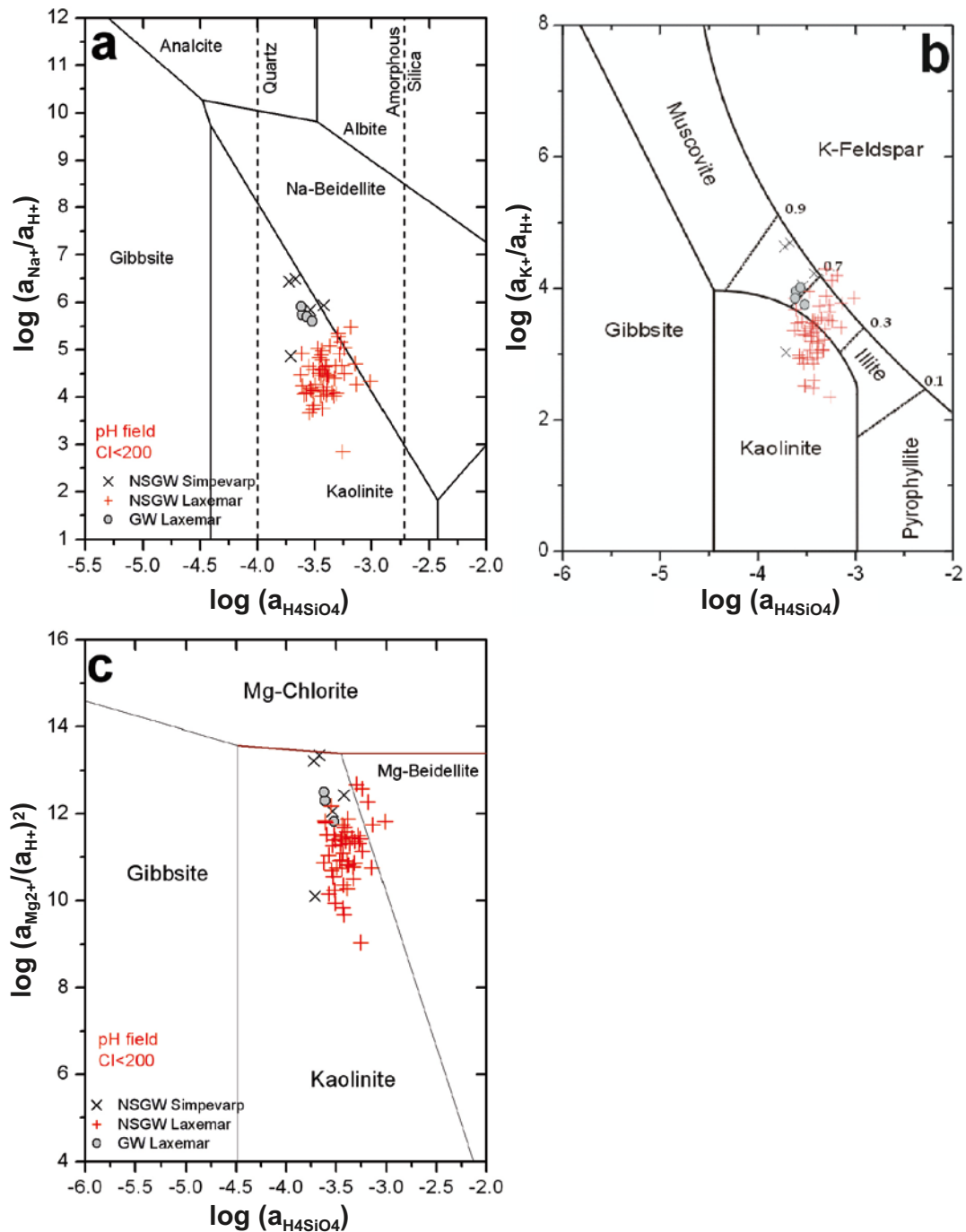
Figure 3-15. *Mineral stability diagrams showing the location of the near-surface groundwaters and dilute groundwaters (with Cl < 200 mg/L) from cored boreholes from Laxemar-Simpevarp area. All the plotted samples have a field measurement for pH. (a) Log (a_{Na+}/a_{H+}) vs. log (a_{H4SiO4}) diagram. (b. log (a_{K+}/a_{H+}) vs. log (a_{H4SiO4}) diagram; illite field is subdivided in three subfields in plot (b) to show the stability of different illite fractions in mixed-layer illite/smectite (0.1, 0.3, 0.7 and 0.9). (c) Log ($a_{Mg2+}/(a_{H+})^2$) vs. log (a_{H4SiO4}) diagram. Activity calculations have been performed with PHREEQC (Parkhurst and Appelo 1999) and the WATEQ4F database (Ball and Nordstrom 2001). The field boundaries have been calculated with data from Drever (1997) in plot (a) and from Helgeson (1969) and Helgeson et al. (1978) in plots (b) and (c).*

Figure 3-16a shows the position of all groundwaters (near surface, shallow and deep) with field pH in the diagram kaolinite-albite-adularia. Most brackish and saline groundwaters are located on the adularia-albite boundary, suggesting a control by this equilibrium situation. This result is very similar to that presented by Grimaud *et al.* (1990) for the Stripa groundwaters but with an important difference: maximum chloride contents at Stripa are below 700 mg/L, whereas Laxemar-Simpevarp groundwaters reach chloride values of 45,000 mg/L (see also Gimeno *et al.* 2006).

This observation is very important as the trend parallel to the adularia-albite boundary defined by the Laxemar-Simpevarp groundwaters includes waters with a very wide range of salinities and affected by different degrees of mixing, which supports the participation of adularia and/or albite in the control of dissolved sodium and potassium.

As expected, most of the near-surface groundwaters fall in the kaolinite stability field. However, some of them fall in the adularia stability field, although far from the adularia-albite boundary. This situation is a consequence of the simplicity of these diagrams, where only the fields for three minerals are considered. As an example, the near-surface groundwaters on the adularia stability field are those located on the illite stability field shown in Figure 3-15b.
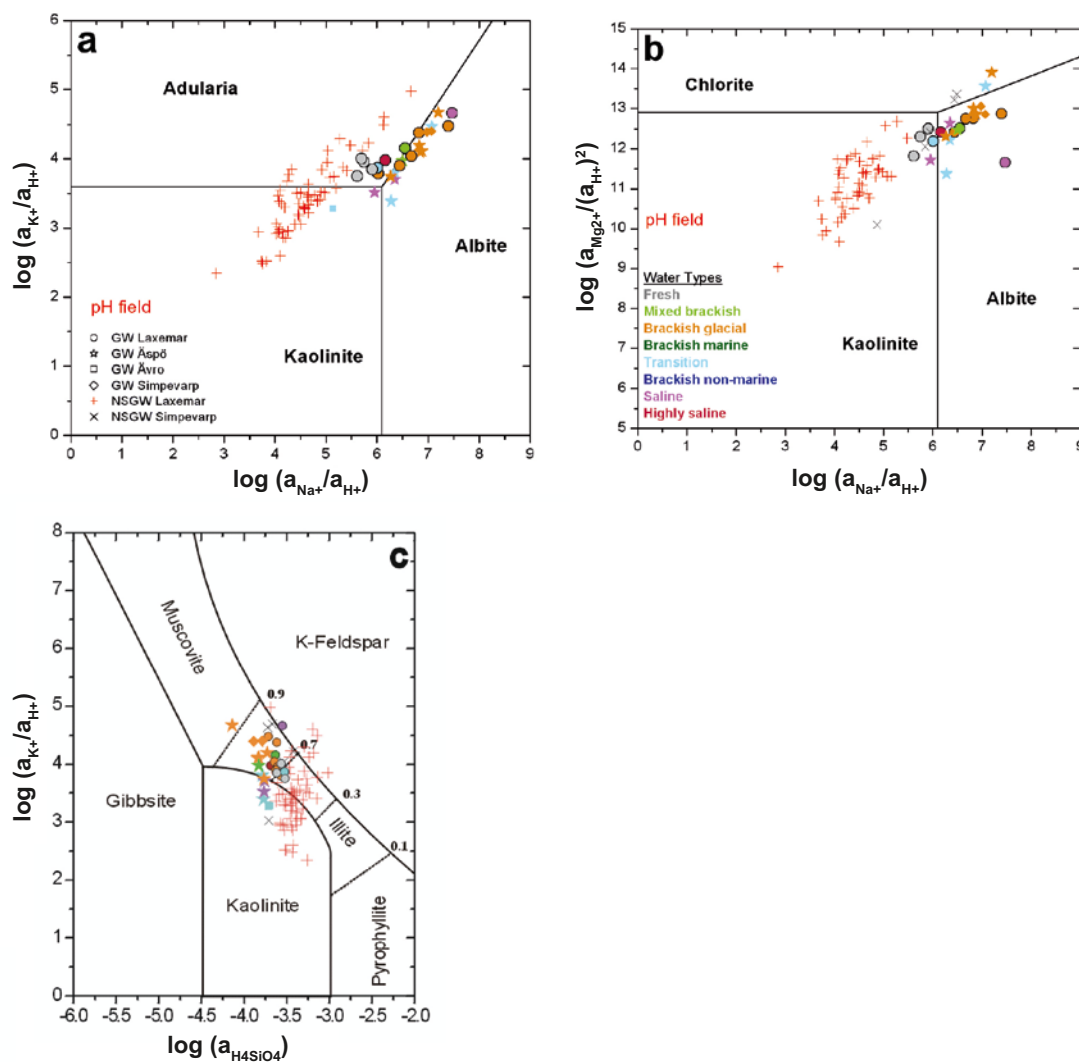
Figure 3-16. *Mineral stability diagrams showing the location of the near-surface groundwaters and dilute groundwaters (with Cl < 200 mg/L) from cored boreholes from Laxemar-Simpevarp area. All the plotted samples have a field measurement for pH. (a). Log (a_{K+}/a_{H+}) vs. log (a_{Na+}/a_{H+}) diagram. (b). Log ($a_{Mg2+}/(a_{H+})^2$) vs. log (a_{Na+}/a_{H+}) diagram. (c) Log (a_{K+}/a_{H+}) vs. log (a_{H4SiO4}) diagram. Activity calculations have been performed with PHREEQC (Parkhurst and Appelo 1999) and the WATEQ4F database (Ball and Nordstrom 2001). Field boundaries have been calculated from Grimaud et al. (1990) data in plots (a) and (b) and from Helgeson (1969) and Helgeson et al. (1978) data in plot (c) (illite field is contoured to show the stability of different illite fractions in mixed-layer illite/smectite).*

With regard to shallow and deep groundwaters from the Laxemar-Simpevarp area, they are located in the illite stability field as shown in Figure 3-16c, supporting an additional control on the dissolved potassium by this phase. The main difference with respect to the near-surface groundwaters is that these deeper waters have longer residence times and they have reached the adularia-albite boundary.

Finally, the diagram with the kaolinite, chlorite and albite stability fields (Figure 3-16b), shows that most of the groundwaters from Laxemar-Simpevarp are in the stability field of albite. In spite of the uncertainties[4], they plot close and parallel to the chlorite boundary, suggesting that this mineral, the most abundant fracture filling phase at all depths, could be a limiting phase for dissolved magnesium (cf. Molinero et al. 2008).

Figure 3-17a, b show the groundwaters from Olkiluoto and Forsmark plotted on these activity diagrams. The results are very similar to those presented for the Laxemar-Simpevarp groundwaters (also shown in the same plots). For example, in Figure 3-17a groundwaters from the three sites plot on the adularia-albite-kaolinite coexistence area, or very close to the adularia-albite boundary. The same happens in the chlorite-albite-kaolinite diagram (Figure 3-17b) where groundwaters from Forsmark and Olkiluoto are superimposed onto those of Laxemar-Simpevarp.

In spite of the simplifications that the use of these diagrams entails, results indicate that the participation of different clay minerals in the control of dissolved magnesium and potassium is plausible in the studied waters, as is the case in other crystalline systems (e.g. Gascoyne 2004). Adularia and albite may also participate, as has also been indicated in other low-temperature crystalline systems such as Stripa (Grimaud et al. 1990) and even Äspö (Trotignon et al. 1999).

These mineral reactions would be superimposed, in most cases, upon different mixing processes. The relationship between mixing and reaction can be analysed by using some of the results obtained in SR-Can (Auqué et al. 2006). In this exercise, the mixing proportions obtained with the hydrogeo-logical model for the present-day state (≈ 2020 AD) of the Forsmark and Laxemar sites were coupled with PHREEQC (Parkhurst and Appelo 1999) mixing and reaction calculations.
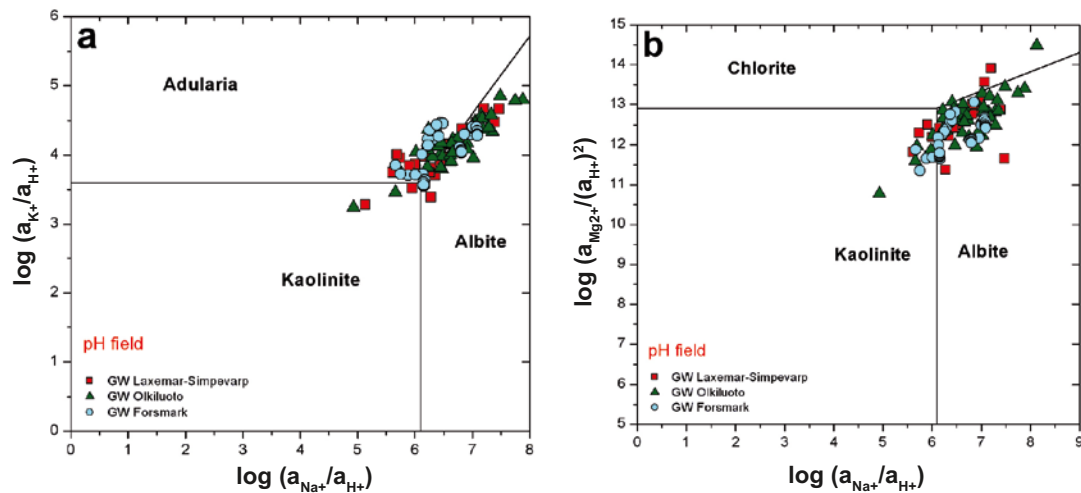
Figure 3-17. *Mineral stability diagrams showing the location of the groundwaters from Laxemar-Simpevarp (red squares), Forsmark (cyan circles) and Olkiluoto (green triangles). All the plotted samples have a field measurement for pH. (a). Log (a_{K+}/a_{H+}) vs. log (a_{Na+}/a_{H+}) diagram; (b). Log ($a_{Mg2+}/(a_{H+})^2$) vs. log (a_{Na+}/a_{H+}) diagram. Activity calculations have been performed with PHREEQC (Parkhurst and Appelo 1999) and the WATEQ4F database (Ball and Nordstrom 2001). The field boundaries have been calculated with data from Grimaud et al. (1990).*

---

[4] It should be taken into account that the chlorite phase used in the diagram is a pure Mg-phase, whereas in fracture fillings chlorite shows a greater compositional complexity, with a significant fraction of Fe(II).

Those hydrological results include the sites in a large regional scale; therefore, they show a larger range of concentrations and mixing proportions than those in groundwaters that have been sampled only in a few boreholes located within the repository candidate volume. Results of *conservative* mixing from the hydrological results for more than 30,000 points (groundwaters) in the Laxemar-Simpevarp regional domain are presented in Figure 3-18 for 2020 AD (a more detailed description of the methodology for simulations can be found in Auqué *et al.* 2006).

The field occupied by the groundwaters, the result of different mixing proportions between different end members (note the chloride contents), in the regional area is restricted to a specific zone around the stability limit between adularia and albite (though not shown, the same happens for Forsmark). The same happens for the chlorite-albite-kaolinite diagram (not shown).

This conclusion does not mean that mineral reactions are not effective. It only means that conservative mixing will constrain the distance to mineral equilibrium and, therefore the intensity of mineral reactions. Note, for instance, that the most dilute synthetic groundwaters (red and orange colours in Figure 3-18) are further away from the adularia-albite boundary. This relationship between the results from mixing and their effects on chemical reactions will also be evaluated in the following compositional systems. The possible influence of cation exchange on the control of dissolved sodium, magnesium and potassium will be assessed next. Since no CEC data are available in the studied system, this analysis will be performed by means of theoretical simulations.

3.2.4 Thermodynamic simulations

After the initial explorative analysis, several simulations have been made to check the feasibility of the different hypotheses put forward in the previous sections. A similar simulation effort has also been made for the rest of the geochemical systems of interest (carbonates, sulphates, silica and fluoride). The basis for these simulations will be described in detail here and this section will be referred to when dealing with the other compositional systems.

General PHREEQC simulations

The main process to be simulated is mixing. This process has taken place between different water types (end members) over time, making the discrimination of the main influences not always easy. In general, the conceptual model suggests that the first mixing event is the input of dilute waters (cold or warm) into bedrock containing very saline groundwaters. Then, during the Littorina period,
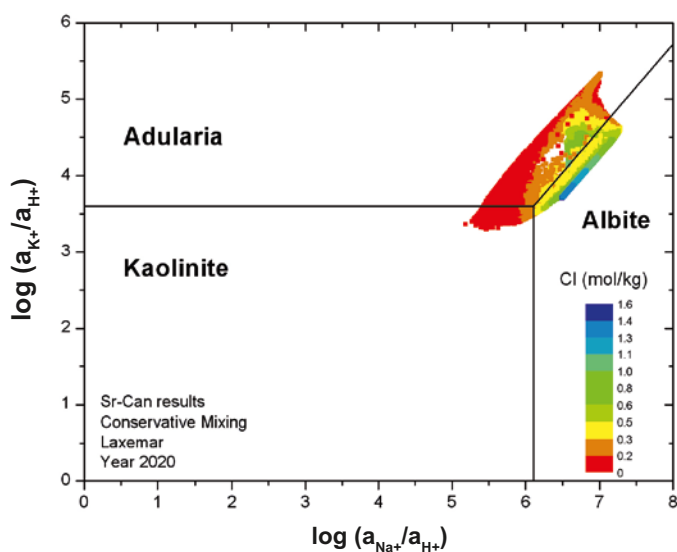
Figure 3-18. Log (a_{K+}/a_{H+}) vs. log (a_{Na+}/a_{H+}) diagram showing the location of the groundwaters obtained from some of the hydrogeochemical simulations performed in Sr-Can (Auqué et al. 2006). The samples are coloured by their salinity (chloride content). The field boundaries have been calculated with data from Grimaud et al. (1990).

marine waters mixed with the already existing groundwaters which display different degrees of salinity depending on the amount of meteoric and/or glacial waters intruded. The final input of warm meteoric waters is more difficult to distinguish, except for their modern isotopic signature and their flushing effect on previous waters.

Taking all these mixing events into account, the following **simulations** have been performed:

- **Simulation 1 (Gl mix #2731)**: a global mixing process between **a very dilute groundwater** (represented by the *Glacial end member*) **and a very saline groundwater** (represented by *sample #2731,* similar to the Deep Saline end member but with field pH measurements). The use of the Glacial end member justifies the input of dilute water, able to overcome the density differences with respect to the pre-existing very saline waters. The unknown detailed chemical composition of this Glacial end member does not add significant uncertainties for the major elements. However, its initial conditions will be better constrained when studying several parameters in the carbonate system (e.g. pH, pCO_2).

- **Simulations 2**: mixing between the Littorina end member (also equilibrated with calcite) and two different waters representative of the different situations that Littorina waters would have found when entering the system:
  - **Simulation 2.1 (Lit mix Gl)**: *Littorina and Glacial* waters.
  - **Simulation 2.2 (Lit mix Brack-Gl)**: *Littorina* waters and the brackish-glacial water already present in the bedrock (result of the earlier mixture between Glacial and the very saline groundwater) with which it could have mixed considering the salinity difference. This water corresponds to a mixing proportion of *90% Glacial and 10%* of *sample #2731* (Cl≈4,500 mg/L *vs.* 6,500 mg/L in Littorina waters).
  - Apart from a process of mixing of Littorina with these two groundwaters (Glacial in Simulation 2.1 and brackish-glacial in Simulation 2.2), other mixing lines between Littorina and intermediate waters could exist, and they should be located between the extreme lines defined by simulations 2.1 and 2.2.

Considering the conceptual model for the evolution of the system, results of simulation 1 will be very useful to understand the behaviour of the deeper and more saline samples (not affected by other mixing processes), while simulation 2 will correspond to those shallower groundwaters affected by the input of Littorina waters.

Calculations explore all the range of mixing proportions between the two end members in intervals of 10% (e.g. 90% Gl and 10% #2731, 80% Gl and 20% #2731, and so on) except for mixing proportions where Glacial dominates, for which the intervals have been reduced to 1%.

As already reported in previous SDM reports, the special features of the Laxemar-Simpevarp area suggest that chemical reactions have a more important influence and that they should be considered in the simulations. Both, equilibrium with calcite, gypsum and fluorite (all together or separately, depending on the system) and cation exchange have been included in the calculations.

For the equilibrium simulations, represented by crosses in the following plots, Na-, Mg- or K-bearing minerals have not been considered due to problems with their thermodynamic data (e.g. different clay minerals; they have roughly been evaluated by stability diagrams in previous sections). For the simulations concerning cation exchange[5], the main limitation is related to the lack of specific information on the type and amount of exchanger in the system. Therefore, only some scoping calculations have been done, assuming a generic exchanger in equilibrium with the different end member waters and then using two different CEC capacities that span the available

---

[5] To properly include cation exchange reactions in the simulations, knowledge of the cation exchange capacity (CEC) of the clay minerals in the fracture fillings and the composition of the exchange complex are necessary. Although this information is not reported to date, available indirect estimates have been used and the exchange complex composition calculated. This composition has been calculated with PHREEQC by assuming equilibrium between a generic exchanger and the water selected as the end member in each simulation. The Gaines-Thomas convention (Gaines and Thomas 1953) has been used together with the selectivity coefficients proposed by Appelo and Postma (2005), both included in the WATEQ4F thermodynamic database (Ball and Nordstrom 2001) distributed with PHREEQC.

data obtained from previous geochemical calculations (Gimeno *et al.* 2008; 0.1 and 0.5 mol/L; they are represented by triangles in the plots). These calculations must be taken with caution as they are based on a very simplified approach (e.g., the same estimated CEC are used for all subareas and depths). Furthermore, all the previous conservative mixing simulations (simulations 1, 2a and 2b) have been repeated in combination with equilibrium reactions and cation exchange in order to explore the effects of different processes in the chemistry of the final water. These simulations are termed "mixing + reaction" and "mixing + cation exchange", respectively.

The chemical contents and saturation states obtained with the different simulations have been compared with the real values measured in the groundwaters. Given the complexity of the system and the simplicity of the simulations, only observations on trends or ranges of values indicative of the effects of the simulated processes should be expected. However, in some cases, the fit of the calculated values with the real ones can be significant.

Specific simulations and results

Figures 3-19 to 3-22 show the results obtained for sodium, magnesium and potassium (respectively) with the different simulations: conservative mixing (spheres), mixing and reaction (crosses), and mixing and cation exchange (triangles), together with the measured values in the groundwaters.

Sodium contents in the conservative mixing simulations (Figure 3-19; spheres) follow linear trends that are, in general, close to the concentrations found in the sampled groundwaters. In the conservative mixing between the dilute water (Gl) and the very saline sample (#2731; black spheres) Na contents are systematically under predicted.

Figure 3-19. *Calculated values of sodium and chloride concentrations obtained with the different conservative mixing (Gl mix #2731, Lit mix Gl, Lit mix Brack-Gl; spheres and lines) and the mixing and equilibrium with calcite, gypsum and fluorite simulations (Gl mix+eq #2731, Lit mix+eq Gl, Lit mix+eq Brack-Gl; crosses). The real values measured in the groundwaters are also shown for comparison (stars: Äspö GW; circles: Laxemar GW, red crosses: Laxemar NSGW; diamonds: Simpevarp GW; black x: Simpevarp NSGW).*

Mixing of Littorina with the already existing more or less dilute waters (with Gl: grey spheres; and with Brack-Gl: red spheres) apparently reproduce some of the values found in the system. Several samples (light orange stars) within the triangular area delimited by Littorina, Gl and Brack-Gl extreme waters could fit other possible mixing lines between Littorina and any water on the line connecting Gl to Brack-Gl. However, their $\delta^{18}O$ values (Figure 3-3c) do not support this possibility. Therefore, processes additional to mixing should be considered.

As expected, mixing and equilibrium with calcite, gypsum and fluorite, does not change the calculated sodium concentration at all (see crosses on circles) in any of the mixtures (Figure 3-19). However, when simulating mixing and cation exchange (Figure 3-20), calculated Na values do change in all the simulations. Figure 3-20a shows the results of mixing and cation exchange produced by the input of very dilute glacial water into a bedrock occupied by saline waters. Sodium values resulting from mixing and cation exchange are always higher than those for conservative mixing and for mixing and equilibrium with calcite, gypsum, and fluorite.

Na contents obtained by mixing+cation exchange (Gl-#2731 mixing; black triangles) match most of the real ones when a CEC of 0.5 mol/L is considered, even in the brackish waters (light orange stars) included in the triangle defined by Littorina, Gl, and Brack-Gl (Figure 3-20b, enlarged area).

The other two simulations, both including Littorina (Figure 3-20b; grey and pale purple triangles), reproduce the change in dissolved sodium concentrations due to the input of marine waters into a system occupied by more dilute waters (Gl to Brack-Gl). Values are lower than the ones predicted by conservative mixing and, in some cases, closer to the measured ones. However, in other cases (e.g. a good number of near-surface groundwaters on the Littorina-Glacial line) the effect of cation exchange is negligible and not necessary to reproduce the measured concentrations. In general, as displayed in the figure, the effect on the final dissolved sodium concentration becomes important only when Littorina proportions in the mixture are higher than 30%. In other words, cation exchange could represent an important control in samples with the highest Littorina signature in the system.

The results from mixing calculations between Glacial and the Highly saline sample #2731 also support that cation exchange plays a significant role in the control of sodium, more so in the dilute segment of the mixing line. Therefore, mixing seems to be the main process in the control of sodium concentrations for the most saline groundwaters. In any case, without more data on the real exchange capacity of the system, all these results are only a qualitative estimation of the importance that this process can have in the system.

Figure 3-20b also shows that there are five samples from the Simpevarp subarea (inside the grey circle with the question mark), with chloride concentrations between 7,910 to 8,560 mg/L, which are not explained by any of the considered simulations. They have clearly higher sodium content than the one expected for their chloride concentration. Higher CEC values in the simulations (around 1.0 mol/L) could explain these higher values of sodium (and also the lower values of dissolved calcium of these groundwaters that will be shown below; Figure 3-46). However, there are not measured data of CEC in the fracture fillings and the existence of such high CEC values have not been deduced in previous works (see the review performed by Gimeno *et al.* 2008). Moreover, these groundwaters show other "uncommon" compositional characters (high sulphate and [11]B values) that must be taken into account and the features of these groundwaters will be revisited later on (see section 3.4.4).

For magnesium and potassium the results obtained with the different simulations are very similar to those for sodium. Conservative mixing simulations reproduce their general trends (Figure 3-21a and 3-22a), indicating a mixing with a non-marine saline end member (sample #2731) and with a marine end member (Littorina). Again, the near-surface groundwaters follow exactly the trend of pure mixing between a very dilute groundwater and the Littorina end member.

As explained for sodium, mixing and reaction assuming equilibrium with calcite, gypsum and fluorite, although not shown, do not change the calculated Mg and K concentrations with respect to conservative mixing. However, when imposing cation exchange, some differences are found.
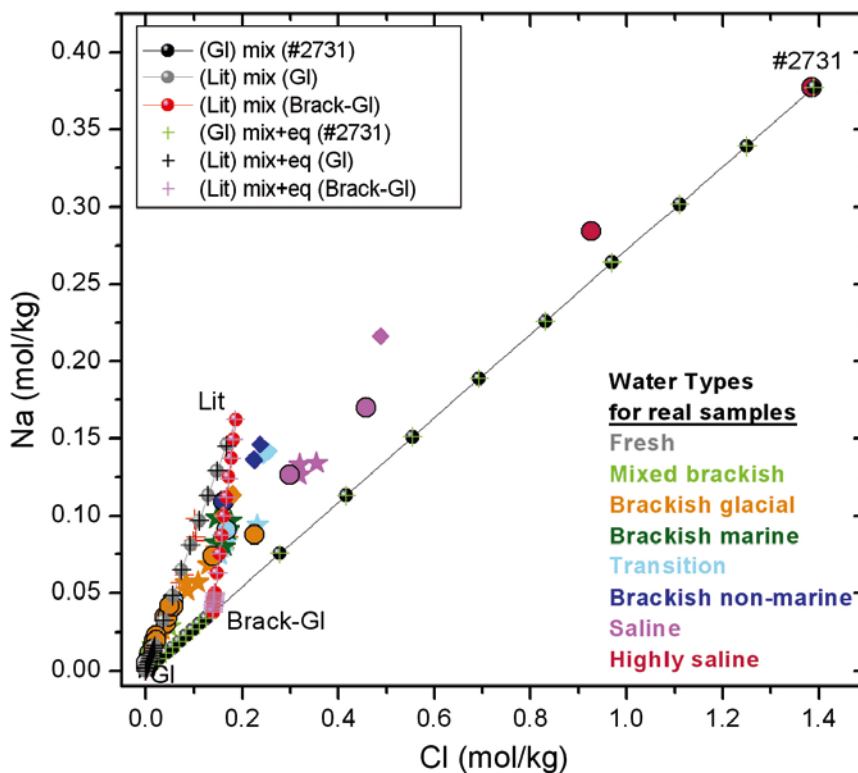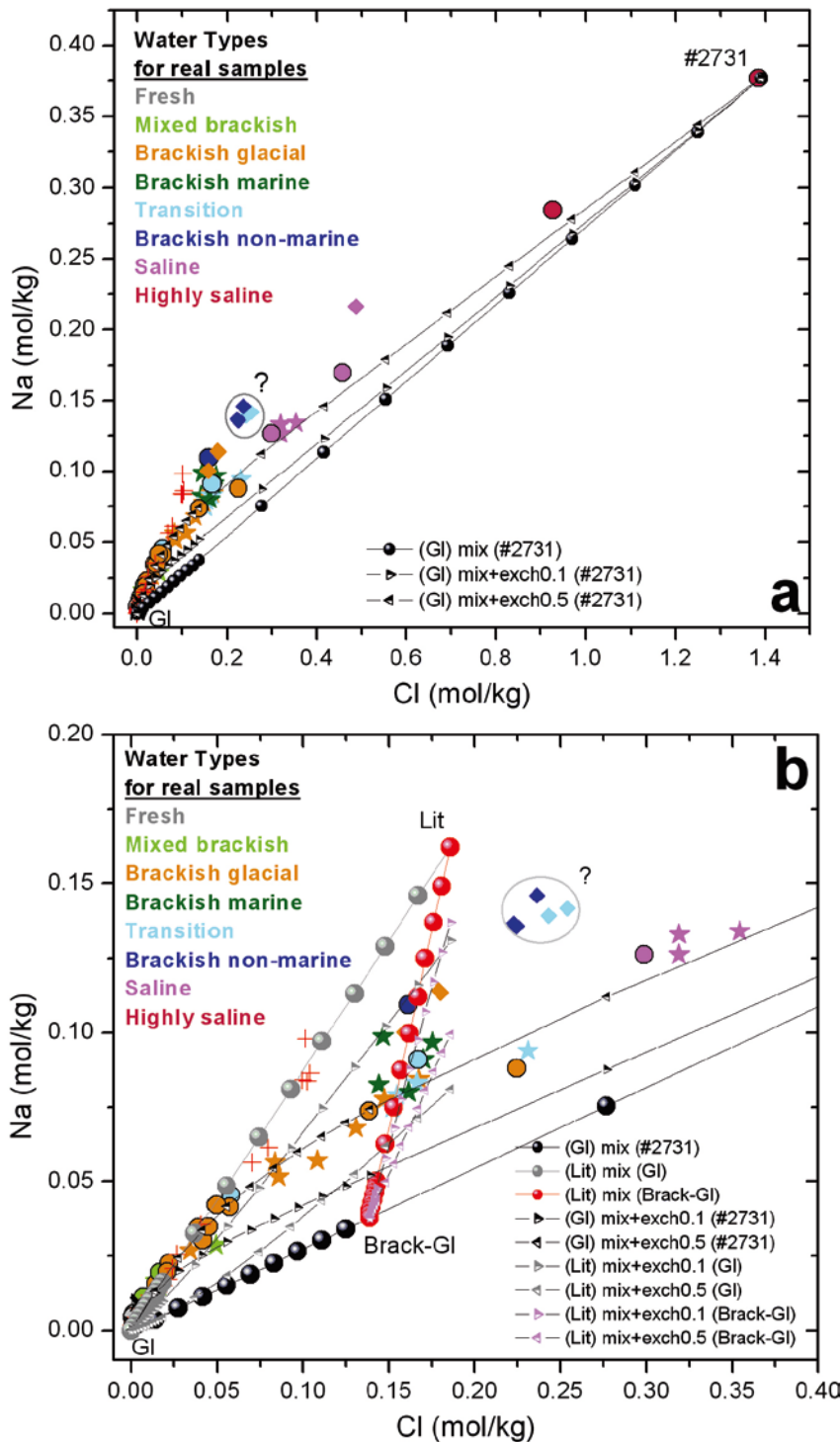
Figure 3-20. *Calculated values of sodium and chloride concentrations obtained with the different conservative mixing (a: Gl mix #2731, Lit mix Gl, Lit mix Brack-Gl) and the mixing and cation exchange simulations (b: Gl mix+exch0.1 #2731, Gl mix+exch0.5 #2731, Lit mix+exch0.1 Gl, Lit mix+exch0.5 Gl, Lit mix+exch0.1 Brack-Gl, Lit mix+exch0.5 Brack-Gl). The real values measured in the groundwaters are also shown for comparison (stars: Äspö GW; circles: Laxemar GW, red crosses: Laxemar NSGW; diamonds: Simpevarp GW; black x: Simpevarp NSGW). Samples grouped inside a grey circle and with a question mark will be described later in the text.*
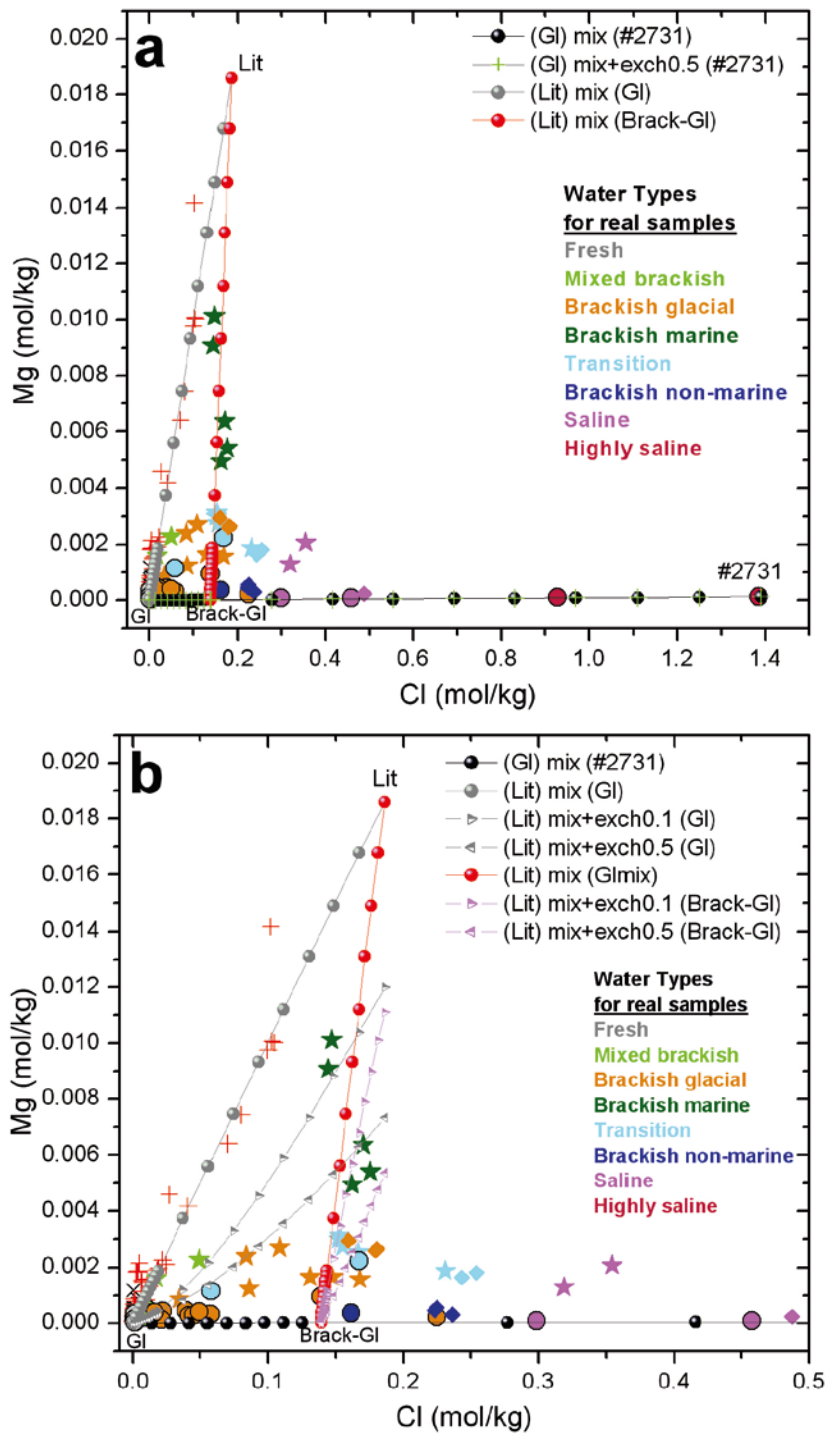
Figure 3-21. *Calculated values of magnesium and chloride concentrations with the different mixing simulations explained in the text. The real values measured in the groundwaters are also shown for comparison (stars: Äspö GW; circles: Laxemar GW, red crosses: Laxemar NSGW; diamonds: Simpevarp GW; black x: Simpevarp NSGW).*
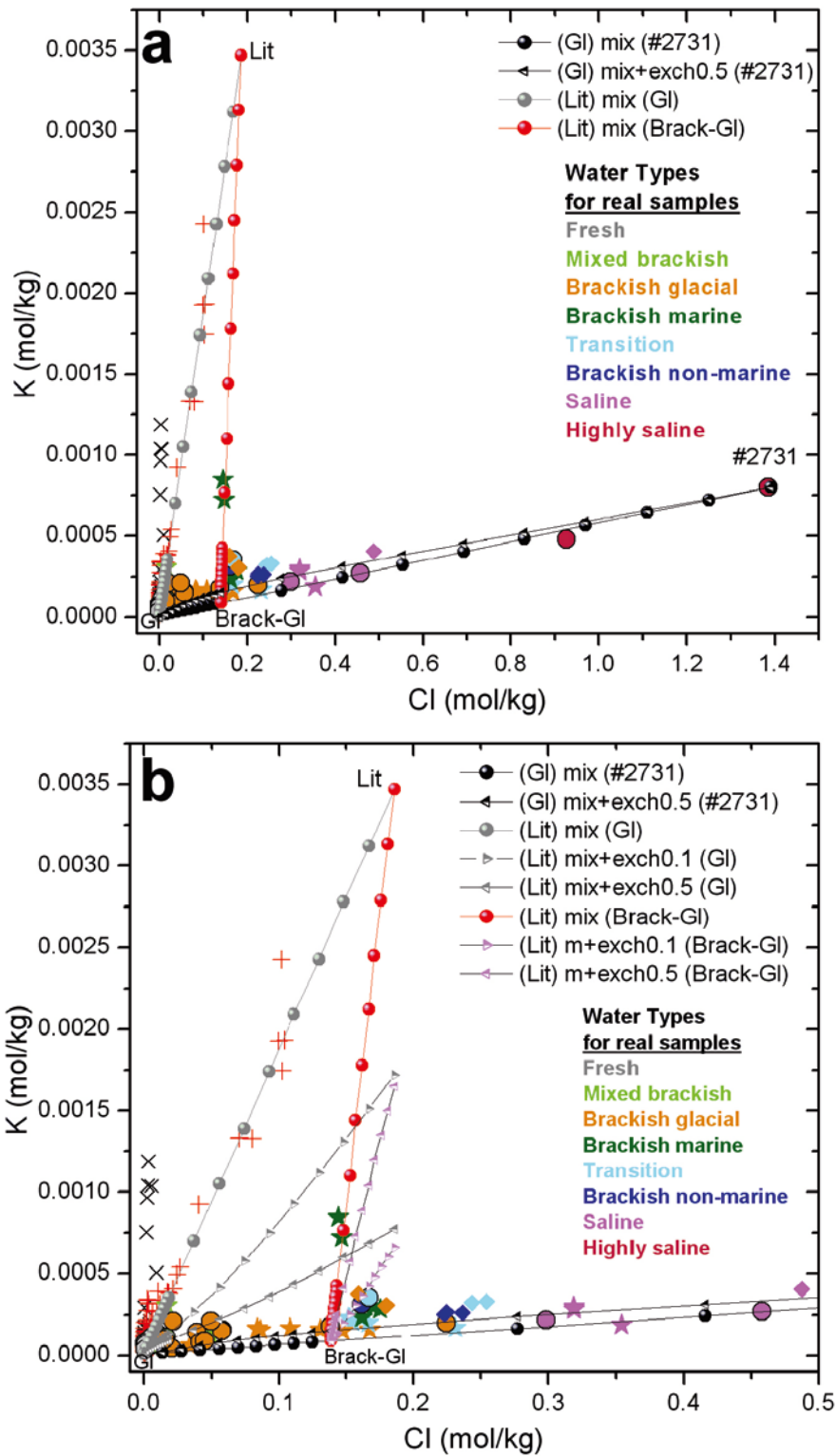
Figure 3-22. *Calculated values of potassium and chloride concentrations with the different mixing simula-tions explained in the text. The real values measured in the groundwaters are also shown for comparison (stars: Äspö GW; circles: Laxemar GW, red crosses: Laxemar NSGW; diamonds: Simpevarp GW; black x: Simpevarp NSGW).*

Magnesium values obtained by mixing and cation exchange between Glacial (Gl) and the saline sample #2731 plot on top of the other two simulations (conservative mixing and mixing + equilibrium). This trend fits very well many real samples, from very dilute to the most saline ones. This means that conservative mixing alone is generally able to explain the very low magnesium values found when salinity is high. However, there are several transition and saline samples (circled) with concentrations higher than those predicted by these simulations which are probably related to dissolution reactions of Mg-bearing minerals.

Potassium differs from magnesium in that the results found by mixing and cation exchange between Gl and #2731 are slightly higher than the ones obtained by mixing, and closer to the values measured in the system when a CEC of 0.5 mol/L is used (Figure 3-22b).

Mixing and cation exchange between Littorina and the two dilute waters (Gl and Brack-Gl) gives magnesium and potassium contents that deviate from those obtained by conservative mixing, suggesting that the effect of cation exchange may be important in groundwaters with a > 20% Littorina contribution (Figure 3-21b and 3-22b). However, the effect of cation exchange in a number of near-surface groundwaters appears to be negligible.

In summary, the effect of cation exchange on magnesium is not intense enough to hide its marine signature in mixtures with Littorina, while the effect on potassium is more difficult to separate from the effects produced by conservative mixing in the more saline samples (Cl > 0.2 mol/kg).

3.2.5   Conclusions

Near-surface groundwaters

Dissolved sodium, potassium and magnesium contents in the near surface groundwater systems at Laxemar-Simpevarp are within the range usually measured in the Swedish context (Tröjbom and Söderbäck 2006a, Tröjbom *et al.* 2008). These contents are controlled by weathering reactions mainly triggered by biogenic CO_2 input. This input of CO_2 promotes a pH decrease and a CO_2 partial pressure increase in the waters, which may favour the dissolution of carbonate or aluminosilicate mineral phases if present in the system.

Na, K and Mg concentrations display a clear increase with the weathering intensity (represented by the alkalinity production) and the incongruent dissolution of aluminosilicates (mainly plagioclase and mafic minerals such as biotite and hornblende) seems to be generally the most important process in their control.

These cations may be partially incorporated into secondary clays and the net effect in the increase of their concentrations depends on the type of the secondary mineral phase. Mineral stability diagrams confirm the stability of kaolinite and illite, and also the participation of smectites in the control of dissolved Na, Mg, K and silica in some groundwaters. Moreover, weathering-induced transformations from illite or chlorite (both present in the overburden) to vermiculite can also participate in the control of dissolved potassium and magnesium.

Other processes affecting the final dissolved concentrations of these elements may be their use as nutrients for plants (e.g. Mg, K) or their participation in cation exchange processes (especially in the case of Mg, Ca and Na). Moreover, some saline near-surface groundwaters from soil pipes located in till below lake and sea sediments seem to be affected by a strong marine influence (e.g. SSM000238 and SSM000239) and/or by discharging deep groundwaters related to the main fracture zones in the area (SSM000241 and SSM000242). Consequently, these waters display large concentrations of sodium (1,900 to 2,230 mg/L), magnesium (151 to 354 mg/L), potassium (50 to 94 mg/L) and silica (up to 75 mg/L).

Groundwaters

Sodium distribution with depth shows similarities with the described chloride trends (section 3.1.1). Moreover, the concentrations of both elements display a positive linear correlation with two different slopes attributable to mixing with a marine end member (roughly following the seawater dilution line) and to mixing with a saline non-marine end member. Groundwaters from the Laxemar subarea show much lower sodium concentrations than groundwaters from the Simpevarp subarea at similar depths,

whereas Äspö groundwaters display intermediate sodium contents. Sodium displays a near-conservative behaviour in the Laxemar subarea samples with large chloride contents (Cl > 10,000 mg/L) as also observed at Forsmark and Olkiluoto. However, samples with Cl < 10,000 mg/L are affected by other mixing processes (mainly with Littorina, although its effects on the sodium contents are less evident than in Forsmark) and by the effects of water-rock interaction, especially in dilute groundwaters down to 500 m depth.

Potassium contents in groundwaters increase very slowly with depth but with values always below the seawater dilution line. This behaviour, showing a global concentration trend towards the saline end member, is common to the four subareas. This may reflect the influence of mixing with a saline (non marine) component in saline groundwaters from Laxemar, as happens at Forsmark and Olkiluoto. The highest potassium contents are found in the shallow groundwaters from Äspö and are restricted to groundwaters with chloride around 5,000 mg/L and with a significant Littorina contribution. The same characteristics, although much clearer, can be observed at Forsmark and Olkiluoto.

Magnesium distribution with depth displays a progressive decrease to values around 2 mg/L at 1,000 m depth, remaining constant thereafter down to the deepest and more saline groundwaters. Since this element has also been used for the definition of the water types (marine indicator), its distribution is clearly suitable for separating the groundwaters affected by marine influence (with the highest magnesium contents) from the rest. This marine influence is clearly different in the different subareas. Groundwaters with the highest magnesium concentrations fall in a narrow range of brackish compositions (~ 3,000–7,000 mg/L Cl) restricted to maximum depths of about 500 m. These waters are considered to represent a significant component of Littorina Sea mixing, although this is less prevalent than at Forsmark or Olkiluoto and mainly limited to Äspö, to some discharge points at Simpevarp and some remnants in the Laxemar subarea (boreholes KLX01, 10 and 15 and HLX38). The decrease of magnesium as the salinity (chloride) increases suggests the influence of a magnesium-depleted saline component.

Apart from the marine influence, the scattering of sodium, magnesium and potassium concentrations in the 1,000–10,000 mg/L chloride concentrations range suggests that aluminosilicate dissolution reactions and also cation exchange could be active in controlling the behaviour of these elements. From the available mineralogical data in fracture fillings, different aluminosilicates could participate in the control of these elements, such as albite, adularia, chlorite and mixed-layer clays like smectite/illite, chlorite/smectite or chlorite/vermiculite. This has been confirmed with the stability diagrams: most of the brackish and saline groundwaters, independently of their salinity or mixing proportions, plot on the adularia-albite limit, suggesting a control of dissolved sodium and potassium by this equilibrium situation; moreover, chlorite, which is the most abundant fracture filling phase at all depths, could be a limiting phase for dissolved magnesium for most of the Laxemar-Simpevarp groundwaters.

The thermodynamic simulations carried out indicate that conservative mixing between a dilute water (Glacial) with a non-marine saline end member (sample #2731) and between a marine end member (Littorina) entering in a more dilute system (Glacial or Brackish-Glacial waters) reproduce the general trends of Na, Mg and K.

However, when including cation exchange (CEC value of 0.5 mol/L) in the simulations of the input of Glacial and very dilute water in a bedrock saturated with saline waters, sodium and potassium values increase, matching better most of the real concentrations in the dilute segment of the mixing line. On the contrary, magnesium values do not differ from the ones obtained with conservative mixing. Simulations reproducing the mixing and cation exchange produced by the Littorina input result in sodium, potassium and magnesium values lower than the ones predicted by conservative mixing and, in some cases, closer to the measured values.

Therefore, mixing seems to be the main process in the control of sodium, magnesium and potassium concentrations for the most saline groundwaters but cation exchange processes may exert an important control over these elements in groundwaters with more than 20–30% of Littorina contribution. In any case, without more data on the real exchange capacity of the system, all these results are only an estimation of what would happen if this process took place in the system.

3.3　Carbonate system

The carbonate system is fundamental to understand the evolution of groundwater parameters such as pH or alkalinity. This is why it has been systematically studied in all the previous SDM phases.

The evolution of this system, though with some peculiarities specific to this area, corresponds to the classical model proposed by Nordstrom *et al.* (1989) for the Stripa groundwaters.

Mineralogical studies of the fracture fillings have confirmed the abundant presence of calcite, an important phase in the pH buffering capacity of the rock system. In addition, the study of these calcites has been an invaluable tool in the understanding of the palaeohydrogeology of the sites (Bath *et al.* 2000, Milodowski *et al.* 2005, Drake and Tullborg 2007).

As in previous SDM stages, the study presented here has focussed on the hydrochemical parameters pH, alkalinity and dissolved calcium, and on the results of geochemical modelling (pCO_2 and calcite saturation index). The study of the near-surface groundwaters has been enlarged with respect to earlier reports, as the carbonate system plays a fundamental role in the hydrochemical characters of the recharge waters. The main uncertainties associated with the carbonate system and their effects on the obtained results are also analysed in detail.

It is important to stress that an important effort has been made to integrate these results with the available mineralogical and isotopic data related to the carbonate system in order to obtain a more complete picture.

3.3.1　Hydrogeochemical data. General trends

General trends of pH, alkalinity and dissolved calcium contents are examined in this section. The pH is highly variable in the near-surface groundwaters. These waters also display the lowest measured values, reflecting the influence of atmospheric and biogenic CO_2 in the soil zone. In the groundwaters, pH values are between 7.2 and 8.6 and do not show any clear trend with depth (Figure 3-23ab), as is the case in other crystalline areas such as Forsmark (Figure 3-24) or Lac du Bonnet (Canada; Figure 16a in Gascoyne 2004), maintaining an important dispersion down to 900 m depth for most of the water types. In the Laxemar subarea, pH values tend to be restricted to a range between 7.5 and 8.5 pH units (Figure 3-23b).

Representing pH with respect to chloride, this trend towards "stabilisation" around pH 8−8.5 in the most saline groundwaters is more evident (Figure 3-23cd), although scattering is also observed. This scattering in pH values is common in other crystalline systems (e.g. Olkiluoto; Figure 5-3 in Pitkänen *et al.* 2004). There is an important gap of data between the saline sample at 1,100 m depth (16,000 mg/L Cl) and the even deeper saline sample at 1,530 m depth (45,000 mg/L Cl), but pH decreases from the former to the latter. The meaning of this decrease has been analysed by thermodynamic simulations to bypass the problem of the lack of data (section 3.3.4).

Alkalinity (HCO_3^-) values also show the widest variability and the highest values in the near-surface groundwaters due to the influence of atmospheric and biogenic CO_2 and to the progress of carbonate and silicate weathering reactions in the overburden (Figure 3-25). In the groundwaters, alkalinity contents show a rapid decrease with depth (Figure 3-25ab) and chloride concentrations (Figure 3-25cd).

High and variable values can be found down to 400 m depth at the Äspö and the Laxemar subareas. In the Laxemar subarea (Figure 3-25d) this behaviour is related to the different hydrology at the borehole locations. The highest values are associated with fresh and "recent" recharging groundwaters (e.g. detectable tritium) although some open-hole mixing effect is also possible in some samples.

The high HCO_3^- values found in the groundwaters of Äspö are clearly associated with groundwaters with a marine (Littorina) signature (chloride concentrations around 5,000 mg/L; Figure 3-25c). Something similar, although even more marked has been observed at Forsmark, where elevated contents of HCO_3^- are found in the waters with an important Littorina contribution (chloride contents around 5,500 mg/L: Figure 3-26b).
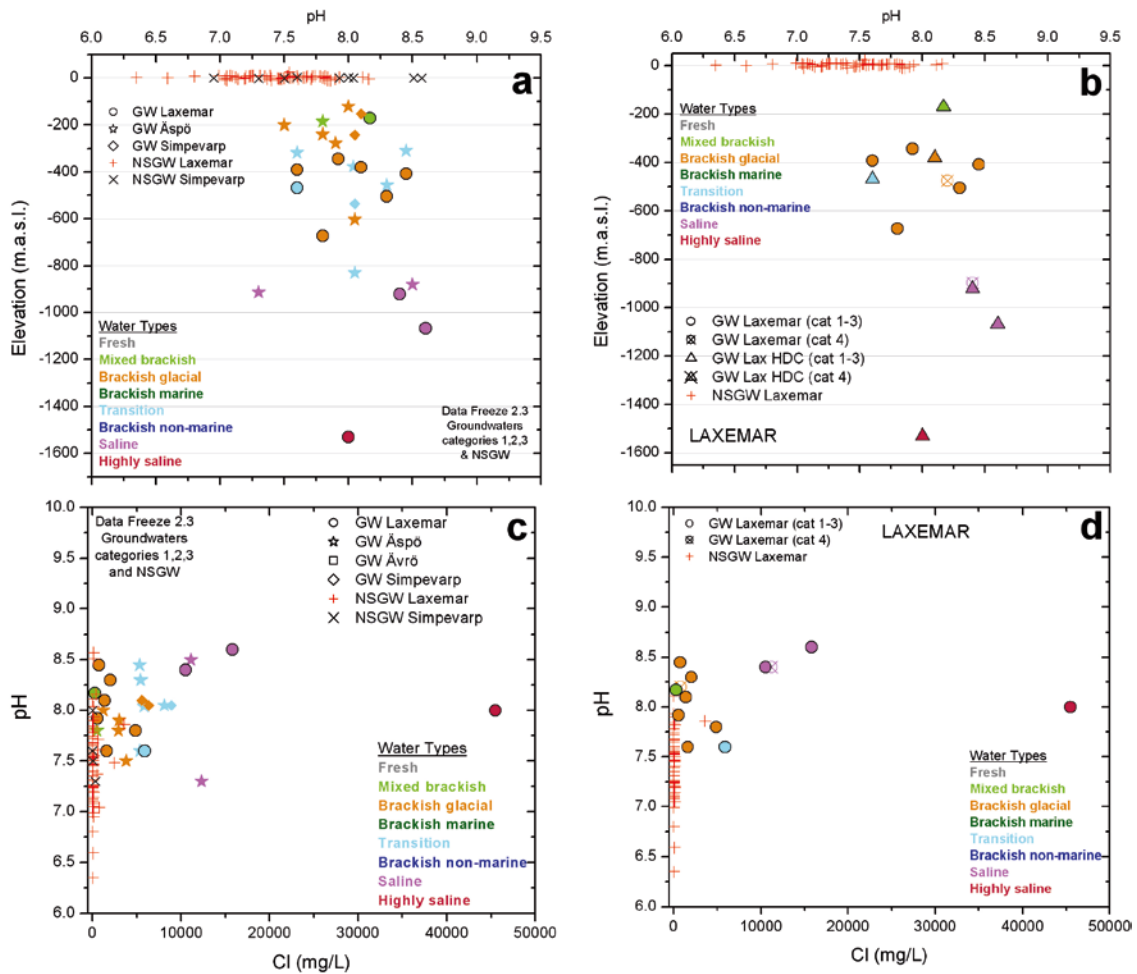
Figure 3-23. *Depth variation of the field pH in the Laxemar-Simpevarp area (a) and in the Laxemar subarea (b) and distribution of these values with respect to chloride contents (c for Laxemar-Simpevarp waters, and d for Laxemar subarea waters).*
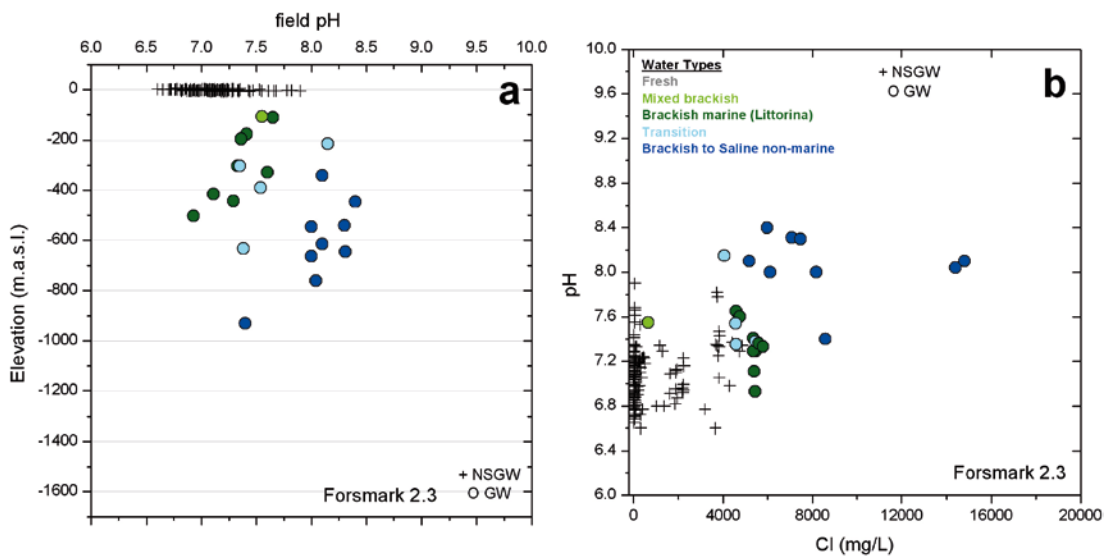
Figure 3-24. *Field pH vs. depth (a) and vs. chloride contents (b) for the Forsmark groundwaters. Representative near-surface groundwaters and groundwaters of categories 1 to 4 are included.*
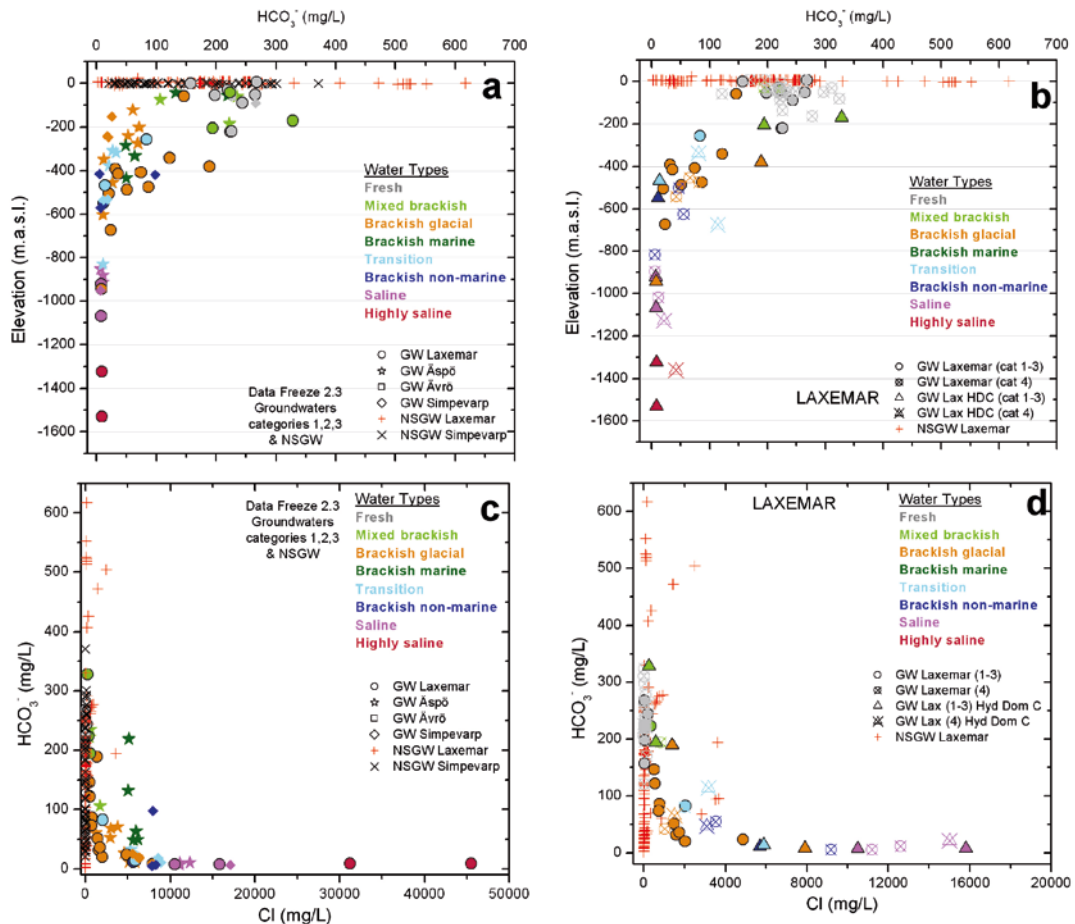
Figure 3-25. *Depth variation of the bicarbonate contents at the Laxemar-Simpevarp area (a) and in the Laxemar subarea (b) and distribution of these values with respect to chloride contents (c) for the Laxemar-Simpevarp waters, and (d) for the Laxemar subarea waters. Note that the chloride concentrations are restricted to 20,000 mg/L (i.e. absence of highly saline groundwaters) in plot (d) for increased resolution at lower salinities in the Laxemar subarea. Note that, as indicated in the keys, Laxemar subarea waters include also category 4 samples (not included in the Laxemar-Simpevarp area plots).*

Average HCO_3^- contents in the present Baltic Sea are around 78.7 mg/L and the estimated value for Littorina waters is 92.5 mg/L, which is lower than the observed values in some of these ground-waters. However, during infiltration of the marine waters through sediments, biological activity promotes an important increase in HCO_3^- contents. For example, Carman and Rahn (1997) found HCO_3^- contents as high as 488 mg/L just 10 cm below the water-sediment interface in the present Baltic Sea.

In the marine sediments, these high HCO_3^- concentrations are usually achieved by equilibrium with calcite. Then, during the circulation of these marine waters in the bedrock, calcite precipitation and aluminosilicate dissolution can occur, lowering the alkalinity. These groundwaters are in equilibrium (or slightly oversaturated) with respect to calcite at present but their HCO_3^- contents remain anomalously high as a result of this marine "inheritance". This inherited marine character of at least part of the HCO_3^- contents in some Forsmark and Laxemar-Simpevarp groundwaters, is in agreement with other marine inheritances very difficult to justify by especial and localised reactions in some Forsmark and Laxemar-Simpevarp groundwaters (high contents of dissolved SiO_2, Mg, Mn, SO_4^{2-} and NH_4^+).

Below 500 m depth (Figure 3-25bc), HCO_3^- contents in the saline groundwaters drastically decrease to a narrow range of values, as it also happens in Forsmark groundwaters (Figure 3-26a), and in Olkiluoto (Figure 5.7 in Pitkänen *et al.* 2004), without any relationship to the chloride concentrations. These characters indicate the existence of a clear mineral solubility control on the contents of this component, superimposed on the effects of mixing.

43
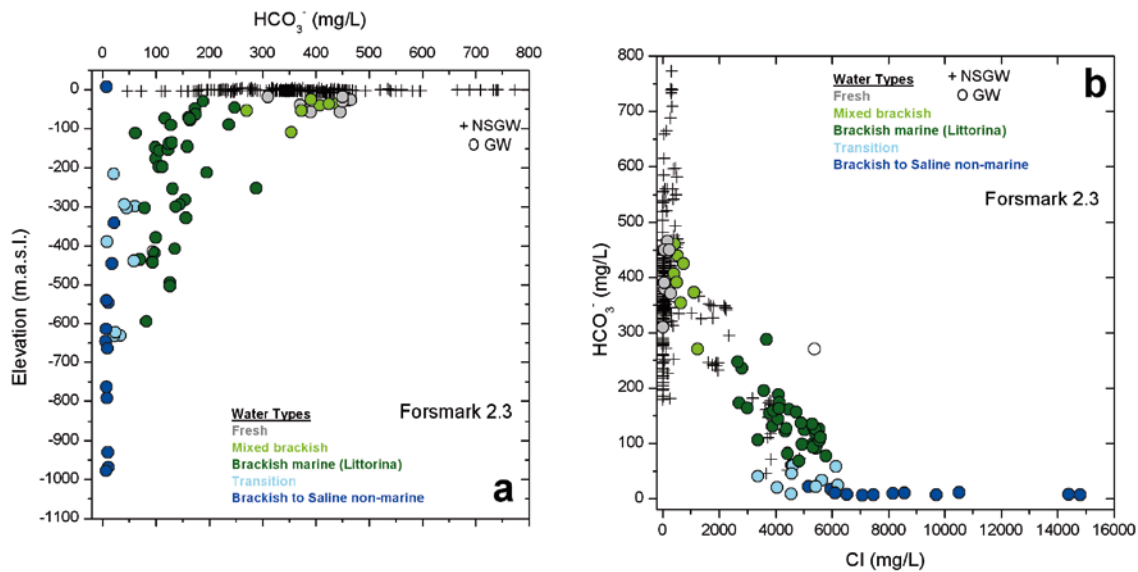
Figure 3-26. *Alkalinity vs. depth (a) and chloride contents (b) for the Forsmark groundwaters. Representative near-surface groundwaters and groundwaters of categories 1 to 4 are included.*

Dissolved calcium in the fresh near-surface groundwaters has maximum concentrations of around 100 mg/L, although they are usually below 80 mg/L. In the groundwaters, Ca contents increase with depth (Figure 3-27ab) and with chloride contents (Figure 3-27cd) towards the value of the Deep Saline end member. More in detail, low Ca concentrations characterise the groundwaters down to 500 m depth in the Laxemar subarea because of the important penetration depth of recharge waters in this zone. In the other subareas, Ca concentrations are higher and show a steeper increase with depth (Figure 3-27ab). From 600 m depth down, calcium contents steadily increase, reaching the maximum value in the Deep Saline end member at the maximum sampled depth (~1,500 m).

Calcium contents are very well correlated with chloride concentration (Figure 3-27cd), at least for groundwaters with chloride contents higher than 5,000 mg/L. As will be shown later, the high Ca content of the mixed waters (derived from the Deep Saline end member) obliterates the effect of mass transfer with respect to equilibration with calcite or gypsum or exchange reactions. This justifies the quasi-conservative behaviour of calcium.

Similar trends and processes can be observed for dissolved calcium at Forsmark (Figure 3-28) and Olkiluoto (Figure 5.5.c in Pitkänen *et al.* 2004). In the case of Forsmark, two main differences can be observed; first, dilute (low Ca) groundwaters are restricted to much shallower depths (less than 100 m); and second, the increase of calcium with depth is broken by two samples with higher calcium concentrations (and higher salinity, Figure 3-28a) at 600–800 m depth. These samples are considered to reflect anthropogenic upconing effects during borehole operation (see section 3.1).

Therefore, two of the main components of the carbonate system (Ca and alkalinity) are mainly related through calcite dissolution-precipitation (section 3.3.3) but their overall trends with respect to chloride concentration and depth are differently affected by this reaction. The very high Ca concentrations in the most saline groundwaters compared with the rest of the water types promotes a mixing-dominated control for this element. Moreover, these high Ca concentrations will be the responsible for calcite oversaturation during the mixing of these saline waters with other more dilute waters, and of the low HCO_3^- contents through the induced precipitation of calcite.
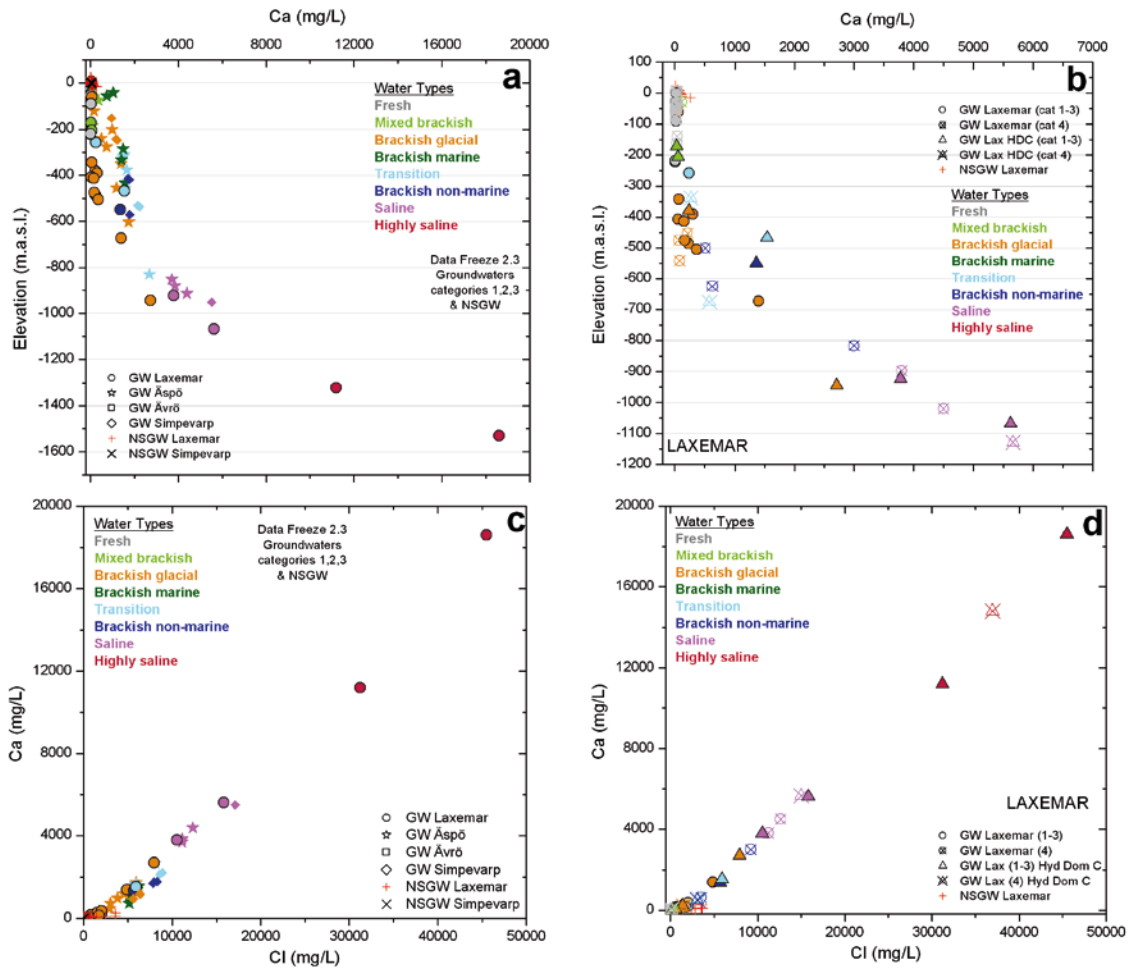
Figure 3-27. *Depth variation of calcium concentrations at the Laxemar-Simpevarp area (a) and in the Laxemar subarea (b); and distribution of these values with respect to chloride contents for the Laxemar-Simpevarp waters (c), and for the Laxemar subarea waters (d). The scales along the axes in the Laxemar subarea plot (b) have been increased to better visualise the shallow to intermediate depths.*
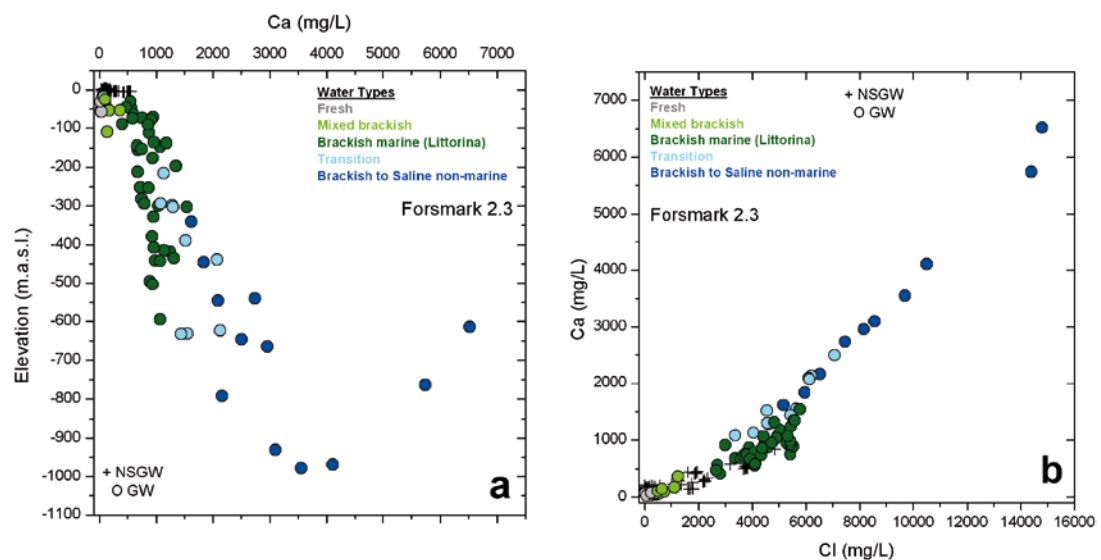
Figure 3-28. *Calcium contents vs. depth (a) and vs. chloride contents (b) for the Forsmark groundwaters. Representative near-surface groundwaters and shallow and deep groundwaters of categories 1 to 4 are included.*

3.3.2 Mineralogical data

Carbonate minerals are evidently the phases of main interest in this system. To date, the only identified carbonate in the mineralogical studies in the overburden and in fracture fillings is calcite[6], although with very different abundances. The available mineralogical information for the overburden (described in section 3.2.2) appears to indicate that calcite is absent or in very low amounts. As this is an issue of special interest, other sources of information have been reviewed in this section to check this.

Mineralogical data from fracture fillings are much more abundant. Calcite occurrence in fracture fillings has been widely recognised in the present Site Characterization Program and also in previous projects. Moreover, as indicated before, isotopic and trace element contents in these calcites have allowed a better understanding of the palaeohydrological history of the sites (Bath *et al.* 2000, Milodowski *et al.* 2005, Drake and Tullborg 2007). Therefore, only the most relevant information has been included in the present study.

Overburden

As reported in section 3.2.2, calcite occurrence in the granitic outcrops of the Laxemar-Simpevarp area (more than 50% of the exposed surface) is always below 0.3%. In the rest of the overburden materials (till deposits and soils), the amount of calcium carbonate is generally very low as well. Determinations performed in 27 till samples have shown values between 0.1 and 0.6% calcium carbonate per dry weight (Tröjbom and Söderbäck 2006a, Tröjbom *et al.* 2008). Only some till samples contain from 2.1 to 4.5% calcium carbonate, probably of marine origin (see Sohlenius *et al.* 2006). The content of calcium carbonate in the glacial clay sediments is also usually low (only in some profiles have high calcium carbonate contents been found, e.g. associated with bands of $CaCO_3$ shells) and also the fine-grained matrix of gyttja lacks $CaCO_3$ (Sohlenius *et al.* 2006). Therefore, although previous studies in the Laxemar subarea failed to identify till deposits containing calcite (e.g. Rudmark *et al.* 2005), it appears that this mineral is present, though in low amounts. Moreover, in the wide bare bedrock exposures in the Laxemar subarea most of the fractures are sealed with chlorite and calcite (Sohlenius *et al.* 2006).

This amount of calcite is not comparable with what is found at Forsmark. Soils and glacial till deposits in that area show an important influence of calcareous materials from Ordovician limestones present on the sea bottom towards the north of the Forsmark area[7] (Lundin *et al.* 2004, SKB 2005b). Limestone clasts and boulders can be observed on the surface of the regolith. Most till samples in the Forsmark area contain between 10–30% calcite (calcium carbonate) per dry weight, which is about 30 times higher than the median value of the Swedish reference data (SKB 2006c). Sandy tills have an average calcite content of 18%, whereas clay-rich till deposits present even higher contents (24%. SKB 2005b). The presence of high contents of calcite in soils has also been indicated at many field locations and the content of calcium carbonate in the < 2 mm fraction can reach 25% by weight (Lundin *et al.* 2004).

The presence of large amounts of calcite is responsible for some of the distinctive characteristics observed in the near-surface groundwaters but also, at a lower scale, in the soils from Forsmark. Soils at Forsmark have pH values (Table 3-1), calcium contents, amounts of exchangeable calcium and calcium weathering rates higher than most Swedish soils (Figure 3-29). On the contrary, the general chemical features of the Laxemar-Simpevarp overburden and soils are much closer to these Swedish average values, especially in the upper soil horizons (SKB 2006a).

The small amounts of calcite in the Laxemar-Simpevarp overburden cause the difference in the characters observed in the near-surface groundwaters and soils compared with those at Forsmark. However, in spite of its low concentration, calcite can imprint a clear compositional character in the near-surface groundwaters, detectable even in their isotopic traits, as shown below (section 3.3.3).

---

[6] A REE-rich carbonate, probably bastnäsite, has also been identified in many fractures although in small amounts (Drake and Tullborg 2005).

[7] Calcite at Forsmark originates from the seafloor of Gävlebukten, a bay to the Baltic Sea located about 100 km north of the Forsmark site and covered by Cambrian and Ordovician sedimentary bedrock. The calcium-rich material was transported from Gävlebukten and deposited in the Forsmark area during the latest glacial period (Tröjbom and Söderbäck 2006a).
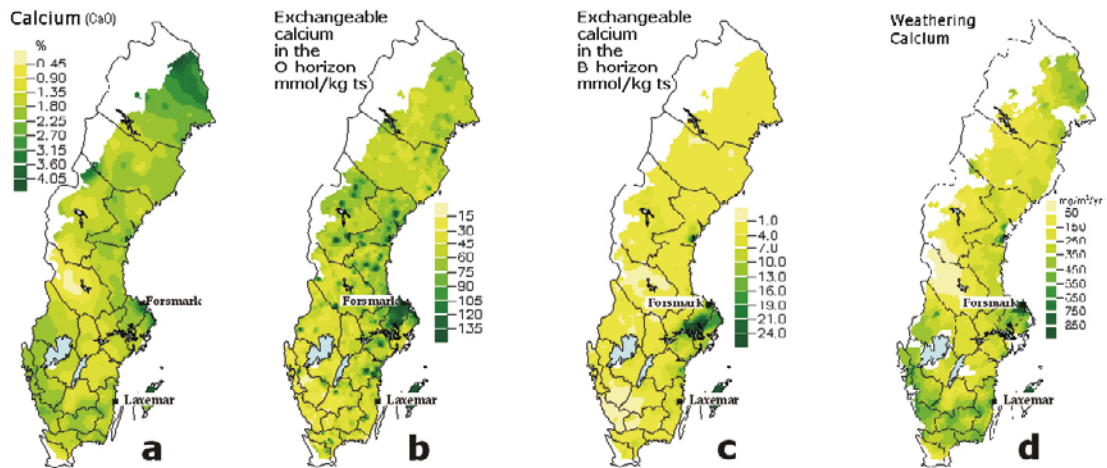
Figure 3-29. Calcium contents (a) and exchangeable calcium in the O-horizon (b), in the C-horizon (c) and calcium weathering rate (d, in mg/m²/yr) in the Swedish soils. From MarkInfo database (Department of Forest Soils, Swedish Univ. of Agricultural Sciences, Uppsala; http://www-markinfo.slu.se/eng/index.html; January, 2009).

Table 3-1. Average values of soil pH in different horizons of the Forsmark and the Laxemar-Simpevarp areas compared with the average values in Swedish soils (data from Lundin *et al.* 2004, 2005).

	Forsmark	Laxemar	Sweden
O-horizon (0–30 cm)	6.2 ± 1.1	4.3 ± 0.7	4.2 ± 0.7
B-horizon (0–10 cm)	6.5 ± 1.0	5.2 ± 0.5	4.9 ± 0.5
B-horizon (10–20 cm)	6.7 ± 0.8	5.3 ±0.4	4.9 ± 0.5
C-horizon (55–65 cm)	7.2 ± 0.9	5.2 ± 0.6	5.3 ± 0.6

Fracture fillings

Calcite fracture fillings phases have been widely studied during the Site Characterization Program and in previous projects as they are basic to a better understanding of the palaeohydrological history of the sites. Moreover, as the amount of calcite dispersed in the overburden is limited, the buffering capacity provided by calcite in the fracture fillings becomes a very important factor in the evolution of the recharge waters. These two topics are briefly described here.

Buffer capacity

Calcite has been found in open fractures in the Äspö, Laxemar and Simpevarp subareas. It is one of the most abundant fracture filling phases (together with chlorite) at all examined depths. Calcite is generally more irregularly distributed on the fracture surfaces than chlorite and calculations performed by Drake and Tullborg (2006a) indicate a calcite mass of 0.27 to 0.41 kg m^{-2} in calcite-coated fractures, with a minimum estimate of 0.0027 kg m^{-2}.

As detected in other zones, recharge waters may induce calcite dissolution in the upper part of the bedrock. For example, recharge groundwaters at Klipperas, undersaturated with respect to calcite, have promoted the complete dissolution of this phase to depths between 20 and 50 m and partial dissolution down to 120 m in fracture zones (Tullborg 1989, Puigdomènech 2001).

At the Äspö island, surface-related dissolution of calcite is evident in the upper 10 m and in some fracture zones down to 50 m. However, calcite has not been totally removed even in the shallowest parts (Tullborg 1989, Puigdomènech 2001). In the Laxemar-Simpevarp area, calcite leaching is observed in the upper 20–30 m although without complete dissolution (Drake and Tullborg 2008). In fact, as indicated above, in the bare bedrock exposures at the Laxemar-Simpevarp area most of the fractures are still sealed with calcite (Sohlenius *et al.* 2006).

Calcite dissolution, though feasible at these shallow levels in the Laxemar and Simpevarp subareas, would probably be very limited due to the fact that recharge waters are already in equilibrium or oversaturated with respect to this mineral. In fact, Wallin and Peterman (1999), studied the isotopic compositions of shallow calcite fracture fillings in the Laxemar-Simpevarp area and concluded that calcite was effectively precipitating from the present-day groundwaters at those levels (around 200 m depth). This circumstance fits also the hydrochemical characters of these waters, as described in the following section. In any case, the detected amounts of calcite in the shallowest levels of the Laxemar and Simpevarp subareas suggest an important buffering capacity (compared with the other aforementioned systems) for future recharge waters.

Palaeohydrological history

Different calcite generations of Palaeozoic age (or older) related to several hydrothermal events and/ or to "warm brines" have been identified (Figure 3-30ab). However, later generations of equant or needle-shaped calcites (Figure 3-30cd) or overgrowths (Figure 3-30b) and more recent, low temperature calcites precipitated in different environments (with varying salinities: e.g. glacial, marine or meteoric influence) have also been identified (Bath *et al.* 2000, Mildowski *et al.* 2005, Drake and Tullborg 2007).
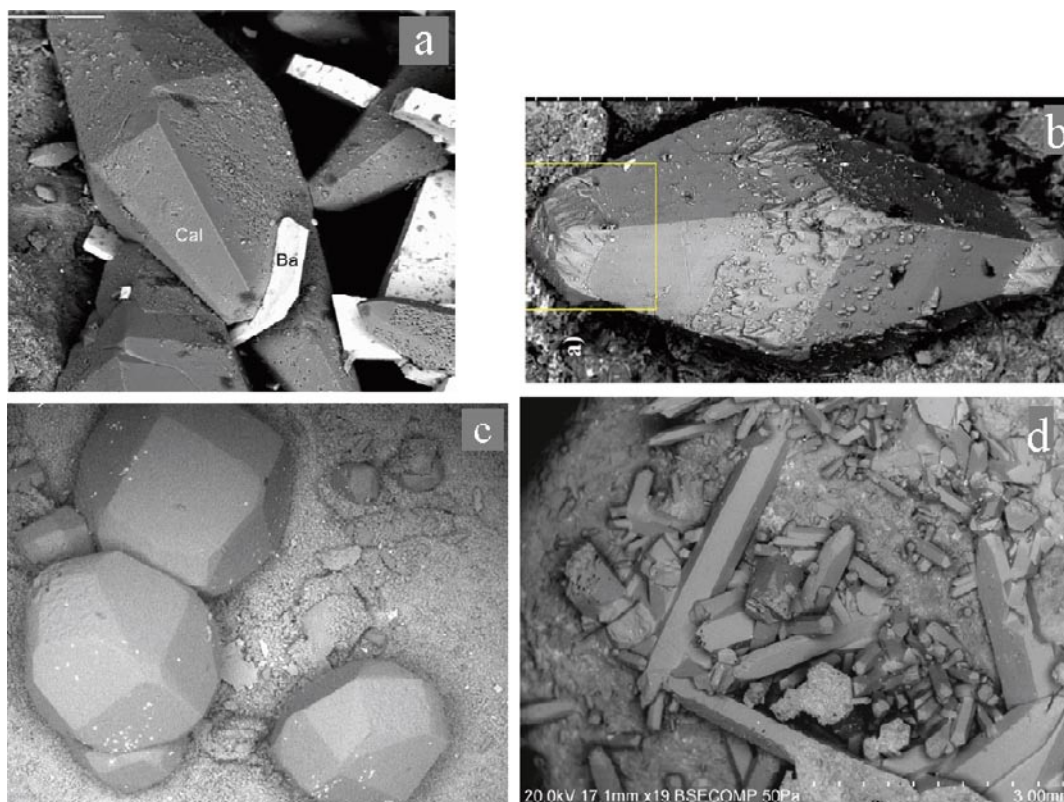
Figure 3-30. *Back-scattered SEM-images of different calcite types in the fracture fillings from the Laxemar-Simpevarp area. (a): scalenohedral calcite (Cal) and barite (Ba) from KLX03 at 457.60–457.75 m, borehole length. Scale marker is 200 µm.(b): scalenohedral calcite with overgrowths of younger calcite from KLX07A at 373.70–373.97 m, borehole length. (c): equant calcite crystals from KLX07A at 696.68–696.83 m, borehole length. (d): needle shaped calcites from KLX08 at 218.29–218.39 m. Taken from Drake and Tullborg (2007).*

The general conceptual model for the Äspö and Laxemar subareas obtained from the calcite studies (e.g. Bath *et al.* 2000, Puigdomènech 2001) indicate that, in the upper 0–100 m of the bedrock, a dynamic situation occurs with dissolution and precipitation of calcite. Below this depth (down to 700–1,000 m) mainly precipitation (or re-crystallisation) of calcite in multiple episodes is detected. Calcites precipitated from brackish, marine waters are found down to 500 m depth, whereas calcites with meteoric-cold climatic signatures can be traced to greater depths (1,000 m), especially in the Laxemar subarea, due to the recharge character of this zone. The hydrogeochemical results and the most recent mineralogical data acquired during the site investigation program support this conceptual model.

Contribution of "biogenic" carbonates, with low $\delta^{13}C$ values, has also been found in the fracture fillings during these investigations. Some samples from the Laxemar subarea have extremely low $\delta^{13}C$ values (–68 to –55‰ at depths between 450 and 670 m) suggesting biogenic activity in the groundwater aquifers causing *in situ* disequilibria. Microbial activity indicates temperatures mostly below 100°C and a low temperature origin for these calcites is suggested, probably formed from waters similar to recent meteoric or brackish Baltic Sea waters at the site (Drake and Tullborg 2007). Similar low $\delta^{13}C$ values have been found in the calcite fillings at Äspö (Tullborg *et al.* 1999), at the Götemar granite (a granite massif that crops out several kilometres north of the Laxemar-Simpevarp area; Drake and Tullborg 2006b), and at Forsmark (Smellie and Tullborg 2005).

This observation is relevant as it supports the existence of long-lived *in situ* biological activity (bacterial fossils have been found in the fracture fillings; Pedersen *et al.* 1997). Microbiological activity, autotrophic or heterotrophic, influences the carbonate system through its effects on the CO_2 (or generating acid metabolites). Therefore, if bacterial activity is ongoing in the present groundwater system, it must represent a source of disequilibrium in the carbonate system. These effects could be important when evaluating the characteristics of the carbonate system (e.g. saturation states) in the groundwaters and they are further discussed below.

3.3.3   Processes. Thermodynamic approach

Calcite is one of the most abundant minerals in fracture fillings and it plays a fundamental role in the pH-buffering of the recharge groundwaters. Moreover, hydrochemical, mineralogical and isotopic data support the hypothesis that calcite precipitation is a common process in deeper groundwaters.

The mineral calcite is particularly important for understanding the carbonate system in the Laxemar-Simpevarp groundwaters and in other similar crystalline systems (e.g. Nordstrom *et al.* 1989, Pitkänen *et al.* 1999, 2004, Iwatsuki *et al.* 2005). Therefore, saturation states with respect to this mineral have been calculated for all the water samples with field pH measurements.

Calcite solubility and carbon speciation are well constrained and the thermodynamic data included in the WATEQ4F database are those proposed by Plummer and Busemberg (1982). The uncertainties associated with their equilibrium constants affect the calcite saturation index by ± 0.15 units. If these maximum thermodynamic errors are, in turn, accumulated to the analytical errors for alkalinity, dissolved calcium and pH (data presented by Nilsson 2008) an overall uncertainty of ± 0.3 units is obtained for the saturation index (slightly lower than that obtained for the Stripa groundwaters by Nordstrom and Ball 1989). This uncertainty range is plotted in all the following graphs containing the calcite saturation index.

CO_2 partial pressure (log pCO_2) is another relevant parameter for understanding the evolution of the carbonate system. CO_2 partial pressure data are also important to evaluate possible uncertainties in measured pH values. For these two reasons, log pCO_2 values, as obtained from speciation-solubility calculations, are also presented in this section.

Near-surface groundwaters

Calcium and HCO_3^- contents in the near-surface groundwaters from the Laxemar-Simpevarp area are within the normal range in the Swedish context (Tröjbom and Söderbäck 2006a, Tröjbom *et al.* 2008). However, in the fresh near-surface groundwaters, calcium and bicarbonate reach maximum values of ~100 and ~550 mg/L respectively, which are lower than those measured in the fresh near-surface groundwaters from Forsmark.

Calcium content, bicarbonate content, and pH are all related through weathering reactions driven by biogenic CO_2 input in the overburden. The decay of organic matter (e.g. plant debris) and root respiration are the main driving forces of weathering reactions as they provide a continuous source of CO_2 in the pedogenic environment (see reaction 3-2-1 in section 3.2.3). In fact, dissolved inorganic carbon (DIC) in most near-surface groundwaters in the Laxemar-Simpevarp area seems to be dominated by this biogenic carbon source (most $\delta^{13}C$ values in the DIC are between –15‰, –20‰; Figure 3-33a).

CO_2 is consumed during the weathering reactions of silicate minerals, liberating calcium (from plagioclase, hornblende, etc) and producing HCO_3^- (Kehew 2001, Appelo and Postma 2005). For example, alteration of anorthite to kaolinite can be expressed as:

$$CaAl_2Si_2O_8 + 2CO_2 + 3H_2O \rightarrow Ca^{2+} + Al_2Si_2O_5(OH)_4 + 2HCO_3^- \qquad (3\text{-}3\text{-}1)$$
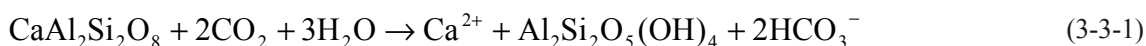
In this type of aluminosilicate incongruent dissolution reaction DIC is only derived from the biogenic CO_2 and the process only changes the distribution of carbonate species, shifting them towards the HCO_3^- field due to the increase in pH (e.g. Clark and Fritz 1997, Appelo and Postma 2005).

If calcite is present in the overburden, the input of biogenic CO_2 will promote undersaturation in the soil waters and calcite will be dissolved through the following reaction

$$CO_{2(g)} + H_2O + CaCO_3 \rightarrow Ca^{2+} + 2HCO_3^- \qquad (3\text{-}3\text{-}2)$$

also increasing dissolved Ca and HCO_3^- in the waters. In this case, an extra source of DIC (from the dissolved calcite) is added to the biogenic input and this fact can facilitate the isotopic identification of calcite dissolution even in almost purely silicate terrains (see section "Calcite dissolution and isotopic trends", below).

As stated in section 3.2.3, weathering intensity during infiltration of surface waters in the overburden is mainly conditioned by the evolution of the waters in open or closed conditions with respect to CO_2. If the consumed CO_2 in weathering reactions is replenished by the input of biogenic CO_2 (reaction 3-3-1; open system conditions to CO_2), weathering reactions will be enhanced, increasing the concentrations of cations and HCO_3^- further than in closed system conditions.

The available mineralogical information on the overburden indicates that major minerals in bedrock outcrops and in till matrix deposits are silicates and aluminosilicates (mainly quartz, plagioclase and potassium feldspar with minor hornblende, illite, vermiculite, chlorite and kaolinite; section 3.2.2) and only small amounts of calcite have been described for this part of the system. Therefore, aluminosilicate weathering reactions would be dominant even for dissolved calcium due to the very low amounts of calcite.

However, the ratio of dissolved calcium to HCO_3^- (Figure 3-31a) identifies an important number of fresh near-surface groundwaters along the 2:1 molar trend typical of reaction 3-3-2, suggesting a clear control by calcite in those waters (as also occurs in the Forsmark area, with much higher amounts of calcite in the overburden; Figure 3-31b).

This 2:1 ratio could also be the result of weathering of some plagioclases such as anorthite (reaction 3-3-1). However, the available mineralogical information indicates that plagioclase is albitic in the granitic rocks and oligoclase in the till deposits. Thus, the corresponding Ca/Na ratio should be between 0.0 (albite) and 0.4 (oligoclase)[8] while this ratio in the near-surface groundwaters is usually higher (Figure 3-32c), again indicating the contribution of calcite.

---

[8] As stated in section 3.2.3, plagioclases and mafic minerals (e.g. amphibole, biotite) react much faster than quartz and K-feldspar. In granitic systems, if plagioclase is present in a greater abundance than these mafic minerals (as it is often the case), the water chemical composition can be mostly explained in terms of plagioclase weathering. Calcium and sodium are then considered to result from plagioclase weathering and the Ca/Na ratio in the waters should be equal to the ratio for the plagioclase present in the parent rock (Garrels and Mackenzie 1967, Banks and Frengstad 2006 and references therein).

As a result of these weathering reactions (involving calcite and aluminosilicates), near-surface groundwaters evolve towards calcite equilibrium with increasing HCO_3^- concentrations (Figure 3-32a) and pH values, although in this case the scatter is large (Figure 3-32b). Most of the measured pH values in the fresh near-surface groundwaters are higher than 6.8, even taken into account that CO_2 partial pressures are higher than the atmospheric value (Figure 3-32c) as a result of biogenic input. Therefore, it can be concluded that weathering reactions, due to their fast kinetics, can compensate this input of acidity, so maintaining a neutral-alkaline pH.

Dissolved calcium in the fresh near-surface groundwaters from the Laxemar-Simpevarp area has, therefore, multiple sources and controls. Aluminosilicate weathering reactions (hornblende and plagioclase dissolution), cation exchange, or even fluorite equilibrium (see section 3.6) may participate. But, in most cases, calcite appears to contribute to the chemical characters of the carbonate system much more than expected considering its small (detected) amount.

Calcite dissolution will be a more effective pH-buffering reaction than aluminosilicate dissolution as it is much faster (at near neutral pH, the dissolution rate of calcite is approximately 7 orders of magnitude faster than the dissolution of plagioclase e.g. White *et al.* 1999a, b). Moreover, most of the waters with the highest HCO_3^- concentrations (e.g. 550 mg/L) and far from the 2:1 trend are in equilibrium with calcite (Figure 3-32b), even at very high CO_2 partial pressures (Figure 3-32c), indicating an effective control of this mineral also in this "extreme" waters (see below).
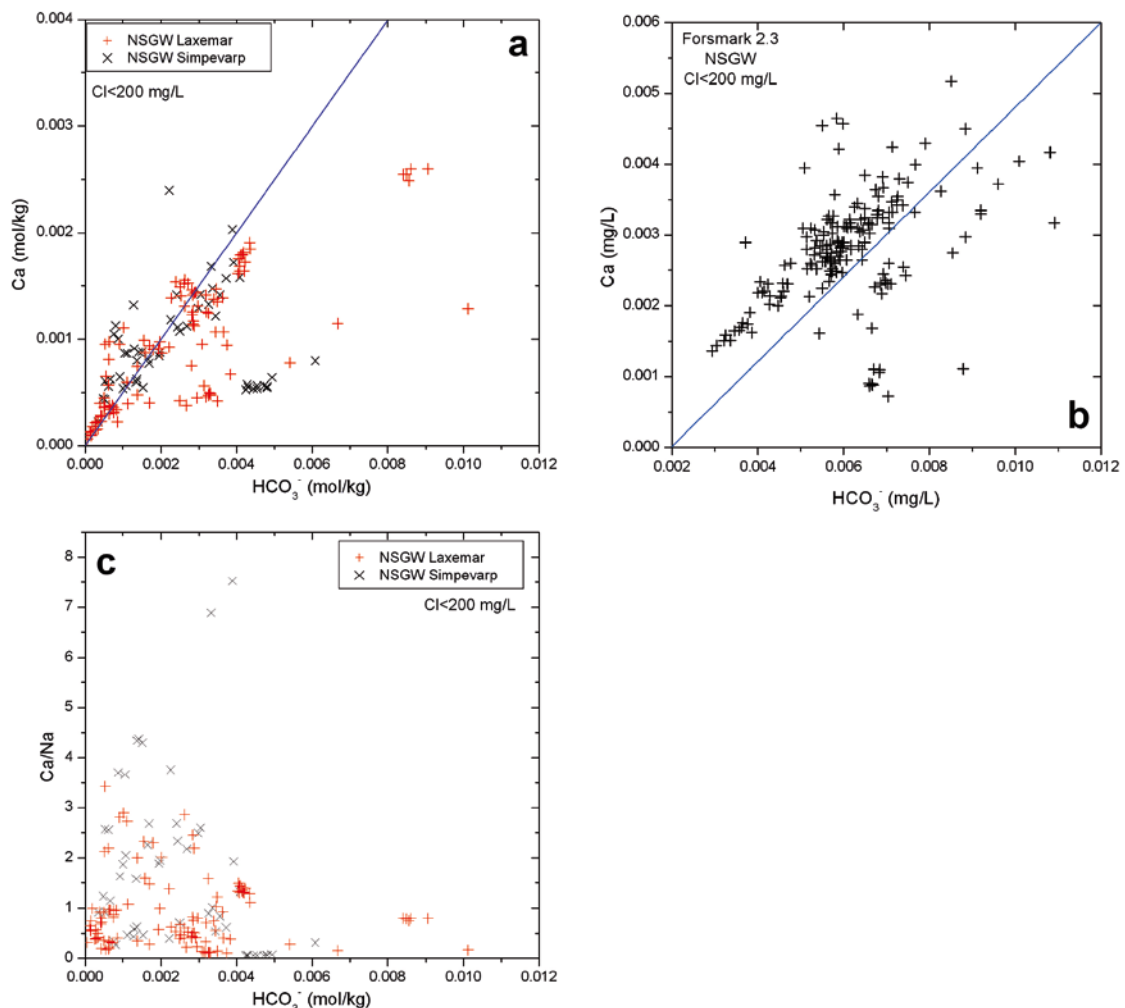
Figure 3-31. *Ca concentration (a) and Ca/Na ratio (b) vs. alkalinity in the fresh near-surface groundwaters at Laxemar-Simpevarp. (c) Ca concentration versus alkalinity at Forsmark. Only fresh (< 200 mg/L Cl) near-surface groundwaters are plotted. Blue line indicates the 2:1 ratio between HCO_3^- and calcium (reaction 3-3-2).*
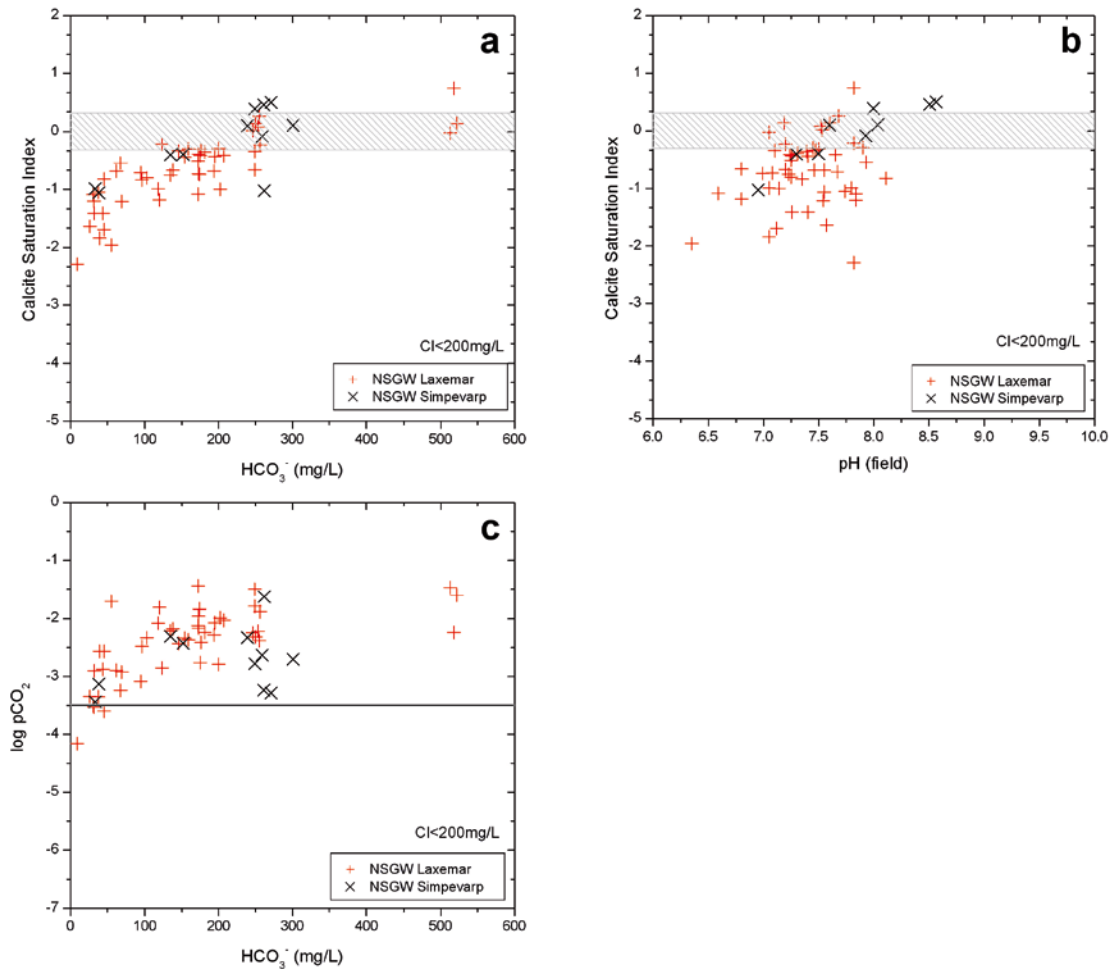
Figure 3-32. *Calcite saturation indices vs. alkalinity contents (a) and pH (b), and CO_2 partial pressures (as log pCO_2) vs. alkalinity contents (c) in the fresh, near-surface groundwaters from Laxemar-Simpevarp area. Only samples with pH values measured in the field and with chloride lower than 200 mg/L are plotted.*

Calcite dissolution and isotopic trends

The available isotopic data relevant to the knowledge of the carbonate system cover some important aspects. In the near-surface groundwaters, isotopic data for dissolved inorganic carbon ($\delta^{13}C$ and ^{14}C) and strontium ($^{87}Sr/^{86}Sr$) help to trace the origin and evolution of dissolved carbon and the influence of the carbonate system on weathering reactions.

As stated above, silicate weathering reactions do not change the biogenic isotopic signature of dissolved inorganic carbon. On the contrary calcite dissolution implies an additional source of carbon (with a different isotopic signature) that must affect the measured values of $\delta^{13}C$ and ^{14}C in the dissolved inorganic carbon (DIC).

$\delta^{13}C$ values in the fresh near-surface groundwaters are mostly between –10 and –21‰, indicating a clear biogenic contribution. However, a weak positive correlation with alkalinity (HCO_3^-) contents can be observed in these waters (Figure 3-33a) suggesting a contribution of $\delta^{13}C$-enriched carbonate phases.

The increase in dissolved bicarbonate produces the dilution of the ^{14}C signal (Figure 3-33b). Most of the high-bicarbonate waters have detectable tritium and ^{14}C decay effects are, therefore, insignificant. All these characteristics are in agreement with a dilution effect promoted by the dissolution of old calcites (containing no ^{14}C) present in the soil cover and in the upper bedrock fractures.

This effect was already observed by Smellie *et al.* (2006) in Laxemar. These authors also proposed that the breakdown of organic material of various ages (some significantly old) can collaborate to the dilution of the ^{14}C signal. Whereas breakdown of old organic material may represent a possible
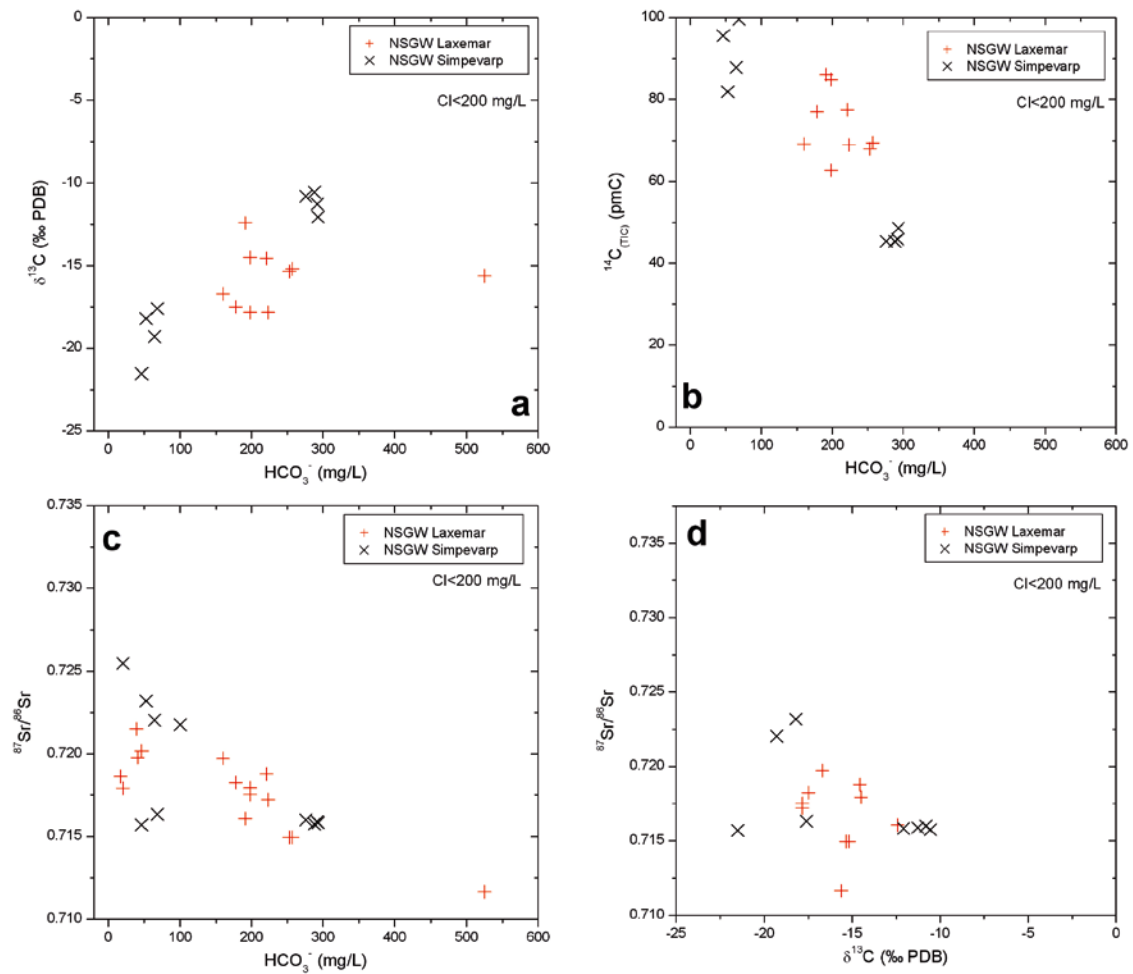
Figure 3-33. *Alkalinity contents (HCO_3^-) vs. $\delta^{13}C$ (a), ^{14}C (b) and $^{87}Sr/^{86}Sr$ (c) values, and $^{87}Sr/^{86}Sr$ vs. $\delta^{13}C$ values (d) in the fresh, near-surface groundwaters from Laxemar-Simpevarp area. Only waters with chloride lower than 200 mg/L are plotted.*

contribution to this trend, it appears that calcite dissolution in CO_2 open system conditions plays an important role, as suggested by the rest of the isotopic trends.

Near-surface groundwaters sampled in soil pipes have low Sr contents but a wide variation in strontium isotopic ratios, from 0.712 to 0.733 (Figure 3-33c). This variation may indicate leaching of minerals with different Rb/Sr ratios in the overburden (Smellie *et al.* 2006). This is totally reasonable, as the $^{87}Sr/^{86}Sr$ ratio is different in different minerals: Sr derived from K-rich minerals (e.g. K-feldspar, biotite) has high $^{87}Sr/^{86}Sr$ ratios, plagioclases (with lower K/Ca ratios) contain Sr with moderate $^{87}Sr/^{86}Sr$ ratios and Sr in calcites has usually much lower $^{87}Sr/^{86}Sr$ ratios (e.g. Cartwright *et al.* 2007 and references therein).

The clear differences in $^{87}Sr/^{86}Sr$ ratios between carbonates and silicates may be used to trace the weathering phases in silicate-dominated areas. If progressive carbonate dissolution occurs, an inverse correlation between $\delta^{13}C$ and $^{87}Sr/^{86}Sr$ would be expected (Katz and Bullen 1996, McNutt 2000, Dogramaci and Herczeg 2002) and a weak correlation can be seen in Figure 3-33d. A clearer inverse correlation can be observed between $^{87}Sr/^{86}Sr$ and alkalinity, even for the samples with the highest alkalinity (Figure 3-33c).

All these observations would confirm that carbonate dissolution participates in the control of the evolution of $^{87}Sr/^{86}Sr$ ratios here and, therefore, the important role played by them in the overburden in the Laxemar-Simpevarp area.

Effects of low amounts of calcite in the weathering environments

In spite of the low proportion of calcite in a silicate-dominated overburden, the effects of its dissolution on the chemical and isotopic composition of the fresh near-surface groundwaters in the Laxemar-Simpevarp overburden has just been demonstrated above. The apparently disproportionated effect has been repeatedly invoked since the classical work by Garrels and Mackenzie (1967) on the study of the weathering processes in granitic environments.

As carbonate minerals are more reactive and soluble than silicate minerals, they tend to regulate the geochemistry of surface waters even when present at trace levels in granitic rocks (Drever and Hurcomb 1986, Anderson *et al.* 1997, Morse and Arvidson 2002, White *et al.* 2005). This effect has been revisited recently in studies of chemical weathering, stressing the importance of the preferential weathering of disseminated or vein calcite in those environments, and the important consequences that it has in the calculation of weathering mass balances (White *et al.* 2005 and references therein).

For example, mass balance calculations performed by Blum *et al.* (1998) on a glacial watershed indicate that 82% of the HCO_3^- flux is derived from the weathering of carbonate minerals and only 18% is derived from silicate weathering, even though the bedrock is predominantly composed of quartz-feldspar gneisses and granites with less than 1% carbonate in the watershed. Other studies have also assessed the relative importance of carbonate *vs.* silicate weathering in controlling $^{87}Sr/^{86}Sr$ ratios, which have been extensively used in estimating continental weathering fluxes and long term CO_2 drawdown (Raymo and Ruddiman 1992, McCauley and De-Palo 1997, Jacobson *et al.* 2002).

The impact of disseminated calcite on solute compositions has also been experimentally documented by leaching granitoid rocks (Stauffer and Wittchen 1991, Clow *et al.* 1997, White *et al.* 1999ab, Jacobson and Blum 2000). Results indicated that initial effluent Ca, alkalinity and $^{87}Sr/^{86}Sr$ were dominated by rapid calcite dissolution, although, as the experiments progressed, the proportion of solutes contributed by silicate weathering increased as calcite was consumed (White *et al.* 2005).

This last observation may have important consequences as field studies have also documented the diminishing effects of calcite with the increasing age of the weathered regolith (Jacobson *et al.* 2002, White *et al.* 2005). The limited amount of calcite present in the overburden from the Laxemar-Simpevarp area will also limit its effects over time. Moreover, the preferential loss of this accessory calcite during weathering may also increase the permeability of the rock, accelerate the subsequent silicate weathering (White *et al.* 2001) and, eventually, change or modify the recharge paths.

Therefore, as it was recommended for the Forsmark site, further studies and estimations on the "durability" of the calcite buffering, integrated into a study of regolith loss to erosion, would be a valuable tool in future predictive calculations for performance assessment.

Comparison between the fresh near-surface groundwaters at Laxemar-Simpevarp and Forsmark

Although calcite has a clear influence in the carbonate system of the near-surface groundwaters in the Laxemar-Simpevarp area, it is not comparable in magnitude to the effects found in the Forsmark area (cf. Gimeno *et al.* 2008).

The extensive presence of limestones in the overburden of the Forsmark area (a feature very uncommon in Swedish soils) promotes important differences in pH, alkalinity, calcium contents and calcite saturation indices in the near-surface groundwaters. These four parameters are compared in Figure 3-34 for Forsmark and Laxemar.

Available field pH data in the fresh near-surface groundwaters do not show clear differences between both areas, although some lower values, as a whole, appear to occur in the Forsmark area (Figure 3-34a). Calcium and bicarbonate contents are clearly higher in Forsmark (Figures 3-34bc) and most of the near-surface groundwaters in this zone are in equilibrium with calcite whereas undersaturation states are much more frequent in the Laxemar-Simpevarp subarea (Figure 3-34d).

The highest alkalinity values found in the Forsmark groundwaters are related to the dissolution of limestones (e.g. reaction 3-3-2), mainly under open conditions with respect to CO_2. But they also depend on the net biogenic CO_2 input to the system, as it facilitates the persistence of more or less prolonged or pervasive CO_2 open system conditions.
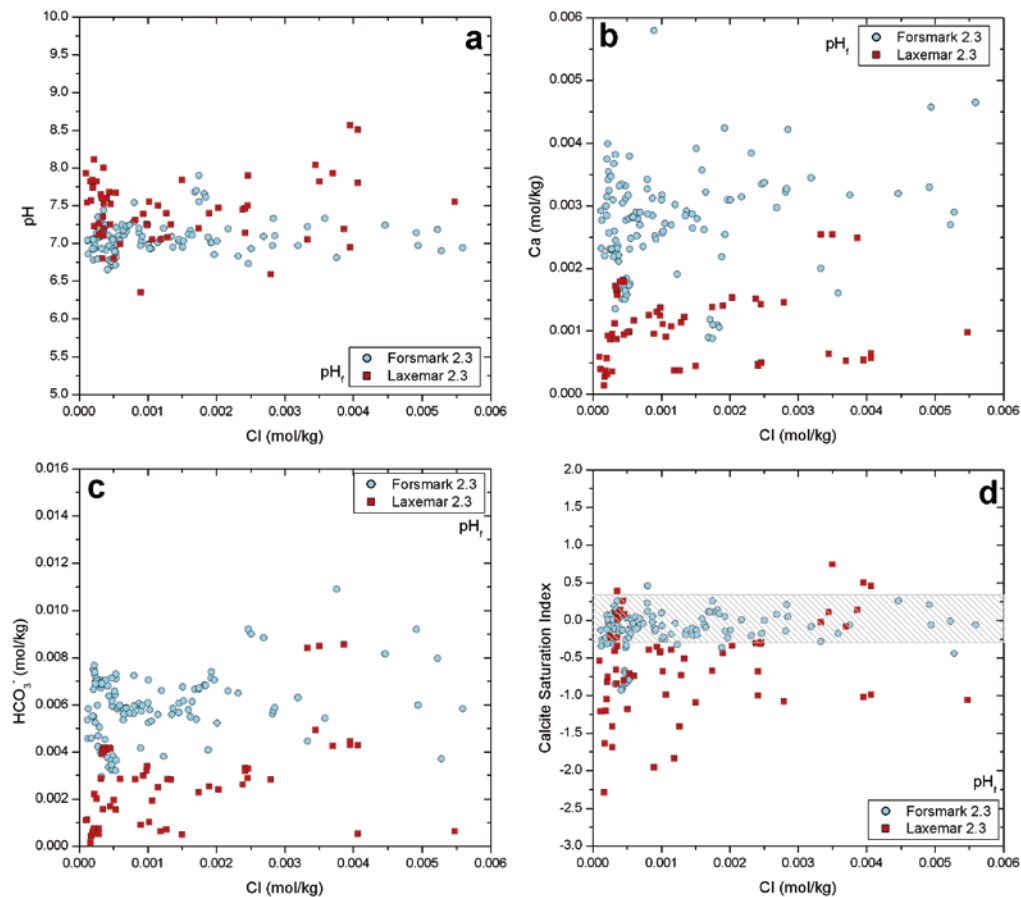
Figure 3-34. *Main chemical features of the carbonate system vs. Cl concentrations for the fresh near-surface groundwaters (with field pH data) from Forsmark and Laxemar-Simpevarp. (a) pH values; (b) Ca concentrations; (c) HCO_3^- concentrations; and (d) calcite saturation index.*

Differences in the development of the soil cover have a critical role in the input of CO_2 and, in general, in the intensity of weathering reactions in crystalline systems (e.g. Oliva *et al.* 2003). As noted before, the Forsmark area contains minor bedrock outcrops (less than 10%) and till deposits and soils dominate the surface. However, in the Laxemar-simpevarp zone, the areas of bare bedrock with associated thin soils are much more abundant (more than 50%, a distinct feature from the rest of Swedish soils; Lundin *et al.* 2005) than the till deposits. Therefore, as a whole, the biogenic CO_2 input seems to be more important in the Forsmark area, favouring the development of higher alkalinities and dissolved calcium.

Apart from differences in the soil cover (both coverage and depth) and vegetation, the temperature, precipitation and mineralogical characters of the overburden could exert a strong influence on the weathering rates of each zone. Weathering reactions and rates control the present and future evolution of the near surface and recharge groundwaters and their study merits further development. This is especially relevant in the Laxemar subarea, where dilute groundwaters (e.g. low dissolved calcium waters) may reach repository depth.

Groundwaters

Calcite saturation indices show the existence of equilibrium or near-equilibrium situations for all the available samples with field pH. Dilute groundwaters rapidly attain equilibrium or slight oversaturation at shallow depths (Figure 3-35ab) and this state is maintained at greater depths in saline groundwaters where mixing processes are effective.

The slight oversaturation detected in some groundwaters from the Laxemar and Äspö subareas between 200 and 500 m depth (Figure 3-35a) may be due to kinetic effects (retarded precipitation of calcite), microbiological activity or problems with the measured pH. These groundwaters have higher-than-atmosphere CO_2 partial pressures (log pCO_2 > –3.5; Figure 3-35cd) and, therefore, they could be affected by out gassing during pH measurement.

All the other samples that are oversaturated with respect to calcite are category 1 to 3 of the saline type (Cl > 10,000 mg/L) at deeper levels (from 900 m depth down; Figures 3-35ab). The presence of a certain degree of oversaturation, with saturation index (SI) values between +0.5 and +1.0, has been commonly reported in deep saline calcium-chloride rich groundwaters from the Fennoscandian Shield (Stripa, Äspö, Laxemar, Olkiluoto; etc; Nordstrom *et al.* 1989, Glynn and Voss 1999, Pitkänen *et al.* 1999, 2004) and it can also be observed in the Lac du Bonnet ground-waters (Figure 3-36a). The origin of this slight oversaturation in such old groundwaters is a debatable matter, as it can be related to problems with pH measurements or other less studied processes (see section 3.3.4). In any case, these equilibrium or quasi-equilibrium situations support the important role of calcite in the control of some key parameters such as pH or alkalinity (Nordstrom *et al.* 1989).
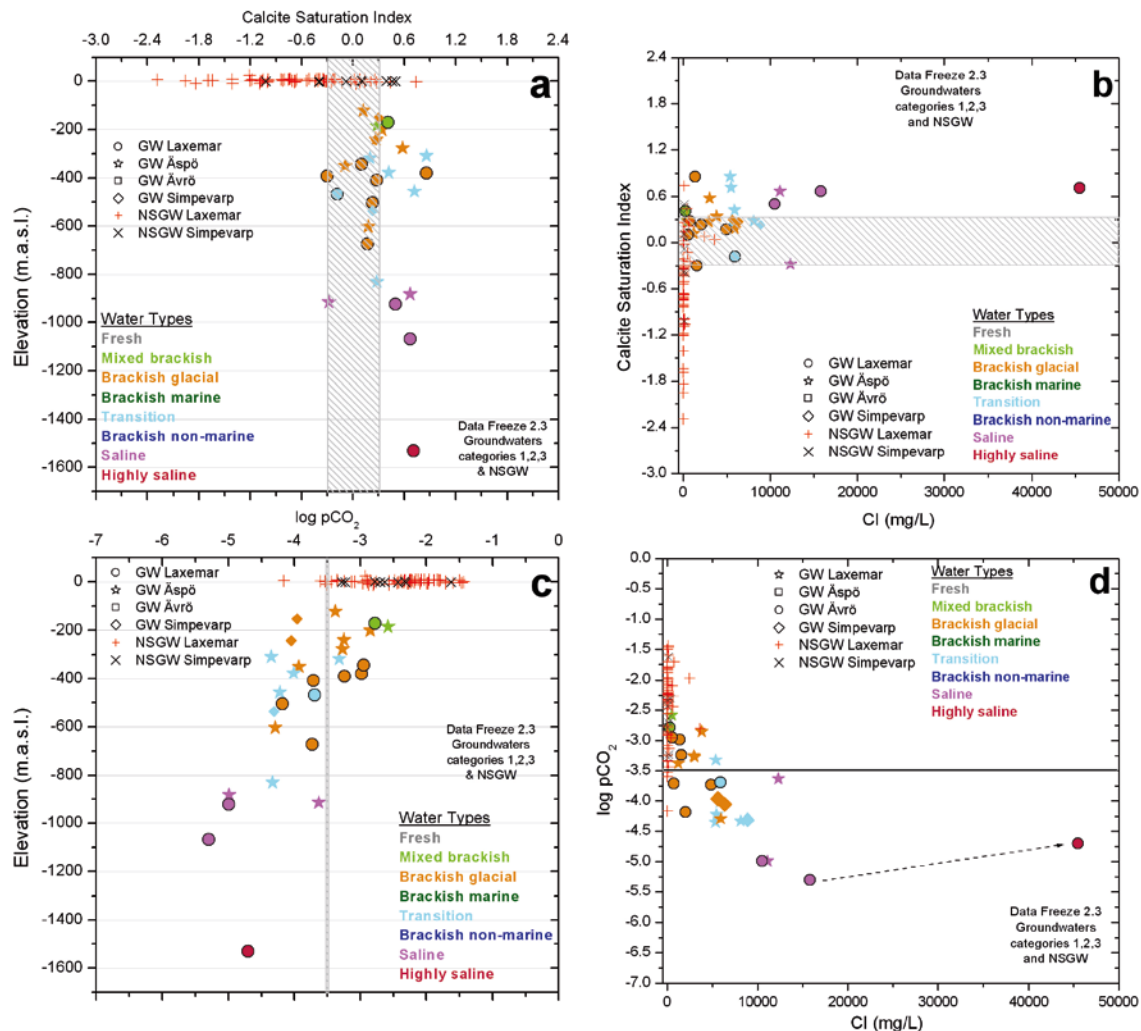
Figure 3-35. *Calcite saturation index vs. depth (a) and chloride contents (b) and calculated CO_2 partial pressure (as log pCO_2) vs. depth (c) and chloride contents (d) in the Laxemar-Simpevarp groundwaters. Results for the near-surface groundwaters are also plotted. Dashed areas correspond to the uncertainty associated with the calcite equilibrium constant accumulated to the analytical errors for alkalinity, dissolved calcium and pH (data presented by Nilsson 2008). The overall uncertainty is ± 0.3 units (slightly lower than that obtained for the Stripa groundwaters by Nordstrom and Ball 1989).*

Calculated CO_2 partial pressures display a progressive decrease with depth (Figure 3-35c) and with chloride content (Figure 3-35d) from the values found in the fresh near-surface groundwaters (most of them with pCO_2 values higher than the atmosphere). Similar trends in the evolution of CO_2 partial pressures with depth and chloride content can be observed, for example, in the Lac du Bonnet groundwaters in Canada (Figure 3-36ab; used analytical data from Gascoyne 2004) and, especially, in the Olkiluoto groundwaters (Figure 3-36cd, Pitkänen *et al.* 2004) where, as also observed in the Laxemar-Simpevarp area, after this initial decrease there is a slight increase in log pCO_2 in groundwaters with chloride around 15,000 mg/L towards the highly saline samples.

The decrease in CO_2 partial pressure observed in the Laxemar-Simpevarp groundwaters can be attributed to calcite dissolution, although restricted to the dilute shallowest groundwaters (dilute groundwaters at 200 m depth have already reached equilibrium or oversaturation with respect to this mineral; Figure 3-35ab).

At greater depths, where groundwaters are also in equilibrium or near-equilibrium with calcite, CO_2 depletion may be associated with aluminosilicate dissolution (a kinetically slow process) and, mainly, to the combined effects of mixing with saline groundwaters and precipitation of calcite (see section 3.3.4). Precipitation of calcite during mixing of dilute and saline groundwaters could keep the alkalinity at the very low levels observed in those groundwaters with Cl > 8,000 mg/L.
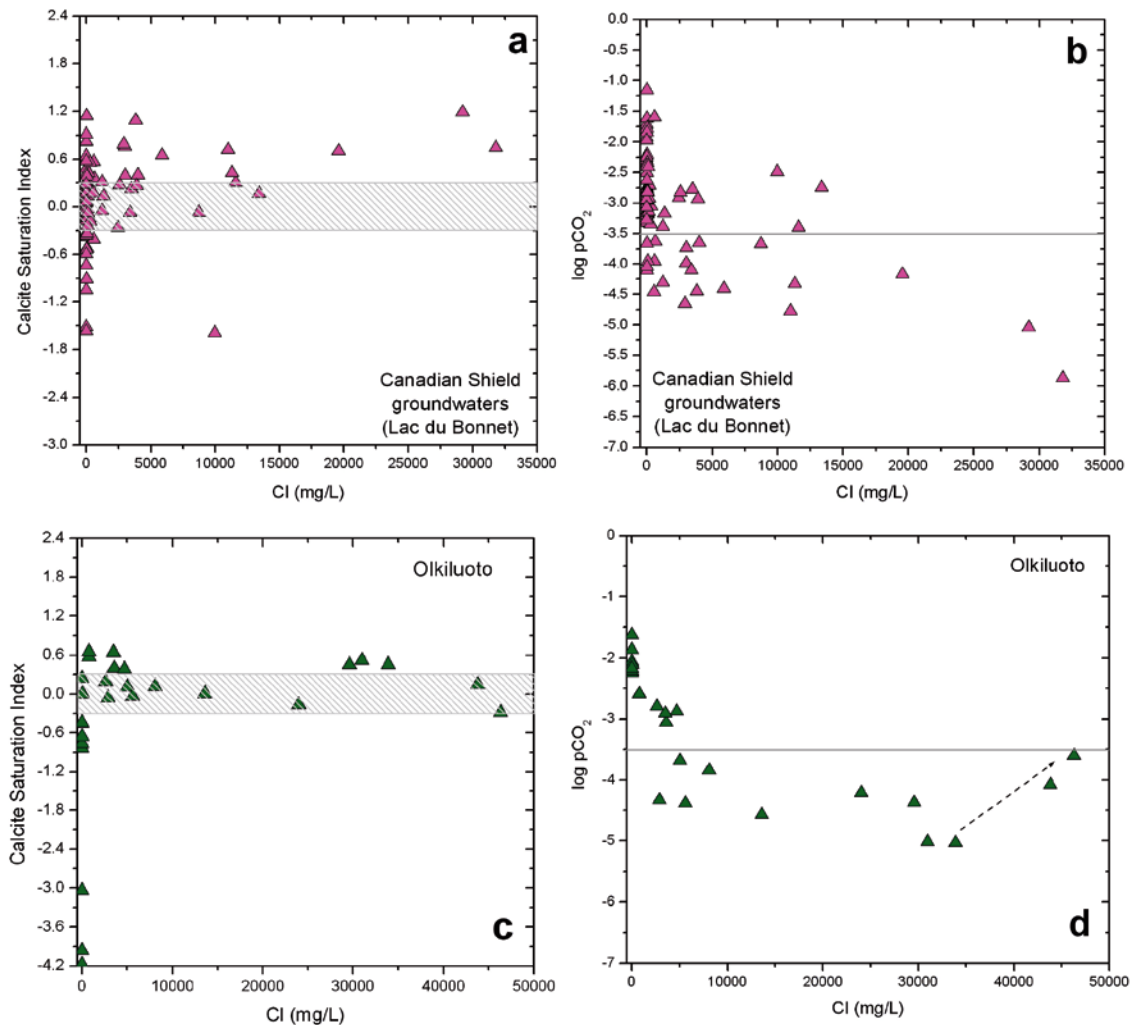
Figure 3-36. *Calcite saturation index (a, c) and calculated CO_2 partial pressure (b, d) as log pCO_2 vs. Cl in the Lac du Bonnet (Canada; a, b) and in the Olkiluoto groundwaters (c and d). Note that different chloride or saturation index scales have been used where appropriate to better visualise and describe the data in question. Dashed areas correspond to the uncertainty of ± 0.3 units associated with the calcite equilibrium constant accumulated to the analytical errors for alkalinity, dissolved calcium and pH.*

3.3.4 Thermodynamic simulations

Following the same structure as in the other sections in this chapter, once the data and calculations have been presented and the hypotetical controls stated, different types of thermodynamic simulations will be presented here. First, an uncertainty analysis of the measured pH values and their effect on speciation-solubility calculations (calcite saturation index) is performed. Then, the same kind of mixing and mixing + reaction simulations are shown, following the scheme already explained in section 3.2.4.

Uncertainties in pH measurement and calcite equilibrium in groundwaters

Groundwaters in the Laxemar-Simpevarp area have CO_2 partial pressures both higher and lower than the atmospheric value. Therefore, pH measurements could be affected by exchange of CO_2 with the atmosphere (CO_2 out gassing or in gassing, respectively) even in on-line pH field measurements.

This problem has been taken into account since the first stage of the Site Characterization Program, especially when pH was measured in the laboratory. Gimeno *et al.* (2004a, c; Simpevarp 1.1 and Forsmark 1.1, respectively) calculated the theoretical (*in situ*) pH for these groundwaters by assuming calcite equilibrium (SI = 0). This approach was also used by Pitkänen *et al.* (2004) for the Olkiluoto groundwaters and, more recently, by other research groups (e.g. Sasamoto *et al.* 2007) to obtain possible values of *in situ* pH in groundwaters over- or undersaturated with respect to calcite, assuming that those apparent saturation states were caused by problems during pH determination in the field and that the equilibrium assumption is *a priori* reliable for groundwaters with long residence times.

Both assumptions and their consequences on the geochemical calculations are explored in this section by performing two different tests with the assistance of the PHREEQC code (Parkhurst and Appelo 1999) and the WATEQ4F database (Ball and Nordstrom 2001):

a) independent estimation of the pH values from $CO_{2(gas)}$ contents for some groundwaters in equilibrium or oversaturated with respect to calcite, and then, a comparison with the measured values to test their reliability; and

b) speciation-solubility calculations assuming calcite equilibrium in all the studied groundwaters and a comparison with the measured pH values.

Evaluation of pH values from $CO_{2(gas)}$ contents

From the thermodynamic and mass/charge balance equations governing the carbonate system, several options may be used to obtain an estimation of the pH value. The most "classical" approach is to obtain the pH value from alkalinity and TIC (total inorganic carbon; e.g. Appelo and Postma, 2005). Unfortunately, TIC values are not available for the studied groundwaters.

However, $CO_{2(gas)}$ contents have been analysed in some groundwater samples and the pH value corresponding to the measured $CO_{2(gas)}$ concentrations can be calculated and compared with the measured ones.

The samples used for these calculations are those with *in situ* pH measurements (from Chemmac) and $CO_{2(gas)}$ data. They include a few samples from the Laxemar and Simpevarp subareas[9] (samples #7953, #10091, #11228, #15008, #5263 and #5288 from KLX03, KLX08, KLX15 and KSH01A boreholes). Several suitable samples from the Forsmark area displaying oversaturation with respect to calcite have also been included (Gimeno *et al.* 2008).

The results are shown in Table 3-2. The calculated pH values for the Laxemar-Simpevarp groundwaters agree very well with the measured ones. Except for one sample (#5263), the differences are smaller than 0.2 pH units. Most of the samples from Forsmark show differences smaller than 0.3 pH units. Therefore, as a whole, these results would indicate good reliability of the pH measurements.

---

[9] The available data from Äspö (pre-investigation phase) have not been included as Smellie and Laaksoharju (1992) mentioned contamination problems in the samples for gasses.

Table 3-2. Calculated values for pH, calcite saturation index and log pCO₂ from CO₂(gas) data compared with those obtained from measured pH values. Groundwater samples from the Laxemar-Simpevarp and Forsmark areas are included.

	Sample #	Elev. SecMid	Cl (mg/L)	CO$_{2(gas)}$ ($\cdot 10^{-5}$ M)	Measured pH	Calculated with measured pH		Calculated from CO$_{2(gas)}$		
						SI calcite	log pCO₂	SI calcite	log pCO₂	pH
Laxemar	7953	−171	259	6.28	8.17	+0.41	−2.78	+0.58	−2.96	8.35
	10091	−380	1,390	8.07	8.10	+0.86	−2.98	+0.68	−2.77	7.90
	11228	−504	11,228	0.318	8.30	+0.23	−4.18	+0.23	−4.18	8.30
	15008	−467	5,890	0.63	7.6	−0.18	−3.69	−0.03	−3.85	7.75
Simpevarp	5263	−152	5,590	3.54	8.1	+0.30	−3.96	−0.36	−3.22	7.4
	5288	−536	8,876	0.36	8.05	+0.23	−4.32	+0.04	−4.1	7.9
Forsmark	4724	−176	5,329	5.34	7.41	+0.20	−2.65	+0.55	−3.02	7.77
	12326	−341	5,160	0.897	8.1	+0.63	−3.84	+0.57	−3.76	8.04
	12354	−442	5,960	0.179	8.4	+0.71	−4.46	+0.71	−4.45	8.39
	8016	−500	5,410	17.9	6.93	−0.12	−2.05	+0.27	−2.45	7.32
	8284	−439	5,330	6.73	7.29	+0.15	−2.55	+0.46	−2.87	7.60
	8273	−628	5,430	2.57	7.38	−0.21	−3.26	−0.22	−3.26	7.37
	8281	−927	8,560	0.717	7.40	−0.27	−3.68	−0.21	−3.74	7.46
	8809	−299	4,560	3.0	7.35	0.0	−2.92	+0.30	−3.25	7.65
	12000	−546	6,100	0.356	8.0	+0.13	−4.29	0.00	−4.12	7.85

However, what is more important is that groundwater samples clearly oversaturated with respect to calcite when using the measured pH maintain this state in the independent CO₂ calculations. This is true for both areas, Laxemar-Simpevarp (e.g. samples #7953 and #10091) and Forsmark (samples #12326 and #12354). Moreover, this agreement is observed for samples with very different compositional characters (e.g. chloride, alkalinity or CO$_{2(gas)}$ contents; Table 3-2) and, therefore, they are not associated with any particular chemical feature or groundwater type.

The oversaturated samples in the Laxemar-Simpevarp area are more diluted and have higher alkalinities than the rest of the samples. They correspond to "shallow" levels in the Laxemar subarea, especially for sample #7953. Therefore, their calcite oversaturation state may be related to a limited residence time, i.e. not enough time to reach equilibrium. However, this explanation cannot be invoked for the rest of oversaturated groundwaters with elevated residence times in neither Laxemar-Simpevarp nor in Forsmark. This is the case for the deepest and more saline samples from the Laxemar-Simpevarp area (Figure 3-35ab). Unfortunately, they do not have CO$_{2(gas)}$ data to check their behaviour, as it has been done for the other groundwaters.

The rest of the samples confirm the equilibrium state with respect to calcite already obtained with the measured pH (in the uncertainty range of ± 0.3 SI units). Only two samples from Forsmark (#4724 and #8284) shift from equilibrium to a slight oversaturation.

As a summary, these results indicate that many of the studied groundwaters are in equilibrium with calcite and confirm the oversaturation state of others.

Evaluation from theoretical pH values at calcite equilibrium

Theoretical pH values have been calculated by assuming equilibrium with respect to calcite for all the groundwater samples with field pH measurement from the Laxemar-Simpevarp area. These theoretical pH values have been obtained with PHREEQC by changing the CO₂ content of each sample to reach calcite equilibrium. The obtained pH and CO₂ partial pressures (as log pCO₂) are compared with the measured pH and the corresponding log pCO₂ (Figures 3-37 and 3-38).

Overall, pH values calculated in equilibrium with calcite cover a range (7.1 to 8.2) slightly narrower than the measured values (7.2 and 8.6), but their evolution with depth and chloride are the same: neither of them show a clear trend. The only difference is that the calculated pH values show less scattering than the measured ones in waters at depths greater than 800 m (Figure 3-37ab) with chloride contents greater than 10,000 mg/L (Figure 3-38ab), whereas calculated pH for the shallower dilute waters show a similar variability to the measured pH.

Something similar happens with the CO_2 partial pressure. Calculated log pCO_2 in equilibrium with calcite are shifted towards higher values (–2 to –4.25) than those obtained with the measured pH (–2.5 to –5.5) but the main trends with depth and chloride content are the same (Figure 3-37cd, and 3-38cd). However, whereas pCO_2 obtained with the measured pH decrease continuously to pCO_2 values around $10^{-5.5}$ down to 1,100 m and up to chloride contents around 16,000 mg/L, pCO_2 values calculated from equilibrium with respect to calcite only decrease down to $10^{-4.2}$ at 600 m depth and 8,000 mg/L Cl, and then values are constant from that depth downwards. In both cases, between the last sample in the decreasing trend (saline waters) and the deepest and more saline groundwaters (highly saline waters) there is a slight increase, as is also observed at Olkiluoto (Figure 3-36d).

This increasing trend of CO_2 partial pressure, together with the decreasing trend observed in pH (not only with the real values but also with those in equilibrium with calcite) in the deepest part of the system between the saline and highly saline groundwaters (Figure 3-22) is much better defined in Olkiluoto (3-36d) due to the greater number of samples. The explanation of this behaviour will be discussed later with different thermodynamic simulations.
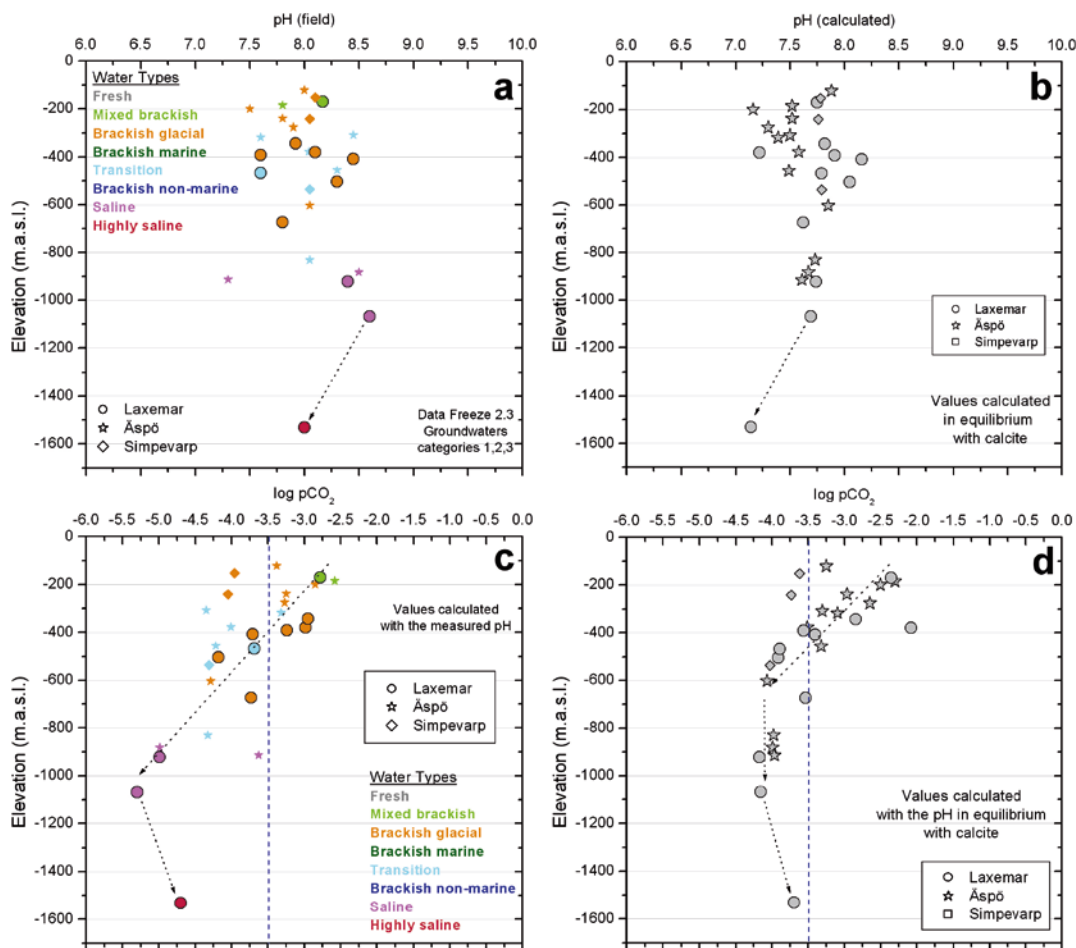
Figure 3-37. *Measured pH values (a) and the corresponding log pCO₂ (c) vs. depth compared with the calculated pH (b) and log pCO₂ (d) values assuming equilibrium with calcite (see text).*
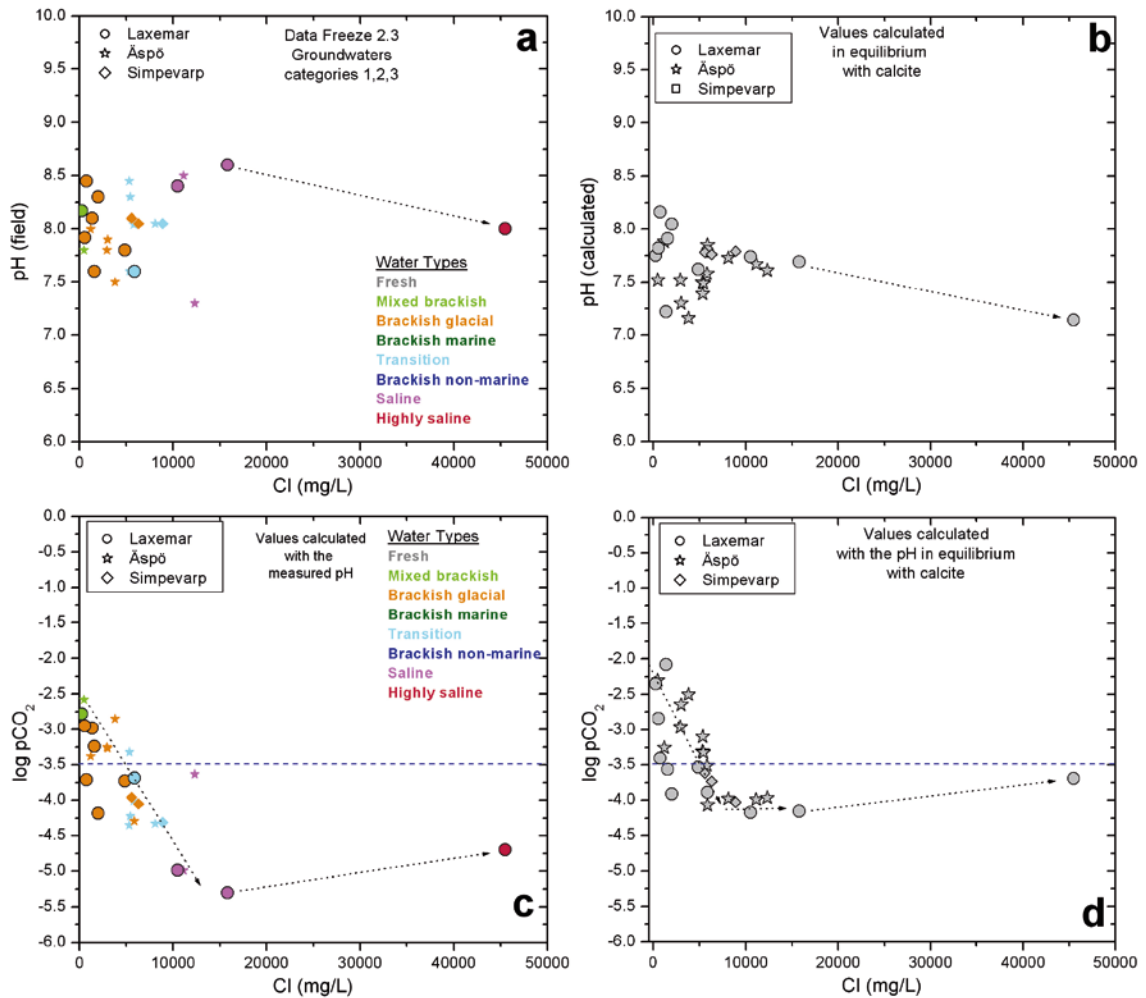
Figure 3-38. *Measured pH values (a) and the corresponding log pCO₂ (c) vs. chloride contents compared with calculated pH (b) and log pCO₂ (d) values assuming equilibrium with calcite (see text).*

With respect to the calcite-oversaturated samples, there are two different situations represented by two different sets of waters:

a) Samples from the Laxemar and Äspö subareas at depths between 200 and 400 m (Figure 3-37c), with higher CO_2 partial pressures than the atmosphere (log $pCO_2 = -3.5$) when considering the measured pH values. When equilibrated with calcite, these samples have even higher log pCO_2 and lower pH (Figure 3-37c, b). Therefore, they could have been affected by out gassing during pH measurement, increasing the pH and producing the oversaturation of calcite. Samples #7953 and #10091 from the Laxemar subarea (Table 3-3) are included in this group as they are oversaturated with respect to calcite and have CO_2 partial pressures higher than the atmosphere. However, as demonstrated above, this out gassing during pH measurement cannot have happened, as calculations performed with the measured $CO_{2(gas)}$ content of both samples give the same pH and the same oversaturation degree with respect to calcite.

b) Saline groundwater samples (Cl > 8,000 mg/L) from deeper levels (from 900 m depth) found at Äspö and Laxemar subareas (Figures 3-35ab). Oversaturation with respect to calcite can only be reached as a result of CO_2 out gassing. This process is possible in waters with CO_2 partial pressure higher than the atmosphere, which is the case of (a) above, but in contrast to those waters, saline groundwaters have very low CO_2 partial pressures when calculated with the measured pH. Even assuming calcite equilibrium, results indicate an increase in CO_2 partial pressure but still below the atmospheric value (Figures 3-37cd). Therefore, these groundwaters are strongly buffered against CO_2 *out gassing,* and atmospheric CO_2 *in gassing* would be highly favoured. In other words, if these groundwaters were in equilibrium with calcite at low P_{CO2} values, CO_2 in gassing would cause an increase in the CO_2 partial pressure and a undersaturation state with respect to calcite (instead of the observed oversaturation).

As a summary, there are several waters whose apparent oversaturation with respect to calcite may be due to modifications in their original pH during measurement. However, there are other samples where the oversaturation is not associated with pH modifications (at least for the tested samples #7952 and #10091) or, if modified, it must have been caused by other processes such as **pressure effects** or **"forced" degassing processes**.

Apparent calcite oversaturation due to **pressure differences** may arise in the deepest samples (1,000–1,500 m depth). However, simple calculations accounting for the pressure effects on the calcite equilibrium constant indicate that groundwaters in equilibrium with calcite at 300 bars (maximum pressure at 1,500 m depth) would appear oversaturated by only +0.2 with respect to this phase at surface conditions, which is not enough to justify the observed oversaturation[10].

Forced degassing has been invoked by Pitkänen *et al.* (2004), who found calcite oversaturation in the most saline and deepest groundwaters at Olkiluoto. These groundwaters have very high total gas content and the authors suggested that they could easily have degassed due to the decrease of pressure in near surface conditions during sampling. Then, minor amounts of CO_2 may be "forced" to evacuate with other gases, raising the pH and the calcite saturation index of the water samples. It is difficult to evaluate this hypothesis in the Laxemar-Simpevarp area as there are no data on the total gas contents in the deepest saline oversaturated groundwaters and the detected amounts in the rest of the sampled groundwaters are much lower than those detected at Olkiluoto.

Discussion

A certain degree of oversaturation with respect to calcite has been commonly reported in different groundwater systems from the Fennoscandian Shield, both near the surface and at depth. These oversaturation states have been frequently related to CO_2 exchange during pH measurement (e.g. Pitkänen *et al.* 1999, 2004) or have simply been attributed to the wide SI uncertainty range of what is considered an equilibrium situation (Gimeno *et al.* 2004b, 2005). In both cases, calcite equilibrium is considered as a reliable situation taking into account the aforementioned pH uncertainties.

However, the verification performed here indicates that the detected oversaturation states in dilute and relatively recent groundwaters from the Laxemar-Simpevarp area or in older groundwaters from the Forsmark area can be considered as true oversaturation states, as they are not affected by uncertainties in the pH measurements. Some of these oversaturation states may be related to a limited residence time, not enough to reach equilibrium. However, some alternative explanations are needed for a small group of shallow groundwaters and mainly for the deeper ones, with longer residence time.

Some authors (Nordstrom *et al.* 1989, Nordstrom and Ball 1989, Glynn and Voss 1999) consider that this oversaturation state can be "real" even in long residence time groundwaters like those from Stripa (ages in excess of 20,000 years, Fritz *et al.* 1989, Andrews *et al.* 1989). They propose a pure "inorganic" justification based on water-rock interaction processes: if dissolution of aluminosilicates is an effective process in these groundwaters, it would promote an increase in pH and in dissolved calcium contents; these increments would be balanced by calcite precipitation when oversaturation levels are high enough to overcome the kinetic barrier to precipitation.

Biological processes may also be involved in promoting oversaturation. Bacterial activity is an ongoing process in the present groundwater system and, necessarily, this activity must represent a source of disequilibrium in the carbonate system. Microbiological activity, auto- or heterotrophic, influences the carbonate system through its effects on the amount of CO_2 (or by generating acid metabolites). It promotes under- or oversaturation states, and therefore, dissolution or precipitation of carbonates, depending on the aquifer or the zone of the aquifer (Chapelle 2001). Under anoxic conditions, different anaerobic bacteria, such as iron reducing bacteria (IRB), sulphate reducing bacteria (SRB) and methanogens usually promote oversaturation and the precipitation of carbonates (e.g. Bennett *et al.* 2000, Postma *et al.* 2007, Konhauser 2007 and references therein). All the aforementioned metabolic groups are present in the studied systems at a wide range of depths.

---

[10] This is a maximum estimate of the effects of pressure differences as it does not take into account the pressure effects on the aqueous carbonate species (Aggarwal *et al.* 1990) which would reduce the oversaturation even more.

For instance, SRB activity has been detected in KLX02 down to 1,160 m depth and in the Forsmark area down to 1,000 m depth in saline groundwaters (Gimeno *et al.* 2008). Although SRB, IRB, or methanogens have not been detected at greater depths, autotrophic and heterotrophic acetogens were detected in significant amounts at 1,350–1,390 m (KLX02 borehole) in some of the most saline and deeper groundwaters from the Laxemar subarea (Haveman and Pedersen 2002).

There are two additional supports to this biological influence. The first one is the mineralogical information, which confirms the precipitation of calcite induced by microbial activity in the fracture fillings (see section 3.3.2). The second support is the observed increase in the oxidation of organic matter by IRB combined with an almost constant calcite oversaturation state (from +0.5 to +1.0, see Figure 4.a in Banwart 1999) throughout the whole Äspö Large-scale Redox Experiment timeframe.

Most of the oversaturated groundwaters in the investigated sites (e.g. Forsmark, Laxemar-Simpevarp or Olkiluoto) display a similar degree of oversaturation with respect to calcite (+0.5 to +1.0) without clear outliers. Similar oversaturation thresholds for calcite precipitation have already been described for many surface systems (e.g. rivers, springs, soils) where a value between +0.6 and +1.0 is observed to be needed before precipitation occurs (Jacobson and Usdowski 1975, Dandurand *et al.* 1982, Suarez 1983, Drysdale *et al.* 2002, Malusa *et al.* 2003) but not in groundwater systems, even in those where calcite is known to be precipitating (e.g. Plummer *et al.* 1990).

Several important points must be highlighted from all the above discussion:

a) problems in pH measurements are not the origin of the detected oversaturation states (at least not always);

b) the "calcite equilibrium approach" to obtain a pH value for the studied groundwaters must be used with caution, as it is based on the assumption of an incorrect pH determination. This assumption may simply hide other types of uncertainties, like the effects of microbiological activity; and

c) these biological effects on the carbonate system have been widely recognized in the microbiological investigations of the sites (e.g. Pedersen *et al.* 1997, Hallbeck 2006, Table 1-4; Laxemar 1.2) but quantitative estimations of the degree of induced disequilibrium have not been obtained and they are usually ignored when evaluating the characters of the carbonate system in the groundwaters.

These uncertainties are not critical to obtain the general picture of the carbonate system in the studied groundwaters. However, they must be clarified in order to obtain a better conceptual model.

Mixing and reaction simulations

As described in section 3.1.7, different mixing and mixing + reaction simulations have been performed based on the general palaeohydrogeological conceptual model. Specific details have been included for the study of the carbonate system:

1. The two basic simulations described in section 3.2.4 (mixing between the Glacial end member water and the highly saline sample #2731, and mixing between the Glacial end member or a Brackish-Glacial water and the Littorina end member) are presented here separately to make clearer the visualization of the results, as each one will be useful for a different set of waters.

2. Since the initial conditions for the Glacial end member are unknown, it has been equilibrated with calcite at different CO_2 partial pressures (log p $CO_2 = -6, -5, -4$, and -3), and therefore, with different pH values.

3. Sample #2731 has been equilibrated with calcite by modifying the CO_2 content. As already explained, the assumption of calcite equilibrium does not change the qualitative trends involving this sample but it does make easier the visualization of the simulation results (especially the evolution of calcite saturation states).

4. The Littorina end member has been equilibrated with calcite in all the performed simulations. A "modified Littorina end member", with higher alkalinity and calcium values, has also been considered in the simulations in order to analyse the relevance of the usual modifications in these parameters during infiltration of marine waters through the bottom sediments. Data for pore waters at 10 cm depth in the present Baltic marine sediments have been taken from Carman and Rahn (1997).

As explained before, considering the conceptual model for the system evolution, the results of simulation 1 (mixing between the Glacial end member water and the highly saline sample #2731) will be very useful to understand the behaviour of the deep saline samples (from 0.4 mol/kg Cl, as a conservative lower limit, to 1.4 mol/kg Cl), not affected by other mixing events. On the other hand simulation 2 (mixing of the Littorina end member with the Glacial end member or with a brackish-glacial water) will correspond to those shallower waters affected by the input of Littorina (from 0 to 0.15 mol/kg Cl). The following parameters in the carbonate system will be analysed in these simulations: calcite saturation state, pH, pCO_2, alkalinity and calcium. The analysis will be focused on the effect of the different CO_2 partial pressures in the Glacial end member and on the effect of considering conservative mixing or additional reactions (calcite equilibrium and cation exchange). Actual data are included in some of the plots for comparison.

Calcite saturation state

Simulation 1: mixing between the Glacial end member and the highly saline sample #2731.

Independent of the value considered for P_{CO2} in the Glacial end member, most mixing proportions reach oversaturation with respect to calcite (Figure 3-39a) but SI remains below +1.0.[11] Oversaturation is more pronounced in waters dominated by the Glacial end member. Therefore, all the simulated mixing paths would promote calcite precipitation, as it is also displayed by the saline and highly saline samples. Although not shown, when including the effects of cation exchange, saturation states increase slightly but the general trend does not change.

Simulations 2: Mixing of the Littorina end member with the Glacial end member; and mixing of the Littorina end member with an already mixed water (90%Gl +10%#2731), considered brackish-glacial (Brack/Gl).

Mixing between Littorina and Glacial (grey symbols) produces a slight undersaturation (within the uncertainty range for equilibrium) except for the case where the Glacial end member has very low P_{CO2} (Figure 3-39b). The slight undersaturation state is more generalized when the "modified Littorina end member" is considered (green symbols; Figure 3-39b). On the contrary, mixing between Littorina and Brackish-Glacial produces oversaturation, especially for mixing proportions with more than 10% Littorina. Cation exchange leads to oversaturation (from 0.8 to +1.2) when superimposed to both types of mixing processes (not shown).

pH and pCO2

Simulation 1: mixing between the Glacial end member and the highly saline sample #2731.

All the conservative mixing simulations, independent of the value of P_{CO2} in the Glacial end member, show a continuous decrease in pH from the dilute end member to the highly saline sample #2731 (black symbols in Figure 3-40). When superimposing calcite equilibrium (grey symbols in Figure 3-40) global pH trends shift towards lower values. pH also decreases monotonously when the Glacial end member is equilibrated at very low P_{CO2} (10^{-6} and 10^{-5} atm). However, in the other two cases, pH decreases first (while the Glacial end member dominates) but increases when the mixture starts to be dominated by the saline end member. Therefore, the observed trend in the real samples (arrow drawn in Figure 3-37) is better reproduced by simulations considering the lowest initial P_{CO2} for the Glacial end member and no equilibrium with calcite.

As already highlighted (Figure 3-38), the general decreasing trend with increasing depth and salinity observed in P_{CO2} becomes an increasing trend from these saline waters to the highly saline end member (arrow drawn in Figure 3-38). This trend is also observed in the Olkiluoto groundwaters (Figure 3-36d). As for pH, only a mixture involving a Glacial end member with a very low P_{CO2} (10^{-6}, 10^{-5}) can reproduce that trend (Figure 3-41).

---

[11] This behaviour is the same independently of the global composition of the glacial end member (e.g. different values of alkalinity, calcium, pH, etc).
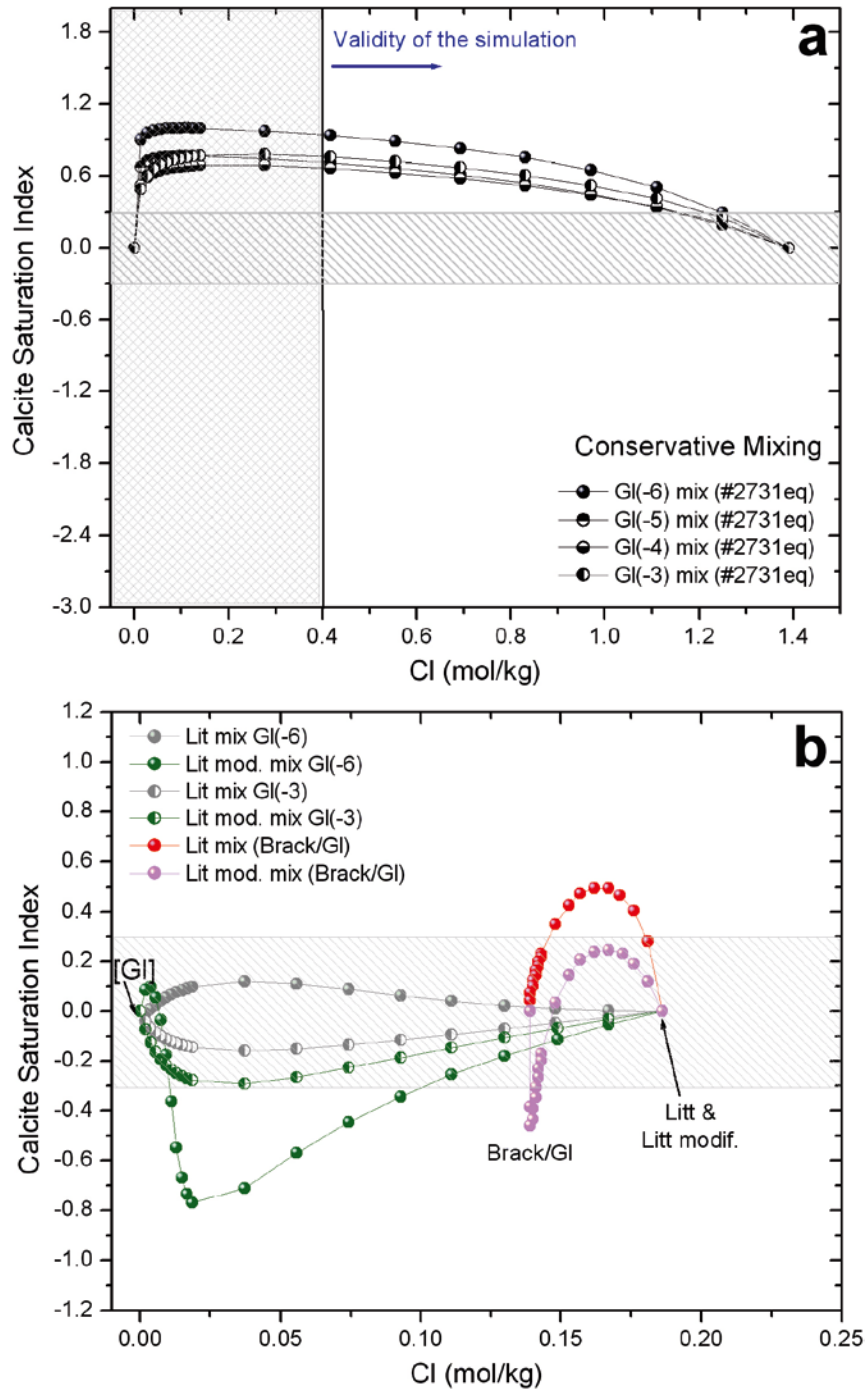
Figure 3-39. *(a) Calcite saturation indices vs. chloride contents obtained from the conservative mixing between the Glacial end member (equilibrated with calcite at different partial pressures, 10^{-6} to 10^{-3} atm) and the Highly saline sample #2731 equilibrated with calcite. The white area indicated as the range of validity for the simulation represents the range of groundwaters (in terms of the Cl contents) in which the obtained results are meaningful. (b) Results of the conservative mixing simulations between a pre-existing Glacial end member (equilibrated with calcite at different CO_2 partial pressures; see text) and a Littorina end member equilibrated with calcite, both unmodified and modified (changing the initial concentrations of alkalinity and dissolved calcium in the end member).*

Figure 3-40. *pH values and chloride obtained from the conservative mixing and mixing + reaction (calcite equilibrium) calculations between the old dilute end member (Glacial) and the highly saline sample #2731. The white area indicated as the range of validity for the simulation represents the range of groundwaters (in terms of the Cl contents) in which the obtained results are meaningful.*
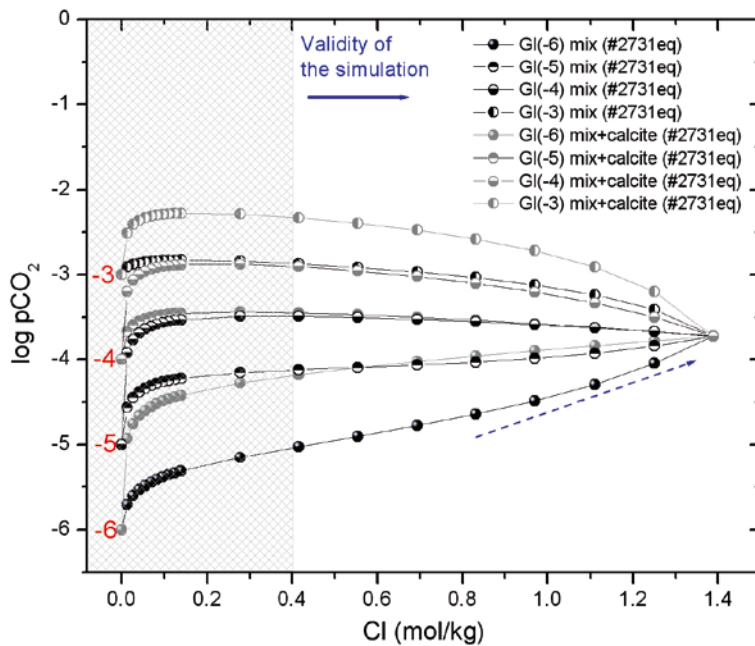
Figure 3-41. *Log pCO_2 values vs. chloride obtained from conservative mixing and mixing + reaction (calcite equilibrium) calculations between the old dilute end member (Glacial) and the highly saline sample #2731. The white area indicated as the range of validity for the simulation represents the range of groundwaters (in terms of the Cl contents) in which the obtained results are meaningful.*

Calcite precipitation produces more important decreases in pH and increases in the CO_2 partial pressure in the mixing + reaction simulations considering a Glacial end-member with very low CO_2 partial pressure (log pCO_2 = –5 and –6) than in the conservative mixing calculations. This means that calcite precipitation produces the expected decrease in the total dissolved carbon together with an increase in the amount of $CO_{2(gas)}$ in the groundwaters proportional to the amount of precipitated calcite, as it can be expressed in the following reaction:

$$Ca^{2+} + 2HCO_3^- \leftrightarrow CaCO_3 + CO_2 + H_2O$$

Simulations 2: Mixing of the Littorina end member with the Glacial end member and mixing of the Littorina end member with an already mixed water (90%Gl +10%#2731), considered brackish-glacial (Brack/Gl).

All the conservative mixing simulations between these end members result in a non-linear decrease in pH as Littorina proportion increases. Changes in these pH trends due to equilibrium reactions can be important but they are always conditioned by the mixing path over which they are superimposed. Calcite re-equilibrium leads to a pH decrease (e.g. Lit mix Gl(–6)) or to a pH increase (Lit mod. mix Gl(–6)) depending on the conservative mixing trend, calcite undersaturation (dissolution) or oversaturation (precipitation).

These effects are even more noticeable in the mixing of Littorina (unmodified or modified) with the Brackish-Glacial water for which, depending on the mixing proportions, waters are over- or under-saturated with respect to calcite. The result is a decrease or an increase in pH when re-equilibrating with this mineral.

The effect of cation exchange on pH depends also on the type of mixing (Figure 3-42 only some of these results are shown as triangles). Mixing between Littorina and Glacial (Gl(–6)) causes a larger pH decrease for larger CEC value. However, when Littorina finds more saline waters (Brackish-Glacial), pH increases as a result of cation exchange.
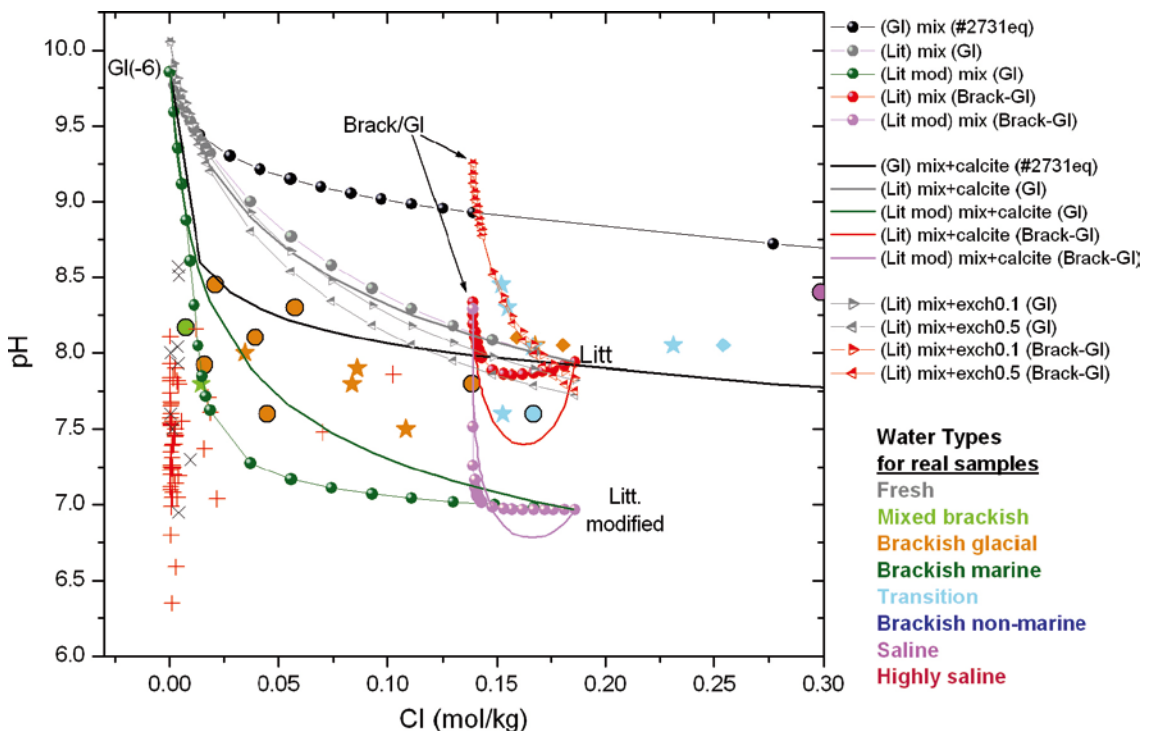
Figure 3-42. pH values vs. chloride obtained from conservative mixing (spheres with lines) and mixing + reaction (calcite equilibrium, lines, and cation exchange, triangles with lines) calculations between the unmodified and modified Littorina and the dilute end member (Glacial or Brackish-glacial). The results for the initial part of simulation 1 are also shown. The real values measured in the groundwaters are shown for comparison (stars: Äspö GW; circles: Laxemar GW, red crosses: Laxemar NSGW; diamonds: Simpevarp GW; black x: Simpevarp NSGW).

In this context, the observed agreement between some real samples and some of these simulated trends must be taken with caution. pH is a very sensitive parameter to calcite equilibrium or to cation exchange; but it is also very sensitive to mixing and to the initial conditions of the involved end members.

Alkalinity

Simulation 1: mixing between the Glacial end member and the highly saline sample #2731.

The alkalinity values measured in the system (around 10 mg/L) are extremely low and almost constant in the most saline groundwaters. In the simulations, only the mixing path involving the Glacial end member with a very low P_{CO2} (10^{-6} or 10^{-5} atm) can reproduce that trend (Figure 3-43a). Imposing equilibrium with calcite over these low- P_{CO2} dilute groundwaters (log P_{CO2} around -6) maintains the low and constant alkalinity values found in groundwaters (Figure 3-43b). Compared with the real data, the rest of the mixing and mixing + reaction simulations do not reproduce the observed trends.

Simulations 2: Mixing of the Littorina end member with the Glacial end member; and mixing of the Littorina end member with an already mixed water (90%Gl +10%#2731), considered brackish-glacial (Brack/Gl).

In contrast to simulation 1, alkalinity results obtained from these different mixing and mixing + reaction simulations do not seem to be significantly affected by calcite equilibrium. (Figure 3-44a). All these mixing cases reproduce some of the contents found in several real samples, mainly when mixing the Glacial end member with very low P_{CO2} or the Brackish-Glacial waters with the modified or unmodified Littorina end member (Figure 3-44b). Therefore, initial conditions in the end members play an important role in the evolution of this parameter. These results agree with the fact that groundwaters with Littorina signature in the Laxemar-Simpevarp area have a high alkalinity in spite of the low Littorina proportion and of the re-equilibrium with calcite. Two facts highlight this result: the low alkalinity of the pre-existing brackish groundwaters and the expected increase in alkalinity of the Littorina waters when passing through the marine sediments (a frequent diagenetic reaction in marine sediments).
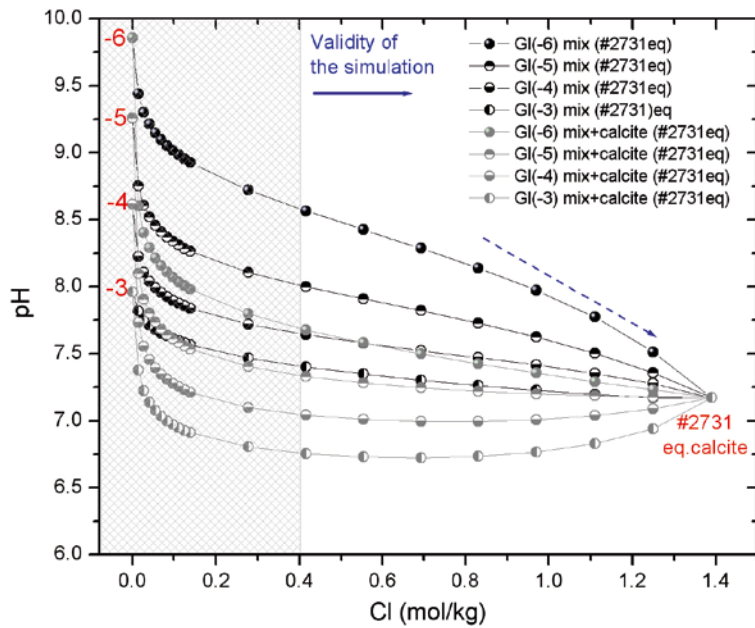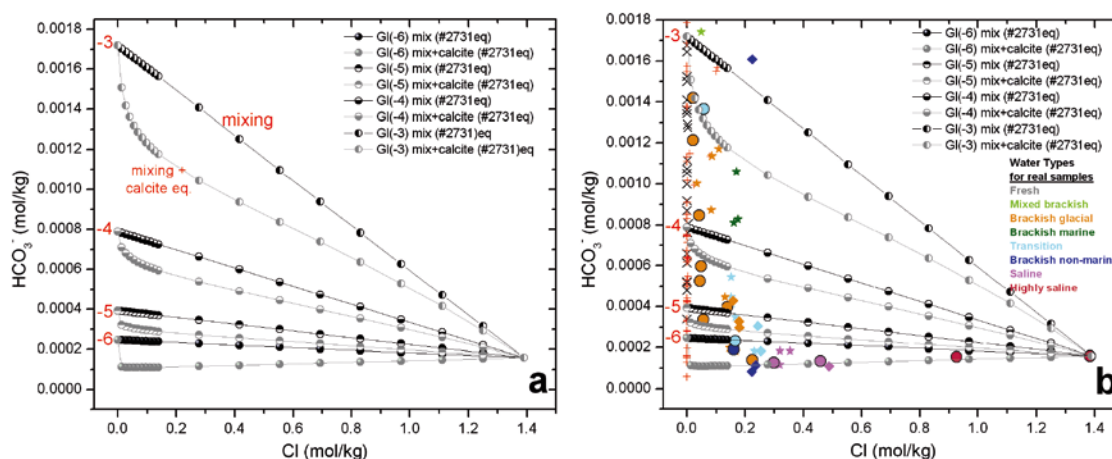

Figure 3-43. *(a) HCO$_3^-$ and chloride contents obtained from the conservative mixing and mixing + reaction (calcite equilibrium) calculations between the old dilute end member (Glacial) and the highly saline sample #2731. (b) Comparison with the contents measured in the real samples (stars: Äspö GW; circles: Laxemar GW, red crosses: Laxemar NSGW; diamonds: Simpevarp GW; black x: Simpevarp NSGW).*
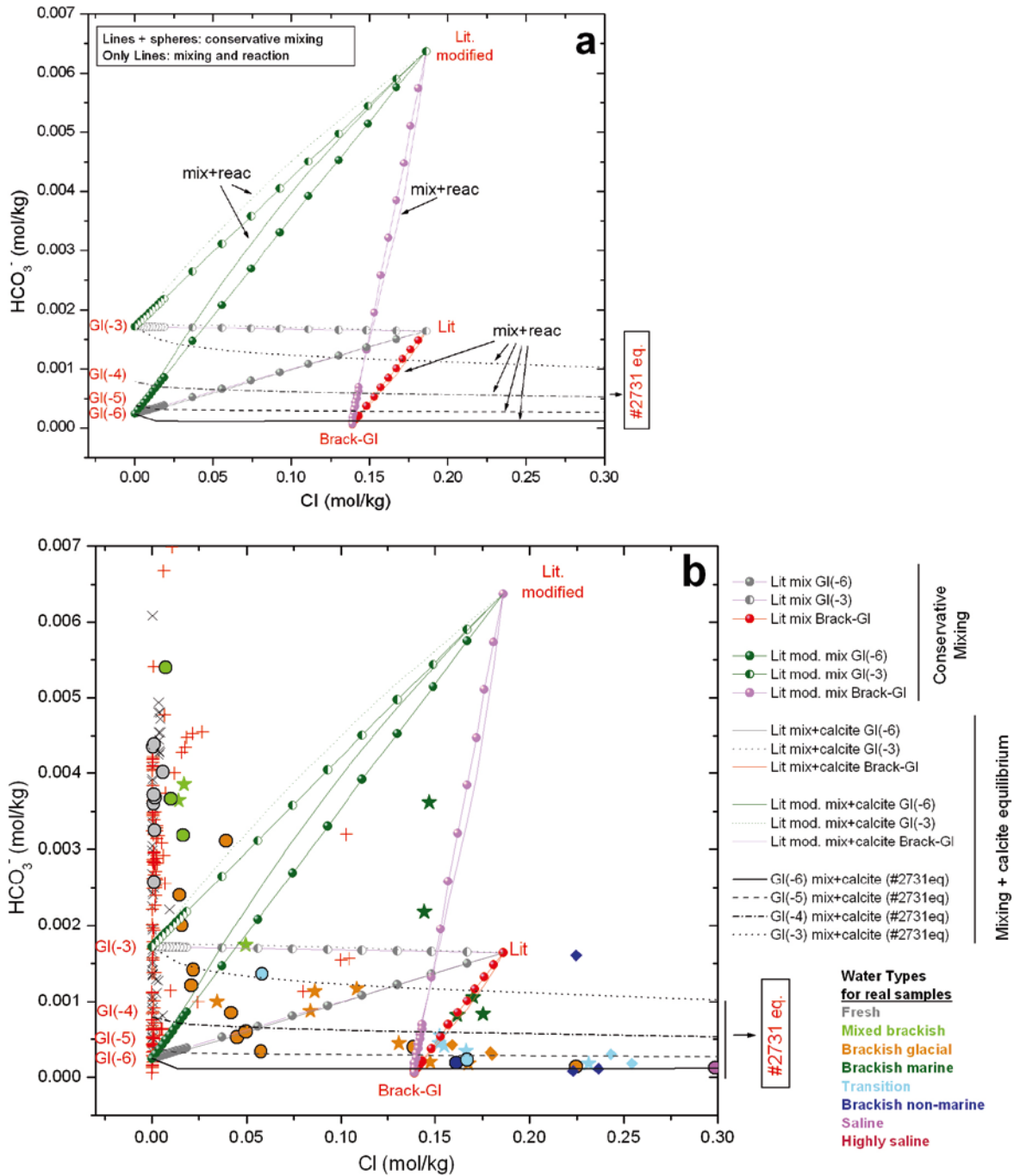
Figure 3-44. *(a) Alkalinity and chloride results in the mixing simulations between Littorina (the original end member and the modified one) and previous groundwaters (Glacial with two different CO$_2$ partial pressures, 10^{-6} and 10^{-3} atm, and the brackish glacial water). Conservative mixing is shown by lines with spheres, and mixing and equilibrium with calcite are shown only by lines. The first steps of four cases corresponding to Simulation 1 mixing and reaction (Glacial and the highly saline sample #2731 with the four different pCO$_2$) are also shown for comparison. (b) Comparison between the alkalinity results shown in Figure 3-43 and the values measured in the real system (stars: Äspö GW; circles: Laxemar GW, red crosses: Laxemar NSGW; diamonds: Simpevarp GW; black x: Simpevarp NSGW).*

Calcium

Simulation 1: mixing between the Glacial end member and the highly saline sample #2731.

Calcium behaviour is completely different from the rest of the parameters considered in the carbonate system and very similar to Na, Mg and K. As it will be shown below, calcium evolution, although affected by the carbonate system (calcite dissolution/precipitation), is mainly controlled by mixing and cation exchange.

Figure 3-45a shows that all the simulations give almost identical results (conservative mixing and mixing + calcite equilibrium) Therefore, for this simulation type, calcium is not affected by either the different P_{CO2} in the dilute end member or by the equilibrium with calcite. That is, this element is mainly controlled by mixing. However, when imposing cation exchange, a decrease in the calculated values for calcium and an improvement in the fitting to measured values are observed (Figure 3-45b).

This behaviour is the complementary evolution to the one observed for sodium (section 3.2.4, Figure 3-20). In any case, mixing (for groundwaters with Cl > 0.2 mol/kg) explains at least 70% of total dissolved calcium in the system.

Simulations 2: Mixing of the Littorina end member with the Glacial end member; and mixing of the Littorina end member with an already mixed water (90%Gl +10%#2731), considered brackish-glacial (Brack/Gl).

Dissolved calcium concentrations obtained during conservative mixing and mixing + calcite equilibrium are identical in all the mixing cases (Gl or brackish glacial and Littorina or modified Littorina), indicating again a predominant control by mixing. Only if cation exchange is included, its effect is clearly observed (Figure 3-46a), even more than for simulation 1 above. Figure 3-46b plots these mixing paths of Littorina with the previous groundwaters and also the first steps of the mixing of simulation 1 for comparison.

As expected, mixing and cation exchange between a dilute water and the highly saline end member produces a decrease in the dissolved calcium content while the same processes when Littorina enters a more diluted system (Glacial or Brackish-Glacial) produces an increase in the Ca concentration.

In this case, as observed for sodium (Figure 3-20b) the same five samples from the Simpevarp subarea (circled) are not explained by any of the simulations considered (Figure 3-46b) because they display lower calcium contents than expected from their chloride concentrations. As stated in section 3.2.4 and in agreement with the sodium contents of these samples (Figure 3-20b), higher CEC values during mixing could explain these calcium contents. However, these groundwaters show other compositional characters that may relate them to freezing processes as discussed in section 3.4.4.
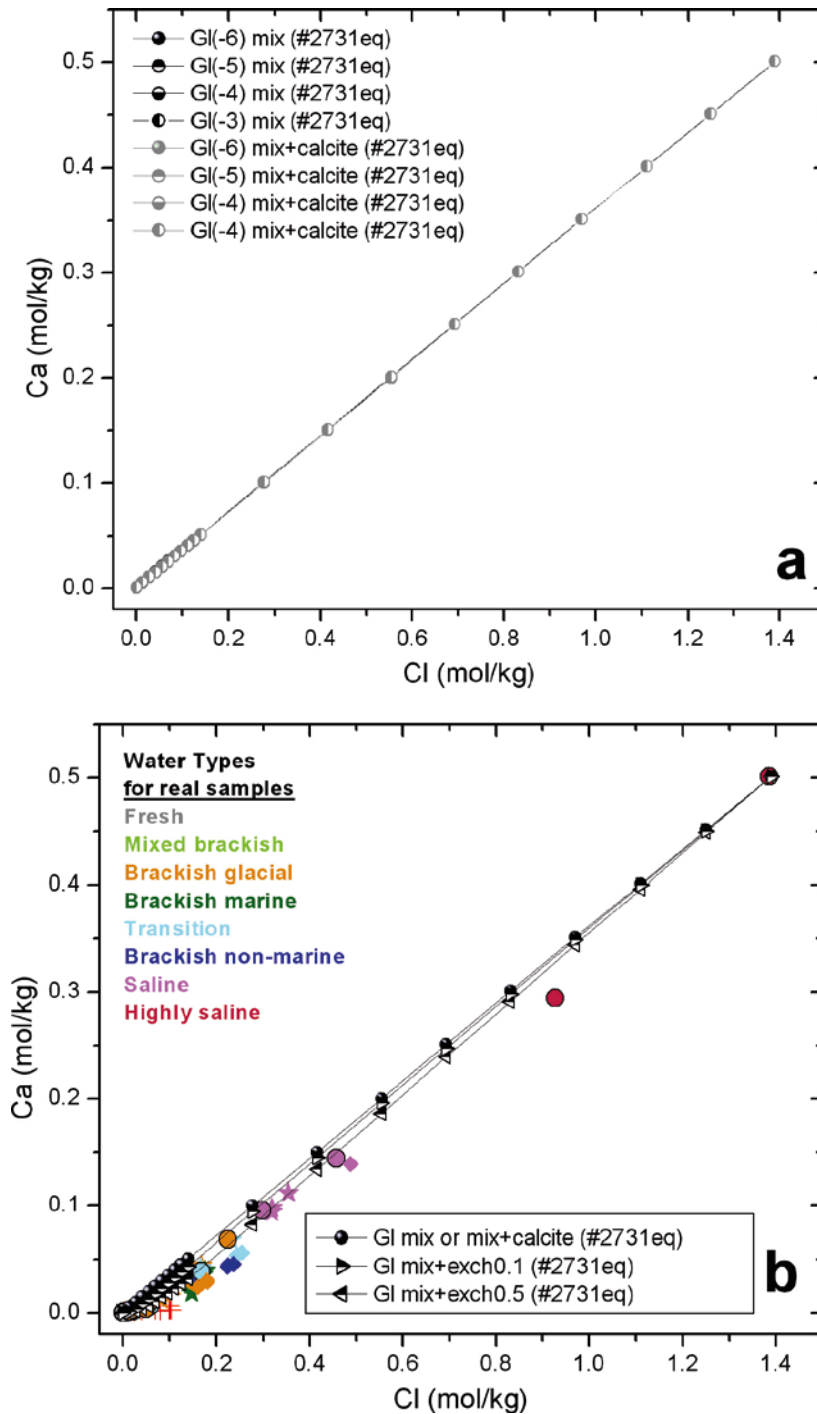
Figure 3-45. *(a) Calcium and chloride contents obtained from the conservative mixing and mixing + reaction (calcite equilibrium) calculations between the old dilute end member (Glacial with different pCO₂) and the highly saline sample #2731 (equilibrated with calcite). Since the results are almost identical for all the cases, only one simulation is plotted. (b) Calcium and chloride contents obtained from the conservative mixing and mixing + cation exchange (two different CEC, 0.1 and 0.5) calculations between the old dilute end member (Glacial with different pCO₂) and the highly saline sample #2731 (equilibrated with calcite). The plot also displays measured values for comparison (stars: Äspö GW; circles: Laxemar GW, red crosses: Laxemar NSGW; diamonds: Simpevarp GW; black x: Simpevarp NSGW).*
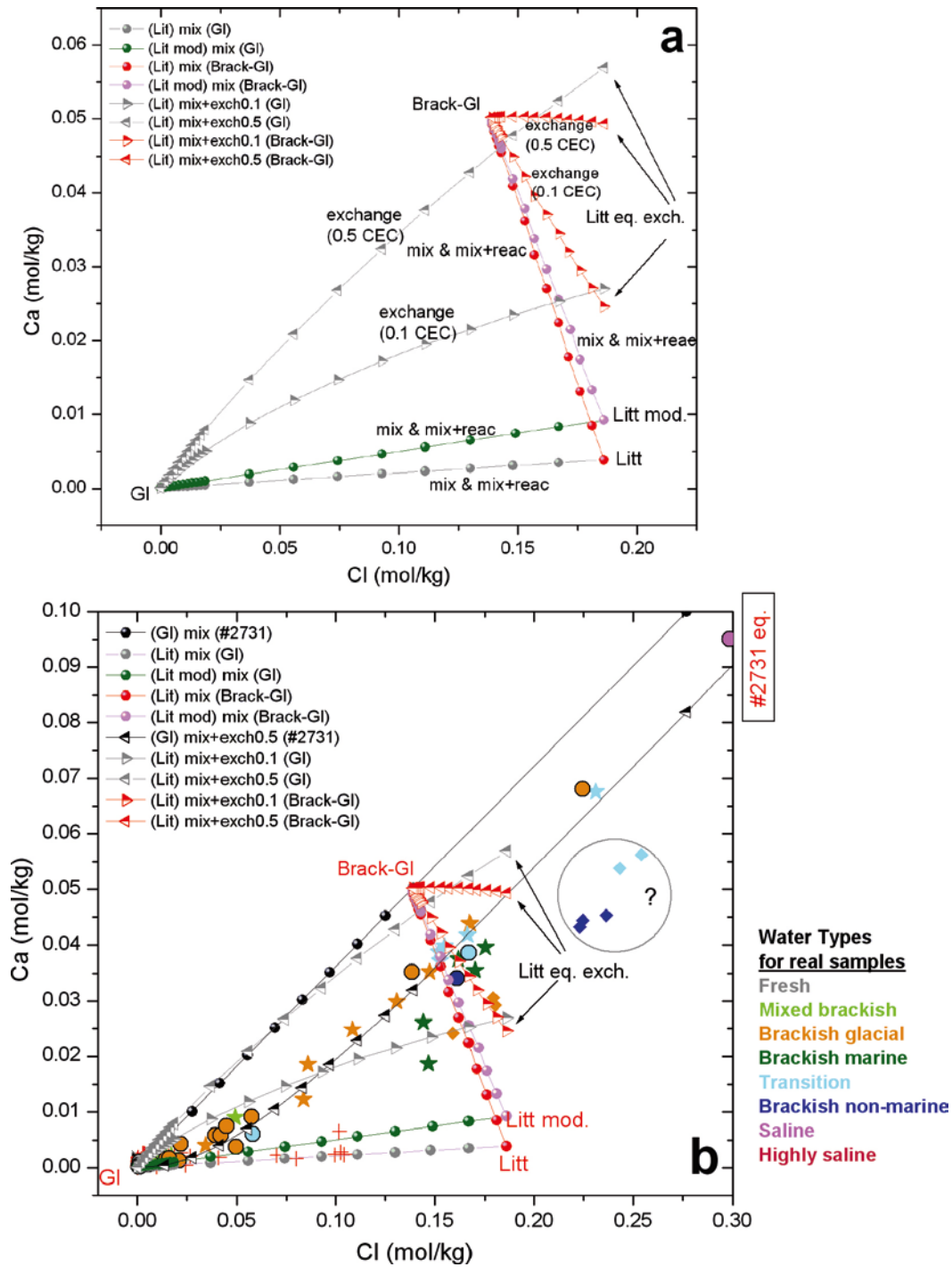
Figure 3-46. (a) Calcium and chloride contents obtained from the conservative mixing calculations between the old dilute end member (Glacial) or the brackish-glacial end member (Brack/Gl) and the Littorina end member (original or modified). Mixing and cation exchange simulations between Littorina and any of the other two dilute end members start with a different Littorina composition as a result of the previous equilibrium with the exchanger. (b) Comparison between measured and calculated calcium values. The first steps of one of the cases corresponding to Simulation 1 mixing and mixing + cation exchange (Glacial and the highly saline sample #2731) are also shown for comparison (stars: Äspö GW; circles: Laxemar GW, red crosses: Laxemar NSGW; diamonds: Simpevarp GW; black x: Simpevarp NSGW). The samples inside the grey circle with a question mark are explained in the text.

Main outcomes

- Mixing of Glacial (or any other dilute groundwater) with the deep and highly saline groundwaters induces calcite oversaturation in the mixed groundwaters due to the very high dissolved calcium concentrations in the highly saline end-member and to the non-linear algebraic effect during mixing (see Wigley and Plummer 1976, for a detailed explanation). This is in agreement with the detection of calcite precipitation and with the occurrence of calcite with cold-climate signatures at these depths (section 3.3.2).

- Calcite precipitation tends to smooth the increase in P_{CO2} and the decrease in pH observed as the highly saline proportion increases during mixing (Figure 3-40 and 3-41). Therefore, the fact that this trend is still recognizable in the groundwaters would support the existence of a Glacial end member with a CO_2 partial pressure low enough to avoid that calcite precipitation obliterates its effects. Mixing and calcite re-equilibrium of these low-P_{CO2} dilute groundwaters (log P_{CO2} around –6) would be able to buffer the low and constant alkalinity values found in these groundwaters (Figure 3-43).

- The dilute groundwaters reaching those depths and mixing with the already present saline groundwaters should have had very low CO_2 partial pressures and high pH values. These characters are in agreement with those of old unmixed Glacial or cold remnants found in other Swedish sites or with those of recent glacial groundwaters (e.g. Grimsel Test Site, Switzerland), corresponding to water-rock interactions that do not change drastically their dilute character but clearly affect their pH and CO_2 partial pressure (see Appendix F).

- Mixing involving Littorina (original or modified) and the two extreme waters with which it could mix when entering the bedrock (Glacial and Brackish-Glacial) show that, most probably, waters will have evolved towards oversaturation states with respect to calcite. Therefore, precipitation of calcite would have been the more frequent process during Littorina intrusion. This is in complete agreement with the identification of calcites with marine signature down to 500 m depth in fracture fillings.

- Dissolved bicarbonate contents induced by these mixing processes are mainly conditioned by the concentrations of marine waters entering the bedrock. Calcite re-equilibrium does not significantly change bicarbonate contents, which justifies the anomalously high HCO_3^- concentrations found in the few waters with clear marine signature.

The calcium contents observed in the saline waters (Cl > 0.2 mol/kg) are better reproduced if mixing between the Glacial and the highly saline sample #2731 end members and cation exchange processes are considered together. This is also valid for less saline waters, such as the brackish-glacial type (at Äspö and Simpevarp), which can be the result of the same mixing between glacial and saline, but with a dominance of the exchange processes on the dissolved calcium contents.

3.3.5 Conclusions

Near-surface groundwaters

The compositional evolution of the near surface and shallow groundwaters is mainly controlled by the existence of weathering reactions. Typical weathering reactions in the subsurface systems are mainly triggered by biogenic CO_2 input derived from organic matter decay (e.g. plant debris) and root respiration. This input of CO_2 promotes a pH decrease and a CO_2 partial pressure increase in the waters, which may favour the dissolution of carbonate or aluminosilicate mineral phases if present in the system.

The intensity of these weathering reactions during infiltration of the surface waters in the overburden is mainly conditioned by the evolution of waters in open or close conditions with respect to CO_2. If the consumed CO_2 is replenished (open system), weathering reactions will be enhanced, increasing the concentrations of cations and HCO_3^- further than in closed system conditions. As the biogenic CO_2 production varies throughout the year (high intensity in summer and low in winter), the intensity of weathering processes is also conditioned by these temporal effects.

Due to this variable influence of atmospheric and biogenic CO_2 and silicate weathering reactions in the overburden, alkalinity (HCO_3^-) and pH values in this part of the system show the widest variability among the Laxemar-Simpevarp groundwaters.

Dissolved calcium in the fresh near-surface groundwaters shows maximum concentrations of around 100 mg/L, although it is usually below 80 mg/L. Aluminosilicate weathering reactions (hornblende and plagioclase dissolution), cation exchange reactions or calcite and fluorite equilibrium may participate in the control of this element in the near surface and shallow groundwaters from Laxemar-Simpevarp. Bicarbonate reaches maximum concentrations around 550 mg/L and calcite equilibrium is only attained for the waters with the largest bicarbonate contents.

Overall, calcite appears to contribute to the chemical and isotopic (C and Sr) characters of the near-surface groundwaters much more than expected by the detected small amounts of this mineral in the Laxemar-Simpevarp overburden. As recommended for Forsmark, further studies and estimations on the "durability" of the calcite buffering are recommended as a valuable tool for future predictive calculations for performance assessment, especially in the Laxemar subarea, where dilute groundwaters have reached the repository depth.

Groundwaters

pH values are between 7.2 and 8.6 in the groundwaters and do not show any clear variation trend with depth. A similar pH behaviour has been observed in other zones with crystalline bedrock like Forsmark or Lac du Bonnet (Canada). For the Laxemar subarea, pH values tend to restrict to a range between 8 and 8.5 pH units in the most saline groundwaters, although scattering is also observed in the rest of groundwaters. There is an important gap in the data between the saline water at 1,100 m depth (16,000 mg/L Cl) and the deepest highly saline water at 1,530 m (45,000 mg/L Cl) but pH decreases from the first to the second one.

Alkalinity contents show a rapid decrease with depth and chloride concentrations. High and variable values can be found down to 400 m depth at the Äspö and Laxemar subareas. As observed in Forsmark, the high HCO_3^- values found in the groundwaters from Äspö are clearly associated with groundwaters with Littorina signature. On the contrary, in the Laxemar subarea they seem to be related to fresh and "recent" (detectable tritium) recharging groundwaters, although open-hole mixing effects are also possible in some samples. Below 500 m depth, alkalinity in the saline groundwaters drastically decreases to a narrow range of values, as also observed in the Forsmark and Olkiluoto groundwaters. This indicates the existence of a clear mineral solubility control on bicarbonate contents superimposed on the effects of mixing.

Calcium concentrations show a clear trend of increasing concentration with depth and chloride contents towards the value of the Deep Saline end-member. Low Ca concentrations characterise the groundwaters down to 500 m depth in the Laxemar subarea because of the important recharge penetration depth in this zone. In the other subareas, calcium concentrations are larger and display a steeper increasing trend with depth. From 600 m depth down, calcium shows a marked and steady increase, achieving the maximum value in the Deep Saline end member at the maximum sampled depth (about 1,500 m).

Thermodynamic simulations also confirm that the high Ca content of the mixed waters (derived from the Deep Saline end member) obliterates the effects of mass transfer with respect to re-equilibrium with calcite or gypsum or exchange reactions. This justifies the quasi-conservative behaviour of calcium for most groundwaters. However, the calcium contents observed in the saline waters (Cl > 0.2 mol/kg) are better reproduced if mixing between the Glacial and the highly saline sample #2731 end members and cation exchange processes are considered together. This is also valid for less saline waters, such as the brackish-glacial type (at Äspö and Simpevarp), which can be the result of the same mixing between Glacial and saline, but with a dominance of the exchange processes on the dissolved calcium contents.

Calculated saturation indices with respect to calcite are close to equilibrium for all the available samples with field-measured pH. Dilute groundwaters rapidly attain equilibrium or slight oversaturation at shallow depths and this state is kept at larger depths in saline groundwaters where mixing processes are effective. The origin of these slight oversaturation states is a debatable matter, as they

can be associated with problems with pH measurements in some samples, with a kinetic inhibition related to oversaturation thresholds for calcite precipitation or with the effects of microbial activity on the carbonate system.

Calculated CO_2 partial pressures display a progressive decrease with depth and with chloride contents from the values found in the fresh, near-surface groundwaters (most of them with pCO_2 values greater than the atmosphere) towards deeper groundwaters. Similar trends in the evolution of CO_2 partial pressures with depth and chloride contents can be observed in the Lac du Bonnet groundwaters (Canada) and, especially, in the Olkiluoto groundwaters where, as also observed in Laxemar-Simpevarp, there is a slight increase in log pCO_2 from groundwaters with chloride around 15,000 mg/L towards the highly saline samples.

The CO_2 partial pressure decrease observed in the Laxemar-Simpevarp groundwaters may be associated with calcite dissolution in the dilute shallowest groundwaters up to 200 m depth, where equilibrium or oversaturation with respect to this mineral is reached. At larger depths, where groundwaters are also in equilibrium or near equilibrium with calcite, the CO_2-depletion may be associated with aluminosilicate-dissolution and, mainly, to the combined effects of mixing with saline groundwaters and precipitation of calcite. Calcite precipitation during mixing of dilute and saline groundwaters could keep the alkalinity at the very low levels observed in the groundwaters with Cl > 8,000 mg/L.

Thermodynamic simulations confirm these conclusions. Mixing of dilute waters with low CO_2 partial pressure (e.g. Glacial with pCO_2 around 10^{-6}) and highly saline deep groundwaters induces calcite oversaturation due to the very high dissolved calcium concentrations in the highly saline end-member and to the non-linear algebraic effect during mixing. This would favour the observed precipitation of calcite with cold climate signatures and would buffer the low and constant alkalinity values. Therefore, the dilute groundwaters reaching those depths and mixing with the already present saline groundwaters should have had very low CO_2 partial pressures and high pH values. These characters are in agreement with those of old unmixed Glacial or cold remnants found in other Swedish sites or with those of recent glacial groundwaters (e.g. Grimsel Test Site, Switzerland), corresponding to water-rock interactions that do not change drastically their dilute character but clearly affect their pH and CO_2 partial pressure.

Simulations of mixing between the original Littorina composition (with larger bicarbonate contents) and the pre-existing groundwaters (from Glacial to Brackish-Glacial) also suggest calcite oversaturation and precipitation during Littorina intrusion. This is in good agreement with the identification of calcites with marine signature found down to 500 m depth in the fracture fillings.

3.4   Sulphate system

The sulphate system in Laxemar-Simpevarp groundwaters differs from what is observed in Forsmark, Olkiluoto and, probably, in the rest of the Scandinavian sites studied to date. Sulphate contents in Laxemar-Simpevarp groundwaters have values higher than 1,000 mg/L in the deepest and more saline waters. These values are the highest analysed up to now in any site of the Swedish and Finnish radwaste programs. Understanding the processes responsible for this peculiar behaviour is, therefore, a key point in the construction of the conceptual model of the hydrogeochemical evolution of the site.

Some of these particularities were analysed in previous SDM reports by Gimeno *et al.* (2004b, 2006). There was proposed for the first time that gypsum participates in the control of dissolved total sulphate in the most saline samples. In fact, gypsum has already been detected in the fracture fillings mineralogy, which can contribute to shed light on some of the uncertainties reported in previous works (e.g. Laaksoharju and Wallin 1997) on the odd behaviour of sulphate in the Laxemar-Simpevarp waters.

However, other processes, together with the palaeohydrological evolution of the site should be taken into account to fully understand the particularities of sulphate. This section focus on the study of the factors that control sulphate contents in the Laxemar-Simpevarp groundwaters, integrating for this purpose the available isotopic, mineralogical and microbiological information.

3.4.1 Hydrogeochemical data. General trends

Apart from sulphate, some other elements can be controlled by the sulphate system in natural groundwaters. These elements include calcium, strontium and barium and therefore, the geochemical trends of these elements are also included in this section.

Near-surface groundwaters

Sulphate contents in the near-surface groundwaters reach maximum values of 480 mg/L in sampling point SSM000238 (Figure 3-47a). However, dissolved sulphate contents in the fresh near-surface groundwaters (Cl < 200 mg/L) are always below 200 mg/L (Figure 3-47b), as is also the case in the Forsmark area.

Several samples from the near-surface groundwaters system from the Laxemar-Simpevarp area are affected by a relict or modern marine sulphate source (as it probably occurs in soil pipes SSM000238 and SSM000239, with Cl concentrations around 2,400–3,600 mg/L and sulphate contents around 130–480 mg/L). Some others, such as SSM000241 and SSM000242, with chloride contents up to 5,000 mg/L Cl and total dissolved sulphate around 20 mg/L (not shown in the plot) display a deep saline signature related to deep groundwaters postulated to be discharging through the main fractures of the area. Their low sulphate contents appear to be associated with very intense biological activity (Tröjbom *et al.* 2008).

To avoid these effects, only near-surface groundwaters with < 200 mg/L Cl (fresh waters) will be considered here. The SO_4^{2-}/Cl ratio in most of these fresh groundwaters is higher than that of sea-water (Figure 3-47b) and, therefore, a non-marine source seems to be the major sulphur contributor (Tröjbom *et al.* 2008).

Even though fertilizers can represent a minor sulphur source in cultivated areas (Tröjbom *et al.* 2008), dissolved sulphate in the near-surface groundwaters seems to originate from two other main sources: atmospheric sulphur deposition (e.g. from burning of fossil fuels) and dissolution of sulphur-bearing minerals (such as pyrite or gypsum). As atmospheric sulphur deposition in this region is not different from the rest of southern Sweden (Tröjbom *et al.* 2008) and dissolved sulphate concentrations in the fresh near-surface groundwaters are twice as high as in streams and lakes (Tröjbom and Söderbäck 2006a), a "mineral" source appears to be necessary.

The correlation between total dissolved sulphate and calcium contents in the fresh near-surface groundwaters does not indicate a clear participation of gypsum dissolution. Instead, isotopic constraints ($\delta^{34}S$ values) support an important contribution from pyrite dissolution to the dissolved sulphate pool in these waters.
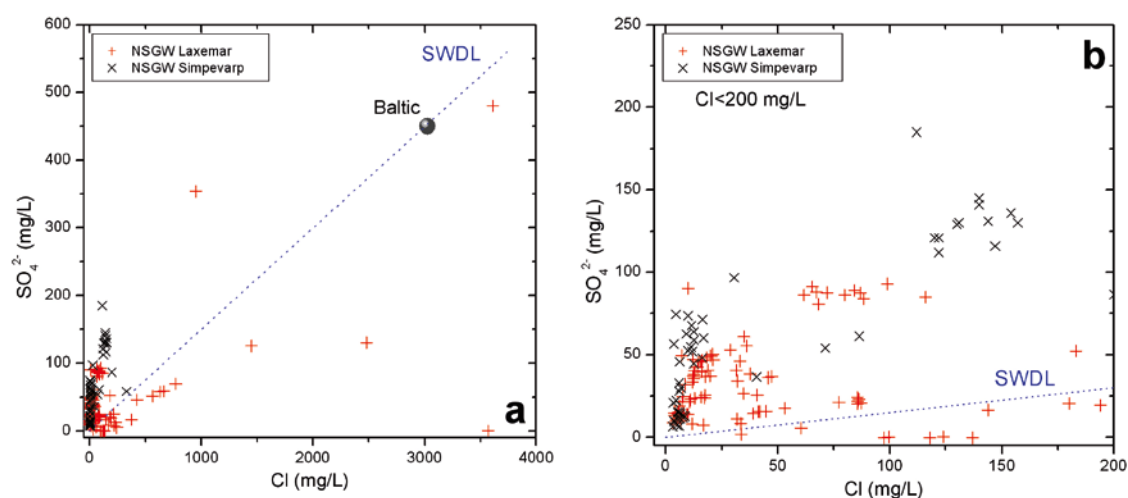
Figure 3-47. *Dissolved sulphate vs. chloride contents in the near-surface groundwaters (NSGW) from the Laxemar-Simpevarp area. (a) Contents in all the representative near-surface groundwaters, with the Baltic end member composition shown as a pink ball; (b) Contents in the fresh near-surface groundwaters (Cl < 200 mg/L). SWDL: Sea Water Dilution Line.*

Sulphur isotope ratios (expressed as $\delta^{34}S$ ‰ CDT) have been measured in near surface, shallow and deep groundwaters from the Simpevarp and Laxemar subareas. Independently of their total dissolved sulphate (Figure 3-48a) or chloride contents, near-surface groundwaters show large variations in sulphur isotopes (–20 to +30‰ CDT), which indicates the existence of multiple sulphur sources. The lowest values (from –20 to –5‰ CDT), possibly reflect the oxidation of sulphides (biogenic pyrite) as a main source of sulphate (Clark and Fritz 1997, Smellie *et al.* 2006, Laxemar 2.1). Some higher values (e.g. up to +15‰ CDT) would indicate atmospheric sulphur deposition at the studied sites (the isotopic signature of atmospheric sulphur in Sweden lies between +3 and +9‰ CDT) possibly with some contribution from the oxidation of sulphides in the overburden.

For the near-surface groundwaters with $\delta^{34}S$ values around +20‰ (the mean value in Baltic Sea waters), they may result from the direct influence of sea water deposition (sea spray). Finally, the highest values (around +30‰ CDT) would indicate the existence, in at least some of the near-surface groundwaters, of sulphate reducing activity modulating the content of dissolved sulphate. Microbial sulphate reduction promotes an increase in the $\delta^{34}S$ values of the remaining dissolved sulphate (Clark and Fritz 1997) but also increases the HCO_3^- content of the waters. This relation is clearly shown in Figure 3-48b, therefore supporting microbial (sulphate reducing) activity.

Thus, based on these isotopic data, a contribution from several sources is expected in most near-surface groundwaters.

Groundwaters

Dissolved sulphate in the Laxemar-Simpevarp area displays two apparent evolution trends with respect to chloride, as Figure 3-49a, b shows: (1) a progressive increase in sulphate with chloride (up to about 10,000 mg/L Cl), clearly suggesting present (Baltic Sea) and past (Littorina Sea) marine effects[12]; and (2) from around 800 mg/L total dissolved sulphate and 9,000 mg/L Cl, a more or less constant sulphate content for a wide range of chloride concentrations (10,000–50,000 mg/L), where the influence of a deep saline water is evident. When total dissolved sulphate is plotted against depth, an overall and continuous increase with increasing depth is observed (Figure 3-49cd), similar to the trends followed by chloride and sodium (Figures 3-1 and 3-6). However, as happened for sodium, the subdivision of the Laxemar-Simpevarp groundwaters into lower and higher sulphate contents at the same depth is also apparent. Low dissolved sulphate concentrations characterise the shallow 0–400 m groundwaters in some groundwaters from the Laxemar and Simpevarp groundwaters and then the concentrations increase progressively with depth; as for most of the Äspö and some Laxemar groundwaters, sulphate increases already from the shallowest depths (Figure 3-49c).
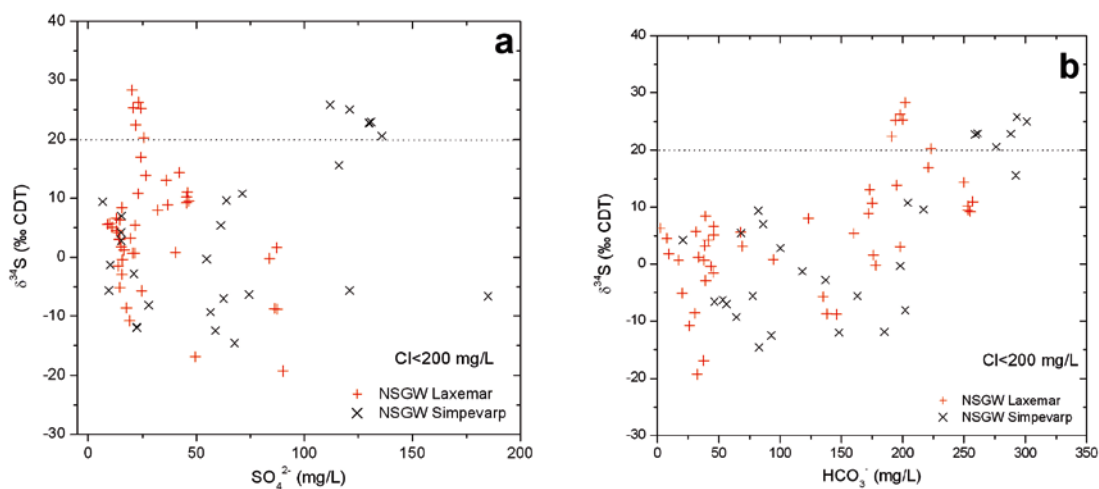
Figure 3-48. *$\delta^{34}S$ values vs. total dissolved sulphate (a) and HCO_3^- contents (b) in the near-surface groundwaters from Laxemar-Simpevarp. Only samples with Cl < 200 mg/L are considered.*

---

[12] In more detail, Äspö and Simpevarp groundwaters show higher salinity (for chloride contents up to 10,000 mg/L) for the same sulphate contents.
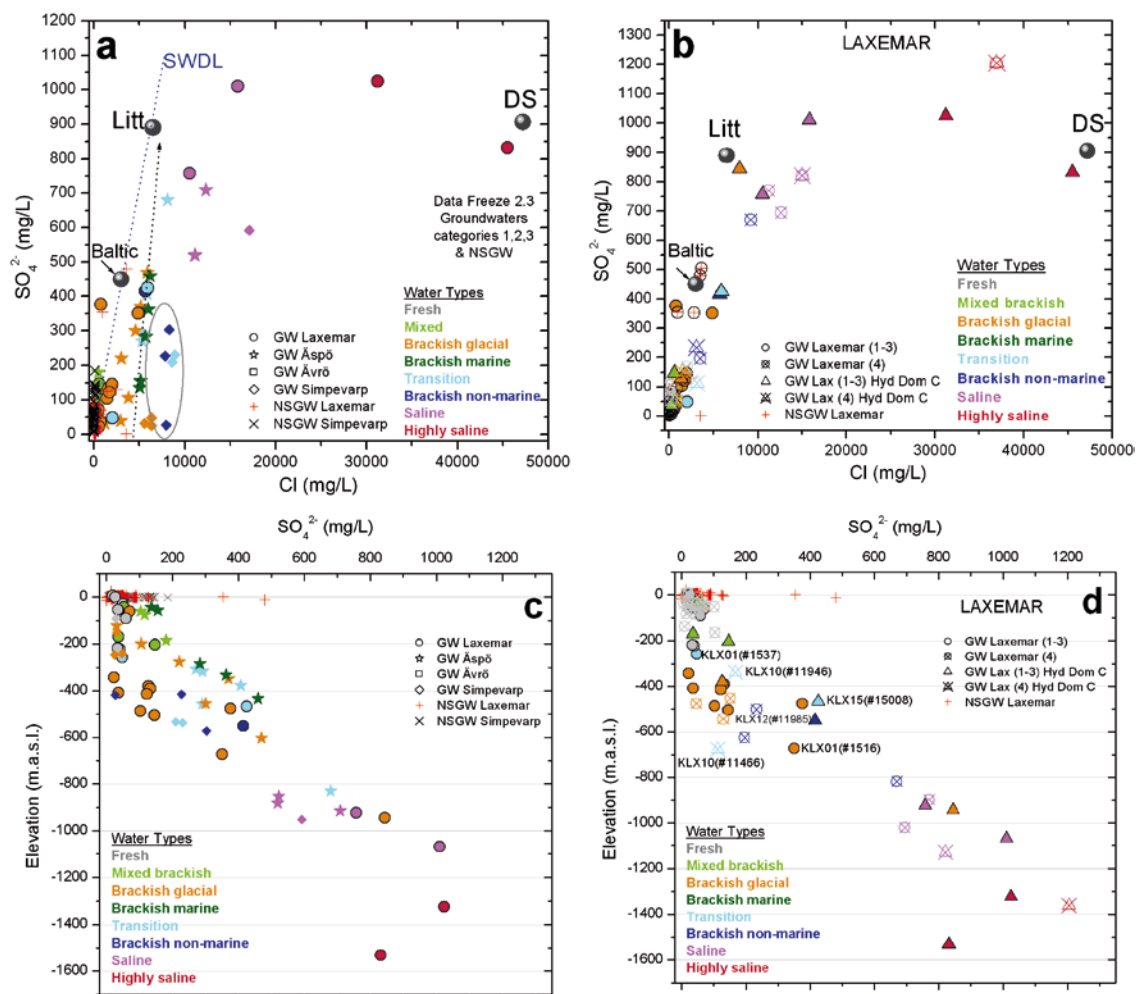
Figure 3-49. *Dissolved sulphate vs. chloride contents (a, b) and depth (c, d) in the Laxemar-Simpevarp groundwaters with categories 1 to 3 (a, c) and in the local Laxemar subarea groundwaters with categories 1 to 4 (b, d). Both near-surface groundwaters (NSGW) and deep groundwaters are plotted. The location of Littorina, Baltic and Deep Saline end members are also shown as grey spheres (plots a and b). In the plots for the local area of Laxemar, an additional symbol has been used to differentiate the waters taken from the Hydraulic domain C (squares). SWDL: Sea Water Dilution Line. The samples labelled in plot (d) indicate the groundwaters from the Laxemar subarea with some traces of Littorina influence.*

In more detail, groundwaters in the first 100 m have sulphate contents lower than 100 mg/L in the Laxemar and Simpevarp subareas and up to 200 mg/L in some Äspö groundwaters with a clear marine signature (Cl contents around 5,000 mg/L). From 100 m down to 400 m depth, total dissolved sulphate concentrations are still below 200 mg/L in Laxemar, where recharge waters dominate, while groundwaters in Äspö can reach sulphate values as high as 500 mg/L at the same depths. In Simpevarp dissolved sulphate is still noticeably low, below 50 mg/L. From 400 m down to 1,600 m depth, the contribution of a deep saline groundwater is evident in all the Laxemar-Simpevarp area, provoking a progressive increase in the concentration of dissolved sulphate.

These overall dissolved sulphate trends, both with respect to Cl and depth, are similar to those in the groundwaters from Lac du Bonnet batholith (Canada; see Figures 7 and 8 in Gascoyne 2004, and Figure 3-50d with respect to chloride), but very different from those observed in other Fennoscandian crystalline systems like Forsmark and Olkiluoto (Figure 3-50abc).

In Forsmark and Olkiluoto, the existence of an important Littorina contribution down to 300–500 m depth gives rise to large total dissolved sulphate contents at these depths followed by a fast decrease (Figure 3-50a for Forsmark). Sulphate distribution with Cl also shows the influence of Littorina in both sites at around 3,000–6,000 mg/L of Cl (brackish marine waters). At higher chloride contents, total dissolved sulphate concentrations drastically decrease to very low values (Figure 3-50bc).
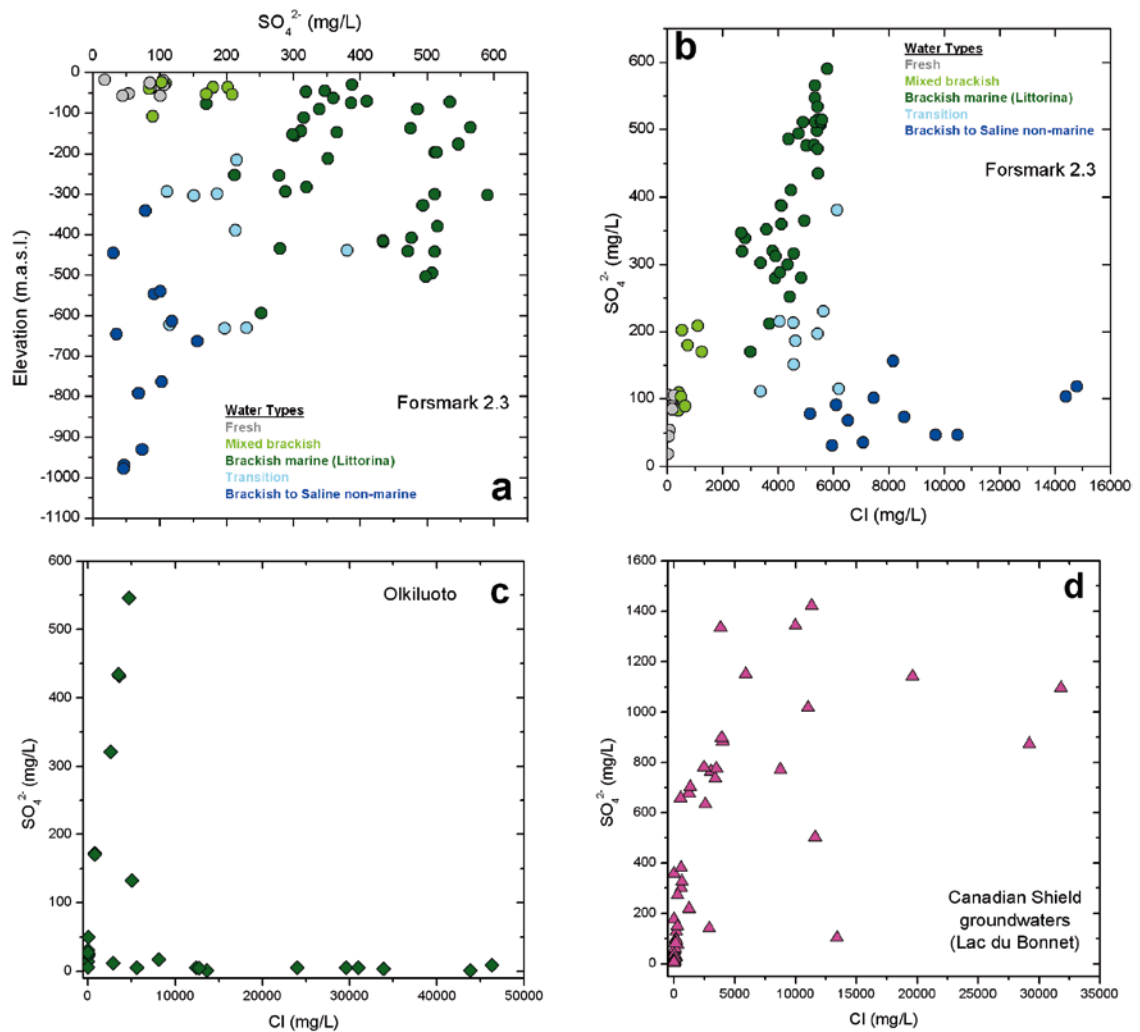
Figure 3-50. Dissolved sulphate vs. depth in groundwaters from Forsmark (a) and vs. chloride in Forsmark (b), Olkiluoto (c) and in the Lac du Bonnet (d). Olkiluoto groundwater data have been taken from Pitkänen et al. (2004) and Canadian groundwaters from Gascoyne (2004). Note that the scales are different.

On the contrary, the Littorina contribution in the Laxemar-Simpevarp area is smaller (samples from the Laxemar subarea with some traces of Littorina signature are labelled in Figure 3-49d), generally more significant in Äspö (see the brackish marine type in some stars in Figures 3-49a and c) where it produces an increase in the concentration of dissolved sulphate already from the shallowest depths.

Therefore, the Littorina contribution seems to be one of the reasons for the observed differences between Laxemar-Simpevarp on one side, and Forsmark and Olkiluoto on the other side[13], but the compositional characters of the Deep Saline end-member have also effects on these trends. The Deep Saline end member in Laxemar-Simpevarp has a total dissolved sulphate concentration of 906 mg/L, whereas in Olkiluoto the equivalent end-member (otherwise with a very similar major-element composition) has very low concentrations (1.2–8.4 mg/L in samples KR4/860/1 and KR4/860/2; Pitkänen *et al.* 2004).

The most saline waters analysed up to now in Forsmark have much lower salinities than these saline end members (Deep Saline end members in the Laxemar-Simpevarp area and Olkiluoto) and the trends are more difficult to discern. However, dissolved sulphate trends are more in agreement with those observed at Olkiluoto (see Appendix F and Gimeno *et al.* (2008) for discussion). Moreover, all

---

[13] In general, the marine influence promotes this type of behaviour in dissolved sulphate. For example, total sulphate contents reach 400 mg/L in groundwaters from Finnsjon with important (mainly) modern marine signatures down to 400 m depth.

the deep saline groundwaters from the Finnish shield with TDS values higher than 20 g/L included in the review by Frape *et al.* (2005) have total dissolved sulphate contents lower than 190 mg/L (and most of them lower than 80 mg/L). It can be concluded that the Deep Saline end member (defined with samples from the Laxemar subarea) seems to have a exceptionally high sulphate content, which is in part responsible for the distinctive behaviour of dissolved sulphate in the Laxemar-Simpevarp area. This very high sulphate content is related to the presence of gypsum in fracture fillings.

Available $\delta^{34}S$ values and total dissolved sulphate contents in the Laxemar-Simpevarp groundwaters are plotted in Figure 3-51. Measured $\delta^{34}S$ values range from +9.1 to +37‰ CDT (even to 48.2‰ in one sample of category 5, #7441 from KLX03). Most of the Simpevarp subarea samples have values from +15 to +25‰ CDT, whereas Laxemar subarea groundwaters display both higher and lower values (Smellie *et al.* 2006).

Values higher than marine ($\delta^{34}S > 20$‰ CDT) are found in groundwaters with Cl$^-$ < 6,500 mg/L (Figure 3-51b) and at depths down to 400 m (Figure 3-51c), in rough agreement with the existence of equilibrium situations with respect to iron monosulphides (see section 4.3.4). These $\delta^{34}S$ values are only found in samples with very low dissolved sulphate concentrations (Figure 3-51a), which can thus be interpreted as being produced *in situ* by sulphate-reducing bacteria.
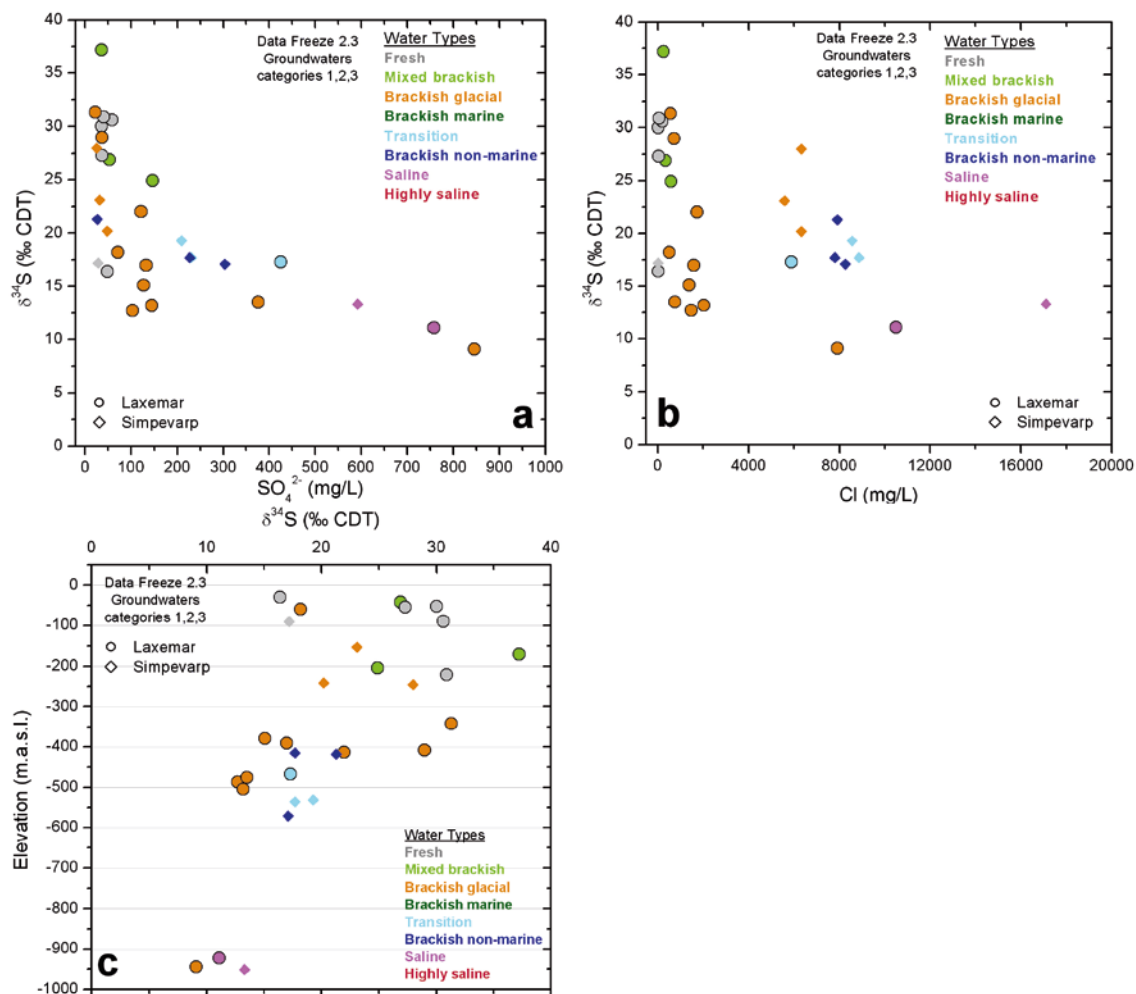
Figure 3-51. *$\delta^{34}S$ values vs. sulphate (a), chloride (b) and depth (c) in the groundwaters from the Laxemar-Simpevarp area. Sulphate and chloride concentrations are restricted to 1,000 and 20,000 mg/L and depth to –1000 m as there are no data for the highly saline groundwaters.*

The highest $\delta^{34}S$ values (+37‰ CDT) have been reported from the Laxemar subarea groundwaters with Cl^- < 500 mg/L and SO_4^{2+} ~ 30 mg/L (HLX14 and KLX03 at 103–218 m and KLX03 at 193–198 m depth). Such extreme $\delta^{34}S$ values are a strong indicator of sulphate reducing activity under closed-system conditions (the closed-system behaviour is also supported by the presence of a glacial melt water component in these samples, indicative of long-term hydraulic isolation; Smellie *et al.* 2008).

Groundwaters with SO_4^{2+} > 250 mg/L display decreasing $\delta^{34}S$ values with increasing sulphate content (Figure 3-51a), consistent with a weaker or non-existent sulphate reducing activity. This decrease does not seem to be due to sulphide oxidation, as it is not supported by fracture mineral investigations (Drake and Tullborg 2004). However, recent sulphur isotope analyses of gypsum samples from fractures in boreholes KLX03 (from +5.9 to +6.8‰ CDT at 533 and 590 m, borehole length, –498 to –554 m.a.s.l.) and KLX08 (from +3.7 to +12.1‰ 795 to 919 m, borehole length, –660 to –765 m.a.s.l.) support the interpretation that gypsum dissolution may lower $\delta^{34}S$ to the observed values in deep saline groundwaters.

The behaviour of Ba and Sr may be coupled to the sulphate system. Dissolved strontium concentrations have a depth distribution very similar to total dissolved sulphate (Figure 3-52ab). However, dissolved strontium vs. chloride (Figure 3-52cd) shows a very good linear correlation, as described for calcium (Figure 3-53a), apparently indicating a control by mixing for both elements. The same strontium-chloride linear correlation is found in Olkiluoto and Forsmark, although the slope is different (Figure 3-53b).
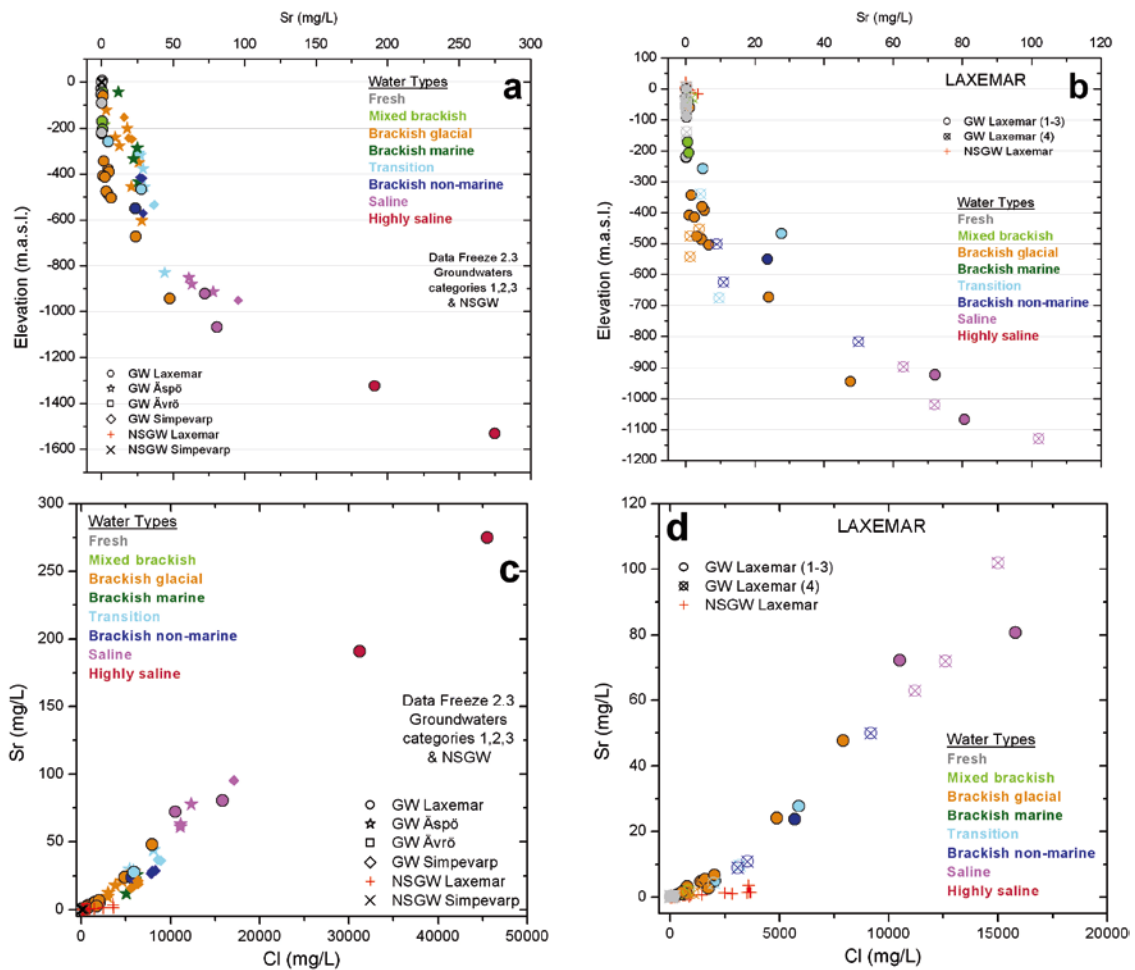
Figure 3-52. Strontium concentrations vs. depth (a, b) and Cl (c, d) contents in the Laxemar-Simpevarp groundwaters (including representative near-surface groundwaters). The scales along strontium, depth and chloride axes have been increased in the Laxemar subarea plots (b and d) to better visualise the shallow to intermediate depths.
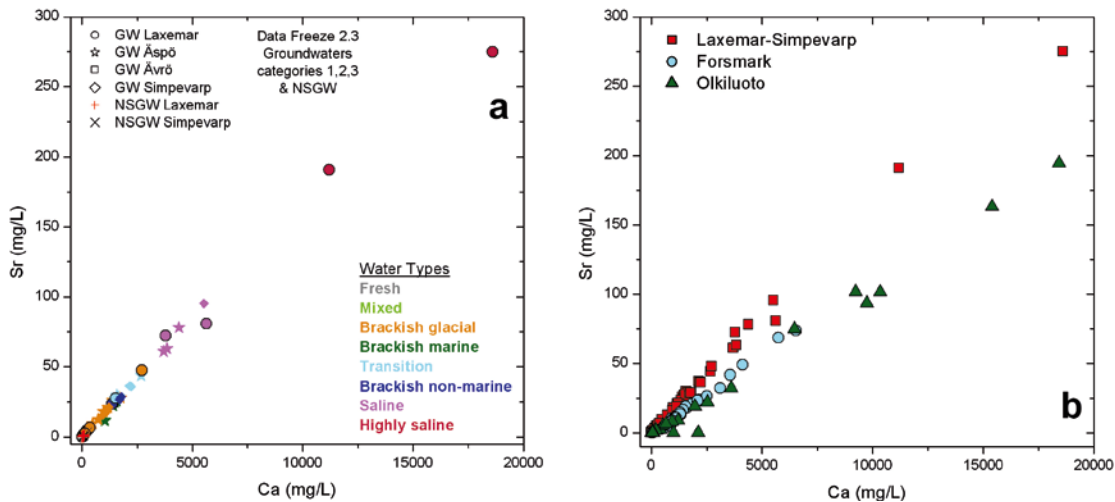
Figure 3-53. *Strontium concentrations vs. Ca contents in the Laxemar-Simpevarp groundwaters (a) and in these waters together with Forsmark and Olkiluoto groundwaters (b)*

The difference in slope is even more evident when the Ca/Sr molar ratio is plotted against chloride (Figure 3-54). The very wide range of variation of the Ca/Sr ratio in near-surface groundwaters (100 < Ca/Sr < 1,000) can be attributed to the weathering of rocks with different Ca/Sr ratios.

As for the deeper groundwaters (Figure 3-54b), Ca/Sr ratios tend to a constant value of ~120 for salinities higher that 0.1 mol/kg Cl in the Laxemar-Simpevarp area. In the Olkiluoto area, on the other hand, the Ca/Sr ratio tends to ~230 (salinities in Forsmark are lower but the final ratio seems to approach that of Olkiluoto). The most interesting observation here is that these ratios agree with those in their respective Deep Saline end-member. This suggests that in saline groundwaters Ca and Sr are mostly inherited from the Deep Saline end-member and controlled by mixing, in spite of the different equilibrium situations in these systems. This hypothesis will be re-addressed later on.

Barium does not show any clear trend either with depth (Figure 3-55a) or with chloride concentration (Figure 3-55b). This suggests the presence of a mineralogical control on dissolved barium (see section 3.4.3, Figure 3-62). The anomalously high Ba concentrations in some groundwaters from
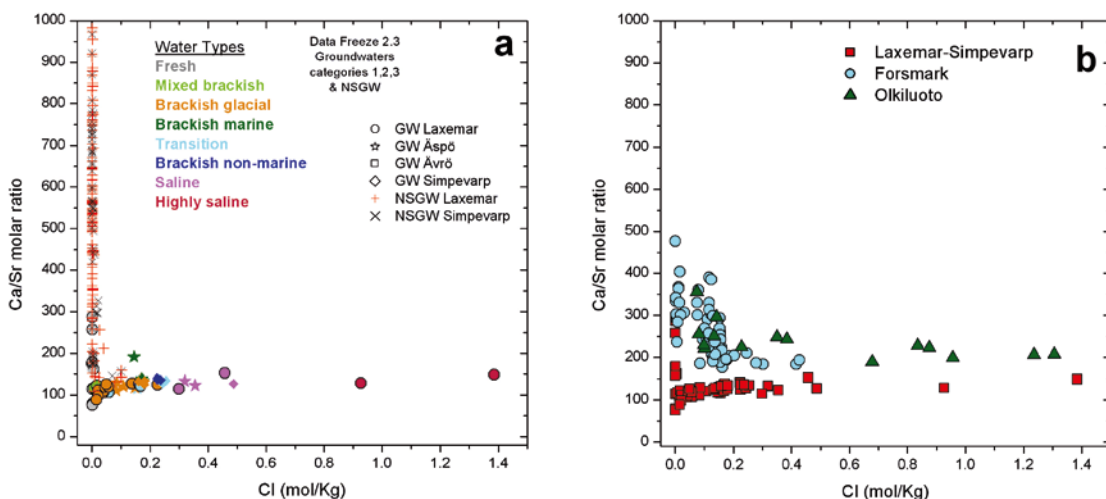
Figure 3-54. *Ca/Sr molar ratios in waters from the Laxemar-Simpevarp area, including the near-surface groundwaters (a) and only deep groundwaters from Laxemar-Simpevarp together with groundwaters from Forsmark and Olkiluoto (b).*

82
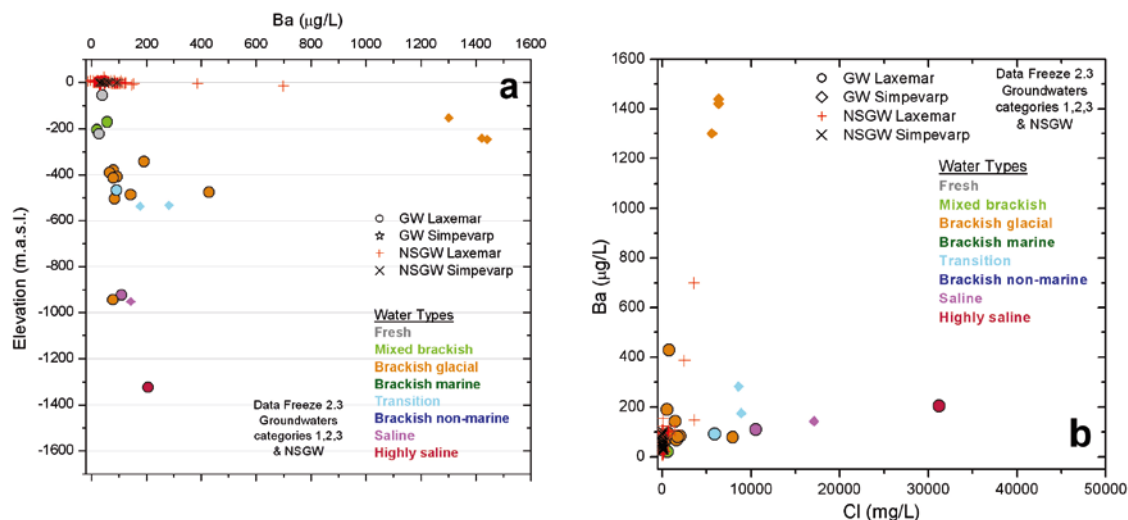
***Figure 3-55.** Barium contents vs. depth (a) and chloride contents (b) in the Laxemar-Simpevarp ground-waters (including the near-surface groundwaters).*

the Simpevarp subarea at around 200 and 400 m depth[14] could be related to analytical problems, but they can also be explained by the presence of harmotome, a soluble Ba-zeolite locally detected in the fracture fillings of the Simpevarp and Laxemar subareas down to 300–400 m depth (Drake and Tullborg 2004, 2006a; see section 3.4.2).

3.4.2 Mineralogical data

The available mineralogical and isotopic information can help to understand the geochemical behaviour of dissolved sulphate and to discover the possible controlling processes. Apart from the identification of important sulphur phases in fractures (gypsum, pyrite, barite and celestite), samples of these fracture fillings have been analysed for major elements and sulphur stable isotopes (expressed as $\delta^{34}S$ ‰ CDT) (Drake and Tullborg 2007).

Overburden

Gypsum has not been identified to date in the overburden, although information is very scarce and restricted to the Laxemar subarea (see section 3.2.2). This phase could appear in some of the scarce outcrops of Littorina sediments now exposed to meteoric weathering (but only if they were pyrite-rich; Öborn and Berggren 1995). However, its occurrence in the rest of the overburden is not very feasible, at least in the amounts needed to participate in the control of dissolved sulphate. This fact would explain the absence of correlation between sulphate and calcium in the near-surface groundwaters and, indirectly, the importance of pyrite as a source of dissolved sulphate.

The groundwater system

Gypsum does not occur frequently in fracture fillings in the Fennoscandian shield. However, from the recent mineralogical studies performed in the Laxemar-Simpevarp area, it is known that this mineral has occasionally been found in low transmissive zones in Simpevarp (KSH03 borehole at 495 and 684 m depth, Drake and Tullborg 2006ab) and more frequently in sealed and open fractures[15] in the Laxemar subarea (boreholes KLX03, KLX06, KLX08, KLX10, KLX12A and KLX17A at depth greater than –360 m.a.s.l., Figure 3-56, Smellie *et al.* 2006, Laxemar 2.1, Drake and Tullborg 2008).

---

[14] Sample at 400 m depth in Simpevarp (#11186, from KSH02) has a barium content of 11.6 mg/L and has not been shown in the plots. It is also oversaturated with respect to barite (SI=1.17).

[15] In the compilation of mineralogical data for SR-Can the estimation is that gypsum represents the 0.5% of the total mineralogy in the sealed fractures and the 0.9% in open fractures at Laxemar. The percentage value represents in how many of the fractures a specific mineral has been identified, following the data reported by Drake *et al.* (2006).
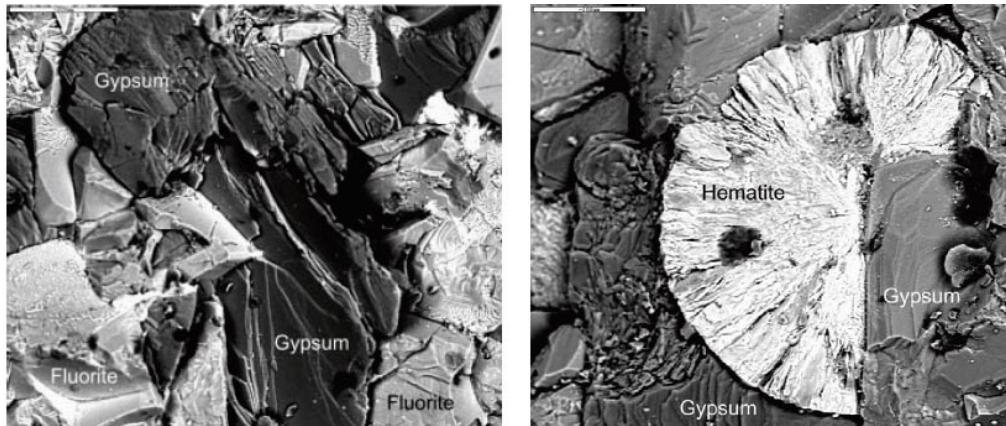
Figure 3-56. *Back-scattered SEM-images of gypsum and fluorite (left) and gypsum with a spherical aggregate of hematite from KLX06 borehole at 789 m, borehole length (right). Scale marker bar is 200 μm. From Drake and Tullborg (2007).*

According to Drake and Tullborg (2007), the paragenesis and the stable isotopes suggest a hydrothermal origin (last crystallization stages) for gypsum and, therefore, an old age (Palaeozoic, several hundred million years ago). Isotopic analyses ($\delta^{34}S$) of fracture gypsum samples from boreholes KLX03 (533 and 590 m, borehole length) and KLX08 (795 to 919 m, borehole length) indicate values from +5.9 to +6.8‰ CDT and from +3.7 to +12.1‰ CDT, respectively (Smellie *et al.* 2006). These values are within the range measured in fracture gypsum in the Eye-Dashwa Lakes pluton (Canada; from +5.3 to + 8.5‰ CDT), which is also interpreted as a late hydrothermal product of similar or even older age (Precambrian, Kamineni 1983). The same range is reported by Fritz *et al.* (1994) for gypsum of magmatic/hydrothermal origin in the Canadian Shield (from 0 to 14‰).

Thus, it appears that gypsum has been present in the fracture fillings for hundreds of millions of years, at least in the Laxemar subarea. Therefore, this mineral could have taken part in the geochemical evolution of the groundwater system even in the oldest brines or deep saline groundwaters. A possible explanation for the smaller amounts detected at the Simpevarp subarea could be that gypsum was formed in all the Laxemar-Simpevarp area but it was almost flushed away in conductive fractures at some subareas (e.g. Äspö and Simpevarp) but kept in some fractures at Laxemar subarea (Drake and Tullborg 2006ab).

Barite ($BaSO_4$) has also been identified as a "late" hydrothermal filling (Figure 3-57) in some fractures at Laxemar subarea (e.g. KLX02, KLX03, KLX04, KLX06, KLX07A, KLX08 and KLX10; Drake and Tullborg 2004, 2005), Simpevarp subarea (KSH01A, KSH01B and KSH03A; Drake and Tullborg 2004, 2006a) and in the Götemar granite (Drake and Tullborg 2006b) over a wide range of depths (50 to 900 m).

Moreover, a quite uncommon barium-zeolite, harmotome, has been identified as a fracture filling mineral in the Simpevarp and Laxemar subareas (Figure 3-57 and 3-58, Drake and Tullborg 2004, 2006a, 2007) down to 300–400 m depth and usually associated with barite[16]. The localised presence of this mineral could explain some of the very high barium concentrations found in the groundwaters from the Laxemar subarea and, especially, from the Simpevarp subarea. However, more studies are needed to check this possibility.

---

[16] Harmotome has not been identified in Forsmark, but this could be because it seems to be an easily dissolved phase, since approximately 90% of the fractures occupied with harmotome are open (Drake and Tullborg 2004).
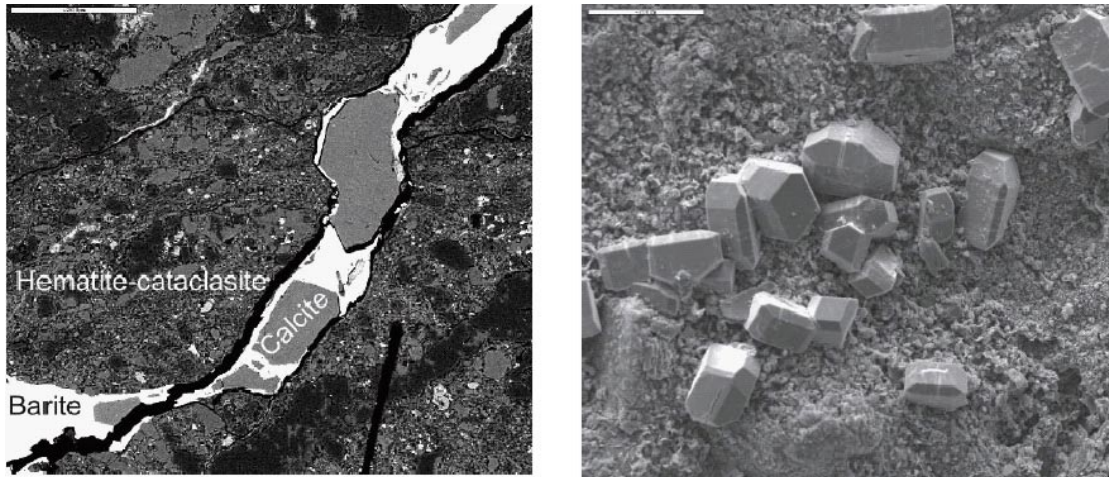
Figure 3-57. *Left: Back-scattered SEM-image of a fracture filled with calcite and barite that cut through earlier formed hematite-cataclasite (KSH03 borehole at Sample 220.15–220.31 m, borehole length). Scale marker bar is 200 µm. Right: Electron image of idiomorphic harmotome crystals (KSH01A borehole at 242 m, borehole length). Scale bar is 200 µm. From Drake and Tullborg (2004, 2006a).*
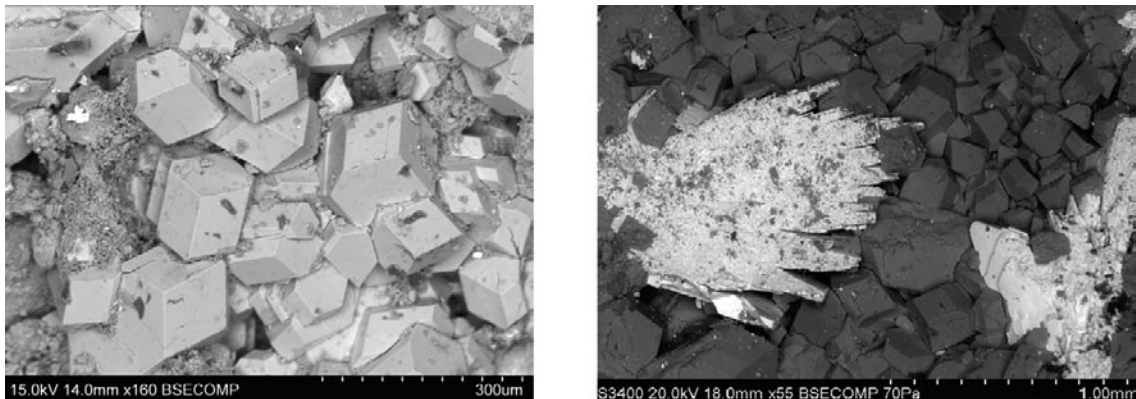
Figure 3-58. *Back-scattered SEM-image of euhedral harmotome (Ba-zeolite) in KLX03 at 266.62–266.71 m, borehole length (left) and in KLX07A (right) at 193.63–193.87 m, borehole length (dark grey) together with barite (bright). From Drake and Tullborg (2007).*

3.4.3 Processes. Thermodynamic approach

Elements such as calcium, strontium, barium and, obviously, sulphate, can be controlled or regulated by sulphate minerals in natural groundwaters. The possible controlling phases are gypsum, celestite and barite (e.g. Nordstrom *et al.* 1985, 1989). The particular characters of the sulphate system in the Laxemar-Simpevarp groundwaters make the assessment of these possible controls necessary. With this goal in mind, saturation states with respect to the aforementioned minerals have been calculated and the results are presented here. The uncertainty ranges considered for these saturation indices are: ± 0.2 SI units for gypsum, ± 0.3 SI units for celestite and ± 0.5 SI units for barite (Langmuir and Melchior 1985, Deustch 1997).

Near-surface groundwaters

The correlation between total sulphate and Ca contents in the fresh near-surface groundwaters does not indicate the participation of gypsum dissolution. In fact, all these waters are clearly undersaturated with respect to this phase (Figure 3-59a).
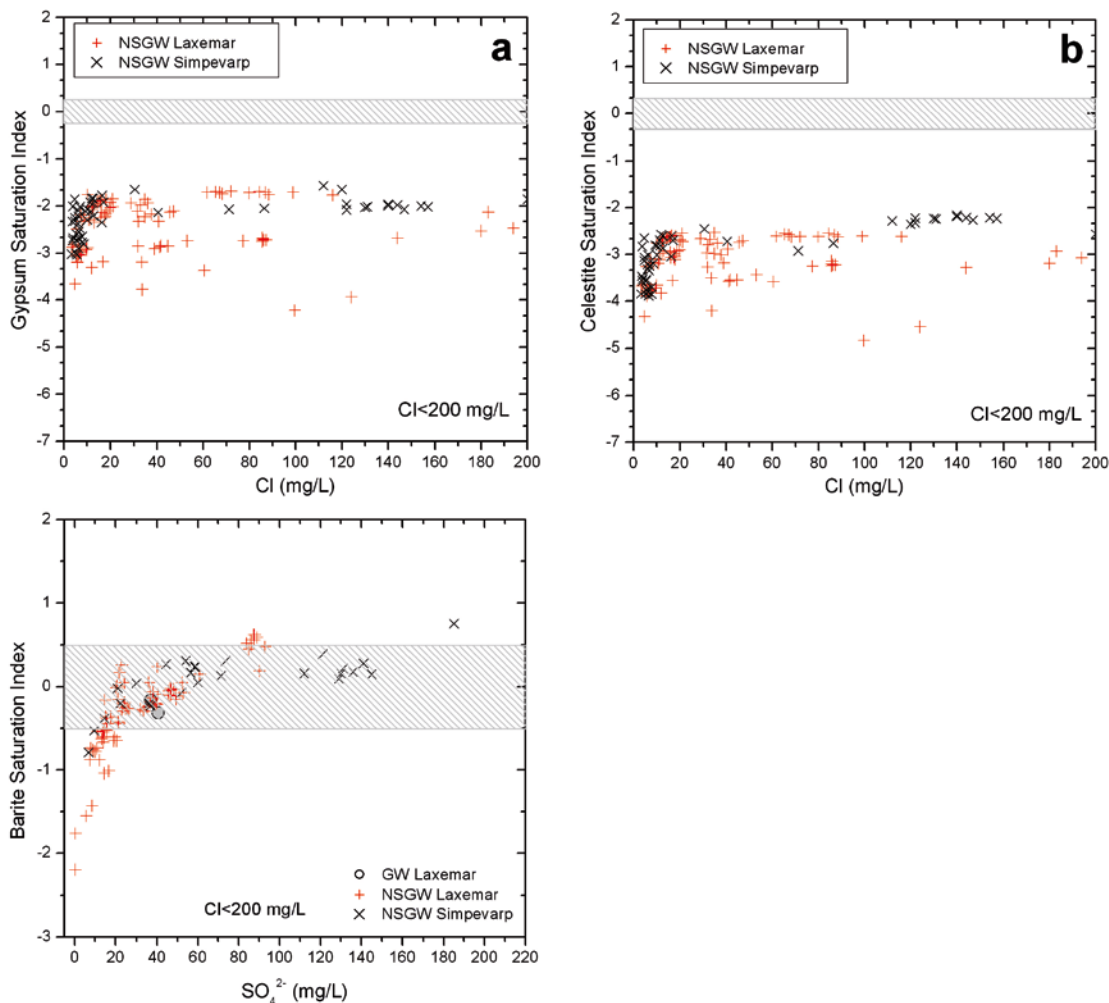
Figure 3-59. *Gypsum (a) celestite (b) and barite (c) saturation indices with respect to chloride (a, b) and sulphate (c) in the fresh near-surface groundwaters at the Laxemar-Simpevarp area with chloride lower than 200 mg/L. Dashed areas represent the uncertainty range.*

Celestite saturation indices indicate that the fresh dilute groundwaters are also clearly undersaturated with respect to this mineral (Figure 3-59b). The same happens with respect to barite in the most diluted waters (SI value below –2.0; Figure 3-59c). However, as sulphate increases, waters quickly evolve towards an apparent equilibrium with respect to barite (within the uncertainty range of ± 0.5 SI units; Figure 3-59c). Therefore, neither calcium nor strontium solubilities are limited by sulphate phases but barium appears to reach a solubility limit in the near-surface groundwaters, also contributing to modulate the dissolved sulphate concentrations.

Other processes can participate in the control of dissolved sulphate in the near-surface groundwaters Based on the $\delta^{34}S$ values, pyrite dissolution and sulphate reduction activity can be invoked for some of these waters. In addition, sorption/desorption processes can also participate actively, at least, in the soils (SO_4^{2-} is known to sorb onto ferric oxyhydroxides; e.g. Dzombak and Morel 1990).

Groundwaters

Groundwater saturation indices with respect to gypsum define a clear trend towards equilibrium as depth or chloride content increase (Figure 3-60ab). Equilibrium situations are reached at depths greater than 800 m in Laxemar, Simpevarp and Äspö (Figure 3-60a). Above this depth a wide variability in the calculated SI values is apparent, especially in the Laxemar subarea (for example, at 500 m depth, SI values for gypsum range from −2.2 to −0.3; Figure 3-60a) but also in some Simpevarp groundwaters. This variability reflects the complex situation shown in Figure 3-49, with recharge groundwaters reaching different depths and also with mixing processes (with marine and non-marine waters) effective at different depths depending on the area.
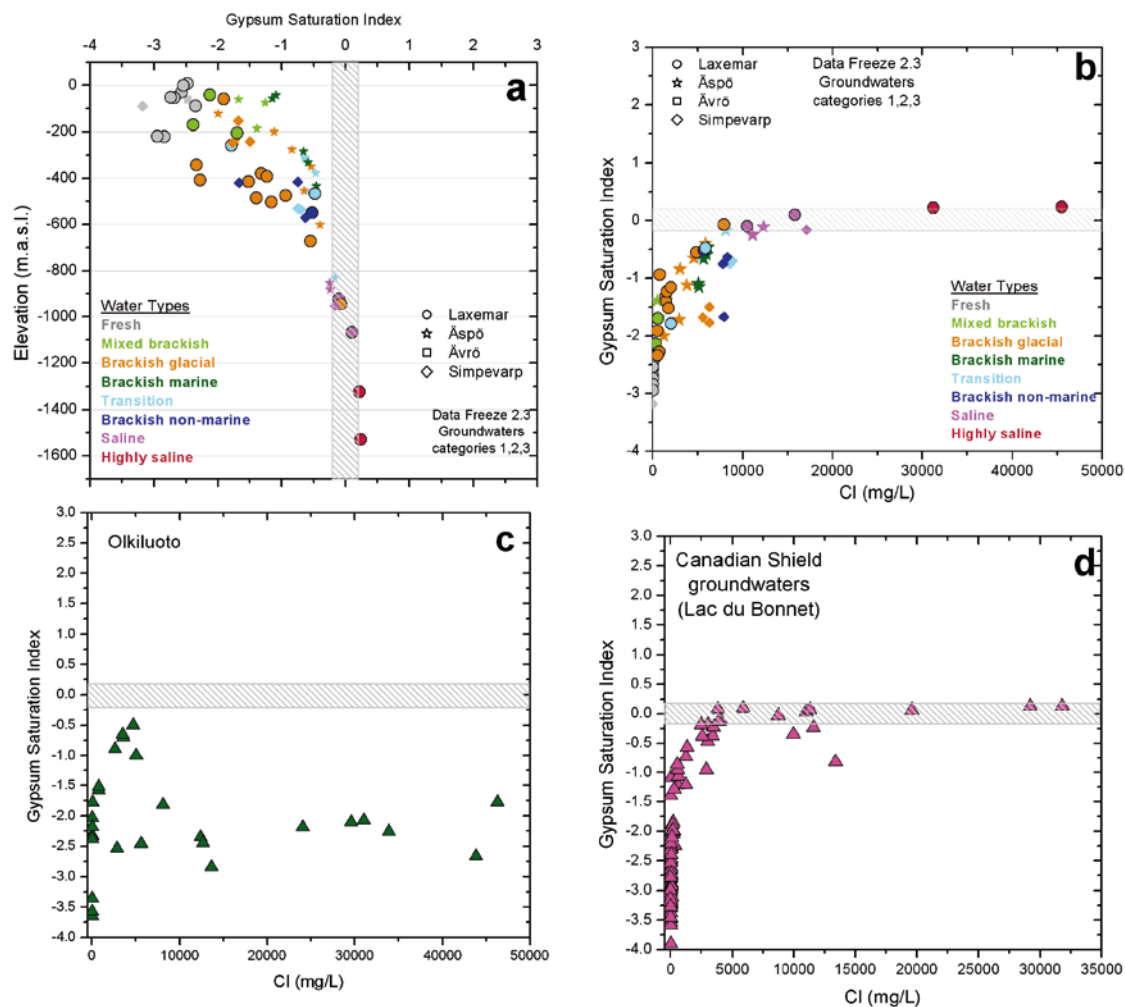
Figure 3-60. *Gypsum saturation index vs. depth (a) and chloride contents (b) in the groundwaters from Laxemar-Simpevarp. For comparison, gypsum saturation index vs. Cl contents for Olkiluoto (c) and Lac du Bonnet Batholith groundwaters (d) are also plotted. Calculations have been performed using the data presented by Pitkänen et al.(2004) for Olkiluoto and by Gascoyne (2004) for Lac du Bonnet Batholith (Canada). Note that chloride scale in plot (c) is different from the others. Dashed areas represent the uncertainty range*

With respect to chloride content (Figure 3-60b), gypsum saturation values also show some differences between the different subareas. Undersaturation decreases with increasing Cl contents (going towards equilibrium) but this trend is clearly different in the Simpevarp subarea, compared with the others, as these waters approach equilibrium at higher salinities. Then gypsum equilibrium is reached by groundwaters with Cl concentrations around 8,000 mg/L at Laxemar and Äspö subareas, whereas it is apparently reached by groundwaters with higher Cl contents (around 17,000 mg/L) at the Simpevarp subarea.

The Laxemar-Simpevarp groundwaters remain in equilibrium with respect to gypsum from around 8,000 mg/L up to near 50,000 mg/L of chloride. This trend strongly suggests the existence of an effective solubility control of dissolved sulphate and introduces a new controlling phase -gypsum- in the Laxemar-Simpevarp groundwater system. A similar limitation of sulphate contents in saline groundwaters was suggested, though not demonstrated with calculations, by Gascoyne (2004) in the Lac du Bonnet Batholith and also attributed to the solubility control exerted by gypsum (Figure 3-60c). The existence of this equilibrium situation would explain the drastic differences observed in dissolved sulphate contents in the more saline groundwaters in other Fennoscandian sites such as Olkiluoto (Figure 3-60d) or Forsmark (not shown).

Based on these results, the hypothesis suggested here is that in the Laxemar-Simpevarp saline groundwaters gypsum equilibrium is superimposed on the mixing between the Deep Saline end member and the much more dilute groundwaters and that this re-equilibration depends on the presence of gypsum in the fracture filling mineralogy.

Gypsum has been identified in the system, but it is unequally distributed with respect to depth and subarea (section 3.4.2). Depending on the amount of gypsum, dissolved sulphate in groundwaters will behave either conservatively (if there is no gypsum available) during mixing with more saline waters or with partial (available gypsum but not enough to reach equilibrium) or total gypsum re-equilibrium (amounts of gypsum enough to reach equilibrium).

Apart from the influence of gypsum, dissolved sulphate in some waters seems to be affected by other reaction processes superimposed on mixing. This is the case of samples from KSH01A (and also some from KLX04), with chloride contents between 5,500 and 8,000 mg/L but with very low dissolved sulphate (lower than 50 mg/L) compared with other samples from the same borehole (Figure 3-49a). This suggests the presence of a sink for dissolved sulphate, probably related to sulphate reduction activity. In fact, sulphate reducing bacteria (SRB) have been detected in some of the samples with anomalously low sulphate contents (sample #5263 from KSH01A) together with higher $\delta^{34}S$ values (above 20‰ CDT) than the values found for the group of waters with 7,800 and 8,800 mg/L Cl (Figure 3-51b).

Sulphate reduction activity is also evident in those less saline groundwaters from the Laxemar-Simpevarp area affected by mixing with a Glacial component (Figure 3-51; section 3.4.1.).

Groundwaters with a Littorina contribution (Cl around 5,000 mg/L) do not reach gypsum equilibrium, as already observed in other systems with larger Littorina participation (e.g. Forsmark or Olkiluoto; Figure 3-60d), but it does increase the concentration of dissolved sulphate with respect to pre-existing waters (section 3.4.4).

As regards Sr-bearing minerals, celestite ($SrSO_4$) saturation indices in Laxemar-Simpevarp groundwaters display a similar trend to gypsum, reaching equilibrium in the most saline samples (Figure 3-61a). Strontianite ($SrCO_3$), on the other hand, is always undersaturated in all groundwaters (Figure 3-61b). Therefore, celestite could be considered as another possible controlling phase in this groundwater system, although it has only been identified in a single fracture filling together with gypsum (KLX17A at 590 m borehole length; Drake and Tullborg 2008). This issue will be discussed in more detail in section 3.4.4.

Most of the groundwaters are in equilibrium with respect to barite (Figure 3-62), as is the case in the recharge waters (Figure 3-49c) and in other low-temperature crystalline systems such as Stripa (Nordstrom *et al.* 1989). However, some of the Laxemar and Simpevarp groundwaters with the highest barium concentrations are clearly oversaturated with respect to barite. As suggested before, more studies are needed to assess the influence of other mineral phases such as harmotome, or the possibility of an analytical error.
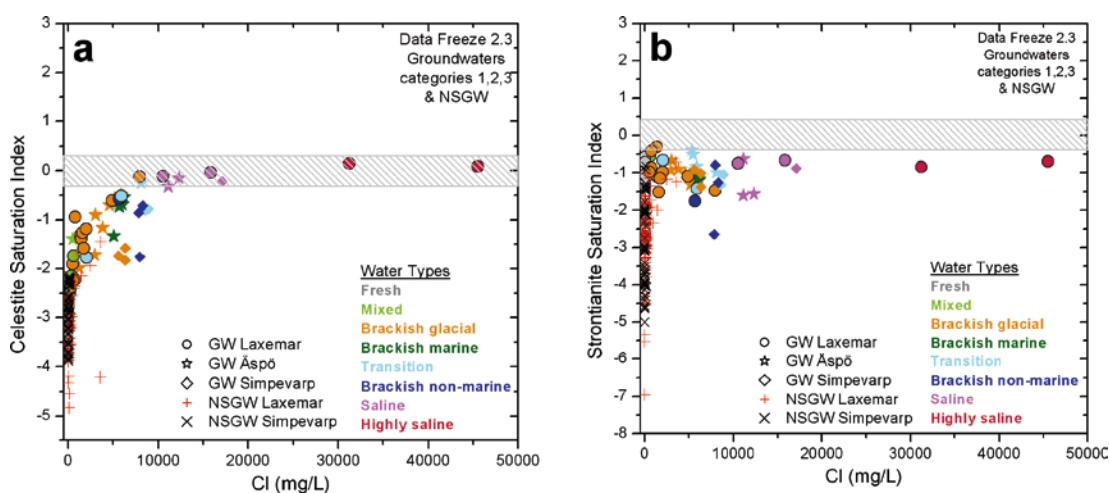
Figure 3-61. *Celestite (a) and Strontianite (b) saturation indices vs. Cl for Laxemar-Simpevarp groundwaters (including near-surface groundwaters). Dashed areas represent the uncertainty range.*
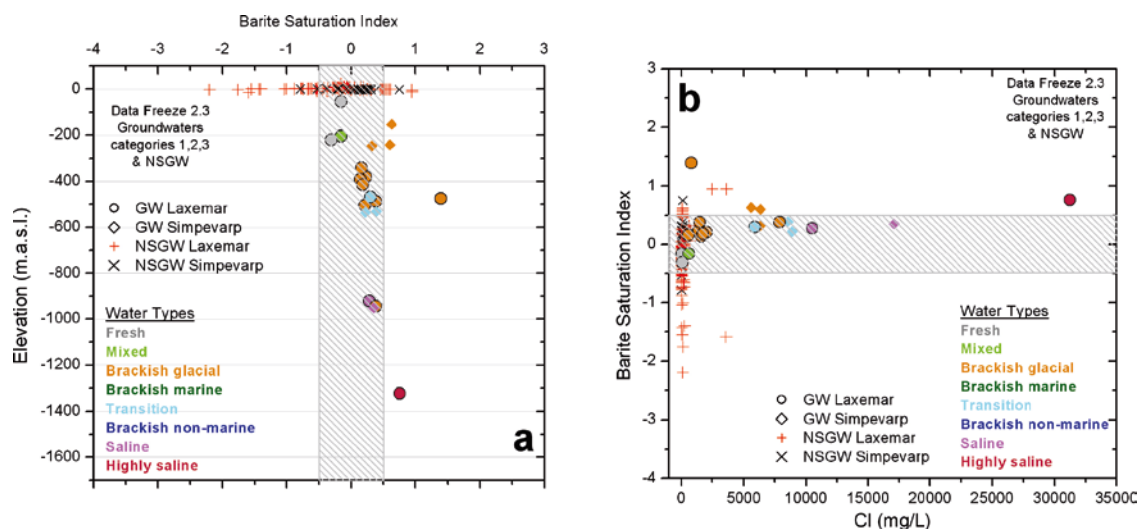
Figure 3-62. *Barite saturation indices vs. depth (a) and chloride contents (b) in the Laxemar/Simpevarp groundwaters (including the near-surface groundwaters). Dashed areas represent the uncertainty range.*

3.4.4 Thermodynamic simulations

The contribution of gypsum and celestite to the control of dissolved sulphate in the most saline groundwaters and of Littorina in some brackish groundwaters (3,000 < Cl < 7,000 mg/L) can be verified by performing different mixing and mixing + reaction simulations. The contribution should be evident in the behaviour of elements such as sulphate, calcium and strontium and in the saturation state of the waters with respect to calcite, gypsum, celestite and strontianite.

Based on the general conceptual model of the system (section 3.2.4), groundwaters in the Laxemar-Simpevarp area are affected by a global process of mixing between a Deep Saline end member and more dilute waters and, then, by the input of marine waters (Littorina Sea stage). Therefore, the same conservative mixing simulations used for the carbonate system will be used here. With regard to mixing + reaction simulations, equilibrium reactions with calcite, gypsum and celestite will be considered.

The processes affecting the sulphate system and their consequences on groundwater hydrochemistry have been assessed by studying separately the results of conservative mixing and mixing + reaction simulations. Results of conservative mixing between the dilute (Glacial) and the saline (#2731) end members play an important role, as they represent the oldest process onto which the rest of the processes are superimposed.

The conservative mixing of a dilute groundwater with progressively higher proportions of a deep saline groundwater (black spheres) increases saturation with respect to gypsum (Figure 3-63a) and celestite (Figure 3-63b). Simultaneously, calcite (as shown in the previous section, 3.3) attains oversaturation (Figure 3-39a). Therefore, disequilibria induced by mixing would produce calcite precipitation and, if present in the system, gypsum and celestite dissolution.

Compared with the SI values of the real samples, the conservative mixing line between the dilute (Gl) and the saline (#2731 sample) end members allows distinguishing between samples whose composition is mainly determined by this mixing process and samples also affected by mixing with other end members and/or by reactions (Figures 3-63ab).

The main reactive process occurring in the system which is able to *decrease* the groundwater saturation state with respect to gypsum and celestite is sulphate reduction. The existence of this process is supported by the presence of SRB in some of the Simpevarp samples located below the conservative mixing line in Figure 3-63a.
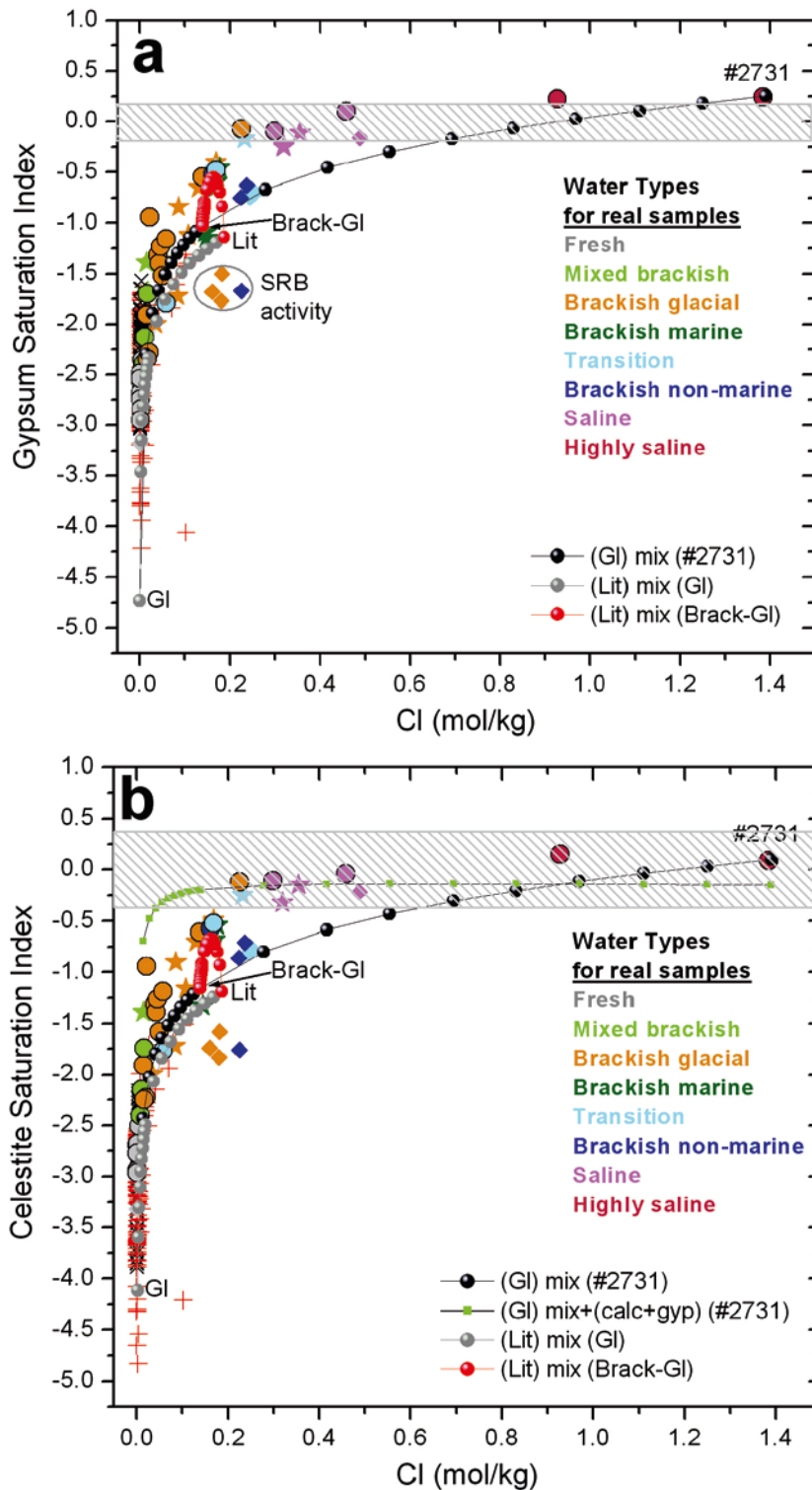
Figure 3-63. *(a) Saturation indices with respect to gypsum (a) and celestite (b) vs. chloride contents for conservative mixing simulations between Glacial end member and sample #2731, Littorina and Glacial, and Littorina and Brackish-Glacial. Measured values are also shown for comparison (stars: Äspö GW; circles: Laxemar GW, red crosses: Laxemar NSGW; diamonds: Simpevarp GW; black x: Simpevarp NSGW). Dashed areas represent the uncertainty range.*

Processes able to *increase* the saturation state are gypsum dissolution and additional mixing with a sulphate-rich end member (Littorina). Gypsum dissolution may shift groundwater saturation to equilibrium (as happens in the most saline samples from Laxemar, Simpevarp and Äspö; Cl > 0.2 mol/kg) or else increase gypsum SI to the (undersaturated) state at which gypsum is completely dissolved (as suggested for some of the samples with Cl < 0.2 mol/kg located close to the conservative mixing line in Figure 3-63a).

There is a set of samples with chloride concentrations near 5,000 mg/L (0.15 mol/kg) whose increase in the gypsum and celestite saturation indices (Figure 3-63ab) could be justified by the input of Littorina. Conservative mixing between Littorina and a Brackish-Glacial water does not reach equilibrium with gypsum or celestite although the saturation states increase towards it (mainly in Äspö and some in Laxemar).

With respect to celestite, results from mixing and mixing + reaction simulations indicate that, if equilibrium with gypsum (or gypsum+calcite) is imposed, the obtained mixed groundwaters are also in equilibrium with respect to celestite (Figure 3-63b). Therefore, celestite equilibrium could be apparent and only derived from mixing and re-equilibrium with gypsum[17]. The implications of this result on the composition of the Deep Saline end member in the Laxemar-Simpevarp area are further discussed in Appendix F.

Next, the effects of mixing and mixing + reaction on the contents of sulphate and strontium[18] are analysed. Figures 3-64 to 21 show the results for the two types of simulations; conservative mixing and mixing + reaction (equilibrium with gypsum and/or calcite and/or celestite), especially for the mixing between the Deep Saline and the Glacial end members.

Calcium and strontium (Figure 3-45b, 3-46b and 3-64) increase linearly with chloride irrespective of the participation of reactions. Changes in the calcium contents imposed by gypsum dissolution or calcite equilibrium are very small compared with the already very high concentrations present in the highly saline water used here as end member (Figure 3-45b, 3-46b). However, the results obtained when assuming cation exchange produce a slight decrease in the calcium content with respect to the previous result, fitting better the measured values (Figure 3-45b, 3-46b).

As expected from its association with calcium, the results obtained for strontium with mixing and mixing + equilibrium reactions (with calcite, gypsum or celestite) are identical and, in general, they reproduce the measured trend (Figure 3-64a, crosses over the spheres). Celestite equilibrium produces very low mass transfers that do not affect the strontium contents obtained by mixing. Only when imposing cation exchange are some modifications observed, resulting in a better fit with the measured values (Figure 3-64b).

In some of the saline samples (Cl > 0.2 mol/kg) and in many brackish-glacial waters (mainly in the Äspö and Laxemar subareas), Sr contents fit an exchange process considering a value of 0.5 mol/L or lower for CEC. This is in agreement with the results from the mixing + cation exchange simulations for sodium (Figure 3-20b) and calcium (Figure 3-45 and 3-46).

Therefore, conservative mixing simulations are able to reproduce the calcium content trend observed in the natural system for saline groundwaters, and also the linear trend of strontium with chloride (independently of the apparent or real equilibrium with celestite). Only cation exchange would be able to change their contents in a maximum proportion of 30% over the concentrations imposed by mixing.

In the case of mixing between Littorina and a Brackish-Glacial water, the two extreme trends of pure mixing and mixing + exchange (red spheres and red triangles in Figure 3-64b) suggest the participation (although in a degree difficult to quantify) of cation exchange to justify the Sr contents of some brackish-marine samples.

---

[17] Contribution of the strontium present in the structure of gypsum is negligible. Measured Sr concentrations in gypsum from some fracture fillings are between 131 and 221 ppm (Drake and Tullborg 2007) and the gypsum dissolution mass transfers calculated in the simulations for the chloride range of interest reach maximum values of $5.0 \cdot 10^{-3}$ mol/kg. Therefore, dissolution of gypsum contributes only with 0.1 or 0.2 mg/L of strontium to solution.

[18] The effects of mixing and mixing and reaction on the calcium content has already been analysed in the previous section.
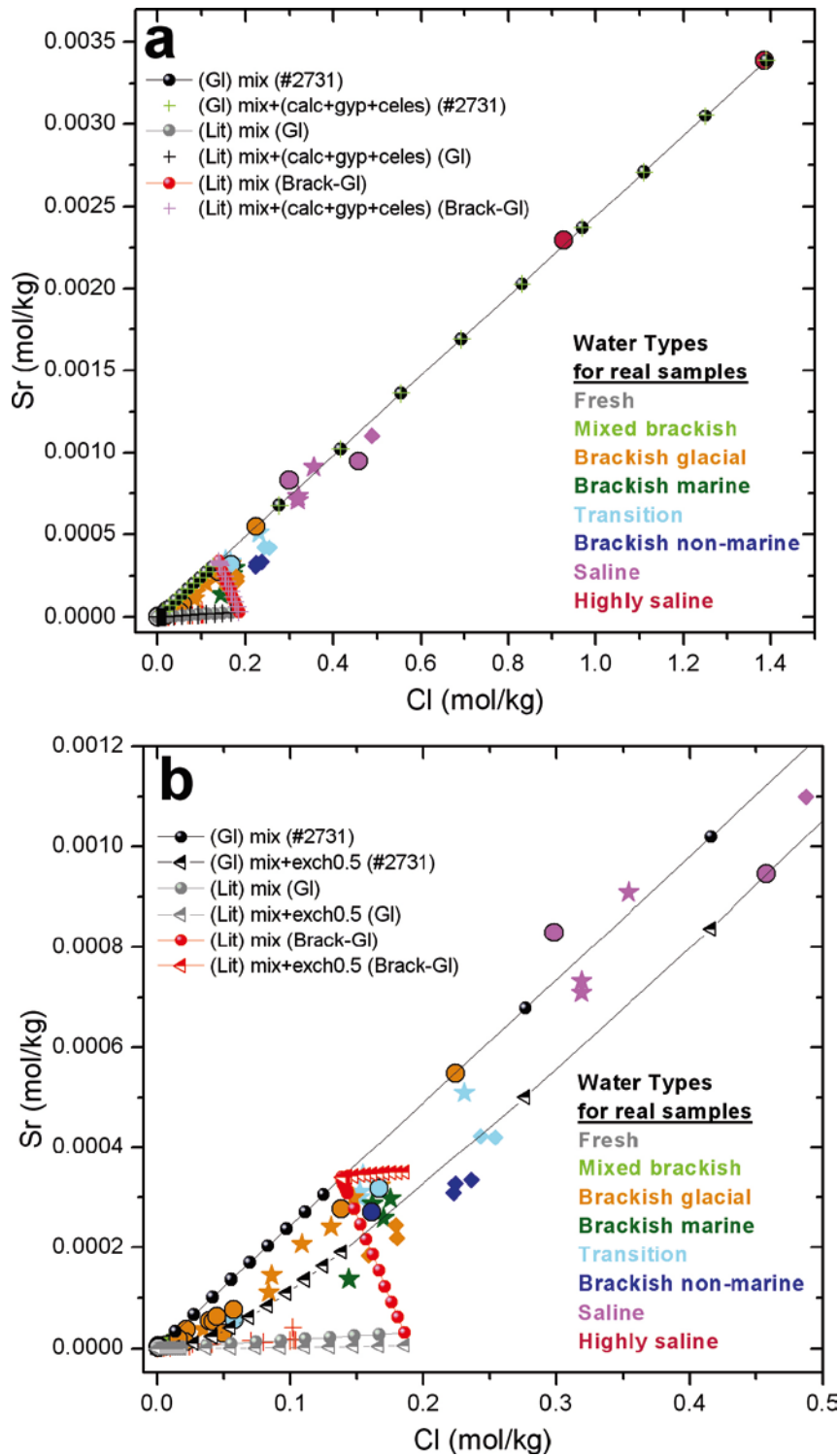
Figure 3-64. *Results for mixing and mixing + reaction simulations between Glacial and #2731, and Littorina and Glacial. (a) Calculated dissolved strontium and chloride concentrations for conservative mixing and for mixing + reaction (equilibrium with calcite, gypsum and celestite); and (b) enlargement of the lower left corner showing dissolved strontium concentrations for conservative mixing and mixing + cation exchange. Measured values are also shown for comparison (stars: Äspö GW; circles: Laxemar GW, red crosses: Laxemar NSGW; diamonds: Simpevarp GW; black x: Simpevarp NSGW).*

For sulphate, conservative mixing between Littorina and the two dilute pre-existing groundwaters (Gl and Brackish-Glacial) produces the expected linear trends with respect to chloride, with a progressive increase of both elements as the mixing proportion of the saline end member increases (Figure 3-65).These conservative trends with respect to sulphate fit well the brackish-marine waters from Äspö (clearly affected by Littorina) and some near-surface groundwaters with very high sulphate contents (in this case Littorina-Glacial mixing would include additional recent meteoric waters mixed with the present Baltic end member).

For more saline waters (Cl > 0.2 mg/L), only simulations that include mixing + gypsum re-equilibration (more exactly, mixing + equilibrium with gypsum+calcite+celestite; green crosses in Figure 3-65) reproduce the observed sulphate behaviour if the uncertainty range of ±0.25 SI units (also plotted in the figure) is taken into account. Sulphate mass transfers associated with gypsum dissolution may be especially relevant for waters with chloride contents between 0.2 and 0.4 mol/kg (Figure 3-65a) and may modify dissolved sulphate contents drastically (from ~0.001 mol/kg in conservative mixing to ~0.01 mol/kg in mixing+gypsum equilibrium).

Finally, Figure 3-65 also shows the same five samples from the Simpevarp subarea (circled), with chloride concentrations between 7,910 to 8,560 mg/L, which are not explained for sulphate by conservative mixing or mixing and gypsum equilibrium paths. The "intermediate" dissolved sulphate concentrations in these samples could represent a situation where gypsum was not abundant enough to allow a complete re-equilibration after mixing and its dissolution only promotes a partial increase in dissolved sulphate.

However, as already shown, these brackish non-marine groundwaters also show higher sodium content than expected for their chloride concentrations (section 3.2.4) when compared with other brackish non-marine groundwater types and, what is more interesting, they also show a clear enrichment in [11]B especially in the 300–550 interval (in boreholes KSH01at 531.5 m and KSH02 at 418.7 and 570.9 m; Figure 3-66). Furthermore, Na-SO_4 type compositions associated with chloride contents ranging from 2,500 to 7,600 mg/L, have been reported from pore waters at similar depth intervals (see Waber $et\ al$. 2009). These occurrences, together with the anomalously high [11]B values (Casanova $et\ al$. 2005, Smellie $et\ al$. 2008), lend to support a freeze-out origin for such pore waters and groundwater types.

The identification of freezing-out processes may be an important point in the overall understanding of the palaeohydrological evolution of the system as traces of this process are very difficult to identify (e.g. Smellie $et\ al$. 2008). However, this hypothesis must be further explored and verified as other processes may explain, at least in part, the compositional characters of these groundwaters (see sections 3.2.4 and 3.3.4).

3.4.5   Conclusions

Near-surface groundwaters

In general, dissolved sulphate contents in the surface (streams, lakes, etc) and near surface ground-water systems at Laxemar-Simpevarp are within the range usually measured in the Swedish context (Tröjbom and Söderbäck 2006a, Tröjbom $et\ al$. 2008). However, there are larger contents (130–480 mg/L) in samples with Cl concentrations around 2,400–3,600 mg/L, affected by a relict or modern marine sulphate source (SSM000238 and SSM000239). On the contrary, samples with a Deep Saline signature (up to 5,000 mg/L Cl) and associated with the deep groundwaters postulated to be discharging through the main fractures of the area, display total dissolved sulphate around 20 mg/L, such as samples SSM000241 and SSM000242. Such low sulphate contents appear to be associated with very intense biological activity.

Dissolved sulphate contents in the rest of near-surface groundwaters are always below 200 mg/L. The SO_4^{2-}/Cl ratio in most of these fresh groundwaters is greater than the seawater ratio and, therefore, a non-marine source seems to be the major sulphur contributor.

Even though fertilizers or atmospheric depositions may represent additional sulphur sources, they cannot fully explain the high sulphur contents in these groundwaters compared to streams and lakes (Tröjbom and Söderbäck 2006a). Therefore, a "mineral" source appears to be necessary.
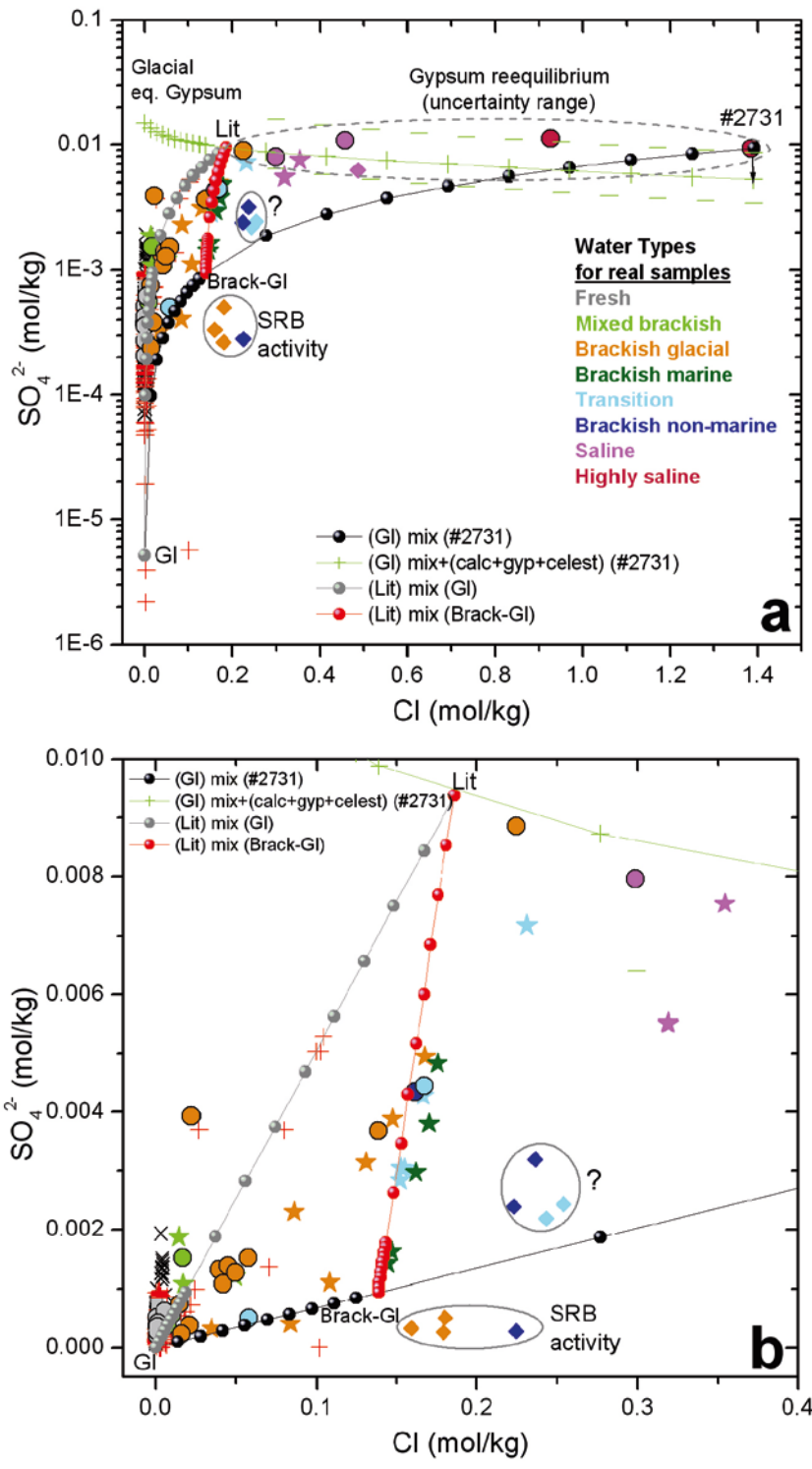
Figure 3-65. *Sulphate and chloride content results (in logarithmic and normal scales, a and b, respectively) for conservative mixing and mixing + equilibrium simulations between the different end members. Measured values are also shown (stars: Äspö GW; circles: Laxemar GW, red crosses: Laxemar NSGW; diamonds: Simpevarp GW; black x: Simpevarp NSGW). The results of gypsum re-equilibration are calculated with an uncertainty range of ±0.25 for gypsum solubility to make these results compatible with the calculated saturation indices from the saline groundwaters. The samples inside the grey circle with a question mark are the same shown for sodium and calcium (Figures 3-20 and 3-46) and are explained in the text.*
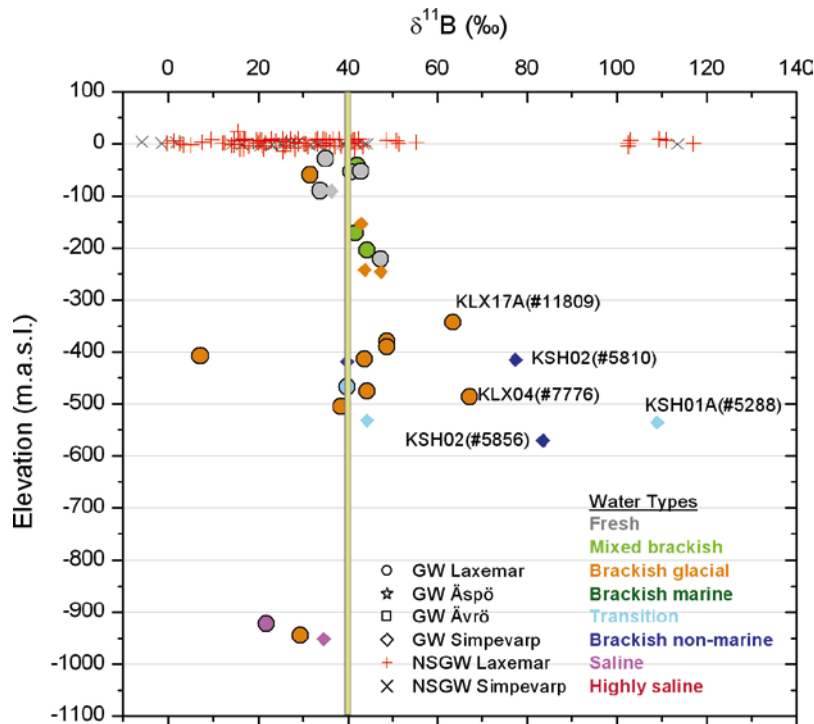
Figure 3-66. *δ¹¹B values as a function of depth for the Laxemar and Simpevarp subareas (vertical yellow column represents the Baltic Sea signature).*

The lack of correlation between total dissolved sulphate and calcium contents in these waters allows discarding a clear participation of gypsum dissolution. Instead, isotopic constraints ($\delta^{34}S$ values measured in dissolved sulphate) support an important contribution from pyrite dissolution (values from –20 to –5‰ CDT) to the dissolved sulphate pool in these waters. The effect of atmospheric deposition, the direct influence from sea water deposition (sea spray) or the existence of sulphate reducing activity are also supported by the range of $\delta^{34}S$ values found in some waters. As a general rule, an overlap among all the sources is expected in most near-surface groundwaters at the site.

All near-surface groundwaters are clearly undersaturated with respect to gypsum and celestite. The same conclusion stands with respect to barite in the most dilute waters. However, waters quickly evolve towards apparent equilibrium situations with respect to this mineral as sulphate concentration increases. Therefore, neither calcium nor strontium solubility is limited by sulphate phases but barium appears to reach a solubility limitation in these near-surface groundwaters, also contributing to modulate the dissolved sulphate concentrations.

Groundwaters

Total dissolved sulphate contents show an overall and continuous increase with depth, similar to the trends observed for chloride or sodium in the groundwaters. As a general trend, low dissolved sulphate concentrations characterise the shallowest 0–400 m groundwaters in Laxemar and Simpevarp groundwaters (values lower than 100 mg/L in the first 100 m depth and up to 200 mg/L between 100 and 400 m depth at Laxemar, and always below 50 mg/L at Simpevarp). With regard to Äspö (and some Laxemar subarea waters), most groundwaters display larger contents (up to 200 mg/L in the first 100 m, groundwaters with clear marine signature, and up to 500 mg/L from 100 m down to 400 m depth), as an inherited character from the Littorina contribution.

From 400 m to 1,600 m depth, the contribution of a deep saline groundwater appears to be effective in all the Laxemar-Simpevarp area, progressively increasing the dissolved sulphate concentrations.

With respect to chloride, dissolved sulphate concentrations in the Laxemar-Simpevarp area display two apparent evolution trends: (1) a progressive increase with chloride (up to about 10,000 mg/L Cl) in a path where the present and past marine effects are evident[19], and (2) almost constant sulphate concentrations around 800 mg/L for groundwaters with evident influence of a deep saline water and with chloride concentrations between 10,000 and 50,000 mg/L.

Similar variation trends with chloride and depth have been described for the Lac du Bonnet batholith (Canada). In contrast, the existence of an important Littorina contribution down to 300–500 m depth in Forsmark and Olkiluoto promotes the presence of the highest total dissolved sulphate contents at those depths (in waters with Cl about 3,000–6,000 mg/L), with a drastic decrease at greater depths and salinities. The different observed sulphate variation trends at depth between Laxemar-Simpevarp and Olkiluoto can be attributed to the different total dissolved sulphate concentration of the corresponding Deep Saline end member (around 906 mg/L for Laxemar-Simpevarp and between 1.2 and 8.4 mg/L for Olkiluoto; Pitkänen *et al.* 2004).

Measured $\delta^{34}S$ values range between +9.1 and +37‰ CDT. Most of the Simpevarp subarea samples have values in the range of +15 to +25‰ CDT, whereas Laxemar subarea groundwaters display both higher and lower values (Smellie *et al.* 2006). $\delta^{34}S$ values greater than in marine waters are found in groundwaters with chloride contents < 6,500 mg/L at depths down to 400 m, in rough agreement with the existence of equilibrium situations with respect to iron monosulphides. Moreover, these samples display the lowest dissolved sulphate concentrations found in these groundwaters. Therefore, they can be interpreted as being diminished by the *in situ* sulphate reduction by SRB. The greatest $\delta^{34}S$ values (+37‰ CDT) are detected in the Laxemar subarea groundwaters with Cl contents below 500 mg/L and with total sulphate around 30 mg/L (HLX14 and KLX03 at 103–218 m and KLX03 at 193–198 m depth). These high values are strong indicators of sulphate-reducing activity under closed conditions. Moreover, the sample with this extreme value showed also a component of glacial melt water, which points towards a clear hydraulic isolation for a long time (Smellie *et al.* 2008).

Groundwaters with total dissolved sulphate contents larger than 250 mg/L display decreasing $\delta^{34}S$ values with increasing sulphate content, indicating weaker or non-existent sulphate-reducing activity. The decrease of the $\delta^{34}S$ signature in these groundwaters seems to be the result of gypsum dissolution.

Groundwater saturation indices with respect to gypsum define a clear trend towards equilibrium with increasing depth and chloride content. Above 900 m depth, groundwaters from Laxemar, Simpevarp and Äspö display a wide variability of calculated SI as a result of the variable depth reached by recharge groundwaters and by marine and non-marine waters. Below 900 m depth, gypsum equilibrium is reached by groundwaters with Cl concentrations around 8,000 mg/L at Laxemar and Äspö, whereas it is apparently reached by groundwaters with higher Cl contents (around 17,000 mg/L) at the Simpevarp subarea. Laxemar subarea groundwaters remain in equilibrium with respect to gypsum from around 8,000 mg/L to near 50,000 mg/L of chloride, which supports the effectiveness of gypsum as a solubility control of dissolved sulphate. The existence of this equilibrium situation would also explain the drastic differences observed in the dissolved sulphate contents of the more saline groundwaters in other Fennoscandian sites such as Olkiluoto or Forsmark.

Gypsum has been identified in the fracture filling mineralogy but it is not equally distributed either with depth or in all subareas. Therefore, groundwaters will be affected by mixing with more saline waters either conservatively (if there is no gypsum available) or with partial or total gypsum re-equilibrium (depending on the amount of available gypsum). Groundwaters with Littorina contribution (Cl around 5,000 mg/L) do not reach gypsum equilibrium, as already observed in other systems with larger Littorina participation (e.g. Forsmark or Olkiluoto).

Apart from the influence of gypsum dissolution, dissolved sulphate contents in some waters seem to be affected by other reaction processes superimposed on mixing, such as microbial sulphate reduction. This is the case for samples from KSH01A (and also some from KLX04), with chloride contents between 5,500 and 8,000 mg/L but with very low dissolved sulphate. SRB have been detected

_____

[19] More in detail, Äspö and Simpevarp groundwaters show higher salinity (for chloride contents up to 10,000 mg/L) for the same sulphate contents.

in some of the waters with anomalously low sulphate contents (sample #5263 from KSH01A) and the available data of $\delta^{34}S$ for some of these groundwaters show larger values (above 20‰ CDT) than the values found for the group of waters with 7,800 and 8,800 mg/L Cl. Sulphate reduction activity is also present in other less saline groundwaters affected by mixing with a Glacial component in the Laxemar-Simpevarp area.

The behaviour of Ba and Sr is closely related to the sulphate system. Barium does not show any clear trend either with depth or with chloride content, which suggests the presence of some mineralogical control on barium behaviour. Most of the groundwaters are in equilibrium with respect to barite, as happens in the possible recharge waters and in other low-temperature crystalline systems, such as Stripa (Nordstrom *et al.* 1989). However, some of the Laxemar and Simpevarp groundwaters at around 200 and 400 m depth display anomalously high Ba concentrations and are clearly oversaturated with respect to barite. This could be related to analytical problems or to the presence of harmotome, a soluble Ba-zeolite locally detected in the fracture fillings of the Simpevarp and Laxemar subareas down to 300–400 m depth. However, more detailed studies are needed to clarify this point.

Dissolved strontium concentrations show a distribution with depth very similar to total dissolved sulphate. As described for calcium, dissolved strontium concentrations display a very good linear correlation with chloride contents, suggesting a control by mixing processes for both elements. The same correlation exists in the Olkiluoto and Forsmark groundwaters although with a different slope which is more evident with the Ca/Sr molar ratio. This ratio shows a very wide range of variation in surface and shallow groundwaters for the three sites, which can be attributed to the weathering of different rocks and minerals with different Ca/Sr ratios. However, the Ca/Sr ratios in deeper and more saline groundwaters show a relatively constant value, although slightly different for each system, which is consistent with the Ca/Sr value in their respective Deep Saline end members. This suggests that, in the more saline groundwaters, Ca and Sr are mostly inherited from the saline end-member and controlled by mixing, in spite of the different equilibrium situations in these systems.

With regard to the Sr-bearing mineral phases, celestite ($SrSO_4$) saturation indices calculated for the Laxemar-Simpevarp groundwaters display a similar trend to gypsum, reaching equilibrium situations in the more saline samples. Therefore, celestite, which has recently been identified in minor amounts in the fracture fillings, could be considered as another possible Sr-controlling phase in this groundwater system.

Thermodynamic simulations of mixing between the deep saline waters and the dilute Glacial end member indicate that disequilibria induced by mixing would produce calcite precipitation and, if present in the system, gypsum and celestite dissolution. Consistent with the observations, calculated calcium and strontium concentrations show a linear increase with chloride irrespective of the presence or absence of reactions. Changes in the simulated Ca or Sr contents imposed by gypsum dissolution or calcite equilibrium are negligible, whereas cation exchange produces a slight decrease in the calcium and strontium contents with respect to the previous results (and in agreement with the calculated increase in sodium), fitting better the measured values analysed in the real samples. This also happens when cation exchange is superimposed on the mixing between Littorina and Brackish/Glacial waters.

Dissolved sulphate concentrations obtained from conservative mixing between Littorina and the pre-existing groundwaters vary linearly with respect to chloride contents, with a progressive increase of both elements as the mixing proportion of the more saline end member increases. It includes brackish-marine waters from Äspö and some near-surface groundwaters with very high sulphate contents. However, for the more saline waters (Cl > 0.2 mol/kg), only the combination of mixing and gypsum re-equilibrium (or equilibrium with respect to gypsum+calcite+celestite) reproduces the observed sulphate behaviour. Sulphate mass transfers associated with gypsum dissolution seem to be especially relevant for waters with chloride contents between 0.2 and 0.4 mol/kg and may modify up to one order of magnitude the contents attributable to conservative mixing.

Finally, some Na-SO_4 groundwaters (and pore waters) with traces of possible freezing-out process have been identified in the Laxemar-Simpevarp area at depths between 300 and 500 m. This important aspect must be verified and further studies are needed.

3.5 The silica system

Previous characterization studies of the Laxemar-Simpevarp area (Gimeno *et al.* 2004ab, 2006) already showed different behaviour of dissolved silica in the near-surface groundwaters and in the deep groundwaters. Dissolved silica contents in the near-surface groundwaters are mainly related to weathering and controlled by mineral reactions with no clear limiting equilibrium situations. On the contrary, dissolved silica in deep groundwaters seems to be generally controlled by equilibrium with respect to chalcedony (a silica phase more soluble than quartz).

The control of the concentration of dissolved silica in these low-temperature groundwaters, even in those with longer residence time, has been assigned to quite different phases and processes (Pitkänen *et al.* 1999, Glynn and Voss 1999). Therefore, a comparison with results from other crystalline systems is especially important here.

This section integrates all the available mineralogical information to better ascertain the factors and controls conditioning the silica contents in the Laxemar-Simpevarp groundwaters. In the following section the main results are presented, including an in-depth assessment of the major uncertainties and their effects on the obtained results (see also Appendix C, section C.3.3).

3.5.1 Hydrogeochemical data. General trends

Silica contents in the Laxemar-Simpevarp area are clearly different in the near surface and in the deep groundwaters (Figure 3-67). Near-surface groundwaters have very high silica contents and show a wide concentration range (from 0 to 75 mg/L; Figure 3.5.1 ab) while deeper and more saline groundwaters display much lower variability, with contents mostly between 4 and 11 mg/L, irrespective of salinity or depth.

Near-surface groundwaters

Chloride contents as high as 5,000 mg/L in some of the near-surface groundwaters from Laxemar-Simpevarp suggest a clear marine influence that may affect dissolved silica concentrations, decreasing or increasing the values attained by weathering.

Silica concentrations in surface Baltic seawaters around Simpevarp are very low, usually below 1 mg/L or less (Tröjbom and Söderbäck 2006ab) as in surface marine waters (Hem 1985). These low concentrations are due to the utilisation of silica by marine organisms (e.g. radiolaria and diatoms) to grow their skeletons (e.g. Blatt 1992). However, near-surface groundwaters affected by marine waters in contact with sediments rich in highly soluble diatom skeletons (made of amorphous silica) can have very high dissolved silica contents. This seems to be case for some near-surface groundwaters in SSM000242 or SSM000239 soil pipes with Cl between 2,480 and 3,570 mg/L and dissolved silica from 43 to 72.5 mg/L (Figure 3-67).

In order to avoid the effects of marine influence, only near-surface groundwaters with chloride contents lower than 200 mg/L will be considered when analysing the processes controlling dissolved silica in near-surface groundwaters (although the elimination of these waters does not affect significantly the range of silica contents).

Near-surface groundwaters from the overburden of similar systems (Forsmark, Olkiluoto and the Canadian Shield) also have a large variability (and some very high silica contents) compared with deeper groundwaters. The maximum silica concentrations in near-surface groundwaters from Forsmark reach 51 mg/L, although they are usually lower than 26 mg/L (Figure 3-68ab). Near-surface groundwaters in Palmottu and in the Canadian Shield reach values of 30 mg/L and 24 mg/L, respectively (Figure 3-68c). Groundwaters from the overburden in Olkiluoto peak at 25 mg/L (Pitkänen *et al.* 2004), but they are usually below 15 mg/L (Figure 3-68d).

Maximum silica contents in the near-surface groundwaters from the Laxemar-Simpevarp area are clearly higher than all these figures. In fact, Tröjbom and Söderbäck (2006a) indicate that the median silica content in the near-surface groundwaters from the Laxemar-Simpevarp area is double than in the near-surface groundwaters from the Forsmark area. Moreover, silica content in waters from lakes and streams in the Laxemar-Simpevarp area are about twice the level measured in most lakes and
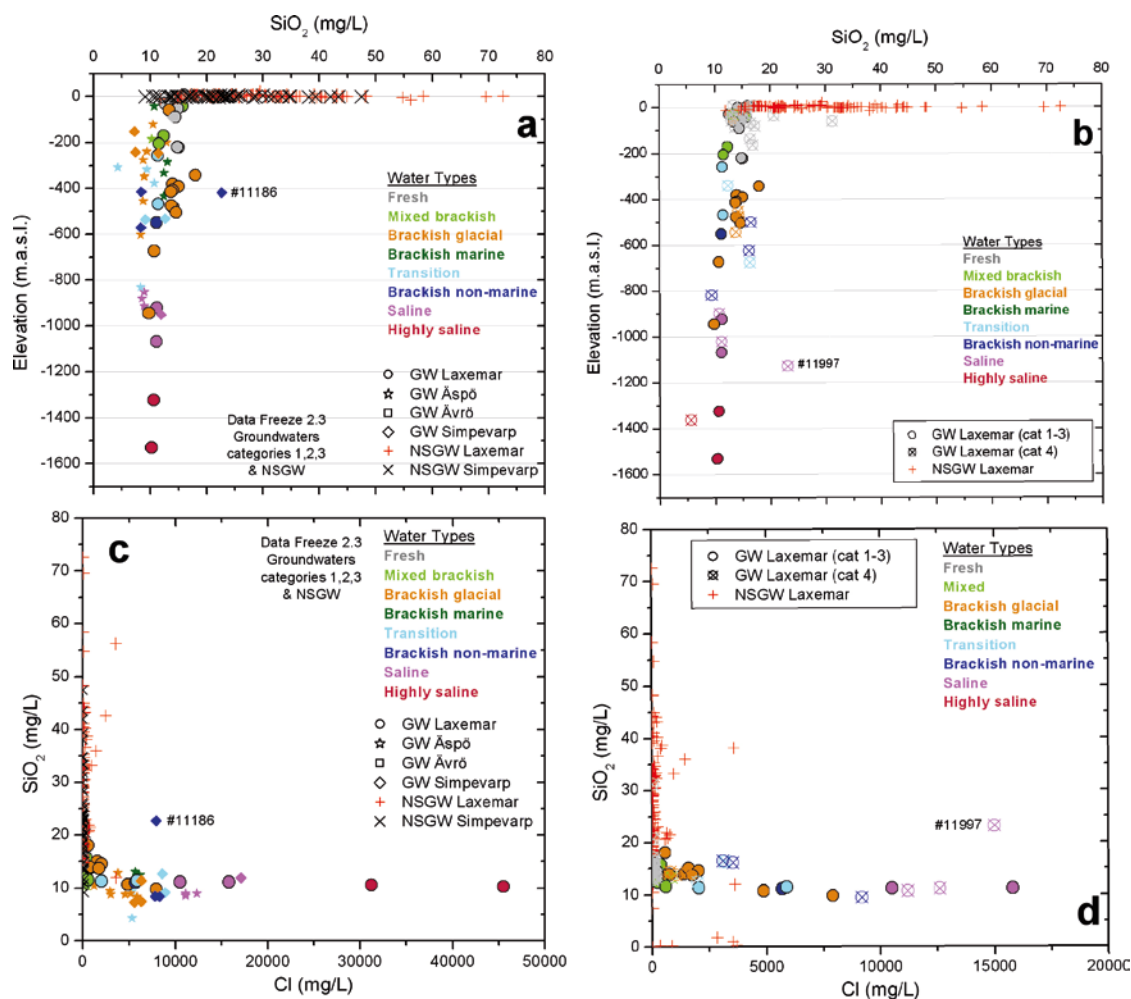
Figure 3-67. *Dissolved silica contents with respect to depth (a, b) and chloride concentration (c, d) in the groundwaters from Laxemar-Simpevarp (a, c) and from the Laxemar subarea alone (b, d). The low variability in the silica contents in the deep groundwaters is only broken by two samples: #11186 in KSH02 borehole at 418.66 m depth (Cl = 7,910 mg/L; plots a and c), and #11997 in KLX02 at 1,129.14 m depth (Cl = 15,000 mg/L; category 4; plots b and d) taken in 2006 and 2007 during the monitoring program. Both have twice the silica contents (around 21–25 mg/L) expected for their depth or chloride content. These values are much greater than the ones analysed before in the same sections. Moreover, the drilling water contents are very large (10.2 and 17.5%, respectively).Therefore, they can be considered "highly uncertain". Note that chloride concentrations are restricted to 20,000 mg/L (i.e. absence of highly saline groundwaters) in plot (d) for increased resolution at lower salinities in the Laxemar subarea.*

streams of Sweden. This suggests a more abundant presence of easily alterable silica phases (see section 3.5.2) and/or more intense weathering of the overburden. The latter interpretation is consistent with the high fluoride contents of these waters (see section 3.6).

Shallow and deep groundwaters

The analysis of dissolved silica trends in the shallow and deep groundwaters in the Laxemar-Simpevarp area shows that most groundwaters with Cl > 3,000 mg/L have silica concentrations around 10 mg/L (Figure 3-69a). A wider variability is evident in the shallowest groundwaters (from 10 to 18 mg/L SiO_2) and in the brackish groundwaters with Cl ~5,500 (from 5 to 13 mg/L SiO_2).

In general, the same behaviour is observed (Figure 3-68) in Forsmark, Olkiluoto, Palmottu (not shown) and the Canadian Shield. The most saline groundwaters (and/or with longest residence time) from all these systems tend to have dissolved silica contents relatively constant within the range 6.4–10.7 mg/L, as in the Laxemar-Simpevarp area.
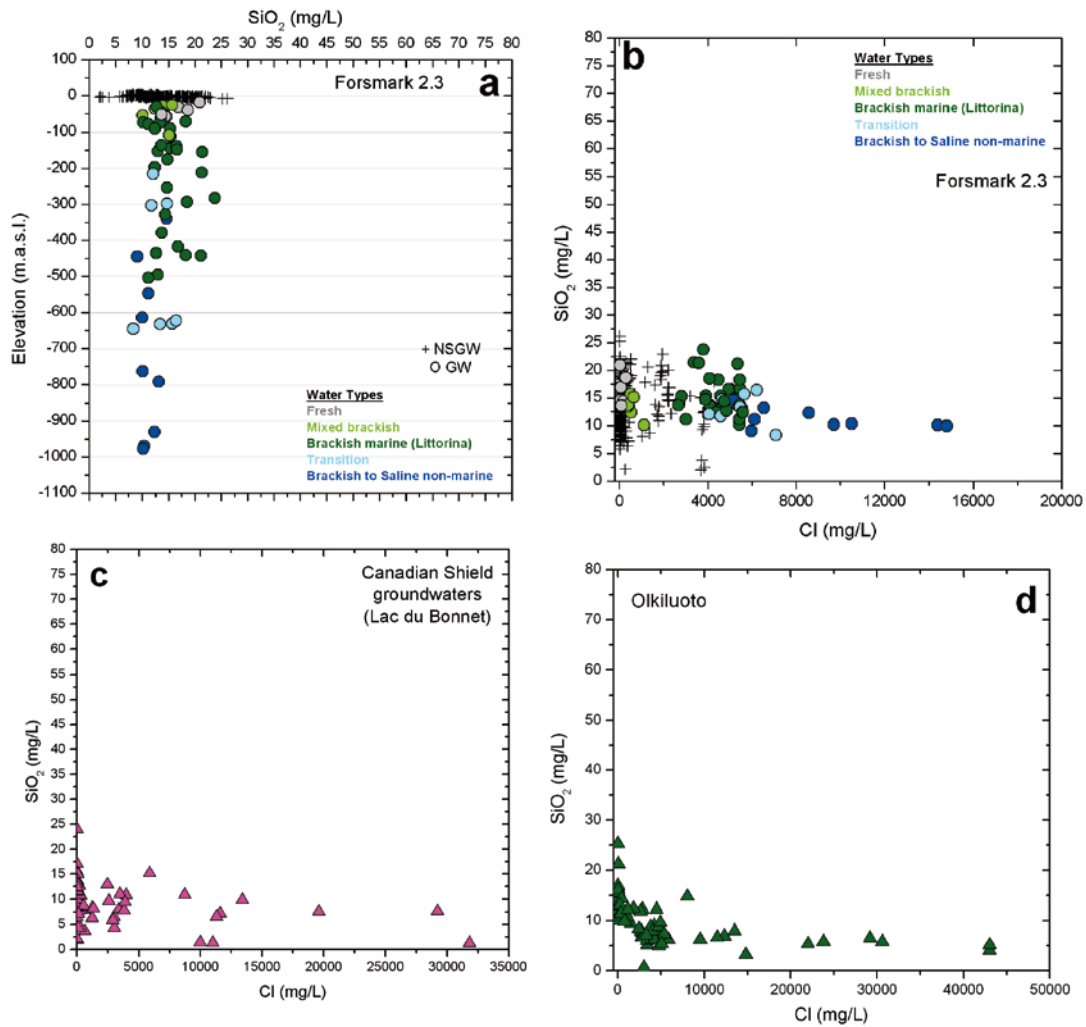
Figure 3-68. *Dissolved silica contents with respect to depth or chloride concentration in the groundwaters from Forsmark (a, b), Canadian Shield (Lac du Bonnet, Gascoyne, 2004; c) and Olkiluoto (Pitkänen et al. 2004) (d). Different chloride scales have been used where appropriate (b, c, d) to better visualise and describe the systems in question.*
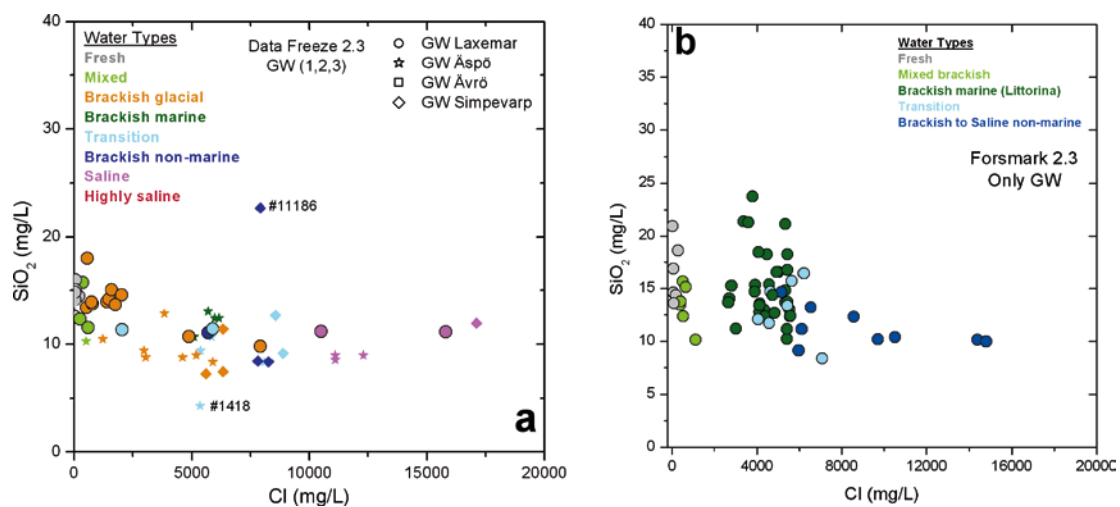
Figure 3-69. *Concentrations of dissolved silica versus chloride concentrations in the groundwaters from Laxemar-Simpevarp (a) and Forsmark (b). Only shallow and deep groundwaters up to 20,000 mg/L Cl are plotted (i.e. absence of highly saline groundwaters from the Laxemar subarea).*

The main difference between silica contents in Forsmark and Laxemar-Simpevarp is that the brackish groundwaters in Forsmark have the highest silica concentrations (up to 25 mg/L), increasing thus the variability range of silica contents (Figure 3-69b). These brackish groundwaters in Forsmark are characterised by an important Littorina contribution and display high and variable contents of total dissolved sulphate, Mg and Mn, inherited from their marine origin (Gimeno *et al.* 2008). In this context, the silica concentrations of these groundwaters can also be easily interpreted as an inherited character.

As already noted for the near-surface groundwaters, high silica concentrations can be acquired by marine waters when passing through bottom sediments with highly soluble diatom skeletons (made of amorphous silica). The dissolution of these skeletons may lead to dissolved silica concentrations as high as 60 mg/L, as seen in sediment pore waters from the present Baltic Sea (e.g. Carman and Rahm 1997). Diatom ooze and diatomaceous muds are frequently present in the Littorina sediments (Burke and Kemp 2002 and references therein) and, therefore, variable but high dissolved silica concentrations are expected in the Littorina marine waters recharging the groundwater system. As these silica-rich recharge waters flow through the bedrock, silica concentrations would decrease by reaction with the fracture filling minerals, especially with clays (e.g. McKenzie *et al.* 1967). However, in the Forsmark area it is clear that these reaction processes have not been able to eliminate the high dissolved silica contents, which remain as a fingerprint of an old mixing process.

In the Laxemar-Simpevarp area, brackish groundwaters with high dissolved silica concentrations (e.g. sample #11466 in KLX10 borehole with 3,610 mg/L Cl and 16.3 mg/L SiO_2) do have a small Littorina contribution, but other samples with higher Littorina mixing proportions in the Äspö and Simpevarp subareas have "normal" silica contents. Therefore, the Littorina imprint on silica seems to have been weaker and/or more easily eliminated (e.g. through sorption processes in fracture-filling clays) in the Laxemar-Simpevarp area.

The opposite effect on silica by "marine" influence can also be observed in some Laxemar-Simpevarp groundwaters. The lowest contents of dissolved silica have been found in KAS02 (Äspö; sample #1418; Figure 3-69a) at 307.68 m depth. This water, with Cl = 5,430 mg/L, has a silica concentration of 4 mg/L, detectable tritium and, in agreement with Glynn and Voss (1999), an important contribution of present Baltic marine waters with depleted silica concentrations due to biological extraction.

Overall, dissolved silica contents in the Laxemar-Simpevarp area (and in the rest of the systems considered above) do not show any kind of correlation with dissolved chloride (Figures 3-67, 3-68 and 3-69) which would indicate the presence of a mineralogical control as a source of this element in the near-surface groundwaters (through weathering reactions) and the presence of a limiting phase in the constant values found in the most saline (or with longer residence time) groundwaters.

3.5.2 Mineralogical data

The available mineralogical information for the overburden and fracture fillings is heterogeneous. Mineralogical data from the bedrock and Quaternary deposits in the overburden are very scarce and they have already been presented in Section 3.2.2. Mineralogical data from fracture fillings are much more abundant and only the most relevant information for the present discussion (mainly silica and clay minerals) has been considered here.

Overburden mineralogy

Quartz is the main mineralogical component in the bedrock and in the clay fraction and matrix of till deposits. It can be predicted that quartz proportions will increase in the future as weathering reactions dissolve the less resistant mineralogy (e.g. plagioclase, hornblende). Microcrystalline quartz, if present, can be a more suitable source of dissolved silica due to its higher solubility; but this source must be very limited as most near-surface groundwaters are oversaturated with respect to chalcedony (as a proxy to microcrystalline quartz).

Some beds of the examined gyttja clays in the overburden contain a significant amount of shells from siliceous fossils (diatoms). The content is so high that it affects the chemical and mineralogical properties of the gyttja clay (Lindborg 2006). Therefore, some contribution of this highly soluble silica polymorphs (amorphous silica) may explain, at least partially, the high dissolved silica concentrations found in the near-surface groundwaters from the Laxemar-Simpevarp area.

From a kinetic point of view, plagioclase and mafic minerals (e.g. biotite and hornblende) react significantly faster than quartz and K- feldspar in crystalline weathering environments (Goldich 1938, Lasaga 1984, White and Brantley 1995, White *et al.* 1998, 2001). Therefore, they should constitute the primary silica source for the near-surface groundwaters in the Laxemar-Simpevarp area.

Silica released from primary minerals is also controlled by the formation of secondary clay minerals. The typical alteration products of weathering in granitic environments, namely kaolinite, illite and vermiculite, have all been identified in the overburden. Kaolinite is usually the first and most common alteration product of aluminosilicate incongruent dissolution. Illitic clays may result from the weathering of micas and feldspars, and vermiculite can be the result of the degradation of biotite, hornblende and other clay minerals (e.g. chlorite or illite; see section 3.2.2). Therefore, all these mineralogical transformations may participate in the control of dissolved silica. This issue is revisited in more detail in section 3.5.3.

Fracture filling mineralogy

From the identified aluminosilicates in fracture fillings, clay minerals are the most probable products of silicate alteration by groundwaters. They may affect dissolved silica concentrations through different mechanisms. The identified clay minerals include mixed-layer clays (smectite/illite, chlorite/smectite, chlorite/vermiculite) that frequently occur in the most superficial fractures (Drake and Tullborg 2005). The relative abundance of clay minerals in open fractures is greater in the Laxemar subarea than in the Simpevarp subarea (see section 3.2.2 for a more detailed description). Moreover, these phases appear in the Laxemar subarea in all studied sections down to 1,000 m depth, whereas they are usually restricted to the upper 300 m in Simpevarp.

All these observations could suggest that the high proportions of clay minerals may be related to preferential groundwater recharge or active circulation paths, especially in the Laxemar subarea. However, this hypothesis must be verified as other explanations are possible.

Therefore, different water-rock interaction processes related to these mineral phases (incongruent dissolution of feldspars with formation of secondary clays, clay mineral transformations, and silica adsorption-desorption reactions in clays; e.g. Langmuir 1997 and references therein) can participate in the control of dissolved silica, at least in the dilute groundwaters of meteoric origin. The observed net effect of these processes is the progressive change of the contents of dissolved silica with depth (and residence time). The possible "final" control by a more stable solid silica phase in long residence groundwaters is difficult to corroborate with the available mineralogical data. Chalcedony (a fibrous microcrystalline quartz variety) has not been identified as a fracture filling mineral in the extensive mineralogical analysis performed neither in Laxemar-Simpevarp nor in Forsmark. The only silica phase identified in fractures is quartz, a ubiquitous mineral both in the granitic rocks and in the fracture mineralogy in the Laxemar-Simpevarp area (Drake and Tullborg 2004, 2005, 2006ab).

Although not in very large proportions with respect to the rest of the fracture minerals, quartz has been identified in the open fractures from Laxemar-Simpevarp at all examined depths (Drake *et al.* 2006). Its origin is hydrothermal, occurring in the early stages of the fracture filling sequence. Quartz usually occurs as coarse-grained idiomorphic crystals (100–200 μm; Figure 3-70), but the existence of polycrystalline, fine-grained quartz crystals has also been reported in fracture fillings and mylonitic zones (e.g. Drake and Tullborg 2005, 2006ab). It has also been identified in the clay mineral fraction used in XRD analyses for phyllosilicate identification and grain sizes of at least < 10 μm exist (Drake and Tullborg 2008). Therefore, quartz crystals have a large variation in grain sizes and, if these grain sizes are small enough, their solubility could reach that of chalcedony and control dissolved silica in groundwaters with longer residence times. This question is analysed in more detail later on.
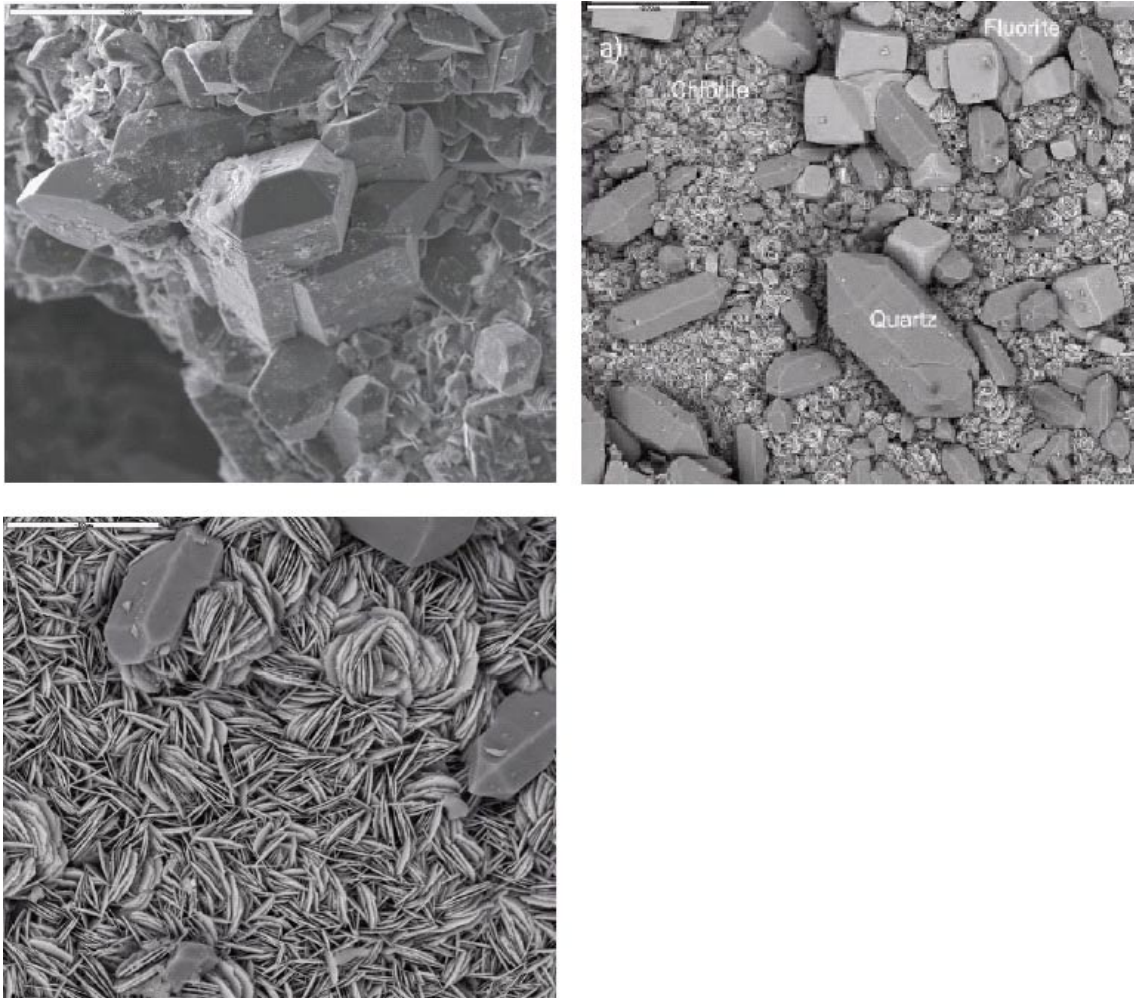
Figure 3-70. Some examples of common quartz crystals in the fracture fillings from the Laxemar-Simpevarp area. Upper left.-SEM image showing idiomorphic quartz crystals growing from the walls of a cavity. Scale bar is 200 µm. (from KA1755A borehole at 208.45–208 m, borehole length; taken from Drake and Tullborg 2005). Upper right.- Back-scattered SEM-images of cubic fluorite crystals, darker quartz crystals and platy, more fine-grained chlorite crystals. Scale bars are 200 µm. (from KKR2 borehole at 367.58–367.73 m, borehole length); and Lower left.- Back-scattered SEM-image of euhedral quartz crystals and platy, more fine-grained, Fe-rich chlorite crystals. Scale bar is 200 µm (surface coating sample in borehole KKR02 at 367.58–367.73 m, borehole length; taken from Drake and Tullborg 2006a)

3.5.3   Processes. Themodynamic approach

Detailed thermodynamic calculations are presented here in order to identify the main processes controlling dissolved silica contents in the Laxemar-Simpevarp groundwaters. As already noted, the general trend suggests the presence of a mineralogical control in the near-surface groundwaters (through weathering reactions) and a limiting phase in the more constant values found in the more saline groundwaters.

The speciation-solubility results presented here are focused on the saturation indices of quartz and chalcedony. The uncertainty range considered for both saturation indices is ± 0.25 SI units (Deutsch 1997).

Near-surface groundwaters

In weathering environments, dissolved silica is mainly controlled by the incongruent dissolution of aluminosilicates. Silica is released from primary minerals (mainly plagioclase and mafic minerals like hornblende) and partially incorporated into secondary clays. The net effect of these reactions on the dissolved silica concentrations depends on the type of the secondary mineral phase formed.

An assessment of the alteration products most likely participating in the control of dissolved silica can be made by using the mineral stability diagrams presented in section 3.2.3. These diagrams show that most fresh near-surface groundwaters fall in the kaolinite stability field (Figure 3-15), supporting the stability of this mineral phase. However, some of the near-surface groundwaters plot near the limit between Na-smectite and kaolinite (Figure 3-15a) and others reach the illite stability field (Figure 3-15b), suggesting also the participation of smectites and illite in the control of dissolved silica. All these results are in agreement with the available mineralogical information and with the general geochemical evolution of weathering in granitic systems.

Apart from the phases included in the activity diagrams, other clay minerals (e.g. vermiculite) and other processes (e.g. sorption-desorption) can participate in the control of dissolved silica in the near-surface groundwaters. The mineralogical analyses performed in the till samples from Simpevarp indicate a significant amount of vermiculite as a result of clay mineral alteration by chemical weathering (Sohlenius *et al.* 2006). Therefore, weathering-induced transformations from illite or chlorite (both present in the overburden) to vermiculite can also contribute to the concentration of dissolved silica.

Sorption-desorption processes involving fine-grained materials in the overburden can also participate in the control of dissolved silica. Surface reactions with clays and aluminium or ferric oxyhydroxides are common in soils (Langmuir 1997 and references therein). Although aluminium and ferric oxyhydroxides are not reported in the available mineralogical information, their presence in the system is very probable in the light of the type of soils that characterise the overburden at Laxemar-Simpevarp (peats, histosols, gleysols and podzols; Lundin *et al.* 2005).

Chalcedony and quartz saturation indices in the near-surface groundwaters (Figure 3-71a) indicate that most of the waters are oversaturated with respect to both phases (SI up to +0.8 for chalcedony and higher than +1.2 for quartz). Something similar is seen in Forsmark (Figure 3-70b) though the maximum degree of oversaturation is lower due to their lower silica contents.

The continuous increase in the oversaturation state with respect to chalcedony as silica increases indicates that it is not a solubility-limiting phase in the near surface environment from both areas. As near-surface groundwaters quickly reach saturation with respect to quartz and chalcedony during weathering, these phases cannot be an important source of dissolved silica.

The higher dissolved silica concentrations in the near-surface groundwaters from Laxemar-Simpevarp suggest the presence of more easily alterable silica phases and/or the existence of more intense weathering processes than in Forsmark or Olkiluoto. The available data on weathering rates (Figure 3-71) confirm that silicon and aluminium weathering rates in the Laxemar-Simpevarp area are faster than in the Forsmark area, which is consistent with the higher aluminium and silica contents found in the former (Figure 3-72). How these characters are conditioned by differences in the mineralogy, soil cover, vegetation, or other factors, merits further studies.
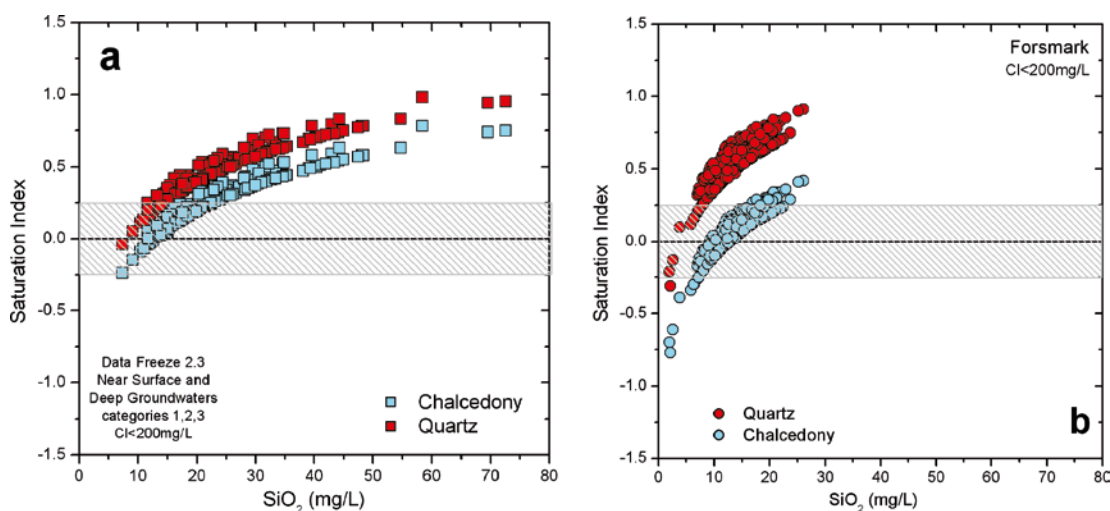
Figure 3-71. Quartz and chalcedony saturation indices vs. dissolved silica in the near-surface groundwaters from the Simpevarp (a) and Forsmark (b) areas. Only near-surface groundwaters with Cl⁻ concentrations below 200 mg/L are plotted. Dashed areas represent the uncertainty range.
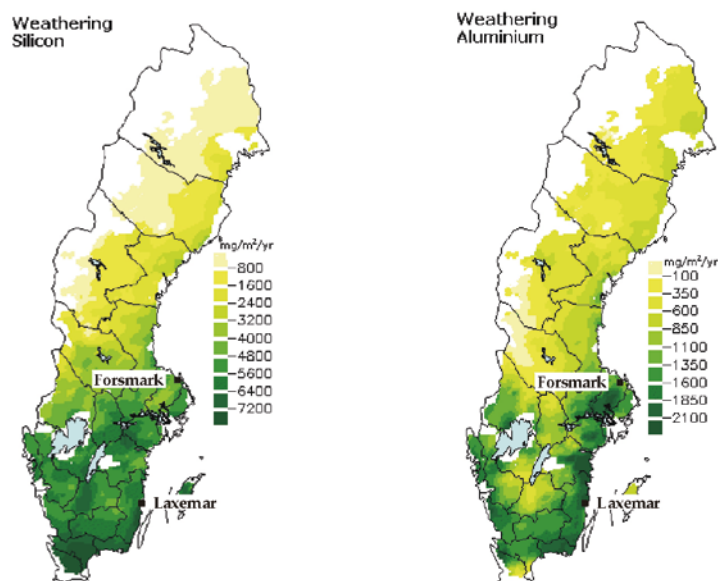
Figure 3-72. Weathering rates for silicon and aluminium (in mg/m2/year) in the Swedish soils. From MarkInfo database (created in the Department of Forest Soils, Swedish University of Agricultural Sciences, Uppsala; http://www-markinfo.slu.se/ eng/index.html; January, 2009).

Shallow and deep groundwaters

Although "marine" influences have been identified in some waters, the behaviour of silica in the shallow and deep groundwaters suggests an important solubility control. The differences reported previously in the distribution of dissolved silica between the near surface (overburden) and the deep groundwaters (Figure 3-67) are also reflected in the chalcedony saturation indices (Figures 3-73 and 3-74). Near-surface groundwaters display a greater variability and a greater degree of oversaturation than deep and more saline groundwaters, which tend to an apparent equilibrium with chalcedony irrespective of depth.

This apparent equilibrium situation is already present in the dilute groundwaters of meteoric origin (Cl < 200 mg/L) at very shallow depths and continue in the saline groundwaters affected by mixing at the same or greater depths. This supports the presence of a clear mineralogical control on dissolved silica through pure water-rock interaction or overlapped with mixing.

Most groundwaters in the Laxemar-Simpevarp area are in equilibrium with respect to chalcedony independent of their salinity (Figure 3-74a), as also occurs in Forsmark (Figure 3-74b) and in other "similar" crystalline environments such as Olkiluoto (Figure 3-74c) and Lac du Bonnet (Canada; Figure 3-74d).

The greater dispersion in the chalcedony SI values (around the considered uncertainty, ± 0.25 SI units) observed in the less saline groundwaters from all these systems (including Laxemar-Simpevarp) may be related to the superposition of other processes in the control of dissolved silica (e.g. aluminosilicate reactions and/or mixing processes like the previously mentioned "disturbance" induced by the Littorina mixing in Forsmark).

Chalcedony may not necessarily represent the mineral controlling dissolved silica concentrations, especially in dilute groundwaters. Feldspars and clay minerals in fracture fillings are probably involved in the control through incongruent dissolution reactions or surface processes whose net effect is to restrict the range of dissolved silica concentrations and the saturation state with respect to chalcedony as depth increases, especially in the most saline waters with longer residence times.
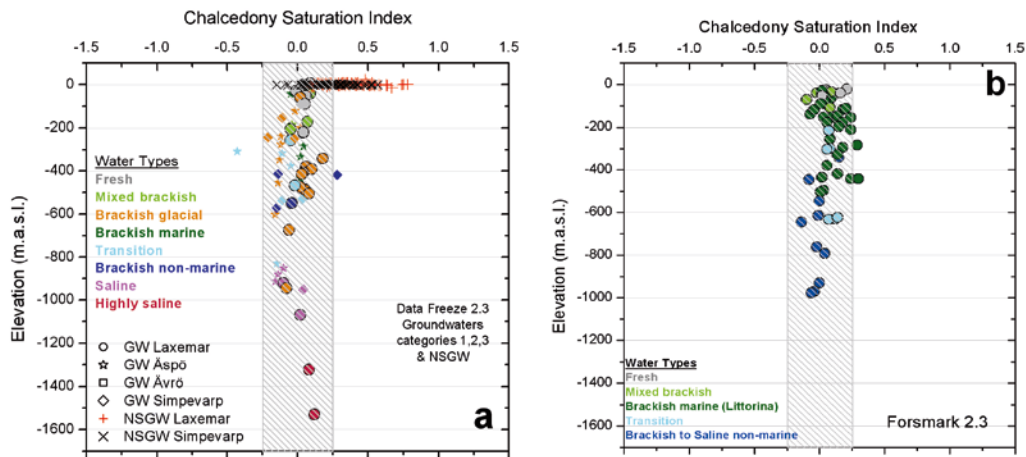
Figure 3-73. *Chalcedony saturation indices vs. depth for all groundwaters in Laxemar-Simpevarp (a), and for groundwaters from the Forsmark area (b). Dashed areas represent the uncertainty range.*
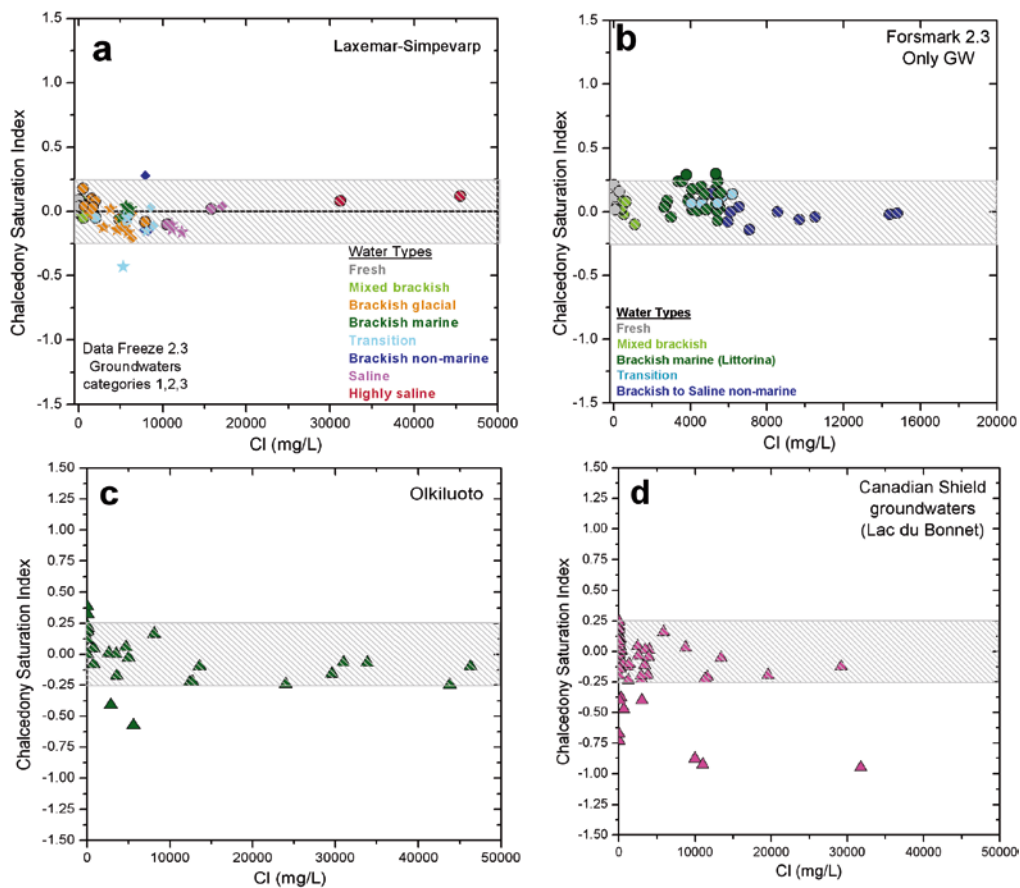
Figure 3-74. *Chalcedony saturation indices vs. chloride contents in the groundwaters from Laxemar-Simpevarp (a), Forsmark (b), Olkiluoto (c) and the Canadian Shield (d). Different chloride scale has been used for Forsmark (plot b) to better visualise and describe the samples. Data for speciation-solubility calculations for the Canadian waters have been taken from Gascoyne (2004) and for the Olkiluoto waters from Pitkänen et al. (1999, 2004). Near-surface groundwaters from Simpevarp and Forsmark zones have not been included. Dashed areas represent the uncertainty range.*

106

Similar apparent equilibrium situations with respect to chalcedony have also been described in other low-temperature systems (Banks *et al.* 2004, Neal *et al.* 2005, Banks and Frengstad 2006), including crystalline environments (Michard *et al.* 1996, Beaucaire *et al.* 1999, Iwatsuki *et al.* 2005). In any case, this equilibrium condition corresponds to (or is deduced from) real dissolved silica concentrations in the studied systems. Therefore, it is not unusual that the assumption of chalcedony equilibrium has also been successfully used in modelling the evolution of groundwaters in low-temperature crystalline systems (Beaucaire *et al.* 1999, Sasamoto *et al.* 2004), including Stripa (Grimaud *et al.* 1990) and Äspö groundwaters (Trotignon *et al.* 1999), without a detailed treatment of the underlying processes.

In all the described systems chalcedony SI approaches equilibrium for groundwaters with Cl > 8,000 mg/L, which correspond to very long residence-time groundwaters (around 1.5 million years as estimated from [36]Cl data in the Laxemar-Simpevarp and Forsmark areas; Louvat *et al.* 1999, Smellie *et al.* 2008). This trend strongly suggests the existence of a "true" equilibrium state with respect to chalcedony (or other silica phase with similar solubility).

Solubility calculations with respect to chalcedony can be interpreted in terms of this fibrous microcrystalline quartz variety (if it is present in the system; e.g. Mahlknecht *et al.* 2006) or, as it occurs in most cases, as a more general microcrystalline quartz phase (not necessarily fibrous), with enhanced solubility due to particle size effects (Heaney and Post 1992, Langmuir 1997). Therefore, to properly analyse this possible equilibrium situation, mineralogical information is needed together with a more detailed analysis of the uncertainties related to particle size on quartz and chalcedony solubility and thermodynamic data. These aspects are discussed next.

3.5.4   Solubility control in the deep groundwaters

The identification of dissolved silica control by equilibrium with SiO_2 phases (quartz or chalcedony) in low temperature systems raises the question about which is the real phase present in the system. Saturation indices indicate equilibrium with a mineral phase with that specific solubility (equilibrium constant) but not the specific type of silica mineral. The solubility identified corresponds to microcrystalline varieties of quartz but they have not been unequivocally found in the natural system. What has been reported is the presence of mega-quartz whose solubility (as it is included in most of the thermodynamic databases) is clearly lower, or microcrystalline varieties of quartz without a precise delimitation of particle size. But even these solubility values must be revisited, as "new" solubility data for quartz have been more recently proposed (Rimstidt 1997).

Therefore, apart from the difficulties related to the effects of the particle size, this problem is even more hampered due to the discrepancies in the thermodynamic data for these phases. These two issues are analysed next in more detail.

New quartz solubility data

The measurement of quartz solubility under low-temperature conditions (21 to 96 °C) by Rimstidt (1997) indicates a considerably greater solubility (log K = −3.746 or 11 ppm as SiO_2 at 25 °C) than previously reported and generally accepted (log K = −4 or 6 ppm of dissolved SiO_2). Although the experiments by Gunnarsson and Arnorsson (2000) seem to have confirmed the findings of Rimstidt (1997), this new solubility value has not generally been incorporated into the thermodynamic databases. Therefore, the consequences of this greater solubility of quartz on natural systems largely remain highly unexplored (a more detailed review of the available solubility data for these phases is presented in Appendix C, section C.3.3). This fact can be due to the difficulties of interpreting the slight differences between the solubility of quartz and chalcedony[20], the other polymorph usually invoked as a candidate in controlling dissolved silica concentrations. In line with this problem, the highly saline groundwaters from the Laxemar-Simpevarp area are possibly some of the low-temperature groundwaters with longest residence times ever analysed. This may offer a good opportunity to verify Rimstidt's (1997) solubility data in a closed system equilibrated with respect to quartz for very long (geological) periods of time.

---

[20] Solubility values for chalcedony in the literature are between 17. 9 and 11.2 mg/L SiO_2 (log K = −3.55 and –3.73) at 25 °C (see Appendix C, section C.3.3).

New speciation-solubility calculations have been performed with PHREEQC (Parkhurst and Appelo 1999) and the WATEQ4F database[21] (Ball and Nordstrom 2001) using the solubility data for quartz proposed by Rimstidt (1997) for the whole set of groundwaters in the Laxemar-Simpevarp and other areas. Results (using both the original solubility data included in WATEQ4F database, and the "new" data from Rimstidt 1997) for the Laxemar-Simpevarp and the Olkiluoto groundwaters are shown in Figure 3-75. Chalcedony saturation indices are also included for comparison.

It is apparent from the figure that the results obtained with the data proposed by Rimstidt (1997) indicate quartz equilibrium in groundwaters with Cl > 15,000 mg/L in both sites. The new saturation indices are just in between those of chalcedony (slightly more soluble) and quartz with the original solubility (slightly less soluble). The difference between the new solubility constant for quartz and the other two is small and within the uncertainty range considered for them.

Although not shown in the plot, calculations were also performed with the Forsmark groundwaters and the groundwaters from the Canadian Shield (Gascoyne 2004) with similar results: groundwaters with higher salinities are in equilibrium with respect to quartz (with Rimstidt's solubility constant) and chalcedony.

Additional data taking into account grain size are necessary to discriminate between both possibilities (control by quartz or chalcedony). As stated above, grain sizes < 10 μm have been identified in the Laxemar-Simpevarp area. The question is whether these grain sizes are indicative of the presence of (mega) quartz or microcrystalline quartz (chalcedony) as the solubility limiting phase.

Microcrystalline quartz (chalcedony) has a greater solubility than (mega)quartz. The "critical" particle size or specific surface at which important changes in solubility occur can be theoretically estimated (Appendix D), The calculations have been performed at 25 °C using a free energy of interface of 3.5×10^{-5} J/cm^2, a molar volume of 22.688 cm^3/mol for quartz (Parks 1984) and considering different roughness factors (1, 2, 5 and 10) in order to include the effects associated with the intrinsic morphological complexity of the mineral.
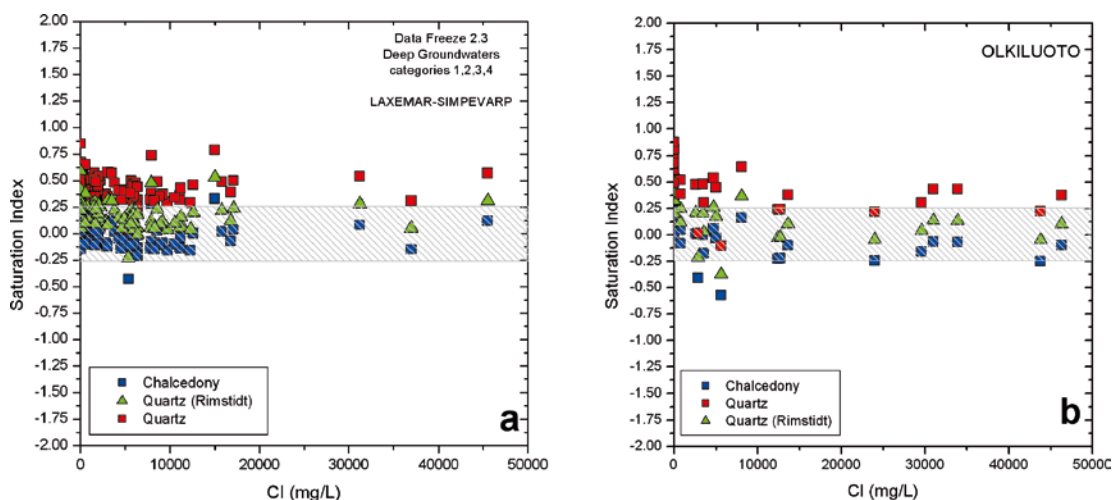
Figure 3-75. Saturation indices with respect to quartz (with the solubility values proposed by Rimstidt, 1997 and with the original values included in the WATEQ4F database) and chalcedony (with the values included in the WATEQ4F database) vs. the chloride contents of the groundwaters from Laxemar-Simpevarp (a) and Olkiluoto (b). Dashed areas indicate the uncertainty range.

---

[21] However the groundwaters of particular interest in this problem are those with greater salinities (as representative of longer residence times). Therefore, the approach used to calculate aqueous silica activity coefficients in WATEQ4F database could be an additional source of uncertainty on the obtained results. This question has been analysed in detail in Appendix B, where it has been proven that the results obtained with the WATEQ4F database are the same as those obtained with the Pitzer approach, *a priori* the most suitable approach for the activity coefficient calculations in these kind of saline solutions.

Figure 3-76 shows that the effect of particle size on solubility is negligible for values larger than 1 μm (10^{-4} cm). However, for particle sizes smaller than 10^{-5} cm the effect might be relevant and its magnitude is directly related to particle roughness (surface area). Theoretical calculations (Appendix D) also show that the microcrystalline quartz involved in the possible control of dissolved silica must have a particle size of 15 nm. Therefore, if chalcedony is responsible for the dissolved silica control in the long residence time groundwaters, it should have this particle size. This size is much smaller than sizes detected in the mineralogical analysis performed to date in the fracture fillings, but its existence cannot be definitively discarded.

However, microcrystalline quartz constituted by small particle sizes tends to re-crystallise, forming larger particles that minimize the excess of Gibbs free energy associated with the solid-water interface. Although this ripening process can be very slow, most Palaeozoic microcrystalline quartz grains in sedimentary rocks have reached crystal sizes larger than 1 μm (Maliva and Siever 1988a, Blatt 1992). As fracture fillings in the Simpevarp and Forsmark areas are of that age or even older, it seems that the present existence of microcrystalline quartz with small particle sizes is not feasible.

Therefore, equilibrium with respect to quartz could be considered as the simpler hypothesis for the deep saline groundwaters from Simpevarp. Similar equilibrium situations have been identified in long residence groundwaters from other crystalline systems (Forsmark, Olkiluoto, Canadian Shield) and it is easier to assume a common control by the ubiquitous mega-quartz instead of a control by a non clearly identified microcrystalline phase and with similar particle size (or solubility) in all these systems. Even though the possible control of the silica contents by quartz instead of by chalcedony in the waters with longer residence time is conceptually relevant, their solubility values are so similar that any of them could be used for predictive calculations.

3.5.5 Conclusions

Two different regimes with respect to the dissolved silica contents and their controls have been identified in Laxemar-Simpevarp groundwaters: one for the near-surface groundwaters and the other for the deeper groundwaters. Near-surface groundwaters display a wide concentration range and the greatest contents of dissolved silica. Deeper groundwaters have a much narrower range of silica concentrations, reaching nearly constant values for the deeper and more saline groundwaters.

Dissolved silica concentrations are not correlated with chloride contents, which would indicate the presence of a mineralogical control as a source of this element (through weathering reactions) in the near-surface groundwaters, or as a limiting phase of the more constant values found in the deeper groundwaters with longer residence time and affected or not by mixing. Therefore, dissolved silica represents a typical reactive component whose control is kinetically or thermodynamically determined by different kinds of heterogeneous processes, possibly overlapped with mixing.
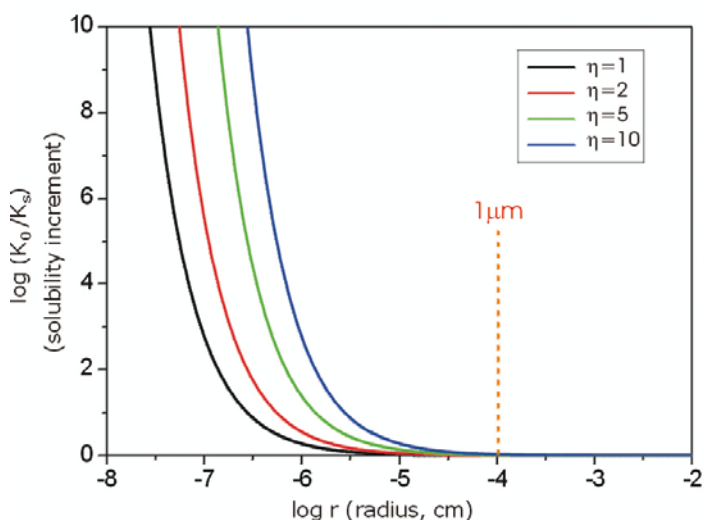
Figure 3-76. *Solubility increment as a function of the radii of ideally spherical particles of quartz. The different curves represent different roughness factors (η). See text for details.*

Silica contents in the near-surface groundwaters are mainly controlled by aluminosilicate weathering reactions. Silica released from primary minerals is partially incorporated into secondary clays and the net effect on the concentration of dissolved silica depends on the type of secondary mineral phase. Plagioclase, hornblende and biotite must constitute the primary silica source for the near-surface groundwaters in the Laxemar-Simpevarp area, as they react significantly faster than the rest of the identified minerals. The released silica is partially incorporated into weathering products, such as kaolinite, smectite, illite and/or vermiculite.

Mineralogical studies performed in the Laxemar subarea indicate the occurrence of high proportions of clay minerals (smectite/illite, chlorite/smectite, chlorite/vermiculite) in open and conductive fractures. The proportion of clay is much higher than that observed in the Simpevarp subarea, which is logical considering the hydrological recharge character of the Laxemar subarea, with dilute groundwaters reacting and reaching greater depths. Moreover, sorption-desorption reactions with fine-grained materials in the overburden (clays and aluminium or ferric oxyhydroxides) and, especially in some of the soils present in the Simpevarp area, can also participate in regulating the dissolved silica concentrations of some near-surface groundwaters.

The mean content (and the greatest values) of dissolved silica in the near-surface groundwaters from the Laxemar-Simpevarp area is larger than in similar waters from other areas (e.g. Forsmark). Lakes and stream waters from this area have twice as much dissolved silica than most Swedish lakes and streams (Tröjbom and Söderbäck 2006a). These observations are in agreement with the faster silica weathering rate in the soils of the Laxemar-Simpevarp area and they indicate the existence of intense weathering in this zone.

The behaviour of dissolved silica changes drastically in deeper groundwaters. At shallow depths the range of silica contents narrows considerably to values around 10 mg/L both in dilute groundwaters and in saline waters affected by mixing. This suggests the predominance of water-rock interaction processes buffering silica concentrations. This predominance has been favoured by the absence of other types of disturbances promoted by the input of marine waters with "extreme" silica contents (as in Forsmark where important inputs of Littorina waters have promoted significant increases in the silica contents, still evident at present time).

As a consequence of the limited dissolved silica variability, most of the groundwaters in the Laxemar-Simpevarp area are in equilibrium or near equilibrium (within the considered uncertainty range of ± 0.25 SI units) with respect to chalcedony or other silica variety with similar solubility. The question of what is the mineral phase controlling the silica solubility in these systems has been carefully evaluated taking into account uncertainties in the thermodynamic data for quartz and chalcedony and the effects of particle size on solubility (quartz *vs.* microcrystalline quartz or chalcedony; see also Appendix C, section C.3.3). The results obtained support a control of dissolved silica by quartz with the "new" solubility data proposed by Rimstidt (1997). As far as we know, these long residence time groundwaters are "the best case" so far supporting a quartz solubility control under low temperature conditions.

Although the control of dissolved silica by chalcedony equilibrium (or other silica phase with similar solubility) has been proposed in other low temperature systems, this silica phase does not necessarily represent the mineral controlling the concentrations of dissolved silica in the dilute groundwaters from the Laxemar subarea. In fact, other water-rock interaction processes related to clays (incongruent dissolution of feldspars, clay mineral transformations, silica adsorption-desorption reactions in clays, etc) may participate in the control of dissolved silica at least in the dilute groundwaters of recent meteoric origin. In any case, the net effect of these heterogeneous processes is the progressive restriction of the dissolved silica range with depth (and residence time).

With respect to the deeper and more saline groundwaters (Cl > 8,000 mg/L), chalcedony or quartz (with the new solubility data) approach equilibrium and similar trends have been reported for Forsmark and Olkiluoto. These saline samples correspond to very long residence-time groundwaters (around 1.5 million years estimated from ^{36}Cl data for groundwaters in Simpevarp and Forsmark areas; Louvat *et al.* 1999, Smellie *et al.* 2008). The old age of these waters strongly suggest the existence of a "true" equilibrium state with respect to a silica phase with this solubility.

The possible control of the silica contents by quartz instead of by chalcedony in the waters with longer residence time, is conceptually important. However, the solubility values for both polymorphs are very similar and, from a pragmatic point of view, any of them could be used for predictive calculations.

3.6 Fluoride system

The analysis of the fluoride system in the Laxemar-Simpevarp area started in the first SDM (Gimeno *et al.* 2004a). However, the amount of available information was then very scarce, especially related to the mineralogy and the dissolved contents in the shallowest groundwaters. Although there are still some important gaps, the information relevant to the study of the fluoride system has increased in the last few years, allowing a more detailed analysis of the evolution of fluoride during mixing and water-rock interaction. The following is a comprehensive analysis of the fluoride system, integrating all the available hydrogeochemical and mineralogical data, and also different geochemical simulations.

3.6.1 Hydrogeochemical data. General trends

Fluoride contents in the Simpevarp-Laxemar area groundwaters are very variable, ranging from 0.2 to 5 mg/L in the near-surface groundwaters and from 1 to 7 mg/L (Figures 3-77ac) in the dilute groundwaters (< 200 m depth).

Although peak values are large compared with other natural systems, they are within the reported range for waters in crystalline rocks. For instance, maximum fluoride contents of around 6.7 mg/L have been reported in the dilute shallow groundwaters of the Canadian Shield (Gascoyne 2004), and values up to 12 mg/L were measured in the Stripa groundwaters (Nordstrom *et al.* 1985), being the most frequent concentration range in shallow groundwaters between 3 and 5 mg/L.

In the Forsmark area, however, the highest fluoride contents (also found in the near surface and shallow groundwaters) only reach 2.5 mg/L (Figure 3-77b, d), and in Lake Finnsjön they are around 3.5 mg/L. The maximum reported in the shallow groundwaters from the overburden in Olkiluoto (~0.8 mg/L; Pitkänen *et al.* 2004) and Palmottu (0.35 mg/L; Blomqvist *et al.* 2000) are even lower.

Therefore, the high fluoride contents in the near surface and shallow groundwaters from Laxemar-Simpevarp are significant in a regional context. In fact, Tröjbom and Söderbäck (2006a) indicate that fluoride concentrations in soil tubes and excavated wells in the Laxemar-Simpevarp area are five times larger than in most excavated wells in Sweden.

Fluoride concentrations in waters from crystalline superficial environments are strongly controlled by the presence of fluoride-bearing minerals and their weathering rates (Frengstad *et al.* 2001, Kim and Yeong 2005)[22]. Thus, the high fluoride concentrations in the near-surface groundwaters from the Laxemar-Simpevarp area suggest the occurrence of either an abundant source of fluoride or an especially intense weathering of the overburden.

As salinity (Cl concentrations) increases in Laxemar-Simpevarp groundwaters, fluoride variability decreases. For chloride contents higher than 5,000 mg/L, fluoride concentrations are always between 1 and 2 mg/L (Figure 3-77c), as also happens in the Forsmark area (Figure 3-77d) and in Finnsjön groundwaters (not shown).

The narrow range of dissolved fluoride in the saline groundwaters, together with the lack of correlation between fluoride and chloride, suggest the existence of a *"mineral solubility control"* on dissolved fluoride in the groundwaters with long residence times.

Therefore, dissolved fluoride concentrations in the Simpevarp and Forsmark groundwaters seem to be controlled by *mineral reaction-controlling processes:* a) as a kinetically-controlled source of fluoride in the shallowest groundwaters with the shortest residence times; and b) as a dissolved fluoride limitant, through equilibrium situations (alone or superimposed on mixing) in the long residence time groundwaters.

---

[22] In fact, fluoride concentrations are used to estimate the weathering rates of some fluoride-bearing minerals like biotite (Navarre-Sitchler and Thyne 2007).
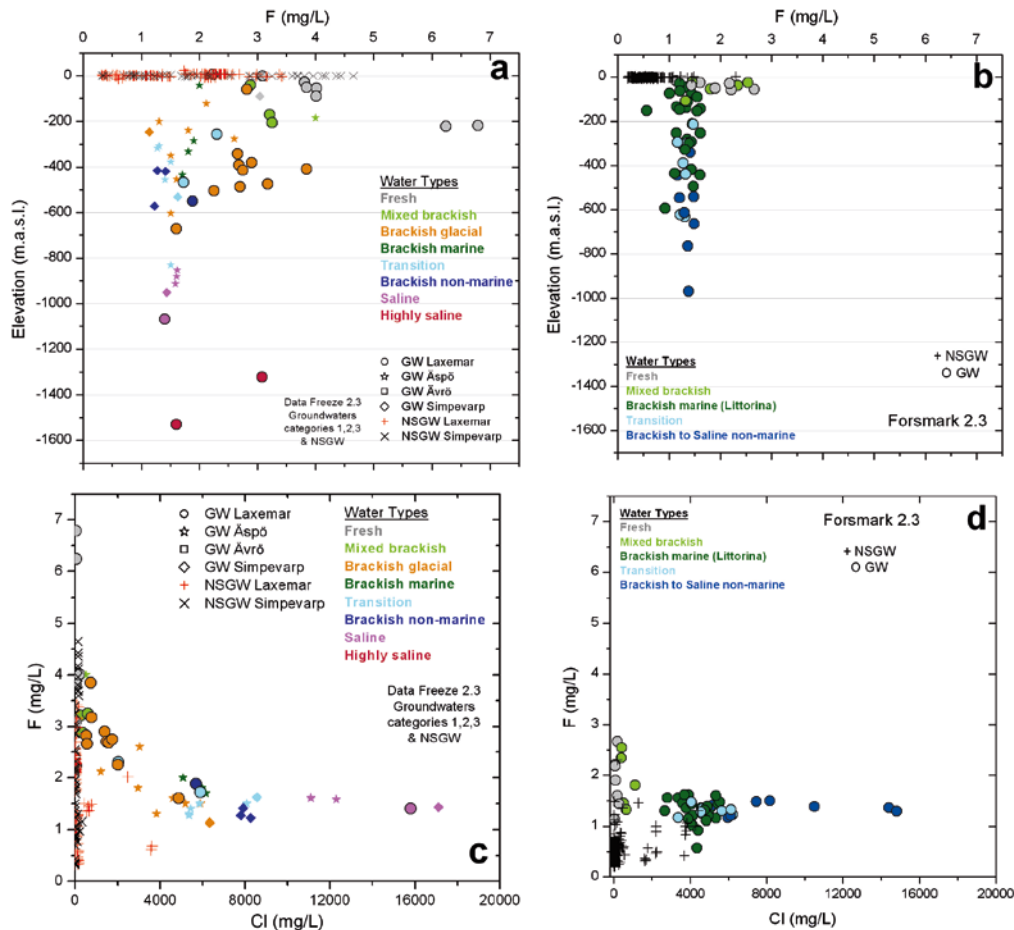
Figure 3-77. *Fluoride contents with respect to depth (a, b) and chloride (c, d) in the Simpevarp (ac) and Forsmark (b, d) area groundwaters, including the near-surface groundwaters. Only shallow and deep groundwaters up to 20,000 mg/L Cl are plotted (i.e. absence of highly saline groundwaters from the Laxemar subarea) in plots c and d.*

3.6.2   Mineralogical data

Fluorite (CaF_2) has generally been considered as the dominant source of dissolved fluoride in groundwaters, especially in crystalline terrains (Deshmukh *et al.* 1995, Saxena and Ahmed 2001). Rock-forming minerals such as amphiboles (e.g. hornblende) and micas (muscovite, biotite) , may contain large amounts of fluorine in their OH^- structural sites (Nordstrom *et al.* 1989, Jacks *et al.* 2005, Chae *et al.* 2006, 2007) and may contribute to the fluoride content in groundwaters. Apatite is another common mineral in crystalline rocks that may contain F.

Overburden

Scarce mineralogical information (and no analytical data of fluoride contents) is available from the Quaternary deposits and the soils in the Laxemar-Simpevarp area. The mineralogical studies by Sohlenius *et al.* (2006) have already been presented in section 3.2.2. There, at least two mineral fluoride sources have been identified: hornblende and micas (keeping aside the anthropogenic sources, such as burning of coal, extraction of aluminium, steel industries or phosphatic fertilizers). Weathering of these minerals may constitute a direct fluoride source for the near-surface groundwaters and also for exchangeable and easily leachable fluoride in clays. Furthermore, all the till samples analysed contain significant amounts of vermiculite, suggesting the existence of clay mineral alteration by chemical weathering (Sohlenius *et al.* 2006) and, therefore, a possible secondary source of fluoride.

Fluorite has been identified as a fracture filling mineral at very shallow levels in the Laxemar-Simpevarp area (see below) and this mineral may represent an additional source of fluoride for the near-surface groundwaters in this area. The observed differences in the contents of dissolved fluoride between the near-surface groundwaters from the Laxemar-Simpevarp and Forsmark areas could be related to this source (fluorite has not been systematically identified in Forsmark). Moreover, variations in the relative content of minerals like biotite and hornblende can also induce significant local changes in the chemistry of soil water, as indicated by Akselsson *et al.* (2006). Clearly, more studies are needed to better constrain this issue.

Fracture fillings

Fluorite has not been identified in the overburden, but this mineral is present in fractures (Figure 3-78) at very different depths, including the shallowest part of the system. For example, fluorite has been identified in the Äspö subarea (KAS04 borehole) at 70 and 185 m borehole section (Drake and Tullborg 2005); in the Laxemar subarea (KLX02 borehole) at 948 m borehole section and also in the ongoing studies of KLX03 and KLX04 boreholes (Drake and Tullborg 2005); and in the Simpevarp subarea (KSH01A borehole at 11, 24, 131, 208, 363, 793, 873 m borehole sections, and KSH03A borehole at 111, 177, 233 and 271 m borehole sections; Drake and Tullborg 2004, 2006a). Fluorite is also frequently found at different depths in the fracture fillings of the Götemar granite (Drake and Tullborg 2006b).
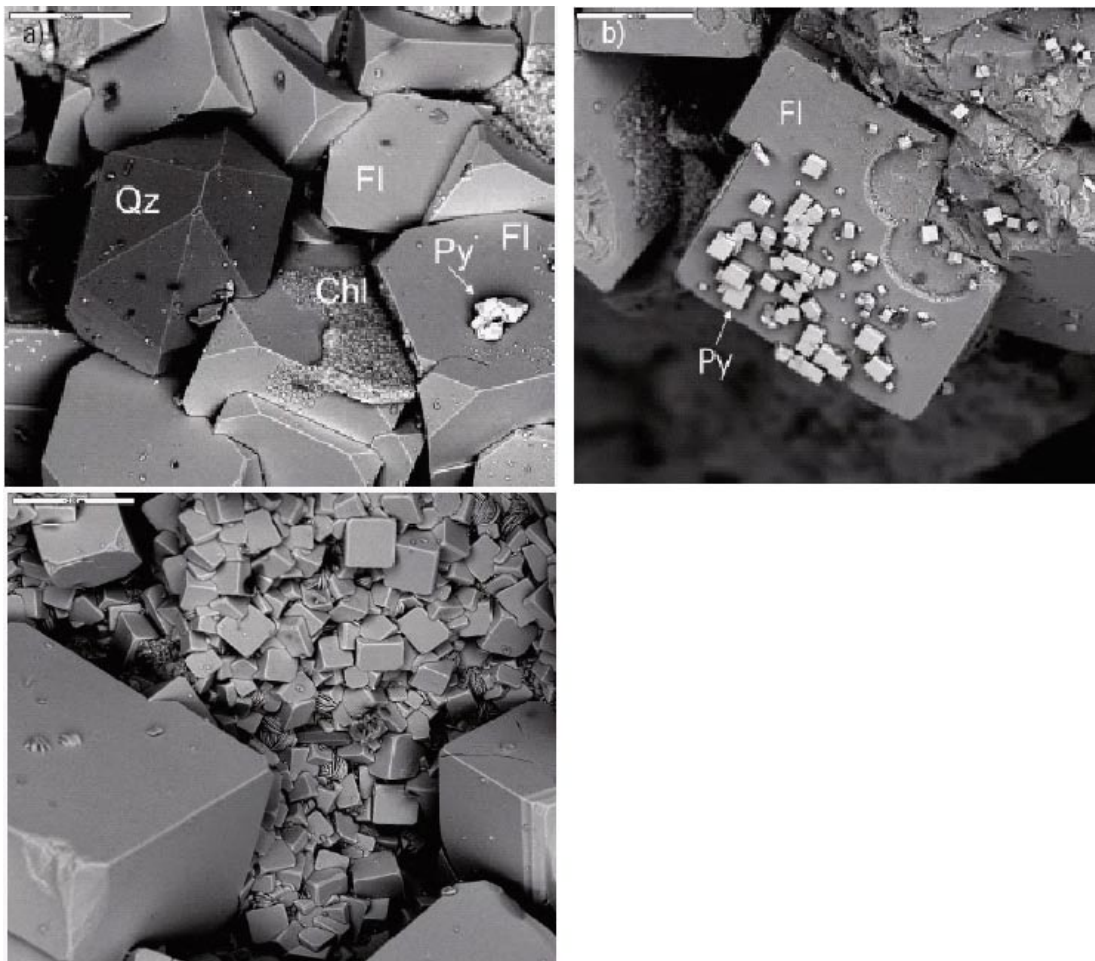
Figure 3-78. *Back-scattered SEM-images of euhedral fluorite (Fl) in fracture fillings. Upper pictures.- Cubic fluorite crystals (Fl) and quartz (Qz only in left) with cubic crystals of pyrite (Py) and a thin cover of chlorite (Chl) on the crystal surfaces. Samples from KKR3 at 54.83–54.86 m, borehole section, and from KKR at 539.04–539.12 m, borehole section. Lower picture.- Euhedral fluorite crystals of variable size in the surface of fracture fillings (KKR03 at 258 m borehole section). Scale bars are 200 µm. Taken from Drake and Tullborg (2006a).*

Drake *et al.* (2006) have estimated that fluorite represents between 0.2 and 0.6% of the fracture minerals (in open and sealed fractures) in the Simpevarp and Laxemar subareas. In open fractures with an aperture ≥ 1 mm, fluorite proportions slightly increase to 0.5 and 3% in Simpevarp and Laxemar, respectively.

Even though these proportions are small, they are much greater than in the Forsmark site, where fluorite has only sporadically been identified (Petersson *et al.* 2004, Sandström *et al.* 2004, Sandström and Tullborg 2005). Fluorite genesis in these areas is associated with several old hydrothermal episodes (as old as 405 ± 27 Ma; Drake and Tullborg 2006a) and it has been available in the system to participate in subsequent interaction processes with different groundwaters.

3.6.3 Processes. Thermodynamic approach

Fluorite is a key mineral to understand the behaviour of dissolved fluoride in crystalline groundwaters (Nordstrom and Jenne 1977, Nordstrom *et al.* 1989; Iwatsuki *et al.* 2005, Chae *et al.* 2007). Therefore, the speciation-solubility calculations presented here are focused on the saturation index of this mineral (the uncertainty range of the saturation index is ± 0.5 SI units; Nordstrom and Jenne 1977, Hem 1985).

Near-surface groundwaters

Fresh near-surface groundwaters have very variable values of the fluorite saturation index (Figure 3-79a). This is consistent with the fact that fluoride and calcium are incorporated in waters in the overburden as a result of weathering of F- and Ca-bearing minerals (aluminosilicates, calcite or fluorite).

The effects of weathering can be estimated from Si-HCO_3^-, and Si-F^- graphs (Figure 3-79bc). As both HCO_3^- and F^- increase as a consequence of mineral dissolution, undersaturation decreases, eventually reaching fluorite equilibrium. The effect of heterogeneity in the dissolution of fluoride sources is also evident from the important variability in the SI values (from undersaturation to equilibrium).

Apart from mineral dissolution, other processes occurring in this weathering environment can contribute to the increase in dissolved fluoride. The near-surface groundwaters with the highest fluoride contents also contain the highest Na concentrations (Figure 3-80a) and usually the lowest Ca concentrations (Figure 3-80b). This suggests that cation exchange may contribute to the increase in dissolved fluoride concentrations. Moreover, as these F-rich near-surface groundwaters have high pH values (Figure 3-80c) and, therefore, high OH^- concentrations, under these conditions the replacement of exchangeable F^- in fluoride-bearing hydroxy-minerals is favoured, increasing thus the F^- content in groundwaters (e.g. Guo *et al.* 2007).

The combined effect of this weathering process eventually drives an important number of near-surface groundwaters to fluorite equilibrium. This equilibrium is then maintained independently of further increases in the concentration of dissolved fluoride (Figure 3-79c), indicating that fluorite equilibrium contributes to the control of dissolved fluoride and calcium in spite of the short residence time of these waters. Therefore, fluoride derived from weathering reactions could be re-precipitating as fluorite at present.

Calcite would also participate in the control of dissolved calcium contents (Figure 3-79d) and, therefore, a clear relationship between pH, alkalinity, calcium and fluoride is established and controlled by both calcite and fluorite in some of the near-surface groundwaters (Nordstrom and Jenne 1977).

Groundwaters

The transition between the near surface and the deeper groundwaters in the Laxemar-Simpevarp area is characterised by a homogenisation of the fluoride contents, evident from 600 m depth down (Figure 3-77a). In comparison, groundwaters in Forsmark already display very constant F^- concentrations at 200 m depth (Figure 3-77b).
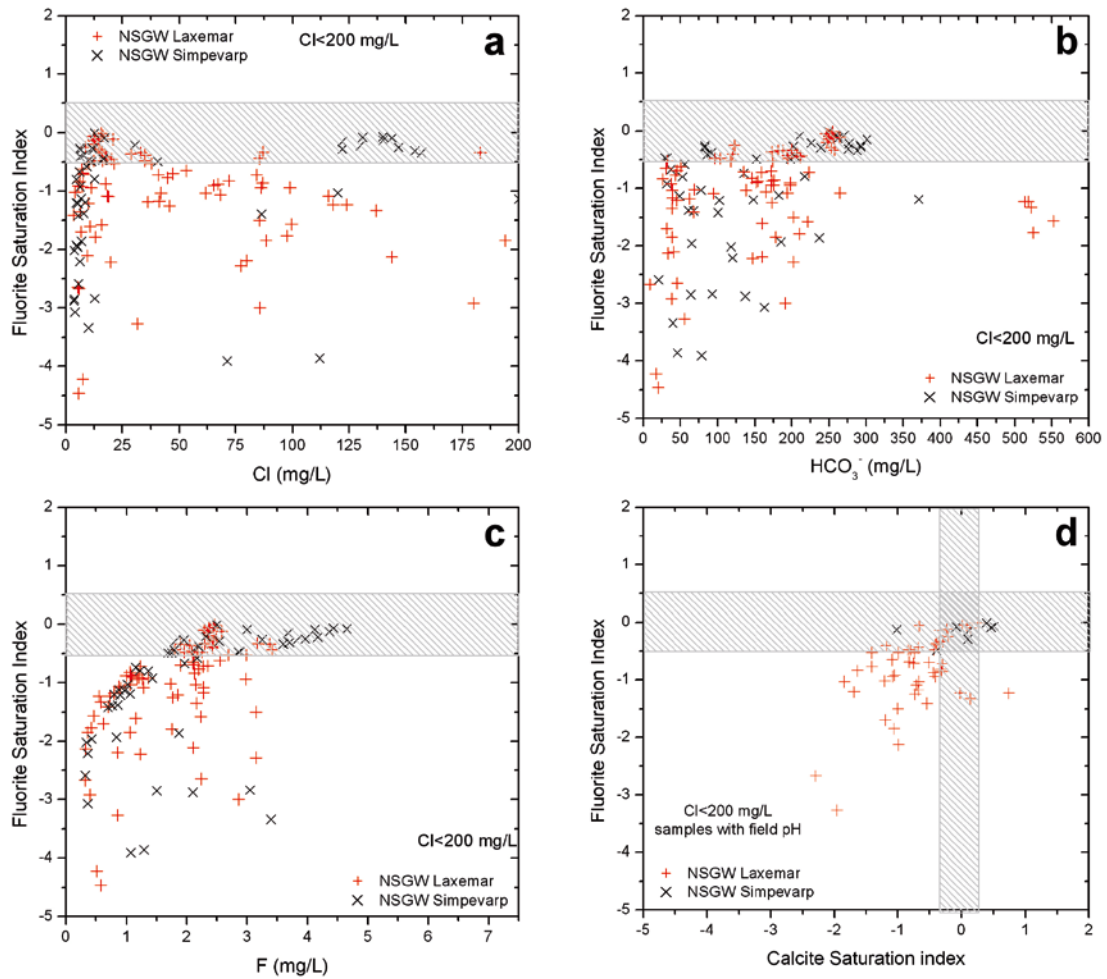
***Figure 3-79.** Fluorite saturation indices with respect to chloride (a), bicarbonate (b), fluoride (c) and calcite saturation index (d) in the fresh near-surface groundwaters with Cl < 200 mg/L from the Laxemar-Simpevarp area. Only waters with field pH measurements were used for plot (d). Dashed areas in plot d correspond to the uncertainty ranges (±0.5 for fluorite and ±0.3 for calcite).*

The existence of very dilute groundwaters (less than 500 mg/L Cl⁻) down to 700 m in the Laxemar-Simpevarp area is well correlated with the variability in fluoride contents down to this depth (in Forsmark, conversely, dilute groundwaters are restricted to shallower levels and "old" brackish-saline groundwaters are found at greater depths).

Independent of this variability, most of the dilute groundwaters in the 100–1,000 m depth range (i.e. with variable residence times) are in equilibrium or near equilibrium with respect to fluorite (Figure 3-81a). This indicates that water-rock interaction is responsible for the equilibrium in those dilute groundwaters that have not suffered significant mixing with more saline groundwaters. Fluorite saturation indices remain close to equilibrium in groundwaters with higher chloride contents (and thus affected by mixing with more saline groundwaters), as also happens in Forsmark (Figure 3-81b).

Fluorite SI values display a trend towards relatively constant values around +1.0 for water salinities between 15,000 mg/L Cl (Figure 3-82a) and 45,000 mg/L Cl (the Deep Saline end-member). This behaviour is also observed in Forsmark (Figure 3-82b), the Canadian Shield (Figure 3-82c), Olkiluoto (Figure 3-82d) and Stripa (Nordstrom *et al.* 1985).
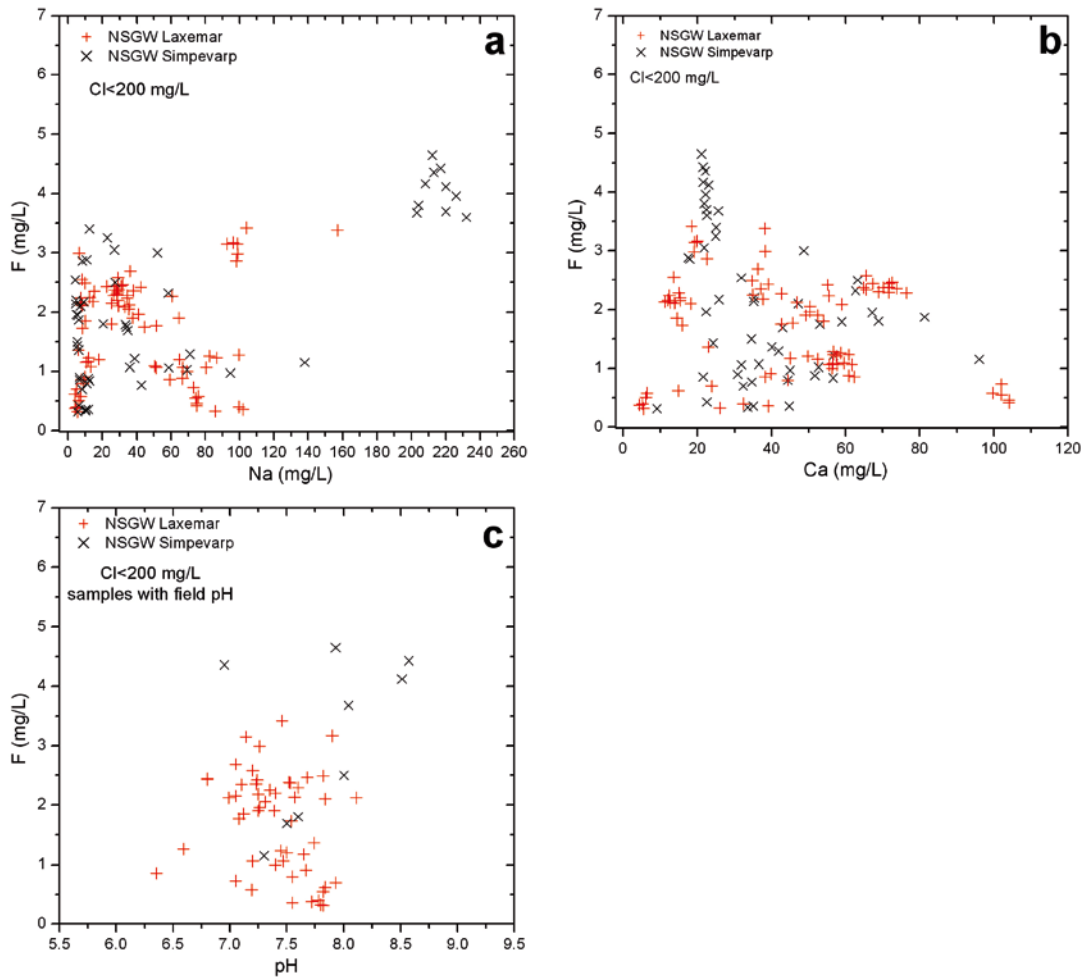
Figure 3-80. *Fluoride contents vs. sodium (a), calcium (b) and pH (c) in the fresh near-surface groundwaters (Cl < 200 mg/L) with field pH data from the Laxemar-Simpevarp area.*
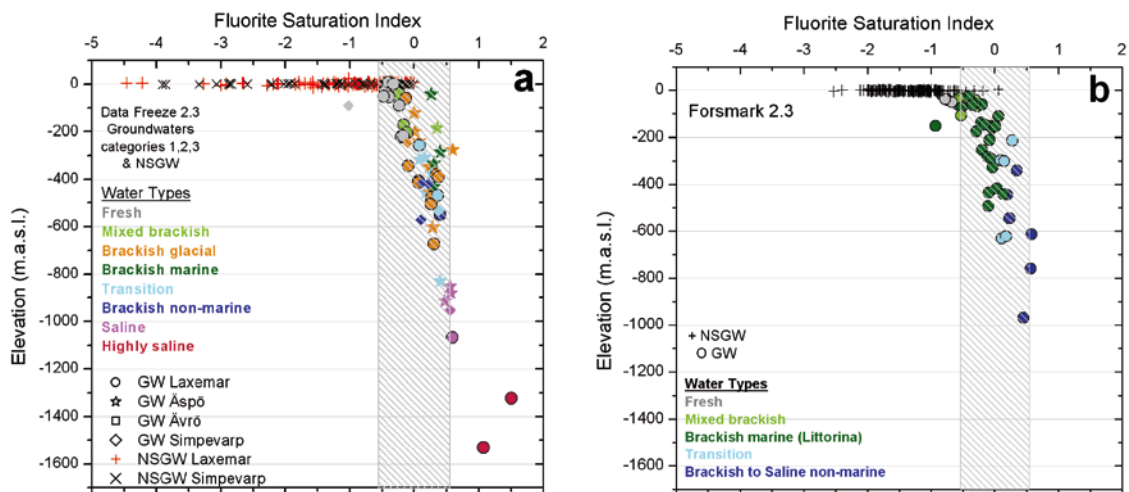
Figure 3-81. *Fluorite saturation index vs. depth in the groundwaters from the Laxemar-Simpevarp (a) and Forsmark (b) areas. Data from near surface and deep groundwaters are included. Dashed areas indicate the uncertainty range.*

Some authors (Nordstrom and Ball 1989, Glynn and Voss 1999) suggest that this oversaturation state is real, putting forward the same reasons as for calcite (section 3.3.4). However, the equilibrium constant for fluorite is not as well known as for calcite. The difference among equilibrium constants in the different thermodynamic databases is around 0.6 log K units[23], and it can be up to one logarithmic unit when considering the values presented in modern reviews on fluorite solubility (see Garand and Mucci 2004).

The uncertainty usually assigned to the fluorite saturation index is ± 0.5 units (taken into account not only the thermodynamic uncertainties, but also the analytical ones). However, if only the K-value variability is considered, the uncertainty should be larger. In fact, other authors have used ±1.0 unit as the SI uncertainty of this phase (e.g. Iwatsuki *et al.* 2005). In the latter case, all reported SI values in the range ±1.0 could be considered as equilibrium situations (Figure 3-82).
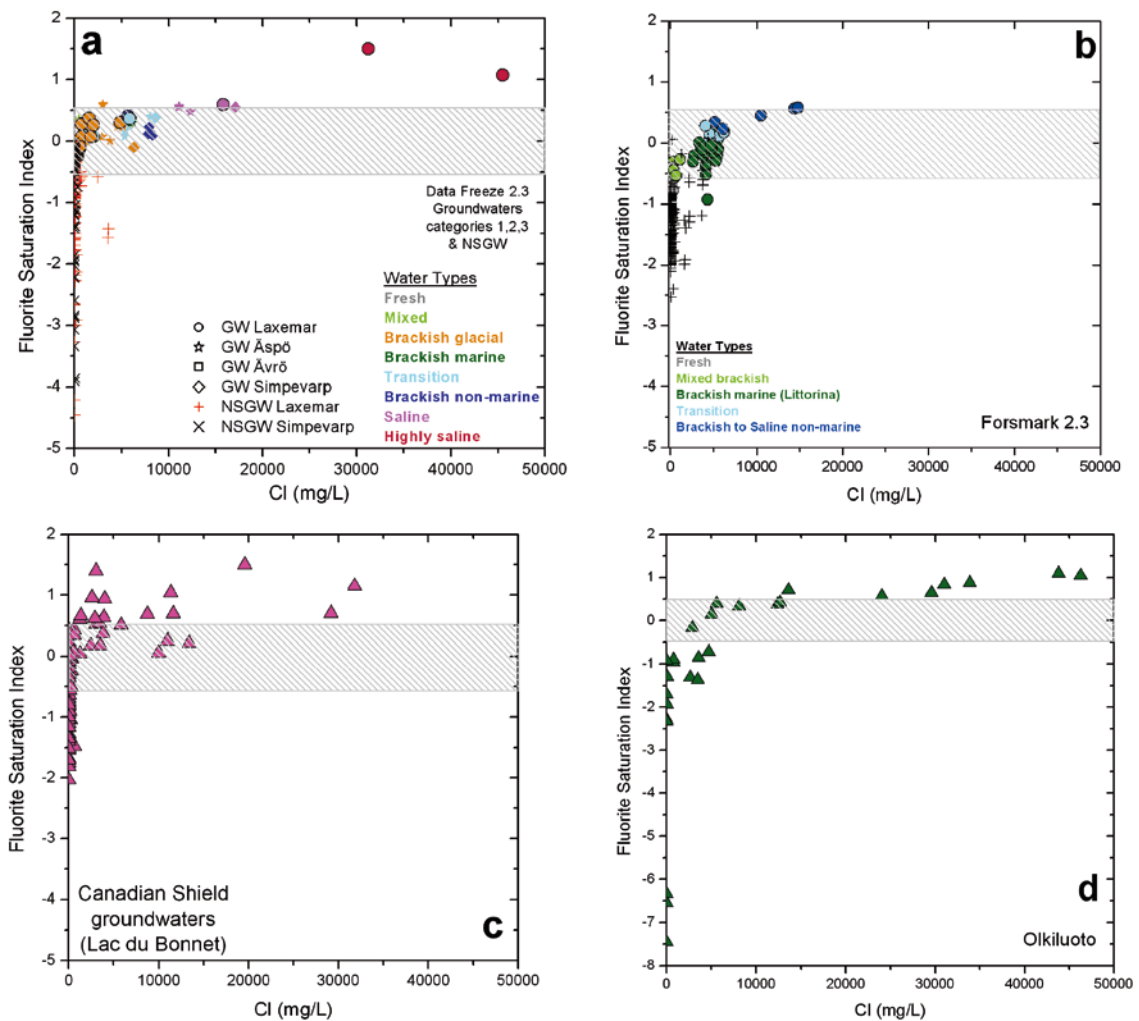
Figure 3-82. Fluorite saturation index vs. Cl concentrations in the groundwaters from Simpevarp (a), Forsmark (b), Canadian Shield (c) and Olkiluoto (d). The scale has been change in plot (d) to better visualise the undersaturation state of the dilute groundwaters. Dashed lines represent the uncertainty associated with SI calculations (Nordstrom and Jenne 1977). Data for speciation-solubility calculations with the Canadian Shield and the Olkiluoto groundwaters have been taken from Gascoyne (2004) and Pitkänen et al. (1999, 2004), respectively.

---

[23] The value at 25°C in the WATEQ4F database used here is log K = −10.6, from Nordstrom *et al.* (1990), while the value considered in SUPCRT 92 (Johnson *et al.* 1992), in the data0.com v8r6 database from EQ3/6 (Wolery and Daveler 1992) or in LLNL database (also distributed with PHREEQC) is log K = −10.03.

At any rate, as highlighted by Nordstrom *et al.* (1985, 1989), the constant values for the fluorite saturation index (slightly oversaturated or in equilibrium) in groundwaters with very different compositions suggest an effective fluorite solubility control on dissolved fluoride concentrations, control that would be extensive to groundwaters affected by mixing processes. In the Laxemar-Simpevarp area, for instance, it would affect the more saline waters from the Laxemar subarea, characterised by a wide range of mixing proportions with the Deep Saline end-member. How this control works through fluorite precipitation-dissolution processes is explored in the next section.

3.6.4 Thermodynamic simulations

Fluorite equilibrium in groundwaters from crystalline systems dominated by pure water-rock interaction processes is considered to be reached mainly by fluorite precipitation (e.g. Nordstrom *et al.* 1985, 1989, Iwatsuki *et al.* 2005). However, in the most saline groundwaters from the Laxemar-Simpevarp area (Cl concentrations from 9,000–10,000 to 45,000 mg/L) fluorite control is superimposed onto the mixing between the Deep Saline end-member and some old groundwaters of meteoric-glacial origin. Under these mixing conditions, fluorite equilibrium can be reached through precipitation or dissolution depending on the proportion of each mixed water (due to the non-linear behaviour of the saturation state during mixing).

In order to assess these processes, different simulations have been carried out by using the end members considered in type 1 simulation (see section 3.2.4), that is, a mixture of the Glacial end member and the highly saline sample #2731. In order to better visualize the effects of mixing on the saturation state of the waters, sample #2731 has been previously equilibrated with fluorite. Since fluoride concentrations in the Glacial end member are not known, four different scenarios have been evaluated:

- negligible dissolved F and undersaturation with respect to fluorite (spheres in Figure 3-83);
- initial fixed undersaturation with SI= −1.5 (F=7.12×10^{-5} mol/kg = 1.85 mg/L; squares) and SI=−2.5 (F=2.38×10^{-5} mol/kg = 0.45 mg/L; triangles in Figure 3-83); and,
- equilibrium with respect to fluorite before mixing (F=3.13×10^{-4} mol/kg = 5.94 mg/L; circles in Figure 3-83).

Dissolved fluoride contents in the dilute end-member obtained under these conditions span almost the whole range of concentrations measured in the real dilute groundwaters in the system (from 0 to 3.3×10^{-4} mol/kg; values in Figure 3-83b at Cl=0 mol/kg).

Additional mixing and reaction simulations have also been carried out by equilibrating the mixed waters with calcite (to check its influence on the fluorite saturation index) or with fluorite (to check the effect on the fluoride content).

Results are rather sensitive to the saturation state and initial fluoride contents in the dilute end-member (Glacial; Figure 3-83ab). On the contrary, the effect of equilibration with calcite is negligible (not shown).

As shown in Figure 3-83a, only when dissolved fluoride is very low in the dilute end-member (spheres), mixing leads to undersaturation with respect to fluorite. Therefore, fluorite dissolution is needed to reach present equilibrium.

In the simulation starting with a fluorite saturation index of −2.5 (squares) in the dilute end-member, the non-linear effect due to mixing produce equilibrium with respect to fluorite in the saline waters, and with a saturation index of −1.5, (numerical) oversaturation is obtained for almost all mixing proportions (triangles). This result is magnified in the last simulation, where equilibrium with fluorite in the dilute end-member has been imposed (circles). In these cases, the evolution during mixing would imply the precipitation of fluorite.

Taking into account the *measured* fluoride contents, the participation of dilute groundwaters with very low (or zero) fluoride concentration in the mixing with saline waters is unlikely. As *calculated* fluoride contents are similar to the ones found in old glacial (or cold meteoric) waters in Sweden (from 1.6 to 5.5 mg/L) and in recent Glacial waters (see Appendix F), the most likely scenario is that mixing of deep saline groundwaters with dilute ones in the Laxemar subarea produced fluorite precipitation.

Fluorite re-equilibrium after mixing (simulated in Figure 3-83b, magenta spheres) modifies the concentration of fluoride, stabilizing its value as it happens in the natural system. However, as observed in the gypsum re-equilibrium process, this re-equilibrium after mixing does not significantly changes the concentration of dissolved calcium, which is basically controlled by mixing.
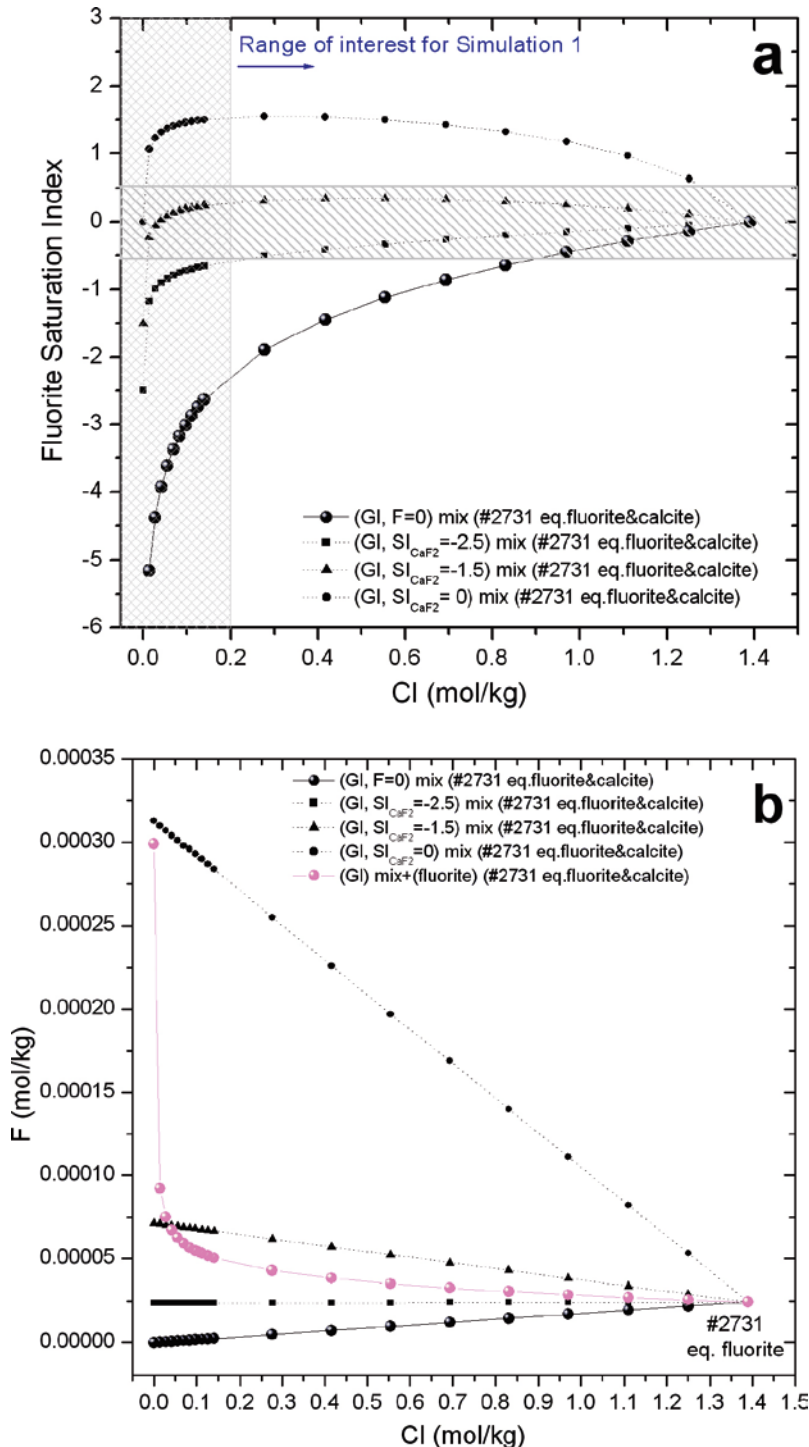
Figure 3-83. *Results of fluorite saturation index (a) and fluoride concentrations (b) with respect to Cl contents for mixing simulations between Glacial and #2731 end members in different simulations (conservative mixing and mixing and reaction). Dashed area indicates the uncertainty range.*

3.6.5 Conclusions

Fluoride contents in the Simpevarp groundwaters seem to be mainly conditioned by mineralogical controls both as sources (through dissolution processes) and as solubility limiting phases (through equilibrium situation with respect to fluorite).

Fluoride contents in the near surface and shallow groundwaters are very high (and variable) due to the weathering and dissolution of F-bearing minerals such as hornblende, micas or fluorite present in the overburden or in fracture fillings at very shallow levels. As a result, waters reach fluorite saturation, and fluoride derived from weathering reactions can be re-precipitating at present as fluorite in some points. Eventually, calcite can also be involved in the control of dissolved calcium in these near-surface groundwaters. Deeper groundwaters in the Laxemar subarea, still dilute but with longer residence times, have less variable fluoride contents, also controlled by fluorite.

Finally, mineralogical control by fluorite is as well effective during all the mixing processes affecting this system. In the case of mixing between old dilute and the most saline waters, different degrees of oversaturation with respect to fluorite in the mixed waters are reached, eventually provoking its precipitation and keeping the control of dissolved fluoride.

Therefore, there is a generalised fluorite control on the concentrations of dissolved fluoride in the Laxemar-Simpevarp area groundwaters. This control superimposes onto the control that calcite exerts on dissolved calcium, giving rise to a clear relationship between pH, alkalinity, calcium contents and fluoride contents.

3.7 Additional mixing and mass balance calculations with M3

As previously reported in earlier SDM reports, the geochemical study of the Laxemar-Simpevarp and Forsmark groundwaters has confirmed the existence of (at least) four end member waters: an old deep saline water, an old marine water (ancient Littorina Sea), a modern meteoric water (Altered Meteoric), and a glacial melt-water. As a result, mixing can be considered the prime irreversible process responsible for the chemical evolution of the Simpevarp and Forsmark groundwater systems. The successive disequilibrium states resulting from mixing conditioned the subsequent water-rock interaction processes and, hence, the re-equilibration pathways of the mixed groundwaters.

However, in the case of the Laxemar-Simpevarp area, the presence of the Littorina end member is much less important as these waters have already been flushed out (see Appendix F). Moreover, in this area, and mainly in the Laxemar subarea, the effects of reactions are more important than in Forsmark. For instance, an especially important component affected by several reactions in the Laxemar-Simpevarp area is dissolved sulphate (section 3.4), which was mainly controlled by mixing (with Littorina) at Forsmark. These two special features (lower Littorina influence and higher effects from reactions) have conditioned the use of the M3 program and a special analysis has been performed here to take reactions into account.

The main purpose of the modelling work presented here is to obtain the contribution of each end member to the chemical composition of every water parcel in the system. Once the first-order effect of mixing has been taken into account via the mixing proportions, water-rock interaction can be used to explain the remaining variability. However, there are many sources of uncertainty that can prevent the accurate calculation of the mixing proportions of a mixing-dominated system (Gómez *et al.* 2008), the type and intensity of the chemical reactions that have taken place on top of, and as a consequence of mixing being the most critical.

The modifications introduced in some elements by the chemical reactions produce deviations in the mixing proportions calculated by M3. These deviations can be more or less important depending on the type of reaction, its extent, and the type of water involved, all unknowns in a study with real water samples.

The uncertainty analysis performed by Gómez *et al.* (2008) concluded that the noise introduced by the reactions (unknown *a priori*) in any study with real waters may produce important effects on the calculated mixing proportions and, therefore, M3 mixing proportions should not be used without first checking their ability to predict conservative elements (that is, elements not involved in chemical reactions).

Nevertheless, once the mixing proportions are calculated, mass balances, also provided by the code (with respect to the conservative elements, especially chloride), can easily help to detect those samples in which reactions have produced a distortion of the calculated mixing proportions.

This analysis (mass balance analysis) has been made using the four end members (Deep Saline, Glacial, Littorina and Altered Meteoric) and the standard set of elements (Na, K, Ca, Mg, HCO$_3$, SO$_4$, Cl, δ^2H and δ^{18}O; Gurban 2008). Then, the alternative suggested by Gómez *et al.* (2008) of using M3 only with those elements that behave conservatively in each system has been used here. The analysis consists in comparing the concentrations of conservative elements found in the systems and the concentrations obtained from the mixing proportions obtained with M3. As the conservative elements are not affected by reactions, the calculated values should be identical to the values measured in the real samples. This approach offers the possibility of obtaining quantitative and reliable mixing proportions and it is very useful when combined with additional methodologies (e.g. classical mass balance and inverse modelling with PHREEQC or similar codes).

Among all the elements used as standard input compositional variables (Na, K, Ca, Mg, HCO$_3$, SO$_4$, Cl, δ^2H and δ^{18}O) only three of them (Cl, δ^2H and δ^{18}O) have an a priori conservative behaviour. However, δ^2H and δ^{18}O are not independent and therefore, an additional conservative element, bromide[24], has been selected. The problem is that the principal component analysis that starts the calculation procedure in M3 needs the number of compositional variables to be equal to or greater than the number of end members (Gómez *et al.* 2008). In all the previous works performed at Forsmark and Laxemar-Simpevarp areas four end members (Deep Saline, Glacial, Littorina and Altered Meteoric) have been used. However, the lack of important Littorina remnants in the Laxemar-Simpevarp area in general, and in Laxemar subarea in particular, allows the use of only three end members: Deep Saline, Glacial and Altered Meteoric. Therefore, with three end members, at least three conservative elements are needed.

3.7.1 Uncertainty analysis

Simulations

Simulations with 3 and 4 end members have been performed:

- Three end members: Deep Saline (DS), Glacial (δ^{18}O = −21‰) (Gl21), and Altered Meteoric (HLX28).

- Four end members: DS, Gl21, HLX28, and Littorina (Litt).

Three different sets of input compositional variables have been used:

- The "standard" set (i.e. Na, K, Ca, Mg, HCO$_3^-$, Cl, SO$_4^{2-}$, δ^2H, and δ^{18}O).

- The standard set without SO$_4^{2-}$.

- The conservative elements Cl, Br, δ^2H, and δ^{18}O.

Combining the two sets of end members with the three sets of input compositional variables, a total of 6 different simulations have been performed. In all simulations an allowance of 0.03 has been used (Gómez *et al.* 2008). The chemical composition for the end members is presented in Table 3-3.

---

[24] Although known that Br is not always a conservative element, its correlation with chloride in the representative samples from Laxemar-Simpevarp is very good (r = 0.989) and therefore, significant deviations from a conservative behaviour are not expected.

Table 3-3. Chemical characterization of the end-member waters.

End-member	Na (mg/L)	K (mg/L)	Ca (mg/L)	Mg (mg/L)	HCO_3^- (mg/L)	Cl (mg/L)	SO_4^{2-} (mg/L)	δ^2H (dev)	$\delta^{18}O$ (dev)	Br (mg/L)
DS	8,500	45.5	19,300	2.12	14.1	47,200	906	−44.9	−8.9	323.6
Gl21	0.17	0.4	0.18	0.1	0.12	0.5	0.5	−158	−21	0.0
Litt	3,674	134	151	448	93	6,500	890	−38	−4.7	22.2
HLX28	110	2.97	11.2	3.6	265	23	35.8	−76.5	−10.9	0.1[*]

(*) The sample from borehole HLX28 that has been taken as Altered Meteoric end-member was not analysed for Br. It has been estimated from Cl assuming a Cl/Br ratio of 200.

Results: deviations and mixing proportions

Deviations. As chloride is considered a conservative element, its content in waters should be explained by pure conservative mixing and the M3 results should give a value similar to the one determined analytically. Therefore the suitability of M3 results in all six simulations can be analysed by checking this.

Figure 3-84 shows the difference between the actual Cl content of a sample and the Cl content computed by M3. This difference is called *deviation* and can be positive or negative. A positive value means that M3 has *underestimated* the Cl content of the sample, and a negative value that M3 has *overestimated* the Cl content. Results in Figure 3-84 are expressed as deviation bars plotted against sample number (upper graphs) and as scatter plots of measured Cl content plotted against computed Cl content. Two additional pieces of information are given for each simulation: (1) the average deviation for the whole dataset, and (2) the coverage (i.e. the percentage of samples that can be explained by mixing the chosen end members). Both figures are important for deciding which simulation is best: the average deviations should be as small as possible (close to zero) and the coverage as large as possible (close to 100%).

In Figure 3-84abcdef, the results for the simulations carried out with 4 end members are given, whereas Figure 3-84ghijkl, give the results for the 3 end-member simulations. By far, the best results are obtained when 3 end members and only conservative elements are used. The average Cl deviation is 50 mg/L (i.e. the difference between the measured and computed Cl content averaged over the 290 samples is 50 mg/L) and the coverage 90% (only 10% of the samples are outside the mixing polyhedron).

It is interesting to note that the results for the 4 end-member, only conservative elements case is much worse in terms of average deviation (–409 mg/L) and coverage (72%), indicating that four input compositional variables seem not to be enough for a simulations with 4 end members, although in theory they should.

Mixing proportions. How different are the computed mixing proportions in the six performed simulations? Are the widely different average deviations (cf. Figure 3-84) also translated into widely different mixing proportions? To answer these questions the amount of the HLX28 end-member in each sample is plotted in Figure 3-85. Quite a large amount of information is incorporated in this figure. Plots with a tan background compare mixing proportions computed with 4 end members; yellow plots compare mixing proportions computed with 3 end members; and blue plots compare mixing proportions computed with 3 and 4 end members.

The rows and columns of the table shown in Figure 3-85 indicate the number of input compositional variables used in the simulation. For example, the upper left plot compares the mixing proportions as computed with 3 and 4 end members (hence the blue background), but always using all the input compositional variables (hence the row and column "all components" labels). In the same way, the tan plot in row "All components" and column "All components except SO_4" compares the mixing proportions (computed with 4 end members) for the corresponding sets of input compositional variables (abbreviated as "All" and "noSO$_4$" on the axis labels).

Starting with the blue plots, where simulations carried out with the same input compositional variables but with different number of end members are compared, we immediately see that when all components or all components except SO_4 are used, the computed mixing proportions (of the HLX28 end-member) are almost identical with 3 and 4 end members, as most samples fall along the diagonal line.

On the other hand, when only conservative elements are used (elements Cl, Br, ^{2}H, and ^{18}O) the mixing proportions computed with 3 and 4 end members are widely different (lower right plot in Figure 3-85). This suggests a breakdown in the simulation when 4 end members and 4 input compositional variables are used.

Now, focussing on the tan plots (4 end-member simulations), it can be seen again how the plots where conservative elements are compared against other sets of input compositional variables, give widely different mixing proportions (large scatter of sample points, away from the diagonal line). This is once more an indication of a failure in the 4 end-member, only conservative elements, simulation. In contrast, the mixing proportions computed with all the components and with all the components except SO_4^{2-} are quite similar.

Finally, looking at the yellow plots, where simulations with 3 end members are compared, discrepancies up to 25% in the mixing proportions (of the HLX28 end-member) can be observed when the results obtained with only conservative elements are compared with the other two sets of input compositional variables. Here resides the real uncertainty in the computed mixing proportions. The "standard" M3 simulations for the Laxemar-Simpevarp site are obtained with all the input compositional variables and 4 end members (DS, Litt, HLX28, and Gl). But Figure 3-84 shows that this simulation has large Cl deviations, suggesting an imperfect fit for the conservative elements. The simulation carried out with 3 end members and only conservative elements has the lowest Cl deviation, and so it is the best suited to compute mixing proportions. In summary, the lower left plot in Figure 3-85 gives the uncertainty in mixing proportions because it compares the "standard" simulation with the "optimal" simulation (in terms of deviation with respect to conservative elements).

Taking the 3 end-member, only conservative elements simulation as the optimal one, we have calculated the composition that each groundwater sample in the Laxemar 2.3 dataset would have only by mixing (of course, mixing the three end-member waters DS, Gl and HLX28). This is plotted in Figure 3-86 for all the "standard" input compositional variables (remember that only conservative elements have been used in the simulations, but once the mixing proportions are obtained, the contents of any element can be calculated).

The plots in Figure 3-86 show the measured concentration of a particular element, say Ca, in the horizontal axis and the computed concentration (via the mixing proportions) on the vertical axis. If all the samples plot, for a particular element, near the red diagonal line, it means that the measured and computed concentrations are identical and, thus, that the content of that element is controlled only by mixing. If, on the other hand, the samples plot away from the diagonal line, this means that reactions have modified the concentration of the element. If the calculated concentration of an element is larger than the measured one, a process that depletes the real sample in that particular element must be called for; if the calculated concentration is lower than the measured one, a process that enriches the real sample in that element would be required.

As expected, the three conservative elements, Cl, δ^2H and δ^{18}O (lower plots in Figure 3-86), show that almost all the samples plot near the red diagonal line. However, there are clear deviations from this line for the rest of the elements.

The plots show the samples coloured by the water type when this information is available, otherwise the symbols are colourless. Na and Ca plot very close to the diagonal line for the saline waters, but show slight deviations for the rest. This means that these elements, in spite of being controlled mainly by mixing (especially for the saline samples), are also affected by reactions. Looking at the position of the samples in the graphs, Na is underestimated in only-mixing calculations while Ca is overestimated, which could be interpreted as a result of cation exchange. This is consistent with what is expected in dilution scenarios of highly saline waters, where calcium replaces sodium in the exchangers (Appelo and Postma 2005) and also with what has been obtained by the thermodynamic simulations presented in sections 3.2 and 3.3.
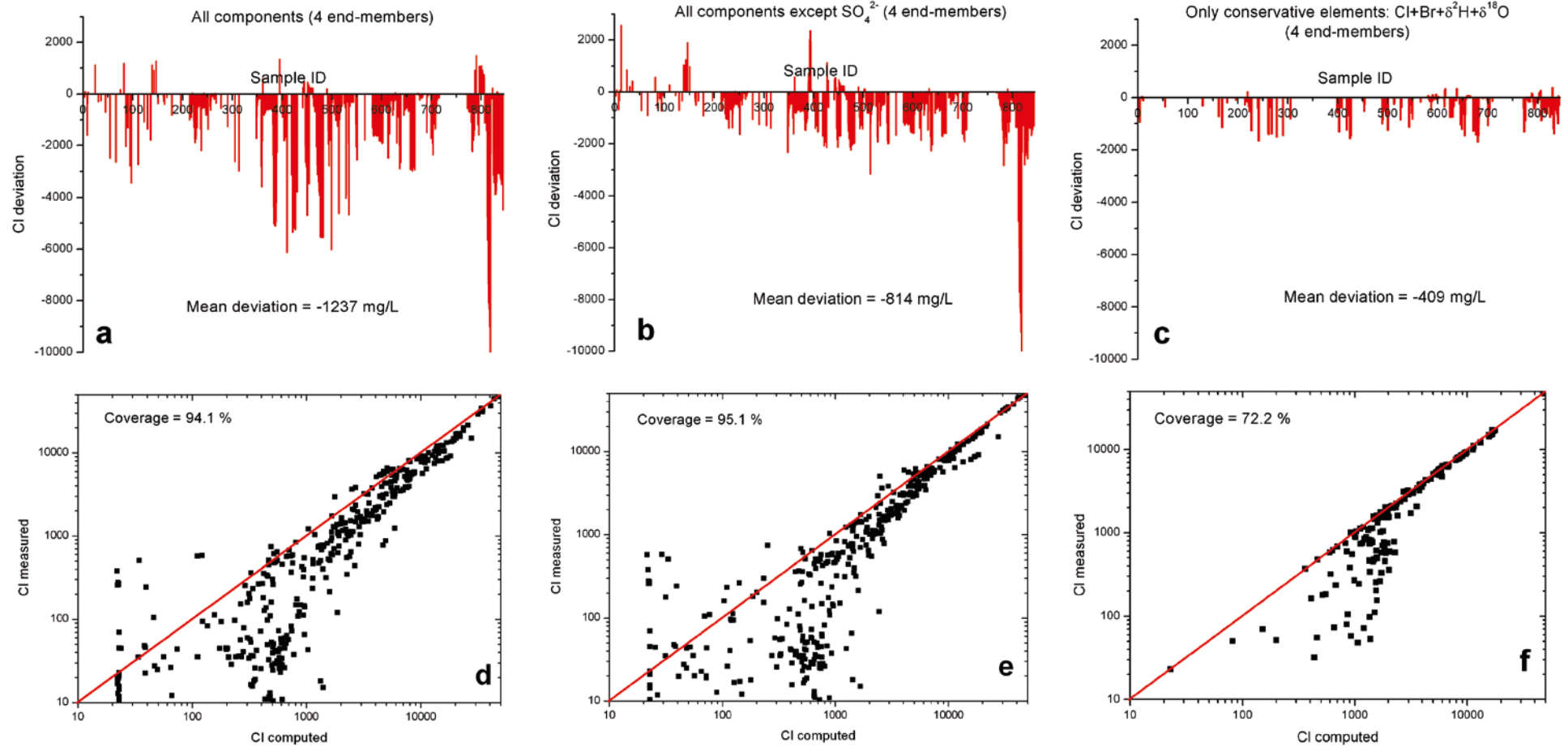
Figure 3-84. *M3 deviations for chlorine obtained using 4 end members (DS + Gl21 + Litt + HLX28) and three different sets of components: the standard set (left), the standard set except sulphate (centre) and only conservative elements (right). Laxemar 2.3 dataset. M3 deviations for chloride.*
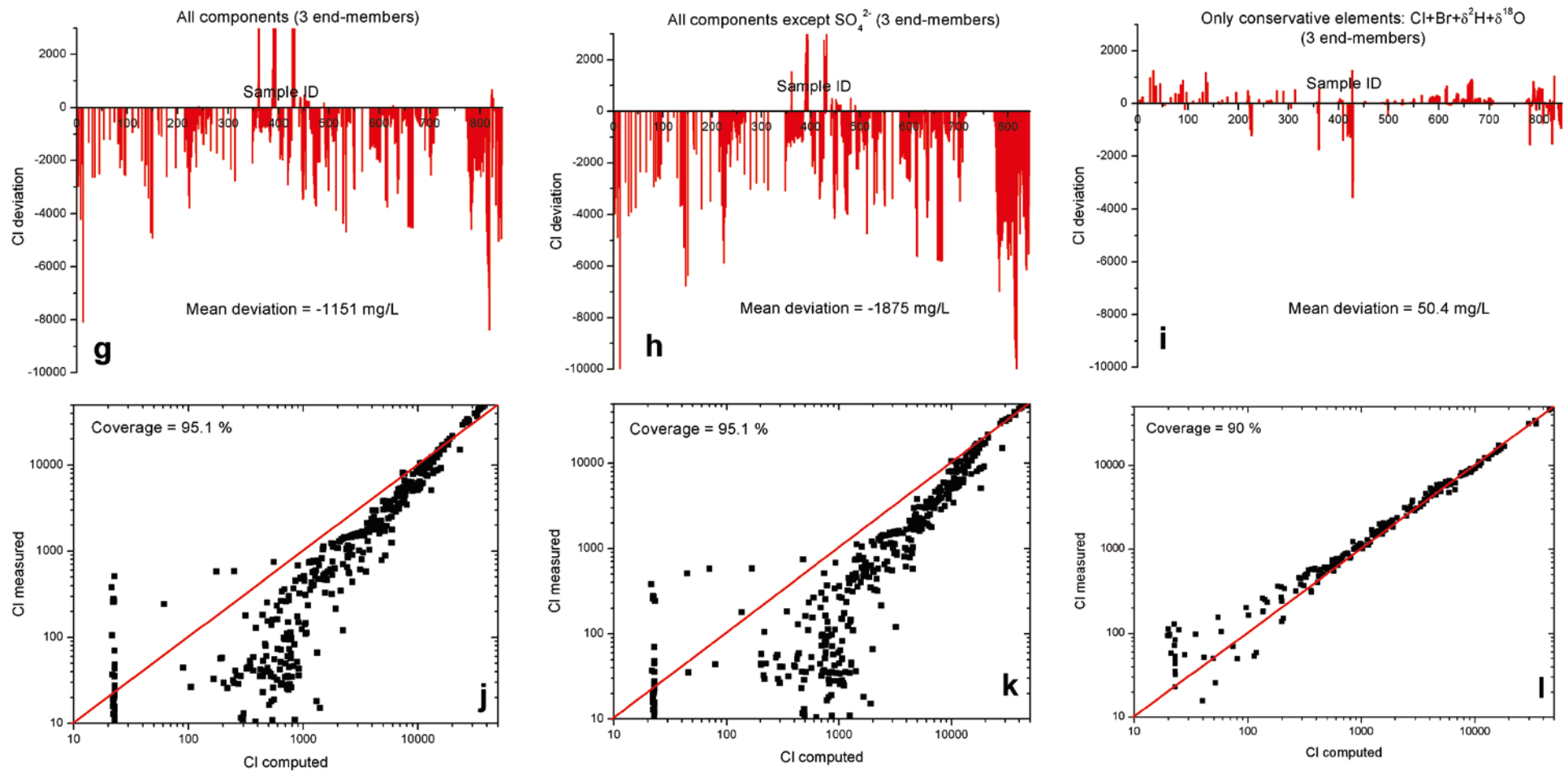
Figure 3-84. Continuation. *M3 deviations for chloride obtained using 3 end members (DS + Gl21 + HLX28) and three different sets of components: the standard set (left), the standard set except sulphate (centre) and only conservative elements (right). Laxemar 2.3 dataset. M3 deviations for chloride.*
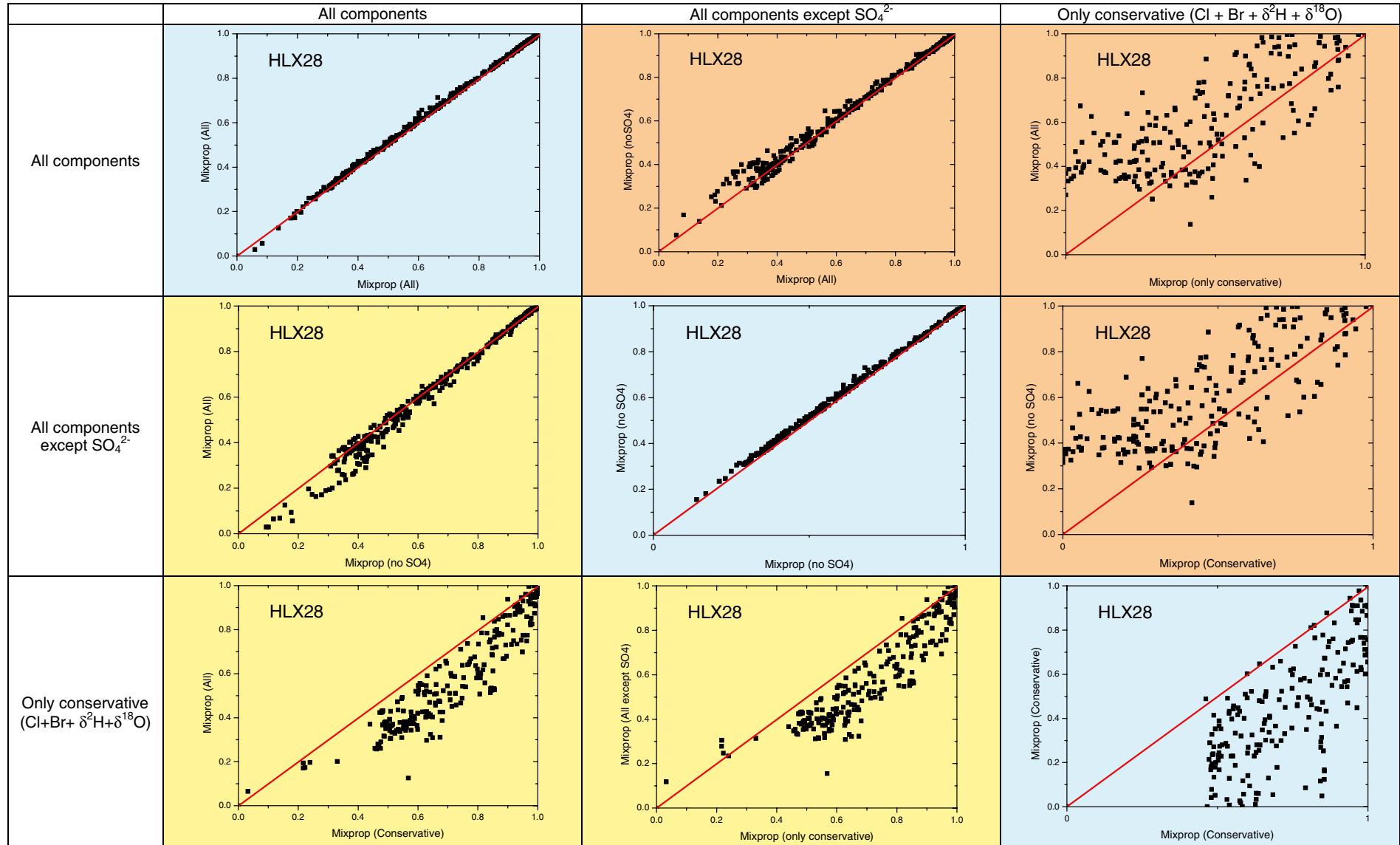
Figure 3-85. *Mixing proportions of the HLX28 end-member in each sample (4 end members in the upper triangle; 3 end members in the lower-triangle, and 4 end member in the vertical axes against 3 end members in the horizontal axes, in the diagonal)*
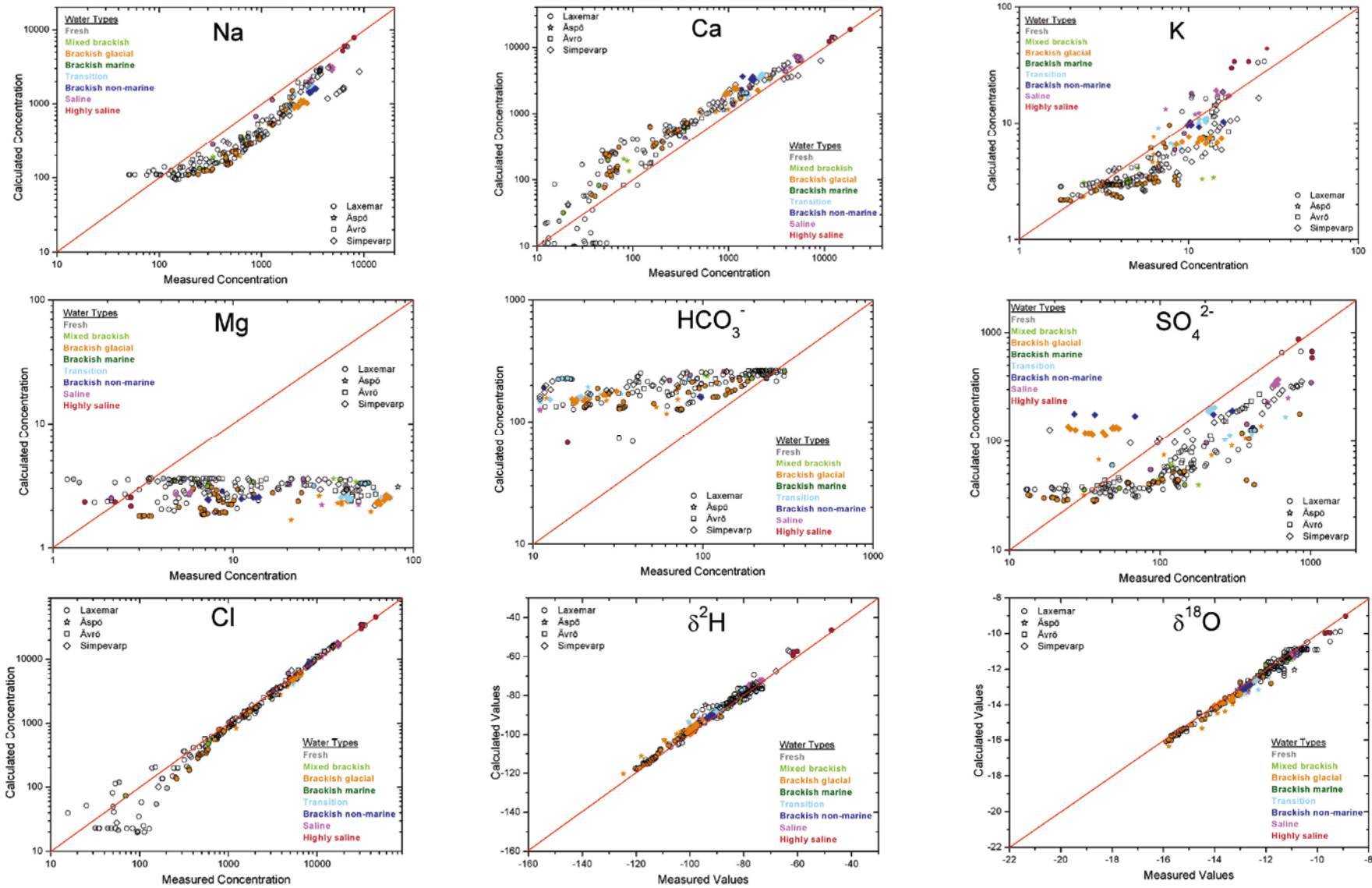
Figure 3-86. *M3 predicted concentration against measured concentration for the case of 3 end members and only conservative elements.*

Potassium shows a fairly good match between the real and the calculated values, which is surprising considering its reactivity in these systems. However, in detail, calculated contents by only-mixing for the more saline waters are overestimated while, in general, the less saline waters are underestimated. Therefore, exchange reactions and aluminosilicate dissolution processes appear to have affected this element (also in agreement with what is reported in section 3.2).

Even sulphate contents are fairly well reproduced for some waters, although for most of them the calculated values underestimate the real ones. An exception to this behaviour are some dilute samples in the Laxemar subarea and some more saline waters in the Simpevarp subarea, where the calculated values are higher than the measured ones. So, in general, dissolved sulphate is affected by the input of additional amounts coming from the dissolution of gypsum or by the depletion related to the presence of sulphate reduction activity (as it has been demonstrated by the thermodynamic simulations reported in section 3.4).

Magnesium and bicarbonate are clearly affected by reactions. The calculated values are very similar independently of the salinity of the sample and they are lower than the measured values in the case of magnesium and higher in the case of bicarbonate.

For bicarbonate, this fact is mainly related to the generalised presence of calcite re-equilibrium, which is the real control of bicarbonate (as indicated in section 3.3). For magnesium the explanation is different, as the results are partially affected by the exclusion of the Littorina end-member in the calculations. The constant values obtained by M3 are the result of mixing three end members with very low and similar magnesium contents. Waters with higher deviations and higher measured values (Äspö, Ävrö and some Simpevarp waters) are those with the higher Littorina proportion in the standard M3 calculation (Figure 3-92, below). For the rest of the groundwaters, the highest measured concentrations of Mg indicate the existence of reactions affecting Mg-bearing minerals (aluminosilicates).

Conclusions from the uncertainty analysis

It is clear that a quantitative assessment of the mixing proportions for each end-member (as already pointed out by Gómez *et al.* 2008), can be obtained when using conservative elements. The results from that simulation guarantee that only pure mixing processes are being considered. Then, once the mixing proportions have been quantitatively obtained, the rest of the elements can be evaluated by comparing their real contents with those obtained theoretically by applying the calculated mixing proportions. The differences between the real and the calculated values can be a good indication of the main kind of chemical reactions affecting their contents.

In the case of Laxemar-Simpevarp this process has been possible as one of the end members (Littorina) has very little (if any) effect in most of the samples. Because of this, only three end members are necessary and therefore, the three really independent conservative elements (Cl, Br and $\delta^{18}O$) are enough to perform the principal component analysis.

However, in spite of the fact that only three end members and only conservative elements give the best results, the original simulation with the whole dataset (standard set) and the four identified end members provides very useful qualitative results for most of the samples included in the system. This is clearly seen in the next section.

3.7.2 Mixing proportions

In this section, the distribution of the mixing proportions with depth is shown in different plots. Samples are coloured by the type of water to see if the different types agree with the dominant end-member as calculated by M3 using the simulation with three end members and only conservative elements.

This analysis has been carried out using two of the simulations considered here: first the "optimal", with three end members and only conservative elements; and second, the "standard" with four end members and the whole set of elements.

Figure 3-87 (a and b) show the mixing proportions sorted by water type; panel (a) shows the results with the first simulation (3 end members, conservative elements) and panel (b) the results with the second simulation (4 end members). As already mentioned, the main difference is the absence of the Littorina end-member in the first simulation, and therefore the absence of the brackish-marine groundwater group. The most conspicuous difference between both simulations is the increase in the contribution of the Altered Meteoric end-member in the first one (compensated by more Glacial and Littorina in the second one). The ranges of mixing proportions obtained with the two simulations for each water type are shown in Table 3-4.
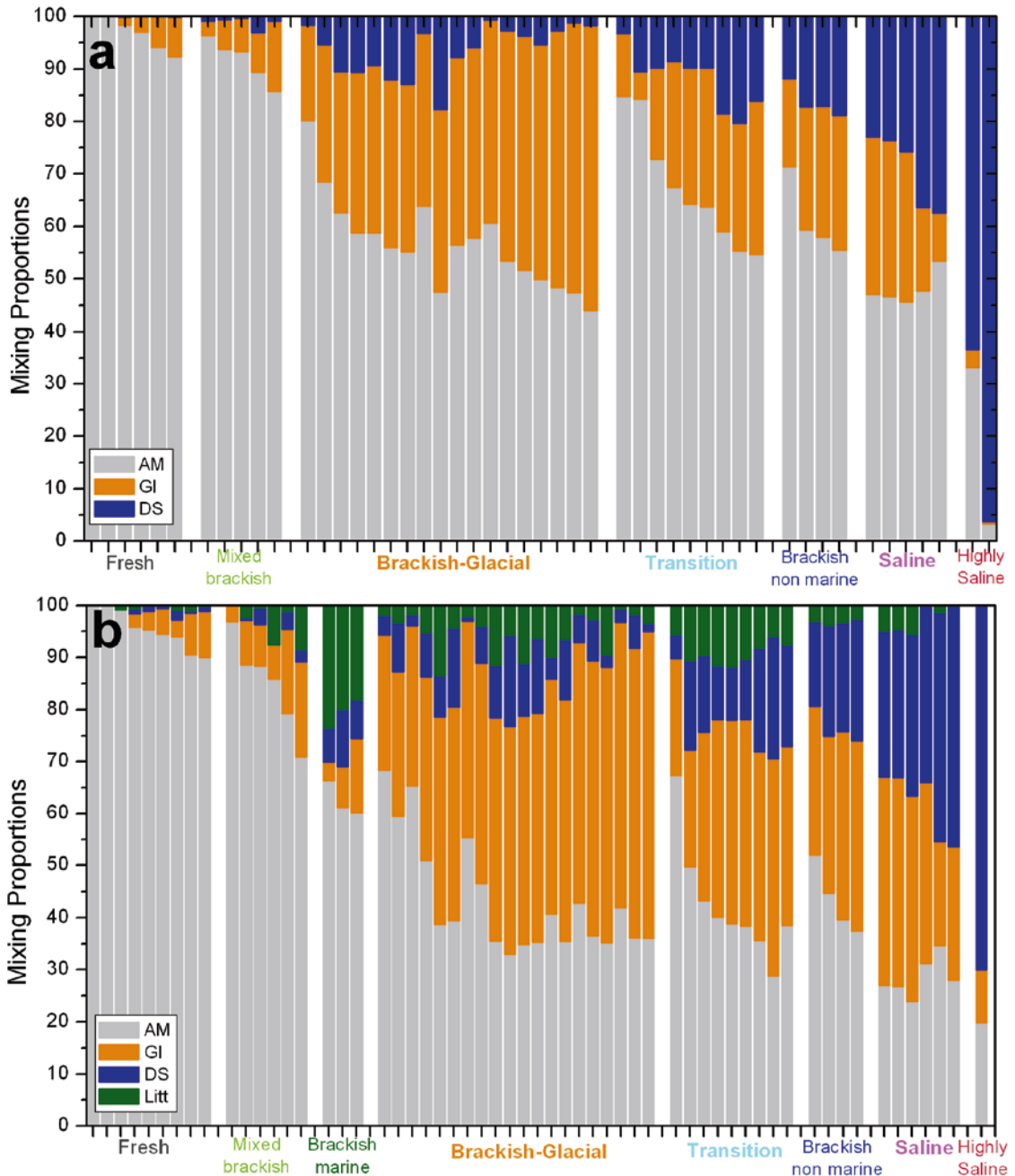
Figure 3-87. Mixing proportions for the different water types considering the samples from Laxemar 2.3 with categories 1, 2 and 3. (a) results from the "optimal" simulation (three end members and only conservative elements); (b) results from the "standard" simulation (four end members and the standard set of elements).

Table 3-4. Ranges of mixing proportions for the different groups of water types and the two different M3 simulations: optimal (3em+cons: 3 end members and only conservative elements) and standard (4em+all: four end members and the standard set of elements).

	Altered Meteoric		Glacial		Deep Saline		Littorina
	3em+cons	4em+all	3em+cons	4em+all	3em+cons	4em+all	4em+all
Fresh	93–100	90–100	0–8	0–9	0–0.2	0–2	0–1
Mixed	86–96	71–97	3–13	3–18	0.4–3	0–3.4	0–9
Brackish marine		60–66		3–14		7–11	18–24
Brackish glacial	44–80	36–68	18–54	26–59	1–18	1–18	0.6–13
Transition	55–85	29–67	5–29	22–42	3.3–20	4–24	5.5–12
Brackish non marine	55–71	37–52	17–26	29–37	12–19	16–23	3–4
Saline	47–53	24–28	9–30	20–40	23–38	28–47	0–5.4
Highly saline	3.2–3.3	20	0.4–3.5	10	64–96	70	0

Figure 3-88 shows the depth dependence of the three end members for the full set of samples. Here, each graph corresponds to a different end-member. Then, Figures 3-89, 3-90 and 3-91 show separately the results for each of the four subareas studied in Simpevarp. In these figures each graph corresponds to a different subarea, with the Altered Meteoric end-member being represented in Figure 3-89, the Glacial end-member in Figure 3-90, and the Deep Saline end-member in Figure 3-91. As the Littorina end-member has not been considered here, samples with Littorina signature (and therefore clearly corresponding to the brackish marine type) do not appear in the plots as they were not included in the mixing polyhedron (out of the coverage, as it was expected).

The main conclusion that can be drawn from these figures is that, in general, and looking at the different subareas separately, the different water types have clear depth dependency and they are very well correlated with the mixing proportions obtained with M3.

Altered meteoric: This is the end-member whose mixing proportion varies most depending on the simulation performed (see above, Table 3-4). In some samples the differences in the mixing proportions can reach 20%. However, independently of this, there is a clear decrease in the percentage of this end member as depth increases (Figure 3-89) and the water evolves towards more saline types (see the colours in the plot). In general, fresh waters (grey circles in the plots) contain between 92 to 100% of Altered Meteoric water and this is clearly observed in the Laxemar subarea. Then, the percentage of this end-member decreases in the different water types, reaching the lowest values in the highly saline waters (from Laxemar) with a range between 3 and 30%.

Another interesting observation is that there is an important amount of the Altered Meteoric end-member (60 to 80%) at the repository level (around 500 m depth) in the Laxemar and Ävrö subareas.

Glacial: The Glacial signature is clearly appreciated in the plots of the different subareas and the agreement with the water types defined is also very good (Figure 3-90). Light orange (salmon) samples, which correspond to the Brackish-glacial water type, have the highest glacial contribution (between 20 and 55%). The rest of the water types have systematically Glacial mixing proportions lower than 30%.

The depth distribution of these waters with Glacial signatures indicates that glacial melt waters have reached depths of around 900 m in Laxemar, whereas they have only penetrated down to 600 m in Simpevarp, and less than 300 m in Äspö.

Figure 3-88. *Depth distribution of the mixing proportions in the four subareas. The mixing proportions have been obtained by M3 with three end members and only conservative elements. (a) Altered Meteoric end-member (AM); (b) Glacial end-member; (c) Deep Saline end-member.*

Deep Saline: The depth trend of this end-member is clearly represented by the Laxemar subarea waters (Figure 3-91). The different water types evolve towards the highly saline waters with increasing depth by increasing the percent of the Deep Saline end-member up to almost 100%. The other subareas show the same increase of Deep Saline percent with depth but only up to a 30% at Äspö island and 40% in the Simpevarp subarea.

It is also interesting to note that, for the same depth (say 1,000 m), the amount of Deep Saline end member is higher in the Simpevarp subarea (40%) than at Äspö island (30%) and in the Laxemar subarea (20%).

In order to check the effect of using the mixing proportions calculated with the "standard" simulation (4 end members and the standard set of elements), another group of plots have been included to show the corresponding results (Figure 3-92).

The results indicate that, although the quantitative values of mixing proportions do not fully agree, the trends and distributions are very similar. Moreover, these results include more samples, even the brackish marine ones with some Littorina signature. Therefore, though qualitative, these results can give very valuable information.
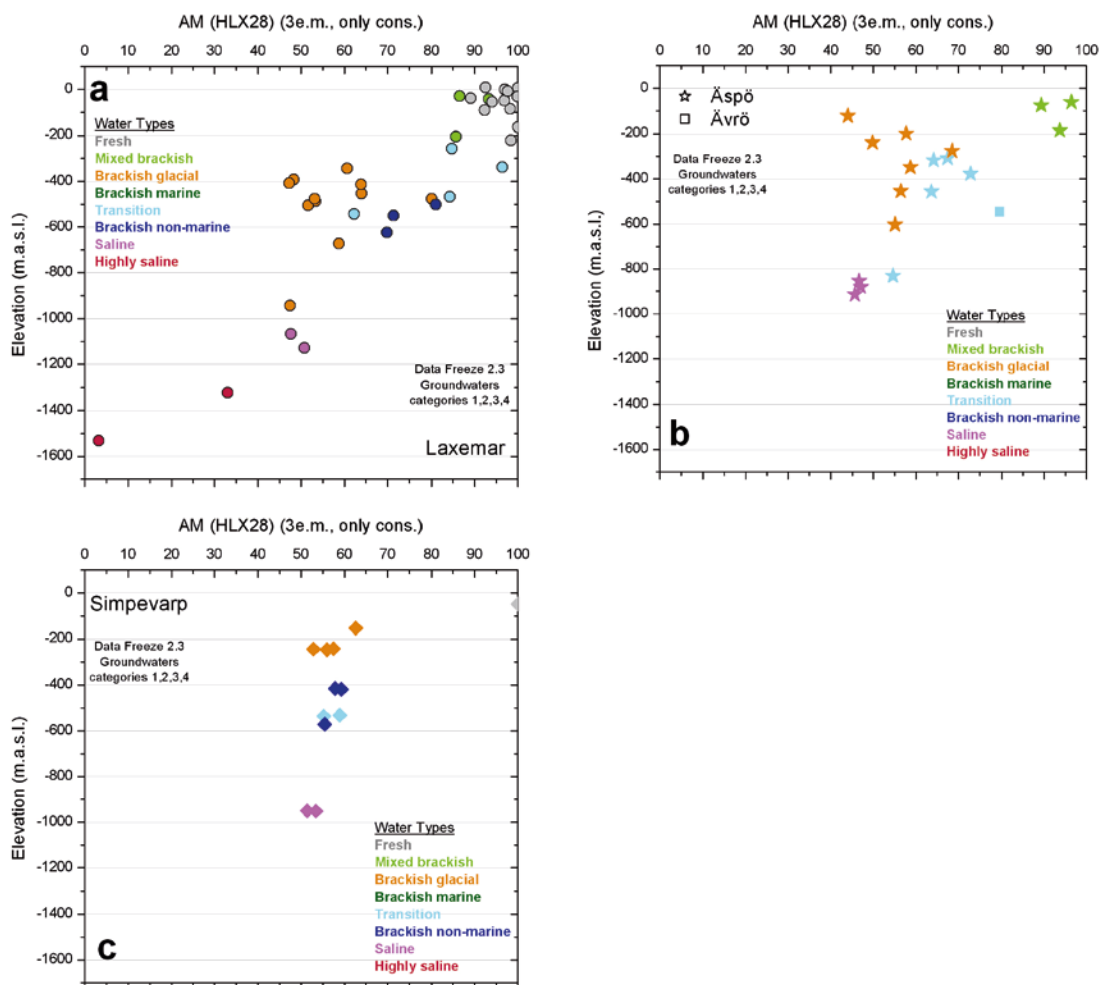
Figure 3-89. *Depth distribution of the Altered Meteoric end-member (AM HLX28) in the four subareas.*
Mixing proportions have been obtained by M3 with three end members and only conservative elements.
(a) Laxemar; (b) Äspö and Ävrö; (c) Simpevarp.

3.7.3 Conclusions

In summary, when chemical reactions only produce slight variations with respect to the chemical composition of the conservative mixing, the reconstruction of chemical compositions from the mixing proportions calculated with M3 are in very good agreement with the measured ones. When chemical reactions produce an important compositional change, the M3 mixing proportions do not reproduce the measured values, and the departure depends on the chemical reaction and/or the type of groundwater. However, this methodology is very useful to obtain the part of the concentration which can be due to mixing and then, to infer what kind of chemical reactions must have occurred to modify (increase or decrease) the final contents. The scatter produced by the non-conservative elements in this kind of statistical analysis influences directly the mixing proportions calculated by the code and their values should be used with caution.

Therefore, in spite of the important qualitative information obtained when using all the elements in the M3 calculations, the quantitative values of mixing proportions must be calculated only with the conservative elements when reactions are important in the system. This procedure offers the possibility of obtaining quantitative and reliable mixing proportions and it is very useful when combined with additional methodologies (e.g. classical mass balance and inverse modelling using PHREEQC or similar codes) as the differences between the real and the calculated values for the non conservative elements can be a good indication of the main kind of chemical reactions affecting their contents.
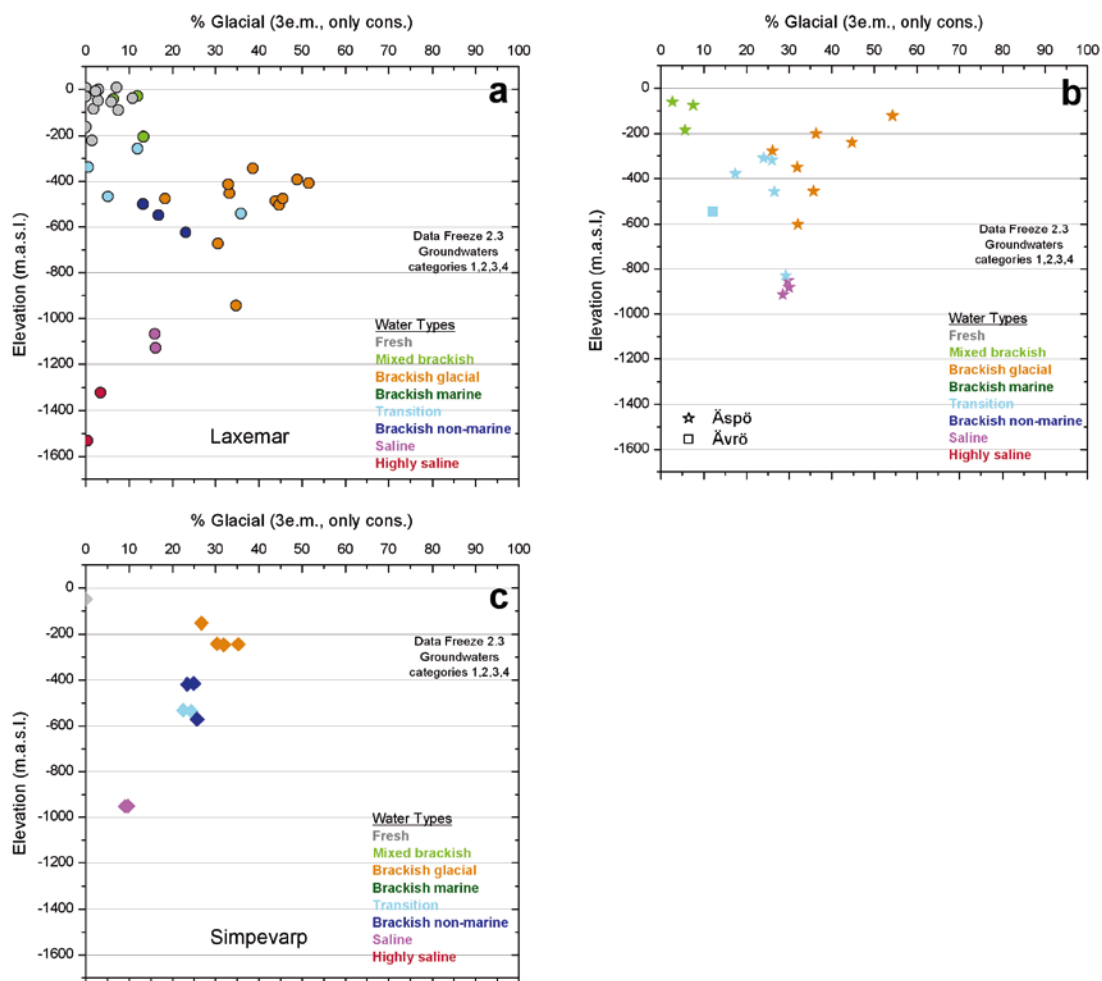
Figure 3-90. *Depth distribution of the Glacial end-member in the four subareas. Mixing proportions have been obtained by M3 with three end members and only conservative elements. (a) Laxemar; (b) Äspö and Ävrö; (c) Simpevarp.*

3.8 Relative importance of mixing and reaction processes

During previous SDM stages in Forsmark and Laxemar-Simpevarp areas, there have been important discussions on the importance of mixing *vs.* heterogeneous reaction processes in the present compositional characters of the groundwaters.

From the results obtained using the inverse modelling approaches (mass balance and mixing calculations performed with PHREEQC and M3, previous works and sections in this chapter) the percentage of a given dissolved element that could be explained by mixing between the considered end members, can be obtained. Then, the percentage not explained by mixing must be due to reactions (water-rock-microbiological reactions). So, the relative importance of mixing and reaction processes are evaluated in terms of the percentage of element explained by one or the other; for example, if the mixing processes explain the 60% of the present concentration for a dissolved element, it can be said that mixing is the main controlling process for this element whereas if mixing explains the 40%, reactions would be the main control.

The dissolved contents of most of the elements in the saline waters are mainly explained by mixing and this statement has been interpreted, in general, as something like "reactions are not important". However, it is exactly the contrary. Reaction mass transfers may be more important in these mixing-controlled crystalline systems than in "pure" water-rock interaction evolutions. And even more important, mixing processes control the direction and extent of most subsequent heterogeneous reactions in the system. This is what is presented next.
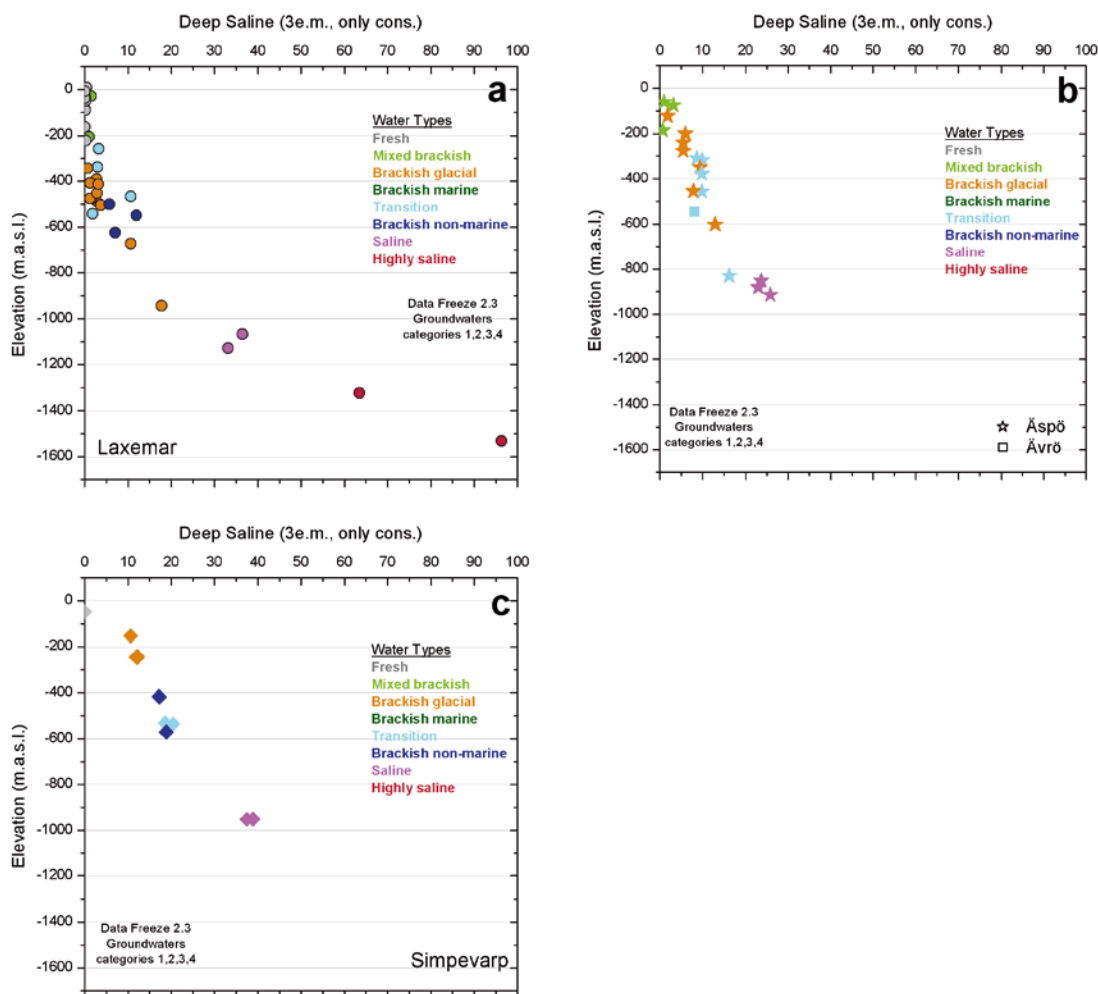
Figure 3-91. *Depth distribution of the Deep Saline end-member in the four subareas. Mixing proportions have been obtained by M3 with three end members and only conservative elements. (a) Laxemar; (b) Äspö and Ävrö; (c) Simpevarp.*

When two solutions are mixed, concentrations in the mixture are volume-weighted averages of the two end members but the thermodynamic activities of the species controlling the water-mineral reactions (e.g. through the ionic activity product) are non-linear functions of the mixing ratio. Therefore, two end members in equilibrium with a solid phase could lead to a mixture either under- or oversaturated with respect to that solid phase. This type of non-linear effects of the mixing over the mineral saturation states affects any mineral (silicates, aluminosilicates; e.g. Hanor 2001) but it has classically been described for carbonates. The carbonate system is especially important in the studied systems, as calcite dissolution/precipitation reactions are kinetically faster than most of the reactions involving aluminosilicates.

Wigley and Plummer (1976) described the most important factors controlling the saturation state of carbonate minerals in water mixtures: ionic strength (salinity), CO_2 partial pressure, temperature and the so called "algebraic effect". The ionic strength effect and the algebraic effect oppose each other and they are superimposed on the rest of the factors making the anticipation of whether over- or undersaturation will result from a mixture, a non-trivial task (Rezaei *et al.* 2005). Mixing of groundwaters, already in equilibrium with respect to calcite, will produce calcite over- or undersaturation in different extent, as a function of the composition and mixing proportions of the mixed groundwaters. Then, as a result of the subsequent re-equilibrium, the dissolved contents of the elements affected by calcite dissolution/precipitation, and even the final pH, will change with respect to the values obtained by conservative mixing. Therefore, even assuming that the re-equilibrium produces important changes in some of the dissolved contents (hiding completely the values imposed by mixing) this re-equilibrium and its extent are the result of mixing. Since the overall evolution of
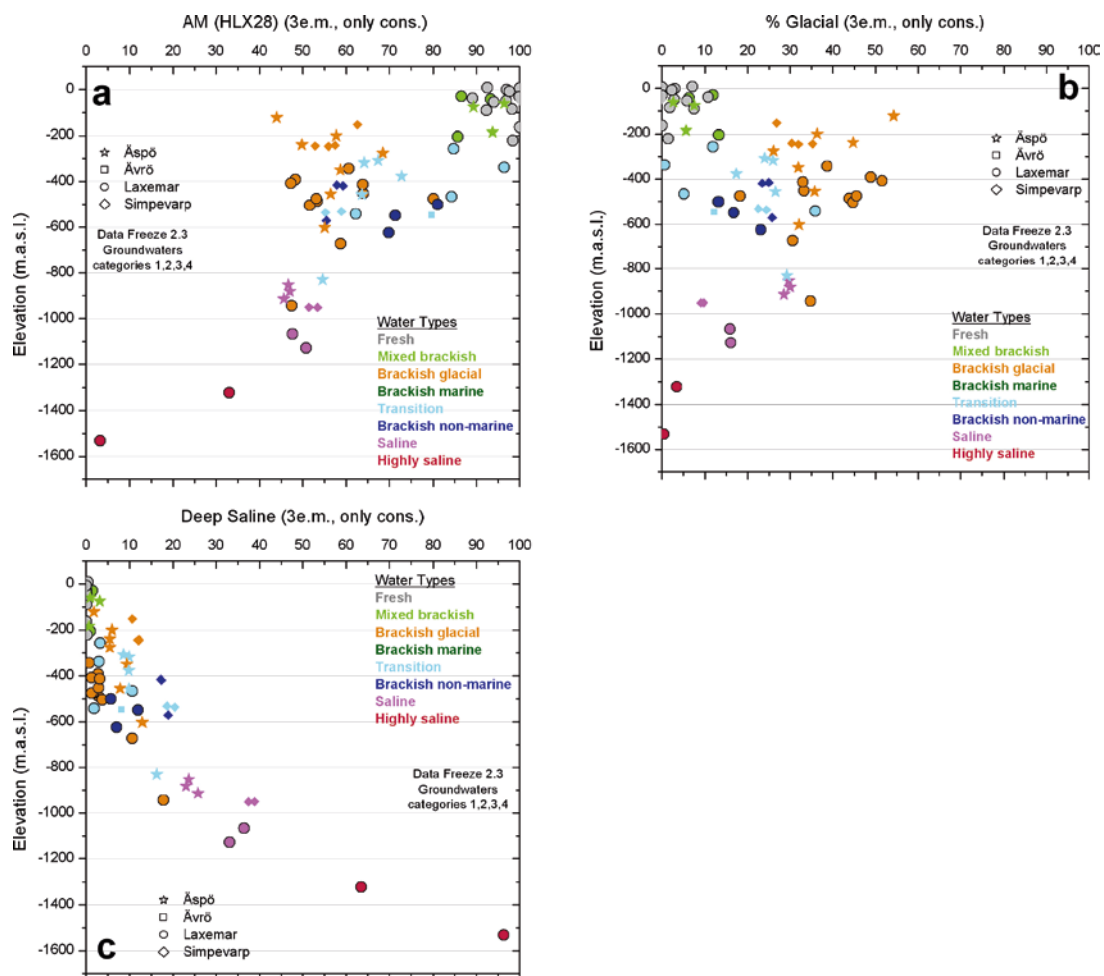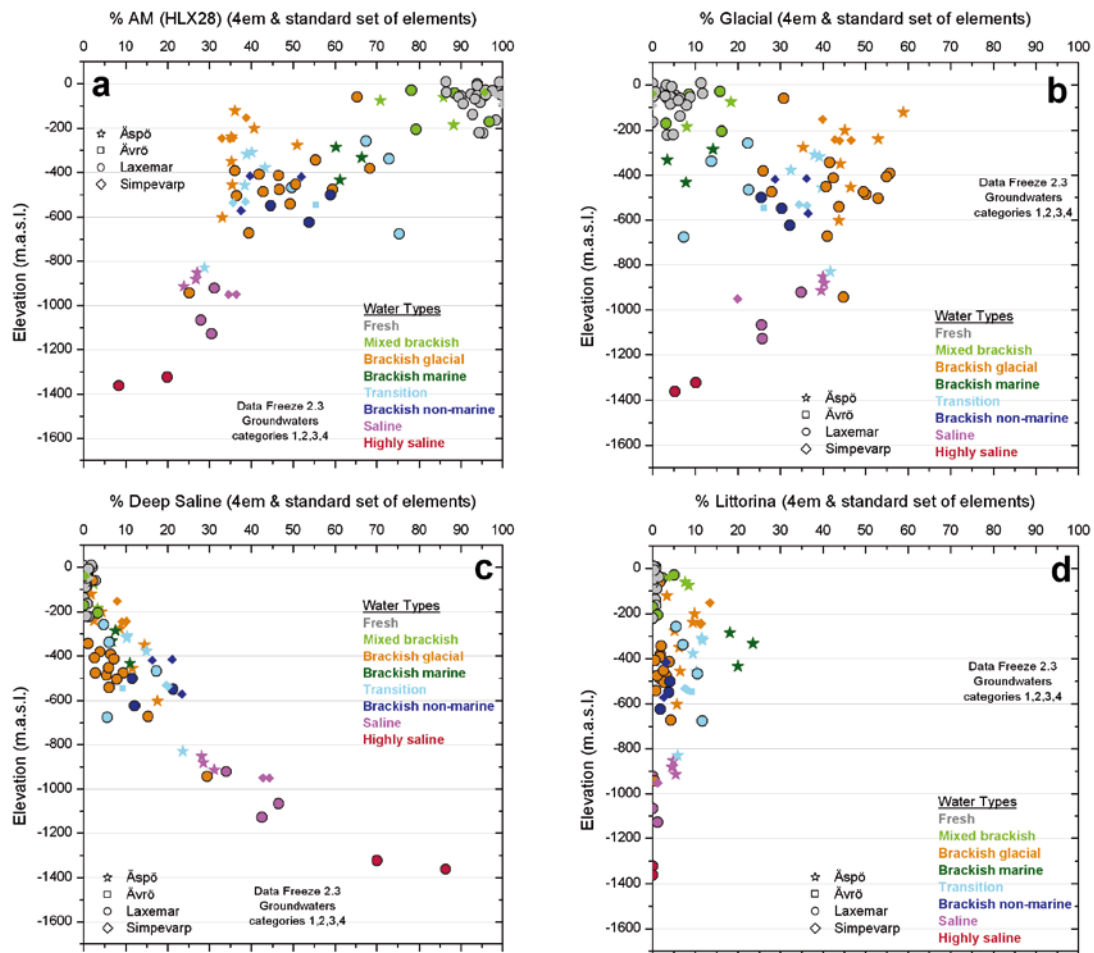
Figure 3-92. *Depth distribution of the mixing proportions in the four subareas. The mixing proportions have been obtained by M3 with four end members and the "standard" set of elements. (a) Altered Meteoric end-member (AM HLX28); (b) Glacial end-member; (c) Deep Saline end-member; and (d) Littorina end-member.*

these processes is highly non-linear, geochemical modelling calculations, such as those presented in different sections, are needed to deal with them.

The effects of mixing on the subsequent re-equilibrium can be expanded for all mineral reactions, including aluminosilicates, if the interaction time is great enough. In fact, the importance of the chloride concentrations (anionic charge concept[25]) in the evolution of rock-buffered waters was recognized long time ago by Helgeson (1970) and chloride has become considered as an independent master variable in determining the water composition in rock-buffered systems since then (Hanor 2001). The anionic charge concept simply states that the final composition of a water in equilibrium with a given mineral assemblage, under similar pressure and temperature conditions, will change as a function of the chloride content (or, in general, anions content) at which the equilibrium is reached. Therefore, for the target groundwater systems, this implies that variations in the chloride concentrations triggered by mixing of waters with contrasting salinities (e.g. the old mixing events between the Deep Saline and Glacial end members) will control the final composition of the mixture after re-equilibrium.

---

[25] This concept has been widely used, as a charge balance constraint, in the study and simulation of the evolution of waters buffered by multimineralic systems through successive partial equilibrium stages, both in high and low temperature conditions (Michard 1987, Michard *et al.* 1996, Chiodini *et al.* 1991, Hanor 1996), including Stripa (Grimaud *et al.* 1990) and Äspö groundwaters (Trotignon *et al.* 1997, 1999). It was also explored by Gimeno *et al.* (2004b) in Simpevarp 1.2.

Mixing processes have also an important control on the subsequent cation exchange reactions, especially if the salinity contrasts between the involved end members produce dilution or concentration of the final mixture. Both, "dilution" (e.g. mixing of Glacial with pre-existing more saline groundwaters) and "concentration" scenarios (e.g. mixing of Littorina with the pre-existing less saline groundwaters) have happened over the palaeohydrological history of the sites. During dilution processes, divalent cations (e.g. Ca^{2+}) are preferentially adsorbed compared with the monovalent ones (e.g. Na^+) whereas in concentration processes, divalent cations are preferentially released from the exchanger to the water while monovalents are adsorbed.

These overall effects are also conditioned by the particular composition of the end members. For example, the infiltration of Littorina waters with high dissolved Mg^{2+} concentrations compared to any pre-existing groundwater, will promote a noticeable enrichment of magnesium in the solid exchanger during mixing, which, in turn will affect the subsequent evolution of the waters in contact.

Therefore, mixing (dilution *vs.* concentration scenarios) may control the overall trends (directions) of the heterovalent exchange processes and even promote drastic modifications in the exchanger compositions that, in turns, would affect subsequent mixing processes.

Finally, the comparison of the compositional characters in the studied groundwaters with those in other groundwaters from crystalline systems only conditioned by pure water-rock interaction can be very helpful to analyse the importance of mixing processes. Several systems studied in the context of the Swedish and Finnish programs (Fjällveden, Klipperas, Gidea, Lansjarv, Stripa, Sweden, and Romuvaara and Kivetty, Finland), all of them interpreted as result of pure water-rock interaction and with long residence times, have been reviewed and Table 3-5 displays the ranges of several compositional parameters.

These groundwaters have very dilute characters with maximum dissolved values lower than the values measured in Laxemar-Simpevarp[26], Forsmark or other systems affected by mixing events with more saline groundwaters. These low dissolved contents indicate that the mass transfers associated with heterogeneous reactions are much smaller than the ones associated with mixing events with more saline waters.

Table 3-5. Some compositional characters of groundwater systems from the Scandinavian Shield controlled by "pure" water-rock interaction processes (Fjällveden, Klipperas, Gidea, Lansjarv, Stripa, Romuvaara and Kivetty) and systems affected by mixing with more saline groundwaters (Laxemar-Simpevarp, Forsmark and Olkiluoto Forsmark).

	Depth	Cl	SO_4^{2-}	Ca	Mg	Na	Mn
Systems controlled by pure water-rock interaction processes							
Fjällveden	124–740	3–170	0.1–7.0	10–42	0.8–5.1	13–310	0.05–0.56
Klipperas	328–909	5.5–43	0.1–4.0	7.9–32	1–4	11–65.0	0.01–0.54
Gidea	97–617	1.5–260	0.1–8.0	8.5–58	1.0–4.4	5–156.0	0.01–0.28
Lansjarv	141–368	0.8–1.5	1.1–4.4	7.7–10.4	1.2–2.0	4.6–11.3	0.0–0.03
Stripa	0–940	22–700	0.1–110	4–170	0.18–5.7	2.5–304	0.0–0.05
Romuvaara	150–457	0.74–109	0.5–8.6	1.7–35.6	0.23–5.0	3.5–65.0	–
Kivetty	60–794	0.47–22	0.2–6.9	6.3–24	0.65–5.3	4.6–40	–
Systems affected by mixing with more saline groundwaters (+ water-rock interaction)							
Laxem-Simp[*]	150–1,530	250–45,500	31–1,010	24–18,600	2.1–71	111–8,030	0.05–1.7
Forsmark[*]	22–980	15.7–14,800	31–565	24–6,520	3.9–287	65–2,300	0.0–2.7
Olkiluoto[**]	58–952	369–45,200	1.2–541	74–18,000	5.6–190	225–954	0.04–2.3

*Values for samples of categories 1 to 4.
** Data from Pitkänen *et al.* (2004)

---

[26] Except for the groundwaters in the Laxemar subarea with a clear meteoric recharge character (without mixing), whose contents are similar to the ones shown in Table 3-6 and have also been interpreted as controlled by water-rock interaction processes.

This does not imply that reaction mass transfers are not important in systems controlled by mixing processes. In fact, reaction mass transfers are much larger in these systems than in the ones simply affected by water-rock interaction. However, the effects of heterogeneous reactions on the hydro-geochemistry of saline mixed groundwaters are usually hidden due to the much greater magnitude of mass transfers produced by mixing.

Therefore, pure water-rock interaction processes may control the compositional characters of some groundwaters in specific evolution moments of the studied systems (e.g. the dilute groundwaters with a meteoric recharge character presently found in the Laxemar subarea down to 500 m depth). However, mixing is the main driving force in the hydrochemical evolution of the sites at large scale, as it represents an important source of disequilibrium that must be relaxed through heterogeneous reactions. Mixing processes also condition the direction and degree of the mass transfers involved in the heterogeneous re-equilibrium processes, especially those with a fast kinetics, calcite dissolution/ precipitation or cation exchange reactions.

Finally, mixing and reaction processes are not alternative "models" able to independently justify the observed compositional evolution of the groundwaters in the sites, and without a clear understanding of the mixing processes and their effects in the past, a predictive assessment of the future evolution is impossible.

4 Redox systems

This chapter provides a general overview of the redox processes controlling some of the important parameters in the system. It summarises the work done in the previous modelling phases, updating the results with the new data from the Laxemar 2.2 and 2.3 data freezes. It includes the presentation of the different redox parameters and the redox modelling concerning the iron, sulphur, manganese and nitrogen systems. As for non-redox systems, several issues suggested by the INSITE group are dealt with here:

- Issue A-1: Modelling of the existence of a relatively shallow "process zone" capable of buffering the meteoric water with respect to redox and cation exchange.
- Issue B-1: Description of models based on reactions and other alternative models.
- Issue E-1: Spatial variability of hydrochemical data.
- Issue G-1: Modelling of redox and pH buffering and water-rock reactions at repository depth.

The redox systems are among the most complicated and discussed items in hydrogeochemistry. Therefore, it has been considered here that the only way to deal with them is to know, understand and interpret all the information related to them (hydrochemical, mineralogical and microbiological) as a whole. This section integrates the results obtained from the potentiometric Eh measurements, redox pair calculations, speciation-solubility calculations, mineralogy and microbiological analyses to identify the main controls of the redox state in groundwaters.

The potentiometric Eh measurement can have both technical and interpretative problems. However, SKB has developed (over the last 25 years) one of the best available methodologies for the measurement of this parameter (Auqué *et al.* 2008) and its careful use can be, at the very least, a qualitative helpful piece of information (Langmuir 1997, Schüring *et al.* 2000) for the study of redox systems. Moreover, potentiometric Eh values can be used to deduce the type of redox-controlling Fe(III)-oxyhydroxide (Fe(III)-oxyhydroxides/Fe(II) are clearly electroactive redox pairs and this methodology has been successfully used in previous works; e.g. Grenthe *et al.* 1992, Banwart 1999, Trotignon *et al.* 2002).

In any case, all the speciation-solubility calculations, conclusions and interpretations of this chapter have been obtained independently of the potentiometric Eh value, or have been confirmed with other data or lines of reasoning using the available mineralogical and microbiological data.

Following the same criteria as in previous reports, a detailed description and discussion of redox systems including the geochemical characterisation of iron, sulphur, manganese and nitrogen systems, is presented here. Although occasionally mentioned, some other important redox indicators (H_2, CH_4) are not discussed at the same detailed level due to the few available data and the associated uncertainties. The available data on CH_4 and H_2 and the need for more detailed studies on both redox components are discussed in Appendix G. Also, in this appendix, the usual uncertainties associated with the study of redox processes, as well as other more particular ones related to the studied systems, are presented.

4.1 Selection of redox data

4.1.1 Selection of representative Eh and pH values

The selection of the pH and Eh values for any specific borehole section has been based on a very careful analysis of the data delivered by Sicada. The whole selection procedure is described in Appendix A.

There are 45 sets of logs in the Laxemar-Simpevarp area (see Table A-3 in Appendix A), corresponding to 16 different packed sections in 3 boreholes from Äspö (KAS02, 03, 04), 4 sections from Ävrö (borehole KAV01), 22 sections in 7 boreholes from the Laxemar subarea (KLX01, 02, 03, 08, 13, 15 and 17) and 3 section from the Simpevarp subarea (borehole KSH01A). They range in depth from 150 to 1,700 m. Twenty one of them passed the initial selection criteria; nine were included in Group 1 and the rest in Group 2 (Table 4-1).

Table 4-1. Eh values selected in the Laxemar-Simpevarp area, where SKB methodology has been used. Data freeze: only the new Laxemar 2.2 and 2.3 data freezes are indicated, the rest of the samples correspond to Laxemar 2.1 data freeze. Category: indicates the category of the sample (see Smellie 2009). Depth: corresponds to the Elevation of the mid section (meters above sea level). The pH and temperature values correspond to the values selected from Chemmac logs, down-hole or surface (see also Appendix A in this contribution). The column called Group indicates the quality of the Eh value as reported in Appendix A.

Data freeze	Borehole	Sample #	Category	Depth (m)	Borehole length (m)	t (ºC)	pH (field meas.)	pe	Eh (mV)	Group
	KAS02	1548	3	−199.8	202–214.5		7.5	−4.49	−257	2
	KAS03	1569	3	−121.8	129–134	10.2	8	−4.62	−260	1
	KAS03	1582	3	−914.0	860–1002	20.5	7.3	−4.63	−270	2
	KAS04	1596	3	−185.1	226–235	10.5	7.8	−5.33	−300	1
	KAS04	1603	3	−275.6	334–343	12.14	7.9	−4.95	−280	1
	KAV01	1384	5	−408.3	420–425	12.9	7.35		−215	1
	KAV01	1379	5	−512.2	522–531	14.9	7		−310	2
	KAV01	1374	4	−546.1	558–563	15	7.4	−3.93	−225	2
	KLX01	1517	5	−440.7	456–461		8.6		−280	2
	KLX01	1516	3	−673.0	680–702		7.8	−4.63	−265	2
	KLX03	7953	1	−170.8	193.5–198.3	8.4	8.17	−4.92	−275	2
	KLX03	10091	3	−379.9	408–415.3	13.1	8.1	−4.75	−270	2
	KLX03	10188	5	−700.6	735–748	19.7	7.5		−220	1
2.2	KLX08	10649	5	−150.4	197–206	8.7	8.1		−266	2
2.2	KLX08	10747	5	−320.0	396.400	12.5	8		−245	1
2.3	KLX13A	11607	3	−408.0	432.439.2	13.9	8.45	−5.04	−287	1
2.3	KLX17A	11809	3	−342.3	416–437.5	12.2	7.92	−5.03	−285	1
2.3	KLX17A	11692	5	−548.0	642–701.1	15.7	8.36	−5.29	−303	2
	KSH01A	5263	2	−152.7	156.5–167	6.3	8.1	−4.51	−250	2
	KSH01A	5266	3	−241.7	245–261.6		8.05	−3.67	−210	2
	KSH01A	5288	3	−536.0	548–565.4		8.05	−4.20	−240	2

Most of the retained Eh values agree very well with the recommended value suggested in previous works or in the specific P-reports where the hydrochemical characterisation of each borehole is summarised (Smellie and Laaksoharju 1992, Grenthe *et al.* 1992, Wacker *et al.* 2004, Bergelin *et al.* 2006, 2008a). P-reports for KLX13[27], KLX15 and KLX17 were not available by the time of reporting this work and Eh values obtained for different sections from these boreholes have been selected by the UZ group.

4.1.2 Selection of samples for redox modelling

As already advanced in previous SDM reports, one of the main problems affecting the available samples for the redox modelling is the high percentage of drilling water in most of them, lower than 10% but usually higher than 1% (the maximum recommended value; e.g. Wacker *et al.* 2004). Small amounts of oxygen (or other dissolved redox component), incorporated with the drilling water or by direct atmospheric contamination, can produce important changes in the redox state of the groundwaters, although they were not detectable during Chemmac logging.

In spite of the important efforts made by the Site Characterisation team, this problem has persisted during the Laxemar 2.2 and 2.3 campaigns. As a consequence, the number of samples suitable for redox modelling is still small (Table 4-2), especially for the last campaigns in the Laxemar subarea. As a trade-off between quality and quantity, only *samples with less than 10% of drilling water* have been used (as in previous phases). This means accepting a level of uncertainty of the original redox characteristics of the system but, at least, this would enable study of whether the mentioned altera-

---

[27] P-report for KLX13 has been recently published and it has been considered in Appendix A.

tions have occurred and their possible effects on the undisturbed conditions. So, for this modelling task, samples with less than 10% of drilling water and enough redox data were selected (Table 4-2), including good Eh and pH data from continuous loggings, analytical data for Fe(II), U, S(-II), Mn and CH$_4$, and microbiological information.

One exception in Table 4-2 is sample #1517 from KLX01A, with potentiometric Eh values but high percentage of drilling water (13%). It has been used in the plots of the Eh values but not for modelling purposes. Samples #11692 (KLX17A), #10649 and #10747 (KLX08) are interpreted as resulting from serious short-circuit during sampling but they are considered for discussion as they have a very complete set of redox data, including microbiological determinations[28].

The selected waters (38 samples) cover a wide range of depths (from 120 to 1,500 m; Table 4-2) and different water types: fresh, mixed brackish, brackish-glacial, transition and saline groundwaters. The samples selected here have been categorised as type 1, 2, 3 and 4 (only some of them are type 5; see Smellie *et al.* 2008b, Laaksoharju *et al.* 2008).

4.2 Redox potential

4.2.1 General trends

Eh values in the Laxemar-Simpevarp area are between –200 and –310 mV (Figure 4-1a) and all measured potentials plot in the reducing zone, close to the lower limit of water stability and roughly parallel to it between pH 7 and 8.6. Something similar happens at Forsmark, though some less reducing values (higher than –200 mV) have been measured (Figure 4-1cd). Overall, the position of most of the selected values in the Eh-pH diagram corresponds to the range defined by Drever (1997) for groundwaters buffered by sulphate-reduction (only some of the most reducing values, below –300 mV, would be below this range).

The distribution of Eh with depth (Figure 4-1b) does not show any evident trend. This conclusion does not change when considering only individual subareas, borehole sections or Group 1 Eh values. This behaviour was already noticed by Nordstrom and Puigdomènech (1986) in their work on different Swedish groundwaters down to 600 m depth, and was also observed in Forsmark (Figure 4-1cd). This is different from what has been found in some other crystalline systems (e.g. in Palmottu, where a similar methodology for Eh measurements was used) and in most aquifers elsewhere, where a marked decrease of redox potential is observed as the residence time and depth of the waters increase (e.g. Drever 1997, Blomqvist *et al.* 2000).

The spatial distribution of Eh with depth plot in Figure 4-2, which is a simplified 3D picture of the site, shows the sparseness and heterogeneous distribution of the data.

As already stated in Laxemar 2.1, this behaviour could be the result of a modification in the original redox state in some groundwaters (perturbation of the system; see below). But, most probably, it can be the consequence of the complex hydrological setting and palaeohydrogeological evolution of the Laxemar-Simpevarp area, where the redox-sensitive elements, the potentials calculated from redox couples or the microbiological populations do not show a clear trend with depth either (see below).

An interesting difference between the Eh data available for the Laxemar-Simpevarp area and for Forsmark is the existence, in the Laxemar subarea, of values for dilute groundwaters barely affected by mixing. These dilute groundwaters (with chloride contents between 260 and 744 mg/L in samples #7953, #111607 or #11809 in KLX03, KLX13A and KLX17A; Table 4-2) display considerably reducing values (–275 to –287 mV) for depths between 170 and 408 m. This fact would indicate the ability of microbial or water-rock interaction processes to create very reducing conditions from shallow depths.

---

[28] During sampling, fracture networks intersecting the boreholes may lead to short-circuiting of the groundwater flow in the surrounding bedrock and also to bypassing the packer systems used to isolate the borehole sections being sampled. This effectively means that the section sampled may have been supplied by mixed groundwaters from higher or lower levels in the bedrock, and/or mixed borehole waters above or below the packer systems (Laaksoharju 2008).
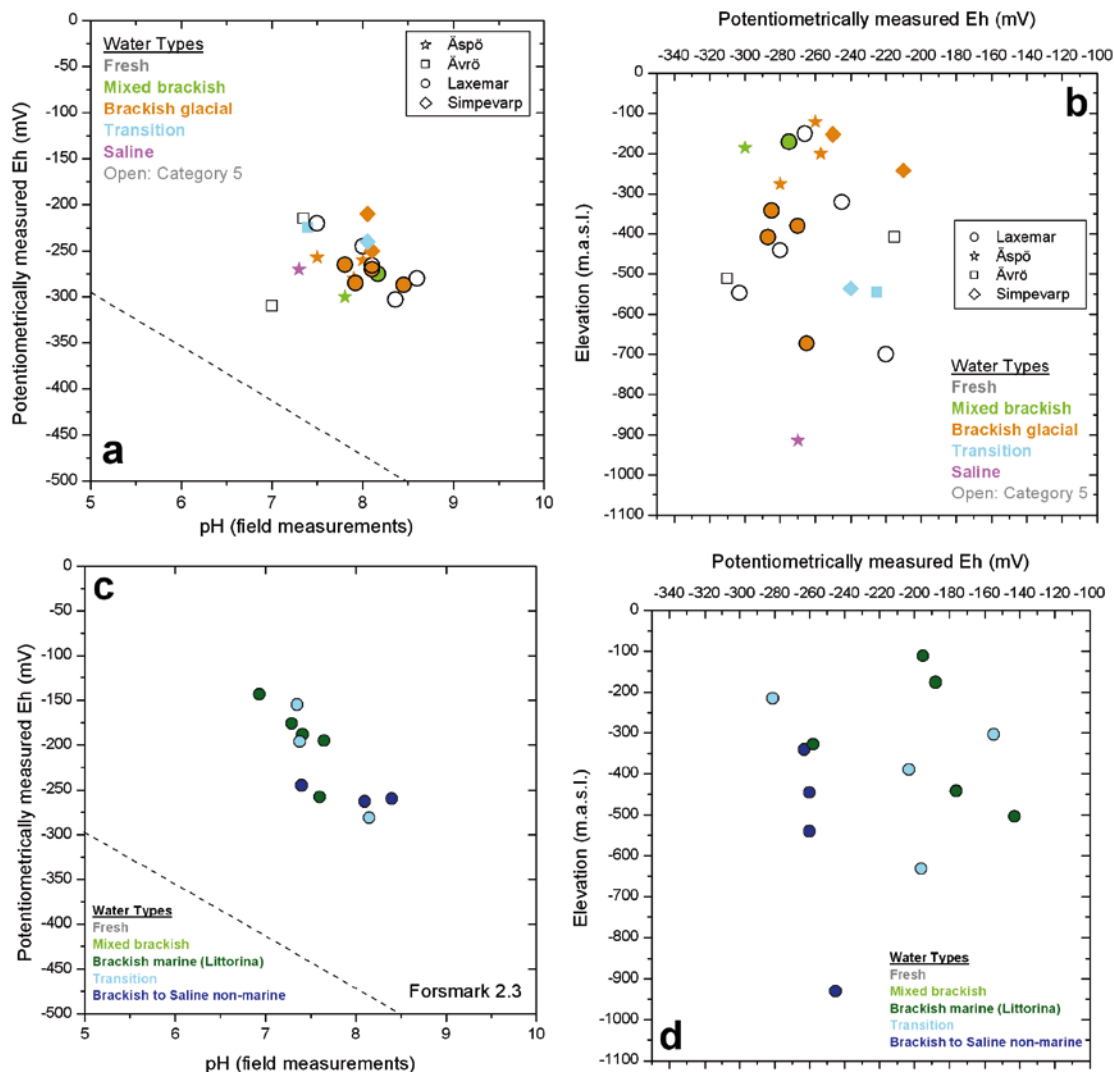
Figure 4-1. *pH-Eh plot and Eh distribution with depth for the groundwaters from Laxemar-Simpevarp (a, b) and Forsmark (c, d) areas respectively.*

Some other waters such as #11692 (KLX17A), #10649 and #10747 (KLX08), even more dilute (Cl between 4.9 and 17 mg/L), with low drilling water percent and measurable tritium values, display even more reducing Eh measurement (from –245 to –303 mV; Table 4-2). Unfortunately these samples were short-circuited during sampling and, therefore, they would correspond to shallower levels. In any case, they would support the existence of very reducing conditions already in the recharge waters with very short residence time.

Therefore, the potentiometrically measured Eh values in the dilute groundwaters are, at least, as reducing as in clearly brackish and saline groundwaters. Even assuming possible perturbations of the original redox environment during the measurements, all the redox potentials at Laxemar-Simpevarp are clearly reducing.

4.2.2 Redox pair modelling

The redox pairs that have been analysed here are the same as in the previous phases (e.g. SKB 2004a, 2005a, 2006a, 2007): the dissolved SO_4^{2-}/HS^- and CO_2/CH_4 redox pairs, and the heterogeneous couples $Fe^{2+}/Fe(OH)_3$, $S_{(c)}/HS^-$, SO_4^{2-}/FeS_{am} and $SO_4^{2-}/pyrite$. These are the most suitable redox pairs for the reducing conditions of these groundwaters and have best performed in similar systems elsewhere in the Scandinavian Shield (see Gimeno *et al.* 2007, 2008, and references therein). Also, they include those that can be participating in the control of the potentiometrically measured Eh at the reducing values in Figure 4-1.
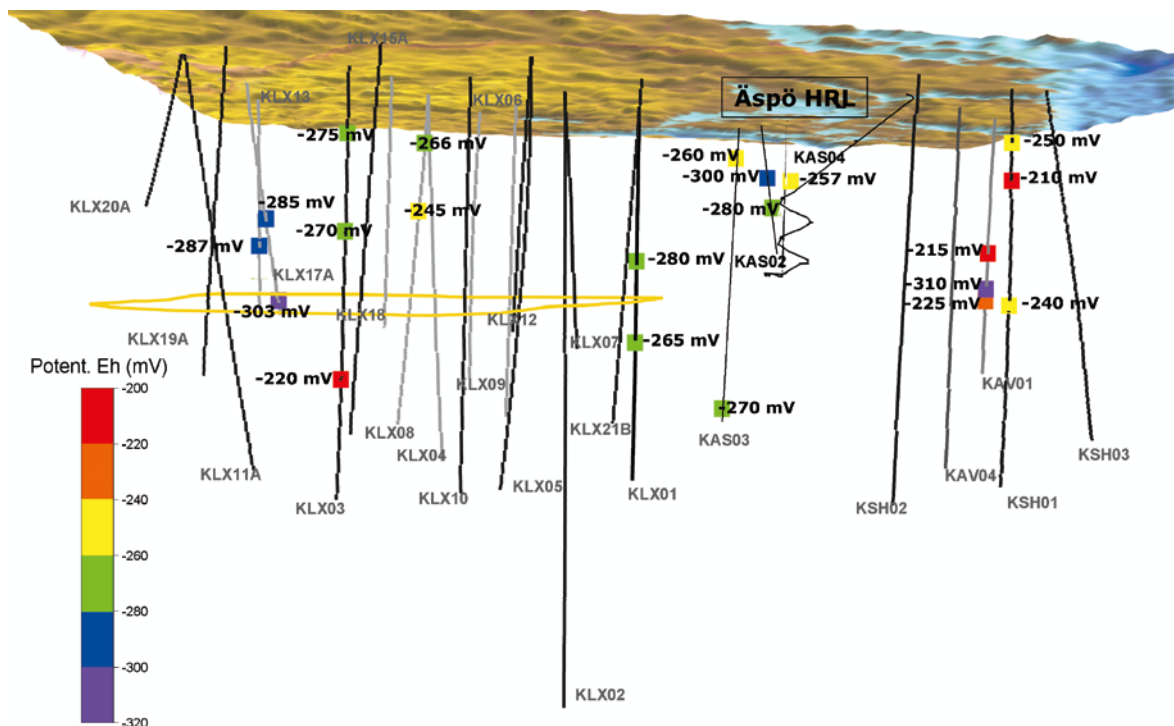
Figure 4-2. *3D distribution of the available potentiometrically measured Eh values drawn on a simplified sketch of the Laxemar-Simpevarp area showing the position of the boreholes. Vertical scale is exaggerated and, therefore, some observations may not be placed at the exact depth. For visual reference, preliminary-selected repository candidate area is marked in yellow (Laxemar) and correspond to 500 m depth.*

PHREEQC and the thermodynamic data included in the WATEQ4F database have been used for the calculations, except in the case of the heterogeneous pair Fe(II)/ Fe(OH)$_3$ for which three different sets of log K values have been used for the solid (see Appendix C, section C.3.1):

1. the set of values proposed by Nordstrom *et al.* (1990) corresponding to amorphous- microcrystalline hydrous ferric oxides, HFOs, or ferrihydrites (log K = 3 to 5,);

2. the value derived from the calibration proposed by Grenthe *et al.* (1992) for a wide spectrum of Swedish groundwaters (log K= −1.1 for a crystalline phase such as hematite or goethite); and

3. the value of log K = 1.2 defined by Banwart (1999) using the same methodology as Grenthe *et al.* (1992) but working with groundwaters from the Äspö large-scale redox experiment, representative of a system affected by recent oxygen intrusion.

The redox potential corresponding to the Fe(II)/ Fe(OH)$_3$ heterogeneous redox pair has been obtained in all these calculations using the above equilibrium constants and the Fe^{2+} activity calculated with PHREEQC[29]. Results obtained with the aforementioned redox couples are summarised in Table 4-3 and Figures 4-3 and 4-4.

Results for iron redox couples

As already reported in Gimeno *et al.* (2007, 2008), the Eh values obtained with the Fe^{2+}/Fe(OH)$_3$ redox pair considering an amorphous or microcrystalline Fe(OH)$_3$ are more oxidising than the measured ones, and they are not included in either the table (Table 4-3) or in the plots.

---

[29] Alternatively, this redox potential can also be calculated with the calibration defined by Grenthe *et al.* (1992) and Banwart (1999) as a function of pH and the total concentration of Fe(II). In previous SDM reports these results have also been presented. However they do not take into account the iron speciation in the groundwaters and, therefore, they do not consider the activity corrections which have been considered for the rest of the redox pairs. Therefore, only the values obtained with PHREEQC have been included here to make all the results comparable.

Table 4-2. Important chemical, physicochemical and microbiological parameters in the selected samples for redox modelling at Laxemar-Simpevarp area. Cat: indicates the category of the sample (see Smellie and Tullborg 2009). Elev.: corresponds to the elevation of the mid part of the sampling interval (m.a.s.l.). DW: represents the percentage of drilling water. The pH data correspond to the field measurements. Ferrous iron, sulphide, uranium and manganese are expressed in mg/L; methane, in ml/L. $\delta^{34}S$ is expressed in ‰ CDT. IRB (iron reducing bacteria), SRB (sulphate reducing bacteria) and MRB (manganese reducing bacteria) are expressed as MPN (most probable number) in cells/mL.

Borehole	Sample	Cat	Elev. (m)	DW (%)	pH	Eh (mV)	Fe(II)	S(–II)	CH$_4$	U (x10^{-3})	Mn(II)	δ^{34}S (‰CDT)	SRB (MPN)	IRB (MPN)	MRB (MPN)
KAS02	1548	3	−199.8	0.81	7.5	−257	0.483	0.5	0.03	−	0.91	−	−	−	−
KAS02	1474	3	−317.2	0.71	7.6	−	0.624	0.15	−	−	0.67	−	−	−	−
KAS02	1428	3	−456.2	0.38	8.3	−	0.941	0.13	−	−	0.73	−	−	−	−
KAS02	1433	3	−523.0	0.28	8.35	−	0.24	0.18	−	−	−	−	−	−	−
KAS02	1560	3	−881.2	0.22	8.5	−	0.049	0.72	0.034	−	0.23	−	−	−	−
KAS03	1569	3	−121.8	0.06	8	−260	0.123	0.71	0.016	−	0.1	−	−	−	−
KAS03	1437	4	−198.7	−	7.65	−	−	0.05	−	−	0.39	−	−	−	−
KAS03	1448	3	−238.9	1.04	7.8	−	−	0.15	−	−	0.35	−	−	−	−
KAS03	1452	3	−602.4	2.23	8.05	−	−	0.05	−	−	0.24	−	−	−	−
KAS03	1455	3	−830.0	2.57	8.05	−	−	0.11	−	−	0.23	−	−	−	−
KAS03	1582	3	−914.0	0.13	7.3	−270	0.077	1.28	0.037	−	0.2	−	−	−	−
KAS04	1596	3	−185.1	0.16	7.8	−300	0.04	1.1	−	−		−	−	−	−
KAS04	1603	3	−275.6	0.52	7.9	−280	0.324	0.41	0.028	−	0.31	−	−	−	−
KAS04	1588	3	−376.7	0.08	8.04	−	0.256	0.6	0.004	−	0.44	−	−	−	−
KAV01	1384	5	−408.3	7.2	7.35	−215	2.49	0.55	−	−	2.8	−	−	−	−
KAV01	1383	5	−512.2	10	7	−310	2.23	1.2	−	−	2.4	−	−	−	−
KAV01	1374	4	−546.1	−	7.4	−225	1.02	0.81	−	−	1.7	−	−	−	−
KSH01A	5263	2	−152.7	2.39	8.1	−250	1.397	0.004	0.06	0.135	0.54	23.1	160	2.1	<0.2
KSH01A	5266	3	−241.7	7.54	8.05	−210	1.301	0.006	−	0.157	0.551	20.2	−	−	−
KSH01A	5288	3	−536.0	10.74	8.05	−240	0.511	−	0.04	0.148	0.484	17.7	3.5	3.3	<0.2
KLX01A	1517	5	−440.7	13	8.6	−280	0.027	0.73	−	−	0.14	−	−	−	−
KLX01	1516	3	−673.0	2.6	7.8	−265	0.029	2.5	0.22	−	0.2	−	−	−	−
KLX01	1773	4	−897.1	0.85	8.4	−	0.052	0.29	−	−	0.09	−	−	−	−
KLX02	2738	4	−298.6	0.22	8.1	−	1.04	0.04	−	−	0.15	−	−	−	−
KLX02	2705	4	−318.1	0.24	8.05	−	0.464	<0.01	−	−	0.14	−	−	−	−
KLX02	2731	3	−1531.0	0.14	8	−	0.426	<0.01	−	−	0.14	−	−	−	−
KLX03	7953	1	−170.8	0.24	8.17	−275	0.251	<0.002	0.87	0.631	0.0618	37.2	<0.2	3.4	1.1
KLX03	10091	3	−379.9	1.88	8.1	−270	0.429	0.007	0.62	0.421	0.107	15.1	220	2.3	280
KLX03	10188	5	−700.6	6.8	7.5	−220	1.0	0.005	−	−	0.27	−	−	−	−
KLX03	10076	1	−922.5	0.04	8.4	−	<0.005	0.09	0.059	<0.01	0.0164	11.1	<0.2	<0.2	2.3
KLX08	10649	5	−150.4	1.4	8.1	−266	0.112	0.004	−	−	0.928	0.0854	39.4	2.3	13	0.4
KLX08	10747	5	−320.0	1.15	8	−245	1.02	0.037	−	−	0.397	0.053	32.7	130	30	17
KLX08	11159	2	−390.7	5.71	7.6	−	0.288	<0.002	−	−	0.0289	0.0877	17	−	−	−
KLX08	11228	3	−504.5	10.7	8.3	−	<0.005	0.01	0.025	0.028	0.0893	13.2	−	−	−
KLX13A	11607	3	−408.0	10.2	8.45	−287	<0.006	0.004	−	−	0.0459	0.0273	29	−	−	−
KLX15A	15008	2	−467.2	4.43	7.6	−	0.548	0.007	0.021	0.144	0.549	17.3	130	140	900
KLX17A	11809	3	−342.3	1.8	7.92	−285	0.69	0.028	−	−	0.116	0.0988	31.3	−	−	−
KLX17A	11692	5	−548.0	0.21	8.36	−303	0.682	<0.006	0.145	0.22	0.025	18.6	3000	280	300

S(–II) < 0.01 will be considered b.d.l.
Fe(II) < 0.05 will be considered b.d.l.

The Eh values calculated with the $Fe^{2+}/Fe(OH)_3$ redox pair using the equilibrium constant proposed by Grenthe *et al.* (1992) are only in agreement (with ±50 mV uncertainty; SKB 2001) with the Eh values measured in 6 samples (Table 4-3; Figure 4-3a), mostly in groundwaters from Äspö, Ävrö and KLX01 borehole, already used by Grenthe *et al.* (1992) when they proposed the calibration. In general, these values are more reducing than the measured ones and the differences between calculated and potentiometrically measured Eh are higher in the shallower waters, irrespective of chloride contents or water type.

The Eh calculated with the same redox pair but using the equilibrium constant proposed by Banwart (1999) show good agreement with the measured values in 9 samples (Table 4-3, Figure 4-3b). In this case, except for one sample, the calculated Eh values are generally less reducing than the measured ones. No relationship has been found between this agreement and the depth or the water type, except that it is better for samples with chloride lower than 5,000 mg/L.

Overall, all these observations suggest that the potentiometrically measured Eh in these ground-waters could be controlled by different iron oxyhydroxides with different solubilities or degree of crystallinity. The $Fe^{2+}/Fe(OH)_3$ heterogeneous redox pair is the most clearly electroactive and, therefore, one of the most feasible to control the Eh measurements in natural systems. However, the variability of the oxyhydroxides solubilities (as a function of their mineralogy, particle size and specific surface area) influences the Eh value obtained (for a review, see Gimeno *et al.* 2007, 2008). This relationship has been successfully used in the literature on this subject (Grenthe *et al.* 1992, Banwart 1999, Trotignon *et al.* 2002) to deduce the type of oxyhydroxide controlling the measured Eh potentials.

The redox potential measured in some brackish to saline groundwaters from Äspö, Ävrö and KLX01 (Laxemar subarea) appears to be controlled by the presence of a clearly crystalline iron oxyhy-droxide, represented by Grenthe's calibration (Figure 4-3a). Therefore, these groundwaters would be in equilibrium or near equilibrium with this type of iron oxyhydroxide (such as the ubiquitous hematite), in agreement with their long residence time, for which low crystallinity phases are not expected (Gimeno *et al.* 2008, and references therein).

Some other groundwaters, mainly in the Laxemar subarea, show a good agreement between their potentiometrically measured values and the ones calculated with the calibration by Banwart (1999, Figure 4-3b). This suggests Eh control by an iron phase with intermediate crystallinity formed by re-crystallisation of an amorphous phase (such as the one considered by Banwart (1999) in the Äspö large-scale redox experiment). In reducing and long residence time groundwaters, this is only possi-ble if there exists a previous oxidising disturbance, that is, a brief oxygen intrusion and precipitation of Fe(III)-oxyhydroxides during the Eh measurements.

Figure 4-3. *Comparison of the Eh values potentiometrically measured with Chemmac and the Eh values calculated with the $Fe^{2+}/Fe(OH)_3$ redox pairs (a) using the equilibrium constant for the hematite defined by Grenthe et al. (1992); and (b) using the equilibrium constant for the solid phase defined by Banwart (1999). The dashed lines indicate the accepted range of Eh variability of ±50 mV.*

In fact, some of the best agreements between potentiometric Eh values and the values calculated with the constant proposed by Banwart (1999) are found in the fresh and "modern" groundwaters represented by the aforementioned "short-circuited" samples #11692 (KLX17A) and #10747 (KLX08). This short-circuit could have had an associated oxygen intrusion during the Eh measurement. However, these groundwaters must correspond to shallower levels, where the presence of low crystallinity Fe(III) oxyhydroxides is possible, and therefore the potentiometric Eh value could represent a natural situation but not at the depths where it was measured.

Apart from these two sets of waters the rest of the samples display measured potential values between the calculated with the Grenthe *et al.* (1992) and Banwart (1999) constants. However, the existence of such variability in the solubilities (or particle size) of the iron oxyhydroxides in the fracture fillings is, for the moment, not very feasible taking into account the hydrothermal origin of the most abundant hematite and the recent investigations on particle size of iron oxyhydroxides.

Results for sulphur and carbon redox couples

Eh values calculated using the electroactive $S_{(s)}/HS^-$ redox couple, in the Laxemar-Simpevarp (Figure 4-4a) or in the Forsmark groundwaters, are invariably higher than the potentiometric Eh values. Therefore, it seems not to be involved in the control of the potentiometric Eh, in contrast to other Swedish groundwaters (Nordstrom and Puigdomènech 1986).

The rest of the sulphur redox couples examined show, in general, a good agreement with the potentiometrically potentiometric Eh values (Table 4-3; Figure 4-4bcd). The results obtained with the homogeneous SO_4^{2-}/HS^- pair and the heterogeneous SO_4^{2-}/FeS_{am} redox buffer agree generally very well with potentiometric Eh values (as in Forsmark; Gimeno *et al.* 2008), whereas the $SO_4^{2-}/$pyrite redox buffer generally gives some less reducing values than the measured ones. In detail:

- The homogeneous pair is generally in between the two heterogeneous pairs, though closer to the amorphous monosulphide.

- Except for the anomalous sample from KAV01 (#1383), the values obtained using the amorphous phase agree with potentiometric Eh values within the ±50 mV uncertainty.

- The same is valid for the homogeneous pair results where, apart from that sample from Ävrö, another sample from Äspö (KAS04, #1596) is slightly out of the uncertainty range. Both exceptions correspond to samples with a potentiometric Eh value lower than -300 mV.

- There are no clear relationships between Eh deviations, chloride contents, depth or water type.

The few Eh values obtained with the non-electroactive pair CO_2/CH_4 are also in very good agreement with the measured values (within ± 50 mV; Figure 4-4e). The higher deviations are associated with the samples with higher chloride contents.

The similar potentials (within ± 50 mV uncertainty) provided by the sulphur (e.g. SO_4^{2-}/HS^- or SO_4^{2-}/FeS_{am}) and the CO_2/CH_4 redox pairs is not strange as the redox windows for these redox pairs are very close, if not overlapping (see, for instance, Kölling 2000). But this situation does not imply the existence of partial redox equilibrium between these couples. For example, the redox potential for the SO_4^{2-}/HS^- redox pair can be calculated for waters with pH > 7 from the equation:

$$pe = \log K - \frac{9}{8} pH + \frac{1}{8} \log \frac{\left[SO_4^{2-} \right]}{\left[HS^- \right]} \tag{4-2-1}$$

and the redox potential for the CO_2/CH_4 pair can be obtained from:

$$pe = \log K - pH + \frac{1}{8} \log \frac{\left[CO_2 \right]}{\left[CH_4 \right]} \tag{4-2-2}$$

These reactions (as well as those of the redox buffers SO_4^{2-}/FeS_{am} or $SO_4^{2-}/$pyrite) involve the transfer of 8 electrons and a difference in the redox potential of only 1/8 pe unit (or 7 mV) would represent a tenfold change in the activity ratios (sulphate/sulphide or CO_2/CH_4 ratios). This result explains the narrow redox windows for these two pairs, as eight orders of magnitude in the activity

ratios could promote only 56 mV of difference in the calculated potential. But it also indicates that the conclusion of a partial equilibrium situation is misleading.

What is really interesting is that the potentiometric Eh values reach the potentials of these windows as CO_2/CH_4 and the sulphate/sulphur redox pairs are *non-electroactive*. Nernstian electrode response can be obtained for certain sulphur redox couples involving native sulphur, hydrogen sulphide and polysulphides (Berner 1963, Boulegue 1978, Macalady *et al.* 1990, Nordstrom 2005). In fact, Nordstrom and Puigdomènech (1986) found that Eh measurements in groundwaters from Fjällveden, Gidea, Lake Finnsjön and Svartboberget (between –50 and –175 mV) agree with the potential calculated from the $S_{(c)}/HS^-$ redox pair as long as polysulphide species were accounted for in the calculation. However, as described above, the values obtained with this redox pair are invariably higher than the potentiometrically measured Eh values for the Forsmark and the Laxemar-Simpevarp groundwaters.

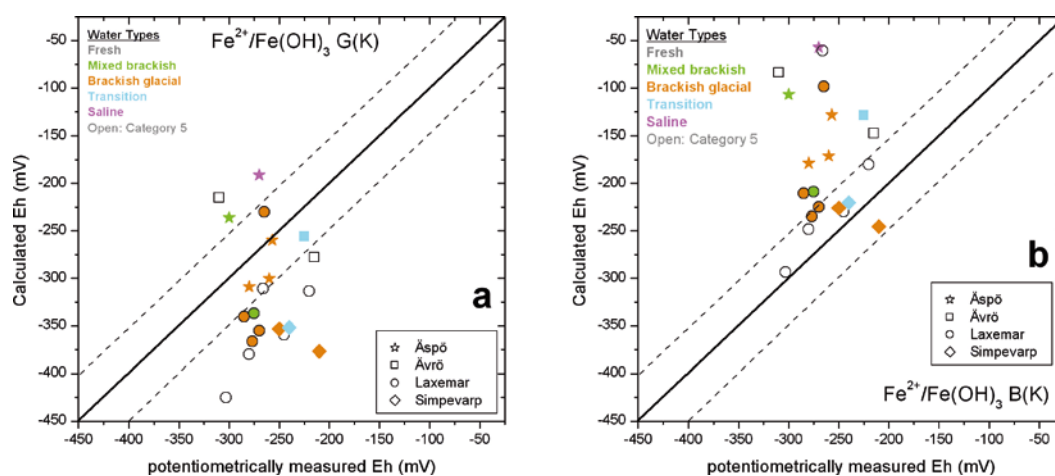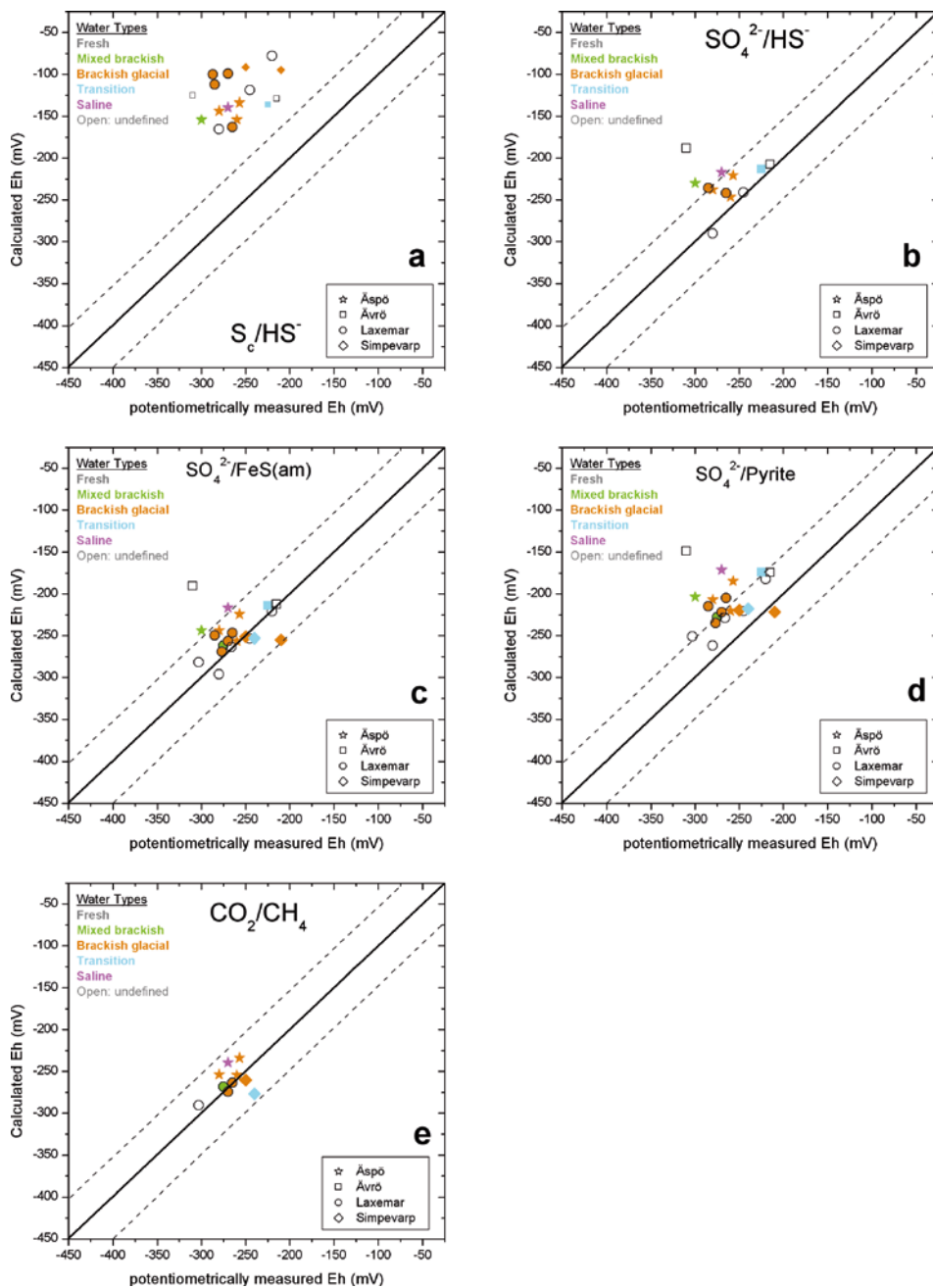**Figure 4-4.** *Comparison of the Eh values potentiometrically measured with Chemmac and the Eh values calculated with the following sulphur and carbon redox pairs. (a)S_c/HS^-; (b) SO_4^{2-}/HS^-; (c) $SO_4^{2-}/FeS(am)$; (d) $SO_4^{2-}/Pyrite$; and (e) CO_2/CH_4;. The dashed lines indicate the accepted range of Eh variability of ±50 mV.*

Table 4-3. Eh values for the selected samples in the Simpevarp area, specifically Äspö, Ävrö and Simpevarp. All these data were already included in the data freeze 2.1. The potentiometrically measured values (column Chemmac) are shown for comparison with the values calculated with the different redox pairs. The redox potential corresponding to the $Fe^{2+}/Fe(OH)_3$ heterogeneous redox pair has been obtained using the correspondent equilibrium constants calculated from the calibrate defined by Grenthe et al. (1992) and Banwart (1999) and the Fe^{2+} activity calculated with PHREEQC.

Subarea	Borehole	Sample	Category	Depth (m)	Cl mg/L	SO_4^{2-}	Fe(II)	S(–II)	CH_4 mL/L	pH	Eh (mV) Chemmac	S_2/HS^-	SO_4^{2-}/HS^-	$SO_4^{2-}/Pyrite$	$SO_4^{2-}/FeS(am)$	CO_2/CH_4	$Fe^{2+}/Fe(OH)_3$ (Grenthe et al. 1992)	(Banwart 1999)
Äspö	KAS02	1548	3	−199.8	3,820	106	0.483	0.5	0.03	7.5	−257	−133.83	−220.5	−184.6	−224.2	−233.8	−259.7	−128.2
	KAS02	1474	3	−317.2	5,360	291	0.624	0.15		7.6		−109.48	−220.7	−187.1	−226.0		−281.6	−150.1
	KAS02	1428	3	−456.2	5,440	290	0.941	0.13		8.3		−122.22	−265.7	−232.5	−265.2		−413.3	−281.6
	KAS02	1433	3	−523.0	6,330	550	0.24	0.18		8.35		−137.81	−267.7	−235.8	−270.1		−386.3	−254.7
	KAS02	1560	3	−881.2	11,100	519	0.049	0.72	0.034	8.5		−142.63	−281.7	−248.3	−283.5	−306.8	−369.7	−237.9
	KAS03	1569	3	−121.8	1,220	31.1	0.123	0.71	0.016	8	−260	−161.80	−246.3	−220.4	−256.5	−254.4	−300.4	−171.1
	KAS03	1448	3	−238.9	2,950	39		0.15		7.8		−153.70	−238.8					
	KAS03	1452	3	−602.4	5,880	470		0.05		8.05		−128.54	−244.8					
	KAS03	1455	3	−830.0	8,080	680	0.047	0.11		8.05		−120.81	−246.6	−218.1	−257.1		−292.2	−160.7
	KAS03	1582	3	−914.0	12,300	709	0.077	1.28	0.037	7.3	−270	−130.33	−216.9	−171.2	−216.5	−239.3	−191.0	−57.0
	KAS04	1596	3	−185.1	508	180	0.04	1.1		7.8	−300	−139.27	−229.8	−203.6	−243.6		−236.1	−106.7
	KAS04	1603	3	−275.6	3,030	220	0.324	0.41	0.028	7.9	−280	−153.98	−237.5	−206.8	−243.6	−253.7	−308.8	−178.6
	KAS04	1588	3	−376.7	5,840	407	0.256	0.6	0.004	8.04		−143.41	−252.3	−216.2	−252.9	−266.7	−333.7	−202.2
Ävrö	KAV01	1384	5	−408.3	350	36	2.49	0.55		7.35	−215	−151.12	−207.5	−174.5	−212.4		−277.8	−147.3
	KAV01	1383	5	−512.2	1,970	118	2.23	1.2		7	−310	−129.07	−188.2	−148.8	−190.5		−215.1	−83.7
	KAV01	1374	4	−546.1	4,300	220	1.02	0.81		7.4	−225	−125.15	−213.2	−174.2	−213.9		−256.0	−128.5
Simpe-varp	KSH01A	5263	2	−152.7	5,590.1	31.71	1.397	0.004	0.06	8.1	−250			−219.4	−251.1	−260.2	−353.4	−225.9
	KSH01A	5266	3	−241.7	6,322.2	48.16	1.301	0.006		8.05	−210			−221.6	−255.0		−376.9	−245.4
	KSH01A	5288	3	−536.0	8,875.7	230.48	0.511		0.04	8.05	−240			−217.7	−253.0	−276.7	−351.8	−220.3

Subarea	Borehole	Sample	Category	Depth (m)	Cl	SO$_4^{2-}$	Fe(II)	S(–II)	CH$_4$	pH	Eh Chem-mac	S$_c$/HS$^-$	SO$_4^{2-}$/HS$^-$	SO$_4^{2-}$/Pyrite	SO$_4^{2-}$/FeS(am)	CO$_2$/CH$_4$	Fe^{2+}/Fe(OH)$_3$ (Grenthe et al.1992)	(Banwart, 1999)
					Mg/l				mL/L									
Laxemar	KLX01	1517	5	−440.7	1,650	103	0.027	0.73		8.6	−280	−165.52	−289.9	−261.7	−296.2		−379.8	−248.3
	KLX01	1516	3	−673.0	4,870	351	0.029	2.5	0.22	7.8	−265	−162.63	−241.6	−204.9	−246.4	−263.4	−230.1	−98.6
	KLX01	1773	4	−897.1	11,200	770	0.052	0.29		8.4		−149.06	−271.5	−240.3	−276.4		−353.9	−222.3
	KLX02	2738	4	−298.6	73	43	1.04	0.04		8.1		−122.25	−246.1	−223.7	−256.7		−381.2	−250.9
	KLX02	2705	4	−318.1	235	84	0.464			8.05				−219.9	−254.8		−354.0	−223.4
	KLX02	2731	3	−1531.0	45,500	832	0.426			8				−212.0	−248.9		−365.2	−232.3
	KLX03	7953	1	−170.8	259	36.6	0.251		0.87	8.17	−275			−228.1	−261.7	−268.2	−337.0	−208.6
	KLX03	10091	3	−379.9	1,390	127	0.429		0.62	8.1	−270	−99.25		−221.9	−256.6	−274.4	−355.3	−224.7
	KLX03	10188	5	−700.6	2,250	232	1.9			7.5	−220	−78.03		−182.3	−221.1		−313.5	−179.9
	KLX03	10076	1	−922.5	10,500	758	−0.005	0.09	0.059	8.4		−133.34	−279.9			−315.7		
	KLX08	10649	5	−150.4	12.6	12.8	0.112			8.1	−266			−228.8	−263.7		−310.7	−60.6
	KLX08	10747	5	−320.0	14.9	14	1.02	0.037		8	−245	−118.81	−241.0	−220.4	−253.7		−359.5	−229.5
	KLX08	11159	2	−390.7	1,590	133	0.288			7.6				−189.8	−229.1		−263.3	−132.8
	KLX08	11228	3	−504.5	2,030	145		0.01	0.025	8.3		−107.65	−254.4			−285.2		
	KLX13A	11607	3	−408.0	744	36.8				8.45	−287	−100.31						
	KLX13A	11541	4	−475.0	774	47.1	0.198			8.2	−277			−234.7	−269.4		−366.7	−234.9
	KLX15A	15008	2	−467.2	5,890	425	0.548		0.021	7.6		−84.49		−185.6	−224.7	−243.1	−275.4	−144.2
	KLX17A	11809	3	−342.3	565	22.9	0.69	0.028		7.92	−285	−112.46	−235.7	−214.8	−249.5		−340.6	−210.3
	KLX17A	11692	5	−548.0	17.1	6.47	0.682		0.145	8.36	−303			−250.7	−281.7	−290.7	−425.1	−293.3

The agreement between the potentiometrically measured Eh and the potentials calculated from the redox buffers SO_4^{2-}/FeS or SO_4^{2-}/pyrite has rarely been found. One of these rare cases is the granitic groundwater system at the Toki granite (Japan) where the potentiometrical Eh values (using a down hole probe) between –260 and –385 mV agree with the potentials obtained from the SO_4^{2-}/pyrite redox couple (JNC 2000, Iwatsuki *et al.* 2005). The authors have considered this pair to control the measured potentials. The other case is Palmottu, where the potentiometrical Eh values (using the same methodology as the one used at Forsmark and Laxemar-Simpevarp areas) from –270 to –320 mV are considered to be controlled by the redox buffers SO_4^{2-}/pyrite and SO_4^{2-}/FeS (Blomqvist *et al.* 2000).

These examples would support the control of the potentiometrically measured Eh in Laxemar-Simpevarp by this type of redox buffer. The important role of both the sulphur system and the micro-bially mediated sulphate reduction on the redox state of the groundwaters has been evidenced by different criteria independent of the potentiometrically measured Eh (evaluation of the saturation state of sulphide minerals, microbiological data, etc) and their influence on the potentiometric determinations of Eh could be reasonable. However, as far the UZ group knows, there is no experimental evidence on the achievement of reversible potentiometric Eh values from the SO_4^{2-}/pyrite and SO_4^{2-}/FeS(am) buffers and the mechanisms by which the electrodes could respond to sulphur or other electroactive species "mediators" generated during sulphate-reduction is presently unknown.

In any case, this is a problem strictly related to the Eh measurements and not to the real importance of the sulphur or CO_2/CH_4 redox pairs as representing effective processes which may contribute to the redox state in many groundwaters at Laxemar-Simpevarp (see below).

4.2.3　Conclusions

Eh values in the Laxemar-Simpevarp area are between –200 and –310 mV and all measured potentials plot in the reducing zone. Something similar happens at Forsmark, though some less reducing values (larger than –200 mV) have been measured. Overall, the position of most of the selected values in the Eh-pH diagram corresponds to the range defined by Drever (1997) for groundwaters buffered by sulphate-reduction (only some of the most reducing values, below –300 mV, would be below this range).

The distribution of Eh with depth does not show any evident trend for any borehole section or studied subarea. This behaviour was already noticed by Nordstrom and Puigdomènech (1986) in their work on different Swedish groundwaters down to 600 m depth, and was also observed in Forsmark. However, it is different to what has been found in other crystalline systems (e.g. in Palmottu, where a similar methodology for Eh measurements was used) and in most aquifers elsewhere, where a marked decrease of redox potential is observed as the residence time and depth of the waters increase (e.g. Drever 1997, Blomqvist *et al.* 2000).

All the redox potentials at Laxemar-Simpevarp are clearly reducing[30] even taking into account the possible perturbations of the original redox environment during the measurements. This would indicate the ability of microbial or water-rock interaction processes to create very reducing conditions even in the shallowest parts of the system.

Results of the available analytical determinations for redox couples in the studied groundwaters, including not only iron and sulphur redox couples, but also the NO_3^-/NO_2^-, NO_3^-/NH_4^+, NO_2^-/NH_4^+, or the MnO_2/Mn^{2+} redox pairs, show the typical redox disequilibrium repeatedly observed in natural waters (Lindberg and Runnells 1984, Langmuir 1997, Stefansson *et al.* 2005) even in long residence time groundwaters (e.g. 25,000–100,000 years; Thorstenson *et al.* 1979, Thorstenson 1984, Stefánsson *et al.* 2005). NO_3^-/NO_2^-, NO_3^-/NH_4^+, NO_2^-/NH_4^+ and MnO_2/Mn^{2+} redox couples provide oxidant Eh values (e.g. from +440 to +150 mV, in the case of NO_2^-/NH_4^+ pair) for the same samples where the sulphur, iron or CO_2/CH_4 redox pairs provide clearly reducing ones.

---

[30] Including some shallow and dilute groundwaters barely affected by mixing or even some short-circuited waters with very short residence time.

This disequilibrium situation among the different redox pairs promotes that an overall Eh value for a groundwater is often impossible to assign (Thorstenson 1984, Nordstrom and Munoz 1985, Langmuir 1997; etc). Therefore, as redox potentials calculated from redox couples are considered the only way to approach meaningful Eh values in natural waters (Thorstenson 1984, Nordstrom and Munoz 1986, Langmuir 1997, Drever 1997, Nordstrom 2005, etc), redox couples with the relevant redox species must be selected.

Under the reducing conditions of the studied groundwaters, the redox pairs used and presented in this section are the most suitable ones. $Fe^{2+}/Fe(OH)_3$ is completely reasonable as ferric oxyhydroxides (mainly hematite) have been found in the fracture fillings and it is an electroactive pair for potentiometric measurements. However, the redox potential defined by this heterogeneous redox pair depends on the mineral phase characters (solubility, particle size, etc) which are not perfectly demarcated yet. Moreover, oxygen intrusion during drilling and sampling may induce low crystallinity oxyhydroxides to precipitate and to become the redox potential controllers. Therefore, the Eh values obtained with this redox pair should be treated with caution.

The results indicate that the potentiometrical Eh values in these groundwaters could be controlled by different iron oxyhydroxides with different solubilities or degree of crystallinity at different depths and locations. The redox potential measured in some brackish to saline groundwaters from Äspö, Ävrö and KLX01 appears to be controlled by the presence of a clearly crystalline iron oxyhydroxide, such as the ubiquitous hematite represented by Grenthe's constant. This is in agreement with the long residence time of these groundwaters, where low crystallinity phases are not expected (Gimeno *et al.* 2004c and references therein). Other groundwaters, mainly in the Laxemar subarea, show a good agreement between their electrode potential measured values and the ones calculated with the solubility value by Banwart (1999). Eh values in these groundwaters could be controlled by the occurrence of an iron phase with an intermediate crystallinity, such as a recent low-crystallinity iron oxyhydroxide re-crystallised from an amorphous one. For the studied system, characterised by reducing and long residence time groundwaters, this situation point towards a brief oxygen intrusion and precipitation of Fe(III)-oxyhydroxides during the Eh measurements.

The presence of dissolved sulphide and sulphate reducing bacteria, as well as the existence of equilibrium situations with respect to amorphous ferrous iron monosulphides (section 4.3.4) in the studied waters, suggest the presence of clearly sulphidic environments. Therefore, the redox potential calculated with the sulphur redox pairs can be considered as representative for these waters. Eh values calculated using the electroactive $S_{(s)}/HS^-$ redox couple, in the Laxemar-Simpevarp or in the Forsmark groundwaters, are invariably larger than the potentiometrically measured Eh values. Therefore, this couple seems not to be involved in the control of measured Eh, in contrast with what happens in other Swedish groundwaters (Nordstrom and Puigdomènech 1986). The rest of the studied sulphur redox couples (SO_4^{2-}/HS^-, SO_4^{2-}/FeS_{am} and $SO_4^{2-}/pyrite$) usually agree within a range of ± 50 mV with the potentiometrically measured Eh values and the same conclusion stands for the few Eh values obtained with the non-electroactive pair CO_2/CH_4.

The potentials of redox pair CO_2/CH_4, very similar to those obtained from the sulphur couples, could be related to the methanogenic activity (samples from the sections KLX03, at 171 and 380 m depth and KLX17A at 342 m depth). However, non-biogenic methane from endogenous sources has also been detected in the other examined sections (Hallbeck and Pedersen 2008b, see also Appendix G). Data are still scarce and, therefore, further studies would be needed to clarify this question.

The surprisingly good agreement between the redox potential obtained with these two sets of non-electroactive redox pairs (sulphur and carbon) and the potentiometrically measured Eh should be further studied.

4.3   Iron and sulphur systems

Iron (II) and iron (III) minerals are widely distributed in the studied systems and the presence of dissolved sulphide and of sulphate reducing bacteria (SRB) has also been reported in these groundwaters. This makes the iron and sulphur systems very important for the understanding of the redox processes in Forsmark and Laxemar-Simpevarp.

An important effort in the characterisation of the sulphur system has been made in previous works (Gimeno *et al.* 2008) as it presents several features very significant for the studied systems:

- The presence of dissolved sulphide in these low temperature groundwaters is related to the presence of sulphate reducing bacteria (while the rest of the dissolved redox indicators for the reducing environment in these systems could have also inorganic origin; Appendix G) although uncertainties in their location or intensity may exist.

- Bacterial sulphate reduction activity in other natural systems at present (surface waters, soils, groundwaters, marine sediments, etc) usually controls the redox processes of the system in which it is developing.

- Finally, the development of this environment in the past can leave clear clues (e.g. sulphide minerals like pyrite).

The relationship between both redox systems is conditioned by the typical bacterial activities of each system (iron reducing and sulphate reducing bacteria) which could have a mutually exclusive effect (dominance of one of the systems) or be effective at the same time. If an electron donor is available (e.g. organic matter), this type of bacterial activity will be conditioned by the presence of the necessary terminal electron acceptors which, in the case of IRB, would be the suitable Fe(III)-bearing minerals.

The iron system may also have an important role in clearly sulphidic environments. For example, the reductive dissolution of ferric oxyhydroxides by hydrogen sulphide may exert a major control on dissolved sulphide contents (Canfield 1989, Canfield *et al.* 1992, Poulton *et al.* 2004), additional to the sulphide precipitation. This process may be especially important in the performance assessment, as the factors controlling dissolved sulphide concentrations are of major concern.

The reductive inorganic capacity of the studied systems is mainly associated with the iron system present in the form of Fe(II)-silicate minerals. But this reductive capacity may be enlarged in the presence of Fe(III)-bearing minerals (e.g. iron oxyhydroxides), if they are suitable for IRB as terminal electron acceptors.

Therefore, the iron system is also of critical importance in the understanding of the present groundwater redox state and its future evolution. More data and detailed studies are needed to deal with this subject in depth. This section presents simultaneously the iron and sulphur systems.

4.3.1 Hydrochemical data

Dissolved Fe(II) and S(–II) display the greater variability and higher contents in the near-surface groundwaters (up to 9 and 5 mg/L, respectively). Maximum iron contents are found in the fresh near-surface groundwaters while maximum sulphide concentrations were detected in the brackish near-surface groundwaters from soil pipe SSM000241 (up to 10 mg/L, not shown in Figure 4-5). Sampled waters in that soil pipe, possibly representing discharges of deep saline/marine groundwaters (Tröjbom *et al.* 2008), also show extremely high HCO_3^- concentrations and very low SO_4^{2-} contents, which support an intense sulphate reducing activity, in agreement with the intense microbial degradation of organic matter indicated by Tröjbom *et al.* (2008) for these waters.

Apart from these exceptions, the highest sulphide contents are close to 1 mg/L, slightly lower than the values found at Forsmark (up to 1.64 mg/L; Figure 4-6), and higher than at Olkiluoto (up to 0.28 mg/L, not shown). Dissolved Fe(II) displays similar values to the near-surface groundwaters from Forsmark (up to 8.7 mg/L) or Olkiluoto (up to 7.4 mg/L, Pitkänen *et al.* 2004). Therefore, dissolved Fe(II) and S(–II) contents in the near-surface groundwaters from the Laxemar-Simpevarp area do not deviate significantly from the ranges found in the same type of waters in other Fennoscandian sites.

The presence of noticeable contents of these elements in many near-surface groundwaters (sulphide was above detection limit in more than 55% of the samples analysed for it) would indicate the occurrence of anoxic environments (post-oxic and sulphidic) already in the more superficial part of the studied area.
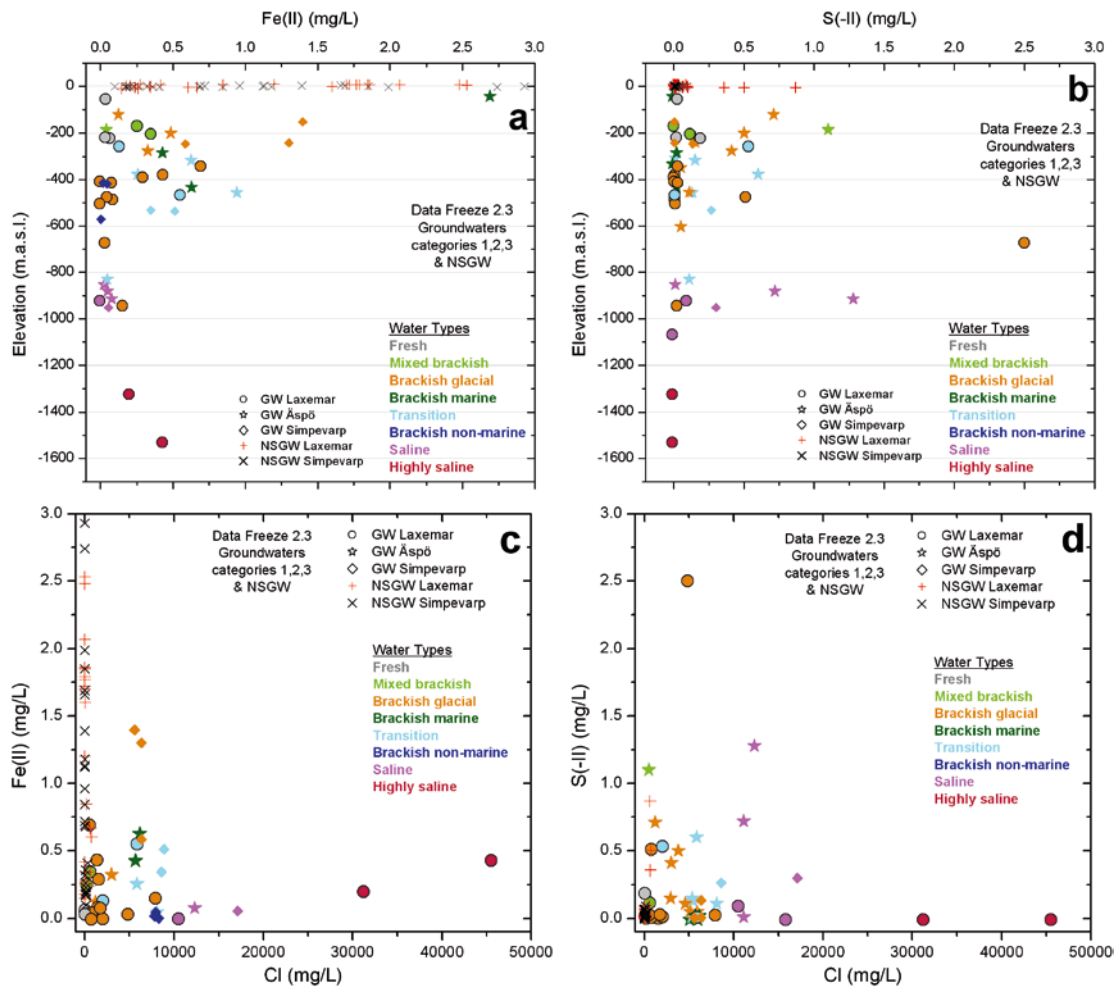
Figure 4-5. *Ferrous iron (a, c) and sulphide (b, d) distribution with respect to depth (a, b) and chloride contents (c, d) in the Laxemar-Simpevarp area groundwaters.*

In the groundwaters, Fe(II) shows a rough decreasing trend from the surface down to 700 m. Below that, the values are lower than 0.2 mg/L except in the deepest highly saline sample (1,500 m depth) where Fe(II) values reach 0.5 mg/L.

There is not a clear evolution trend of dissolved sulphide with depth. There are variable but significant amounts down to 900 m depth with maximum of 2.5 mg/L at 700 m depth. High sulphide contents are mainly associated with groundwaters from Ävrö and Äspö; values between 1 and 1.25 mg/L can be found down to 900 m depth in the more saline samples from Äspö (Figure 4-5b). The already mentioned highest value of 2.5 mg/L S(-II) has been measured in the Laxemar subarea, but in general S(-II) contents are noticeably lower than in the other subareas, mostly below 0.5 mg/L and in many cases below detection limit (the case of the deepest and most saline waters).

There is no correlation between Fe(II) or S(–II) and chloride (Figure 4-5cd). A local maximum for both elements (and also in dissolved Mn; see section 4-4) is observed at around 5,000–6,000 mg/L Cl in groundwaters with certain marine influence, mainly in Simpevarp (including Ävrö) and Äspö.

Forsmark and Olkiluoto groundwaters show a similar distribution of these elements with depth. Dissolved Fe(II) in Forsmark reach the highest values in the brackish marine groundwaters, decreasing to similar contents to those found at Laxemar-Simpevarp at 1,000 m depth (Figure 4-6a). Ferrous iron is also enriched (concentrations higher than 1 mg/L) in the Olkiluoto groundwaters with a significant marine component at shallow levels (down to 200 m) and then decrease at greater depths. However, in contrast to Forsmark and Laxemar-Simpevarp, the deepest and more saline waters in Olkiluoto display the largest values of Fe(II) (more than 3 mg/L see Figure 5–16c in Pitkänen *et al.* 2004).
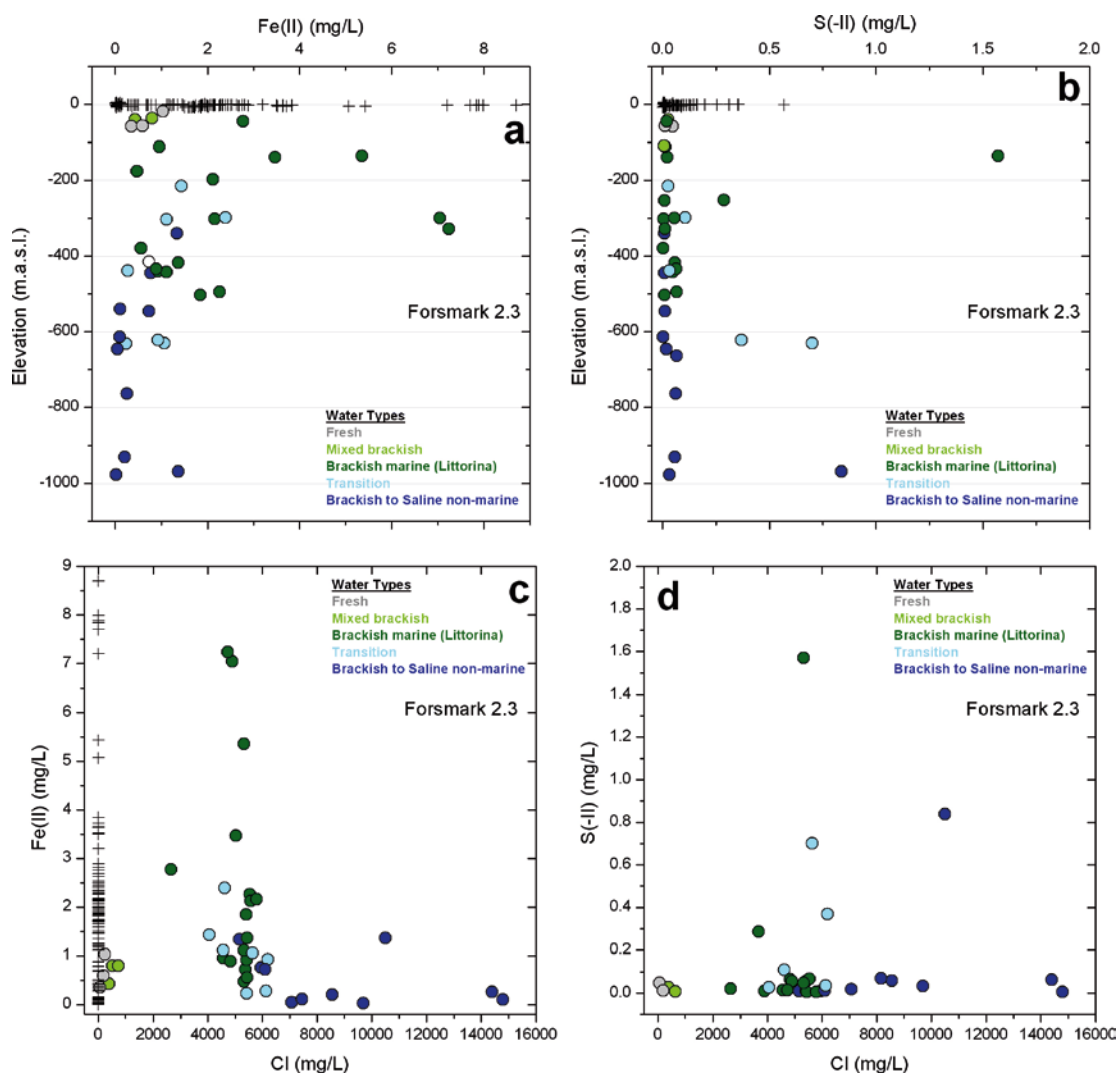
Figure 4-6. *Ferrous iron (a, c) and dissolved sulphide concentrations (b, d) with respect to depth (a, b) and chloride contents (c, d) in the Forsmark groundwaters (including near-surface groundwaters).*

Dissolved sulphide concentrations in the Forsmark and Olkiluoto groundwaters reach the highest values in the brackish groundwaters with an important Littorina component and at relatively shallow levels (near 1.6 mg/L at 150 m depth in Forsmark, Figure 4-6a; and up to 12 mg/L in the Olkiluoto area at 400 m depth). Some sulphidic groundwaters are found in Forsmark at 600 m (0.3–0.6 mg/L) and 1,000 m depth (0.8 mg/L) while sulphide is undetectable from 500 m depth down at Olkiluoto.

Distribution of dissolved Fe(II) and S(–II) with respect to chloride in the Forsmark (Figure 4-6c) and Olkiluoto groundwaters does not show any correlation either, except the presence of a wide range of concentrations in Littorina-rich groundwaters with 5,500 mg/L of chloride.

In summary, there is a high number of samples with significant sulphide contents (e.g. > 0.2 mg/L) in the Laxemar-Simpevarp area (mainly at Äspö and Ävrö) but this is slightly different at the Laxemar subarea where the number of samples with S(–II) > 0.2 mg/L is much lower (except for the sample with the maximum of 2.5 mg/L). These values are well in the ranges for Forsmark or Olkiluoto (where values of 12 mg/L have been measured) or other low temperature groundwater systems in crystalline aquifers[31].

---

[31] Nordstrom and Puigdomènech (1986) indicated sulphide contents up to several tenths of mg/L in the Swedish sites studied by them; up to 3.5 mg/L were determined in Palmottu (Blomqvist *et al.* 2000); up to 4.49 mg/L were analysed in the Toki Granite groundwaters (Mizunami Underground Laboratory, Japan; Iwatsuki *et al.* 2005).

4.3.2 Mineralogical data

Mineralogical studies constitute one of the most important parts in the understanding of the geochemical evolution in the studied groundwaters. This important role becomes even more relevant for redox processes. The amount and characters of the minerals involved in this kind of processes supply basic information for the understanding of the factors conditioning the present situation and the palaeohydrological or future evolution of the redox state (see Appendix G for discussion).

An important issue related to the redox mineralogy of the systems is the assessment of the reducing capacity. Migration of superficial oxidizing groundwaters to the deeper bedrock may occur, for instance, during deglaciation events and it could adversely affect the chemical stability of the repository. Therefore, it is important to show that sufficient inorganic reducing capacity is provided by the fracture coatings and fracture wall rock. Since iron and sulphur minerals are critical in the assessment of the reducing capacity, the available data on these minerals are reviewed below.

A second issue is the determination of the maximum penetration depth of the oxidizing waters (redox front) at present and over the palaeohydrological history of the system. The fracture filling mineralogy and geochemistry (see Drake and Tullborg 2008) can be used to trace the situation of these redox fronts and, therefore, also the depths to which the reducing capacity may be diminished. The study of redox-sensitive Fe-minerals, such as pyrite and specially Fe-oxides and Fe-oxyhydroxides (e.g. goethite), can be used for this purpose and the obtained results on this subject are also summarised below.

Overburden and shallow bedrock: reducing capacity and traces of oxygen penetration

The oxic conditions in the surface waters will change to anoxic and reducing when passing through the soil cover and/or the near surface bedrock fractures. Both degradation of organic matter and the interaction with Fe(II)-minerals can consume the dissolved oxygen in the fresh, near-surface groundwaters in the overburden and the shallowest bedrock. Therefore, this superficial zone constitutes the first layer where the redox buffering processes are able to act over the recharge waters and where traces of old or recent oxidising events could remain.

As described in chapter 3 (section 3.2), the overburden in the Laxemar-Simpevarp zone is dominated by areas of bare bedrock with very thin soils (leptosol) if any. This is a distinctive feature with respect to other Swedish sites (Lundin *et al.* 2005). The rest of the surface is covered by till and clayey deposits and soils (peat soils and histosols dominate in the zone although gleysols, podzols, umbrisols and regosols are also frequent; Lundin *et al.* 2005). Therefore, these two lithologic units (soils and sediments, on one hand, and the shallow bare bedrock, on the other) will show different textural, biological, hydraulic and geochemical features with different effects on the type and intensity of the redox processes.

Soils and sediments

In the available mineralogical data for the till and clay deposits (see section 3.2.2) the presence of hornblende and chlorite has been usually noted. Several facts suggest that pyrite, although not detected, is also present: (1) the gyttja clay sediments (fine-grained clay and silt sediments, mainly deposited in the Littorina Sea period at the bottom of the sea) usually contain iron sulphides once formed in an anoxic environment some centimetres below the marine water-sediment interface (e.g. Sohlenius and Öborn 2004); and (2) sulphur isotope ratios ($\delta^{34}S$) measured in dissolved sulphate, indicate the oxidation of sulphides (pyrites) as the main source of sulphate in some near-surface groundwaters (see section 3.4.1).

Apart from these minerals contributing to the reducing capacity of the system, the presence of some other redox sensitive minerals may be easily deduced. This is the case of Fe-oxyhydroxides, on which there is no mineralogical information but whose presence is almost certain considering the existing soils:

1. an essential feature of podzolic soils is the development of spodic horizons, that is, accumulations of metal–humus complexes and secondary, low crystallinity Fe, Al and Al–Si oxides and oxyhydroxides in the B horizon, ferrihydrite (and also goethite) being the most important iron mineral phase in this type of soils (Schwertmann and Taylor 1989, Schwertmann 1993, Karltun *et al.* 1998);

2. in hydromorphic soils (soils influenced by water, such as gleysols and histosols, periodical or permanently water-saturated soils, respectively), the redoxomorphic processes (redox element remobilization) are responsible for their main soil features. Therefore, is not strange that lepidocrocite, often associated with goethite, occurs in this type of soils in humid temperate climates (Schwertmann 1993). Moreover, natural occurrence of green rusts (mixed ferrous/ferric hydroxides) has been observed in gleysols (Trolard et al. 1997, Berthelin et al. 2006).

Interaction of Fe(II)-minerals with dissolved oxygen in waters produces different Fe(III)-oxides, -hydroxides and – oxyhydroxides (collectively termed as Fe(III) oxyhydroxides in this section). These secondary ferric minerals are ubiquitous in sediments and soils formed in the presence of oxygen and they often occur in fractures and pore spaces as a result of low-temperature weathering[32].

The occurrence of these poorly-crystalline Fe-oxyhydroxides in the soils of the Laxemar-Simpevarp area would be limited to the shallowest part of the profiles (usually, from cm to dm below the surface) exposed temporally (e.g. seasonally) or permanently to the action of oxidising meteoric waters. However, oxygen penetration is limited by the biological activity as the biological degradation of organic matter in the soil layer drastically increases the reducing capacity in the overburden. This is the reason why the occurrence of the poorly-crystalline Fe(III)-oxyhydroxides in the soils of the Laxemar-Simpevarp area is limited to the shallowest part of the profiles.

Reducing conditions are produced in peat soil, gleysol and histosol by prolonged water saturation of soil material in the presence of organic matter. These reducing conditions are reached just below the water table and promote the mobilization of reduced species of iron and manganese through the edaphic profile and may partially explain the high Fe(II) contents found in some near-surface groundwaters. Moreover, sulphidic mineral formation (monosulphides and pyrite) can be an active process in histosols under these reducing conditions (Fanning et al. 1993, Todorova et al. 2005), supporting the results obtained in the speciation-solubility calculations (see section 4.3.4).

Therefore, in the areas with a thick soil cover, the recharge groundwaters will be reducing through the soil profile before reaching the bedrock.

Shallow bedrock and redox front

The outcrops of bare bedrock in the Laxemar-Simpevarp area are dominated by the Ävrö granite and quartz monzodiorites and show low proportions of pyrite and other sulphides. However, they show variable although significant amounts of biotite, chlorite and hornblende as the main minerals able to buffer the input of oxygen-rich waters. More important, however, is the type of minerals present in near surface fracture fillings as the potential oxidation effects of the meteoric waters in the overburden will be favoured in water-conducting fracture zones of bedrock outcrops.

A detailed study of shallow fracture fillings (upper 100 m depth) has been performed by Drake and Tullborg (2008) in two sites with exposed bedrock outcrops from the Laxemar subarea. The results indicate the presence of high amounts of old, low-temperature crystalline goethite[33] in the uppermost

---

[32] Several properties of Fe-oxyhydroxides (e.g. grain size; see Dideriksen et al. 2007) make possible the distinction between low-temperature and hydrothermal genesis, or even between "recent" and "old" low temperature formation. In low-temperature oxic environments, poorly-crystalline Fe-oxyhydroxides (ferrihydrite, lepidocrocite) quickly precipitate and often age to crystalline hematite or goethite. The presence of poorly-crystalline Fe-oxyhydroxides is indicative of present oxic (or alternating oxic-anoxic conditions) because their recrystallization kinetics towards the more crystalline and stable phases (goethite and hematite) can be very fast, in the order of days to years, when the groundwaters are alkaline, reducing (Houben 2003, Schwertmann and Murad 1983, Stipp et al. 2002) and have high contents of dissolved Fe(II) (Pedersen et al. 2005). In any case, crystalline iron-oxyhydroxides can remain stable even when solutions become reducing, as is the case in the fracture fillings of the Laxemar-Simpevarp zone. Therefore, Fe(III)-oxyhydroxides may be used as markers of recent or old oxidising conditions for tracing the depth of the dissolved oxygen penetration (redox front) at Laxemar-Simpevarp.

[33] This distinctive high proportion of crystalline goethite at shallow levels (uppermost 20–40 m interval) has been identified in the Forsmark area as well (Drake et al. 2006). Identification of high proportions of crystalline goethite only in the shallowest part of the system suggests a low temperature origin for goethite instead of a hydrothermal origin (the most common origin for hematite as the most abundant oxyhydroxide at all depths in the studied system). This low temperature origin has been confirmed by Dideriksen et al. (2007).

10–25 m of the boreholes and, occasionally, deeper down to c. 80 m in a few highly fractured sections. They also indicate the occurrence of other Fe-oxyhydroxides. Between 0 and 20 m depth these oxyhydroxides are recent and of low-temperature origin whereas those occurring deeper are older and have either low-temperature or hydrothermal origins. Above 20 m depth, pyrite crystals are altered and/or partially replaced by goethite and clay minerals in fractures and in the adjacent wall rock, whereas below this depth, the intensity of alteration decreases and pyrite is generally unaltered.

Additional data from other sites confirm these observations. With regard to the occurrence of goethite, mineralogical and isotopic studies of iron oxyhydroxides performed by Dideriksen *et al.* (2007) in KAS02 (Äspö), KOV01 (Oskarshamn) and KFM02A (Forsmark) boreholes indicate the presence of well-crystallised but very fine-grained Fe-oxyhydroxides (mainly goethite), typical of old, low-temperature genesis, at depths reaching between 5 and 19.5 m at Äspö (KAS02 borehole) and 100 m depth in the KOV01 borehole.

Recent, low temperature Fe-oxyhydroxides (such as poorly-crystalline lepidocrocite or ferrihydrite, frequently described as "rust"; Landström and Tullborg 1990) have also been identified in the fracture fillings of other areas (e.g. Klipperas), usually in the upper tens of meters, together with crystalline goethite or hematite (Tullborg pers. comm.).

Therefore, the occurrence of recent, low temperature Fe-oxyhydroxides indicates that the present redox front in the Laxemar subarea is located at about 15–20 m depth, in a zone affected by seasonal and annual variations in the recharge waters. The identification of old, low temperature goethite down to 80 m depth in the Laxemar subarea indicates the possible maximum penetration depth of oxygenated groundwaters in the past (within the last 300,000 years; Drake and Tullborg 2008).

Although the presence of low temperature Fe-oxyhydroxides at greater depths cannot be discarded (Dideriksen *et al.* 2007), these estimations of penetration depths are in agreement with the results of previous studies using different methodologies (Puigdomènech 2001, Tullborg *et al.* 2003).

In any case, all these oxidising episodes have not been intense enough to exhaust the reducing capacity of fracture filling minerals, not even in the shallowest part of the system where chlorite and pyrite are still present.

Bedrock and fracture fillings

One of the most important issues for long term disposal safety is the reducing capacity of the surrounding materials against the input of oxygen-rich waters. This subject has been the main aim of different studies and modelling calculations in the framework of the site characterisation programs and the performance assessment exercises in Canada and the Scandinavian Shield (e.g. SITE-94, SR-95 o SR-Can; Arthur 1996, Glynn and Voss 1999, Guimerá *et al.* 1999, 2006, Gascoyne 1999, Luukkonen 2006). They consider Fe(II)-bearing aluminosilicates (biotite, chlorite) and sulphides (pyrite) as the main inorganic redox buffers against penetration of oxygenated waters in glacial scenarios.

Directly related to the reducing capacity of the bedrock and fracture fillings is the existence of an apparently widespread red-staining alteration associated with the presence of hematite. The available information on all these issues is reviewed and summarised here.

Chlorite and pyrite

The most important Fe(II)-bearing minerals in the plutonic rocks (Ävrö granite, quartz monzodiorite and fine-grained dioritoid) from the Laxemar-Simpevarp area are chlorite, biotite, magnetite and, subordinately, hornblende and pyroxene. Average values of chlorite + biotite (% vol) in the most abundant rocks are between 8–18%, amphibole between 0.1 and 12% and pyroxenes between 2.3–3.7% in fine grained dioritoids and gabbro-diorites. Pyrite is only found in very small amounts (always below 0.26 vol %; mean value is below 0.1 vol %). However, in the fracture fillings, chlorite and pyrite (this last one more common than in the bedrock) appear to be the main Fe(II)-bearing minerals.

Chlorite is formed at different hydrothermal stages in fracture fillings (Drake and Tullborg 2007) and represents, together with calcite, the most frequent mineral in all the fracture fillings examined at the Laxemar and Simpevarp subareas, in sealed (around 30 %[34]) and especially in open fractures (70%). It is found at all depths, including the first 100 m (although in lower amounts between 0 and 20 m depth).

The typical width of a chlorite coating in a chlorite-bearing open fracture has been estimated as ~ 0.25 mm, which gives a mass between 0.65 and 0.83 kg m^{-2}, lower than the estimations performed for the Forsmark area (with chlorite mass between 1.30 and 1.65 kg m^{-2}). A minimum estimate of the chlorite content is a 0.1 mm thick coating covering 5% of the fracture surface and thus the minimum amount of this mineral would be around 0.015 kg m^{-2}, similar to the proposed value for the Forsmark area (Drake *et al.* 2006).

To date, no detailed chemical analyses on the contents of Fe (II) and Fe(III) in the fracture fillings have been carried out in the Laxemar-Simpevarp area investigations. However, Mössbauer analyses of chlorite from a fracture filling and from gouge material have been carried out during the Redox Experiment at the nearby Äspö HRL. The values from these analyses are thought to be representative also for the candidate area as well (Tullborg 1995, Drake *et al.* 2006). The oxidation factor (Fe^{3+}/Fe$_{tot}$) for chlorite varies between 0.329 and 0.437 in the samples examined in that experiment and therefore, Fe(II) would make up more than 55% of the total Fe content in all of the samples. Moreover, this proportion may be minimised as the examined samples contain trace amounts of epidote (a silicate mineral that exclusively incorporates Fe(III)), which might enhance the oxidation factor. The only additional data regarding other fracture fillings (Drake *et al.* 2006) indicate that, in fractures with chlorite/corrensite and hematite with a mean value of Fe$_{tot}$ content of 6% (calculated from chemical analyses in bulk fracture fillings), the amount of Fe(II) can represent more than half (3.6%) of the total iron content. Additional information of Fe(II)/Fe(III) in the fracture coatings for chlorite and clay minerals from fracture coatings and gouge material would be needed as they may provide the largest inorganic reducing capacity in the systems (Drake and Tullborg 2006a).

Pyrite is the main sulphide mineral in fractures at the Laxemar-Simpevarp area, representing more than 95% of all sulphides (other identified sulphides are chalcopyrite, galena, sphalerite and very rarely argentite). Pyrite occurs as two main varieties in the Laxemar-Simpevarp area (Figure 4-7): (a) anhedral or subhedral crystals of early-formed hydrothermal pyrite; and b) later formed anhedral to euhedral crystals (in narrow, sealed fractures) or euhedral, cubic crystals (when occurring on open fracture surface). Pyrite crystals, unevenly distributed on the fracture surfaces, are less than 0.2 mm in size.

Pyrite is much more abundant in sealed fractures at the Laxemar subarea (7%) than at the Simpevarp subarea (1%) and the same happens in the open fractures but with higher proportions in both subareas (18% at Laxemar subarea and 5% at Simpevarp subarea)[35]. Pyrite is more common in fractures with an aperture larger than 1 mm (22% in Laxemar subarea and 8% in Simpevarp subarea) and is distributed in almost all examined sections although more abundantly in the intervals 300–400 m and 600–900 m in the Simpevarp subarea, and 300–700 m in the Laxemar subarea.

The pyrite content in fractures is difficult to estimate quantitatively, since its presence varies widely on the fracture surfaces. A rough estimation of the maximum mean amount of pyrite, based on a surface coverage of 0.5% and a crystal side of 0.2 mm, in an average pyrite-bearing fracture, is 0.005 kg m^{-2} fracture surface. A minimum estimate is around 0.0005 kg m^{-2}. Similar values have been proposed for the Forsmark area (see Drake *et al.* 2006 for details).

The presence of unaltered sulphides (mostly pyrite) in the fracture fillings, although unevenly distributed in the fracture surfaces, may be taken as an indicator of stable reducing conditions in the system. Moreover, additional important information can be obtained from the detailed study of this phase.

---

[34] The percentage value represents in how many of the fractures a specific mineral has been identified, following the data reported by Drake *et al.* (2006).

[35] For comparative purposes, pyrite at Forsmark is also more common in open fractures (9%) than in closed fractures (3%).
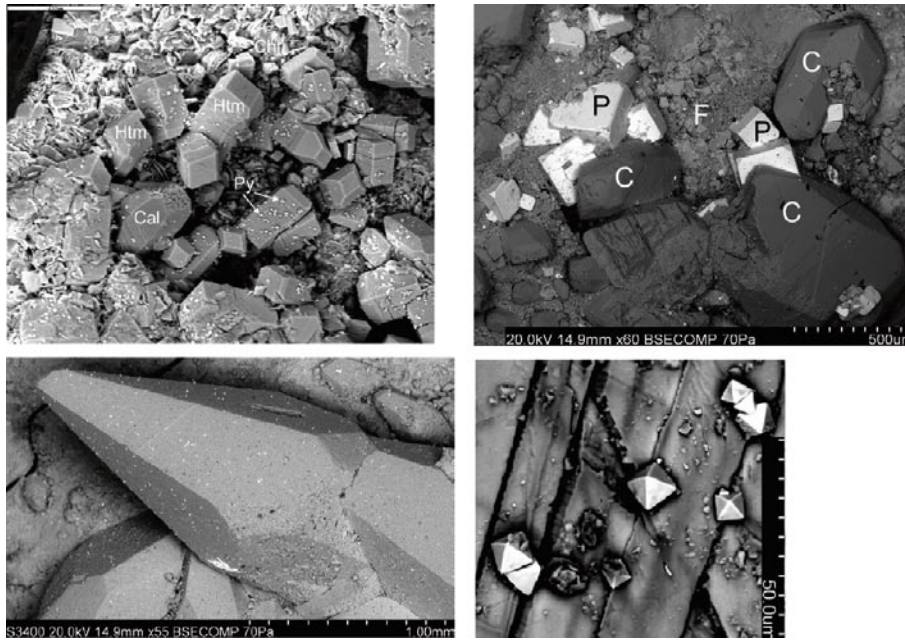
Figure 4-7. *Back-scattered SEM-images of different pyrite habits and textures in the fracture fillings. Upper left- Euhedral pyrite crystals (Py) growing on the surfaces of harmotome (Htm) and calcite(Cal) crystals. Aggregates of chlorite/corrensite (Chl) are also present. Scale bar is 200 µm (from KLX03 at 195.95–196.15 m, borehole length. Upper right-.Cubic pyrite (P), equant calcite (C) and cubic fluorite (F) in KLX07A at 356.93–356.96 m, borehole length. Lower left- Scalenohedral calcite with pyrite (small bright spots) and barite (small aggregate of bright crystals, lower part of the image) on the surface. Sample from KLX07A at 346.73–346.82 m, borehole length. Lower right- Euhedral pyrite crystals on top of calcite. Sample KLX08 at 108.24–108.33 m, borehole length. From Drake and Tullborg (2007).*

In the last mineralogical investigations (Drake and Tullborg 2007, 2008), $\delta^{34}S$ has been analysed in pyrite samples from different generations in the fracture fillings from the Laxemar-Simpevarp area. The younger[36] pyrite samples have higher $\delta^{34}S$ values (+54 to +55‰ CDT except for one sample which has –42 ‰) than the early hydrothermal ones. The extremely negative $\delta^{34}S$ value (–42‰), found in KLX08 borehole at 707 m depth is typical for microbial reduction of sulphate. The same origin has been suggested for pyrites with negative values (from –16‰ to –26‰) found at 200–500 m depth in Äspö (Tullborg *et al.* 1999).

Likewise, pyrites with the highest $\delta^{34}S$ values may indicate the presence of sulphate reduction activity. The samples with highest $\delta^{34}S$ values (around +54.5 ‰ CDT) in the Laxemar-Simpevarp zone were found in the KLX07A borehole at 300 m depth. Pyrites with such high $\delta^{34}S$ values (+46.6 to + 60.8‰ CDT) have also been found in the fracture fillings from the Götemar granite at 213–214 m in the KKR02 borehole (Drake and Tullborg 2006b). These values are too high to be explained by thermochemical fractionation and these pyrites probably correspond to a late stage product of a microbial sulphate reduction process in a closed system with a limited sulphate source[37]. Microbial sulphate reduction can take place at temperatures up to 100–120°C and these temperatures overlap with those estimated for the formation of those younger pyrite samples (Drake and Tullborg, 2006a, 2007). Moreover, microbial (sulphate reduction) influence in the fracture system is also indicated in all the studied systems by low $\delta^{13}C$ values found in calcites of the same generation and/or of the same samples (see Drake and Tullborg 2008 for a detailed description).

---

[36] The word "younger" refers to mineral phases which could have been formed from the Late Palaeozoic to recent, possibly Quaternary, times (Drake and Tullborg 2006a, b, 2007, 2008).

[37] Sulphate reducing bacteria usually produce ^{34}S-depleted sulphide. In a "closed" system with a limited reservoir of sulphate, preferential loss of the lighter isotope from the reservoir influence the isotopic composition of the unreacted source material in that the ^{34}S-composition of residual sulphate steadily increase with sulphate consumption (Rayleigh distillation). In this context, extremely enriched H_2S may be incorporated in the last fraction of deposited pyrite (Drake and Tullborg 2006a and references therein).

All these data would indicate that, although with possible large local (or temporal) variations, the bacterial sulphate reduction activity has been present in the studied systems for a long time and at least down to 800 m. The occurrence of this kind of bacterial activity has been identified at present down to 1,000 m depth.

Hematite

The fractured crystalline groundwater systems of the Scandinavian Shield show a wide variety of oxyhydroxides, ranging in crystallinity from amorphous phases or ferrihydrites (in the overburden and shallowest part of the bedrock) to those fully crystalline phases found in deeper fracture fillings. Overall, this variety of oxyhydroxides will show a wide stability, solubility and reactivity, mainly controlled by their mineralogy, crystallinity, degree of hydration, impurities and particle size (see e.g. Langmuir and Whittemore 1971, Postma 1993, Cornell and Schwertmann 2003).

As already described, the available mineralogical studies indicate the presence of hematite widely distributed in the fracture fillings. Except at the shallowest depths, the hydrothermal crystalline hematite form is the dominant iron oxide. Hematite occurs in sealed and open fractures and in all examined sections (down to 1,000 m depth) in the Laxemar-Simpevarp and Forsmark areas. Up to now, this is completely different from what has been found in other sites such as Olkiluoto (Finland), where hematite (or other oxyhydroxides) has not been identified in the fracture fillings (Pitkänen *et al.* 2004) except at very shallow levels.

Hematite (as well as calcite, chlorite, clay minerals, and pyrite) is more abundant in open fractures (25% in Simpevarp and 13% in Laxemar subareas) than in sealed fractures (7% in Simpevarp and 5% in Laxemar subareas), and mainly in fractures with an aperture larger than 1 mm (38% in Simpevarp and 20% in Laxemar subareas). Hematite proportion in the open fractures with apertures greater and smaller than 1 mm (9-15%) at Forsmark is similar to that at the Laxemar subarea but lower than at the Simpevarp subarea.

Hematite appears in different situations, with different morphologies and textures (Figure 4-8) and its genesis is associated with different old hydrothermal stages (e.g. Drake and Tullborg 2007). It can be identified by XRD (X-ray Diffraction) but in many cases it is below the detection limit of this technique (Drake and Tullborg 2004, Sandström *et al.* 2004) and its presence must be identified by other techniques. Using Scanning Electron Microscopy (SEM) hematite has been found as continuous fillings in small fractures, as mineral inclusions inside other mineral phases, as small microcrystalline and spherical aggregates filling in voids or in the fracture surface or as thin coatings on other mineral surfaces (Drake and Tullborg 2004, 2005, Sandström *et al.* 2004, Drake and Tullborg 2007, 2008).

One of the most common observations related to hematite in the fracture fillings is the presence of red staining overgrowths, also present in the altered wall rock. These red coloured zones are produced by the presence of microcrystals or micrograins of hematite (Drake and Tullborg 2007) as it also occurs with reddish colours in soils or in sedimentary rocks[38]. In the studied systems red staining is related to the formation of minute hematite grains during hydrothermal alteration stages (at temperatures about 250–400 °C) associated with the intrusion of the Götemar and Uthammar granites nearby and at least older than 1,100 Ma and probably ca. 1,400 Ma (Drake *et al.* 2008).

Macroscopic observation of this red-staining alteration may suggest a decrease in the reducing capacity (e.g. Fe(II) contents) of the system. This issue has been analysed by Drake and Tullborg (2008) and Drake *et al.* (2008). They indicate that the red-stained rock adjacent to fractures show major changes in mineralogy, moderate changes in chemistry (e.g. K-enrichment, Ca-depletion and constant Fe_{tot}) but very small changes in the oxidation factor (Fe(III)/Fe_{tot} ratio) compared to the reference, unaltered rock.

---

[38] In the very well-known sedimentary *Red Beds* the red colour origin is associated with the presence of hematite particles smaller than 2 μm dispersed in the material (eg. Blodgett *et al.* 1993).
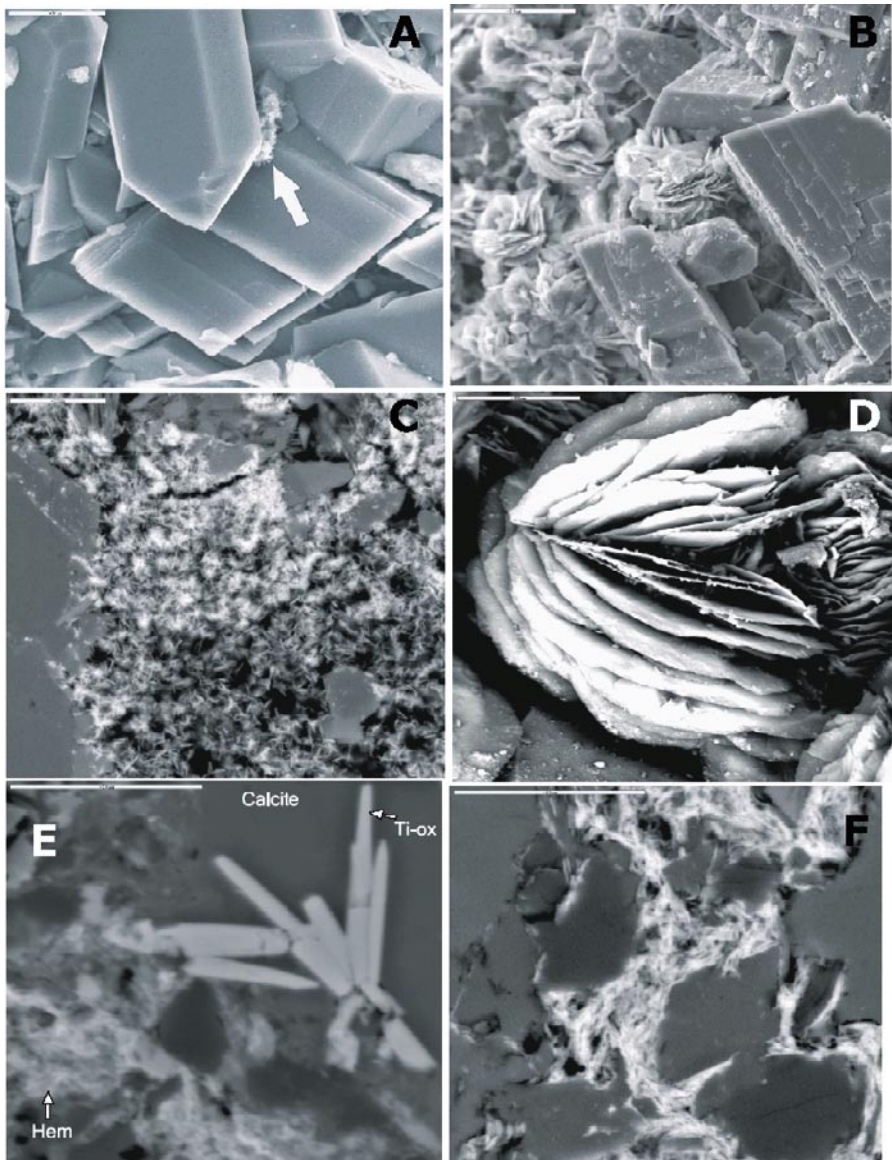
Figure 4-8. Different hematite habits and textures in the fracture fillings. A.- Idiomorphic adularia crystals with small aggregates of hematite crystals (indicated by the arrow) in a sample taken at 208.45–208.50 m depth in KA1755A borehole (Äspö); the scale bar corresponds to 20 µm. B.- Laminar aggregates of hematite (left part in light grey) associated with idiomorphic quartz and adularia crystals in a sample taken at 208.5 m depth in KAS04 borehole (Äspö); the scale bar corresponds to 50 µm. C.- Aggregates of microcrystalline hematite crystals associated with adularia in a sample taken at 17.7–17.85 m depth in KAS04 borehole; the scale corresponds to 20 µm. D.- Leafy crystals of hematite in a sample taken at 831 m depth in borehole KLX03 (Laxemar); the scale bar corresponds to 50 µm. E.- Backscattered electron image of hematite stained mylonite (Hem); hematite shows fibrous-irregular habits; the scale bar corresponds to 20µm (borehole KSH01A at 363.5 – 363.7 m). F.- Fine-grained hematite crystals in a cataclasite with an intense red staining (borehole KAS04 at 17.70 – 17.85 m); the scale bar corresponds to 20µm. Taken from Drake and Tullborg (2004, 2005).

In fact, the occurrence of the reddish colour is not the result of very high proportions of hematite[39] but of dispersed amounts of very small grains. Therefore, red-staining only promotes a very limited decrease in reducing capacity, if any, and would not promote negative effects on this important feature to the disposal safety. On the contrary, the increased amount of small hematite crystals as well as the increased porosity observed in the red-stained rock may result in enhanced retention of radio-nuclides due to an increased sorptivity and diffusion close to the fracture (Drake *et al.* 2008).

Related to this, although hematite is in volumetrically low proportions, as it is on the external surface of the fracture fillings it can present a high surface to contact groundwaters depending on its particle size[40]. Therefore, there is a noticeable variability in the particle size of the hematite in the fracture fillings, some in the range lower than one micron. This may be also important to their solubility (with variations of four orders of magnitude; Appendix C, section C.3.1). The study carried out in the Scandinavian Shield by Grenthe *et al.* (1992) can help in narrowing the range of solubilities for this crystalline phase. This study on the factors controlling the reducing redox state of several Swedish groundwaters of long residence time allowed the indirect determination of the solubility of the iron oxy-hydroxides involved in the redox control and for reaction:

$$Fe(OH)_{3(s)} \leftrightarrow Fe^{3+} + 3OH^- \hspace{4cm} (4\text{-}3\text{-}1)$$

a value of log K = –43.1 was obtained. This value would be in the lower range of the solubility values obtained for crystalline hematite (and/or goethite) and would suggest the presence of surface areas not exceedingly large for these phases (see the review in Appendix C, section C.3.1).

No additional estimations exist to confirm this value, as the measurement of the surface areas for particular minerals (e.g. hematite) in the fracture fillings is extremely difficult. However, the surface area (or particle size) of the hydrothermal hematite (or other crystalline oxyhydroxide present in the fracture fillings) can also be relevant to the understanding of its behaviour as a TEA (*Terminal Electron Acceptor*) in the bacterial processes of iron reduction or to estimate its behaviour in the surface processes of radionuclide retention. These are the reasons why an estimation of these values has been performed and reported in Appendix D.

Using the equations described in Appendix D on the relations between particle size (or surface area) and solubility, the minimum particle size from which the effects on the equilibrium constant of hematite (or goethite) start to be important can be estimated. Figure 4-9 shows the results for hematite (goethite results are superimposed almost perfectly and are not plotted). As shown, the effects of particle size on the solubility are negligible for values higher than $1\mu m$ (10^{-4} cm). At that point, the surface area loses its relevance for solubility independent of the roughness.

---

[39] The hematite percent in the *red beds* is usually below the detection limit of XRD (eg. Grygara *et al.* 2003).

[40] This parameter is also responsible for the colour: the reflectivity of the red zone in the spectrum decreases as the particle size increases. Hematite particles between tenths and several hundreds of nanometres show very brilliant red colours, while in the micrometric range (1–5 µm) the tonality becomes darker purple red (Kerker *et al.* 1979, Schwertmann 1993). Moreover, in these ranges, morphology also affects the colour: fibrous crystals give more yellowish tonality than the tabular ones (Hund 1981). Hematite crystals larger than 5 µm show grey tonality. Detailed characterisation of colours has been classically used as a method to identify the type and features (e.g. grain size) of the Fe-oxyhydroxide present in materials such as soils in which the variability in this type of phases is very high (e.g. Bigham and Ciolkosz 1993, Cornell and Schwertmann 2003, and references therein). Although a systematic study on the different colours and tonalities in the fracture fillings has not been performed, there are some interesting observations on this. Drake and Tullborg (2004) indicate the presence of two different reddish pigmentations in the fracture fillings from the KSH01A borehole: the first one constituted by brilliant red hematite micro crystals and the second one formed by isolated and bigger hematite crystals associated with magnesium chlorite and with a dark red towards brown colour. These characters would indicate that the particle size in the first case must be in the nanometrical range (below 1 micron), and the second one must be in the micrometric range (below 5 µm). SEM observations support these deductions. Drake and Tullborg (2004, 2005) have reported the presence of small microcrystalline aggregates of hematite with leafy habits grouped in relatively spherical particles (Figure 4-8A, 4B and 4D). The size of these aggregates is varied (see the scale in photographs 4-8A and 4D) but the smallest (Figures 4-8A and 4C), due to their intricate planar morphology, might have a very high surface area. The presence of these aggregates has been described even in the surface of the fracture fillings (Figure 4-8A). Several SEM observations have also been made on the reddish pigmentation in the fracture fillings (Figures 4-8E and F). This hematite also appears as dense aggregates of micrometric or smaller particles or crystals with fibrous-leafy habits. All these observations indicate the noticeable variability in the particle size of the hematite in the fracture fillings.
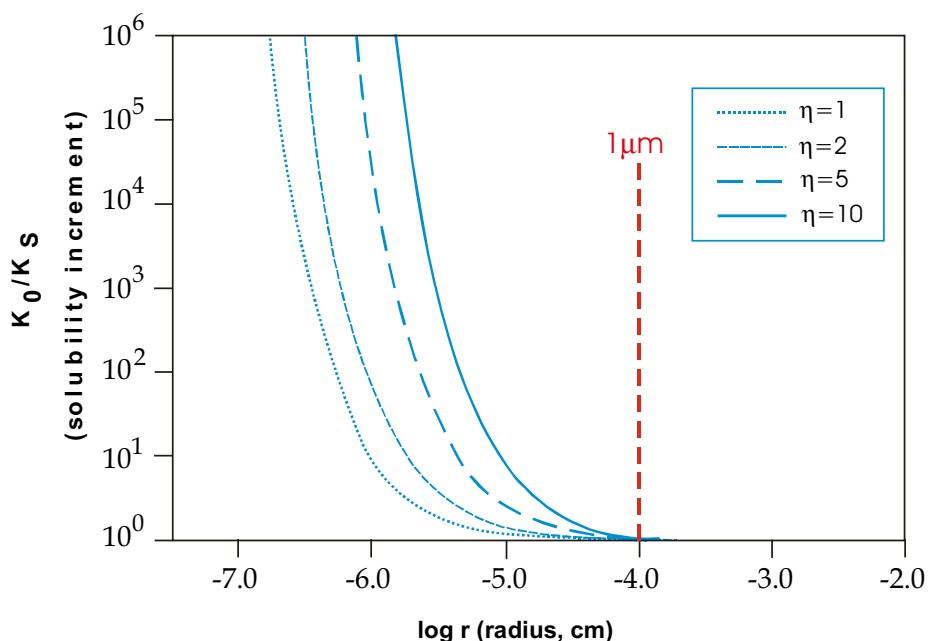
Figure 4-9. *Solubility excess as a function of the radii of ideally spherical particles of hematite. The different curves represent different roughness factors (η). See Appendix D.*

However, for smaller particle sizes, and mainly below 0.1 µm, the effects might be really important and their magnitude is directly related to the particle roughness (surface area). Therefore, the crystal morphology or the degree and shape of the particles-aggregates become especially important in this range of sizes, whose presence in the system, at least below 1 micron, has been recently confirmed (Dideriksen *et al.* 2007).

The estimation of the hematite (and goethite) surface area in these systems could be made knowing their solubility product. If the value of pK = 43.1 deduced by Grenthe *et al.* (1992) is accepted as a representative value for the hematite solubility in the system, the surface area obtained for hematite would be 62.7 m²/g and for goethite, 77.3 m²/g. These values would represent a significant surface taken into account the wide-spread of hematite in the outermost part of fracture coatings. But probably they represent a maximum estimation, as crystals or aggregates of hematite in the micrometric range, and therefore with lower surface areas (possibly as low as 2 to 3 m²/g; Langmuir 1997), are also present in the fracture fillings.

The results obtained from the calculation of the hematite particle size (ideally spherical) assuming the solubility value proposed by Grenthe *et al.* (1992), indicate that the oxyhydroxide would be constituted of 0.01 µm particles. This size is in the lower limit of the particles sizes determined in typical soil hematite at low-temperatures, and at hydrothermal temperatures the expected size would be larger (Cornell and Schwertmann 2003). All these results appear to be supported by the recent work by Dideriksen *et al.* (2007). They determined the particle size of hydrothermal hematite in samples from KOV01 and KAS02 boreholes and they found particle sizes as low as 0.08 µm and even lower for the old, low-temperature samples (mostly very fine-grained crystalline goethite but also hematite[41]). Unfortunately, they were not able to determine with precision the particle size for the old, low-temperature samples, although they probably approach surface areas near the calculated above. However, this type of old, low-temperature crystalline oxyhydroxides is less abundant than the hydrothermal hematite and, therefore, the effects of its greater surface area are much more localised.

---

[41] The theoretical solubility for hematite with particle size of 0.08 µm would be of around pK= 43.9, near the value determined by Grenthe *et al.* (1992) and clearly indicative of a crystalline hematite with low surface area.

Overall, all these results suggest the existence of crystalline (hydrothermal) hematite with variable but not exceedingly low particle size and, therefore, with surface areas not very large. Only locally, low-temperature crystalline goethite and hematite can show significant surface areas with a rough estimate of 62–77 m^2/gr. The calculated solubility from the particle size measured for hydrothermal hematite does not show important discrepancies with the value calculated by Grenthe *et al.* (1992) from potentiometrically measured Eh values in long residence time groundwaters (see Appendix D).

Implications for the redox buffering capacity

All data and results presented above are directly or indirectly related to the important issue of the reducing capacity of the materials that constitute the final barrier in the disposal concept, the geosphere. Therefore, the main conclusions are presented here from this perspective.

Two domains are involved in the redox buffering capacity of the overburden in the Laxemar-Simpevarp area: bare bedrock zones and the soil-sedimentary cover.

In the areas with a thick soil cover the recharge groundwaters will be reduced by the biological degradation of organic matter through the soil profile before reaching the bedrock. This situation is especially clear for the hydromorphic soils (peat soil, hystosol and gleysol) dominant in the overburden, where very reducing redox conditions, produced by prolonged water saturation of soil material in the presence of organic matter, may be reached just below the water table.

In water-conducting fracture zones of bedrock outcrops the potential oxidation effects of the recharge waters can be much more important. The mineralogical and geochemical studies performed in the shallow fracture fillings of these zones (Drake and Tullborg, 2008) indicate, however, that the present redox front in the Laxemar subarea is located at about 15–20 m depth.

Penetration of oxygenated groundwaters in the past (within the last 300,000 years) has been identified by the presence of old, low temperature goethite at variable depths: from 5 to 20 m in the Äspö subarea and down to 80 m depth in the Laxemar subarea or 100 m in the KOV01 boreholes (Dideriksen *et al.* 2007, Drake and Tullborg 2008). The greatest penetration depths are associated with highly transmissive fracture zones (Laxemar subarea) or with areas with a higher topography (KOV01 borehole). Although the presence of low temperature Fe-oxyhydroxides at greater depths cannot be excluded (Dideriksen *et al.* 2007), these estimations are in agreement with the results of previous studies using different methodologies (Puigdomènech 2001, Tullborg *et al.* 2003).

In any case, these present or past oxidising episodes have not been intense enough to exhaust the reducing capacity of fracture filling minerals, even in the shallowest part of the system where chlorite and pyrite are still present.

The largest reducing capacity is apparently provided by the Fe(II)-bearing Al-silicates which, in the fracture coatings and gouge material, are chlorite and also clay minerals (corrensite, smectite, mixed layer clays, illite/smectite). Together with calcite, these are usually the most frequent minerals identified in the fracture fillings. Pyrite and other sulphides are more common in fracture fillings than in the bedrock and also S^{2-} contribute to the reducing capacity. However, pyrite is very irregularly distributed in the fracture fillings and its estimated proportions are much lower than those of chlorite and other clay minerals.

The chlorite analysis performed in the Äspö subarea indicates that Fe(II) would make up more than 55% of the total Fe content in all of the samples. However, there are no data for the Laxemar subarea or for other Fe-minerals in fractures. Therefore, additional information of Fe(II)/Fe(III) in the fracture coatings for chlorite and clay minerals from fracture coatings and gouge material would be needed (Drake and Tullborg 2006).

The presence of unaltered sulphides (mostly pyrite) in the fracture fillings, although unevenly distributed in the fracture surfaces, has been identified in almost all the examined sections. This may be taken as an indicator of stable reducing conditions in the system even at shallower levels.

The particle size for hydrothermal hematite determined by Dideriksen *et al.* (2007) and the theoretical calculations performed in this section indicate the existence of variable but not exceedingly large surface areas for this mineral and also a solubility value close to that deduced by Grenthe *et al.* (1992). The red-staining alteration observed in the rock adjacent to the fractures and in the fracture fillings is not the result of very high proportions of hematite but it is associated with the particle size of dispersed amounts of this mineral. Therefore, this red-staining alteration only promotes a very limited decrease in the reducing capacity, if any (Drake *et al.* 2008, Drake and Tullborg 2008).

As a whole, all these data indicate that the system has kept a noticeable reducing capacity over the time and at present. However, more quantitative data are needed on the amounts and compositions of the minerals involved in order to transfer this fact to predictive calculations on the system evolution.

Moreover, a more refined concept of the buffering capacity should include the effects of microbial activities in groundwaters. Different types of microbial activities are found at present and are deduced to be active in the past. For example, stable isotopes confirm that pyrite has been formed at different events with gradually lower temperatures and increasing biogenic influence. Activity of sulphate reducing bacteria appears to be present in Forsmark and Laxemar-Simpevarp zones a long time ago and down to 800 m depth.

The importance of microbial activities in maintaining the redox conditions of a repository, buffering the oxygen-rich groundwaters intrusion, has been long recognised (Puigdomènech 2001 and references therein). However, they are not included in the predictive calculations for glacial scenarios, as the factors controlling the presence of different metabolic groups, their mutual relations and their quantitative effects on the groundwaters still present numerous uncertainties. Some of them will be presented later.

4.3.3 Microbiological data

Much effort has been made in the microbiological site characterisation during the different SDM stages in the Forsmark and Laxemar-Simpevarp areas (e.g. Hallbeck 2006, 2007, Laxemar 2.1 and Forsmark 2.1, respectively). The latest updates correspond to the works of Hallbeck and Pedersen (2008a) for the Forsmark 2.2–2.3 and Hallbeck and Pedersen (2008b) for the Laxemar and Simpevarp subareas in the present Laxemar 2.2.–2.3 stage. Thanks to these works, there has been a great improvement in the degree of knowledge on the microbiological processes and their influence on the redox state of these crystalline systems.

Some uncertainties on the activities of different metabolic groups are presently known (e.g. Hallbeck and Pedersen 2008abc). However, some other important problems and uncertainties, not explicitly treated in earlier works, can only be identified by integrating the microbial results with the mineralogical data and the geochemical modelling results.

Most of these questions affect the microorganisms involved in the usual degradation of organic matter: Do they act in sequence? Are different metabolisms segregated in distinct zones or do they act concomitantly? Are the metabolic groups detected at depth active under pristine conditions or is their presence (or metabolic intensity) induced or modified by drilling and sampling operations?

These questions affect especially the iron and sulphur redox systems[42] and their related "typical" microbial processes: dissimilatory iron and sulphate reduction. Therefore, the main results on the iron reducing bacteria and sulphate reduction bacteria are summarised in this section to state the problems and issues that will be analysed in detail later on.

Apart from the microbiological data for the Laxemar and Simpevarp subareas delivered in the last data freeze, the previously available data on the IRB and SRB contents (most probable numbers, MPN) from the Äspö island and the Laxemar subarea (KLX01 and KLX02 boreholes) have been included as well (Gimeno *et al.* 2006, Hallbeck 2006).

---

[42] Also the manganese and the nitrogen system (and their related microbial activities, manganese and nitrate reducing bacteria) are affected by this type of uncertainties (see sections 4.4 and 4.5).

Results of microbiological analysis for IRB and SRB

IRB and SRB populations (expressed as most probable numbers, MPN in Figure 4-10) detected in the Laxemar-Simpevarp groundwaters do not show any specific trend with respect to depth or to their metabolic products (dissolved Fe(II) and S(–II); Figure 4-5) as has been observed at Forsmark or Olkiluoto (Gimeno *et al.* 2007, Hallbeck 2007, Pedersen 2008).

IRB data

Microbial data at the Simpevarp subarea were determined in borehole KSH01A at 153, 242 and 536 m depth and the MPN of IRB at these sections were very low (2.1 to 3.3 cell/mL). Previous data were available for KLX02 and KLX03 boreholes (Laxemar subarea). At 700 m in KLX03 and 1,100 m depth in KLX02, the data indicated the presence of 50 and 300 cell/mL of IRB, respectively. At deeper levels (between 1,300 and 1,500 m in KLX02) the results indicated the absence of IRB (Haveman and Pedersen 2002, Hallbeck 2006). Data from the last data freeze indicate that the highest numbers of IRB are found in borehole KLX15A, 467 m and KLX17A, 342 and 548 m depth with 140, 240 and 280 cell/mL, respectively.

Using the classification of measured MPN values proposed in Hallbeck (2006, see Table 1-2), it could be said that, in general, there are not significant enough numbers of IRB (higher than 50 cell/mL) to promote effects on the chemistry of the groundwaters. Something similar occurs at Olkiluoto, where the last data presented by Pedersen (2008) showed that, from the 21 samples analysed, only 4 displayed MPN of IRB higher than 15 cell/mL and only two of them had contents higher then 50 cell/mL (around 100 and 300 cell/mL) at 80 and 300 m depth.

These results at Olkiluoto could be explained, *a priori*, by the very limited availability of Fe(III)-oxyhydroxides at depth[43] (Pitkänen *et al.* 2004, Pedersen 2008) as terminal electron acceptors for the IRB activity. Iron oxyhydroxides (mainly hematite) are widely distributed at all depths in the Laxemar-Simpevarp area and, therefore, a more active presence of IRB would be expectable.
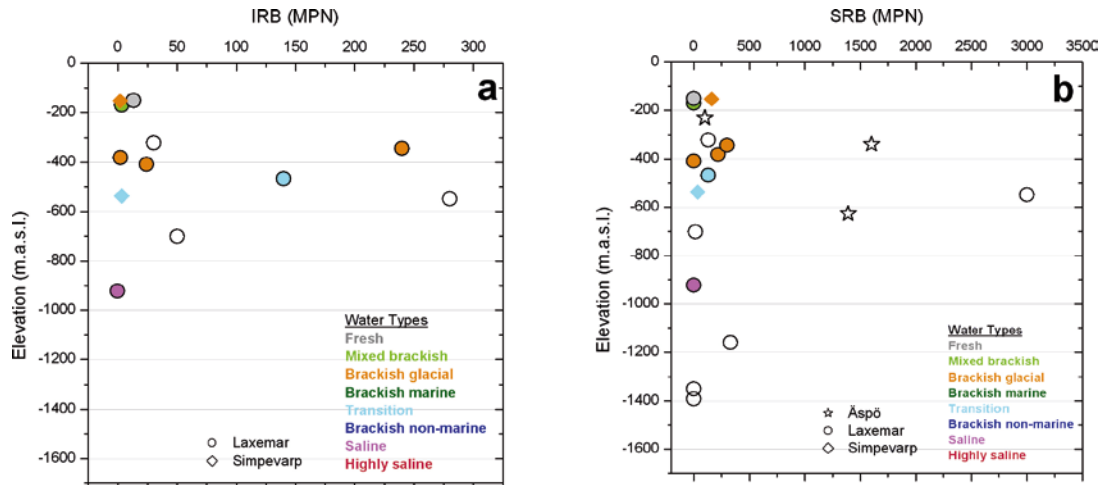
Figure 4-10. *Most Probable Number distribution with depth of iron reducing bacteria (a) and sulphate reducing bacteria (b) in the Laxemar-Simpevarp area groundwaters. Open symbols correspond to samples without a defined water type.*

---

[43] Mineralogical studies performed in the Olkiluoto fracture fillings indicate the absence of iron oxyhydroxides except at very shallow depths (Pitkänen *et al.* 2004, Pedersen 2008). This absence may be related to sampling problems and, probably, some amounts of these minerals may be present in the fracture fillings. However, it seems that these amounts must be noticeably lower than the amounts detected at Laxemar-Simpevarp or Forsmark areas.

More samples with significant IRB populations were identified at Forsmark (Figure 4-11ab), where hematite is also distributed at all depths in the fracture fillings. The highest value is found at shallow levels (MPN near 4,000 cells/mL in KFM01A at 111.75 m depth) but important values are also found at greater depths in KFM10A at 214 m depth, in KFM01D at 341 and 445 m depth, KFM08A at 546 m depth and KFM10A at 328 m depth (MPN from 80 to 1,600 cells/mL). Hallbeck and Pedersen (2008a) also indicate the existence of values around 1,600 cell/mL at 664 m in the KFM08D borehole.

These results indicate that the presence or the abundance of Fe(III)-oxyhydroxides in the studied systems do not have a direct relationship with the proportion of cultivated IRB or with their effects. Therefore, other factors must condition the IRB activity in the systems at depth and some of these factors may be related to anthropogenic disturbances.

For instance, the highest number of IRB found in borehole KLX17A at 548 m in the Laxemar subarea corresponds to very dilute groundwaters (Cl = 17 mg/L) with measurable amounts of tritium and produced by a short-circuit during sampling. Therefore, the detected IRB would correspond to shallower levels or may be enhanced at depth by the short-circuit. Oxygen intrusion problems in the Forsmark area and formation of poorly-crystalline iron oxyhydroxides have been detected and this type of disturbance may also enhance the IRB activity (Gimeno *et al.* 2008).

Therefore, the interpretation of samples with significant numbers of IRB in the Laxemar-Simpevarp area has many unknowns and uncertainties which make it difficult to state the active presence of these microorganisms at the indicated depths under pristine conditions.

SRB data

The available microbiological data from Äspö indicate the occurrence of SRB with significant values of MPN in many of the studied sections. They have been identified (Figure 4-10b) at 230.5 m and 338.5 m depth in borehole KAS04 (MPN between 100 and 1,600 cells/ml), at 450 m coexisting with other bacterial groups (Haveman and Pedersen 2002) and at 626 m in KAS03 (1,390 cells/ mL; Pedersen 1997). That is, SRB activity seems to be widely distributed in depth and, overall, this situation coincides with the clearest sulphidic signature (represented by higher dissolved sulphide concentrations; Figure 4-5b) of these groundwaters.

This relationship between SRB activity and dissolved sulphide contents is not so clear at the Laxemar and Simpevarp subareas. The highest dissolved sulphide concentrations were found at the Laxemar subarea in KLX01 borehole at 673 m depth (2.5 mg/L of S(–II)) where Hallbeck (2006) indicated an MPN for the SRB extremely high (56,000 cells/mL; not plotted in Figure 4-10b).
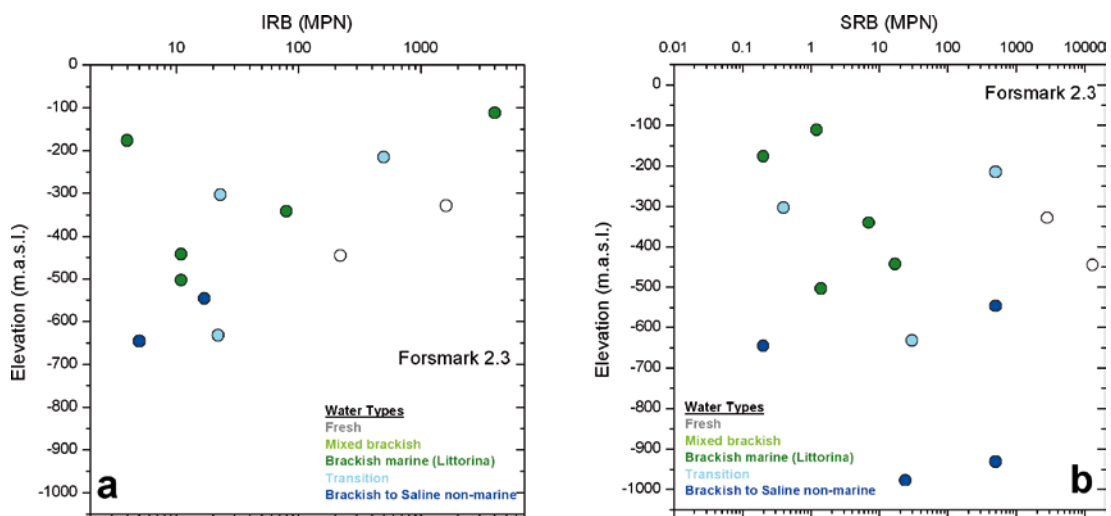
Figure 4-11. *Most Probable Number of iron reducing bacteria (a) and sulphate reducing bacteria (b) distribution with depth in the Forsmark groundwaters. Open symbols correspond to samples without a defined water type.*

However, dissolved S(–II) in the rest of the sections, where SRB have been found in the Laxemar subarea boreholes (KLX02, KLX03, KLX08, KLX15A and KLX17A), is in most cases below detection limit while the SRB contents vary in a wide range:

- Previous microbiological data for KLX02 correspond to 1,160, 1,350 and 1,390 m (Haveman and Pedersen 2002) and the reported MPN for the SRB at 1,160 m depth is 330 cells/mL, whereas SRB could not be cultured at 1,350 and 1,390 m depth (the most saline samples).

- In the three sections sampled from KLX03 borehole, SRB were found only at 380 m depth (MPN values of 220 cells/mL).

- In KLX08 borehole at 150 and 300 m depth and in KLX15A at 467 m depth, MPN values of 2.3, 130 and 130 cell/mL have been obtained, respectively.

- In KLX017A at 352 and 548 m depth, the obtained MPN values were 100 and 3,000 cells/mL, respectively.

The available data for the Simpevarp subarea (borehole KSH01A), indicate that the MPN for SRB at 153 and 536 m depth are 160 and 35 cell/mL, respectively, also in groundwaters with dissolved sulphide below the detection limit.

Overall, in contrast to IRB, significant numbers of SRB (higher than 50 cells/mL; Hallbeck 2006) to influence the chemistry of the groundwaters from the Laxemar-Simpevarp zone, are widely distributed with depth showing a peak around 380–700 m depth[44]. However, dissolved sulphide in some of these waters is very low. Several factors may influence this. First, amorphous ferrous monosulphide precipitation may produce an important decrease of dissolved sulphide in environments with low rates of sulphate reduction and/or high contents of dissolved Fe(II) (see section 4.3.4). Second, disturbances during sampling (e.g. associated with flushing, pumping, etc) can drastically decrease the pristine dissolved sulphide concentrations[45]. Finally, other types of disturbances associated with the sampling activities may promote misleading interpretations; this is the case of the aforementioned results from KLX17A at 548 m, affected by a short-circuit during sampling and where the highest IRB (280 cell/mL) and very high SRB values (3,000 cell/mL; the second in the ranking of the Laxemar-Simpevarp area) were determined.

This could explain the lack of correlations found between the MPN of SRB and the dissolved sulphide contents in these groundwaters and represents an important uncertainty on the extent of the sulphate reducing activity and on its effects on the related inorganic processes (see section 4.3.4). In any case, as the only source of dissolved sulphide in low-temperature systems is bacterial activity, higher sulphide contents would confirm the predominant role played by these microorganisms in the Laxemar-Simpevarp groundwaters.

Discussion

The number of samples with significant amounts of IRB in the Laxemar-Simpevarp subarea is very low and apparently restricted to the 350–550 m depth interval. In contrast, significant SRB activity (usually one order of magnitude higher) appears to be more frequent and widely distributed with depth. Therefore, as a whole, SRB activity appears to be more important than IRB activity in the Laxemar-Simpevarp area.

The only sections where MPN of both, IRB and SRB, were significantly high correspond to boreholes KLX15A and KLX17A between 350 and 550 m, suggesting that both metabolic groups are active at these depths (Hallbeck and Pedersen 2008b). However, the two samples in KLX17A

---

[44] The highest SRB values at Forsmark are in the same range although in less samples.

[45] For instance, during the monitoring program in the KLX15A borehole at 467 m depth, dissolved sulphide concentrations were well above detection limit (and even reaching 21.5 mg/L) whereas in the sample for this depth in the 2.3 data freeze, dissolved sulphide was below detection limit. In other boreholes sampled during the monitoring program, similar results were obtained. In KLX18A at 452 m depth with a dissolved sulphide concentration of 1.43 mg/L in the data freeze, values between 7.98 and 1.23 were measured during the monitoring period. In KLX019A at 414 m depth with an initial value of 0.027 mg/L S(–II), concentrations between 0.018 and 0.973 mg/L were measured during the monitoring. Similar disturbing effects have been documented at the MICROBE site in the Äspö hard rock laboratory (Hallbeck and Pedersen 2008c).

show tritium contents and the sample with the highest IRB contents at 548 m is the product of a short-circuit.

Other metabolic groups have also been found (e.g. manganese reducing bacteria, acetogens) in significant numbers in these sections with high IRB and SRB contents. Hallbeck and Pedersen (2008b) indicate that there is no obvious explanation for these high numbers of microorganisms at the sampled depths. The same situation was described at Forsmark where high populations of IRB (together with other microorganisms) were found at depths between 300 and 650 m (Hallbeck and Pedersen 2008a). In both cases a natural or induced mixing (during drilling and pumping activities) of different groundwaters is suggested, although possible contamination by flushing water is also indicated, at least for some sections, in the Forsmark area.

This situation represents a serious problem in the understanding of the redox processes. In natural systems, the degradation of organic matter by microorganisms may proceed through separated zones, dominated by individual metabolic groups and organised in terms of their Gibbs free energy yield (Langmuir 1997, Appelo and Postma 2005). In this classical redox zonation scheme, a competitive exclusion between different metabolics groups is produced (Lovley and Goodwin 1988). However, this segregation in zones is not always observed and concomitant activities of different metabolic groups in the same zones have also been reported in sediments and sedimentary aquifers. This is the case of iron and sulphate reducing bacteria (e.g. Postma and Jakobsen 1996, Jakobsen and Postma 1999). Therefore, the coexistence or exclusion among different types of bacteria in the Laxemar-Simpevarp groundwaters should be determined to constrain their influence in the observed redox situation.

4.3.4 Processes. Thermodynamic approach

Speciation-solubility calculations have been performed with the PHREEQC code (Parkhurst and Appelo 1999) and the WATEQ4F database (Ball and Nordstrom 2001) to identify some of the effective processes controlling dissolved iron and sulphide concentrations. Saturation indices have been calculated for siderite and amorphous Fe(II)-monosulphides, phases whose control on Fe(II) and S(–II) has been identified in the studied systems (e.g. Gimeno *et al.* 2006) and in other similar systems (e.g. Chen and Liu 2005, Jakobsen and Cold 2007).

Under the "iron mono-sulphides" term the amorphous mono-sulphide ($FeS_{(am)}$ or $FeS_{(ppt)}$), more properly named disordered mackinawite (Wolthers *et al.* 2003, 2005) or nanocrystalline mackinawite (Rickard 2006, Rickard and Luther III 2007)[46], the ordered or crystalline mackinawite (tetragonal FeS) and greigite (Fe_3S_4) are included. Only amorphous monosulphide and crystalline mackinawite have been considered in this work.

The amorphous monosulphide is the most soluble of the iron sulphides and it is the first phase that typically precipitates in most natural aqueous systems (Chen and Liu 2005, Rickard and Morse 2005, Rickard and Luther III 2007), with fast precipitation kinetics (seconds; Rickard 1989, 1995). Mackinawite (the crystalline monosulphide) is slightly less soluble but its precipitation kinetics is also fast (in order of days; Rickard 1989). It is also common to find this crystalline phase as a result of the re-crystallisation of amorphous monosulphides, which is also a fast process (Rickard 1995, Wilkin and Barnes 1997, Benning *et al.* 2000), and it can affect the composition of the solution in contact which would re-equilibrate to the activity product of crystalline mackinawite (Chen and Liu 2005). A detailed description of the thermodynamic data used for these phases can be found in Appendix C (section C.3.2).

An uncertainty range of 5% of the log K value (Deustch 1997) has been fixed for siderite, which is ±0.55[47]. The uncertainty range for monosulphides ($FeS_{(am)}$ and mackinawite) has been ± 0.36 as recommended by Gimeno *et al.* (2006).

---

[46] The term amorphous monosulphide has been kept on here to avoid terminological problems as it has been used in earlier reports.

[47] The solubility value of siderite used in the calculations is the one included in WATEQ4F database (Ball and Nordstrom 2001), log K =–10.89. This value is similar to the more recent experimental values proposed by Jensen *et al.* (2002), from –11.03 ± 0.1 to –10.34 ± 0.15 under anaerobic conditions.

Near-surface groundwaters

As stated above, dissolved Fe(II) and S(–II) in near-surface groundwaters indicate the presence of anoxic environments with effective reductive dissolution of Fe-silicates (e.g. Fe(III)-bearing clay minerals) or ferric oxyhydroxides (post-oxic environment) and bacterial S(–II) production (sulphidic environment) already in the very shallow parts of the system. This is conditioned by the biological and microbial activity developed in the overburden and mainly in the soils, where organic matter decay may lead to complete redox sequences (from oxic to post-oxic, sulphidic and methanic environments) at centimetre or metre scales. IRB and SRB activities are the main contributors of Fe(II) and S(–II) in the near-surface groundwaters. Dissimilatory iron reducing bacteria can reduce the poorly-crystalline iron oxyhydroxides using organic matter (e.g. acetate, equation 4-3-2) or hydrogen (equation 4-3-3) as electron donors:
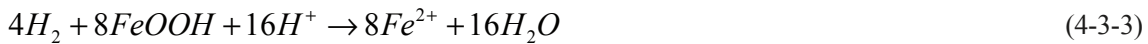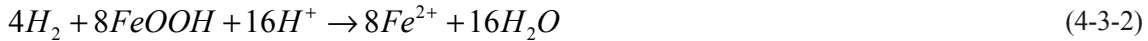
$$4H_2 + 8FeOOH + 16H^+ \rightarrow 8Fe^{2+} + 16H_2O \tag{4-3-2}$$

$$4H_2 + 8FeOOH + 16H^+ \rightarrow 8Fe^{2+} + 16H_2O \tag{4-3-3}$$

and sulphate reducing bacteria can reduce the dissolved SO_4^{2-} through the reactions:

$$CH_3COO^- + SO_4^{2-} + 3H^+ \rightarrow H_2S + 2CO_2 + 2H_2O \tag{4-3-4}$$

$$4H_2 + SO_4^{2-} + 2H^+ \rightarrow H_2S + 4H_2O \tag{4-3-5}$$
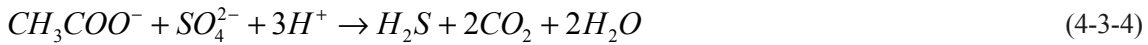
Sulphate reduction processes can indirectly contribute to the dissolved Fe(II) through the reaction:

$$H_2S + 2FeOOH + 4H^+ \rightarrow S^0 + 2Fe^{2+} + 4H_2O \tag{4-3-6}$$
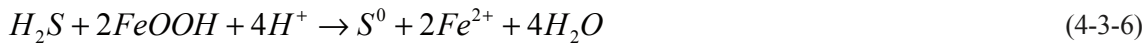
All these reactions may be sources of dissolved Fe(II) and S(–II). However, additional processes can be involved in the control of these compounds. Speciation-solubility results indicate that most of the near-surface groundwaters are in equilibrium or oversaturated with respect to siderite (Figure 4-12a), with maximum S.I. values around +1.0. The same was observed in the Forsmark near-surface groundwaters (Figure 4-12b), though with a consistently lower degree of oversaturation. These results support the effective precipitation of siderite and, therefore, its involvement in the control of dissolved Fe(II). An equilibrium control at such constant oversaturation levels (between +0.5 and +2.0) has been described for other anaerobic groundwater and aquatic systems as a kinetic inhibition of the ongoing precipitation that is compensated by the oversaturation (Jensen *et al.* 2002, Jakobsen and Cold 2007 and references therein).
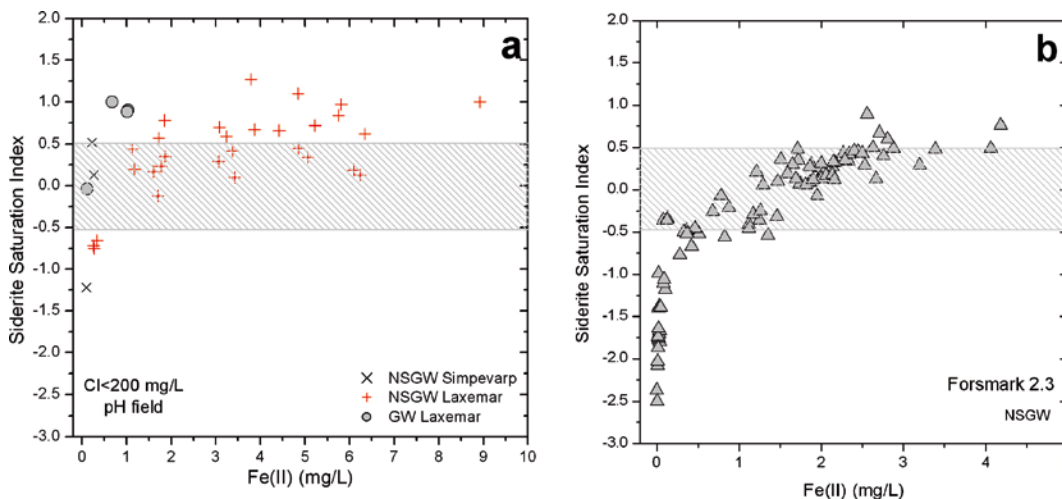
Figure 4-12. Siderite saturation index vs. ferrous iron in the Laxemar-Simpevarp (a) and Forsmark (b) fresh near-surface and shallow groundwaters with chloride lower than 200 mg/L and pH measurements from the field. Note that Fe(II) scale is different in the two plots. The dashed areas indicate the uncertainty range.

Most near-surface groundwaters are undersaturated with respect to the "amorphous" FeS (Figure 4-13a). However, this phase reaches equilibrium in almost all waters with dissolved sulphide contents higher than 0.04 mg/L, including the brackish near-surface groundwaters of soil pipe SSM000241 with the highest S(–II) contents (between 3.6 and almost 5 mg/L; not shown in plot)[48].

These equilibrium situations would suggest the effective precipitation of these phases (see Appendix C.3.2) through reaction:

$$Fe^{2+} + H_2S \rightarrow FeS + 2H^+ \qquad (4\text{-}3\text{-}7)$$

and the unmistakable presence of microbial sulphate reduction, which had already been deduced from the δ^{34}S in the dissolved sulphate of some near-surface groundwaters (see section 3.4.1).

Most of the near-surface groundwaters undersaturated with respect to the amorphous FeS are in equilibrium with respect to the less soluble mackinawite (Figure 4-13b). This result can indicate a lower intensity of the sulphate reduction or its periodic variations (dissolved sulphide in the near-surface groundwaters can vary considerably between sampling campaigns; Tröjbom *et al.* 2008) allowing the formation of the amorphous monosulphides at one time and their rapid recrystallisation to mackinawite when intensity decreases.

All these observations imply that there are zones in the overburden where dissolved Fe(II) may be controlled by equilibrium with amorphous FeS and siderite. The dissolved sulphide from SRB activity is clearly limited by amorphous FeS precipitation in some near-surface groundwaters but also in some deeper fresh groundwaters, indicating the extension of the sulphidic environment in some meteoric groundwaters (not affected by mixing) in the Laxemar subarea.

Groundwaters

Siderite saturation indices decrease with depth and chloride from the equilibrium values found in the near-surface groundwaters (Figure 4-14ab), which indicates that this phase does not play a controlling role on Fe(II) in deeper groundwaters.

Groundwaters with the highest oversaturation values (up to +1.0) are mainly associated with the fresh groundwaters from the Laxemar subarea down to 500 m depth. This oversaturation can be interpreted as an inherited character from the recharge through the overburden which has not been relaxed yet (siderite precipitation kinetics is much slower than calcite precipitation; Jensen *et al.* 2002). Recharge waters at Forsmark do not reach levels as deep as at the Laxemar subarea.
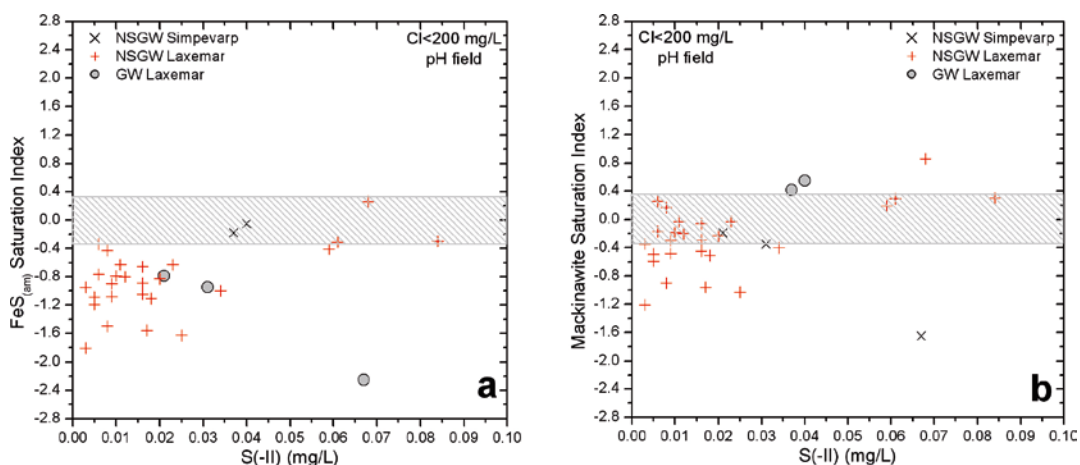
Figure 4-13. *Amorphous monosulphide (a) and crystalline mackinawite (b) saturation index vs. dissolved sulphide in the Laxemar-Simpevarp near-surface groundwaters with chloride lower than 200 mg/L and pH measurements from the field. The dashed areas indicate the uncertainty range.*

---

[48] Although not shown, this equilibrium situation with respect to amorphous FeS has also been identified in the near-surface groundwaters from Forsmark.
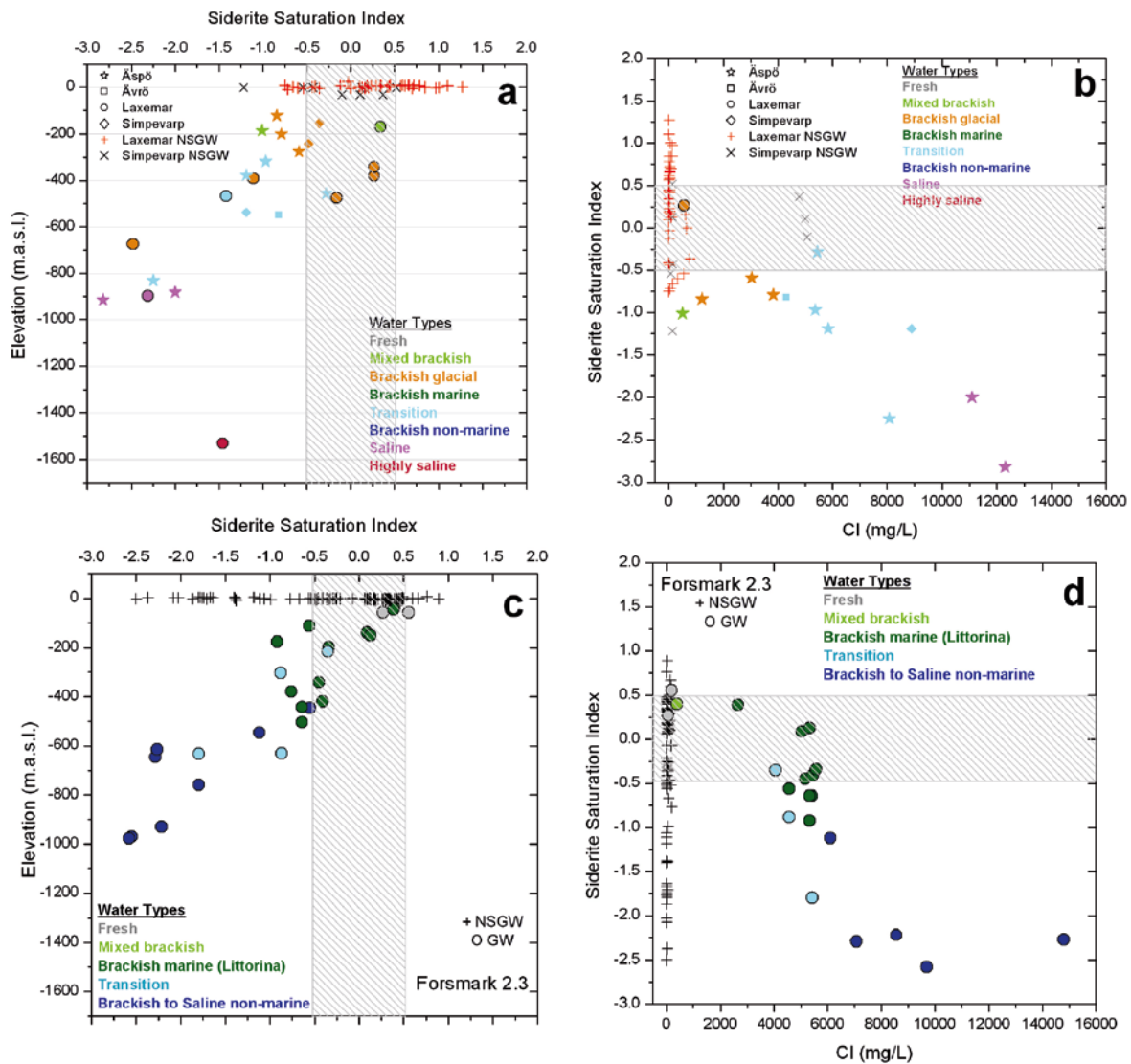
Figure 4-14. *Siderite saturation index vs. depth (a, c) and chloride contents (b, d) in the Laxemar-Simpevarp (a, b) and Forsmark (c, d) groundwaters (including near-surface groundwaters). Dashed areas indicate the uncertainty range.*

Therefore, siderite saturation indices decrease almost linearly with depth (Figure 4-14c) and display a step around 5,500 mg/L Cl (Figure 4-14d) in groundwaters with clear Littorina contribution.

Equilibrium situations with respect to Fe(II)-monosulphides can be observed down to 600 m depth, mainly in groundwaters from Äspö and Simpevarp, but also in some from the Laxemar subarea (Figure 4-15c). At greater depths, in groundwaters with chloride contents higher than 7,000 mg/L, this equilibrium situation appears to be less frequent but clearly reached by some groundwaters from the Äspö zone at 900 m depth. The equilibrium with respect to amorphous monosulphides is observed in groundwaters with highly variable chloride contents (fresh to saline; Figure 4-15a), as also happened at Forsmark.

This implies that equilibrium must be imposed by common factors at all sites independent of the evolution history and the type of system. The most obvious factor is the activity of sulphate-reducing bacteria. The second is the existence of an iron source in the system with enough intensity to keep the waters saturated with respect to these metastable phases. The activity of SRB is necessary to supply H_2S to the waters. The occurrence of these micro-organisms depends on the presence of anoxic conditions, the nutrient supply, the competition with other biological groups, etc. All these factors can interact with each other in order to enhance their activity in very different hydrogeo-chemical systems.
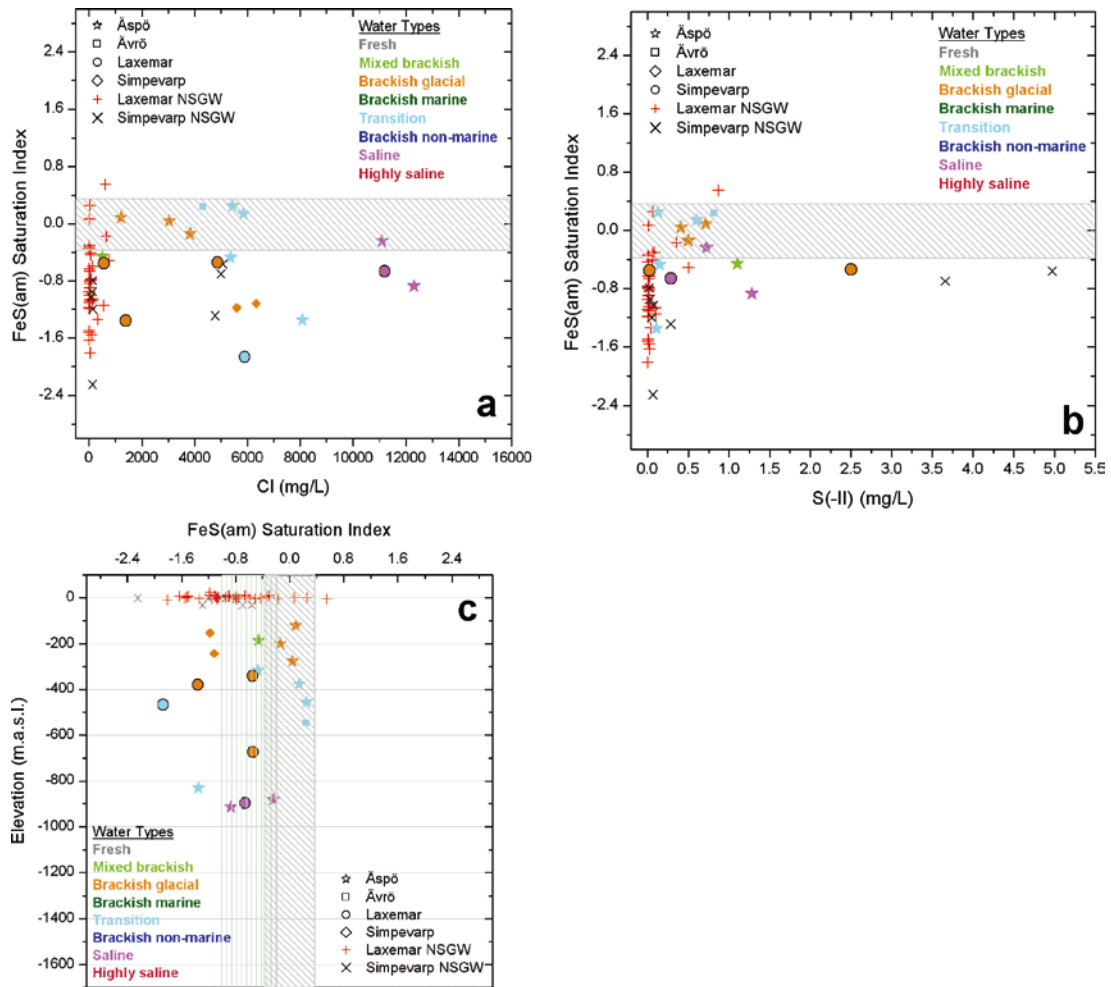
Figure 4-15. *Saturation indices for ferrous iron monosulphide (FeS) in the Laxemar-Simpevarp ground-waters as a function of chloride (a), sulphide (b) and depth (c) The shaded zones represent the uncertainty range (±0.36 units) for the amorphous (light grey inclined lines) and the microcrystalline phase (light green vertical lines).*

The importance of these two factors (SRB and an iron source) has been demonstrated in many low temperature natural systems with active precipitation of sulphides. The predominance of one or the other is responsible for the development of waters with high or low sulphide contents (Wilkin and Barnes 1997, Hurtgen *et al.* 1999, etc).

Equilibrium with respect to the amorphous iron monosulphides found in the Laxemar-Simpevarp groundwaters has important implications. The metastability of the amorphous iron monosulphides, becoming mackinawite or pyrite in a "short time"[49], has been demonstrated in the field and in the laboratory. Therefore, the occurrence of this equilibrium indicates a continuous and present supply of H_2S by the SRB activity. When dissolved Fe(II) (or a source for this component) is also present, waters become oversaturated with respect to the amorphous monosulphides and they can precipitate, maintaining the equilibrium in the system. Therefore, the equilibrium observed in Laxemar-Simpevarp waters corresponds to a present monosulphide precipitation process.

---

[49] Recrystallization of amorphous monosulphide to mackinawite starts in a matter of days and can last up to two years (Rickard 1995, Wilkin and Barnes 1997). More recent works (Benning *et al.* 2000) suggest a shorter time (several months). Transformation to pyrite can be accomplished in a time span from hours to decades (eg. Hurtgen *et al.* 1999). Even the longest time span is short compared to the residence time of the studied groundwaters (e.g. 10^2–10^4 years).

This active precipitation process is not equally present in all the subareas. Most of the Äspö and Ävrö groundwaters are clearly in equilibrium with monosulphides. In Laxemar, only some samples from categories 4 and 5 from KLX01, KLX02 and KLX08 boreholes are in the same situation, although another three samples (from KLX01, and KLX17) are close to equilibrium with respect to this amorphous phase but in equilibrium with mackinawite. In the rest of the boreholes in the Laxemar subarea and in the Simpevarp subarea, many sampled waters are not sulphidic and, *a priori*, cannot be in equilibrium with these phases. As the precipitation of monosulphides is conditioned by the activity of SRB and the concentration of Fe(II), these two topics are discussed below.

Most of the waters from Äspö and Ävrö have a sulphidic signature and are in equilibrium with iron monosulphides. Microbiological studies in Äspö indicate that SRB activity seems to be widely distributed in depth. Therefore, it may supply the necessary dissolved sulphide to reach equilibrium with respect to iron monosulphides. The Fe(II) content of these groundwaters is also significant (Table 4-2), which suggests the existence of a Fe(II) source (hematite) together with a long-lasting SRB activity. Therefore, the characters found at Äspö point to an active precipitation of amorphous iron monosulphides. The presence of waters in equilibrium with this phase at 930 m depth indicates that the biological activity of SRB extends at present down to that depth. It is expected that in Ävrö groundwaters (as they are similar to Äspö) a noticeable activity of SRB and an iron source also exist.

The groundwaters in the Laxemar subarea can be both sulphidic and non-sulphidic. The three waters from the KLX01 borehole (400 m to 900 m depth) are in equilibrium (or close to) with amorphous monosulphides. Microbiological data are restricted to 673 m depth (sample #1516, with 2.5 mg/L of HS$^-$, the most sulphidic water among the subareas) and the MPN for the SRB is the highest, with 56,000 cells/mL (Hallbeck 2006). Obviously, the effects of this bacterial population on the water chemistry must be very important and the H$_2$S supply, together with the precipitation of iron monosulphides, must be able to keep the dissolved Fe(II) contents at the low levels found in these waters (0.029 mg/L Fe(II)). Nevertheless, the presence of Fe(II), although in low concentrations, suggests the existence of a source of iron (hematite[50]) that compensates for the biological effects of the SRB and decreases the high H$_2$S content associated with their activity.

Waters from KLX02 and KLX03 boreholes are less sulphidic and dissolved S(–II) is in many cases below detection limit. Sample #2738 (at 298 m depth) from KLX02 and 0.04 mg/L S(–II), is the only sample in equilibrium with the amorphous monosulphide. At depths greater than 1,000 m, dissolved sulphide is below detection limit (Figure 4-5b). Haveman and Pedersen (2002) reported an MPN value of 330 cells/mL for SRB at 1,160 m, whereas these bacteria were not detected at 1,390 m depth. This absence of SRB is in agreement with these waters being the most saline in the Scandinavian Shield and supports the suggestion from Haveman and Pedersen (2002) that the salinity is one of the possible limiting factors in SRB activity. In general, using the equilibrium state of monosulphides as a proxy for SRB activity, these bacteria could be present at depths down to 900 m (Figure 4-15c), close to the maximum depth (1,093 m) at which this type of bacteria has been found or the maximum depth with dissolved sulphide above detection limit (KLX03 at 922 m depth).

The two samples from KLX03 (#10091 and #10188 with sulphide below detection limit) are undersaturated even when considering the reporting limit. Microbiological information available for 380 m depth indicates MPN values of 220 cells/mL for SRB.

Significant numbers of SRB have been detected in KLX08, KLX15 and KLX17 but only one sample from KLX08 at 320 m depth is in equilibrium with respect to the amorphous monosulphide.

Therefore, the identification of an equilibrium situation with respect to the amorphous monosulphides in groundwaters can be used as an indicator of the activity of SRB. However, the absence of equilibrium does not preclude this activity. SRB can be active but other factors may affect the monosulphide equilibrium such as: (1) the absence of iron oxides, (2) the disturbance of dissolved sulphide during sampling, or (3) the low activity of SRB producing insufficient H$_2$S to reach the

---

[50] This section was re-sampled one year later (sample 1633 from 1989) and the chemical composition was very similar (even in pH and Eh) showing the same equilibrium with respect to iron monosulphides. The main difference was the lower dissolved S(–II) and the higher Fe(II) contents. There are no microbiological analyses from this sampling but it seems that the SRB activity had decreased and was unable to keep the Fe(II) levels as low as the ones found in 1988.

amorphous monosulphide solubility product (though it is enough to reach mackinawite equilibrium in some cases). More detailed studies are needed to constrain these possibilities but, due to these problems, a direct correlation between SRB and equilibrium with iron monosulphide may not be found.

Discussion

The relationship between the iron and sulphur systems through monosulphide precipitation is evident in the near surface and deep groundwaters from the studied systems. It is especially important in the groundwaters as, in spite of the uncertainties, the presence of dissolved sulphide and iron oxyhydroxides in the fracture fillings is clear. Equilibrium with respect to amorphous monosulphides may be able to control the dissolved sulphide contents in groundwaters, which is a major concern for performance assessment.

Other processes may be deduced as well. The reductive dissolution of ferric oxyhydroxides by hydrogen sulphide (sulphidisation; reaction 4-3-6) may also exert a major control on dissolved sulphide contents (Canfield 1989, Canfield *et al.* 1992, Poulton *et al.* 2004). This reaction occurs due to the oxidation of dissolved sulphide at the mineral surface, followed by the release of the produced Fe(II) to solution. Subsequent reaction with additional dissolved sulphide may produce FeS precipitation again.

The extent to which iron minerals are able to control dissolved sulphide contents depends on the reactivity and abundance of the particular minerals present (Canfield 1989, Canfield *et al.* 1992, Raiswell and Canfield 1996). Iron minerals display a wide variability in terms of their reactivity towards dissolved sulphide, ranging from reactive Fe(III)-oxyhydroxides (with very fast kinetics, Poulton *et al.* 2004) to essentially unreactive Fe-silicates (Canfield *et al.* 1992, Dos Santos Afonso and Stumm 1992, Raiswell and Canfield 1996). Thus, the availability of hematite in the fracture fillings may play an important role in the buffering of the dissolved sulphide in groundwaters and this potential role would merit further studies.

The SRB-mediated precipitation of amorphous monosulphides and its coupling with other organic and inorganic geochemical processes should be taken into account in the safety assessment. Its potential influence on the genesis of colloidal phases is only one of the many important consequences because, independently of the iron monosulphides occurring as mineral or colloidal phases, their capacity to retain pollutants is very high. However, as the stability of the iron monosulphides under any hydrogeochemical perturbation is low, their behaviour should be carefully assessed.

4.3.5   Additional processes and calculations

Understanding of the links between the iron and sulphate reducing bacteria is also needed to evaluate the relationship between the iron and sulphur redox systems. The relationship between IRB and SRB is not always mutually exclusive as the classical redox zones scheme[51] suggests. Both metabolic groups have been identified as being concomitantly active in the same points in sediments or aquifers (e.g. Postma and Jakobsen 1996, Jakobsen and Postma 1999, Blodau and Peiffer 2003, Park *et al.* 2006, Jakobsen and Cold 2007), which could be extrapolated to other metabolic groups in systems with limited organic matter (e.g. Jakobsen and Postma 1999).

Taking into account the problems associated with the dissolved redox indicators of the involved processes (Appendix G), the identification of a coexistence or mutual exclusion between IRB and SRB in the Laxemar-Simpevarp groundwaters is not possible from hydrochemical data alone. Moreover, microbiological analyses where IRB and SRB have been detected, suggesting the simultaneous activity of both, have many uncertainties.

---

[51] Redox zones, understood as the result from the segregation of different terminal accepting processes (TEAP's) in separate zones during degradation of organic matter (and, therefore, the dominance of several types of metabolisms over others), is thermodynamically explained in terms of Gibbs free energy yield or redox potentials for each involved reaction. In the presence of multiple TEAPs, microorganisms are assumed to use the thermodynamically most favourable TEAP first until that species is exhausted and then other TEAPs are used sequentially in order of decreasing free energy yield (or redox potential) for each reaction (e.g. Stumm and Morgan 1996, Appelo and Postma 2005).

Fe(III)-oxyhydroxides or Fe(III)-clays may be used as terminal electron acceptors (TEA's) by iron reducing bacteria. Both are widely present in the fracture fillings of the Laxemar-Simpevarp and Forsmark areas at all depths. Therefore, *a priori*, it could be thought that these groundwater systems would represent something like the "IRB paradise". However, the opposite appears to occur and only locally have high numbers of IRB been detected.

This section analyses the processes affecting the Fe(III)-oxyhydroxides and Fe(III)-clays as terminal electron acceptors (TEA) for the IRB activity, to solve this apparent contradiction. A general bioenergetics approach of the possible TEAP`s (*Terminal Electron Accepting Process*) for IRB, SRB and methanogenic activities is presented. Then, a partial equilibrium approach for iron and sulphate reduction is used to infer the effects of the stability of Fe(III)-oxyhydroxides on the predominance of iron and sulphate reduction processes. The potential use of Fe(III) present in phyllosilicates by IRB is also examined, as this process remains almost totally unexplored in crystalline systems. Finally, a conceptual model for the IRB activity in oxygen intrusion scenarios is proposed.

Energetics of the possible TEAP`s

In the aforementioned classical redox zonation, the order of preference is usually assumed to be $O_2 > NO_3^- > Mn(IV)$ -oxides $> Fe(III)$ -oxides $> SO_4^{2-} > CO_2$ from tabulated free energy values (ΔG^0) or redox potentials in standard conditions ($E^{0\prime}$, pe_0 (W), depending on the authors). As these standard conditions are not usually met in natural systems with variable chemical conditions, relating the sequential use of multiple TEAP's to tabulated values may be misleading. Therefore, the energy yield (ΔG_r) of the TEAP`s, using an adequate substrate (e.g. acetate, formate, etc) must be calculated explicitly from the concentrations and activities of the involved reactants and products in the studied systems (e.g. Jakobsen and Postma 1999, Park *et al.*2006).

The obtained energy for each TEAP is then compared with the respective threshold energy requirements[52] for the reaction to proceed. All TEAP's characterised by a free energy value lower than the threshold value are presumed to be active. Therefore, it is a test to identify the active TEAP's in the system and ideally it will become a judgement of whether a process dominate (e.g. redox processes are segregated in separate zones) or several processes can occur concomitantly (e.g. the redox zonation is diffuse or non-existent).

Unfortunately, this type of calculation cannot be quantitatively performed here as there are no data available on the contents of the organic substrates (acetate, formate, etc). However, the potentials calculated for the redox pairs related to the target TEAP's can be used to obtain a qualitative idea of the available energy yields for different metabolisms under the actual present conditions of these groundwaters.

Selected redox pairs

The selected redox pairs to perform the calculations are those directly related to dissimilatory iron and sulphate reduction and with methanogenesis. For these two last metabolisms, the chosen redox couples are SO_4^{2-}/HS^- and CO_2/CH_4. For iron reduction processes several redox pairs are used, considering a low crystalline $Fe(OH)_3$ phase (($Fe(OH)_3 B(K)$, from Banwart 1999), and a crystalline $Fe(OH)_3$ ($Fe(OH)_3 G(K)$, from the data proposed by Grenthe *et al.* 1992).

As IRB may also use the structural Fe(III) in clay minerals as terminal acceptor, the Fe(III)-clay/Fe(II)-clay redox pair proposed by Banwart (1999) is also used as a proxy of these processes. Fe(III)-clay/Fe(II)-clay redox couple is based on the reversible one-electron transfer between oxidised and reduced smectites. For this reaction, the conditional redox potential (Eh, V) proposed by Banwart (1999) as a function of pH at 10°C is defined by the equation

$$Eh = 0.280 - 0.056\ pH \tag{4-3-8}$$

As in section 4.2.2, the redox potentials for the selected redox couples are obtained with PHREEQC (Parkhurst and Appelo 1999) from the activities of the involved dissolved elements calculated at the measured physico-chemical conditions in the groundwaters.

---

[52] A threshold energy level exists for the TEAP´s, corresponding to the minimum energy necessary for microorganisms to store the gained energy as ATP (e.g. Jakobsen and Postma 1999).

Calculated Eh values for these redox couples in the Laxemar-Simpevarp groundwaters are shown in Figures 4-16 and 4-17 as redox ladders separated by water types. Redox ladders are a classical graphical representation of oxidation-reduction reactions arranged in order of decreasing oxidation potentials. In the ladder, the oxidised species of all couples having more positive Eh values can theoretically oxidise the reduced species of couples having more negative Eh values (e.g. Langmuir 1997) and the most thermodynamically favoured process is the one with the highest potential difference. Therefore, the position of the couples in the redox ladder indicates the amount of free energy available for a particular redox reaction.

As the "reference" couple (organic matter-CO_2) cannot be calculated properly due to the non-existence of data on the adequate organic substrates, the potential of this redox pair is assumed to be always the lowest in all the represented ladders (shadowed area at the bottom of the plots).

Results

As shown in Figures 4-16 and 4-17, reduction of structural Fe(III) in clays (blue diamonds) as terminal acceptor for microbially mediated organic matter oxidation would be the most energetically favoured redox reaction in almost all examined samples. Therefore, if that structural Fe(II) was bioavailable, IRB activity would be strongly favoured in almost all examined groundwaters.

The oxidation of organic matter by a poorly-crystalline $Fe(OH)_3$ (($Fe(OH)_3$ B(K), green dots in Figures 4-16 and 4-17) would be the second most energetically favourable redox reaction. On the contrary, the oxidation of organic matter by the crystalline $Fe(OH)_3$ ($Fe(OH)_3$ G(K), red squares) present in the groundwater system, would be the least favourable one in almost all cases.

This result indicates the important effect that the type of Fe(III)-oxyhydroxide present in the system, has to enhance the IRB activity over the rest of the metabolic groups. The presence of a low crystalline oxyhydroxide (like the one defined by Banwart 1999), is possible if the system has undergone a temporal intrusion of waters with dissolved oxygen but it is impossible in the pristine conditions of these reducing groundwaters with long residence time. However, an oxygen intrusion could produce the precipitation of these low crystallinity oxyhydroxides and then it could justify IRB activity (as the most thermodynamic favourable process) in places where it did not exist before.
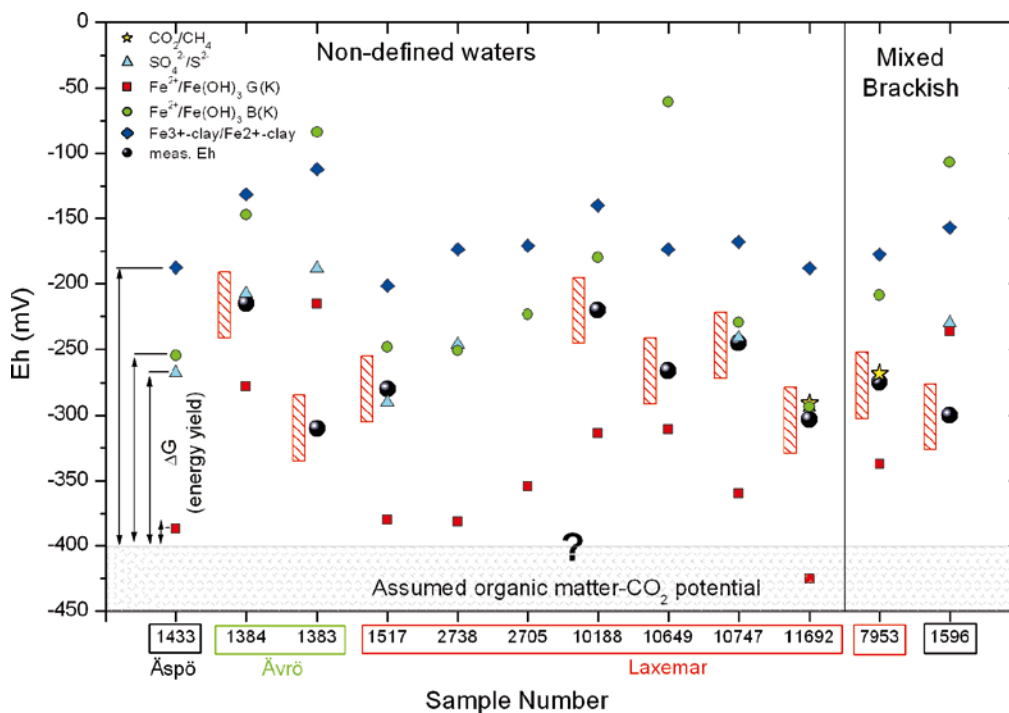
Figure 4-16. Comparison of the Eh values calculated with redox pairs involved in different possible TEAP´s for the Laxemar-Simpevarp groundwaters. Potentiometrically measured Eh (the red dashed rectangle indicate the accepted range of Eh variability of ±50 mV) and results for CO_2/CH_4, SO_4^{2-}/HS^-, two different $Fe^{2+}/Fe(OH)_3$ and Fe(III)-clay/Fe(II)-clay are also shown. Several samples without a defined water type and the group of mixed groundwaters are displayed here.
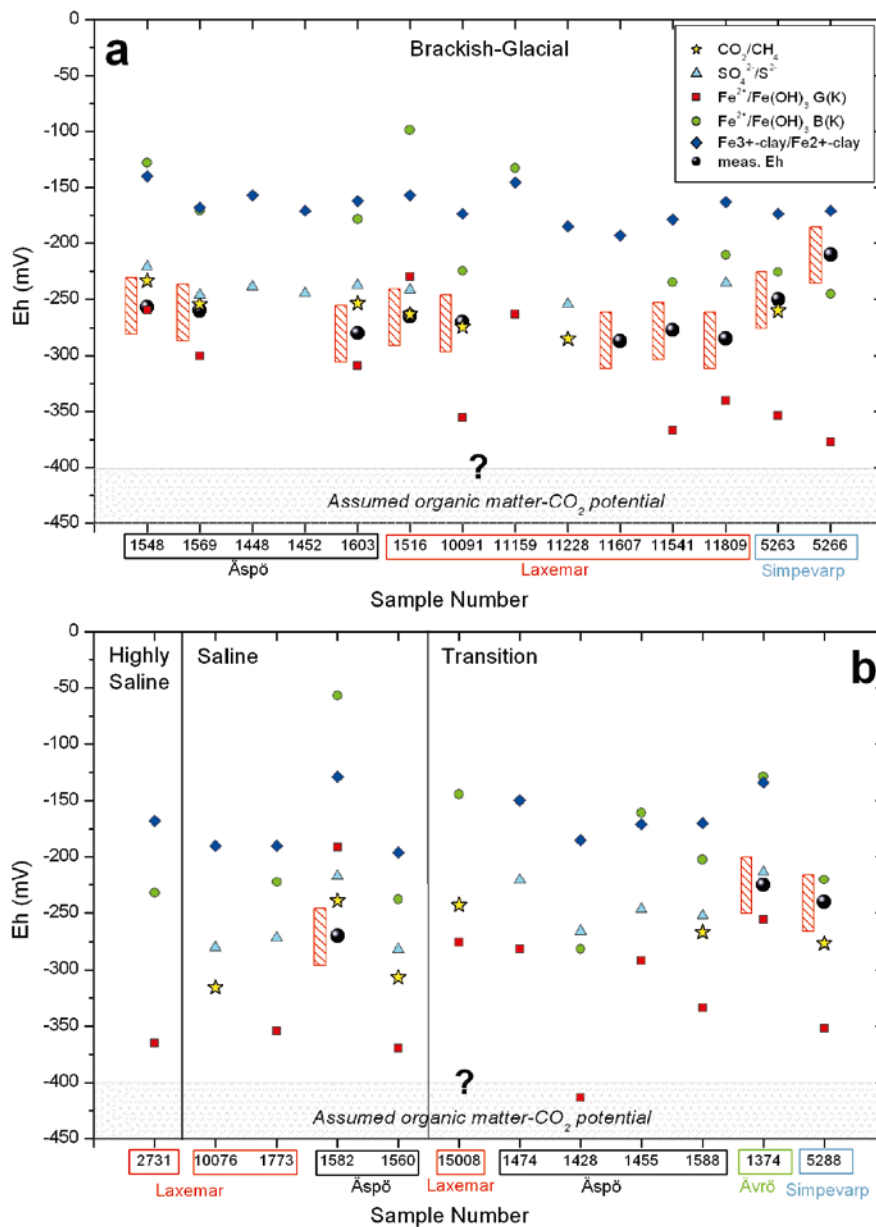
Figure 4-17. *Comparison of the Eh values calculated with redox pairs involved in different possible TEAP′s for the Laxemar-Simpevarp groundwaters. Potentiometrically measured Eh (the red dashed rectangle indicate the accepted range of Eh variability of ±50 mV) and results for CO_2/CH_4, SO_4^{2-}/HS^-, two different $Fe^{2+}/Fe(OH)_3$ and Fe(III)-clay/Fe(II)-clay are also shown. (a) group of brackish-glacial groundwaters; (b) group of highly saline, saline and transition groundwaters.*

In some of the examined samples the heterogeneous iron pair proposed by Banwart is close to or overlaps the value corresponding to the SO_4^{2-}/HS^- redox pair (cyan triangle). This is the case of samples #11692 (KLX17A) and #10747 (KLX08), the result of a short-circuit during sampling and, probably, corresponding to shallower levels. The agreement between these two calculated potentials would indicate that the amount of energy for IRB and SRB is similar and, therefore, both could theoretically be active at the same time in these samples. This has been confirmed with the microbiological analyses.

The comparison between the potentials obtained with SO_4^{2-}/HS^- and CO_2/CH_4 suggests that sulphate reduction would be the process with the highest energy yield in all the samples, and therefore the thermodynamically favoured process. However, for some samples, especially for the brackish-glacial groundwaters from Äspö (#1548, #1569, #1603; Figure 4-17), the energetic yield for both processes is similar and they may occur simultaneously (as observed in different environments; Kuivila *et al.* 1989, Jakobsen and Postma 1999, Park *et al.* 2006).

Discussion

The previous results indicate the existence of significant differences between the iron (Fe(III)-clay/ Fe(II)-clay and low crystalline $Fe(OH)_3/Fe^{2+}$ pairs) and the sulphur redox couples in the groundwaters. The free energy available from iron redox pairs is noticeably higher than from sulphur pairs. In terms of their use as TEAP's by iron and sulphate reducing bacteria, these differences would strongly favour the activity of iron reducing bacteria and, probably, they would inhibit sulphate reduction until bioavailable Fe(III) is exhausted.

This situation would lead to a generalised domain of IRB in the studied systems, which is the opposite of what has been observed up to now. This is due to the fact that bioavailability of Fe(III) in the solids is very limited or non-existent, in spite of the ubiquitous presence of Fe(III)-clays (e.g. chlorites) in the fracture fillings. Therefore, some type of limitation must exist for the use of Fe/III) in clays by IRB. This aspect is further discussed in section "*Reduction of Fe(III) in phyllosilicates*".

With respect to the iron oxyhydroxides, the results indicate that the type of Fe(III)-oxyhydroxide present in the system is a critical issue to favour or limit the IRB activity over the rest of the metabolic groups: poorly-crystalline Fe(III) oxyhydroxides would thermodynamically favour the IRB activity whereas crystalline Fe(III) oxyhydroxides would indirectly favour the rest of metabolic groups.

The existence of low crystallinity Fe(III)-oxyhydroxides in reducing groundwaters with long residence times is difficult to justify and the actual data on the Fe(III)-oxyhydroxides in the fracture fillings support the existence of crystalline phases (goethite and, mainly, hematite) with low surface areas. The result is that, under the pristine conditions of deep groundwaters with long residence time, the IRB activity would be seriously disfavoured. Without bioavailable Fe(III)-electron acceptors, sulphate reduction would be the most predominant TEAP from a thermodynamic point of view and, therefore, one of the major processes regulating redox conditions in the groundwaters.

The bioenergetics approach to redox processes presented in this section provides qualitative results. However, it is very useful to state the problems and conditionings associated with the activity of the different metabolic groups. A quantitative treatment, with data for the electron donors (acetate, formate, H_2, etc) should be explored to obtain the values of the free energy for the involved TEAP`s and a better assessment of the controlling processes (Appendix G).

Partial equilibrium calculations

Following the work by Postma and Jakobsen (1996), some simple thermodynamic calculations could be useful to discriminate between several redox processes assuming a partial equilibrium between them and analysing their implications for what has been observed in the natural system.

This approach is especially useful for iron and sulphate reduction coupled to organic matter oxidation. Oxidation of organic matter (using carbohydrate, CH_2O, as a proxy) with ferric iron oxyhydroxide can be represented by:

$$4Fe(OH)_3 + CH_2O \rightarrow 4Fe^{2+} + HCO_3^- + 7OH^- + 3H_2O \qquad (4\text{-}3\text{-}9)$$

and sulphate reduction activity is usually represented by a generic reaction such as:

$$2CH_2O + SO_4^{2-} + OH^- \rightarrow 2HCO_3^- + HS^- + H_2O \qquad (4\text{-}3\text{-}10)$$

or

$$2CH_2O + SO_4^{2-} \rightarrow 2HCO_3^- + HS^- + H^+ \qquad (4\text{-}3\text{-}11)$$
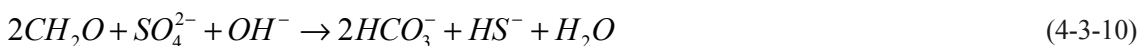
The assumption of partial equilibrium between iron and sulphate reduction implies that the energy yield from both processes is the same and then, the effects of different iron oxyhydroxides (which plays a critical role on the favourability of iron and sulphate reduction) can be easily explored.

Development of equilibrium reactions between iron and sulphate reduction processes

According to Postma and Jakobsen (1996), the reduction of Fe(III)-oxyhydroxides can be represented by the general half reaction:

$$Fe(OH)_3 + 3H^+ + e^- \rightarrow Fe^{2+} + 3H_2O \tag{4-3-12}$$
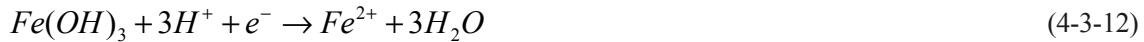
and the sulphate reduction process can be written as equation (4-3-13) with H_2S as the dominant species at pH < 7, or as equation (4-3-14) with HS^- as the dominant species at pH >7.

$$SO_4^{2-} + 8e^- + 10H^+ \leftrightarrow H_2S + 4H_2O \tag{4-3-13}$$

$$SO_4^{2-} + 8e^- + 9H^+ \leftrightarrow HS^- + 4H_2O \tag{4-3-14}$$

Equations (4-3-13) and (4-3-14) are mutually related through reaction (4-3-15):

$$H_2S \leftrightarrow HS^- + H^+ \tag{4-3-15}$$

Equilibrium reaction for the two redox couples can be obtained from reaction (4-3-12) and reactions (4-3-13) or (4-3-14). For example, combining (4-3-12) and (4-3-14), the final reaction is:

$$8Fe^{2+} + SO_4^{2-} + 20H_2O \leftrightarrow 8Fe(OH)_3 + HS^- + 15H^+ \tag{4-3-16}$$

Apart from this, sulphate reducing environments are commonly found to be in equilibrium or near equilibrium with FeS (Postma and Jakobsen 1996, Appelo and Postma 2005 and references therein). The existence of this heterogeneous equilibrium has been identified in Laxemar-Simpevarp and in Forsmark groundwaters (Gimeno *et al.* 2008). This equilibrium can be written as:

$$H^+ + FeS \leftrightarrow Fe^{2+} + HS^- \tag{4-3-17}$$

Therefore, there are two different reactions (4-3-16) and (4-3-17) which combine sulphur and iron couples. The next step is to put both reactions together and this can be done eliminating either Fe^{2+} or HS^-. Both options may be valid in natural systems since, due to the insolubility of FeS, anoxic environments are dominated by either Fe(II) or dissolved S(–II) (Postma and Jakobsen 1996, Appelo and Postma 2005):

- For Fe(II)-dominated environments (eliminating HS⁻) reactions (4-3-16) and (4-3-17) can be combined as:

$$9Fe^{2+} + SO_4^{2-} + 20H_2O \leftrightarrow 8Fe(OH)_3 + FeS + 16H^+ \tag{4-3-18}$$

- For sulphidic environments (eliminating Fe^{2+}) and depending on the pH, the combination of reactions (4-3-16) and (4-3-17) gives: at pH > 7 where sulphate reduction proceeds following reaction (4-3-14):

$$8FeS + SO_4^{2-} + 20H_2O \leftrightarrow 8Fe(OH)_3 + 9HS^- + 7H^+ \tag{4-3-19}$$

  whereas at pH < 7 and taken into account reaction (4-3-13):

$$8FeS + SO_4^{2-} + 20H_2O + 2H^+ \leftrightarrow 8Fe(OH)_3 + 9H_2S \tag{4-3-20}$$
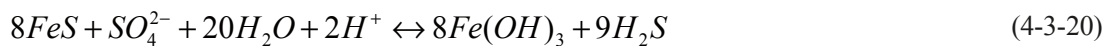
Equilibrium constants for reactions (4-3-13), (4-3-14) and (4-3-15) are those included in the WATEQ4F database distributed with PHREEQC (Parkhurst and Appelo 1999) and for reaction (4-3-17) a value for log K =–3 is used (see Appendix C). Different oxyhydroxides (Figure 4-18), ranging from less crystalline and more soluble phases (hydrous ferric oxides –HFO- or ferrihydrites) to more crystalline and less soluble oxyhydroxides (e.g. hematite), are considered in calculations:

- amorphous and microcrystalline ferrihydrite (in the terminology of Nordstrom *et al.* 1990) with log K values of –37 and –39, respectively, for the reaction

$$Fe(OH)_3 \rightarrow Fe^{3+} + 3OH^- \tag{4-3-21}$$

- lepidocrocite with log K = –40.9 for reaction (4-3-21). This solubility is also the value deduced by Banwart *et al.* (1994) and Banwart (1999), using the same approach as Grenthe *et al.* (1992), for the iron oxyhydroxide produced by a brief oxidising disturbance in the Äspö large-scale redox experiment (REX; Banwart 1999);

- the oxyhydroxide solubility (log K= –43.1 for reaction 4-3-21) deduced by Grenthe *et al.* (1992) from Eh, pH and Fe(II) data of a wide spectrum of deep groundwaters in Sweden. In agreement with the mineralogical observations in fracture fillings, this solubility value corresponds to a crystalline phase such as goethite or, most probably, hematite (the most frequent oxyhydroxide found in fracture fillings in the Laxemar-Simpevarp and Forsmark areas; Figure 4-18); and

- hematite, with a log K = –44.0 as the lower solubility limit of all oxyhydroxides considered in calculations.

- The calculations were carried out at two different SO_4^{2-} concentrations, 10^{2-} and 10^{4-} M, which cover the range found in the Laxemar-Simpevarp groundwaters.

Results

For Fe(II)-dominated environments, simultaneous equilibrium between sulphate reduction, Fe-oxide reduction and FeS is described in terms of the dominant species by reaction (4-3-18). This relation is displayed for the different iron oxyhydroxides in Figure 4-19 as a function of pH and $\log(aFe^{2+})$ and for the two SO_4^{2-} concentrations used in calculations, which gives a range indicated by two parallel lines with the same colour. These two lines indicate an equal free energy yield of Fe(III)-reduction and sulphate reduction. On the left side of the equilibrium zone, for a given oxyhydroxide (lower pH or lower Fe^{2+} activities than those assumed at the equilibrium condition), iron reduction is favoured (reaction 4-3-18 tends to proceed to the left). On the right side, sulphate reduction would take place.
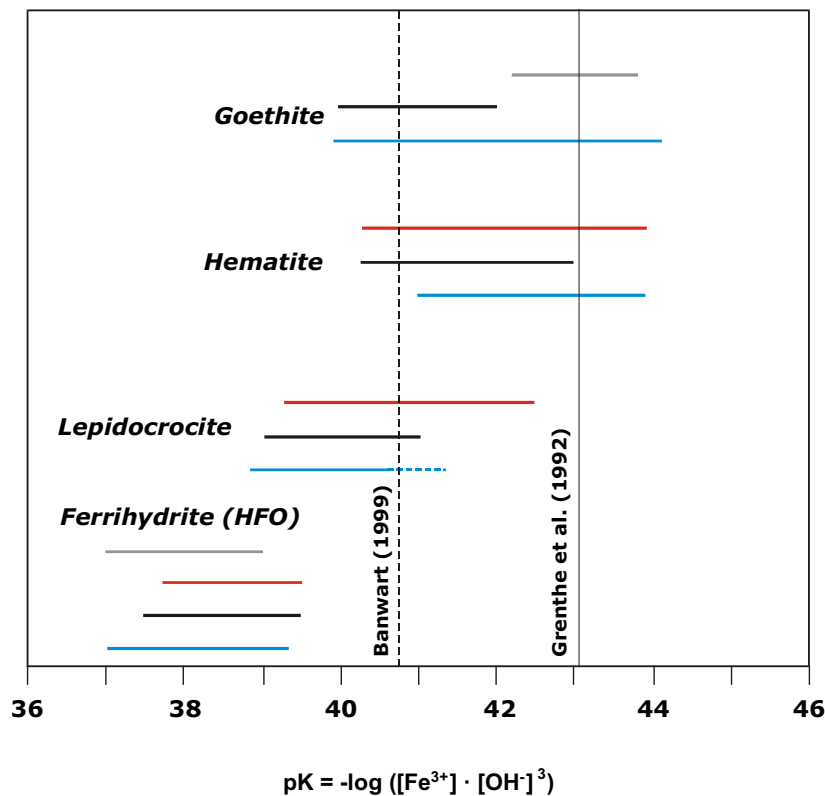
Figure 4-18. Reported solubility ranges at 25 °C for the main ferric oxyhydroxides. Blue lines represent the ranges obtained by Langmuir (1969; 1997); black lines correspond to the values suggested by Appelo and Postma (2005) from an analysis of Cornell and Schwertmann (2003) data; red lines represent the ranges reported in Bonneville et al. (2004); and, finally, grey lines represent the range of values proposed by Nordstrom et al. (1990). The most recent solubility ranges obtained by Majzlan et al. (2004) for 2-line and 6-line ferrihydrite (values between 37.5 and 39.5) coincide with the ranges shown in the plot for this phase. The values reported by Macalady et al. (1990) for goethite (pK=44.15) and hematite (pK=44.0) are in agreement with the less soluble extreme of the range shown in the plot for these minerals. Empirical values deduced by Grenthe et al. (1992; pK=43.1) and Banwart (1999; pK = 40.9) for different Swedish groundwaters are also indicated.
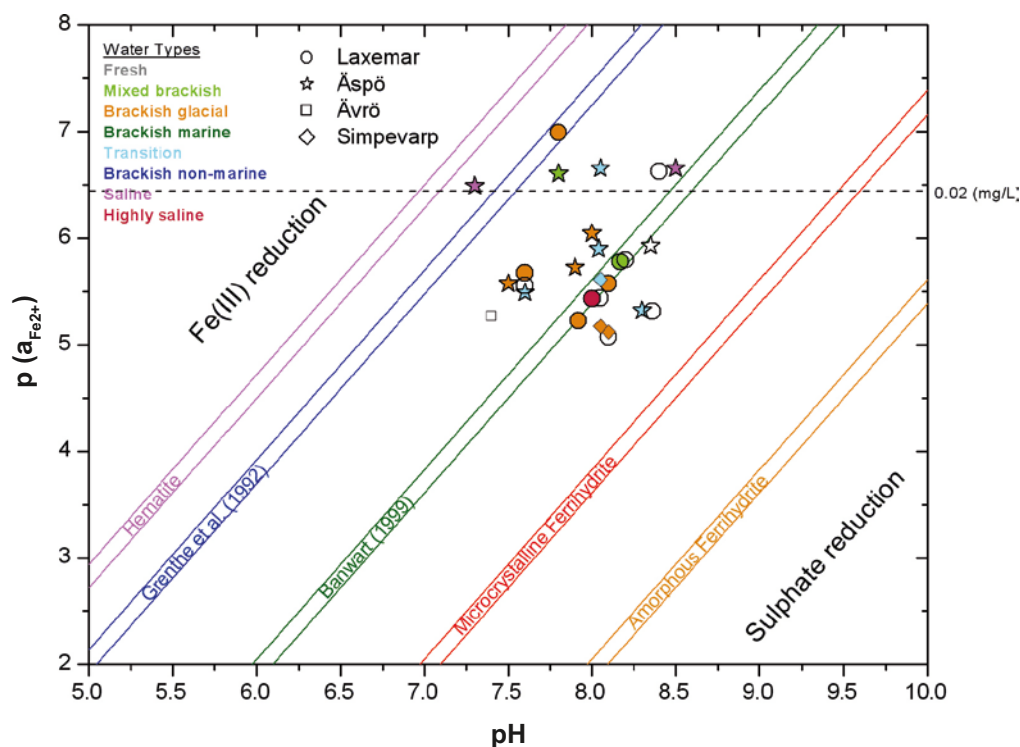
Figure 4-19. *Fe^{2+} activity vs. pH diagram showing the stability relations for simultaneous equilibrium between Fe(III) and sulphate reduction at equilibrium with FeS in Fe(II)-dominated environments. Zones between lines with the same symbols correspond to this partial equilibrium for different oxyhydroxides calculated at SO_4^{2-} concentrations between 10^{2-} and 10^{4-} M (reaction 9). On the left side of the equilibrium zone for a given oxyhydroxide iron reduction is favoured and on the right side sulphate reduction would take place. Detection limit (0.02 mg/L) for analytical concentrations of dissolved Fe(II) is shown for reference.*

Similarly, results for sulphidic environments (reactions 4-3-19 and 4-3-20) are shown in Figure 4-20 as a function of HS⁻ activity (results with total dissolved sulphide or mS(–II) are the same) and pH and the two sulphate concentrations used for calculations. Above the equilibrium zone for a given oxy-hydroxide, dissolved sulphide concentrations are lower than the assumed equilibrium condition and sulphate reduction is favoured (reactions 4-3-19 and 4-3-20 shift to the right). Below the equilibrium zones iron reduction is favoured.

Both plots show the minor influence of sulphate concentration on the equilibrium and the major influence of pH on the relative stability of iron and sulphate reduction. But they mainly demonstrate the important effect of the stability (and/or the specific surface) of iron oxyhydroxides on the presence of iron or sulphate reducing environments. In the presence of ferrihydrites (amorphous HFO or iron oxides with very high surface areas) iron reduction is favoured under most aquatic conditions. However if hematite or goethite are present sulphate reduction is sometimes more favourable (Postma and Jakobsen 1996, Peiffer 2000, Appelo and Postma 2005). That is, as the stability of iron oxides increases (and/or surface area decreases), sulphate reduction becomes increasingly favourable.

These diagrams also show the relative stability of the oxyhydroxides involved. In Fe(II) dominated environments (Figure 4-19), equilibrium zones are dependent on pH. For most waters with pH > 7 and dissolved iron above detection limit only the most crystalline (and low surface area) oxyhydrox-ides (hematite or goethite) are stable as iron reduction is not favoured in these waters. The rest of the phases, if present under these conditions, will be well inside the iron reduction field and will tend to disappear.

In sulphidic environments equilibrium zones are less sensitive to pH (Figure 4-20) but the position of the equilibrium lines indicate the same as in the case of Fe(II)-dominated environments. The stability zones for amorphous to microcrystalline ferrihydrites correspond to dissolved sulphide concentrations
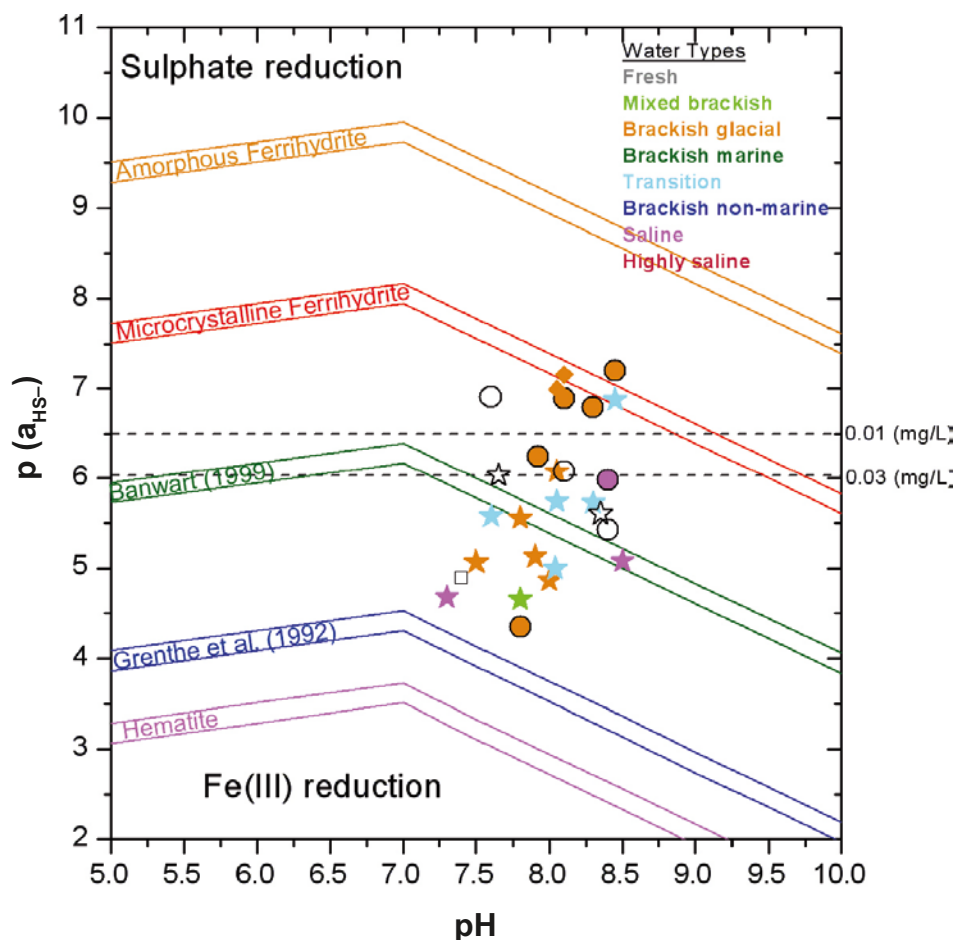
Figure 4-20. *The negative logarithm of the HS⁻ activity (p(a_{HS⁻})) vs. pH diagram showing the stability relations for simultaneous equilibrium between Fe(III) and sulphate reduction at equilibrium with FeS in sulphidic environments. Coloured lines correspond to this partial equilibrium for different oxyhydroxides calculated at SO_4^{2-} concentrations between 10^{-2} and 10^{-4} M (reactions 4-3-19 and 4-3-20). Above this equilibrium zones sulphate reduction is favoured and below iron reduction would take place. Samples location does not change when using S(–II) total values. Detection (0.01 mg/L) and reporting limit (0.03 mg/L) for analytical concentrations of dissolved sulphides are indicated for reference.*

below sulphur detection limit (0.01 mg/L). Therefore, ferrihydrites are not stable in waters containing measurable dissolved sulphides and only more crystalline oxyhydroxides could be stable under these conditions. At pH values between 7 and 9, only waters with dissolved sulphide activities higher than 1×10^{-2} M, that is, outside the plot below the lower limit shown is the y axes, could have potential for reducing all suite of iron oxides, including the more stable and crystalline ones.

According to this, Laxemar-Simpevarp groundwaters are located in the area where the only stable Fe(III)-oxyhydroxides would be the more crystalline and less soluble phases, as observed in the system, and therefore, sulphate reduction is the most favourable processes.

The wide distribution of groundwater samples in the field between the microcrystalline ferric oxides and the crystalline phase defined by Grenthe *et al.* (1992) indicates that these waters could only be in partial equilibrium if a broad spectrum of iron oxyhydroxides with different solubilities or surface areas exists. This has neither been identified in the fracture fillings, nor expected in waters with long residence time.

Assuming that the pristine Fe(III)-oxyhydroxide mineralogy in the groundwater system mainly consists of phases with the solubility proposed by Grenthe *et al.* (1992), only some groundwaters from the Äspö island and the Laxemar subarea (the nearest to the Grenthe's solubility in the diagrams) could be in situations close to partial equilibrium.

In summary, partial equilibrium situations between iron and sulphate reduction processes in most groundwaters from the Laxemar-Simpevarp area would not be frequent since iron reduction is totally unfavourable with respect to sulphate-reduction in most cases.

Discussion

The results obtained in this section emphasise, again, the critical importance of the stability of iron oxyhydroxides on the predominance of iron and sulphate reduction processes and, therefore, in the development of segregated redox zones in natural systems.

The use of ferric oxyhydroxides as TEAP's by iron reducing bacteria (and its ability to compete with other terminal electron accepting processes like sulphate reduction) strongly depends on their crystallinity, particle size and surface area. These characters provide different thermodynamic stabilities that affect the energy that may be gained from iron reduction. The less crystalline phases (e.g. ferrihydrite and lepidocrocite) constitute the primary source (Bonneville *et al.* 2004, Pedersen *et al.* 2005 and references therein) and, therefore, their absence would be an important limitation in the activity of these microorganisms.

Some experimental studies have shown that the more crystalline hematite or goethite can be used by IRB if they show surface areas similar to those typical for amorphous Fe(III)- hydroxides[53] (Roden and Zachara 1996, Roden 2003). However, the data obtained for the hematite-goethite found in the fracture fillings indicate surface areas much lower than those typical of amorphous Fe(III)-oxyhydroxides ($400–600$ m^2/g; Cornell and Schwertmann 2003). Therefore, the absence of amorphous iron oxyhydroxides with the suitable characters in the fracture fillings from Laxemar-Simpevarp, would limit the competitive success of iron reducers in favour of sulphate-reduction or other metabolic processes such as methanogenesis. In terms of the development of a redox zonation, this result is also important, as the segregation of Fe(III) and sulphate reduction in distinct redox zones (like the post-oxic and sulphidic zones in Berner's scheme; Berner 1981) is also strongly affected by the suite of iron oxyhydroxides present in the environment.

In environments containing a broad spectrum of iron oxyhydroxides (such as marine or lake sediments, soils, or, possibly, the Laxemar-Simpevarp overburden), Fe(III) and sulphate reduction may proceed simultaneously once the most unstable iron phases are absent or have dissolved completely (if ferrihydrite is present, Fe(III) reduction is strongly favoured in most conditions). In this situation, the boundary between zones of iron and sulphate reduction could be very diffuse and different degrees of overlapping can be observed (Postma and Jakobsen 1996, Jakobsen and Postma 1999). In environments with only iron oxyhydroxides of a confined stability range, as appears to occur in most of the groundwater system of the Laxemar-Simpevarp area, the development of segregated redox zones of Fe(III) and sulphate reduction is expected.

Apart from these thermodynamic considerations, kinetics constraints and other additional processes may limit the use of the Fe(III)-oxyhydroxides by IRB in the studied systems. Fe(III)-oxyhydroxides undergo structural transformations when entering an anoxic environment and they become dynamic phases able to transform from the least stable, poorly-crystalline and high surface area iron oxides towards more stable, crystalline and low surface area oxyhydroxides. This re-crystallization process has been studied in the laboratory and in natural systems and the obtained rates range from months to several years (Schwertmann and Murad 1983, Langmuir 1997, Stipp *et al.* 2002, Houben 2003), very fast in the context of the residence time of the studied waters. Even more, the presence of dissolved Fe(II) in the groundwaters has noticeable catalytic effects, increasing the transformation rates (Pedersen *et al.* 2005). This means that the Fe(II) initially produced by a hypothetic reduction of ferrihydrite by IRB (or any other inorganic process) would cause an autocatalytic transformation of the remaining pooly crystalline Fe(III)-oxyhydroxides into less reactive phases.

---

[53] This fact appears to be related to the use of nutrient-rich conditions to optimise the IRB growth during experiments (Lovley *et al.* 2004, Weber *et al.* 2006). In fact, under nutrient-limited conditions, similar to those occurring in natural subsurface environments, Glauser *et al.* (2003) did not observe reduction of crystalline goethite and hematite.

Therefore, the presence of poorly-crystalline Fe(III)-oxyhydroxides is not feasible under the pristine reducing conditions of Laxemar-Simpevarp groundwaters. Although these phases could have formed under oxygen intrusion events, they must have re-crystallised over the time to more crystalline phases not bioavailable for the IRB, in agreement with the mineralogical observations.

The presence of dissolved Fe(II) in the groundwaters has additional effects, as it can be affected by sorption processes and it is known that the presence of Fe(II) in the surface of iron oxyhydroxides[54] inhibits microbial Fe(III) reduction (Roden and Urrutia 2002). Therefore, in the long residence time and reducing groundwaters from Laxemar-Simpevarp, Fe(II) sorbed on the oxyhydroxides (from old IRB activities or inorganic dissolution of iron phases) may represent another inhibiting factor for the present IRB activity.

Reduction of Fe(III) in phyllosilicates

Iron phyllosilicates have usually been considered as poorly reactive or unreactive iron phases for dissimilatory Fe(III)-reducers (Postma 1993, Larsen and Postma 2001, Hyacinthe *et al.* 2006). However, the structural ferric iron in clay minerals can be reduced either inorganically or biologically and several authors have demonstrated that IRB not only reduce Fe(III)-oxyhydroxides but also Fe(III)-phyllosilicates as electron acceptors for respiration.

Microbially-mediated reduction of octahedral Fe(III) in smectites is known (Stucki *et al.* 1987, Wu *et al.* 1988) and more recent experimental studies confirm this possibility both for structural Fe(III) in clay minerals (e.g. smectite, nontronite, chlorite, illite) as the sole electron acceptor (Kostka *et al.* 1996, 2002, Jaisi *et al.* 2007) or in the presence of Fe(III)-oxyhydroxides (Kukkadapu *et al.* 2006).

Although indirectly mentioned elsewhere (e.g. Banwart 1999, Trotignon *et al.* 2002), the potential use of Fe(III) in phyllosilicates by IRB remains totally unexplored in crystalline systems and it can be an important aspect in the overall understanding of microbial activity. Fracture fillings contain significant amounts of different clay minerals, with chlorite as the most abundant and the still scarce data on Fe(II) and Fe(III) contents in chlorites indicate the presence of important amounts of ferric iron potentially available for IRB activity.

The results obtained with the Fe(III)-clay/Fe(II)-clay redox pair proposed by Banwart (1999) suggest that microbial reduction of Fe(III) in clays would be the most thermodynamically favourable metabolism in groundwaters. Therefore, the existence of this additional TEAP, if effective, would implicate that the presence of IRB activity is impossible in the absence of adequate Fe(III)-oxyhydroxides.

However, the generalised and dominant presence of clay minerals and, specifically, chlorites in the fracture fillings from the Laxemar-Simpevarp or Forsmark areas would imply that the IRB activity should be much more frequent than observed in the groundwaters and, as stated before, a limiting factor should exist for the use of clay minerals as TEA.

Experimental studies indicate that the relative reducibility of Fe(III) in clays, either inorganic or biologically, depends on the chemistry and structure of the clay mineral. Smectite seems to be the most reducible, followed by chlorite and finally illite (Kukkadapu *et al.* 2006, Jaisi *et al.* 2007). Therefore, the type or the relative proportions of clay minerals (and/or the amounts of Fe(III) in their structures) may limit the extent of microbial Fe(III) reduction. Unfortunately, the available data on these characters in the fracture fillings are still very scarce. However, reducibility of structural Fe(III) in clay minerals is known to decrease sharply when even small amounts of Fe(II) are sorbed on their surface, compromising the IRB activity probably due to physical blockage of the electron transfer chain (Jaisi *et al.* 2007).

---

[54] Cell enzymatic activity of IRB is also diminished by the presence of sorbed Fe(II) on cell surfaces. This type of sorption is another important factor responsible for controlling the extent of microbial reduction of iron oxy-hydroxides. The effects of this inhibition are expected to be more severe under nutrient-limited (non-growth) conditions, because cells would have little chance to remove sorbed Fe(II) by reproduction (Urrutia *et al.* 1998, Roden and Urrutia 2002).

Therefore, in groundwaters with long periods under permanently reducing conditions, the accumulation of aqueous and surface-bound Fe(II) is possible from both biotically induced or inorganic reactions. This accumulation will finally limit the Fe(III) oxide reactivity toward enzymatic reduction, particularly in situations where removal of Fe(II) end-products is slow compared to the kinetics of reduction or dissolution. Hence, although more detailed studies are needed, all lines of reasoning appear to indicate that in long-residence time groundwaters (in reducing conditions or without recent mixing events able to produce the desorption of Fe(II) from clays), the use of the structural Fe(III) in clays by IRB would be inhibited.

Oxygen intrusion scenarios and IRB activity: a conceptual model

All the data presented above suggest that the IRB activity at present in the Laxemar-Simpevarp groundwaters must be restricted to the shallowest levels, where a broad spectrum of Fe-oxyhydroxides (including low crystalline phases) exists. At deeper levels, the characters of Fe-oxyhydroxides and clays in the fracture fillings do not seem to be suitable to support the active presence of this type of microorganisms.

However, under specific evolutionary scenarios (in the past or in the future), the presence of IRB is, at least temporally, feasible. This is the case of oxygen intrusion scenarios. All the modelling studies performed on this issue have considered only inorganic redox buffers against penetration of oxygenated waters (Fe(II)-bearing aluminosilicates and sulphides). However, although the relevance of microbial activities for maintaining the reducing conditions of a repository, and for buffering the intrusion of O_2-rich groundwater, has been recognised (e.g. Pedersen and Karlsson 1995, Banwart 1999, Trotignon *et al.* 2002, Puigdomènech 2001) the effects of microbial activity have not been included in the predictive calculations of the performance assessment exercises.

The results and deductions obtained in the previous sections allow establishing a possible evolutionary model and evaluating the consequences on the IRB behaviour under oxygen intrusion scenarios. In this model (Figure 4-21), the input of O_2-rich recharging groundwaters into a reducing basement promotes the precipitation of amorphous, low crystallinity oxyhydroxides (e.g. ferrihydrite, the first oxyhydroxide usually precipitating under these conditions). Moreover, the change in the solution chemistry (e.g. ionic strength) would promote the desorption of the previously sorbed Fe(II) in clays.

As reducing conditions return, the presence of a low crystalline Fe-oxyhydroxide strongly favours microbial Fe(III) reduction if organic matter (from the recharging groundwaters or from the "Deep biosphere") or hydrogen are available as electron donors.

Therefore, a stage of IRB activity can be predicted in oxygen intrusion scenarios (Figure 4-21) as this input will produce the precipitation of the Fe(III)-oxyhydroxide suitable for their activity. But the extent and rate of dissimilatory Fe(III) reduction will be affected by different inhibition effects, most of them associated with their own metabolic activity. Sorption or surface-precipitated biogenic Fe(II) in mineral surfaces of Fe-oxyhydroxides and clays will promote important inhibitory effects on the extent of microbial reduction (Figure 4-21). During the later stages of the reduction process under permanently reduced conditions, the accumulation of aqueous and surface-bound Fe(II) is expected to limit the Fe(III) oxide or clay reactivity toward enzymatic reduction, particularly in situations where removal of Fe(II) end-products is slow compared to the kinetics of reduction (Roden 2004, 2006, Kukkadapu *et al.* 2006).

Moreover, the reactivity of the Fe(III)-oxyhydroxides will change significantly over time after the onset of anaerobic conditions, due to preferential dissolution of the more reactive oxide phases and the fast transformations of the poorly-crystalline ferric oxides towards the more crystalline and stable ones (also favoured by the presence of dissolved Fe(II); Pedersen *et al.* 2005). Therefore, the easily bioavailable iron oxyhydroxides will decrease, and the remnant oxyhydroxides, crystalline and with low surface areas, will not be available as TEA for the IRB in the usual nutrient-limited conditions of aquifers.

Therefore, based on this conceptual model, one can predict that the extent of the IRB activity is necessarily limited in time. Initially their activity will be limited by the effects of their own metabolism (input of dissolved Fe(II) to the groundwaters) on the TEA. During this "IRB stage" other metabolic groups can be concomitantly active (at least when the less crystalline iron oxyhydroxides disappear).
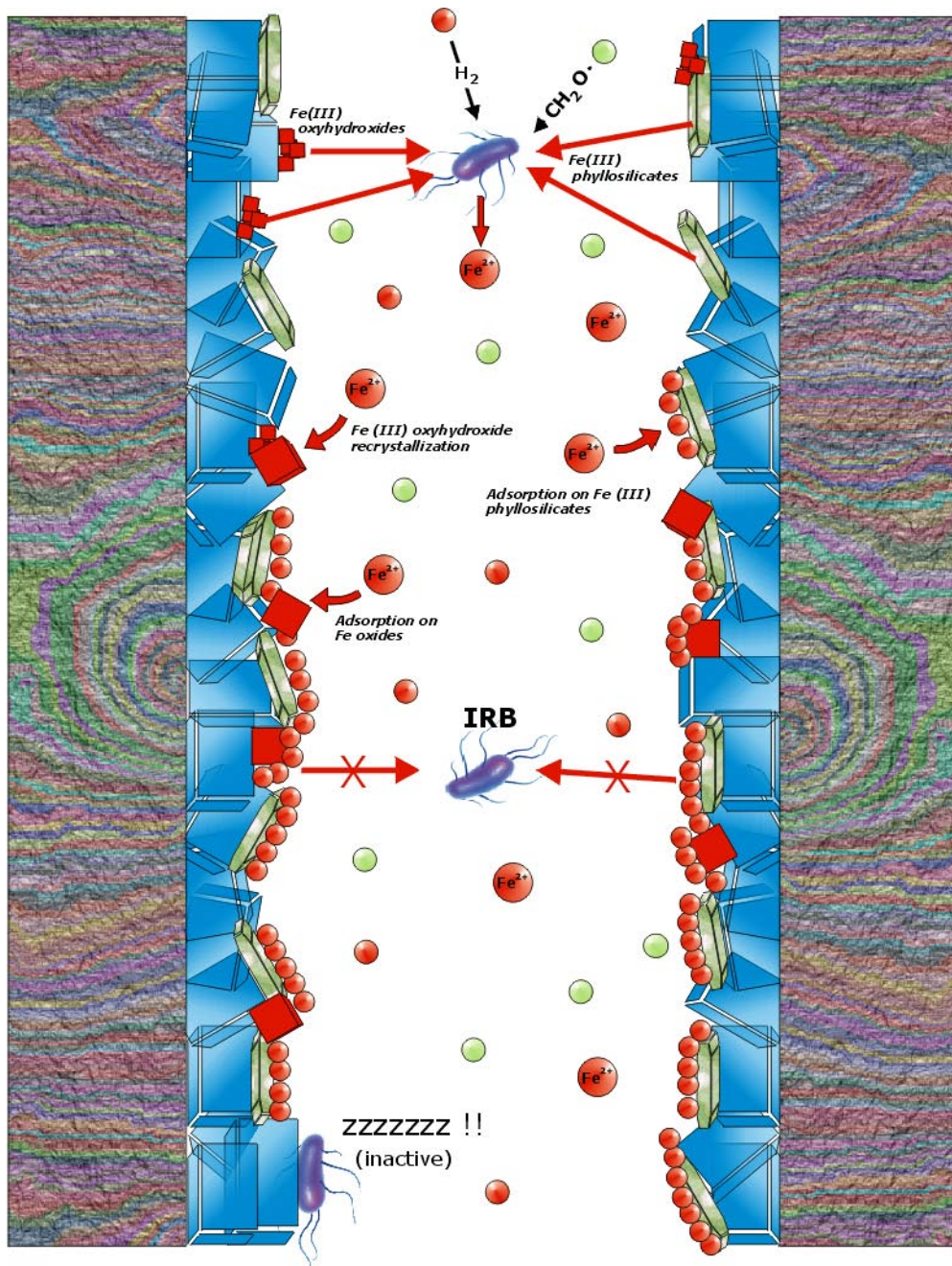
Electron acceptors

⬡ Fe(II)–Fe(III) *phyllosilicates*

⬥ Fe(III) oxyhydroxides

Electron donnors

● Organic matter

● Hydrogen

Figure 4-21. *Schematic representation of the limiting processes for the use of Fe(III)-oxyhydroxides and Fe(III)-phyllosilicates as electron acceptors by iron reducing bacteria. These processes will constrain the extent and rate of dissimilatory Fe(III) reduction in oxygen intrusion scenarios. Schematic representation of the limiting processes for the use of Fe(III)-oxyhydroxides and Fe(III)-silicates as electron acceptors by iron reducing bacteria. Preferential dissolution of the more reactive oxide phases, fast transformations of the poorly-crystalline ferric oxides towards the more crystalline and stable ones (favoured by the presence of dissolved Fe(II)) and sorption processes of dissolved Fe(II) on iron oxyhydroxides and Fe(III) clay minerals or on cell surfaces, control the extent and rate of dissimilatory Fe(III) reduction processes.*

Finally, IRB activity would cease and it would be replaced by other microorganisms (sulphate reduction bacteria or methanogens). This last stage would probably correspond to the present situation of the groundwater system.

This conceptual model is supported by the results obtained by Banwart (1999) and Trotignon *et al.* (2002) in the framework of the REX project. The studies performed in the large-scale redox experiment carried out at the Äspö Hard Rock Laboratory indicate that, after a brief oxidising disturbance, a low crystallinity Fe-oxyhydroxide was formed in the system. This oxyhydroxide re-crystallised with time (less than three years) to the "intermediate" solubility iron oxyhydroxide deduced by Banwart (1999). Significant IRB populations were observed but no evidence of sulphate reduction was found (Banwart, 1999 and references therein), probably because IRB, with the suitable TEA, outcompete the SRB activity (Fe(III)-clays may also be involved in the iron reduction processes; Banwart 1999).

In the supporting laboratory experiment of the REX project, waters with dissolved oxygen were injected periodically in a core section extracted from the REX borehole (Trotignon *et al.* 2002). Several results of this experiment are of special interest:

- The Eh potential measured during different O_2 "pulses" of the experiment (spanning 6–12 days) are in agreement with a calculated Fe(OH)$_3$ log K of –38, in the range of ferrihydrites (Figure 4-15). However, during the long anoxic periods between pulses (up to three months) the system reached equilibrium with crystalline goethite.

- During the anoxic periods a noticeable increase in IRB activity was detected correlated with strong increases in dissolved Fe(II). No SRB activity was detected.

- A strong increase in SRB activity was detected at the end of the experiment with the onset of marked reducing conditions.

All these results are in agreement with the proposed model. Oxygen intrusion promotes the precipitation of amorphous, low crystalline Fe(III) oxyhydroxides. Once the reducing conditions are re-established, these oxyhydroxides are used as TEA by IRB that outcompete SRB (and methanogens). Preferential dissolution of these more reactive, low crystalline Fe(III) oxyhydroxides and the fast transformations of the remaining ferric oxides, in the presence of dissolved Fe(II), promotes the shift towards equilibrium with the less reactive and bioavailable goethite. In this situation (and, probably, also acting other inhibitory effects of IRB activity such as sorption of dissolved Fe(II) on oxyhydroxides and clay minerals) dissimilatory iron reduction is not favoured and it is replaced by microbial sulphate reduction.

A noticeable result of this experiment is that SRB present in the core section from Äspö survived the dissolved oxygen pulses and, when suitable conditions return, they re-colonised the experimental setup.

4.3.6 Conclusions

Iron (II) and iron (III) minerals are widely distributed in the studied systems and the presence of dissolved sulphide and of SRB has also been reported in these groundwaters. This makes the iron and sulphur systems very important for understanding the redox processes in Forsmark and Laxemar-Simpevarp.

In the near-surface groundwaters, dissolved **Fe(II) and S(–II)** contents from the Laxemar-Simpevarp area do not deviate from the ranges found in the same type of waters in other Fennoscandian sites. Dissolved Fe(II) displays similar values as the near-surface groundwaters from Forsmark (up to 8.7 mg/L) or Olkiluoto (up to 7.4, Pitkänen *et al.* 2004). Speciation-solubility calculations show that most of the near-surface groundwaters are in equilibrium or oversaturated with respect to siderite (FeCO3). This suggests the effective precipitation of siderite and its involvement in the control of dissolved Fe(II).

As a general trend, maximum contents of sulphide are close to 1 mg/L, slightly lower than the values found at Forsmark (up to 1.64 mg/L), and higher than at Olkiluoto (up to 0.28 mg/L). For most of the near-surface groundwaters with dissolved sulphide contents greater than 0.04 mg/L,

speciation-solubility calculations indicate the existence of equilibrium with respect to "amorphous" FeS, which points towards its effective precipitation in these waters associated with the unmistakable presence of microbial sulphate reduction, as also deduced from $\delta^{34}S$ values in some near-surface groundwaters.

In the deep groundwater system, dissolved **Fe(II)** concentrations decrease roughly from the surface down to 700 m depth. Below that depth, the values are lower than 0.2 mg/L except in the deepest highly saline sample, where Fe(II) values reach 0.5 mg/L, which represents a slight increase in the contents of this element compared with the contents found at 1,000 m depth. For dissolved **S(–II)**, there is not a clear evolution trend with depth. There is a large number of samples with significant sulphide contents (e.g. > 0.2 mg/L) in the Laxemar-Simpevarp area (mainly at Äspö and Ävrö), whereas at the Laxemar subarea the number of samples with S(–II) > 0.2 mg/L is much smaller, probably related to disturbances during sampling.

Speciation-solubility calculations indicate that siderite saturation indices decrease in the deep groundwaters with increasing depth and chloride contents, which indicates that this phase is not playing a controlling role on dissolved Fe(II) concentrations in this part of the system. With regard to Fe(II)-monosulphides, equilibrium situations can be observed down to 600 m depth, mainly in groundwaters from Äspö and Simpevarp, but also in some groundwaters from Laxemar. This equilibrium situation appears to be less frequent at greater depths but is clearly reached at 900 m depth by some groundwaters with very variable chloride contents from Äspö, as also observed in Forsmark. As is also the case for the near surface groundwater system, the equilibrium with respect to the amorphous and metastable iron monosulphides found in most Simpevarp groundwaters suggests the presence of an iron source combined with a continuous and present supply of H_2S produced by SRB activity.

Understanding of the links between iron and sulphate reducing bacteria is also required to know the relationship between the iron and sulphur redox systems. The available data on IRB and SRB, as typical metabolic groups associated with the iron and sulphur system, appear to indicate that the SRB activity is more important and widely distributed than the IRB activity in the Laxemar-Simpevarp zone, in spite of the uncertainties associated with sampling.

The number of samples with significant amounts of IRB in the Laxemar-Simpevarp area is very low and restricted to the 350–550 m depth interval. Furthermore, these data are affected by many unknowns and uncertainties and the deduction of concomitant activities of iron and sulphate reducing bacteria at these depths is, at least, problematic.

This problem can be generalised to the rest of the anaerobic metabolic processes involved in organic matter degradation. The simultaneous identification of different metabolic groups at the same section is frequent in microbiological research and, in some occasions, almost the whole suite of anaerobic microbes (iron reducing bacteria, manganese reducing bacteria, sulphate reducing bacteria and methanogens) has been cultured. Several questions arise: Does it mean that all these groups are simultaneously active? Are some of the groups cultured in the laboratory induced by sampling operations or favoured by cultivation methods but they are not active in the pristine conditions? Which one is induced and which one is really active?

To increase the knowledge of the redox processes in the studied systems it is necessary to answer these questions. To know whether there are zones dominated by individual functional groups of microbes (excluding other groups) or zones where more than one group is active is a basic requirement to properly model the evolution of redox processes.

Using a general bioenergetics approach of the possible TEAP`s for IRB, SRB and methanogenic activities and a partial equilibrium approach for iron and sulphate reduction, some interesting conclusions have been obtained on the expected dominance of iron or sulphate reduction processes. Results indicate that present IRB activity in the Laxemar-Simpevarp groundwaters is restricted to the shallowest levels, where a broad spectrum of Fe-oxyhydroxides (including low crystalline phases) exists. At deeper levels, in spite of the abundance of Fe(III)-oxyhydroxides and clays in the fracture fillings, their characters do not seem to be suitable for their use as TEA by IRB. This would favour the activity of other metabolic groups, such as sulphate reducing bacteria or methanogens.

The main factors determining whether iron or sulphate reduction is energetically more favourable are pH and, especially, the stability of iron oxyhydroxides in the system. The different thermodynamic stabilities of Fe(III)-oxyhydroxides (conditioned by their mineralogy, particle size or surface area) affect the energy that may be gained from iron reduction and, therefore, influence the metabolic rates and the competition between iron and sulphate reducers (or methanogens), at least in low substrate (electron donor) conditions.

Iron reducing bacteria in natural systems subdued to that electron donor limitation (e.g. in aquifers) have only been found to compete successfully with SRB or methanogens in the presence of ferrihydrite or similar poorly-crystalline iron minerals. But the reactivity of the Fe(III)-oxyhydroxides changes significantly over time after the onset of anaerobic conditions due to: (i) the preferential dissolution of the most reactive oxide phases; (ii) the fast transformation of the poorly-crystalline ferric oxides to more crystalline and stable phases (Houben 2003, Schwertmann and Murad 1983, Stipp *et al.* 2002, Pedersen *et al.* 2005); and (iii) the accumulation of surface-associated biogenic or non-biogenic Fe(II). All three processes limit the activity of IRB and promote sulphate reduction (or methanogenesis).

Mineralogical studies in Forsmark and Laxemar-Simpevarp areas support the existence of crystalline phases (old low-temperature goethite and, mainly, hydrothermal hematite) with low surface areas. As expected in long time residence time groundwaters in permanently reducing conditions, amorphous or low crystalline oxyhydroxides have not been found except under disturbed (oxygen intrusion) conditions at the boreholes (e.g. Dideriksen *et al.* 2007).

Iron reducing bacteria can also use the Fe(III) in clay minerals as TEA for respiration, but this process remains totally unexplored in crystalline systems in spite of the abundance of these minerals in the fracture fillings. However, reduction of structural Fe(III) in clay minerals decrease when even small amount of surface sorbed Fe(II) is present in the clays. Therefore, and as it occurs for iron oxyhydroxides, the reduction of structural Fe(III) in clay minerals could be importantly inhibited by sorbed Fe(II), making its use as TEA by IRB very difficult.

All these observations may explain why IRB have not been frequently found in the microbiological analyses performed at Laxemar-Simpevarp, except at shallow levels. They would also suggest that some problems may have occurred during the sampling of the populations at greater depths.

Under these conditions, sulphate reducing bacteria and methanogens would be favoured in the groundwater system. Preliminary calculations on the energy yield for both processes indicate that SRB activity is thermodynamically favoured in most of the examined samples but concomitant SRB activity and methanogenesis is also possible in some cases.

All these findings have been summarised in a conceptual model for the evolution of IRB activity during oxygen intrusion scenarios, in agreement with the results obtained in the REX project. Obviously, this model is very preliminary, but it includes some key geochemical processes, usually ignored, that need further study for the understanding of the relationships between the different metabolic groups and their influence on the redox processes in the studied system.

The rate and extent of Fe(III) oxide reduction are governed by complex surface-chemical and physiological interactions that are only poorly characterised yet. Quantification of the IRB inhibitory effects is important for the understanding of the geochemical and microbiological relations and a prerequisite for the development of predictive (e.g. reactive transport) calculations including microbiological processes.

4.4   Manganese system

In previous SDM reports for the Laxemar-Simpevarp groundwaters the detailed study of the geochemical behaviour of Mn was not addressed. This type of study was performed by Gimeno *et al.* (2007, 2008) in Forsmark 2.1 and included the available Laxemar-Simpevarp groundwaters for comparison.

The data and results for the Laxemar-Simpevarp area are framed here in the broader picture of other crystalline systems in the Scandinavian Shield. Moreover, the main uncertainties associated with the processes able to control dissolved manganese in the Laxemar-Simpevarp groundwaters are also analysed in more detail.

4.4.1   Hydrochemical data

Manganese concentrations in near surface and deep groundwaters from the Laxemar-Simpevarp area vary from very low ($< 3\times10^{-3}$ mg/L, reporting limit, Nilsson 2008) to more than 2.5 mg/L. (Figure 4-22a). The highest values are found at shallow depths in brackish near surface and shallow groundwaters from Simpevarp and Äspö (Figure 4-22a) with clear marine influences (Cl about 4,000–5,500 mg/L; Figure 4-22b).

Apart from these exceptions, maximum values found in the overburden are reached in the fresh near-surface groundwaters (up to 1.5 mg/L; Figure 4-22ab). Manganese concentrations in these waters are high compared with the median values of non–disturbed shallow groundwaters in Sweden as is also the case with iron concentrations (Tröjbom and Söderbäck 2006a).

Manganese contents show variable but high values in groundwaters with Cl contents around 5,500 mg/L and down to 500 m depth (Figure 4-22ab). These groundwaters have a clear Littorina signature and correspond mainly to Äspö and Simpevarp. Deeper and more saline groundwaters have lower manganese contents (< 0.25 mg/L). Overall, the distribution of manganese concentrations with depth shows a similar pattern to that of dissolved Fe(II) (Figure 4-5a) also showing variable and high contents down to 600 m depth and very low values at greater depth.

There is no clear trend between dissolved manganese and chloride contents except for the local maximum seen at around 5,500 mg/L Cl (as occurs with other elements; Figure 4-22b) in the aforementioned groundwaters with marine influence.

In the Forsmark area (Figure 4-23a), manganese contents in the groundwaters show a similar variability, reaching maximum concentrations near 3 mg/L. The highest variability and values are found in some brackish near-surface groundwaters and groundwaters with chloride contents around 4,000–5,500 mg/L and with an important Littorina signature. Deeper and more saline groundwaters have lower manganese contents (< 0.25 mg/L).

At Olkiluoto similar trends are found. Dilute, near-surface groundwaters in the overburden show variable and high Mn contents (up to 2.2 mg/L, Figure 4-23b) and this is also the case for waters with a chloride concentration of 4,000–5,000 mg/L (up to 1.2 mg/L; Figure 4-23b). The only difference is that, in this system, maximum Mn levels of around 2.3 mg/L have been measured in two very saline samples (Cl = 44,000 mg/L) at 900 m depth.
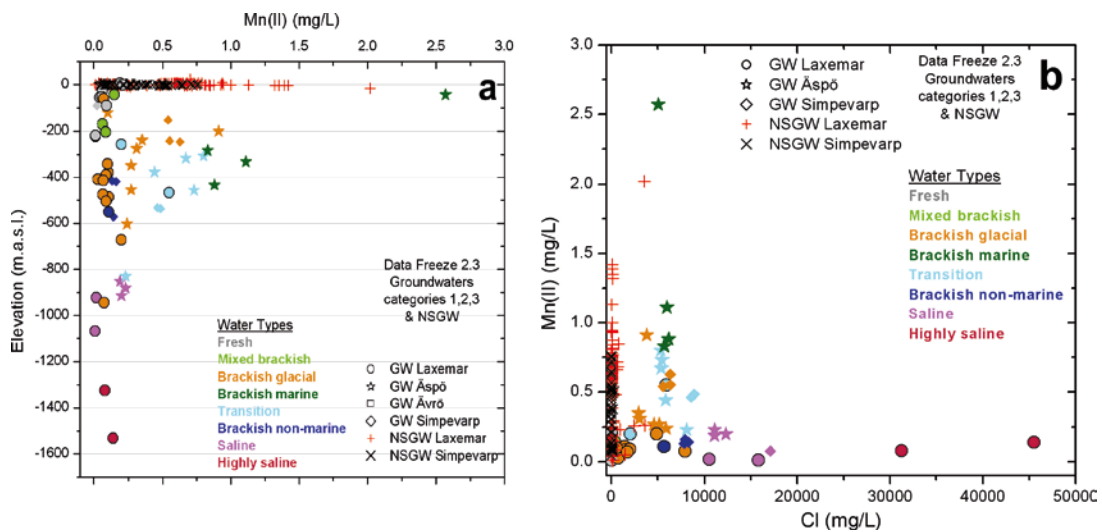
Figure 4-22. *Manganese content distribution with respect to depth (a) and chloride (b) in the Laxemar-Simpevarp area groundwaters.*

In the Finnsjön area, at depths between 100 and 700 m, maximum Mn concentrations reach 1.3 mg/L and, again, variable and relatively high Mn contents are associated with waters with Cl content between 3,000 and 5,000 mg/L (Figure 4-23c) with an old (Littorina) or modern (Baltic) marine contribution.

Near-surface groundwaters in the overburden from Palmottu (Finland) show Mn concentrations reaching 0.44 mg/L. Maximum Mn contents of 1.2 mg/L are found in the shallow groundwaters (100–200 m depth), where Cl contents are very low (Figure 4-23d). Deep groundwaters never exceed 0.2 mg/L of Mn. Stripa groundwaters have very low Mn levels, with maximum values of 0.05 mg/L and often below the detection limit (Nordstrom *et al.* 1985). Finally, groundwaters studied by Gascoyne (2004) in the Canadian Shield have always low Mn concentrations (below 0.7 mg/L).

From this short review of Mn concentrations in crystalline systems, some important conclusions can be drawn. The high variability and contents of Mn in soil pipes and dilute near-surface groundwaters in all the reviewed systems can be considered normal and related to the intrinsic variability in mineralogy, intensity of weathering and redox conditions in the superficial environment. The Mn variability in groundwaters with Cl contents in the range 3,000–5,500 mg/L and showing clear Littorina contribution in some of the studied systems (Laxemar-Simpevarp, Forsmark, Olkiluoto and Finnsjön), is related to a common event in the palaeohydrogeological history of those systems: a Littorina recharge period, not detected in the other groundwater systems (e.g. Palmottu and Stripa).
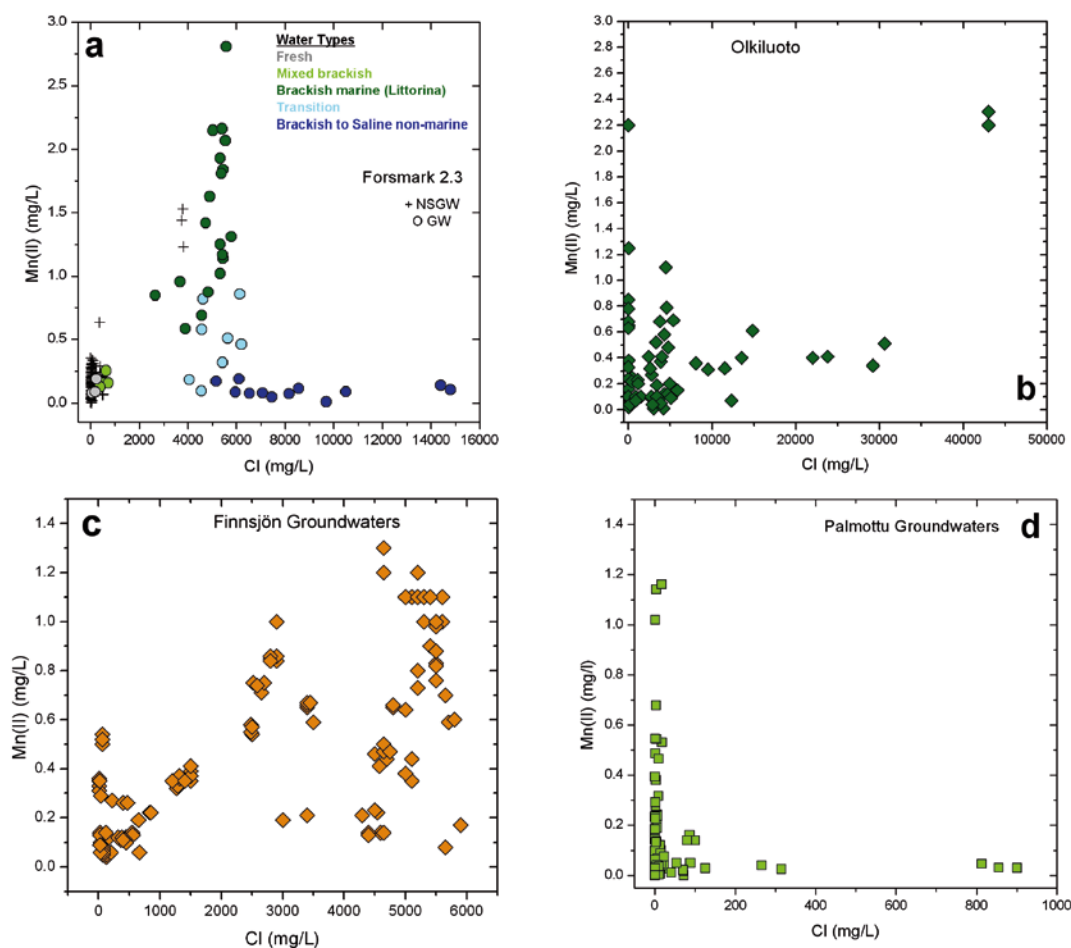
Figure 4-23. Manganese distribution with respect to chloride in different Nordic Sites. (a) Forsmark area (Sweden); (b) Olkiluoto (Finland); (c) Finnsjön (Sweden); and (d) Palmottu (Finland). Different scales have been used where appropriate to better visualise and describe the different systems.

4.4.2 Mineralogical data

Manganese may occur as manganese oxides or oxyhydroxides, as carbonate minerals (rhodochrosite or in solid solution with siderite or calcite) and also as a trace constituent in many other minerals. It can be associated with iron minerals, usually iron oxyhydroxides or mixed Mn-Fe oxyhydroxides, or in chlorites and other clays. Moreover, manganese is also known to substitute calcium in calcite.

In the overburden, Mn can be present as a minor component in rock-forming silicate minerals such as amphiboles, biotites or chlorites, all of them present in bedrock outcrops and till deposits of the Laxemar-Simpevarp area. As a result of weathering reactions, manganese may associate with different secondary minerals or appear as Mn-oxyhydroxides in oxic environments.

Although the available mineralogical data for soils are still very scarce, the existence of Mn(IV) oxyhydroxides is almost certain taking into account the existence of redoxomorphic soils. Moreover, Drake and Tullborg (2008) have recently identified the presence of manganese oxyhydroxide in the more superficial part of the fracture fillings at 10 m depth. However, there is no trace of Mn oxyhydroxides in deeper fracture fillings, neither in Laxemar-Simpevarp nor in Forsmark. This absence is reasonable as Mn-oxyhydroxides are not stable under reducing conditions for a long time, especially if dissolved Fe(II) or S(–II) are present (Appelo and Postma 2005).

Manganese is mainly associated with calcite and clay minerals (e.g. chlorite, corrensite) in the fracture fillings. Total manganese contents (MnO) in fracture filling calcites are occasionally high, with concentrations up to 4 wt.% (median concentration is ~0.3 wt.%). Manganese contents in clay minerals are usually between 0.1 and 0.3 wt.% in corrensite and between 0.3 and 0.7 wt.% in chlorite (Drake and Tullborg 2008).

Chemical analysis of bulk fracture filling material (Drake and Tullborg 2008) shows a positive correlation between manganese and iron, also suggesting the presence of manganese in chlorite and clay minerals. The highest Mn concentrations (up to 6.27% wt. MnO) are found in the upper ~50 m and, especially, in the upper 10 m, in samples with Mn-oxyhydroxides and Mn-rich mixed-layer clays. Manganese concentrations in the deeper bulk fracture filling material are always below 0.4 wt. % (Figure 4-24a).

4.4.3 Microbiological data

Microbiological analyses from the overburden in the Laxemar-Simpevarp area are not available yet. However, the presence of Mn(IV) oxides or oxyhydroxides (the terminal electron acceptor, TEA, for manganese reducing bacteria, MRB) in soils and in the fracture fillings at the shallower levels would favour the active presence of this bacterial metabolic group in the near-surface groundwaters. In fact, MRB have been frequently found in the overburden at Olkiluoto (Pedersen 2008).

Some groundwaters analysed for MRB (Figure 4-24b) show MPN numbers high enough to influence their chemistry (see Table 1-2 in Appendix 2 from Hallbeck 2006). The highest numbers (MPN between 280 and 900 cells/mL) were found at depths between 380 and 548 m in boreholes KLX03 (#10091), KLX15A (#15008) and KLX17A (#11692). However, the presence of these high numbers is not correlated with the observed Mn(II) concentrations in the groundwaters (Figure 4-24a). The same occurs in the Forsmark area, where some of the groundwaters with high dissolved Mn(II) concentrations show MPN of MRB below detection limit, whereas others with low Mn(II) contents show very high MNP values (see Figure 3.5.16 in Gimeno *et al.* 2008).

Several reasons may explain this lack of correlation. First, increases in dissolved Mn(II) do not necessarily imply the presence of dissimilatory manganese reduction because manganese oxides can also be inorganically reduced (see reactions 4-4-1 and 4-4-2) by dissolved Fe(II) (Postma 1993, Postma and Jakobsen 1996), by dissolved sulphides (Yao and Millero 1993) or even by some metabolic products excreted by bacteria (e.g. siderophores) or by other dissolved components.

$$H_2S + 4MnO_2 + 2H_2O \rightarrow SO_4^{2-} + 4Mn^{2+} + 6OH^- \qquad (4\text{-}4\text{-}1)$$

$$2Fe^{2+} + MnO_2 + 2OH^- \rightarrow 2FeOOH + Mn^{2+} \qquad (4\text{-}4\text{-}2)$$
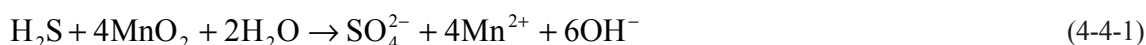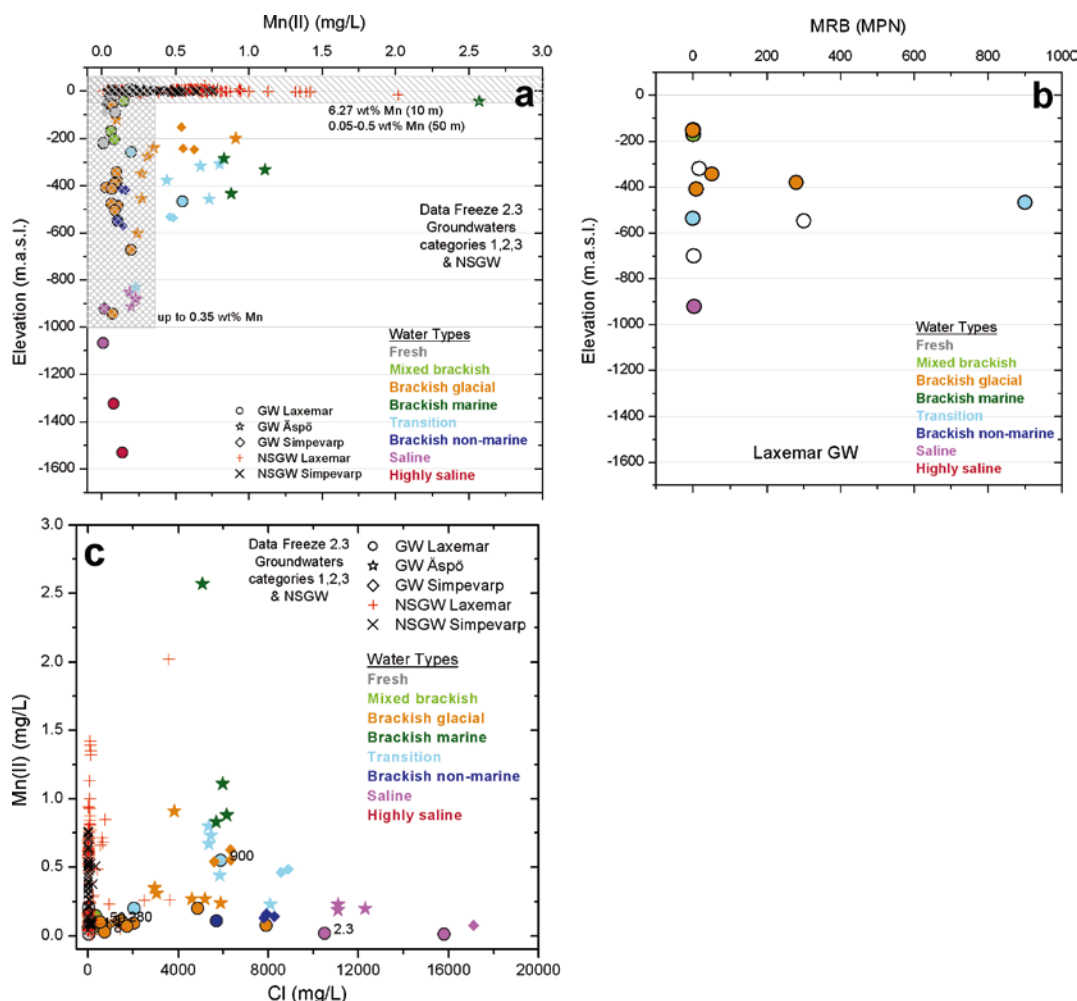
Figure 4-24. *Dissolved manganese distribution with respect to depth (a; including a sketch of the contents in the bulk fracture filling), and to chloride (c) and most probable number of MRB in different Laxemar-Simpevarp groundwater samples vs. depth (b). These numbers are also indicated in plot (c), where the highly saline waters are not shown to better visualise the less saline samples. Open symbols correspond to samples without a defined water type.*

Second, most of the known dissimilatory iron-reducing bacteria can reduce manganese as well, only switching to the reduction of Mn oxides or oxyhydroxides when they become available (Nealson and Saffarini 1994). This fact was already noted by Hallbeck and Pedersen (2008ab) to explain the good correlation found between the MPN of IRB and MRB both in Laxemar-Simpevarp and in the Forsmark areas. But it would represent an uncertainty in knowledge of the microbiological activity at depth: are the detected MRB really active or are IRB switching to manganese reduction favoured by cultivation methods?

Finally, MRB bacteria may use a wide number of Mn oxides and oxyhydroxides as TEA, including MnO_2 oxides, mixed valence and trivalent oxides and hydroxides. However, none of them has been identified at this site yet and the absence of these minerals would represent the main limitation to the active presence of these microorganisms in the groundwaters of the studied systems.

One could even claim for the ability of MRB to use the manganese present in the phyllosilicates (as IRB do with the Fe(III) in these phases). However, there are no data on the presence of the oxidised forms in clay minerals, Mn(IV) or Mn(III), necessary for MRB, and most important, the use of the structural manganese in clays by MRB still remains to be demonstrated. Therefore, the active presence of MRB and its effects on the groundwater composition must be considered with caution.

194

4.4.4   Processes. Thermodynamic approach

Speciation-solubility calculations have been performed with the PHREEQC code (Parkhurst and Appelo 1999) and the WATEQ4F database (Ball and Nordstrom 2001). Results indicate strong undersaturation with respect to all Mn oxides and oxyhydroxides included in that database.

Since the only Mn mineral that reaches equilibrium in the studied groundwaters is rhodochrosite ($MnCO_3$), it is the only mineral discussed in this section. An uncertainty range of ± 0.5[55] has been considered for the rhodochrosite saturation index.

Near-surface groundwaters

Many near-surface groundwaters display significant contents of dissolved manganese that, together with the presence of dissolved Fe(II) or S(–II) (see section 4.3.4), confirm the existence of reducing environments with effective Mn(II) mobilization. This mobilisation may be due to inorganic processes or to microbial Mn reduction of organic matter by MRB.

Under anoxic conditions, inorganic dissolution of Mn-bearing minerals and reductive dissolution of manganese oxyhydroxides may increase manganese concentrations in the near-surface groundwaters. Manganese oxyhydroxides react quickly with dissolved S(–II) and Fe(II) (Postma 1985, Yao and Millero 1993), producing an increase in the dissolved Mn(II) and the precipitation of ferric oxyhydroxides (reactions 4-4-1 and 4-4-2). These reactions are perfectly feasible in the near-surface groundwaters, as significant amounts of Fe(II) and S(–II) have been measured (probably in some soils characterised by oxic-anoxic alternating periods; e.g. gleysols).

Likewise, dissimilatory manganese reducing bacteria can reduce manganese oxyhydroxides using hydrogen or organic matter (e.g. acetate) as electron donors and increasing also the dissolved Mn concentrations in the near-surface groundwaters:

$$MnO_2 + H_2 + 2H^+ \rightarrow Mn^{2+} + 2H_2O \tag{4-4-3}$$

$$CH_3COO^- + 4MnO_2 + 3H_2O \rightarrow 2HCO_3^- + 4Mn^{2+} + 7OH^- \tag{4-4-4}$$
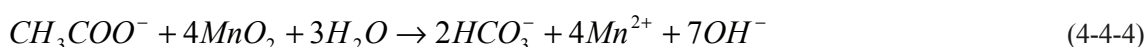
However the concentration of dissolved manganese from these sources may be controlled by other processes, such as cation exchange, sorption or carbonate precipitation, which can limit the final dissolved manganese content (Watson *et al.* 2003, Massmann *et al.* 2004). Among all these processes, the one most clearly present in the near-surface groundwaters is rhodochrosite precipitation. There is an equilibrium situation in most of the near-surface groundwaters from the Laxemar-Simpevarp area, including the brackish groundwaters from soil pipe SSM000241 with 3000 mg/L HCO_3^- (not shown in the plots; Figure 4-25 and 4-26).

Rhodochrosite has not been detected yet in the available mineralogical data from the overburden. However, this mineral has also been suspected or identified as a possible Mn(II)-sink in sedimentary aquifer systems (Matsunaga *et al.* 1992, Massmann *et al.* 2004) and in laboratory studies on microbial organic carbon reduction of Mn(IV) (e.g. Lovley and Phillips 1988) where it was reported that the Mn(II) produced was quickly precipitated as $MnCO_3$. More recently, Amirbahman *et al.* (2003) reached similar conclusions in column experiments designed to simulate the biogeochemical processes resulting from microbial oxidation of organic matter.

Therefore, dissolved manganese control by rhodochrosite in the near-surface groundwaters is feasible in a context where the biogenic CO_2 input and the aluminosilicates and calcite weathering reactions can produce important alkalinity increases.

---

[55] The solubility value of rhodochrosite used in the calculations is the one included in WATEQ4F database (Ball and Nordstrom 2001), log K = –11.13. This value is very similar to the more recent values proposed by Jensen *et al.* (2002). The uncertainty range has been fixed at 5% of the log K value.

Groundwaters

As already indicated, the sources of manganese in the fracture fillings are mainly calcite and clay minerals (e.g. chlorite, corrensite). Calcite dissolution is not expected to be very important in manganese control as groundwaters at very shallow levels are already in equilibrium (or slightly oversaturated) with respect to this phase.

Additional controls on dissolved manganese contents in groundwaters may involve surface processes or solubility constraints. Overall, dissolved manganese follows a roughly similar trend with depth to iron (Figures 4-5), with variable and high values from the surface to 500 m in the brackish groundwaters and very low values in the deeper, more saline waters (Figure 4-22a). This similar behaviour is also shown in Figure 4-25a and it could be an indication of the "simultaneous" control by iron phases with traces of manganese (oxyhydroxides, clays) or by the operation of surface processes between dissolved manganese and iron oxyhydroxides.

However, the positive correlation between dissolved Fe(II) and Mn(II) shows very different slopes depending on the location (subarea; Figure 4-25a). Most of the Laxemar subarea groundwaters define a shallow slope while waters from Simpevarp and Äspö display a noticeably steeper slope.

The same differences can be observed between HCO_3^- and dissolved manganese. Groundwaters with low manganese contents (below 0.5 mg/L), mainly from Laxemar subarea, keep these low values independently of the alkalinity increase (Figure 4-25b). However, Mn and alkalinity increase together in the samples from Äspö (those with the highest manganese contents) up to this last parameter reaches values around 140 mg/L. This correlation could be explained by the activity of Mn-reducing bacteria (MRB) that produce Mn(II) but also HCO_3^- due to the oxidation of organic matter (see reaction 4-4-4). However, as already indicated in section 4.1.3, the existence of this type of bacterial activity is unclear, especially considering that they should be restricted to waters with very specific chloride contents around 5,500 mg/L (Figure 4-22b). Therefore, some other process must be conditioning this correlation.

Rhodochrosite saturation indices decrease towards clear undersaturation with depth and chloride content (Figure 4-26ab). The few groundwaters still in equilibrium with this mineral correspond to dilute waters with meteoric origin but at 400 m depth in the Laxemar subarea, and to brackish groundwaters with Littorina signature characterised by Cl contents about 5,500 mg/L. The presence of dilute groundwaters still in equilibrium with rhodochrosite at depths of around 400 m can also be observed in the Palmottu groundwaters (Figure 4-27ab) but also showing an overall trend towards undersaturation as the depth increases.
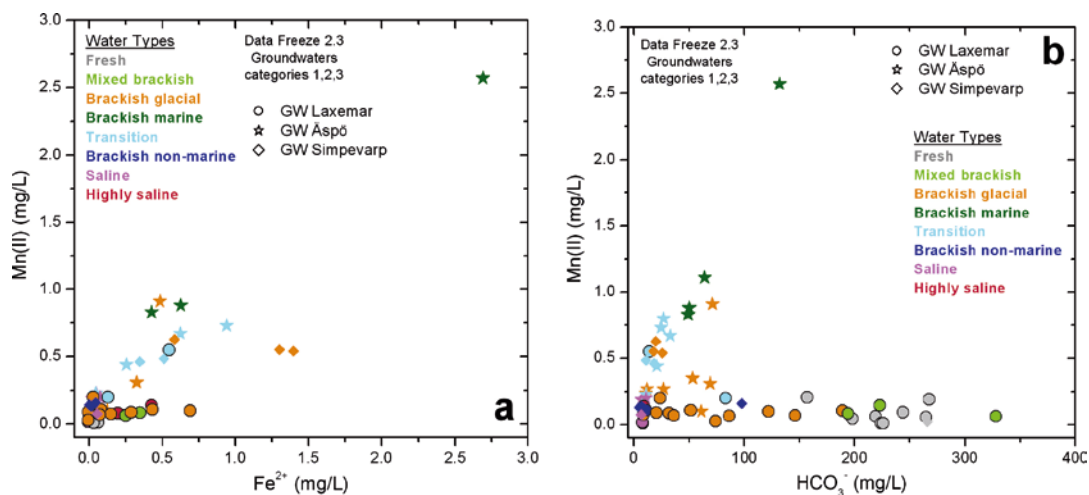
Figure 4-25. *Manganese contents in Laxemar-Simpevarp groundwaters with respect to ferrous iron concentration (a) and alkalinity (b).*
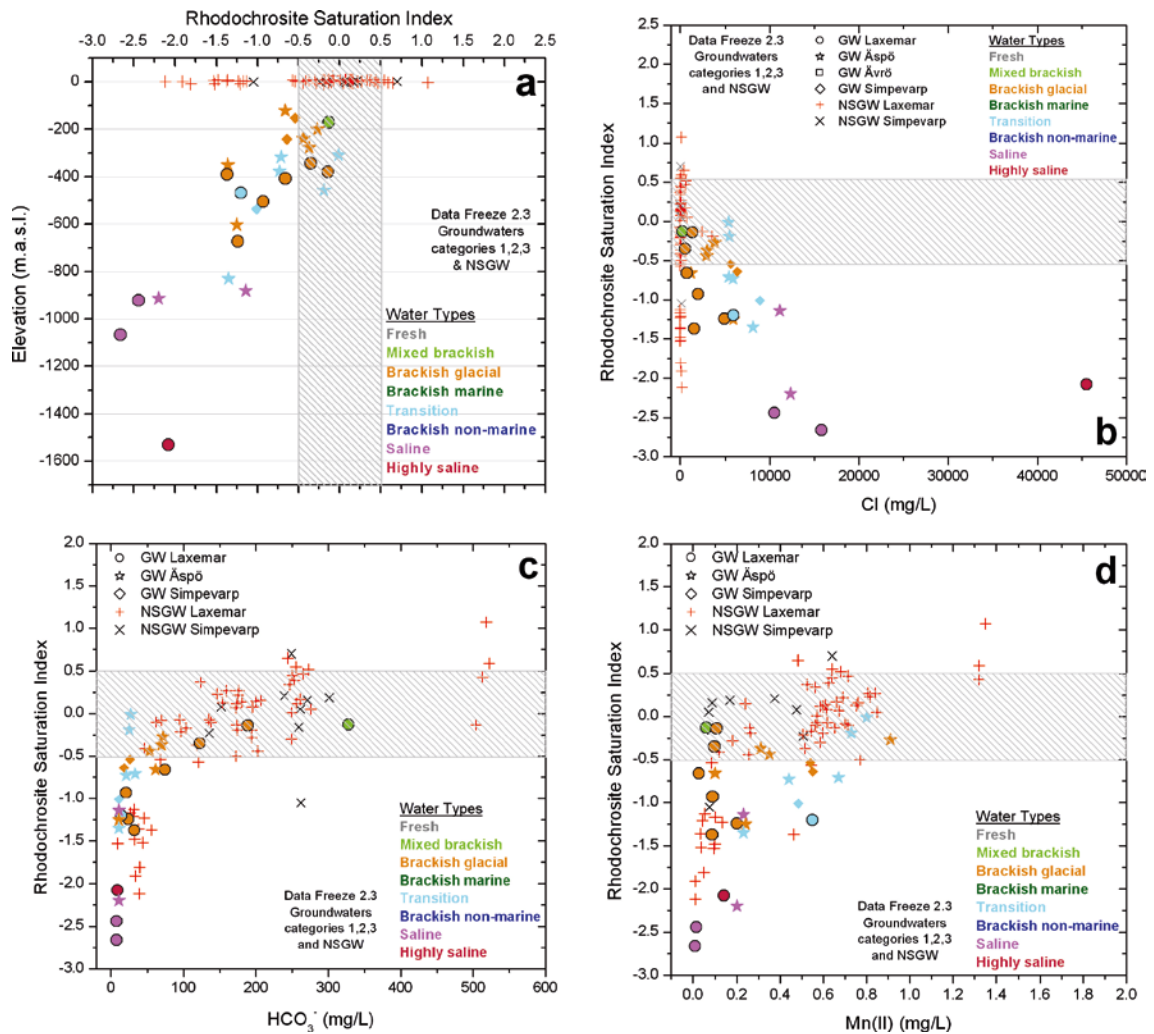
Figure 4-26. Rhodochrosite saturation index in Laxemar-Simpevarp groundwaters with respect to different parameters. (a) depth; (b) Cl contents; (c) alkalinity and (d) manganese concentrations.

The presence of brackish groundwaters in equilibrium with rhodochrosite can also be observed in Forsmark and Olkiluoto. Only some of the groundwaters with a significant contribution of the Littorina end-member (in the range of Cl contents between 3,500 and 5,500 mg/L and Mn contents up to 1.2 mg/L; Figure 4-27cd) reach equilibrium with this mineral. The rest of the groundwaters are clearly undersaturated with respect to this phase, including the most saline groundwaters with the largest Mn contents at Olkiluoto (2.3 mg/L, Figure 4-27d).

These results show that equilibrium with rhodochrosite is not common in deep and old groundwaters in these crystalline systems. Only those groundwaters with a clear Littorina signature reach equilibrium. Figure 4-28 shows the relationship between manganese content and rhodochrosite saturation index with Littorina proportion as calculated by M3 (n-pc mixing algorithm) for the Laxemar-Simpevarp and Forsmark groundwaters.

As it is clear from the plots for Forsmark, saline waters with low Littorina proportion (< 14%) have low Mn contents and are clearly undersaturated with respect to rhodochrosite. When the Littorina proportion reaches 40–50%, waters start to be in equilibrium with rhodochrosite, together with high but variable Mn contents, perhaps related to inorganic re-equilibrium processes after the mixing event.
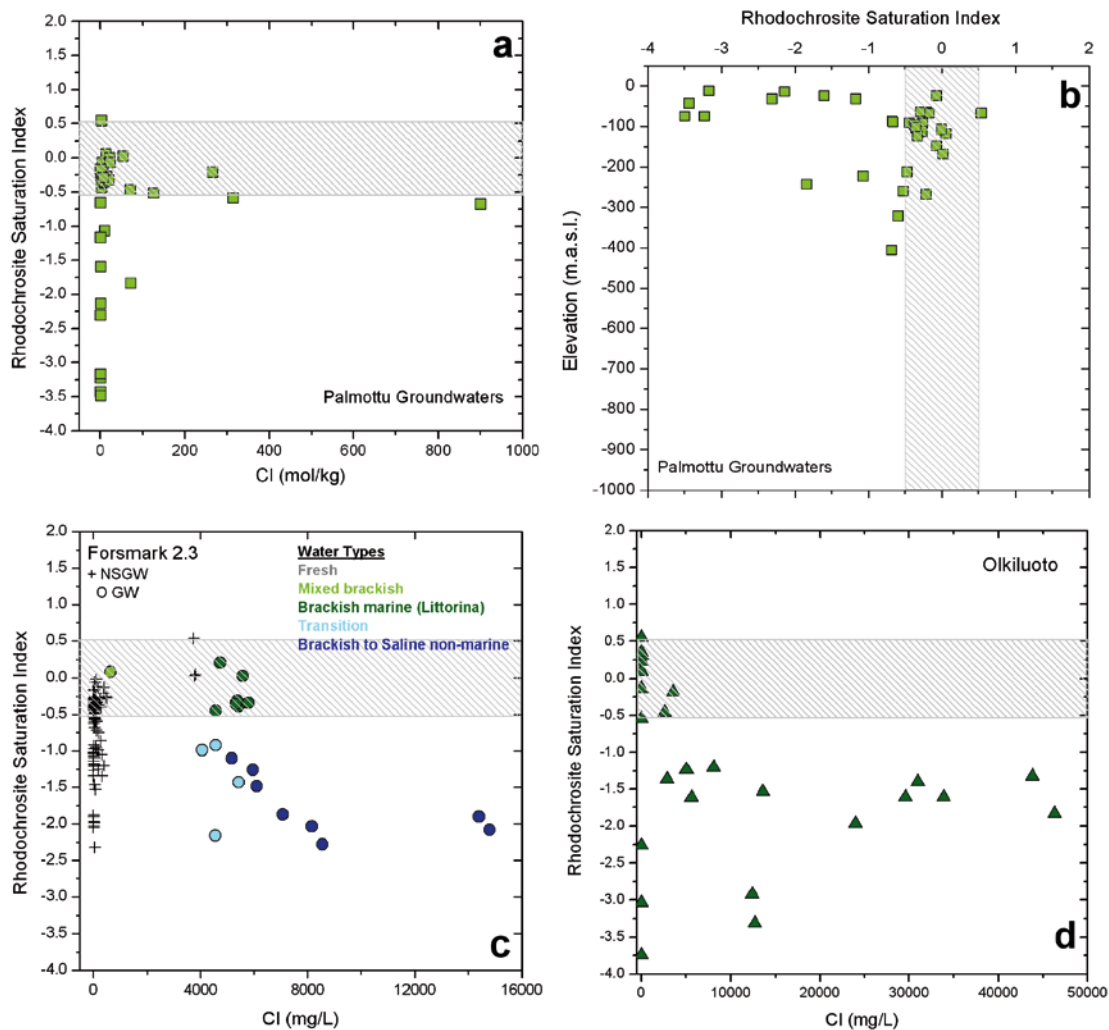
Figure 4-27. *Rhodochrosite saturation indices in the groundwaters from different sites. (a) and (b) Palmottu (Finland); (c) Forsmark (Sweden); and (d) Olkiluoto (Finland). Different chloride scales have been used where appropriate to better visualise and describe the systems in question.*

For the Laxemar-Simpevarp groundwaters, Littorina proportions are much lower than in Forsmark or Olkiluoto. However, dissolved manganese shows a clear correlation with Littorina proportions[56] (Figure 4-28a) and groundwaters with 10–13% of Littorina reach rhodochrosite equilibrium[57].

All this lines of evidence suggests a clear link between manganese concentrations, equilibrium with rhodochrosite and the Littorina signature in the Laxemar-Simpevarp groundwaters, even considering the present lower remnants of this end member. Therefore, this relationship can be interpreted as an inheritance of the hydrochemical conditions imposed by rhodochrosite formation during the infiltration of Littorina waters through the marine sediments (authigenesis of Mn-carbonates was an active process in the Baltic Sea since 7,000–8,000 year ago; Kulik *et al.* 2000, Neumann *et al.* 2002 and references therein), in the same way as already proposed by Gimeno *et al.* (2006, 2008) for Forsmark (see also Appendix F).

---

[56] Manganese is not considered in the set of elements used by M3.

[57] Unfortunately, samples from Äspö with the clearest Littorina signatures do not have field measurements of pH and have not been considered in the rhodochrosite analysis.
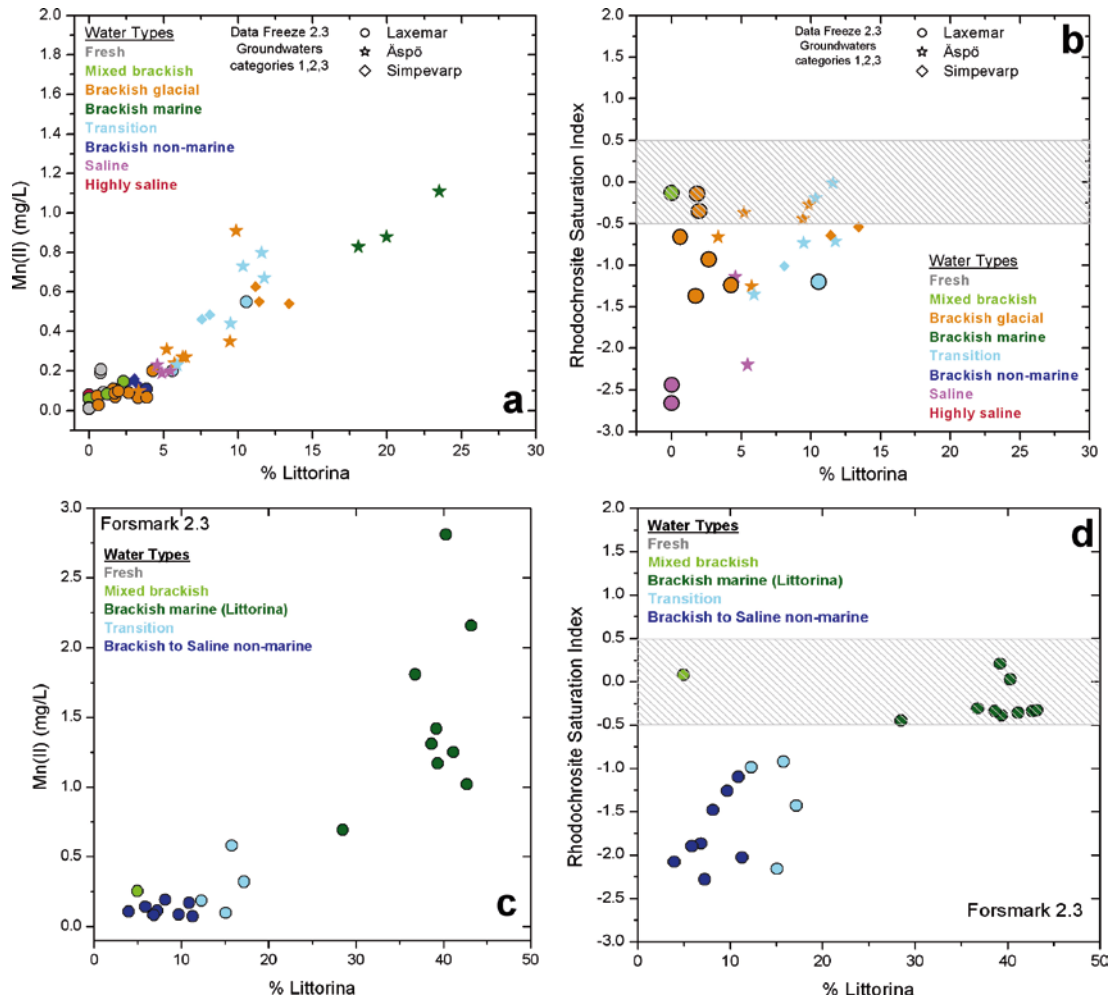
Figure 4-28. *Manganese concentrations (a and c) and rhodochrosite saturation indices (b and d) with respect to the Littorina proportion in Laxemar-Simpevarp (a and b) and Forsmark (c and d) groundwaters. Note that the number of samples in plot (b) is lower than in plot (a) as only samples with pH field measurements have been used to calculate the saturation indices. Different manganese and Littorina percent scales have been used where appropriate to better visualise and describe the systems in question.*

4.4.5 Conclusions

The dissolved manganese contents in the fresh near-surface groundwaters from the Laxemar-Simpevarp area are elevated compared to the median values of shallow groundwaters in Sweden although similar concentrations are found in other crystalline systems (e.g. Olkiluoto, Palmottu). This high variability and concentrations can be considered as normal and related to the intrinsic variability of factors in weathering processes in the superficial environment (weathering intensity, mineralogical differences, redox conditions, biological activity, etc).

Weathering of amphiboles, biotites or chlorites (or possible relict rhodochrosite in outcrops of Littorina sediments) is the main Mn source in the overburden of the Laxemar-Simpevarp area. Under oxic conditions, dissolved manganese would precipitate in secondary phases, mainly as insoluble Mn(IV)-oxyhydroxides, present in soils and in the fracture fillings of the overburden. High dissolved manganese contents found in many fresh near-surface groundwaters (together with the presence of dissolved Fe(II) or S(–II)) confirm the existence of reducing environments with effective Mn(II) mobilization at very shallow levels. This mobilisation, due to both inorganic processes and manganese reduction of organic matter by MRB, would increase the manganese concentrations in the near-surface groundwaters. However, the concentrations of dissolved manganese appear to be limited by the precipitation of rhodochrosite, a carbonate phase in equilibrium in most of the near-surface groundwaters. Other processes like cation exchange or surface complexation can be also effective in the control of dissolved manganese.

Manganese concentrations in deeper groundwaters appear to be controlled or affected by different processes. Low Mn contents and a trend towards undersaturation with respect to rhodochrosite can be observed in the groundwaters from the Laxemar subarea. Overall, dissolved manganese follows a roughly similar trend with depth to iron and the mineralogical studies of the fracture fillings also suggest the association of iron and manganese with chlorite and clay minerals. Therefore, manganese contents appear to be controlled by iron phases with traces of manganese (oxyhydroxides, clays; e.g. through the operation of surface processes between dissolved manganese and these phases).

In the Simpevarp and Äspö subareas, some brackish groundwaters (and some near-surface groundwaters with discharge characters) between 200 and 500 m depth with Cl contents around 5,500 mg/L and a significant Littorina contribution have variable but high Mn concentrations and are in equilibrium with rhodochrosite. These characteristics, also observed in the brackish groundwaters from Forsmark or Olkiluoto, represent the inheritance of rhodochrosite formation during Littorina infiltration through the marine sediments.

Water-rock interaction processes after mixing with the pre-existing groundwaters at depth may have modified the original manganese or HCO_3^- values of these marine waters. However, and in spite of the minor Littorina contribution in Laxemar-Simpevarp, some of these brackish groundwaters still show this inheritance in the manganese contents (as well as in other components such as SO_4^{2+}, Mg^{2+}, silica, NH_4^+ etc). Below 500 m depth, low Mn contents and undersaturation with respect to rhodochrosite are also found in the groundwaters from the Simpevarp-Äspö subareas.

The influence of microbiological processes (MRB) is feasible in the near surface and shallow "recent" groundwaters, but it is uncertain in the deeper waters with longer residence time. The main problem is the absence in the fracture fillings of the TEA (manganese oxyhydroxides) needed by these organisms. Except at very shallow levels, the presence of manganese oxyhydroxides has not been identified in either Laxemar-Simpevarp or in Forsmark. This absence is reasonable, as manganese oxides (in contrast with hematite) are not especially stable under reducing conditions over long time periods. It represents a serious limitation for the active presence of MRB in the groundwaters and the identification of this metabolic group at depths greater than 100–150 m may have been produced by disturbances of the pristine conditions during sampling (short-circuit, artificial mixing, etc).

4.5   The nitrogen system (nitrate, nitrite and ammonium)

The study of the redox processes in previous work on the Laxemar-Simpevarp area has focussed on the most important compositional systems (those related to iron, sulphide and manganese) to understand the effective redox processes, mostly under generalised reducing conditions.

From the beginning of the site characterisation work, the low measured concentrations of NO_3^- and NO_2^- in the groundwaters indicated that nitrate reduction was not a critical process and the relatively high NH_4^+ concentrations would confirm the generalised reducing character of most of them. Therefore, the explicit treatment of the nitrogen system has not been included in the previous site descriptive models.

In this final report on the Laxemar-Simpevarp area, the main characters of the nitrogen system are also evaluated to complete the treatment of the redox processes. As this is the first time that this compositional system has been presented, some general remarks are also introduced in the description below.

Available analytical data for dissolved nitrogen in different oxidation states include NO_2^-, NO_3^-, NH_4^+ and N_{total} in the near-surface groundwaters (soil pipes). The same data have been measured in the groundwater samples except for N_{total} contents.

When analysing the data it must be taken into account that the detection (or reporting) limits for those components have changed over the different sampling campaigns stored in Sicada. For example, for the Äspö groundwaters (in the hydrogeochemical pre-investigations stage) the indicated detection limits are 0.01 mg/L for NO_3^-, 0.001 mg/L for NO_2^- and 0.005 mg/L for NH_4^+ (Smellie and Laaksoharju 1992). For much more recent sampled subareas (e.g. Laxemar, Simpevarp) the reporting limits are 0.2 μg/L for NO_3^-, 0.1 μg/L for NO_2^- and 11 μg/L for NH_4^+ (Nilson 2008).

Soil nitrogen contents in the overburden (and, therefore, in the recharge waters) can fluctuate depending on the soil type and/or with waste or fertilizer management. Nitrate contents (NO_3^-) in these waters can be especially significant. It is a conservative anion, only stable under oxidising conditions and it disappears when the system reaches very low oxygen contents (Kehew 2001, Appelo and Postma 2005). Moreover, NO_3^- contents in groundwater systems characterised by very low concentrations (as occurs in many crystalline systems) has led to their use as indicator of sample contamination (Gascoyne 2004). Ammonium (NH_4^+) is less mobile than NO_3^- (e.g. it participates in exchange reactions) and represents a stable nitrogen form under reducing conditions. Therefore, some information can be gained from the particular properties and "contrasting" behaviour of those nitrogen species.

4.5.1 Hydrochemical data

In natural waters nitrogen occurs in various oxidation states from nitrate (+V) to ammonium (–III) and the transformation between those species is almost exclusively facilitated by microorganisms (Kehew 2001). Organic nitrogen is converted to ammonium (ammonification process) and, under oxidising conditions, ammonium is oxidised to nitrite (NO_2^-) or further oxidised to nitrate (NO_3^-) by specialised nitrifying bacteria (two-step nitrification process). These processes occur under aerobic conditions (e.g. in the soil zone above the water table) affecting decaying organic matter as well as excess ammonium from fertilizers or wastes (Hallberg and Keeney 1993).

Under anaerobic conditions, nitrate is the most thermodynamically-favoured electron acceptor for the oxidation of organic substrates and it is used by nitrate reducing bacteria (NRB) for respirative energy production. This nitrate reduction process (denitrification) occurs in different steps, each of which is catalysed by specific NRB, producing nitrite, nitrous oxide, ammonium or nitrogen gas (Hallberg and Keeney 1993, Chapelle 2001)

The nitrification-denitrification cycle is broken in aerobic-anaerobic transitions. Under aerobic conditions, nitrification may lead to nitrate accumulation whereas under anaerobic conditions, nitrification is blocked and nitrate is depleted by denitrification processes. This usually results in an overall depletion of nitrogen species in anaerobic groundwater systems (Chapelle 2001).

The distribution of the different nitrogen species contents with depth is interpreted here in this context. This distribution displays for near-surface groundwaters a much wider variability and higher concentrations than for groundwaters (Figure 4-29). Overall, this distribution is similar to that found in other crystalline environments (Forsmark, Olkiluoto or Lac du Bonnet, Pitkänen *et al.* 2004, Gascoyne 2004), but, in detail, some differences can be observed for some of these components among these sites, both in the near surface and in the deeper groundwaters.

Near-surface groundwaters

As has been stated, nitrate, nitrite and ammonium nitrogen concentrations show the widest variability and highest concentrations in the near-surface groundwaters, where nitrate contents reach 11 mg/L, though most of them are below 1 mg/L (Figure 4-29ab). Only one sample reaches a value for nitrite as high as 1 mg/L, while the others are clearly below 0.03 mg/L (Figure 4-29cd). Finally, NH_4^+ can reach very high values (300 to 600 mg/L in the soil pipes SSM000241 and SSM000242, not shown in Figure 4-29ef) but most of the available data are below 4 mg/L).

The most saline waters from the overburden (with Cl > 500 mg/L) do not have significant amounts of NO_2^- and NO_3^-. The maximum variability is found in the fresh near-surface groundwaters. On the contrary, the highest NH_4^+ contents are associated with the near-surface groundwaters with high chloride contents, especially to the aforementioned SSM000241 and SSM000242 soil pipes (Cl contents from 3,500 to 5,000 mg/L). These samples, possibly representing discharges of deep saline/marine groundwaters, show also some unusual hydrochemical characters (extremely high HCO_3^- concentrations, very low SO_4^{2-} contents, high sulphide concentrations detected during the sampling period, etc) interpreted by Tröjbom *et al.* (2008) as due to a especially intense microbial degradation of organic matter. The very high NH_4^+ concentrations would support this hypothesis.

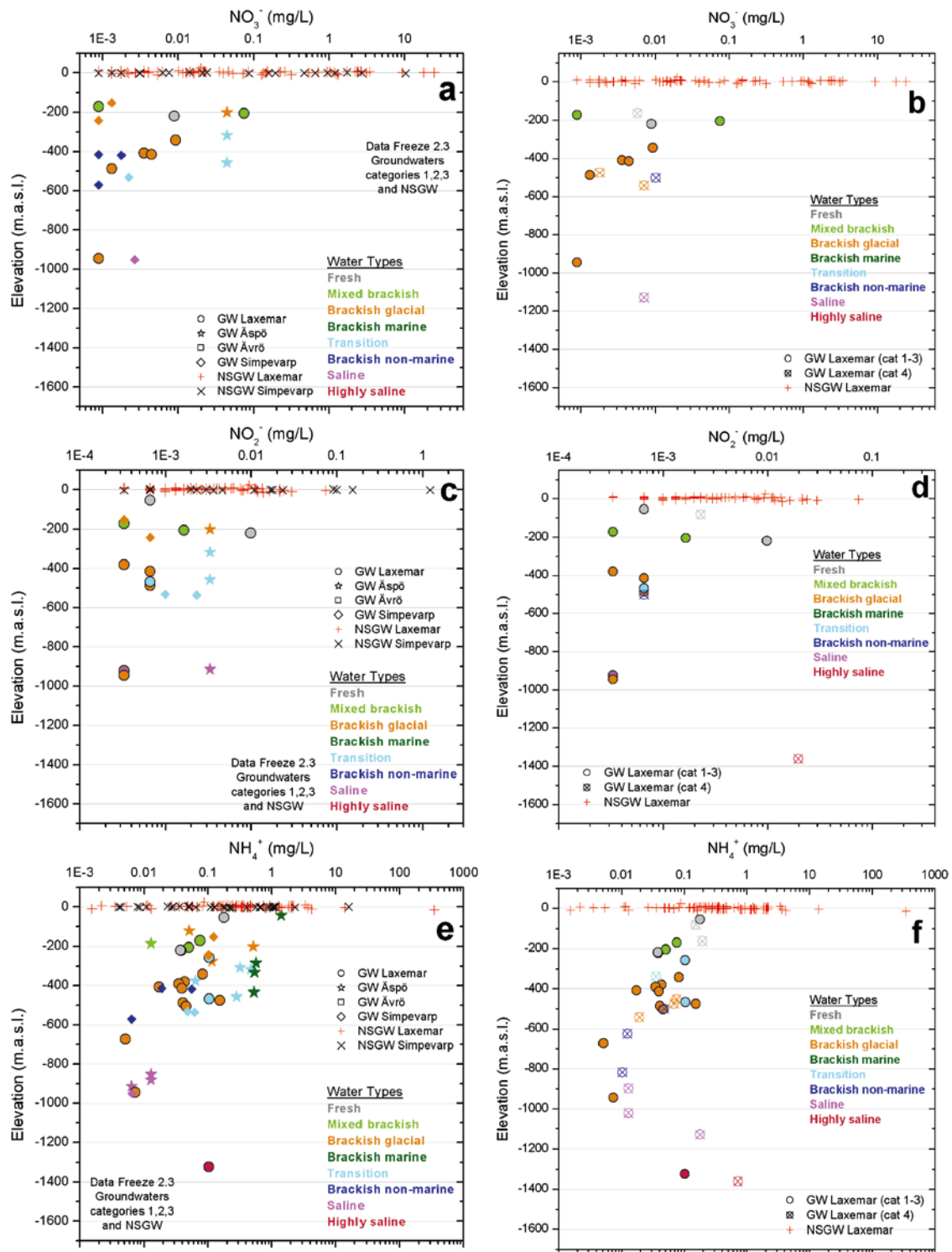**Figure 4-29.** *Concentrations of NO$_2^-$ (a, b), NO$_3^-$ (c, d) and NH$_4^+$ (e, f) vs. depth in the groundwaters from the Laxemar-Simpevarp area. Representative near-surface groundwaters (NSGW) and groundwaters from all the subareas and corresponding to categories 1, 2 and 3 (a, c, e panels) and only Laxemar (subarea) groundwaters of categories 1 to 4, (b, d, f panels) are included separately.*

Except for these cases, the contents of these components in the fresh near-surface groundwaters (Cl < 200 mg/L) from Laxemar-Simpevarp do not differ very much from the contents found in equivalent waters from other sites. For example, in Forsmark near-surface groundwaters, the maximum values determined are 2 mg/L for NO_3^-, 0.15 mg/L for NO_2^- and 10 mg/L for NH_4^+. In the Lac du Bonnet Batholith (Canada), the near-surface groundwaters show NO_3^- concentrations up to 5.6 mg/L although most of them are below 0.5 mg/L (Gascoyne 2004). Near-surface groundwaters in the overburden from Olkiluoto show some lower values, below 0.2 mg/L for NO_3^- and NH_4^+ (Pitkänen *et al.* 2004).

Nitrogen contents show a temporal variability possibly related to seasonal variations in the biological activity. The major contribution to the total nitrogen in the fresh, near-surface groundwaters from the Laxemar-Simpevarp area is generally represented by ammonium and/or by dissolved organic nitrogen and only in some samples nitrate dominates the total nitrogen contents. The important NH_4^+ contribution is the usual situation in anaerobic or forest soils (as well as in recently fertilized soils; Bohn *et al.* 2001). NO_2^- contents are mostly at trace levels and the NO_3^- concentrations are mostly below 3 mg/L, as occurs in natural, uncontaminated systems.

The atmospheric pool and the degradation of organic matter are considered by Tröjbom *et al.* (2008) as the major sources of N in the near-surface groundwaters from Simpevarp, but some contribution from weathering is also possible. The largest reservoir of nitrogen in the Earth's surface is associated with igneous rocks, where it occurs as ammonium within potassium-rich silicates both in rock-forming minerals and in secondary weathering products (Krohn *et al.* 1998, Holloway *et al.* 2001). Moreover, exchangeable NH_4^+ is usually present in anaerobic soils (Bohn *et al.* 2001) and, therefore, cation exchange reactions can participate in the regulation of dissolved ammonium in the near-surface groundwaters.

Deep groundwaters

As already mentioned, the variability range and contents of the nitrogen species drastically decrease in the deeper groundwaters (Figure 4-29). NO_3^- and NO_2^- contents are very low and in many cases below detection limit. The highest analysed contents are 0.01 mg/L at 200 m depth in a mixed-brackish groundwater (Figure 4-29).

These extremely low contents of nitrate and nitrite have also been observed in other crystalline environments such as the crystalline batholith of Lac du Bonnet, Canada (Gascoyne 2004), Olkiluoto (Pitkänen *et al.* 2004) and Forsmark (maximum contents of dissolved NO_3^- and NO_2^- are around 0.025 mg/L and 0.005 mg/L, respectively). This situation is in agreement with nitrate instability in the generalised reducing conditions found in those groundwaters (e.g. Kehew 2001) and with the aforementioned usual depletion of nitrogen species observed in anaerobic groundwater systems.

Compared with the contents in the near-surface groundwaters, NH_4^+ contents in the deep groundwaters from Laxemar-Simpevarp are also in a more restricted range. The greatest variability is shown in the first 500 m depth with contents up to 1.1 mg/L in the brackish marine groundwaters with Cl contents between 4,000 and 6,000 mg/L (Figure 4-30a) located in Äspö (mainly from KAS02 and KAS06 boreholes).

Something similar happens in Forsmark and Olkiluoto. In the Forsmark groundwaters, high NH_4^+ values (from 1 to almost 4 mg/L) are found down to 500 m depth (Figure 4-30c) systematically associated with brackish marine groundwaters with chloride concentrations between 5,000 and 5,500 mg/L, showing the highest Littorina contribution (Gimeno *et al.* 2008). This association also occurs in the Olkiluoto area where groundwaters with high Littorina contribution also show variable and high NH_4^+ concentrations (with maximum values near 0.9 mg/L, Pitkänen *et al.* 2004).

All these observations indicate that the high NH_4^+ concentrations found in these groundwaters represent an inherited character from their old marine signature. Seawater shows very low NH_4^+ concentrations (usually well below 0.05 mg/L in the available samples from the Baltic Sea) but increasing ammonium concentrations with depth in the interstitial waters from marine sediments is a common observation. In marine sediments with organic matter, bacterial activity promotes the transformation of organic nitrogen compounds and the formation of NH_4^+. It also occurs in the present sediments of the Baltic Sea, where NH_4^+ concentrations from 4 to 16 mg/L are frequent (Carman and Rahm 1997).

Therefore, infiltration of the recharging Littorina waters through marine sediments can easily justify important increments in dissolved NH_4^+, as already proposed by Pitkänen *et al.* (2004). The minor contribution and the flushing out of the Littorina groundwaters in the Laxemar-Simpevarp area could explain the less marked signature in the NH_4^+ concentrations with respect to that observed in the Forsmark groundwaters. Cation exchange processes can also produce significant decreases in NH_4^+ concentrations (Appelo and Postma 2005) during the circulation of these marine waters through the fractured bedrock. However, these reaction processes have not been able to completely mask the marine signature in either Simpevarp or Forsmark groundwaters. Moreover, reducing conditions preclude the bacterial nitrification of ammonium (Chapelle 2001, Appelo and Postma 2005) and, therefore, favour the presence of NH_4^+ in the groundwaters.

In the saline groundwaters sampled between 1,100 and 1,400 m depth, NH_4^+ concentrations are meaningful, especially in the most saline and deepest sample (Figures 4-29ef and 4-30ab) with almost 0.8 mg/L of dissolved NH_4^+. Again, a similar situation has been described by Pitkänen *et al.* (2004) for the most saline and deepest samples at Olkiluoto. As a marine (Littorina) contribution at these depths is not possible, other processes should be invoked to explain the origin of these deep NH_4^+ concentrations. Pitkänen *et al.* (2004) suggest an origin related with high hydrocarbon contents but more studies are needed on this subject.
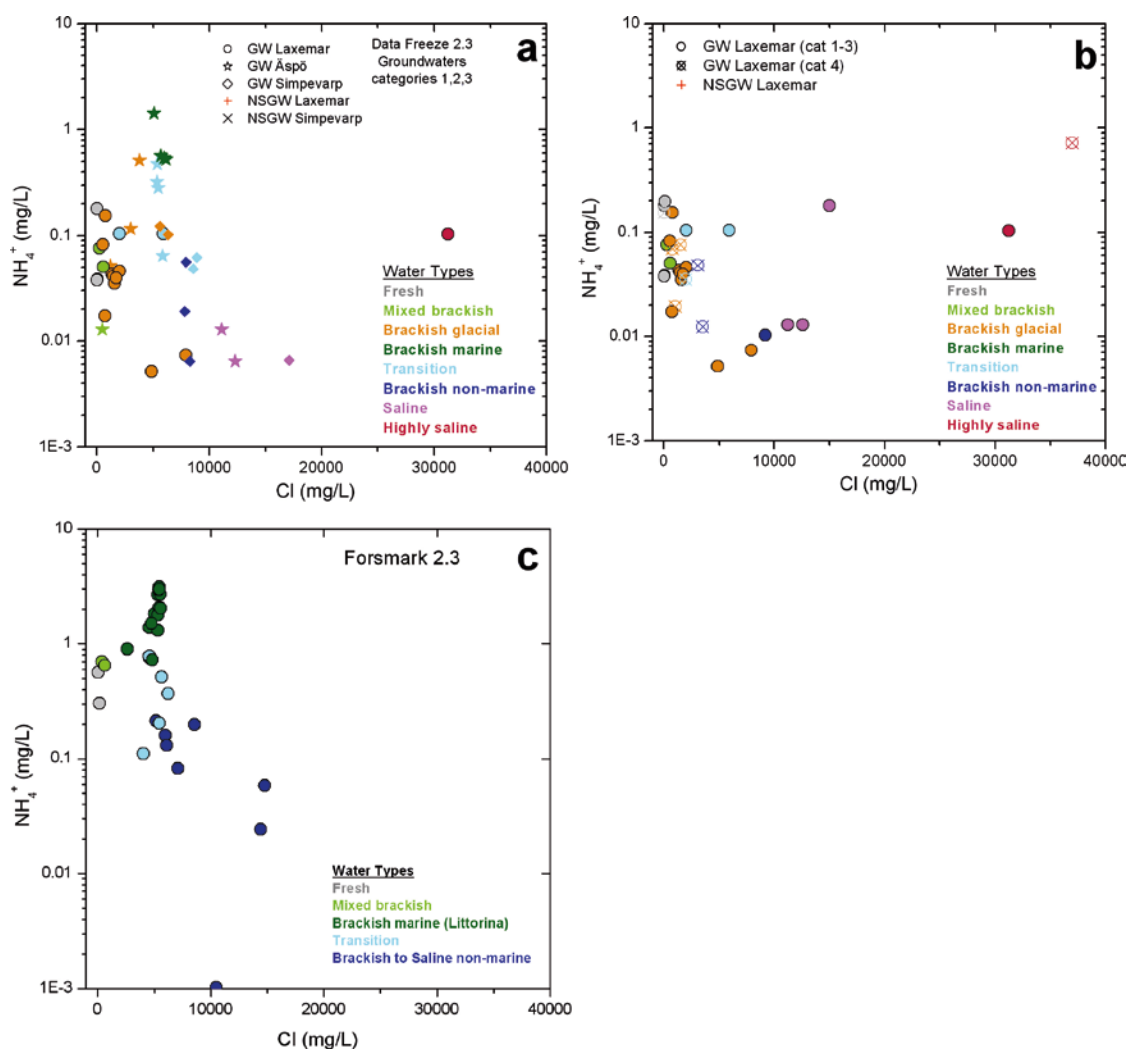
Figure 4-30. *Logarithmic scale of NH_4^+ versus chloride concentration in the groundwaters of Laxemar-Simpevarp area (a), in the Laxemar subarea alone (b) and in the Forsmark area (c). Variable and high NH_4^+ contents are found in the groundwaters with clear Littorina signature.*

4.5.2 Microbiological data

Unfortunately, microbiological analyses from the overburden in the Laxemar-Simpevarp area are not available yet. However, as the transformation between nitrogen species is almost exclusively facilitated by microorganisms, different microbiological nitrogen-related activities are expected to occur, such as ammonification and nitrification processes under aerobic conditions and denitrification processes (by nitrate reducing bacteria; NRB) in the anaerobic zones of the overburden (e.g. NRB has been identified in the overburden from Olkiluoto, Pedersen 2008)

As stated above, nitrate concentrations in the near-surface groundwaters are mostly in the range of "non-contaminated" natural systems (nitrate concentrations mostly below 1 mg/L). Nitrate is the most thermodynamically favoured electron acceptor for the oxidation of organic substrates under anaerobic conditions and NRB activity is expected to reduce drastically the concentration of this component in the recharge waters.

The detected NO_3^- contents in the fresh and/or shallow groundwaters affected by meteoric inputs (with maximum concentration of 0.016 mg/L and mostly below 0.002 mg/L) are consistent with the absence of contamination. Moreover, they suggest the establishment of anoxic conditions very rapidly at shallow depth in the system, in agreement with the deductions from other redox parameters.

Data on the presence of NRB have been obtained in the last microbiological analyses performed in the Laxemar-Simpevarp groundwaters. Most probable numbers (MPN) of NRB have been represented in Figure 4-31. MPN values are high (usually higher than 500 cells/mL and reaching 9,000 cells/mL) in fresh and saline groundwaters to about 700 m depth. However, nitrate concentrations (the TEA for NRB) are extremely low in these groundwaters (Figure 4-29ab). The presence of detectable but also very low nitrite contents (Figure 4-29cd) suggests the existence at present of some NRB activity at these depths, but this is a debatable matter, mainly at the rates suggested by MPN data.

Nitrate concentrations appear too depleted in the overburden and recharge groundwaters to sustain such high NRB activity at depth. Moreover, under anoxic conditions and in the presence of nitrate, bacterial nitrate reduction is by far the most favoured heterotrophic respirative pathway even independent of fermentative bacteria (Appelo and Postma 2005, Konhauser 2007). If the low nitrate contents detected in the groundwaters were produced by such intense NRB activity, this metabolic activity would probably outcompete the other heterotrophic metabolic bacterial groups that have been detected at the same levels. A similar problem was detected in the Forsmark area, where high MPN of NRB were detected in groundwaters with very low nitrate concentrations (Hallbeck and Pedersen 2008a).
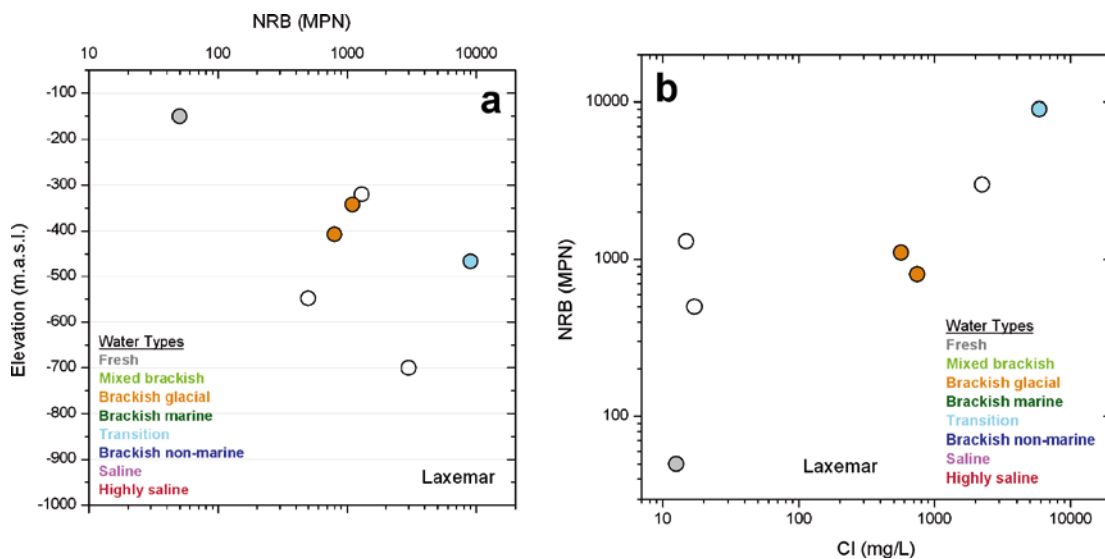
Figure 4-31. Most probable numbers (MPN) of NRB vs. depth (a) and chloride contents (b) in the Laxemar-Simpevarp groundwaters. Open symbols represent samples without a defined water type.

The origin of this problem may be related to the fact that the number of NRB might have been enhanced by the own culture method used in laboratory for their detection, switching the metabolic pathway of other bacteria (e.g. IRB or especially, acetogens; see Appendix G) towards nitrate reduction. Therefore, the presence of nitrate reducers in a sampled section does not necessarily indicate that they actually exist in the system (Hallbeck and Pedersen 2008a). This situation represents another example of the complexities arising from the study and interpretation of microbiological data.

4.5.3 Conclusions

The behaviour of nitrogen species in groundwater systems is strongly affected by the existence of aerobic or anaerobic conditions. The observed evolution in the Simpevarp groundwaters show the general depletion of nitrogen usually observed in anaerobic groundwater systems as residence time and/or depth increase.

The higher contents and variability in NO_2^-, NO_3^- and NH_4^+ concentrations are associated with the near-surface groundwaters in the overburden, where the oxic/anoxic transition appears to occur. Nitrogen from the atmosphere, from the degradation of organic matter and, probably, from aluminosilicate weathering, is subject to different microbiologically-mediated processes, such as ammonification, nitrification and denitrification. This justifies the existence of a wider range of contents of nitrogen species in the near-surface groundwaters and explains the temporal variability in their concentrations observed in the monitored soil pipes (associated with the seasonal changes in the biological activity).

In some possible discharge zones of saline groundwaters, very high nitrogen concentrations (mainly as NH_4^+) can be found associated with an especially intense biological activity. However, the concentration of nitrogen species in the fresh near-surface groundwaters is usually within the range found in surface, uncontaminated systems.

Groundwaters show very low (if any) nitrate and nitrite concentrations, in agreement with their reducing conditions. Shallow groundwaters from meteoric origin also show this character, indicating the development of an anoxic environment very soon after groundwater infiltration.

Meaningful ammonium concentrations are present in the groundwaters, mainly in the first 500 m depth. The highest variability and concentration values are associated with the few groundwaters with a Littorina signature in the Laxemar-Simpevarp area. This association also occurs in the Forsmark and Olkiluoto zones and represents an "inherited" marine character associated with the transport of Littorina waters through the marine sediments during recharge. Ammonium is not a conservative component and reaction processes (e.g. exchange reactions) can reduce the NH_4^+ concentrations during circulation of these marine waters through the fractured bedrock. However, these reactions are not able to completely mask the marine signature in the Laxemar-Simpevarp, Forsmark or Olkiluoto groundwaters. This is favoured by the stability of dissolved ammonium in reducing environments. Moreover, it supports the likely existence of reducing conditions in these groundwaters for a long time span.

5   Summary and conclusions

The main processes determining the global geochemical evolution of the Laxemar-Simpevarp groundwaters system are mixing and reaction processes. Mixing has taken place between different types of waters (end members) over time, making the discrimination of the main influences not always straightforward. Several lines of evidence suggest the input of dilute waters (cold or warm), at different stages, into a bedrock with pre-existing very saline groundwaters. Subsequently, marine water entered the system over the Littorina period (when the topography and the distance to the coast allowed it) and mixed with pre-existent groundwaters of variable salinity. In the Laxemar subarea mainland, the Littorina input occurred only locally and it has mostly been flushed out by the subsequent input of warm meteoric waters with a distinctive modern isotopic signature.

In addition to mixing processes and superimposed to their effects, different chemical reactions have taken place in the system due to the interaction between waters, minerals and/or microbial activity (e.g. aluminosilicate and carbonate dissolution/precipitation, cation exchange, gypsum dissolution, main redox reactions, etc).

In this context, some elements such as chloride or $\delta^{18}O$ behave conservatively (only dependant on mixing) while others are affected by chemical reactions to differing degrees, especially the redox-sensitive elements. Therefore, the general conclusions on the geochemical behaviour of two sets of elements (conservative and non-conservative, including redox) are summarised below.

5.1   Conservative elements: chloride, $\delta^{18}O$ and δ^2H

These parameters have been used for water type definition. Chloride concentration is a salinity indicator and it shows the transition from the more dilute groundwaters at shallow depths to the highly saline waters at the deepest parts. Moreover, since chloride is usually conservative in groundwaters, its evolution is suitable for comparison when studying the hydrochemical evolution trends of other elements, ranging from conservative to non-conservative. Moreover, chloride can be used as a tracer of the main irreversible process operating in this system (i.e. mixing) as proposed in earlier reports.

$\delta^{18}O$ is also a conservative component that can be used to trace mixing processes, to distinguish between recharge waters corresponding to cold or warm climates and, therefore, to separate the groundwaters affected by glacial influence from the rest.

As a general rule, chloride concentrations increase with depth but some specific points can be highlighted (Figure 5-1):

a) the dilute nature of recharge meteoric waters determines chloride concentrations < 500 mg/L up to average depths of around 500 m in the Laxemar subarea, followed by a marked and steady rise in salinity, which in KLX02 achieves 47g/L Cl at the maximum sampled depth;

b) dilute recharge meteoric waters for the Äspö and Simpevarp subareas are restricted to around 100 m depth;

c) at the Simpevarp subarea there is a marked increase in salinity from around 8,000–9,000 mg/L Cl at 600 m to 17,000 mg/L Cl down to 1,000 m;

d) the greater salinity between 100–600 m at the more coastal Äspö and Simpevarp sites could be explained by potential discharge hydraulic conditions in those locations.

With regard to $\delta^{18}O$, there is a wide range of variation for waters down to 600 m (Figure 5-1; grey dashed area) from −16‰ to −7‰. As also described for Forsmark, the heaviest values appear in the brackish-marine type waters (especially in Äspö). The lightest values are associated with brackish waters with a significant Glacial component, whereas fresh, mixed, transition and brackish-non marine types display intermediate values. From 900 m down, $\delta^{18}O$ values tend to increase towards the values of the Deep Saline end member (−8‰; Figures 5-1 and 5-2). Such enrichment has also been observed in Olkiluoto from 500 m down and in deep brines of the Canadian Shield.
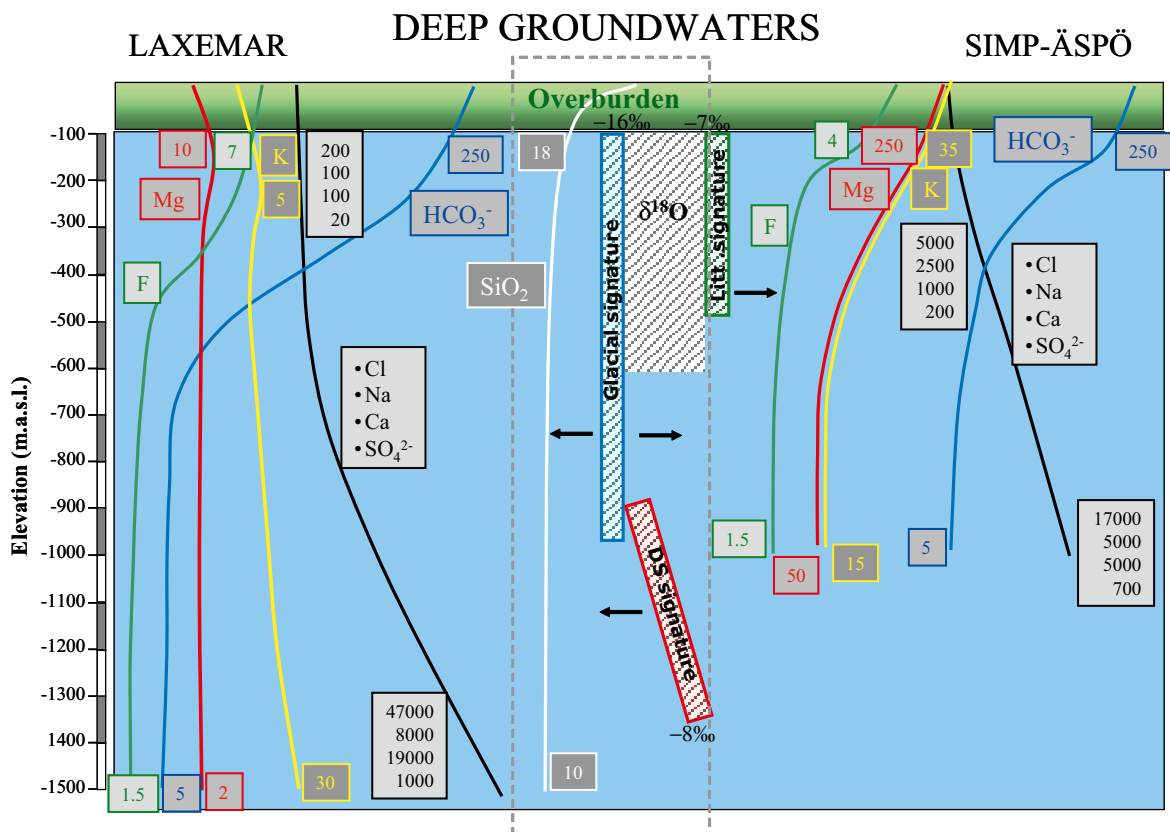
Figure 5-1. *Simplified sketch of the evolution of the dissolved contents of the major components with depth. Maximum contents in the shallowest and deepest parts of the bedrock system (in light blue) are shown in mg/L besides the trend lines and with the same colours. Left zone shows the evolution observed in the Laxemar subarea, while right zone displays the evolution in the Simpevarp and Äspö subareas. The middle part of the profile (indicated by the dashed gray vertical rectangle) shows the common evolution of silica and isotopic composition with depth for both subareas.*

Except for some near-surface groundwaters with very large $\delta^{18}O$ values and for the dilute recharge meteoric groundwaters at Laxemar, the isotopic composition and chloride contents in the rest of the groundwaters can be explained as resulting from mixing between the Deep Saline, Glacial, Littorina and Altered Meteoric end members (Figure 5-2).

Clear differences between the different waters emerge from their isotopic composition. Fresh, mixed brackish, brackish non-marine, transition and saline waters plot within the range between –13‰ and –10‰ $\delta^{18}O$ following the GMWL. Groundwaters with clear Glacial signature plot also on the GMWL but with lower $\delta^{18}O$ values. The deviation of Baltic Sea waters from the GMWL isotopic composition is typical of evaporation effects which, to a lesser extent, have influenced some of the near surface waters and the brackish-marine groundwaters from Äspö. Finally, highly saline waters display enrichment in $\delta^{18}O$ usually attributed to very intensive water/rock interactions under near-stagnant conditions.

5.2   Non conservative elements

This group includes the elements whose concentrations are more or less influenced by the existence of chemical reactions. Water-rock interactions are clearly more important at Laxemar-Simpevarp than at Forsmark, especially in the shallowest parts of the system.
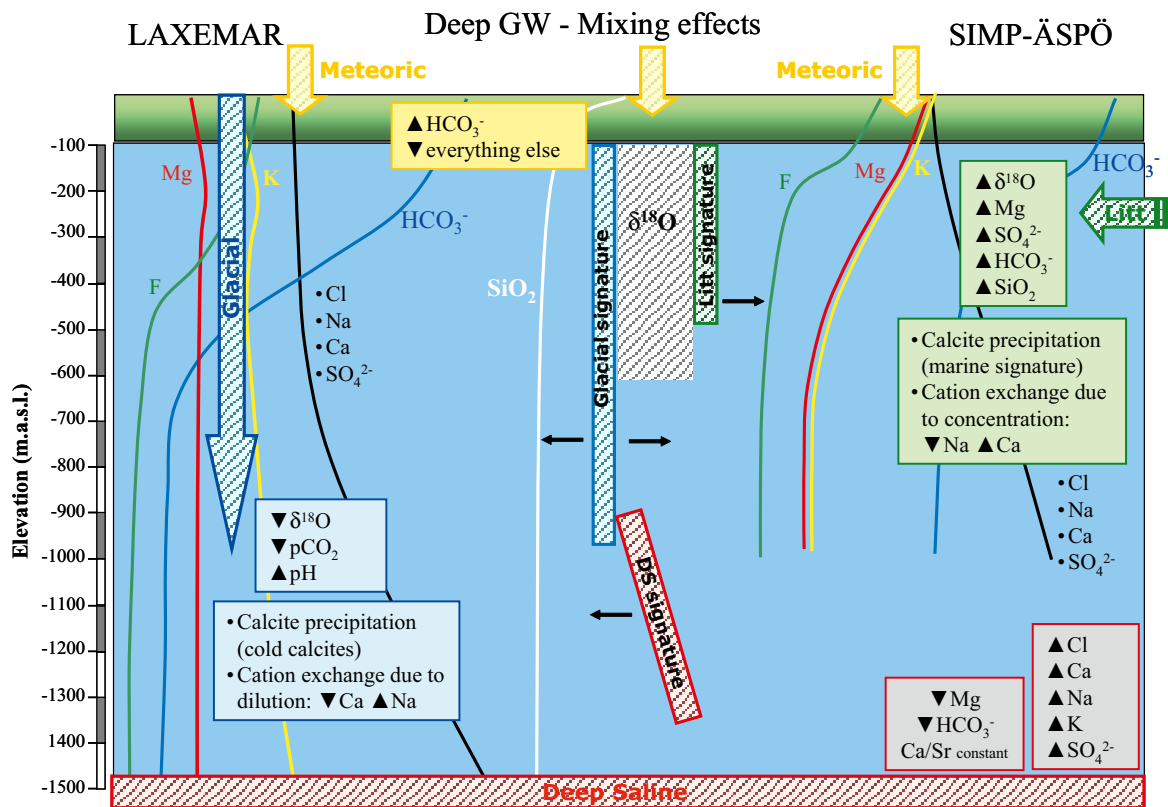
Figure 5-2. *Simplified sketch of the effects of mixing with different end members on the dissolved contents of the major components. The temporal sequence could be as follow: First, the presence of deep saline waters (red rectangle in the deepest part of the bedrock) conditions high contents of chloride, calcium, sodium, potassium and sulphate, low values of magnesium and bicarbonate, and a more or less constant Ca/Sr ratio. Then, the input of dilute waters (meteoric or glacial waters) over the time, creates a concentration profile from the surface down to depth. The cold climate signature will decrease the oxygen-18 signature and waters with low pCO_2 and high pH values will enter the system. The different mixtures will promote calcite precipitation and cation exchange due to dilution (decrease of calcium and increase of sodium in waters). The following water type entering the system is a marine water (Littorina) that, after several diagenetic processes in the marine sediments, will pass to the bedrock down to different depths depending on the coast proximity (more in Simpevarp and Äspö) and on the salinity of the pre-existing waters (Glacial to brackish-glacial waters). The higher density of these Littorina waters will displace the previous dilute waters and the result will be more concentrated waters enriched in magnesium, sulphate, bicarbonate and silica. Calcite will precipitate and the cation exchange will produce the decrease of sodium and the increase of calcium in the waters. Oxygen-18 signatures will also increase. Finally, the continuous input of meteoric waters will produce a superimposed dilution profile (more marked in the recharge areas such as Laxemar).*

To study the behaviour of non-conservative elements, two different subsystems with different hydrological and geochemical processes can be distinguished: the overburden (near surface/shallow and intermediate system down to 150 m depth) and the deep bedrock system (below 150 m depth).

The overburden is dominated by water-rock interactions between the recharge meteoric waters and the bedrock, till sediments and soils. The results of these processes determine the hydrochemistry of the waters recharging the deep groundwater system. But there are also places in this upper part which are influenced by marine inputs or deep discharges.

In the deep part of the system (below 150 m depth), mixing processes usually dominate and the effects of reactions between the groundwaters and the minerals in the fracture fillings will be superimposed on mixing signatures.

5.2.1 Near-surface groundwaters

Dissolved sodium, potassium, magnesium, calcium, bicarbonate and sulphate contents in the surface (streams, lakes, etc) and near surface groundwater systems at Laxemar-Simpevarp are within the range usually measured in the Swedish context (Tröjbom and Söderbäck 2006a, Tröjbom *et al.* 2008). However, silica and fluoride contents in near-surface groundwaters display higher values in this system.

The compositional evolution of the near surface and shallow groundwaters is mainly controlled by the existence of weathering reactions. Typical weathering reactions in the subsurface systems are mainly triggered by biogenic CO_2 input derived from organic matter decay (e.g. plant debris) and root respiration. This input of CO_2 promotes a pH decrease and a CO_2 partial pressure increase in the waters, which may favour the dissolution of carbonate or aluminosilicate mineral phases if present in the system (Figure 5-3).

In carbonate or aluminosilicate dissolution reactions, cations (Na, Ca, Mg, K, etc), silica and alkalinity are released (Figure 5-3). The intensity of these weathering reactions during infiltration of the surface waters in the overburden is mainly conditioned by the evolution of waters under open or closed conditions with respect to CO_2. If the consumed CO_2 is replenished (open system), weathering reactions will be enhanced, increasing the concentrations of cations and HCO_3^- further than under closed system conditions. As the biogenic CO_2 production varies throughout the year (high intensity in summer and low in winter), the intensity of weathering processes is also conditioned by these temporal effects. Due to this variable influence of atmospheric and biogenic CO_2 on silicate weathering reactions in the overburden, alkalinity (HCO_3^-), fluoride, major cations, silica and pH values in this part of the system show the greatest variability among the Laxemar-Simpevarp groundwaters.

Na, K and Mg concentrations display a clear increase with the weathering intensity, which also causes an increase in the alkalinity production. The incongruent dissolution of aluminosilicates (mainly plagioclase and mafic minerals such as biotite and hornblende) seems to be generally the most important process in their control.

Figure 5-3. *Simplified sketch of the main processes affecting the fresh near-surface groundwaters indicating the maximum representative dissolved contents of the main components (outliers excluded).*
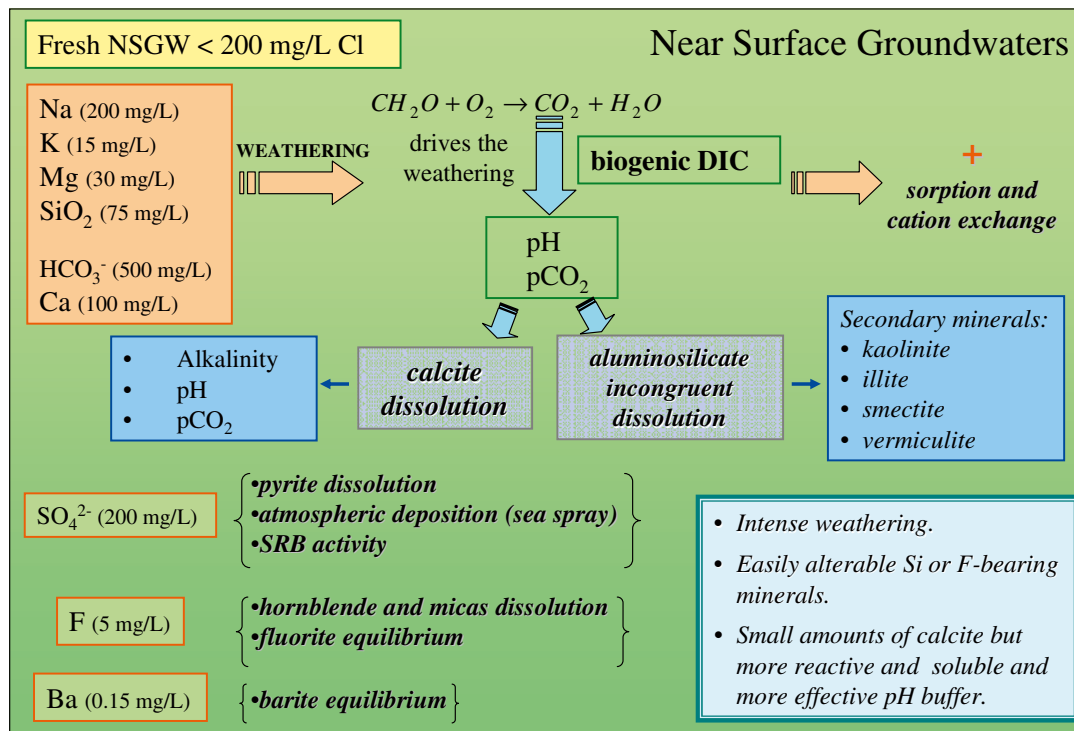
These cations may be partially incorporated into secondary clays and the net effect in the increase of their concentrations depends on the type of the secondary mineral phase (Figure 5-3). Mineral stability diagrams confirm the stability of kaolinite and illite and also the participation of smectites in the control of dissolved Na, Mg, K and SiO_2 in some groundwaters. Moreover, weathering-induced transformations from illite or chlorite (both present in the overburden) to vermiculite can also participate in the control of dissolved potassium and magnesium.

Other processes affecting the final dissolved concentrations of these elements may be their use as nutrients for plants (e.g. Mg, K) or their participation in cation exchange processes (especially in the case of Mg, Ca and Na). Moreover, some saline near-surface groundwaters from soil pipes located in till below lake and sea sediments seem to be affected by a strong marine influence (e.g. SSM000238 and SSM000239) and/or by discharging deep groundwaters related to the main fracture zones in the area (SSM000241 and SSSM000242). Consequently, these waters display large concentrations of sodium (1,900 to 2,230 mg/L), magnesium (151 to 354 mg/L), potassium (50 to 94 mg/L) and silica (up to 75 mg/L).

Dissolved calcium in the fresh near-surface groundwaters shows maximum concentrations of around 100 mg/L, although it is usually below 80 mg/L. Calcite and aluminosilicate weathering reactions (hornblende and plagioclase dissolution), cation exchange reactions or calcite and fluorite equilibrium may participate in the control of this element in the near surface and shallow groundwaters from Laxemar-Simpevarp (Figure 5-3). Bicarbonate reaches maximum concentrations around 500 mg/L and calcite equilibrium is only attained for the waters with the largest bicarbonate contents. Overall, calcite appears to contribute to the chemical and isotopic (C and Sr) characters of the near-surface groundwaters much more than expected from the detected small amounts of this mineral detected in the Laxemar-Simpevarp overburden (Figure 5-3).

Sulphate concentrations are larger (130–480 mg/L) in samples with Cl concentrations around 2,400–3,600 mg/L, affected by a relict or modern marine sulphate source (SSM000238 and SSM000239). On the contrary, samples with a possible Deep Saline signature (up to 5,000 mg/L Cl) and probably associated with the deep groundwaters discharging through the main fractures of the area, display total dissolved sulphate of around 20 mg/L, such as samples SSM000241 and SSM000242. Such low sulphate contents appear to be associated with very intense biological activity.

Dissolved sulphate contents in the rest of the near-surface groundwaters are always below 200 mg/L, as in the Forsmark area. The SO_4^{2-}/Cl ratio in most of these fresh groundwaters is greater than the seawater ratio and, therefore, a non-marine source seems to be the major sulphur contributor. The lack of correlation between total dissolved sulphate and calcium contents in these waters allows discarding control by dissolution. Instead, isotopic constraints ($\delta^{34}S$ values of dissolved sulphate) support an important contribution from pyrite dissolution (values from –20 to –5‰ CDT) to the dissolved sulphate pool in these waters. The effect of atmospheric deposition or the direct influence from seawater deposition (sea spray) or even the existence of sulphate reducing activity (Figure 5-3) are also supported by the range of $\delta^{34}S$ values found in some waters.

Neither calcium nor strontium solubility are limited by precipitation of sulphate phases but barium appears to reach a solubility limitation (barite) in these near-surface groundwaters, also contributing to modulate the dissolved sulphate concentrations (Figure 5-3).

As indicated above, higher values and variability of silica and fluoride concentrations have been found in the near-surface groundwaters of Laxemar-Simpevarp compared with other systems. This would indicate a more important presence of easily alterable silica and fluoride-bearing minerals, and/or a more intense weathering in the Laxemar-Simpevarp overburden. Dissolved fluoride is mainly controlled by hornblende and micas dissolution and fluorite participates as solubility-limiting phase (Figure 5-3).

Dissolved silica concentrations are mainly controlled by the incongruent dissolution of aluminosilicates (although dissolution of amorphous silica -diatoms- in marine sediments outcrops may also play an important role). Silica is released from primary minerals (mainly plagioclase and mafic minerals such as hornblende) and partially incorporated into secondary clays. The net effect of these reactions on the increase of dissolved silica concentrations depends on the type of the secondary

mineral phase formed. According to the results from the mineral stability diagrams already describe above, these phases could be kaolinite, illite, smectites and vermiculite. Sorption-desorption processes involving fine-grained materials in the overburden can also participate in the control of dissolved silica. Surface reactions with clays and aluminium or ferric oxyhydroxides are common processes in soils (Langmuir 1997 and references therein).

Chalcedony and quartz saturation indices in the near-surface groundwaters indicate that most of the waters are oversaturated with respect to both phases. The continuous increase in the oversaturation state with respect to chalcedony and quartz as the silica increases indicates that these phases are not solubility-limiting phases for this element in the near-surface groundwaters from both zones. It can be predicted that the quartz content will increase proportionally in the future as weathering reactions dissolve the less resistant mineralogy (e.g. plagioclase, hornblende).

The variable and high dissolved Fe(II), S(–II) and Mn(II) concentrations in near-surface groundwaters indicate the presence of anoxic environments with effective reductive dissolution of Fe-silicates (e.g. Fe(III)-bearing clay minerals) or ferric and manganese oxyhydroxides (post-oxic environment) and bacterial S(–II) production (sulphidic environment) already in the very shallow parts of the system. These reducing conditions are conditioned by the biological and microbial activity developed in the overburden and mainly in the soils, where organic matter decay may lead to complete redox sequences (from oxic to post-oxic, sulphidic and methanic environments) at the centimetre to metre scale.

Different bacterial metabolic activities (IRB, SRB and MRB) may contribute to the dissolved Fe(II), S(–II) and Mn(II) concentrations. But inorganic processes are also involved in the control of these elements: reduction of ferric and manganese oxyhydroxides by dissolved sulphides as well as siderite and rhodochrosite equilibrium or iron monosulphide precipitation have been identified as the main effective processes.

In the exposed bedrock outcrops of the overburden, the reducing capacity is lower than in the soils and therefore, oxygenated waters may reach greater depths. The occurrence of recent, low-temperature Fe(III)-oxyhydroxides indicates that the present redox front in the Laxemar subarea is located at about 15–20 m depth, in a zone affected by seasonal and annual variations in the recharge waters. The identification of old, low-temperature goethite down to c. 80 m depth, indicates the possible maximum penetration depth of oxygenated groundwaters in the past through highly fractured sections. However, these oxidising episodes have not been intense enough to exhaust the reducing capacity of fracture filling minerals in the shallowest part of the system, where chlorite and pyrite are still present.

5.2.2 Deep groundwaters

Sodium, potassium and magnesium

Sodium distribution with depth shows similarities with the described chloride trends (Figure 5-1). Moreover, the concentrations of both elements display a positive linear correlation with two different slopes attributable to mixing with a marine end member (roughly following the seawater dilution line) and to mixing with a saline non-marine end member. Groundwaters from the Laxemar subarea show much lower sodium concentrations than groundwaters from the Simpevarp subarea at similar depths (see the black trends in the left and the right parts of Figure 5-1), whereas Äspö groundwaters display intermediate sodium contents. Sodium displays a near-conservative behaviour in the Laxemar-Simpevarp samples with large chloride contents (Cl > 10,000 mg/L), as also observed at Forsmark and Olkiluoto. However, samples with Cl < 10,000 mg/L are affected by other mixing processes (mainly with Littorina, although its effects on the sodium contents are less evident than in Forsmark) and by the effects of water-rock interaction, especially in dilute groundwaters down to 500 m depth.

Potassium contents in the Laxemar subarea groundwaters increase very slowly with depth (yellow trend in the left part of Figure 5-1) but with values always below the seawater dilution line. This behaviour shows a global concentration trend towards the saline end member (Figure 5-2). This may reflect the influence of mixing with a saline (non marine) component in saline groundwaters from Laxemar, as happens at Forsmark and Olkiluoto. In the right part of Figure 5-1 (Simpevarp-Äspö

subareas), potassium shows the highest contents in the shallow groundwaters from Äspö and they are restricted to groundwaters with chloride contents around 5,000 mg/L and with a significant Littorina contribution. The same characteristics, although much clearer, can be observed at Forsmark and Olkiluoto.

A similar behaviour can be appreciated for magnesium. In the Laxemar subarea, magnesium distribution with depth displays a progressive concentration decrease to values around 2 mg/L at 1,000 m depth, remaining constant thereafter down to the deepest and more saline groundwaters (red trend in the left part of Figure 5-1). Again, the decrease of magnesium as the salinity (chloride) increases suggests the influence of a magnesium-depleted saline component (Figure 5-2). However, in the Simpevarp subarea (right part of Figure 5-1), the highest magnesium contents have been found, associated with brackish compositions restricted to maximum depths of about 500 m. These waters are considered to represent a significant component of Littorina Sea waters (Figure 5-2).

Apart from the marine influence, the scattering of sodium, magnesium and potassium concentrations in the 1,000–10,000 mg/L chloride concentrations range suggests that aluminosilicate dissolution reactions and also cation exchange (Figure 5-4) could be active in controlling the behaviour of these elements as happens in the near-surface groundwaters. From the available mineralogical data in fracture fillings, different aluminosilicates, such as albite, adularia, chlorite and mixed-layer clays like smectite/illite, chlorite/smectite or chlorite/vermiculite, which has been confirmed with the stability diagrams, could participate in the control of these elements.

The thermodynamic simulations carried out indicate that mixing seems to be the main process in the control of the sodium, magnesium and potassium concentrations for the most saline groundwaters. On the other hand, cation exchange processes may exert an important control over these elements in fresh and brackish groundwaters (with more than 20–30% of Littorina contribution). In any case, without more data on the real exchange capacity of the system, all these results are only an estimation of what would happen if this process took place in the system.

Carbonate system

pH values are between 7.2 and 8.6 in the groundwaters and do not show any clear variation trend with depth. A similar behaviour for pH has been observed in other crystalline areas such as Forsmark or Lac du Bonnet (Canada). For the Laxemar subarea, pH values tend to be restricted to a range between 8 and 8.5 in the most saline groundwaters, although some scatter is also observed in the rest of the groundwaters.

Alkalinity contents show a sharp decrease with increasing depth (Figure 5-1) and chloride concentration. High and variable values can be found down to 400 m depth at the Äspö and Laxemar subareas. As observed in Forsmark, the high HCO_3^- values found in the groundwaters from Äspö are clearly associated with groundwaters with a Littorina signature (Figure 5-2). On the contrary, in the Laxemar subarea they seem to be related to fresh and "recent" recharging groundwaters, although open-hole mixing effects are also possible in some samples. Below 500 m depth, alkalinity in the saline groundwaters drastically decreases to a narrow range of values, as also observed in the Forsmark and Olkiluoto groundwaters. This indicates the existence of a clear mineral solubility control on bicarbonate contents superimposed to the effects of mixing.

Calcium concentrations show a clear increasing trend with depth and chloride content towards the value of the Deep Saline end-member (Figures 5-1 and 5-2). Low Ca concentrations characterise the groundwaters down to 500 m depth in the Laxemar subarea because of the important recharge penetration depth in this zone. In the other subareas, calcium concentrations are higher and display a steeper increase with depth. From 600 m depth down, calcium concentrations show a marked and steady increase, achieving the maximum value in the Deep Saline end member at the maximum sampled depth (about 1,500 m).

Thermodynamic simulations also confirm that the high Ca content of the mixed waters (derived from the Deep Saline end member) obliterates the effects of mass transfer with respect to re-equilibrium with calcite or gypsum or cation exchange reactions (Figure 5-4). This justifies the apparent quasi-conservative behaviour of calcium for groundwaters with chloride contents higher than 0.2 mol/kg. However, the calcium contents observed in these saline waters are better reproduced if mixing

(between the Glacial and the highly saline end members) and cation exchange processes are considered together. This is also valid for less saline waters, such as the brackish-glacial type (at Äspö and Simpevarp), which can be the result of the same mixing between Glacial and saline, but with the exchange processes dominating the dissolved calcium contents.

Calculated saturation indices with respect to calcite show the close proximity to equilibrium for all the available samples with field-measured pH. Dilute groundwaters rapidly attain equilibrium or slight oversaturation with respect to calcite at shallow depths and this state is maintained at greater depths in saline groundwaters where mixing processes are effective.

Calculated CO_2 partial pressures display a progressive decrease with depth and with chloride contents from the values found in the fresh, near-surface groundwaters (most of them with pCO_2 values greater than the atmosphere). Similar trends in the evolution of CO_2 partial pressures with depth and chloride content can be observed in the Lac du Bonnet groundwaters and in the Olkiluoto groundwaters. This decrease may be associated with calcite dissolution in the dilute shallowest groundwaters up to 200 m depth, where equilibrium or oversaturation with respect to this mineral is reached. At greater depths, where groundwaters are also in equilibrium or near equilibrium with calcite, the CO_2-depletion may be associated with aluminosilicate-dissolution and, mainly, with the combined effects of mixing with saline groundwaters and precipitation of calcite.

Thermodynamic simulations confirm these conclusions. Mixing of highly saline deep groundwaters and dilute waters with high pH and low CO_2 partial pressure (e.g. Glacial end member with pCO_2 around 10-6, Figure 5-2), induces calcite oversaturation due to the very high dissolved calcium concentrations in the highly saline end-member and to the non-linear algebraic effect during mixing. This would favour the observed precipitation of calcite with cold climate isotopic signatures and would buffer the low and constant alkalinity values.

Simulations of mixing between the original Littorina composition (or with larger bicarbonate contents) and the pre-existing groundwaters (from Glacial to Brackish-Glacial) also suggest calcite oversaturation and precipitation during Littorina intrusion. This is in good agreement with the identification of calcites with marine signature found down to 500 m depth in the fracture fillings.
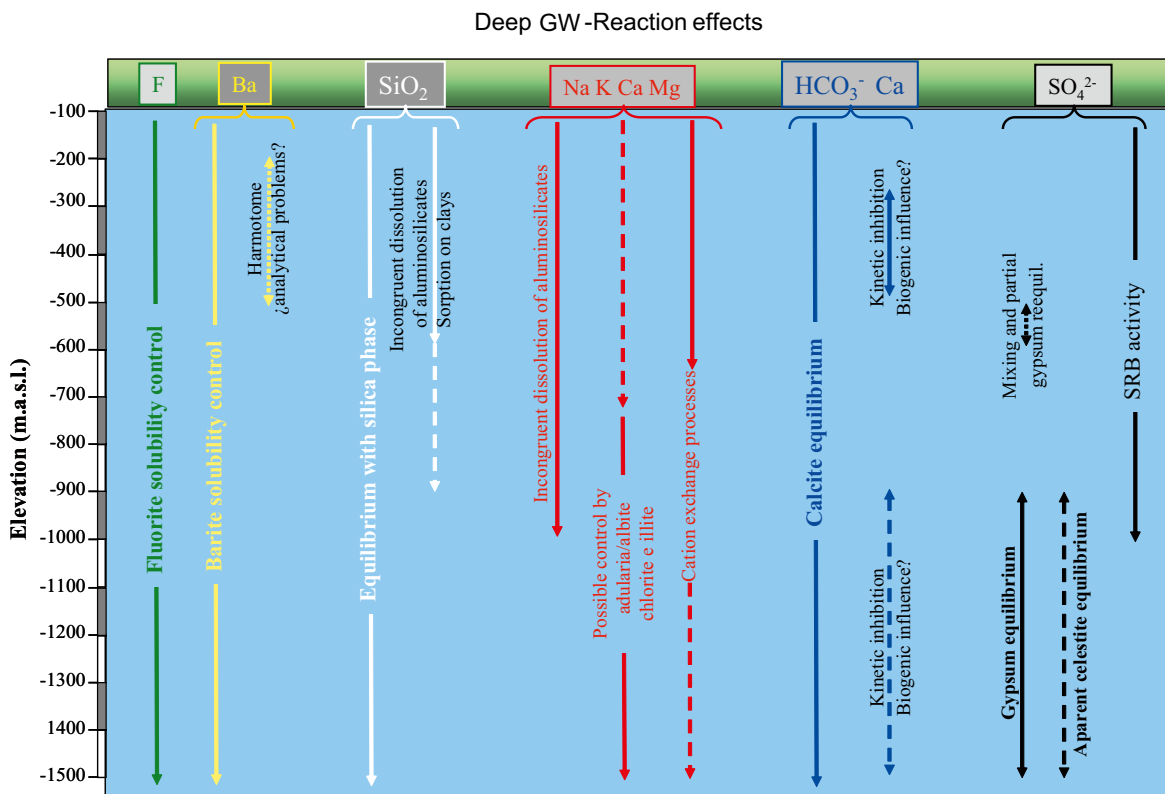
Figure 5-4. *Simplified sketch of the effects of reactions on the dissolved contents of the major components.*

Silica system

In contrast with the wide range of silica contents found in the near-surface groundwaters, most deep groundwaters with Cl > 3,000 mg/L show silica concentrations within a narrow range around 10 mg/L (white trend in the common area of Figure 5-1). However, greater variability is displayed by the shallowest waters (from 10 to 18 mg/L SiO_2) and by the brackish waters with Cl around 5,000–5,500 (from 5 to 13 mg/L SiO_2). In general, similar silica behaviour is observed in Forsmark, Olkiluoto, Palmottu and in the Canadian Shield groundwaters. The main difference with respect to Laxemar-Simpevarp waters is that brackish groundwaters at Forsmark have the highest silica concentrations (up to 25 mg/L), as inherited from the significant Littorina contribution.

Different water-rock interaction processes related to clays (incongruent dissolution of feldspars, clay mineral transformations, silica adsorption-desorption reactions in clays, etc; Figure 5-4) can participate in the control of dissolved silica, at least in the dilute groundwaters of recent meteoric origin. In any case, the net effect of these heterogeneous processes leads to a progressive restriction of the dissolved silica range with depth and residence time. As a consequence, most of the old groundwaters in the Laxemar-Simpevarp area are in equilibrium or near equilibrium with respect to chalcedony or another silica variety with similar solubility.

The question of what mineral phase is controlling the silica solubility in these systems has been carefully evaluated taking into account the uncertainties in the thermodynamic data for quartz and chalcedony and the effects of particle size on solubility. The results obtained support control of dissolved silica by quartz with the "new" solubility data proposed by Rimstidt (1997). However, even though the possible control of the silica content by quartz instead of by chalcedony in the waters with longer residence time is conceptually important, the solubility of both polymorphs is so similar that either of them could be used for predictive calculations.

Sulphate system

Total dissolved sulphate contents show an overall and continuous increase with depth (Figure 5-1), similar to the trends observed for chloride and sodium in the groundwaters. As a general trend, low dissolved sulphate concentrations characterise the shallow 0–400 m groundwaters in Laxemar and Simpevarp subareas. With regard to Äspö (and some waters from the Laxemar subarea), most groundwaters display higher sulphate contents (up to 200 mg/L in the first 100 m, groundwaters with clear marine signature, and up to 500 mg/L from 100 m down to 400 m depth), as an inherited character from the Littorina contribution (Figure 5-2).

From 400 m to 1,600 m depth, contribution of a deep saline groundwater appears to be effective in all the Laxemar-Simpevarp area, increasing progressively the dissolved sulphate concentrations (Figure 5-2).

With respect to chloride, dissolved sulphate concentrations in the Laxemar-Simpevarp area display two apparent evolutionary trends: (1) a progressive increase with chloride (up to about 10,000 mg/L Cl) in a path where the present and past marine effects are evident[58], and (2) almost constant sulphate concentrations around 800 mg/L for groundwaters with evident influence of a deep saline water and with chloride concentrations between 10,000 and 50,000 mg/L.

Similar variation with chloride and depth has been described for the Lac du Bonnet batholith. In contrast, the existence of an important Littorina contribution down to 300–500 m depth in Forsmark and Olkiluoto promotes the presence of the largest total dissolved sulphate contents at those depths (in waters with Cl about 3,000–6,000 mg/L), with a drastic decrease at greater depths and salinities. The different observed sulphate trends at depth in Laxemar-Simpevarp and Olkiluoto can be attributed to the different total dissolved sulphate concentration of the corresponding Deep Saline end member (around 906 mg/L for Laxemar-Simpevarp and between 1.2 and 8.4 mg/L for Olkiluoto, Pitkänen *et al.* 2004).

---

[58] More in detail, Äspö and Simpevarp groundwaters show higher salinity (for chloride contents up to 10,000 mg/L) for the same sulphate contents than Laxemar subarea groundwaters.

Measured $\delta^{34}S$ values agree with the existence of equilibrium situations with respect to iron mono-sulphides in some samples, together with the indication of in situ sulphide generation by sulphate-reducing bacteria. In other waters, $\delta^{34}S$ values indicate a weaker or non-existent sulphate-reducing activity together with the influence of gypsum dissolution.

Groundwater saturation indices with respect to gypsum define a clear trend towards equilibrium with increasing depth and chloride content. The existence of this equilibrium situation would also explain the drastic differences observed in the dissolved sulphate contents of the more saline groundwaters in other Fennoscandian sites like Olkiluoto or Forsmark.

Gypsum has been identified in the fracture filling mineralogy but it is not equally distributed with either depth or subarea. Therefore, groundwaters will be affected by mixing with more saline waters either conservatively (if gypsum is not available) or with partial or total gypsum re-equilibrium (depending on the amount of available gypsum). As already observed in other systems with a greater Littorina presence (e.g. Forsmark or Olkiluoto) groundwaters with a Littorina contribution (Cl around 5,000 mg/L) do not reach gypsum equilibrium. Apart from the influence of gypsum dissolution, dissolved sulphate in some waters seems to be affected by other reaction processes superimposed on mixing, such as microbial sulphate reduction by SRB (Figure 5-4).

The behaviour of Ba and Sr is closely related to the sulphate system. Barium does not show any clear trend with either depth or chloride, which suggests the presence of some mineralogical control. Most of the groundwaters are in equilibrium with respect to barite, as happens in the possible recharge waters and in other low-temperature crystalline systems, such as Stripa (Nordstrom *et al.* 1989).

Dissolved strontium concentrations show a distribution with depth very similar to total dissolved sulphate. As described for calcium, dissolved strontium concentrations display a strong linear correlation with chloride content, suggesting a control by mixing processes for both elements. The same correlation has been observed in the Olkiluoto and Forsmark groundwaters, although with a different slope. The Ca/Sr molar ratio shows a very wide range of variation in surface and shallow groundwaters for the three sites, which can be attributed to the weathering reactions of different rocks and minerals with different Ca/Sr ratios. However, the Ca/Sr ratios in deeper and more saline groundwaters show a relatively constant value, although slightly different for each system, but con-sistent with the Ca/Sr value in their respective Deep Saline end members (Figure 5-2). This suggests that, in the more saline groundwaters, Ca and Sr are mostly inherited from the saline end-member and controlled by mixing, in spite of the different equilibrium situations in these systems.

With respect to the Sr-bearing mineral phases, celestite ($SrSO_4$) saturation indices calculated for the Laxemar-Simpevarp groundwaters display a similar trend to gypsum, reaching equilibrium in the more saline samples. Celestite has recently been identified in minor amounts in the fracture fillings. Therefore, this mineral could be considered as another possible Sr-controlling phase in this groundwater system.

Thermodynamic simulations of mixing between the deep saline waters and the dilute Glacial end member, indicate that disequilibria induced by mixing would produce calcite precipitation and, if present in the system, gypsum and celestite dissolution. Consistent with the observations, calculated calcium and strontium concentrations show a linear increase with chloride irrespective of the presence or absence of reactions. Changes in the simulated Ca or Sr contents imposed by gypsum dissolution or calcite equilibrium are very small, whereas cation exchange produce a slight decrease in the calcium and strontium contents with respect to the previous result (and in agreement with the calculated increase in sodium), fitting better the measured values analysed in the real samples.

Dissolved sulphate concentrations obtained from conservative mixing between Littorina and the pre-existing groundwaters vary linearly with respect to chloride content, with a progressive increase of both elements as the mixing proportion of the more saline end member increases. This happens in the brackish-marine waters from Äspö and some near-surface groundwaters with very high sulphate contents. However, for the more saline waters (Cl > 0.2 mg/L), only the combination of mixing and gypsum re-equilibrium (or equilibrium with respect to gypsum+calcite+celestite) reproduces the observed sulphate behaviour.

Fluoride system

In the Laxemar-Simpevarp area, the fluoride contents in groundwater near surface and shallow dilute groundwaters (< 200 m depth) are very high and variable, up to 7 mg/L (green trend in Figure 5-1). This is due to weathering and dissolution of F-bearing minerals such as hornblende, micas or fluorite present in the overburden or in fracture fillings at very shallow levels. As a result, waters reach fluorite saturation and fluoride derived from weathering reactions can be re-precipitating at present as fluorite in some points.

Below 200 m depth at the Simpevarp subarea and 400 m depth at the Laxemar subareas, as salinity increases, fluoride variability decreases. Groundwaters that are still dilute but with longer residence times at the Laxemar subarea show less variable fluoride contents than shallower waters, as resulting from the fluorite solubility control. For chloride contents greater than 5,000 mg/L, fluoride concentrations are always between 1 and 2 mg/L, as in the Forsmark and Finnsjön groundwaters. Mineralogical control of fluorite is also effective during all the mixing processes affecting this system.

Therefore, there is a generalised fluorite control on the dissolved fluoride in the Laxemar-Simpevarp area groundwaters (Figure 5-4). It will be superimposed on the calcite control of dissolved calcium, giving rise to a clear relationship between pH, alkalinity and calcium and fluoride contents, which will be controlled by both phases. However, fluorite re-equilibrium during mixing does not produce significant changes on the dissolved calcium concentrations, which are mainly controlled by mixing in the saline groundwaters.

Redox systems

All the potentiometrically measured Eh values in the Laxemar-Simpevarp area, including some shallow and dilute groundwaters barely affected by mixing, are clearly reducing even taking into account the possible perturbations of the original redox environment during the measurements. This would indicate the ability of microbial or water-rock interaction processes to create very reducing conditions even in the shallowest parts of the system.

The interplay between **the iron and sulphur systems** exerts the main control over the redox processes that promote these reducing conditions in the Laxemar-Simpevarp groundwaters. For the iron system, the widespread presence of Fe(II) and Fe(III) minerals has been detected in the studied systems and these phases play a fundamental role in the overall reducing capacity of the system. The reductive dissolution of ferric oxyhydroxides by hydrogen sulphide is a kinetically fast process that may exert a major control on dissolved sulphide contents in addition to the amorphous ferrous iron monosulphide precipitation. These processes may be especially important in the performance assessment, as the factors controlling dissolved sulphide concentrations are of major concern in the Swedish Spent Fuel disposal design.

The long residence times of groundwaters under reducing conditions and the actual data on the Fe(III)-oxyhydroxides in the fracture fillings support the existence of crystalline phases (goethite and, mainly, hematite). The high degree of crystallinity and low surface areas of these ferric phases have probably limited their use as TEAP's by iron reducing bacteria (IRB) in the Laxemar-Simpevarp groundwater system. Additionally, in these long time maintained reducing conditions, the use the Fe(III) in clay minerals as TEA for respiration by IRB could be importantly inhibited by sorbed Fe(II). These results suggest that, under the pristine conditions of deep groundwaters with long residence time, the IRB activity would be seriously disfavoured and may explain why IRB have not been more frequently found in the microbiological analyses performed at Laxemar-Simpevarp. Therefore, the active presence of IRB should be associated with temporal perturbations of the system (oxygen intrusion scenarios). But even in that case the extent of the IRB activity will be necessarily limited in time by the effects of their own metabolism (increase of dissolved Fe(II)) on the TEA. Furthermore, these results also emphasise that the analysis of the IRB inhibitory effects is important for the understanding of the geochemical and microbiological relations and that further studies are needed.

With regard to the sulphur system, the results of the monitoring program indicate that the measured dissolved sulphide concentration may be affected (diminished) by disturbances during sampling operations, especially in the groundwaters from the Laxemar subarea. Therefore, the groundwater intervals with measurable dissolved sulphide concentrations are, probably, greater than the available data suggest at present. Even with this uncertainty, equilibrium with respect to amorphous monosulphides in groundwaters occurs widely down to 900 m, close to the maximum depth at which SRB have been found and at which dissolved sulphide is detectable.

Bioenergetic and partial equilibrium approaches indicate that, without bioavailable Fe(III)-electron acceptors, sulphate reduction would be the most predominant TEAP from a thermodynamic point of view and, therefore, one of the major processes regulating redox conditions in the groundwaters. In this sense, the sulphur redox couples (SO_4^{2-}/HS^-, SO_4^{2-}/FeS(am) and SO_4^{2-}/pyrite) can provide representative redox potential values (in most cases coincident with the potentiometrically measured Eh) for these sulphidic environments with active SRB activity. The key role played by SRB in the stabilisation of these reducing conditions over time appears to be supported by the isotopic values ($\delta^{34}S$) found in pyrites from the fracture fillings in the Laxemar-Simpevarp zone.

Besides bacterial activity, the largest inorganic reducing capacity is apparently provided by the presence of Fe(II)-bearing Al-silicates (chlorite and clay minerals, such as corrensite, smectite, mixed layer clays, illite/smectite) and by the minor and irregularly distributed amounts of pyrite. These Fe(II)-bearing minerals in the fracture fillings have been identified at all depths and even in the shallowest part of the system, which suggests that the system has maintained a noticeable reducing capacity over time and still does so at present.

As regards *the manganese system,* the concentrations of this element in groundwaters are variable and they appear to be controlled by different processes in different subareas.

In the groundwaters from the Laxemar-Simpevarp area, low Mn contents and undersaturation with respect to rhodochrosite can be observed. Dissolved manganese contents follow a roughly similar trend with depth to iron and the mineralogical studies of the fracture fillings also suggest the association of manganese with iron phases (oxyhydroxides, clays).

Additionally, some brackish and near-surface groundwaters with significant Littorina contribution in the Simpevarp-Äspö subareas show variable but high Mn concentrations and reach equilibrium with respect to rhodochrosite. These characteristics, also observed in the brackish groundwaters from Forsmark or Olkiluoto, represent the inheritance of the hydrochemical conditions imposed by rhodochrosite formation during Littorina infiltration through the marine sediments.

Most groundwaters analysed for MRB show MPN values which are not large enough to influence their chemistry. Even for the samples with large MPN values, the active presence of MRB and its effects on the composition of deep groundwaters should be considered with caution since, as also observed in Forsmark, it is not correlated with the observed Mn(II) concentrations in groundwaters. Moreover, none of the Mn oxides and oxyhydroxides that MRB may use as TEA has been identified in the deep groundwater system to date. Although the presence of manganese oxyhydroxides has recently been identified in the fracture fillings of the more surficial part (at 10 m depth), they have not been found deeper in either Laxemar-Simpevarp or Forsmark. This is consistent with the existence of reducing conditions and with the presence of dissolved Fe(II) and S(–II), which are known to diminish the stability of manganese oxyhydroxides. The lack of a mineral phase that can be used as TEA by MRB probably represents a major limitation to the active presence of these microorganisms in the studied groundwaters. Therefore, the identification of MRB at depths greater than 100–150 m is subjected to many uncertainties (see also Appendix G) and may be due to disturbances of the pristine conditions during sampling (short-circuit, artificial mixing, etc).

Finally, the behaviour of the *nitrogen system* is strongly determined by the existence of aerobic or anaerobic conditions. The observed evolution in the Simpevarp groundwaters shows the general depletion of nitrogen usually observed in anaerobic groundwater systems as residence time and/or depth increase. The largest contents and variability in NO_2^-, NO_3^- and NH_4^+ concentrations are associated with the near-surface groundwaters in the overburden, where the oxic/anoxic transition appears to occur, whereas deep groundwaters show very low (if any) nitrate and nitrite concentrations, in agreement with their reducing character.

More data and detailed studies are needed on ***methane and hydrogen*** gas distribution in the Laxemar-Simpevarp and Forsmark areas. As discussed in Appendix G, these gases may have both organic and inorganic origin and they may participate or control the redox state of the groundwater system at different depths, under different conditions and with variable rates depending on their origin. They also act as substrates for different autotrophic and heterotrophic metabolisms, especially the hydrogen, which may play an important role in the regulation of microbial activities. Therefore, the distribution of these gasses may help to clarify the distribution and mutual relationships of different metabolic groups in the groundwater system.

5.3   Conclusions

- The present hydrochemistry of groundwaters in the Laxemar-Simpevarp areas is mainly a result of mixing, driven by the climate changes, of different groundwaters with different origins (deep groundwater, glacial water, Littorina Sea water and meteoric water). The own composition of these end members affects some of the chemical characters of the groundwaters in the system: (1) low magnesium and bicarbonate contents and high sulphate concentrations in the waters with important deep saline signature, (2) very low values of $\delta^{18}O$ in the waters with glacial signature, (3) high values of magnesium, ammonium, manganese and other elements in waters with important Littorina signature, and (4) tritium presence and very low values of most chemical components (except bicarbonate) in the waters affected by the meteoric recharge.

- Hydrogeologically the Laxemar subarea is an area of groundwater recharge with systematic changes in groundwater chemistry with depth which accompany increasingly lower hydraulic conductivity values and lower groundwater flow rates in the bedrock. The Simpevarp subarea is mainly an area of groundwater discharge. In general, these hydrogeological characters are transferred to the depths of influence of the different water types. This explains why meteoric, glacial and deep saline influences are found deeper in the Laxemar subarea than in Simpevarp subarea, while Littorina reaches greater depths in the Simpevarp subarea than in the Laxemar subarea (where its influence is clearly weaker).

- Geochemically, weathering reactions are the main processes in the near-surface groundwaters. These weathering processes clearly persist down to 200 m depth but some mixing processes have also been recognised. From 200 m down, mixing is the main irreversible process in the bedrock and, apart from the effects due to the chemical composition of the different end members, it has triggered different chemical reactions. pH and Eh are controlled to a large extent by chemical reactions and microbial activity.

- Chloride concentration increases continuously with depth and allows characterising the transition depths between different water types at the different subareas.

- Oxygen-18 signature is a clear indicator of cold climates and of the input of glacial waters at different depths, reaching 1,000 m depth but mainly concentrated around the 350 to 600 m depth interval.

- Na, K and Mg are mainly controlled by the incongruent dissolution of aluminosilicates and by the effects of mixing with end members enriched or depleted in these cations (increase or decrease of the contents due to conservative mixing and cation exchange produced by the dilution or concentration scenarios developed by mixing). In the deepest, more saline and with longer residence time groundwaters, equilibrium control by aluminosilicates is possible.

- Ca is also affected by aluminosilicate incongruent dissolution but equilibrium with calcite and fluorite and cation exchange are both important in the control of its contents in the shallow groundwaters. Progressive mixing with a Ca-rich end member with increasing depth obliterates the effect of mass transfers due to re-equilibrium with calcite and gypsum or cation exchange. In any case, these chemical reactions are also important processes.

- Alkalinity contents and pH values show the greatest variability in the overburden due to the variable influence of atmospheric and biogenic CO_2 and their influence on weathering reactions. Then, pH values tend to be restricted to a range between 8 and 8.5 in the saline groundwaters and alkalinity tends to decrease with increasing depth and salinity. Ultimately, both parameters are mainly controlled by calcite equilibrium.

- Sulphate concentrations are affected by atmospheric and sea-water deposition in the shallow waters but also by pyrite dissolution. With increasing depth, mixing with brackish-marine and saline non-marine end members, together with gypsum and barite re-equilibrium, control the sulphate content. Microbially-mediated sulphate reduction may also contribute to the control of sulphate concentrations from the near-surface groundwaters to depths around 900 m.

- Silica contents are mainly controlled by the incongruent dissolution of aluminosilicates and by sorption-desorption processes in the overburden. In the deeper groundwaters the concentrations of this element are in equilibrium or close to equilibrium with chalcedony or another silica variety with similar solubility.

- Fluoride contents are controlled by hornblende and micas dissolution and fluorite participates as solubility-limiting phase, mainly below 200 m depth.

- To evaluate the redox system is one of the most important requirements for repository safety assessment, but also one of the most complicated tasks in hydrogeochemistry. For the analyses of the site investigation data, an integrated modelling approach was applied. The potentiometric Eh measurements, the redox pairs calculations, the speciation-solubility calculations and other thermodynamic calculations (bioenergetic estimations and partial equilibrium approach for the iron and sulphur systems) were combined with the available mineralogical and microbiological information. This integrated approach has allowed identifying some of the main controls of the redox state in groundwaters, as well as the main uncertainties still present.

- Anoxic environments are present in the near-surface system, with effective reductive dissolution of Fe-silicates or ferric and manganese oxyhydroxides (post-oxic environment) and bacterial S(–II) production (sulphidic environment). These reducing conditions are conditioned by the biological and microbial activity developed in the overburden and mainly in the soils. Different bacterial metabolic activities (IRB, MRB and SRB) may contribute to the dissolved Fe(II), S(–II) and Mn(II) concentrations. However, inorganic processes are also involved in the control of these elements. Reduction of ferric and manganese oxyhydroxides by dissolved sulphides as well as siderite and rhodochrosite equilibrium or iron monosulphide precipitation have been identified as the main effective processes.

- Few data exist for the redox characterisation of the shallow groundwater system but the potentio-metrical Eh values are between –250 and –280 mV, indicating clear reducing conditions in the dilute groundwaters barely affected by mixing, even taking into account the possible perturbations of the original redox environment during the measurements. Contents of ferrous iron and sulphide confirm the occurrence of post-oxic and sulphidic environments. Thus, all the data would indicate the ability of microbial or water-rock interaction processes to create very reducing conditions even in the shallowest parts of the system.

- Deeper down, all the Eh values potentiometrically measured are clearly reducing (–245 to –303 mV) and the redox conditions seem to be mainly controlled by the interplay between the iron and sulphur systems that promote these reducing conditions in the Laxemar-Simpevarp groundwaters. More data and detailed studies are needed to integrate the role of methane and hydrogen, and also on the spatial distribution and the simultaneous or competitive exclusion relations of *in situ* active metabolic processes.

- Recommendations for the future:
  - As the studied fractured systems show a complex palaeohydrological history that favours the existence of hydrogeochemical heterogeneities, a higher spatial resolution in the sampling network would be necessary to obtain a sample volume ideally smaller than the system heterogeneities. This higher spatial resolution would improve the overall knowledge of the system and it should be focussed on solving some of the uncertainties and problems detected (samples apparently affected by freezing-out processes, the gap between the saline and highly saline samples, etc).
  - More efforts are needed to minimise the disturbing effects during sampling (especially on the dissolved redox indicators and microbiological data).
  - Data on cation exchange capacity (CEC) in the fracture fillings are needed to verify the importance of the exchange processes deduced from the performed simulations.

– The influence of the microbial activities on the carbonate system must be clarified and, if possible, quantified to solve some uncertainties and to obtain a more refined model for the evolution of the system.

– More data and detailed studies on the methane contents and its isotopes are needed to better constrain the methanogenic activity vs. the "endogenous" origin of this component and to obtain a clear picture of the distribution of methane with depth.

– The apparently highly variable hydrogen contents need to be constrained with better detection limits to characterise the nanomolar range of this element and its influence on the different metabolic activities and/or in the development of different redox zones.

– The *in situ* active metabolic processes, their simultaneous or competitive exclusion relations, the factors that control their spatial distribution and their corresponding rates of activity must be clarified, as microbial metabolic activities are the ultimate engine that drives most redox reactions in aquatic systems. These aspects would also need a better knowledge on the fluxes of metabolic substrates in the system and on the interfacial properties of the available Fe and Mn oxyhydroxides.

References

Aggarwal P K, Gunter, W D and Kharaka, Y K (1990). Effect of pressure on aqueous equilibria. In: D.C. Melchior and R.L. Bassett (eds.), Chemical Modeling of Aqueous Systems II. American Chemical Society Symposium Series, Washington, D.C., American Chemical Society, pp. 87–101.

Akselsson C, Holmqvist J, Kurz, D and Sverdrup H (2006). Relations between elemental content in till, mineralogy of till and bedrock mineralogy in the province of Småland, southern Sweden. Geoderma, 136, 643–659.

Amirbahman A, Schönenberger R, Furrer G and Zobrist J (2003). Experimental study and steady-state simulation of biogeochemical processes in laboratory columns with aquifer material. Journal of Contaminant Hydrology, 64. 169–190

Anderson S P, Drever J I, and Humphrey N F (1997). Chemical weathering in glacial environments. Geology, 25, 399–402.

Andrews J N, Hussain N and Youngman M J (1989). Atmospheric and radiogenic gases in groundwaters from the Stripa granite. Geochim. Cosmochim. Acta, 53, 1831–1841.

Appelo C A J and Postma D (2005). Geochemistry, Groundwater & Pollution. Balkema, Rotterdam, The Netherlands, 2nd edition, 649 p.

Arthur R C (1996). SITE-94. Estimated rates of redox-front migration in granitic rocks. SKI Report 96:35, 27 p.

Auqué L F, Gimeno, M J, Gómez J, Puigdomènech I, Smellie J and Tullborg E-L (2006). Groundwater chemistry around a repository for spent nuclear fuel over a glacial cycle Evaluation for SR-Can. SKB Technical Report TR-06-31, 123 pp.

Auqué L F, Gimeno M J, Gómez J and Nilsson A-C (2008). Potentiometrically measured Eh in groundwaters from the Scandinavian Shield. Applied Geochemistry, 23, 1820–1833.

Ball J W and Nordstrom D K (2001). User's manual for WATEQ4F, with revised thermodynamic data base and test cases for calculating speciation of major, trace, and redox elements in natural waters. U.S. Geological Survey, Open File Report 91–183, USA.

Banks D and Frengstad B (2006). Evolution of groundwater chemical composition by plagioclase hydrolysis in Norwegian anorthosites. Geochim. Cosmochim. Acta, 70, 1337–1355.

Banks D, Parnachev V P, Frengstad B, Holden W, Karnachuk, O V and Vedernikov A A (2004). The evolution of alkaline, saline ground- and surface waters in the southern Siberian steppes. Applied Geochemistry, 19, 1905–1926.

Banwart S A (1999). Reduction of iron (III) minerals by natural organic matter in groundwater. Geochim. Cosmochim. Acta, 63, 2919–2928.

Banwart S, Gustafsson E, Laaksoharju M, Nilsson A-C, Tullborg E-L, Wallin B, (1994). Large-scale intrusion of shallow water into a vertical fracture zone in crystalline bedrock: initial hydrochemical perturbation during tunnel construction at the Äspö Hard Rock Laboratory, southeastern Sweden. Water Resour. Res., 30, 1747–1763.

Bath A, Milodowski A, Ruotsalainen P, Tullborg E-L, Cortés Ruiz A, Aranyossy J-F (2000). Evidences from mineralogy and geochemistry for the evolution of groundwater systems during the quaternary for use in radioactive waste repository safety assessment (EQUIP project). EUR report 19613.

Beaucaire C, Gassama N, Tresonne N and Louvat D (1999). Saline groundwaters in the hecinian granites (Chardon Mine, France): geochemical evidence for the salinity origin. Appl. Geochem, 14, 67–84.

Bennett P C, Hiebert F K and Robert-Rogers J (2000). Microbial control of mineral-groundwater equilibria: Macroscale to microscale. Hydrogeol. J, 8, 47–62.

Benning L G, Wilki R T and Barnes H L (2000). Reaction pathways in the Fe-S system below 100 °C. Chemical Geology, 167, 25–51.

Bergelin A, Berg C and Wacker P (2006). Oskarshamn site investigation. Complete chemical characterisation in KLX03. Results from four investigated borehole sections: 193.5–198.4 m, 408.0–415.3 m, 735.5–748.0 m, 964.5–975.2 m. SKB P-06-08, 106 pp.

Bergelin A, Nilsson K, Lindquist A and Wacker P (2008). Oskarshamn site investigation. Complete chemical characterisation in KLX08. Results from four investigated borehole sections: 197.0–206.6 m, 396.0–400.9 m, 476.0–485.6 m, 609.0–618.5 m. SKB P-06-308, 109 pp.

Berner R A (1963). Electrode studies in hydrogen sulfide in marine sediments. Geochim. Cosmochim. Acta, 27, 563–575.

Berner R A (1981). A new geochemical classification of sedimentary environments. J. Sediment. Petrol., 51, 359–365.

Berthelin J, Ona-Nguema G, Stemmler S, Quantin C, Abdelmoula M and Jorand F (2006). Bioreduction of ferric species and biogenesis of green rusts in soils. C. R. Geoscience, 338, 447–455

Bigham J M and Ciolkosz E J (1993). Soil color. SSSA Special Publication number 31, Soil Science Society of America Inc., Madison, Wisconsin, USA.

Blatt H (1992). Sedimentary Petrology. W.H. Freeman and Co., New York, 514 pp.

Blodau C and Peiffer S (2003). Thermodynamics and organic matter: constraints on neutralization processes in sediments of highly acidic waters. Appl. Geochem., 18, 25–36.

Blodgett R H, Crabaugh J P and McBride E F (1993). The color of Red Beds. A geologic perspective. In: J.M. Bigham and E.J. Ciolkosz (eds.), Soil color. Soil Science Society of America Special Publication Number 31, pp. 127–159.

Blomqvist R, Ruskeeniemi T, Kaija J, Ahonen L, Paananen M, Smellie J, Grundfelt G, Pedersen K, Bruno J, Pérez del Villar L, Cera E, Rasilainen K, Pitkänen P, Suksi J, Casanova J, Read D and Frape S (2000). The Palmottu Natural Analogue Project. Phase II: transport of radionuclides in a natural flow system. European Commission, Final Report, Phase II, EUR-19611, 171 p.

Blum J D, Gazis C A, Jacobson A D and Chamberlain P G (1998). Carbonate versus silicate weathering in the Raikhot watershed within the High Himalayan Crystalline Series. Geology, 26, 411–414.

Bohn H L, McNeal B L and O´Connor G A (2001). Soil Chemistry. John Wiley & Sons, Inc., 3rd Edition, 307 p.

Bonneville S, Van Cappellen P and Behrends T (2004). Microbial reduction of iron (III) oxyhydroxides: effects of mineral solubility and availability. Chem. Geol., 212, 255–268.

Boulegue J (1978). Electrochemistry of reduced sulphur species in natural waters. Geochim. Cosmochim. Acta, 42, 1439–1445.

Burke I T and Kemp A E S (2002). Microfabric analysis of Mn-carbonate laminae deposition and Mn-sulfide formation in the Gotland Deep, Baltic Sea. Geochim Cosmochim. Acta, 66, 1589–1600.

Canfield D E (1989). Reactive iron in sediments. Geochim. Cosmochim. Acta, 53, 619–632.

Canfield D E, Raiswell R, and Bottrell S (1992). The reactivity of sedimentary iron minerals toward sulfide. Am. J. Sci. 292, 659–683.

Carman R and Rahm L (1997). Early diagenesis and chemical characteristics of interstitial waters and sediments in the deep deposition bottoms of the Baltic Proper. Journal of Sea Research, 37, 25–47.

Cartwright I, Weaver T and Petrides B (2007). Controls on 87Sr/86Sr ratios of groundwater in silicate-dominated aquifers: SE Murray Basin, Australia. Chem. Geol., 246, 107–123

Chae G T, Yun S T, Kwon M J, Kim S Y and Mayer B (2006). Batch dissolution of granite and biotite in water: implication for fluorine geochemistry in groundwater. Geochem. J., 40, 95–102.

Chae G T, Yun S T, Mayer B, Kim K H, Kim S Y, Kwon J S, Kim K and Koh Y K (2007). Fluorine geochemistry in bedrock groundwater of South Korea. Science of the Total Environment, 385, 272–283.

Chapelle F H (2001). Ground-water microbiology and geochemistry. John Wiley & Sons, Inc. 2nd edition, 477 p.

Chen W F and Liu T K (2005). Ion activity products of iron sulfides in groundwaters: implications from the Choshui fan-delta, Western Taiwan. Geochim. Cosmochim. Acta, 69, 3535–3544.

Chiodini G, Cioni R, Guidi M and Marini L (1991). Chemical geothermometry and geobarometry in hydrothermal aqueous solutions: a theoretical investigation based on a mineral-solution equilibrium model. Geochim. Cosmochin. Acta, 55, 2709–2727.

Clark I and Fritz P (1997). Environmental isotopes in hydrogeology. CRC Press LLC, 328 p.

Clow D W, Mast M A, D W, Bullen T D and Turk J T (1997). Strontium 87/strontium 86 as a tracer of mineral weathering reactions and calcium sources in an alpine/subalpine watershed, Loch Vale, Colorado. Water Resources Res., 33, 1335–1351.

Cornell R M and Schwertmann U (2003). The iron oxides. Wiley-VCH, Weinheim, Germany. 2nd edition, 664 p.

Dandurand J L, Gout R, Hoefs J, Menschel G, Schott J and Usdowski E (1982). Kinetically controlled variations of major components and carbon and oxygen isotopes in a calcite-precipitating spring. Chem. Geol., 36, 299–315.

Deshmukh A N, Valadaskar P M and Malpe D B (1995). Fluoride in environment: a review, Gondwana Geol Mag, 9, 1–20.

Deutsch W J (1997). Groundwater geochemistry. Fundamentals and applications to contamination. Lewis Publishers, New York, 221 pp.

Dideriksen K, Christiansen B C, Baker J A, Frandsen C, Balic-Zunic T, Tullborg E K, Mørup S and Stipp S L S (2007). Fe-oxide fracture fillings as a palæo-redox indicator: Structure, crystal form and Fe isotope composition. Chemical Geology, 244, 330–343.

Dogramaci S S, Herczeg A L (2002). Strontium and carbon isotope constraints on carbonate-solution interactions and inter-aquifer mixing in groundwaters of the semi-arid Murray Basin, Australia. J. Hydrology, 262, 50–67.

Dos Santos Afonso M and Stumm W (1992). Reductive dissolution of iron(III) (hydr)oxides by hydrogen sulfide. Langmuir, 8, 1671– 1675.

Drake H and Tullborg E-L (2004). Oskarshamn site investigation. Fracture mineralogy and wall rock alteration Results from drill core KSH01A+B. SKB P-04-250, 120 p.

Drake H and Tullborg E-L (2005). Oskarshamn site investigation. Fracture mineralogy and wall rock alteration. Results from drill cores KAS04, KA1755A and KLX02. SKB P-05-174, 69 p.

Drake H and Tullborg E-L (2006a). Oskarshamn site investigation. Fracture mineralogy. Results from drill core KSH03A+B. SKB P-06-03, 65 p.

Drake H and Tullborg E-L (2006b). Oskarshamn site investigation. Fracture mineralogy of the Götemar granite. Results from drill cores KKR01, KKR02 and KKR03. SKB P-06-04, 61 p.

Drake H and Tullborg E-L (2007). Oskarshamn site investigation. Fracture mineralogy Results from drill cores KLX03, KLX04, KLX06, KLX07A, KLX08 and KLX10A. SKB R-07-74, 132 p.

Drake H and Tullborg E-L (2008). Fracture mineralogy of the Laxemar site. Final report. SKB R-08-99.

Drake H, Sandström B and Tullborg E-L (2006). Mineralogy and geochemistry of rocks and fracture fillings from Forsmark and Oskarshamn: Compilation of data for SR-Can. SKB R-06-109, 105 p.

Drake H, Tullborg E-L and Annersten H (2008). Red-staining of the wall rock and its influence on the reducing capacity around water conducting fractures. Appl. Geochem., 23(7), 1898–1920.

Drever J I (1997). The Geochemistry of Natural Waters: Surface and Groundwater Environments. 3rd ed., Prentice Hall, New York, USA, 436 p.

Drever J I and Hurcomb D R (1986). Neutralization of atmospheric acidity by chemical weathering in an alpine drainage basin in the North Cascade Mountains. Geology, 14, 221–224.

Drysdale R N, Taylor M P and Ihlenfeld C (2002). Factors controlling the chemical evolution of travertine-depositing rivers of the Barkly karst, northern Australia. Hydrol. Process., 16, 2941–2962.

Dzombak D and Morel F M (1990). Surface complexation modeling. Hydrous ferrric oxide. Wiley & Sons, New York, USA, 393 p.

Fanning D S, Rabenhorst M C and Bigham J M (1993). Colors of acid sulfate soils. In: J.M. Bigham and E.J. Ciolkosz (eds.), Soil color. Soil Science Society of America Special Publication Number 31, pp. 91–108.

Frape S K and Fritz P (1987). Geochemical trends for groundwaters from the Canadian Shield. In: P. Fritz and S.K. Frape (eds.), Saline Water and Gases in Crystalline rocks. Geol. Assoc. Can. Spec. Pap., 33, pp. 19–38.

Frape S K, Blyth A, Blomqvist R, McNutt R H and Gascoyne M (2005). Deep fluids in the continents: II. Cryslalline Rocks. In: J.I. Drever (ed.). Surface and ground water, weathering, and soils. Treatise on Geochemistry, vol 5. pp. 541–580. Elsevier.

Frengstad B, Banks D and Siewers U (2001). The chemistry of Norwegian groundwaters: IV. The pH-dependence of element concentrations in crystalline bedrock groundwaters. The Science of the Total Environment, 277, 101–117

Fritz P, Fontes J-C H, Frape S K, Louvat D, Michelot J-L, and Balderer W (1989). The isotope geochemistry of carbon in groundwater at Stripa. Geochim. Cosmochim. Acta, 53, 1765–1775.

Fritz P, Frape S K, Drimmie R J, Appleyard E C and Hattori K (1994). Sulfate in brines in the crystalline rocks of the Canadian Shield. Geochim. Cosmochim. Acta, 58, 57–65.

Gaines G L and Thomas H C (1953). Adsorption studies on clay minerals. II. A formulation of the thermodynamics of exchange adsorption. J. Chem. Phys. 21, 714–718.

Garand A and Mucci A (2004). The solubility of fluorite as a function of ionic strength and solution composition at 25°C and 1 atm total pressure. Marine Chemistry, 91, 27–35.

Garrels, R.M. (1967). Genesis of some ground waters from igneous rocks. In: P.H. Abelson (Ed.), Researches in Geochemistry. Wiley, New York, pp. 405–420.

Garrels R M and Mackenzie F T (1967). Origin of the chemical compositions of some springs and lakes. In: W. Stumm (Ed.), Equilibrium Concepts in Natural Water Systems. Advances in Chemistry Series, 67, American Chemical Society, Washington, DC, pp. 222–242.

Gascoyne M (1999). Long-term maintenance of reducing conditions in a spent fuel nuclear fuel repository. A re-examination of critical factors. SKB R-99-41, 56 p.

Gascoyne M (2004). Hydrogeochemistry, groundwater ages and sources of salts in a granitic batholith on the Canadian Shield, southeastern Manitoba. Applied Geochemistry, 19, 519–560.

Gimeno M J, Auqué L F and Gómez J (2004a). Explorative analysis and mass balance modelling. In: SKB (2004), Hydrogeochemical evaluation of the Simpevarp area, model version 1.1. SKB R-04-16, Appendix 2, pp. 121–164.

Gimeno M J, Auqué, L F and Gómez J (2004b). Mass balance modelling. In: SKB (2004), Hydrogeochemical evaluation of the Simpevarp area, model version 1.2. Preliminary site description of the Simpevarp area. SKB R-04-74, Appendix 4, pp. 289–352.

Gimeno M J, Auqué L F and Gómez J (2004c). Explorative analysis and Mass balance modelling. In: M. Laaksoharju (ed.), Hydrogeochemical evaluation of the Forsmark site, model version 1.1. SKB R-04-05, Appendix 2, pp. 113–160.

Gimeno M J, Auqué L F and Gómez J (2005). PHREEQC modelling. Contribution to the model version 1.2. In: SKB (2005), Hydrogeochemical evaluation. Preliminary site description. Forsmark area, version 1.2. SKB R-05-17, Appendix 3, pp. 263–322.

Gimeno M J, Auqué L F and Gómez J (2006). Mass balance modelling. In: SKB (2006), Hydrogeochemical evaluation. Preliminary site description. Laxemar subarea, version 2.1. SKB R-06-70, Appendix 3, pp. 175–210.

Gimeno M J, Auqué L F and Gómez J (2007). Water-rock interaction modelling issues. In: SKB (2007), Hydrogeochemical evaluation of the Forsmark site, modelling stage 2.1-issue report. SKB R-06-69, Appendix 3, pp. 131–187.

Gimeno M J, Auqué L F, Gómez J and Acero P (2008). Water-rock interaction modelling and uncertainties of mixing modelling. SDM-Site Forsmark. SKB R-08-86, 212 pp.

Glauser S, Weidler P G, Langley S and Beveridge T J (2003). Controls on Fe reduction and mineral formation by a subsurface bacterium. Geochim. Cosmochim. Acta, 67, 1277–1288.

Glynn P D and Voss C I (1999). SITE-94. Geochemical characterization of Simpevarp ground waters near the Äspö Hard Rock laboratory. SKI Report 96-29, SKI, Stockholm, Sweden, 210 p.

Goldich S S (1938). A study on rock weathering. Journal of Geology, 46, 17–58.

Gómez J B, Laaksoharju M, Skårman E and Gurban I (2006). M3 version 3.0: Concepts, methods, and mathematical formulation. SKB TR-06-27.

Gómez J B, Auqué L F and Gimeno M J (2008). Sensitivity and uncertainty analysis of mixing and mass balance calculations with standard and PCA-based geochemical codes. Appl. Geochem., 23 (7), 1941–1956.

Grenthe I, Stumm W, Laaksoharju M, Nilsson A-C and Wikberg P (1992). Redox potentials and redox reactions in deep groundwater systems. Chem. Geol., 98, 131–150.

Grimaud D, Beaucaire C and Michard G (1990). Modelling of the evolution of ground waters in a granite system at low temperature: the Stripa ground waters, Sweden. Applied Geochemistry, 5, 515–525.

Grygara T, Dedecekb J, Kruiverc P P, Dekkersc M J, Bezdickaa P and Schneeweiss O (2003). Iron oxide mineralogy in late Miocene red beds from La Gloria, Spain: rock-magnetic, voltammetric and Vis spectroscopy analyses. Catena, 53, 115–132.

Guimerá J, Duro L, Jordana S and Bruno J (1999). Effects of ice melting and redox front migration in fractured rocks of low permeability. SKB TR 99-19, 86 p.

Guimerá J, Duro L and Delos A (2006). Changes in groundwater composition as a consequence of deglaciation . Implications for performance assessment. SKB R-06-105, 56 p.

Gunnarsson I and Arnorsson S (2000). Amorphous silica solubility and the thermodynamic properties of H4SiO4° in the range of 0° to 350°C at Psat. Geochim. Cosmochim. Acta, 64, 2295–2307.

Guo Q, Wang Y, Ma T and Ma R (2007). Geochemical processes controlling the elevated fluoride concentrations in groundwaters of the Taiyuan Basin, Northern China. J. Geochem. Explor., 93, 1–12.

Gurban I (2008). Forsmark Site: M3 modelling and 2D visualisation of the hydrochemical parameters in Forsmark groundwater. In: Kalinowski, B. (ed). Background complementary hydrogeochemical studies. Site descriptive modelling, SDM-Site Laxemar. SKB R-08-111.

Hallbeck L (2006). Explorative analyses of microbes, colloids and gases. In: SKB (2006) Hydrogeochemical evaluation. Preliminary site description. Laxemar subarea, version 2.1. SKB R-06-70, Appendix 2.

Hallbeck L (2007). Microbial, gas and colloid issues. In: SKB (2007) Hydrogeochemical evaluation of the Forsmark site, modelling stage 2.1-issue report. SKB R-06-69, Appendix 2.

Hallbeck L and Pedersen K (2008a). Explorative analysis of microbes, colloids and gases. SDM-Site Forsmark. SKB R-08-85.

Hallbeck L and Pedersen K (2008b). Explorative analysis of microbes, colloids and gases. SDM-Site Laxemar. SKB R-08-109.

Hallbeck L and Pedersen K (2008c). Characterization of microbial processes in deep aquifers of the Fennoscandian Shield. Appl. Geochem., 23(7), 1796–1819.

Hallberg G R and Keeney D R (1993). Nitrate. In: W.M. Alley (ed.), Regional Ground-Water Quality. Van Nostrand Reinhold, New York. Chapter 12, pp. 297–322.

Hanor J S (1996). Variations in chloride as a driving force in siliciclastic diagenesis. In: L.J. Crosey, R. Loucks and M.W. Totten (eds.) Siliciclastic Diagenesis and Fluid Flow: Concepts and Applications. SEPM Special Publication 55, Society for Sedimentary Geology, pp. 3–12.

Hanor J S (2001). Reactive transport involving rock-buffered fluids of varying salinity. Geochim. Cosmochim. Acta, 21, 3721–3732.

Haveman S and Pedersen K (2002). Distribution of culturable microorganisms in Fennoscandian Shield groundwater. FEMS Microbiology Ecology, 39, 129–1337.

Heaney P J and Post J E (1992). The widespread distribution of a novel silica polymorph in microcrystalline quartz varieties. Science, 255, 441–443.

Helgeson H C (1969). Thermodynamics of hydrothermal systems at elevated temperatures. Am. J. Sci., 267, 729–804.

Helgeson H C (1970). Description and interpretation of phase relations in geochemical processes involving aqueous solutions. Am. J. Sci., 268, 415–438.

Helgeson H C, Delany J M, Nesbitt H W and Bird D K (1978). Summary and critique of thermodynamic properties of rock forming minerals. Am. J. Sci., 278-A.

Hem J D (1985). Study and interpretation of the chemical characteristics of natural water. U.S. Geological Survey Water-Supply Paper 2254, 264 p.

Holloway J M, Dahlgren R A and Casey W H (2001). Nitrogen release from rock and soil under simulated field conditions. Chem. Geol., 174, 403–414.

Houben G J (2003). Iron oxide incrustations in wells. Part 1: genesis, mineralogy and geochemistry. Appl. Geochem., 18 (6), 927–939.

Hund F (1981). Inorganic pigments: basis for colored, uncolored and transparent properties. Angew. Chem. Int. Edit., 20, 723–730.

Hurtgen M, Lyons T, Ingall E D, Cruse A (1999). Anomalous enrichments of iron monosulphide in euxinic marine sediments and the role of H2S in iron sulphide transformations: examples from Effingham inlet, Orca Basin, and the Black Sea. Am. J. Sci., 299, 556–588.

Hyacinthe C, Bonneville S and Van Cappellen P (2006). Reactive iron(III) in sediments: Chemical versus microbial extractions. Geochim. Cosmochim. Acta, 70, 4166–4180.

Iwatsuki T, Furue R, Mie H, Ioka S and Mizuno T (2005). Hydrochemical baseline condition of groundwater at the Mizunami underground research laboratory (MIU). Appl. Geochem., 20, 2283–2302.

Jacks G, Bhattacharya P, Chaudhary V and Singh K P (2005). Controls on the genesis of some high-fluoride groundwater in India. Applied Geochemistry, 20, 221–228.

Jacobson A D and Blum J D (2000). Ca/Sr and 87Sr/86Sr geochemistry of disseminated calcite in Himalayan silicate rocks from Nanga Parat: Influence on river-water chemistry. Geology, 28, 463–466.

Jacobson A D, Blum J D, Chamberlain C P, Poage M A and Sloan V F (2002). Ca/Sr and Sr isotope systematics of a Himalayan glacial chronosequence: Carbonate versus silicate weathering rates as a function of landscape surface age. Geochim. Cosmochim. Acta, 66, 13–27.

Jacobson R L and Usdowski E (1975). Geochemical controls on a calcite precipitating spring. Contrib. Mineral. Petrol., 51, 65–74.

Jaisi D P, Dong H and Liu C (2007). Influence of biogenic Fe(II) on the extent of microbial reduction of Fe(III) in clay minerals nontronite, illite, and chlorite. Geochim. Cosmochim. Acta, 71, 1145–1158.

Jakobsen R and Cold L (2007). Geochemistry at the sulfate reduction–methanogenesis transition zone in an anoxic aquifer. A partial equilibrium interpretation using 2D reactive transport modeling. Geochim. Cosmochim. Acta, 71, 1949–1966

Jakobsen R and Postma D (1999). Redox zoning, rates of sulfate reduction and interactions with Fe-reduction and methanogenesis in a shallow sandy aquifer, Rømø, Denmark. Geochim. Cosmochim. Acta, 63, 137–151.

Jensen D L, Boddum J K, Tjell J C and Christensen T H (2002). The solubility of rhodochrosite (MnCO3) and siderite (FeCO3) in anaerobic aquatic environments. Applied Geochemistry, 17, 503–511.

JNC (2000). H12: Project to establish the scientific and technical basis for HLW disposal in Japan. Supporting Report 3, Safety Assessment of the Geological Disposal System. TN1410 2000-004, Japan Nuclear Cycle Development Institute, Japan.

Johnson J W, Oelkers E H and Helgeson H C (1992). SUPCRT92: a software package for calculating the standard molal thermodynamic properties of minerals, gases, aqueous species and reactions from 1 to 5000 bars and 0 to 1000°C. Comp. Geosci., 18, 899–947.

Kamineni D C (1983). Sulfur-isotope geochemistry of fracture-filling gypsum in an archean granite near Atikokan, Ontario, Canada. Chem. Geol., 39, 263–272.

Karltun E, Bain D C, Gustafsson J P, Mannerkoski H, Murad E, Wagner U, Fraser A R, McHardy W J and Starr M (1998). Surface reactivity of poorly ordered minerals in podzol B horizons. Geoderma, 94, 265–288.

Katz B G and Bullen T D, 1996. The combined use of 87Sr/86Sr and carbon and water isotopes to study the hydrochemical interaction between groundwater and lakewater in mantled karst. Geochim. Cosmochim. Acta, 60, 5075–5087.

Kehew A E (2001). Applied chemical hydrogeology. Prentice Hall, 368 p.

Kerker M, Scheiner P, Cooke D D and Kratohvil J P (1979). Absorbance index and color of colloidal hematite. J. Colloid Interf. Sci., 71, 176–187.

Kim K and Jeong G Y (2005). Factors influencing natural occurrence of fluoride-rich groundwaters: a case study in the southeastern part of the Korean Peninsula. Chemosphere, 58, 1399–1408.

Kölling M (2000). Comparison of different methods for redox potential determination in natural waters. In:L. Schüring, H.D. Schulz, W.R. Fischer, J. Böttcher and W.H.M. Duijnisveld (eds), Redox. Fundamentals, processes and applications. Springer. Chapter 4, 42–54.

Konhauser K (2007). Introduction to geomicrobiology. Blackwell Publishing, 425 p.

Kostka J E, Stucki J W, Nealson K H and Wu J (1996). Reduction of structural Fe(III) in smectite by a pure culture of Shewanella putrefaciens strain MR-1. Clays Clay Miner., 44, 522–529.

Kostka J E, Dalton D D, Skelton H, Dollhopf S and Stucki J W (2002). Growth of Iron(III)-reducing bacteria on clay minerals as the sole electron acceptor and comparison of growth yields on a variety of oxidized iron forms. Applied and Environmental Microbiology, 68, 6256–6262.

Krohn M D, Evans J and Robinson G R Jr, (1998). Mineral-bound ammonium in black shales of the Triassic Cummock Formation, Deep River basin, North Carolina. U.S. Geological Survey Bulletin, 1776, 86–98.

Kuivila K M, Murray J W, Devol A H and Novelli P C (1989). Methane production, sulfate reduction and competition for substrates in the sediments of Lake Washington. Geochim. Cosmochim. Acta, 53, 409–416.

Kukkadapu R K, Zachara J M, Fredrickson J K, McKinley J P, Kennedy D W, Smith S C and Dong H (2006). Reductive biotransformation of Fe in shale–limestone saprolite containing Fe(III) oxides and Fe(II)/Fe(III) phyllosilicates. Geochim. Cosmochim. Acta, 70, 3662–3676.

Kulik D, Kersten M, Heiser U and Neumann T (2000). Application of Gibbs energy minimization to model early-diagenetic solid-solution aqueous-solution equilibria involving authigenic rhodochrosites in anoxic Baltic Sea sediments. Aquatic Geochemistry, 6, 147–199.

Laaksoharju M and Wallin B (Ed) (1997). Evolution of the groundwater chemistry at the Äspö Hard Rock Laboratory. Proceedings of the second Äspö International Geochemistry Workshop, Äspö, Sweden, June 6–7, 1995. SKB 97-04, Stockholm, Sweden.

Laaksoharju M, Smellie J, Tullborg E-L, Gimeno M, Hallbeck L, Molinero J and Waber N (2008). Bedrock hydrogeochemistry, Forsmark. Site descriptive modelling. SDM-Site Forsmark. SKB R-08-47.

Laaksoharju M (Ed) (2008). Bedrock hydrogeochemistry, Laxemar. Site descriptive modelling. SDM-Site Laxemar. SKB R-08-93.

Landström O and Tullborg E L (1990). The influence of fracture mineral/groundwater interaction on the mobility of U, Th, REE and other trace elements. SKB Technical Report 90-37, 71 p.

Langmuir D (1969). The Gibbs free energies of substances in the system Fe-O2-H2O-CO2 at 25 °C. Geological Survey Research, 1969. U.S.G.S. Prof. Paper, Vol. 650-B, pp. B180–B184.

Langmuir D (1997). Aqueous environmental geochemistry. Prentice Hall, 600 p.

Langmuir D and Melchior D (1985). The geochemistry of Ca, Sr, Ba and Ra sulfates in some deep brines from the Palo Duro Basin, Texas. Geochim. Cosmochim. Acta, 49, 2423–2432.

Langmuir D and Whittemore D O (1971). Variations in the stability of precipitated ferric oxyhydroxides. In: J.D. Hem (Ed.), Nonequilibrium Systems in Natural Water Chemistry. Advances in Chemistry Series, 106. Amer. Chem. Soc., Washington, D.C. Chapter 8, pp. 209–234.

Larsen O and Postma D (2001). Kinetics of the reductive bulk dissolution of lepidocrocite, ferrihydrite, and goethite. Geochim. Cosmochim. Acta, 65, 1367–1379.

Lasaga A C (1984). Chemical kinetics of water-rock interactions. Journal of Geophysical Research, 89, 4009–4025.

Lindborg T (ed) (2006). Description of surface systems. Preliminary site description Laxemar subarea – version 1.2. SKB R-06-11,

Lindberg R D and Runnells D D (1984). Ground water redox reactions: an analysis of equilibrium state applied to Eh measurements and geochemical modeling. Science, 22, 92–927.

Louvat D, Michelot J L and Aranyossy J F (1999). Origin and residence time of salinity in the Äspö groundwater system. Appl. Geochem., 14, 917–925.

Lovley D R and Goodwin S (1988). Hydrogen concentrations as an indicator of the predominant terminal electron-accepting reactions in aquatic sediments. Geochim. Cosmochim. Acta, 52 (12), 2993–3003.

Lovley D R and Phillips E J P (1988). Novel mode of microbial energy metabolism: organic carbon oxidation coupled to dissimilatory reduction of iron or manganese. Appl. Environ. Microbiol. 54, 1472–1480.

Lovley D R, Holmes D E and Nervin K-P (2004). Dissimilatory Fe(III) and Mn (IV) reduction. Advances in Microbial Physiology, 49, 219–286.

Lundin L, Lode E, Stendahl J, Melkerud P-A, Björkvald L and Thorstensson A (2004). Soils and site types in the Forsmark area. SKB Report R-04-08, 102 p.

Lundin L, Lode E, Stendahl J, Björkvald L and Hansson J (2005). Oskarshamn site investigation. Soils and site types in the Oskarshamn area. SKB R-05-15, 96 p.

Luukkonen A (2006). Estimations of Durability of Fracture Mineral Buffers in the Olkiluoto Bedrock. Posiva Working Report 2006-107, 38 p.

Macalady D L, Langmuir D, Grundl T and Elzerman A (1990). Use of model-generated Fe3+ ion activities to compute Eh and ferric oxyhydroxide solubilities in anaerobic systems. In: D.C. Melchior and R.L. Basett (Editors), Chemical Modeling of Aqueous Systems II. A.C.S. Symp. Ser. 416. Amer. Chem. Soc., Washington, D.C., pp. 350–367.

Mahlknecht J, Garfias-Solis J, Aravena R and Tesch R (2006). Geochemical and isotopic investigations on groundwater residence time and flow in the Independence basin, Mexico. Journal of Hydrology, 324, 283–300.

Majzlan J, Navrotsky A and Schwertmann U (2004). Thermodynamics of iron oxides: Part III. Enthalpies of formation and stability of ferrihydrite (~Fe(OH)3), schwertmannite (~FeO(OH)3/4(SO4)1/8), and ε-Fe2O3. Geochim. Cosmochim. Acta, 68, 1049–1059.

Maliva R G and Siever R (1988). Pre-Cenozoic nodular cherts: evidence for Opal-CT precursors and direct quartz replacement. Am. J. Sci., 288, 798–809.

Malusa J, Overby S T and Parnell R A (2003) Potential for travertine formation: Fossil Creek, Arizona. Appl. Geochem., 18, 1081–1093.

Massmann G, Pekdeger A, Merz C (2004). Redox processes in the Oderbruch polder groundwater flow system in Germany. Appl. Geochem., 19 (6), 863–886.

Matsunaga T, Karametaxas G, von Gunten H R and Lichtner P C (1992). Redox chemistry of iron and manganese minerals in river-recharged aquifers: A model interpretation of a column experiment. Geochim. et Cosmochim. Acta, 57, 1691–1704.

McCauley S E and DePalo D J (1997). The marine 87Sr/86Sr and 18O records, Himalayan alkalinity fluxes and Cenozoic climate models. In Tectonic Uplift and Climate Change (ed. W. F. Ruddiman). Plenum Press.

McKenzie F T, Garrels R M, Bricker O P and Bickley F (1967). Silica in sea water: control by silica minerals. Science, 155, 1404–1405.

McNutt R H (2000). Strontium isotopes. In: Cook, P.G., Herczec, A.L. (Eds.), Environmental Tracers in Subsurface Hydrology. Kluwer Academic Publishers, Boston, pp. 233–260.

Melkenud P-A, Olsson M and Rosén K (1992). Reports in forest ecology and forest soils Number 65. SLU. Uppsala.

Michard G (1987). Controls of the chemical composition of geothermal waters. In: H.C. Helgeson (Editor), Chemical Transport in Metasomatic Processes. NATO (North Atlantic Treaty Org.). ASI (Adv. Sci. Inst.). Ser. C. 218: 323–353.

Michard G, Pearson F J Jr and Gautschi A (1996). Chemical evolution of waters during long term interaction with granitic rocks in northern Switzerland. Appl. Geochem., 11, 757–774.

Milodowski A E, Tullborg E-L, Buil B, Gomez P, Turrero M-J, Haszeldine S, England G, Gillespie M R, Torres T, Ortiz J, Zacharias E, Silar J, Chvatal M, Strand L, Sebek O, Bouch, J, Chenery S R, Chenery C, Sheperd T J and Mc Kervey J A (2005). Application of Mineralogical, Petrological and Geochemical tools for Evaluating the Palaeohydrogeological Evolution of the PADAMOT Study Sites. PADAMOT Project Technical Report WP2.

Molinero J, Salas J, Arcos D and Duro L (2008). Integrated hydrogeological and geochemical modelling of the Laxemar-Simpevarp area during the recent Holocene (last 8000 years). In: Kalinowski, B. (ed.), Background complementary hydrogeochemical studies. SKB R-08-111.

Morse J W and Arvidson R S (2002). The dissolution kinetics of major sedimentary carbonate minerals. Earth-Science Reviews, 58, 51–84.

Navarre-Sitchler A and Thyne G (2007). Effects of carbon dioxide on mineral weathering rates at earth surface conditions. Chem. Geol., 243, 53–63.

Neal C, Neal M, Reynolds B, Maberly S C, May L, Ferrier R C, Smith J and Parker J E (2005). Silicon concentrations in UK surface waters. Journal of Hydrology, 304, 75–93.

Nealson K H and Saffarini D (1994). Iron and manganese in anaerobic respiration: environmental significance, physiology and regulation. Annual Reviews of Microbiology, 48, 311–343.

Neumann T, Heiser U, Leosson M A and Kersten M (2002). Early diagenetic processes during Mn-carbonate formation: evidence from the isotopic composition of authigenic Ca-rhodochrosites of the Baltic Sea. Geochim. Cosmochim. Acta, 66, 867–879.

Nilsson A C (2008). Laxemar site investigation: Quality of hydrochemical analyses (DF version 2.3. In: Kalinowski, B. (ed.), Background complementary hydrogeochemical studies. SKB R-08-111.

Nordstrom D K (2005). Moldeling low-temperature geochemical processes. In: J.I. Drever (ed.), Surface and ground waters, weathering, and soils. Treatise on Geochemistry, 5. Elsevier, pp. 37–72.

Nordstrom D K and Ball J W (1989). Mineral saturation states in natural waters and their sensitivity to thermodynamic and analytical errors. Sci. Geol. Bull., 42 (4), 269–280.

Nordstrom D K and Jenne E A (1977). Fluoride solubility in selected geothermal waters. Geochim. Cosmochim. Acta, 41, 175–188.

Nordstrom D K and Munoz J L (1985). Geochemical Thermodynamics. 2nd Ed. The Benjamin/Cummings Publ. Co., Menlo Park, California, 477 pp.

Nordstrom D K and Puigdomènech I (1986). Redox chemistry of deep ground-waters in Sweden. SKB TR 86-03, 30 p.

Nordstrom D K, Andrews J N, Carlsson L, Fontes J C, Fritz P, Moser H and Olsson T (1985). Hydrogeological and hydrochemical investigations in boreholes. Final report of the Phase I geochemical investigations of the Stripa groundwaters. Stripa Project Technical Report 85-06. SKB, Sweden.

Nordstrom D K, Ball J W, Donahoe R J and Whittemore D (1989). Groundwater chemistry and water–rock interactions at Stripa. Geochim Cosmochim Acta, 53, 1727–1740.

Nordstrom D K, Plummer L N, Langmuir D, Busenberg E, May H M, Jones B F and Parkhurst D (1990). Revised chemical equilibrium data for major water-mineral reactions and their limitations. In: Melchior, D.C. and Basset, R.L. (Eds.) Chemical Modeling of Aqueous Systems II. ACS Symp. Ser. pp. 398–413.

Öborn I and Berggren D (1995). Characterization of jarosite-natrojarosite in two northern Scandinavian soils. Geoderma, 66, 213–215.

Oliva P, Viers J, and Dupre B (2003). Chemical weathering in granitic environments. Chemical Geology, 202, 225–256.

Park J, Sanford R A and Bethke C M (2006). Geochemical and microbiological zonation of the Middendorf aquifer, South Carolina. Chem. Geol., 230, 88–104.

Parkhurst D L and Appelo C A J (1999). User's Guide to PHREEQC (Version 2), a computer program for speciation, batch-reaction, one-dimensional transport, and inverse geochemical calculations. Water Resources Research Investigations Report 99-4259, 312 p.

Parks G A (1984). Surface and interfacial energy of quartz. J. Geophys. Res., 89, 3997–4008.

Pedersen H, Postma D, Jakobsen R and Larsen O (2005). Fast transformation of iron oxyhydrosxides by the catalytic action of aqueous Fe(II). Geochim. Cosmochim. Acta, 16, 3967–3977.

Pedersen K (1997). Investigations of subterranean microorganisms and their importance for performance assessment of radioactive waste disposal. Results and conclusions achieved during the period 1995 to 1997. SKB-TR-97-22, 284 pp.

Pedersen K (2008). Microbiology of Olkiluoto Groundwater. 2004–2006. Posiva, 2008-02, 156 p.

Pedersen K and Karlson F (1995). Investigations of subterranean microorganisms- their importance for performance assessment of radioactive waste disposal. SKB TR 95-10, 222 pp.

Pedersen K, Ekendahl S, Tullborg E-L, Furnes H, Thorseth I-G and Tumyr O (1997). Evidence of ancient life at 207 m depth in a granitic aquifer. Geology, 25, 827–830.

Peiffer S (2000). Characterization of the redox state of aqueous systems – towards a problem oriented approach. In: Schuering, J., Schulz, H.D., Fischer, W.R., Boettcher, J., Duijnesveld, W.H.M. (Eds.), Redox–Fundamentals, Processes and Measuring Techniques. Springer Verlag, Berlin.

Petersson J, Berglund J, Danielsson P, Wängnerud A Tullborg E-L, Mattsson H, Thunehed H, Isaksson H and Lindroos H (2004). Forsmark site investigation. Petrography, geochemistry, petrophysics and fracture mineralogy of boreholes KFM01A, KFM02A and KFM03A+B. SKB P-04-103, 48 p.

Pitkänen P, Luukkonen A, Ruotsalainen P, Leino-Forsman H and Vuorinen U (1999). Geochemical modelling of groundwater evolution and residence time at the Olkiluoto site. Posiva report 98-10, 184 p.

Pitkänen P, Partamies S and Luukkonen A (2004). Hydrogeochemical interpretation of baseline groundwater conditions at the Olkiluoto site. Posiva report 2003-07, 159 p.

Plummer L N and Busemberg E (1982). The solubilities of calcite, aragonite and vaterite in CO2-H2O solutions between 0 and 90 °C, and an evaluation of the aqueous model for the system CaCO3- CO2-H2O. Geochim. Cosmochim. Acta, 46, 1011–1040.

Plummer L N, Busby J F, Lee R W and Hanshaw B B (1990). Geochemical modeling of the Madison Aquifer in parts of Montana, Wyoming and South Dakota. Water Resour. Res., 26(9), 1981–2014.

Posiva (2005). Olkiluoto Site Description 2004. Posiva 2005-03, 122 p.

Postma D (1985). Concentration of Mn and separation from Fe in sediments. I. Kinetics and stoichiometry of the reaction between birnessite and dissolved Fe(II) at 10 °C. Geochim. Cosmochim. Acta, 49, 1023–1033.

Postma D (1993). The reactivity of iron oxides in sediments: a kinetic approach. Geochim. Cosmochim. Acta, 57, 5027–5034.

Postma D, and Jakobsen R (1996). Redox zonation: Equilibrium constraints on the Fe(III)/SO4-reduction interface. Geochim. Cosmochim. Acta, 60, 3169–3175.

Postma D E, Larsen F, Thi Minh Hue N, Duc M T, Hung Viet P, Quy Nhan P and Jessen S (2007). Arsenic in groundwater of the Red River floodplain, Vietnam: Controlling geochemical processes and reactive transport modeling. Geochim. Cosmochim. Acta, 71, 5054–5071.

Poulton S W, Krom M D and Raiswell R (2004). A revised scheme for the reactivity of iron (oxyhydr)oxide minerals towards dissolved sulfide. Geochim. Cosmochim.Acta, 68, 3703–3715.

Puigdomènech I (2001). Hydrochemical stability of groundwaters surrounding a spent nuclear fuel repository in a 100,000 year perspective. SKB Technical Report 01-28, 83 p.

Raiswell R and Canfield D E (1996). Rates of reaction between silicate iron and dissolved sulfide in Peru Margin sediments. Geochim. Cosmochim. Acta, 60, 2777–2787.

Raymo M E and Ruddiman W F (1992). Tectonic forcing of late Cenozoic climate. Nature, 359, 117–122.

Rezaei M, Sanz E, Raeisi E, Ayora C, Vazquez-Sune E, Carrera J (2005). Reactive transport modeling of calcite dissolution in the fresh-salt water mixing zone. J. Hydrol., 311 (1–4), 282–298.

Rickard D T (1989). Experimental concentration-time curves for the iron (II) sulphide precipitation process in aqueous solutions and their interpretation. Chem. Geol., 78, 315–324.

Rickard D T (1995). Kinetics of FeS precipitation. Part 1, competing reaction mechanisms. Geochim. Cosmochim. Acta, 59, 4367–4379.

Rickard D T (2006). The solubility of FeS. Geochim. Cosmochim. Acta, 70, 5779–5789.

Rickard D T and Luther III G W (2007). Chemistry of Iron Sulfides. Chem. Rev., 107, 514–562

Rickard D T and Morse J W (2005). Acid volatile sulfide (AVS). Marine Chemistry, 97, 141–197.

Rimstidt D D (1997). Quartz solubility at low temperatures. Geochim. Cosmochim. Acta, 61, 2553–2558.

Roden E E (2003). Fe(III) oxide reactivity toward biological vs. chemical reduction. Environ. Sci. Technol., 37, 1319–1324.

Roden E E (2004). Analysis of long-term bacterial vs. chemical Fe(III) reduction kinetics. Geochim. Cosmochim. Acta, 68, 3205–3216.

Roden E E (2006). Geochemical and microbiological controls on dissimilatory iron reduction. C. R. Geoscience, 338, 456–467.

Roden E E and Urrutia M M (2002). Influence of biogenic Fe(II) on bacterial crystalline Fe(III) oxide reduction. Geomicrobiol. J., 19, 209–251.

Roden E E and Zachara J M (1996). Microbial reduction of crystalline iron (III) oxides: influence of oxide surface area and potential cell growth. Environ. Sci. Technol., 30, 1618–1628.

Rudmark L, Malmberg Persson K and Mikko H (2005). Oskarshamn site investigation. Investigation of Quaternary deposits 2003–2004. SKB P-05-498.

Sandström B and Tullborg E-L (2005). Forsmark site investigation. Fracture mineralogy. Results from fracture minerals and wall rock alteration in boreholes KFM01B, FM04A, KFM05A and KFM06A. SKB P-05-197, 151 p

Sandström B, Savolainen M and Tullborg E-L (2004). Forsmark site investigation. Fracture mineralogy. Results from fracture minerals and wall rock alteration in boreholes KFM01A, KFM02A, KFM03A and KFM03B. SKB P-04-149, 93 p.

Sasamoto H, Yui M and Arthur R C (2004). Hydrochemical characteristics and groundwater evolution modeling in sedimentary rocks of the Tono mine, Japan. Physics and Chemistry of the Earth, 29, 43–54.

Sasamoto H, Yui M and Arthur R C (2007). Estimation of in situ groundwater chemistry using geochemical modelling: a test case for saline type groundwater in argillaceous rock. Physics and Chemistry of the Earth, 32, 196–208.

Saxena V K and Ahmed S (2001). Dissolution of fluoride in groundwater: a water–rock interaction study. Environ Geol., 40, 1084–1087.

Schüring J, Schlieker M and Hencke J (2000). Redox Fronts in Aquifer Systems and Parameters Controlling their Dimensions. In: J. Schüring, H.D. Schulz, WR. Fischer, J. Böttcher and W.H.M. Duijnisveld (eds.) Redox: Fundamentals, Processes and Applications. Springer-Verlag Berlin Heidelberg New York, 251 pp.

Schwertmann U (1993). Relations between iron oxides, soil color, and soil formation. In: J.M. Bigham and E.J. Ciolkosz (eds.), Soil color. Soil Science Society of America Special Publication Number 31, pp. 51–69.

Schwertmann U and Murad E (1983). Effect of pH on formation of goethite and hematite from ferrihydrite, Clays and Clay Minerals, 31, 277–284.

Schwertmann U and Taylor R M (1989). Iron oxides. In: J.B. Dixon and S.B. Weed. Minerals in soil environments. Soil Sci. Soc. Am. Book Series 1, Madison, Wisconsin, USA, pp. 379–438.

SKB (2001). Site Investigations: Investigation Methods and General Execution Programme. SKB TR-01-29.

SKB (2004a). Hydrogeochemical evaluation of the Simpevarp area, model version 1.1. SKB R-04-16, 398 pp.

SKB (2004b). Hydrogeochemical evaluation for Simpevarp model version 1.2. Preliminary site description of the Simpevarp area. SKB R-04-74, 463 p.

SKB (2005a). Hydrogeochemical evaluation Preliminary site description. Forsmark area, version 1.2. SKB R-05-17, 403 p.

SKB (2005b). Preliminary site description. Forsmark area – version 1.2. SKB R-05-18, 752 p.

SKB (2006a). Hydrogeochemical evaluation. Preliminary site description Laxemar subarea, version 1.2. SKB R-06-12, 435 pp.

SKB (2006b). Hydrogeochemical evaluation. Preliminary site description Laxemar subarea, version 2.1. SKB R-06-70, 337 pp.

SKB (2006c). Site descriptive modelling. Forsmark stage 2.1. Feedback for completion of the site investigation including input from safety assessment and repository engineering. SKB R-06-38, 444 p.

Smellie J A T and Laaksoharju M (1992). The Äspö Hard Rock Laboratory: Final evaluation of the hydrogeochemical pre-investigations in relation to existing geologic and hydraulic conditions. SKB TR 92-31, 239 p.

Smellie J A T and Tullborg E-L (2005). Explorative analysis and expert judgement of major components and isotopes. Contribution to the model version 1.2 In: Hydrogeochemical evaluation. Preliminary site description. Forsmark area. Version 1.2. SKB R-05-17, 403 p.

Smellie J, Tullborg E-L and Waber N (2006). Explorative analysis and expert judgement of major components and isotopes. Contribution to the model version 2.1. In: SKB(2006), Hydrogeochemical evaluation. Preliminary site description. Laxemar subarea, version 2.1. SKB R-06-70, 337 p.

Smellie J and Tullborg E-L (2009). Documentation related to categorisation of the extended data freeze Laxemar 2.3 groundwater samples.In: Kalinowski (ed) Background Complementary hydrogeochemical studies. Site descriptive modelling SDM-Site Laxemar. SKB R-08-111.

Sohlenius G and Öborn I (2004). Geochemistry and partitioning of trace metals in acid sulphate soils in Sweden and Finland before and after sulphide oxidation. Geoderma, 122, 167–175.

Sohlenius G and Rudmark L (2003). Forsmark site investigation. Mapping of unconsolidated Quaternary deposits. Stratigraphical and analytical data. SKB P-03-14, 29 pp.

Sohlenius G, Bergman T, Snäll S, Lundin L, Lode E, Stendahl J, Riise A, Nilsson J, Johansson T and Göransson M (2006). Oskarshamn site investigation. Soils, Quaternary deposits and bedrock in topographic lineaments situated in the Simpevarp subarea. SKB P-06-121, 180 pp.

Stauffer R E and Wittchen B D (1991). Effects of silicate weathering on water chemistry in forested, upland, felsic terraine of the USA. Geochim. Cosmochim. Acta, 55, 3253–3271.

Stefánsson A, Arnórsson S and Sveinbjörnsdóttir A E (2005). Redox reactions and potentials in natural waters at disequilibrium. Chem. Geol., 221, 289–11.

Stipp S L S, Hansen M, Kristensen R, Hochella J M F, Bennedsen L, Dideriksen K, Balic-Zunic T, Léonard D and Mathieu H J (2002). Behaviour of Fe-oxides relevant to contaminant uptake in the environment. Chemical Geology, 190, 321–337.

Stucki J W, Komadel P and Wilkinson H T (1987). Microbial reduction of structural iron(III) in smectites. Soil Sci. Soc. Am. J., 51, 1663–1665.

Stumm W and Morgan J J (1996). Aquatic Chemistry. Chemical equilibria and rates in natural waters. 3rd ed., John Wiley & Sons, New York, USA, 1022 p.

Suarez D L (1983). Calcite supersaturation and precipitation kinetics in lower Colorado River, All American canal and east highland canal. Water Resour. Res., 19, 653–661.

Thorstenson D C (1984). The concept of electron activity and its relation to redox potentials in aqueous geochemical systems. USGS Open-File Report 84-072, U.S. Geol. Survey, Denver, Colorado, USA.

Thorstenson D C, Fisher D W, and Croft M G (1979). The geochemistry of the Fox Hills-Basal Hell Creek aquifer in Southwestern North Dakota and Northwestern South Dakota. Water Resour. Res., 15, 1479–1498.

Todorova S G, Siegel D I and Costello A M (2005). Microbial Fe(III) reduction in a minerotrophic wetland – geochemical controls and involvement in organic matter decomposition. Appl. Geochem., 20, 1120–1130.

Tröjbom M and Söderbäck B (2006a). Chemical characteristics of surface systems in the Forsmark area. Visualization and statistical evaluation of data from surface waters, precipitation, shallow groundwater, and regolith. SKB R-06-18, 230 p.

Tröjbom M and Söderbäck B (2006b). Chemical characteristics of surface systems in the Simpevarp area. Visualization and statistical evaluation of data from surface waters, precipitation, shallow groundwater, and regolith. SKB R-06-19, 164 p.

Tröjbom M Söderbäck B and Kalinowski B (2008). Hydrochemistry in surface and shallow groundwater. Site descriptive modelling. SDM-site, Laxemar. SKB R-08-46.

Trolard E, Genin J M R, Abdelmoula M, Bourrié G, Humbert B and Herbillon A (1997). Identification of a green rust mineral in a reductomorphic soil by Mossbauer and Raman spectroscopies. Geochim. Cosmochim. Acta, 61, 1107–1111.

Trotignon L, Beaucaire C, Louvat D and Aranyossy J F (1997). Equilibrium geochemical modelling of Äspö groundwaters: a sensitivity study to model parameters. In: M. Laaksoharju, B. Wallin (Editors), Evolution of the Groundwater Chemistry at the Äspö Hard Rock Laboratory. Proceedings of the Second Äspö International Geochemistry Workshop, June 6–7, 1995. SKB ICR-97-04.

Trotignon L, Beaucaire C, Louvat D and Aranyossy J F (1999). Equilibrium geochemical modelling of Äspö groundwaters: a sensitivity study of thermodynamic equilibrium constants. Appl. Geochem, 14, 907–916.

Trotignon L, Michaud V, Lartigue J-E, Ambrosi J-P, Eisenlohr L, Griffault L, de Combarieu M and Daumas S (2002). Laboratory simulation of an oxidizing perturbation in a deep granite environment. Geochim. Cosmochim. Acta, 66, 2583–2601.

Tullborg E L (1989). The influence of recharge water on fissure-filling minerals. A study from Klipperas, southern Sweden. Chem. Geol., 76, 309–320.

Tullborg E-L (1995). Mineralogical/Geochemical Investigations in the Fracture Zone. In: S. Banwart (Ed.), The Redox experiment in block scale. Chapter 4. SKB PR-25-95-06, pp. 81–101.

Tullborg E-L, Landström O and Wallin B (1999). Low-temperature trace element mobility influenced by microbial activity. Indications from fracture calcite and pyrite in crystalline basement. Chem. Geol., 157, 199–218.

Tullborg E-L, Smellie J A T and MacKenzie A B (2003). The use of natural uranium decay series studies in support of understanding redox conditions at potential radioactive waste disposal sites, MRS, Scientific basis for Nuclear Waste Management XXVII vol. 807, pp. 571–576.

Urrutia M M, Roden E, Fredrickson J K and Zachara J (1998). Microbial and geochemical controls on synthetic Fe(III) oxide reduction by Shewanella alga strain BrY. Geomicrobiol. J., 15, 269–291.

Wacker P, Berg C and Bergelin A (2004). Oskarshamn site investigation. Complete hydrochemical characterisation in KSH01A.Results from four investigated sections, 156.5–167.0, 245.0–261.6, 586.0–596.7 and 548.0–565.4 metres. SKB P-04-12, 72 p.

Wallin B and Peterman Z (1999). Calcite fracture fillings as indicators of paleohydrology at Laxemar at the Äspö Hard Rock Laboratory, southern Sweden. Appl. Geochem., 14, 953–962

Watson I A, Oswald S E, Ulrich Mayer K, Wu Y and Banwart S A (2003). Modelling kinetic processes controlling hydrogen and acetate concentrations in aquifer-derived microcosm. Environ. Sci. Technol., 37, 3910–3919.

Weaver C E (1989). Clays, Muds, and Shales. Developments in Sedimentology, n° 44. Elsevier, New York.

Weber K A, Achenbach L A and Coates J D (2006). Microorganisms pumping iron: anaerobic microbial iron oxidation and reduction. Nature Rev. Microbiol., 4, 752–764.

White A F and Brantley S L (1995). Chemical weathering rates of silicate minerals: an overview. In: A. F. White and S. L. Brantley (ed.), Chemical Weathering Rates of Silicate Minerals. Reviews in Mineralogy and Geochemistry, vol. 31.Mineralogical Society of America, pp. 1–22.

White A F, Blum A E, Schulz M S, Bullen T D, Harden J W and Peterson M L (1996). Chemical weathering of a soil chronosequnece on Granitic Alluvium. 1. Reaction rates based on changes in soil mineralogy. Geochim. Cosmochim. Acta, 60, 2533–2550.

White A F, Blum A E, Schulz M S, Vivit D S, Stonestrom D A, Larsen M , Murphy S F and Eberl D (1998). Chemical weathering in a tropical watershed, Luquillo Mountains, Puerto Rico: I. Long-term versus short term weathering fluxes. Geochim. Cosmochim. Acta, 62, 209–226.

White A F, Blum A E, Bullen T D, Vivit D V, Schulz M and Fitzpatrick J (1999a). The effect of temperature on experimental and natural weathering rates of granitoid rocks. Geochim. Cosmochim. Acta, 63, 3277–3291.

White A F, Bullen T D, Vivit D V and Schulz M S (1999b). The role of disseminated calcite in the chemical weathering of granitoid rocks. Geochim. Cosmochim. Acta, 63, 1939–1953.

White A F, Bullen T D, Schulz M S, Blum A E, Huntington T G and Peters N E (2001). Differential rates of feldspar weathering in granite regoliths. Geochim. Cosmochim. Acta, 65, 847–869.

White A F, Schulz M S, Lowenstern J B, Vivit D V and Bullen T D (2005). The ubiquitous nature of accessory calcite in granitoid rocks: implications for weathering, solute evolution, and petrogenesis. Geochim. Cosmochim. Acta, 69, 1455–1471.

Wigley T M L and Plummer L N (1976). Mixing of carbonate waters. Geochim. Cosmochim. Acta, 40, 989–995.

Wilkin R T and Barnes H L (1997). Pyrite formation by reactions of iron monosulfides with dissolved inorganic and organic sulfur species. Geochim. Cosmochim. Acta, 60, 4167–4179.

Wolery T J and Daveler S A (1992). EQ6, a computer program for reaction path modelling of aqueous geochemical systems: theoretical manual, user's guide and related documentation (version 7.0). Lawrence Livermore National Laboratory. UCRL-MA-110662 PT IV, 338 p.

Wolthers M, van der Gaast S J and Rickard D (2003). The structure of disordered mackinawite. Am. Miner., 88, 2007–2015.

Wolthers M, Charlet L, van der Linde P R, Rickard D and van der Weidjen C H (2005). Surface chemistry of disordered mackinawite (FeS). Geochim. Cosmochim. Acta, 69: 3469–3481.

Wu J, Roth C B and Low P F (1988). Biological reduction of structural iron in sodium-nontronite. Soil Sci. Soc. Am. J., 52, 295–296.

Yao W and Millero F J (1993). The rate of sulfide oxidation by $\delta MnO2$ in seawater. Geochim. Cosmochim. Acta, 57, 3359–3365.

Review of Chemmac logs in the Laxemar-Simpevarp area (including Äspö, Ävrö, Simpevarp and Laxemar)

A.1   Introduction and motivation of this Appendix

This document presents the final Eh and pH values selected by the group of the University of Zaragoza for modelling purposes explaining, when necessary, the differences with the values suggested or reported by other authors.

The only P-report with Chemmac[59] information from the Laxemar-Simpevarp area (including Simpevarp, Äspö, and Laxemar subareas) available from the beginning of the SDM phase was the one corresponding to KSH01 borehole (Simpevarp; Wacker *et al.* 2004), but it was published well after the data had been delivered in the corresponding data freeze. After that, the next available drafts of new P-reports corresponding to the Chemmac logs in boreholes KLX03 (Bergelin *et al.* 2006) and KLX08 (Bergelin *et al.* 2008a) were not accessible, in a draft version, until two months after the delivery of Laxemar 2.2 data freeze (that is, March, 2007). This means that in all the cases, the University of Zaragoza was the group that recommended the values to be used in these previous data freezes. In this appendix the selection made by the UZ is compared with the one presented in the aforementioned P-reports. The problem is the same with the new Chemmac logs delivered with the Laxemar 2.3 data freeze: the corresponding P-reports are not available yet, and the UZ group has recommended the selected Eh values while expected for them. The exception is the P-report corresponding to KLX13A (Bergelin *et al.* 2008b) which appeared one year after the delivery of the extended Laxemar 2.3 data freeze (that is, December, 2008). The values recommended there are also compared with the UZ selection.

The inclusion of different subareas (Äspö, Ävrö, and Laxemar), with data from previous sampling campaigns, quite separate in time, added new methodological difficulties to this task:

- Chemmac logs available for Äspö, Ävrö and Laxemar subareas, prior to SDM phase, were provided by Sicada in form of raw data.

- Eh and pH data for KAS boreholes (Äspö), KAV borehole (Ävrö) and KLX01-02 boreholes (Laxemar) had been previously used in different SKB reports (Smellie and Laaksoharju 1992, Laaksoharju *et al.* 1995), some scientific papers (e.g. Grenthe *et al.* 1992) and even in SKI's SITE-94 Performance Assessment (Glynn and Voss 1999). But in all these works the Eh values were merely reported, rejected or used without indication of the criteria employed to do it.

- Chemmac methodology has evolved (and improved) with time and the same could be valid for the criteria used for selection of representative Eh values.

Therefore the UZ group decided to re-analyse all the available continuous logs for the Laxemar-Simpevarp area (and also for the Forsmark and some other Swedish sites, Auqué *et al.* 2008) in order to select a high-quality Eh, pH and temperature datasets based on a common and well defined set of criteria to create a database as complete as possible which can be used for geochemical modelling. After this revision, the selected and rejected values were compared with the aforementioned P-reports and previous works, and, with some exceptions, the degree of concordance was very good.

The selection criteria handled are summarised in Section 2 and the explanation of the different decisions taken when selecting Eh and pH values are included here in Sections 3 and 4. Section 3 is focussed on the available logs obtained, prior to the start of the SDM phase, in Äspö, Ävrö and Laxemar subareas. There are not available P-reports for these logs and the representative Eh values obtained in this review were compared with the Eh data used in previous works (see above). Section 4 is dedicated to the logs obtained during the different SDM phases. Results are evaluated and compared with the information in the available P-reports. In these cases, the plots shown have been taken directly from the report.

---

[59] The Chemmac measurement facilities include a communication system, measurement application and flow-through cells with electrodes and sensors at the surface (surface Chemmac) and downhole (borehole Chemmac; eg. Wacker *et al.* 2004).

An additional comment is worth including here. It refers to the origin of the data used for the plots performed by the University of Zaragoza (UZ). They come from the Sicada deliveries for each data freeze. The way Sicada stores the data makes impossible to plot the electrode readings as a function of time (as P-reports do). So, all the graphs plot Eh (and pH) as a function of measurement number, irrespective of the actual time interval between measurements. But in all the cases the final decisions could have been taken independently of this.

A.2   Selection criteria defined by the UZ

Chemmac methodology of measurement, and selection criteria used by UZ have been describe in detail in Auqué *et al.* (2008). Here a short summary is presented.

Basically, the measurement methodology involves continuous logging of Eh for long periods of time in isolated packed-off sections in a borehole. Eh is measured simultaneously by three electrodes (Au, Pt and C electrodes) in the borehole and three electrodes at the surface against Ag/AgCl double junction gel-filled reference electrodes in both cases. Apart from Eh, the logging also includes other parameters such as pH, dissolved oxygen, conductivity and temperature.

The selection of a potentiometric Eh value for a borehole section must be based on a careful analysis of the readings obtained with the different electrodes at depth and at the surface, the logging time, the pH, the conductivity, and the dissolved oxygen values. The basic assumption is that the measured potential corresponds to the equilibrium potential and this fact can only be demonstrated when the different electrodes give identical readings. Ideally, the Eh values selected as representative should only be those obtained simultaneously and within a small Eh range (50 mV) by the four or six electrodes normally used over a long period of time. However this criterion is too restrictive: There can be undesirable effects selectively affecting one electrode, or technical problems affecting one of the two measurement cells (down-hole and surface cells).

Taking into account all these issues, we decided to apply the following selection criteria:

- Eh logs longer than 3 days (actually, most logs are longer than a week);

- Eh logs with stable (i.e. not changing over time) and similar readings (range smaller than 50 mV) for several electrodes in the long term; and

- Eh logs with simultaneous and stable pH readings (in order to minimize the uncertainty associated with pH in geochemical modelling).

The set of Eh logs that fulfilled these criteria is then classified according to the quality of the redox values. We have defined two groups of representative Eh values depending on the number of electrodes giving similar readings (50 mV):

- Group 1 Eh values: stable and similar readings in at least three electrodes, two of them at depth.

- Group 2 Eh values: stable and similar readings in two electrodes, at depth or at the surface.

These groups reflect the difference in the quantity and the quality of the information used to define the representative Eh value. Group 1 includes Eh values with the most reliable information, i.e., based on electrode readings at depth. Group 2 Eh values include good quality values but limited by frequent log interruptions, different recording times for the different electrodes, or other technical difficulties. In other words, they are considered less reliable values.

A.3   Review of the existing information for Äspö (KAS boreholes), Ävrö (KAV boreholes) and Laxemar (KLX01 and KLX02 boreholes) prior to the SDM phase

All available Sicada Chemmac loggings from sampling campaigns **prior to the start of the SDM phase** in Äspö, Ävrö and Laxemar subareas have been included in this review. The target boreholes and sections are indicated in Table A-1. At the end of the document the final table (Table A-2) with all the selected data including the values taken **during the SDM phase** is presented.

With respect to the pre-existing values, only the Eh and pH values gathered in Table A-1 fulfil the selection criteria defined in Section 2 and they are thus chosen as representative. As the Table shows, there are several sections with Chemmac measurements but with no representative Eh value. The logs corresponding to these sections (with no values in Table A-1) are collected at the end of this appendix A.

As indicated above, the representative Eh values obtained in this review were compared with the Eh data used in previous works (Smellie and Laaksoharju 1992, Grenthe *et al.* 1992, Laaksoharju *et al.* 1995). As Table A-1 shows, the agreement between the Eh values selected for modelling in ChemNet and the values reported previously is fairly good.

Table A-1. Borehole sections with Chemmac measurements before the start of the SDM phase. Sections with Eh data show the selected values in this review and in previous works in Äspö (KAS boreholes), Ävrö (KAV borehole) and Laxemar (KLX01 and KLX02 boreholes) where SKB methodology (Chemmac) has been used. Bold figures are Group 1 values; the rest are Group 2 values. The pH values in last column are those selected from Chemmac loggings, down-hole or at the surface, following the same criteria as for the Eh values.

Subarea	Borehole	Sample represen-tative	Depth (elev. secmid)	Borehole section (m)[1]	Eh value (mV) selected as representative		Reference	pH selected as represent.
					This work	Previous works		
Äspö	KAS02	1548	−200	202–214	−257	−260	Smellie and Laaksoharju (1992)	7.5
		1419[2]	−308	314–319	−380	−400	Smellie and Laaksoharju (1992)	8.45
		1474	−317	308–344				7.6
		1428	−456	463–468		−220	Delivered by Sicada	8.35±0.05
		1433	−523	530–535		−310	Smellie and Laaksoharju (1992)	8.35
		1560	−881	860–924		−150	Delivered by Sicada	8.5
	KAS03	1569	−122	129–134	**−260**	−270	Smellie and Laaksoharju (1992)	8.0
		1437	−199	196–222				7.65
		1448	−239	248–251				7.8
		1445	−454	453–480				
		1452	−602	609–623				8.05
		1455	−830	690–1002				8.05±0.05
		1582	−914	860–1002	−270	−270	Smellie and Laaksoharju (1992)	7.3±0.1
	KAS04	1596	−185	226–235	**−300**	−300	Smellie and Laaksoharju (1992)	7.8±0.1
		1603	−276	334–343	**−280**	−280	Smellie and Laaksoharju (1992)	7.9
		1588	−377	440–480				8.04±0.04
Ävrö	KAV01[3]	1391	−408	420–425	**−215**		Grenthe *et al.* (1992)	7.35
		1383	−512	522–531	−310		Grenthe *et al.* (1992)	7.0±0.1
		1374	−546	558–563	−225		Grenthe *et al.* (1992)	7.4±0.2
		1354	−675	635–743				8.15
Laxemar	KLX01	1537		272–277				
		1528	−441	456–461	−280			8.6±0.1
		1516	−673	680–702	−265			7.8±0.2
		1773	−897	910–921				8.4
	KLX02	2738	−299	315–321				8.1
		2705	−318	335–340				8.05±0.05
		2712	−778	798–802				7.75
		3035	−1069	1090–1096				8.6
		2731	−1531	1420–1700		−300	Delivered by Sicada	8.0±0.1

[1] All the references to depth in this document refer to the borehole length as it is clearer to find the exact samples we are talking about.

[2] The sample representative of this borehole section is #1418 but the sample used for modelling #1419 is almost the same, with the same percent of drilling water and with iron contents that the other does not have.

[3] The samples from KAV01 are not highlighted as representative.

Also, rejected values are in agreement with what was previously rejected in previous works. For example, all Eh measurements in KLX02 borehole prior to 1995 were rejected in agreement with recommendations made by Laaksoharju *et al.* (1995). The only two noticeable discrepancies are presented in Section 3.2.

Next we present the selected (section A.3.1) and rejected values (section A.3.2) for modelling also indicating the values that have been rejected in spite of having considered them to be acceptable in previous SDM phases.

Then, in Section 4, the data taken during the different SDM phases are presented and compared with the P-reports (when available).

A.3.1   Eh and pH values selected for redox modelling

The sections with representative values are two sections in KAS02 (202–214 and 314–319), two sections in KAS03 (129–134 and 860–1,002), two sections in KAS04 (226–235 and 334–343), three sections in KAV01 (420–425, 522–531 and 558–563), and two sections in KLX01 (456–461 and 680–702).

KAS02 at 202–214 m borehole length

The Eh value proposed in the previous work (Smellie and Laaksoharju 1992) is –260. This value is in agreement with the one proposed by the University of Zaragoza which is Eh = −257 mV (Figure A-1a). The pH value for this section is pH = 7.5 (Figure A-1b).

KAS02 at 314–319 m borehole length

Chemmac log has stable readings of two electrodes. The final and stabilised Eh readings after 12 days of measurements correspond to the Pt electrode down-hole and at the surface, but both readings are out of the accepted range of 50 mV (–320 mV with the Pt electrode at depth, and –400 mV with the Pt electrode at the surface; Figure A-2a). So, it should have been discarded following our criteria. However, relatively stable values with the three electrodes (Pt, Au and C) were obtained over the first period of measurement (−370 to −400); moreover, the value of −380 mV is the most reducing value reported up to now for this area and it was included by Grenthe *et al.* (1992) as part of the dataset used for them to define their redox fit for the $Fe(OH)_3/Fe^{2+}$ redox pair. For all these reasons, we have tentatively included it as a Group 2 Eh value in some discussions.
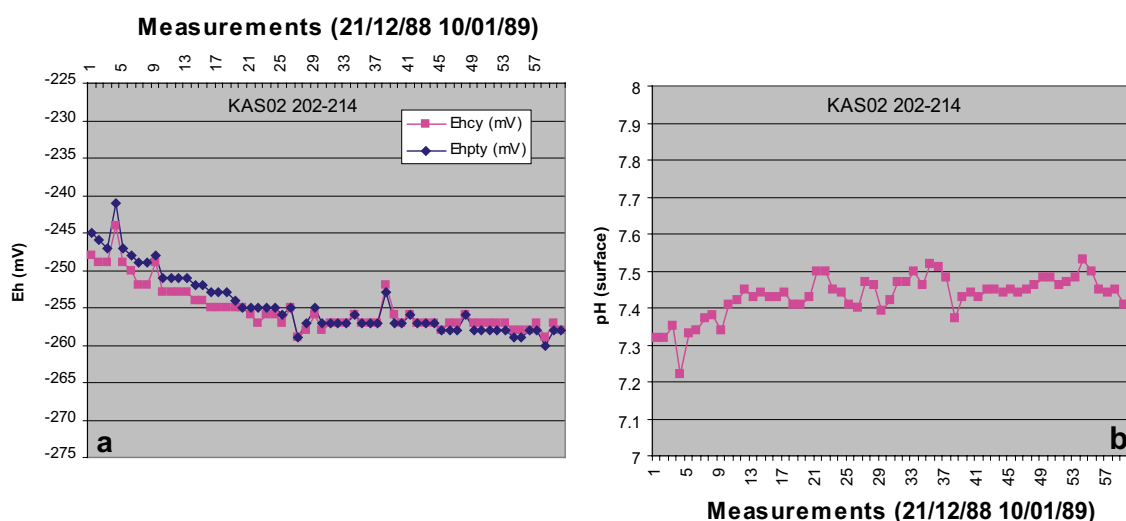
Figure A-1. *(a) Redox potential measurements (Eh) in KAS02 (section 202–214 m) by platinum, glassy and carbon electrodes at the surface (Ehpty and Ehcy). (b) Measurements of pH by one glass electrode at the surface (Phy). X axis indicates de number of measurements, and the title the time interval. This is the same for the rest of the plots in this document.*

The pH selected for this section has been 8.45 (Figure A-2b). Borehole electrodes seem to stabilise at the end of the logging but for a long period they show values near to the selected one (note that precision of pH electrodes usually is not better than 0.05 pH units). Besides, the surface electrode tends to converge with the others also at the end of the measurements.

KAS03 at 129–134 m borehole length

The Eh value proposed in the previous work (Smellie and Laaksoharju, 1992) is −270 mV which is in agreement with the one proposed by the University of Zaragoza (Eh = −260; Figure 3a). The pH value for this section is pH = 8 (Figure A-3b).
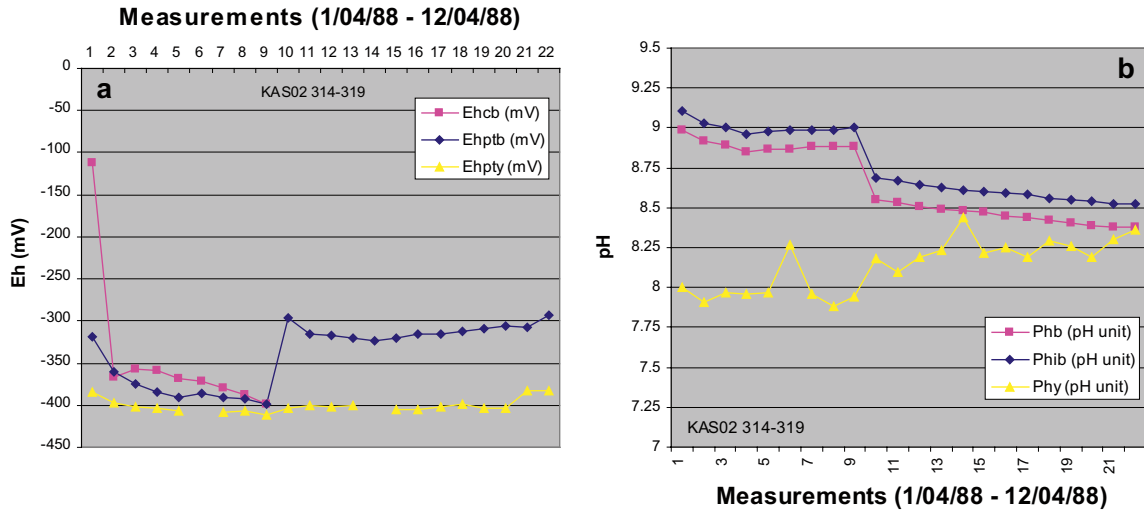
Figure A-2. *(a) Redox potential measurements (Eh) by different electrodes at KAS02 in section 314–319 m (borehole section). (b) Measurements of pH by two glass electrodes in the borehole section (Phb and Phib) and one glass electrode at the surface (Phy).*
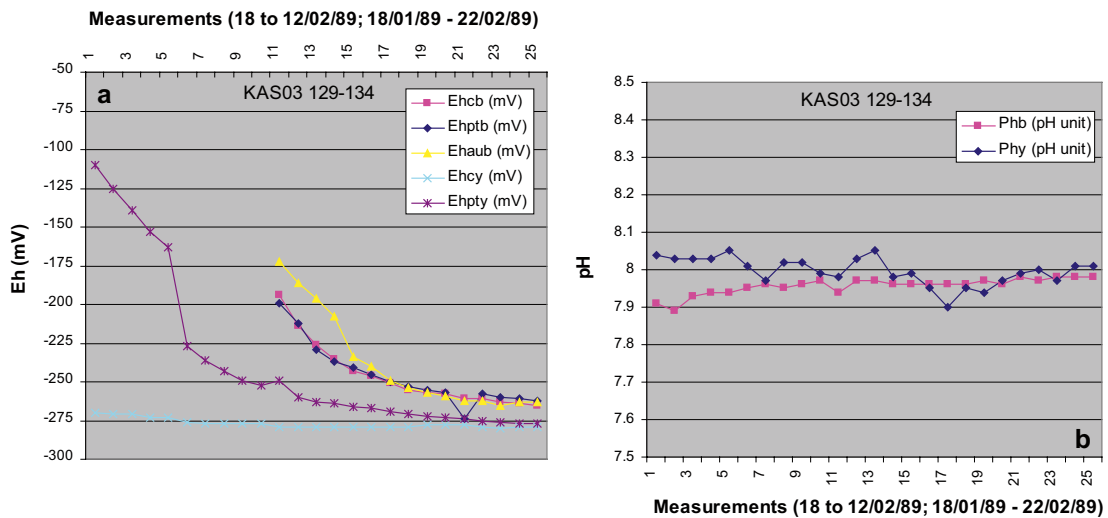
Figure A-3. *(a) Redox potential measurements (Eh) by glassy carbon, gold and platinum electrodes in the borehole section and at the surface at KAS03 in section 129–134 m (borehole section). (b) Measurements of pH by one glass electrode in the borehole section (Phb) and one glass electrode at the surface (Phy).*

243

KAS03 at 860–1,002 m borehole length

The Eh value proposed in the previous work (Smellie and Laaksoharju 1992) is −270 mV which is in agreement with the one proposed by the University of Zaragoza (Figure A-4a). The pH value for this section is pH = 7.3±0.1 (Figure A-4b).

KAS04 at 226–235 m borehole length

The Eh value proposed in the previous work (Smellie and Laaksoharju 1992) is −300 mV which is in agreement with the one proposed by the University of Zaragoza (Figure A-5a). The pH value for this section is pH = 7.8±0.1 (Figure A-5b).

Figure A-4. *(a) Redox potential measurements (Eh) by glassy carbon and gold electrodes in the borehole section and glassy carbon and platinum at the surface at KAS03 in section 860–1002 m (borehole section). (b) Measurements of pH by one glass electrode in the borehole section (Phb) and one glass electrode at the surface (Phy).*

Figure A-5. *(a) Redox potential measurements (Eh) by glassy carbon and gold electrodes in the borehole section and glassy carbon and platinum electrode at the surface at KAS04 in section 226–235 m (borehole section). (b) Measurements of pH by one glass electrode in the borehole section (Phb) and one glass electrode at the surface (Phy).*

KAS04 at 334–343 m borehole length

The Eh value proposed in the previous work (Smellie and Laaksoharju 1992) is −280 mV which is in agreement with the one proposed by the University of Zaragoza (Figure A-6a). The pH value for this section is pH = 7.9 (Figure A-6b).

KAV01 at 420–425 m borehole length

The Eh value obtained for this section was used by Grenthe *et al.* (1992) and from their plots a value around −215 can be deduced. It is in agreement with the one proposed by the University of Zaragoza (Figure A-7a). The pH value for this section is pH = 7.35 from the borehole electrode (Figure A-7b) but a value of 7.15 ±0.2 could be used for uncertainty analysis.

Figure A-6. *(a) Redox potential measurements (Eh) by glassy carbon, platinum and gold electrodes in the borehole section and glassy carbon and platinum electrode at the surface at KAS04 in section 334–343 m (borehole section). (b) Measurements of pH by one glass electrode at the surface.*

Figure A-7. *(a) Redox potential measurements (Eh) by glassy carbon, platinum and gold electrodes in the borehole section and glassy carbon and platinum electrode at the surface at KAV01 in section 420–425 m (borehole section). (b) Measurements of pH by one glass electrode at depth and another electrode at the surface.*

KAV01 at 522–531 m borehole length

The Eh value obtained for this section was used by Grenthe *et al.* (1992) and from their plots a value around −310 can be deduced. It is in agreement with the one proposed by the University of Zaragoza (Figure A-8a). The pH value for this section is pH = 7.0 ±0.1 (Figure A-8b).

KAV01 at 558–563 m borehole length

The Eh value obtained for this section was used by Grenthe *et al.* (1992) and from their plots a value around −225 can be deduced. It is in agreement with the one proposed by the University of Zaragoza (Figure A-9a). The pH value for this section is pH = 7.4 ±0.2 (Figure A-9b).
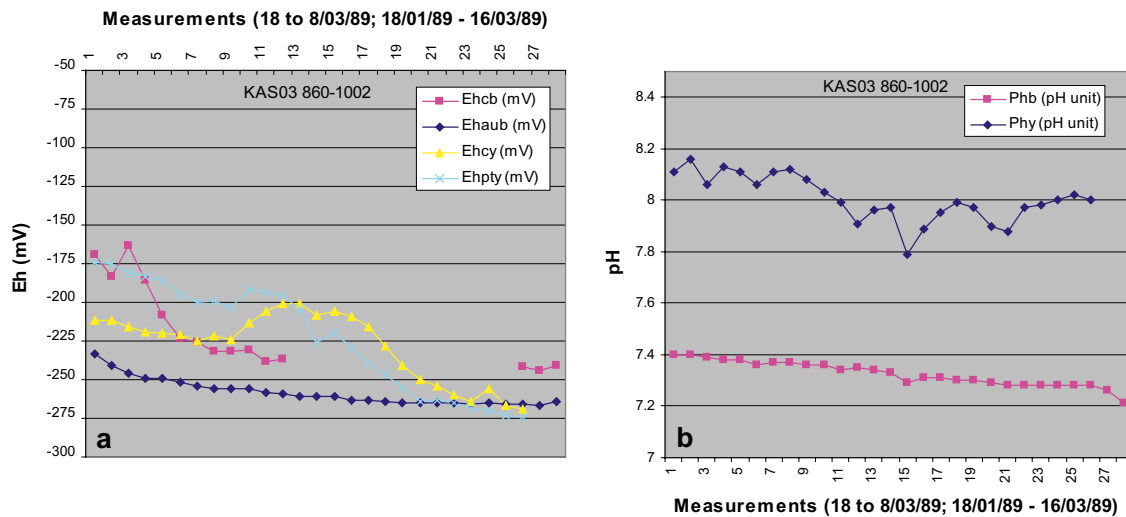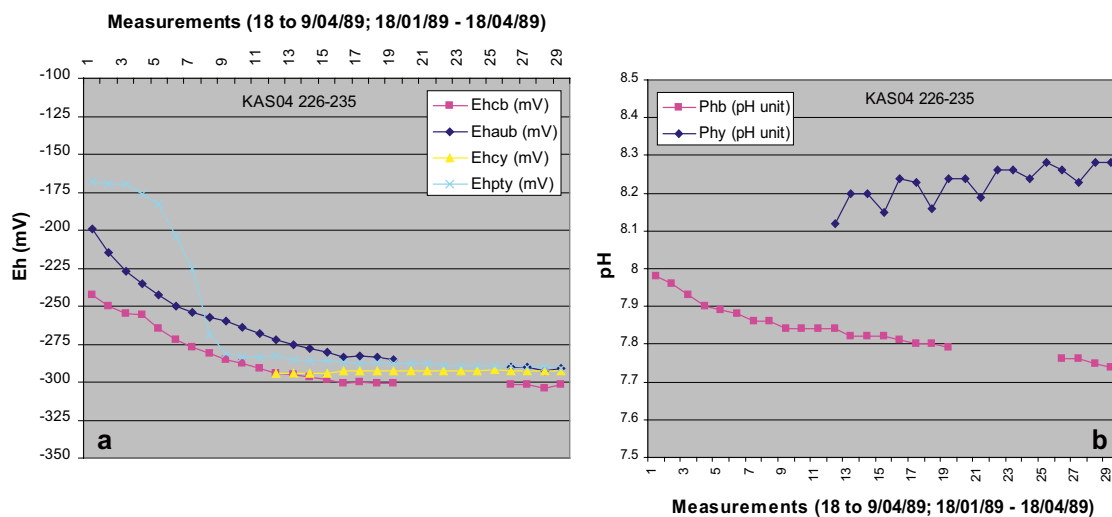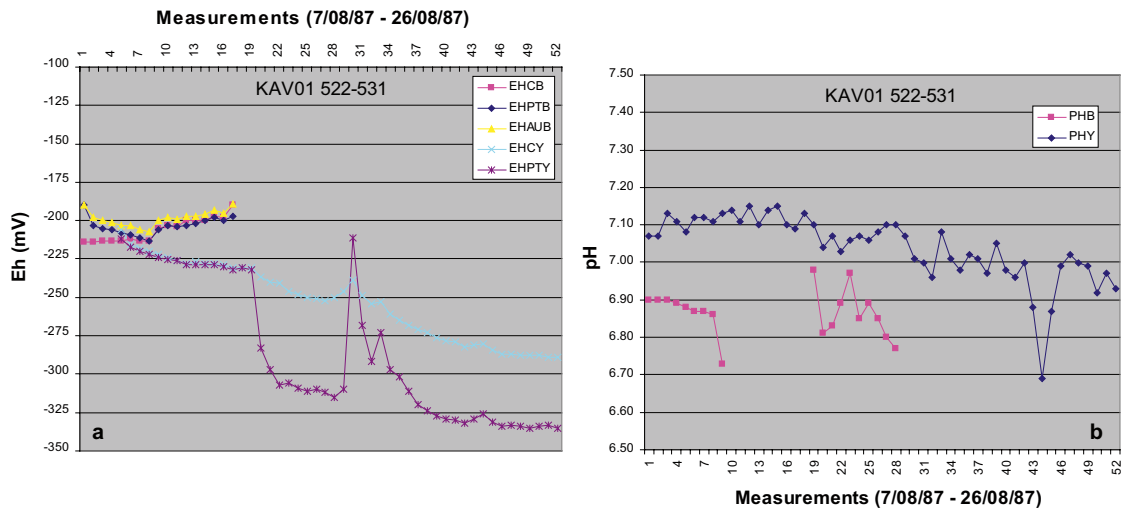

Figure A-8. (a) Redox potential measurements (Eh) by glassy carbon, platinum and gold electrodes in the borehole section and glassy carbon and platinum electrode at the surface at KAV01 in section 522–531 m (borehole section). (b) Measurements of pH by one glass electrode at depth and another electrode at the surface.

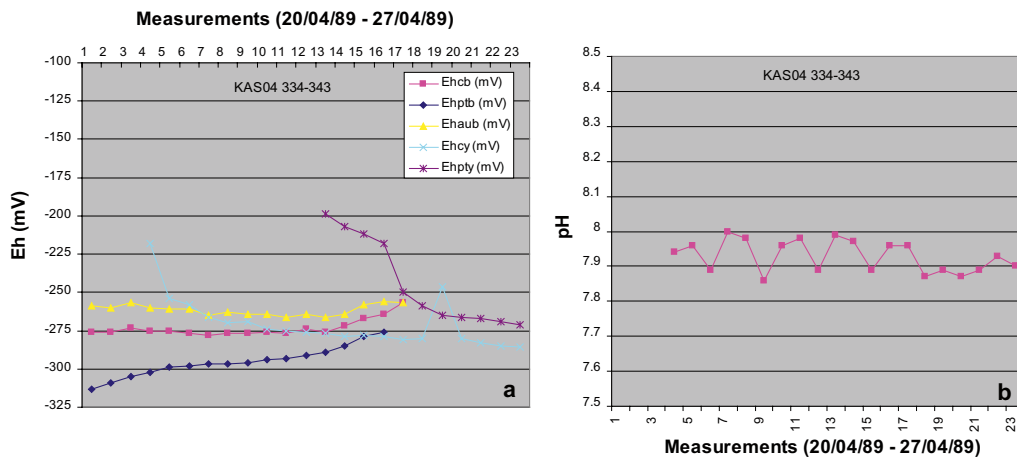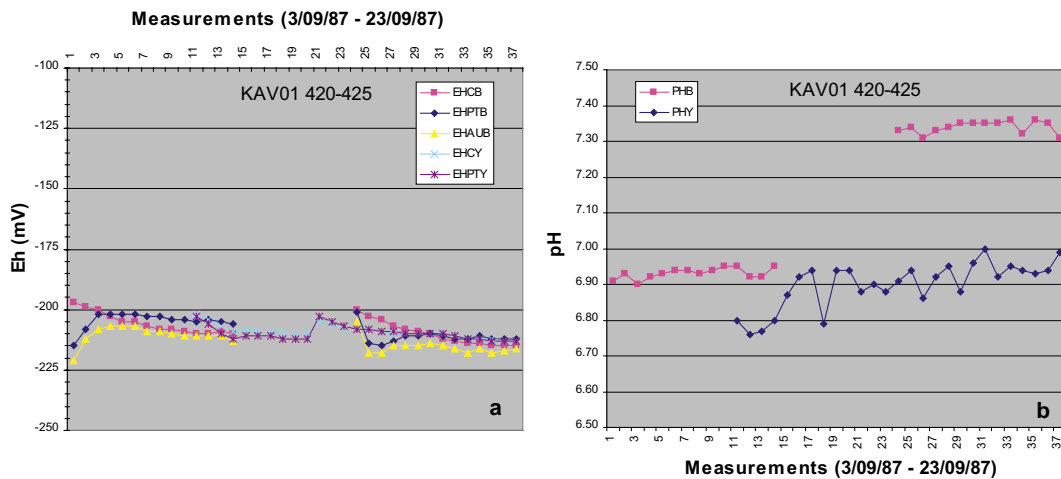*Figure A-9. (a) Redox potential measurements (Eh) by glassy carbon and platinum electrodes in the borehole section and at the surface at KAV01 in section 558–563 m (borehole section). (b) Measurements of pH by one glass electrode at depth and two electrodes at the surface.*

KLX01 at 456–461 m and 680–702.11 borehole lengths

The Eh values reported for these sections are –280 mV and –265 mV and they were marked as doubtful in Simpevarp 1.2 (SKB 2004)[60] as they do not strictly fulfil the indicated criteria (Figure A-10): difference of slightly more than 50 mV (60 mV, Fig A-10a) and poor temporal overlap of the readings (Figure A-10b). However, with some flexibility they could be considered as Group 2 representative values. The pH values selected have been 8.6 and 7.8±0.2 for the 456–461 section and the 680702 section respectively (Figure A-10c and A-10d).

A.3.2   Eh values rejected for redox modelling

Here we indicate the sections whose Eh values have been rejected for modelling. We describe in detail the reasons for rejecting some values previously considered representative. But in the cases where the rejection made by the University of Zaragoza agrees with the decision taken by others in previous works the plots are simply included at the end of this Appendix.

KAS02 at 308–344 m borehole length

The values obtained for this section have been rejected in previous works and also here by the University of Zaragoza (see plots at the end of this appendix A). Although the measurement period is something short a pH value of 7.6 can be considered (Tables A-1 and A-3).
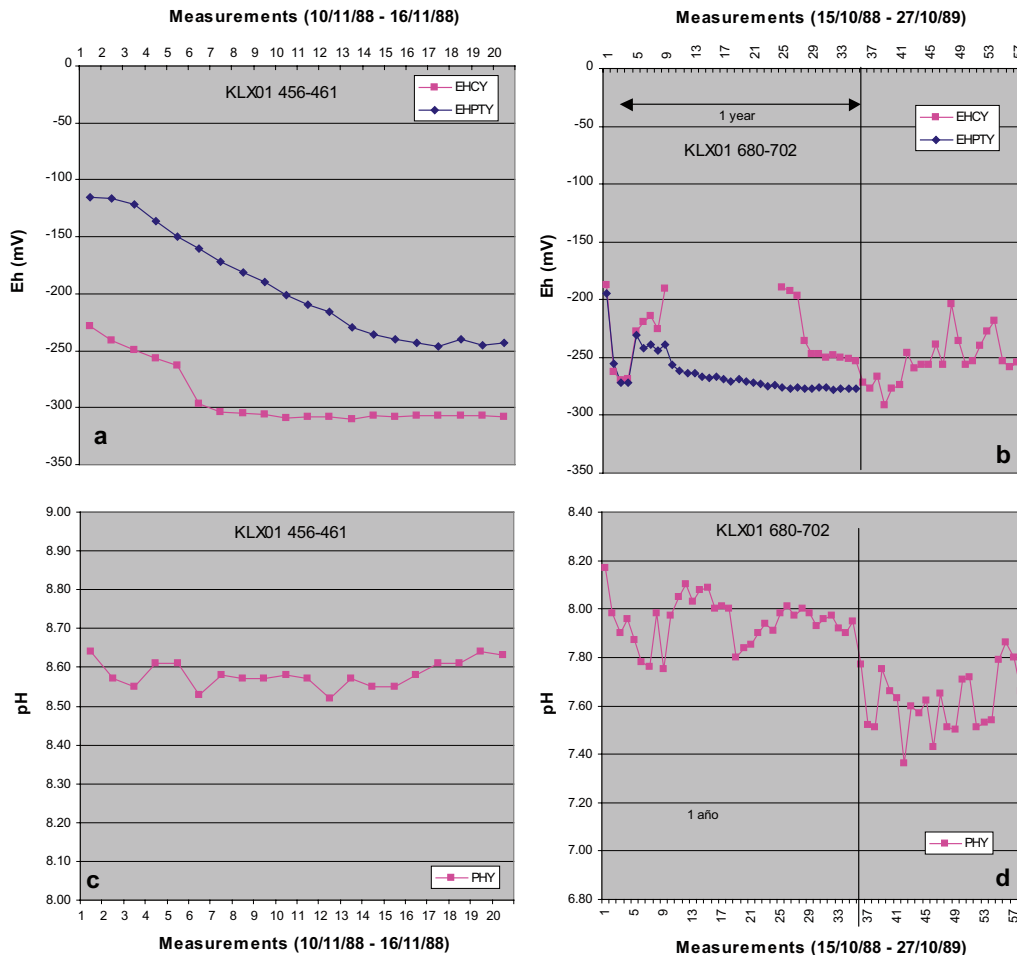
Figure A-10. *Redox potential measurements at surface with different electrodes at KLX01 in section 456–461 m (a) and section 680–702 m (b). pH logs at surface for the same sections (c and d).*

---

[60] A value of –275 was indicated in Simpevarp 1.2 for this section due to a typing error.

KAS02 at 463–468 m borehole length

Smellie and Laaksoharju (1992) reported a value of –290 mV whereas we have eliminated the value due to the lack of stability in the measurements (Figure A-11a). There are readings for the three electrodes at depth and for two electrodes (Pt and C) at the surface. At depth the readings follow a decreasing trend with time, but with no stabilisation: C-electrode reading ends at about –300 mV (the other two at –190 and –260 mV). At the surface the C electrode has a very short measurement interval, whereas the Pt electrode has a relatively stable plateau at –150 mV in the middle of the measuring interval, but not at the end. Due to these problems we have eliminated this value from the representative data Table. The pH value selected is 8.35±0.05 (Figure A-11b).

KAS02 at 530–535 m borehole length

The Eh value proposed in the previous work (Smellie and Laaksoharju 1992) is –310 mV but it has been rejected by the University of Zaragoza as the readings do not fulfil the proposed criteria (Figure A-12a). The pH value for this section is pH = 8.35 (Figure A-12b).
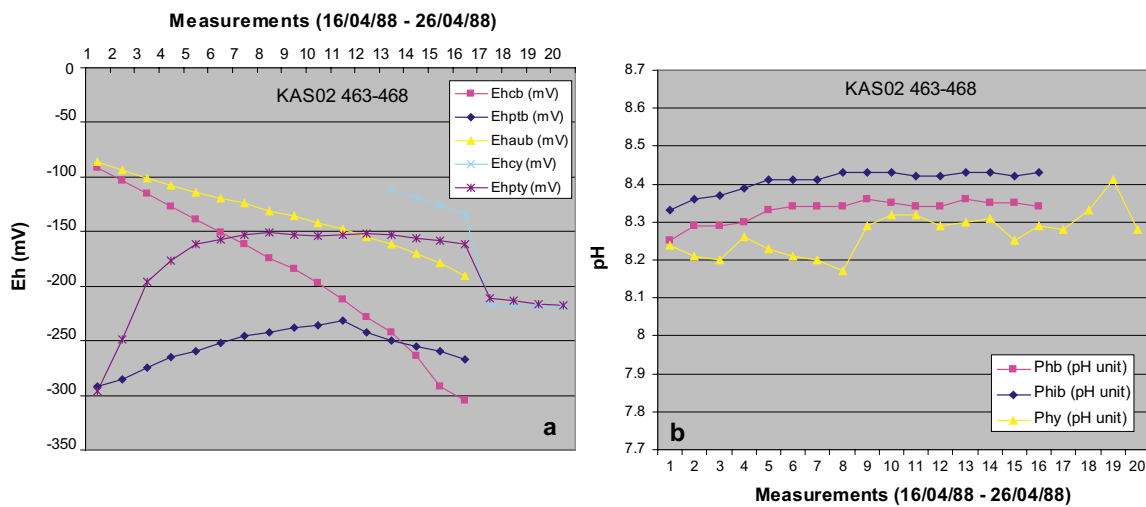
Figure A-11. *(a) Redox potential measurements (Eh) at depth and surface with different electrodes at KAS02 in section 463–468 m (borehole section). (b) Measurements of pH by two glass electrodes in the borehole section (Phb and Phib) and one glass electrode at the surface (Phy) by one glass electrodes at the surface (Phy).*
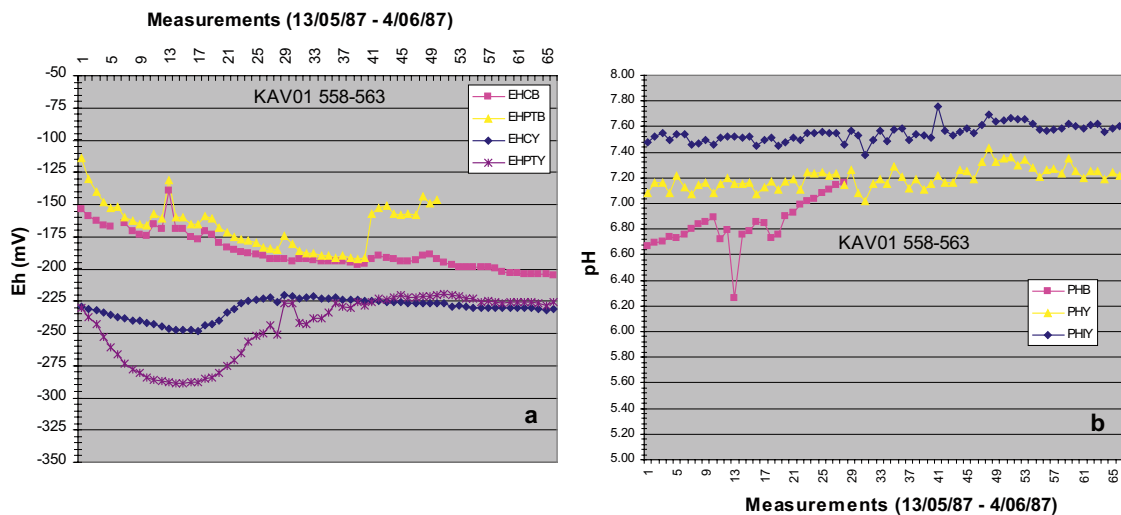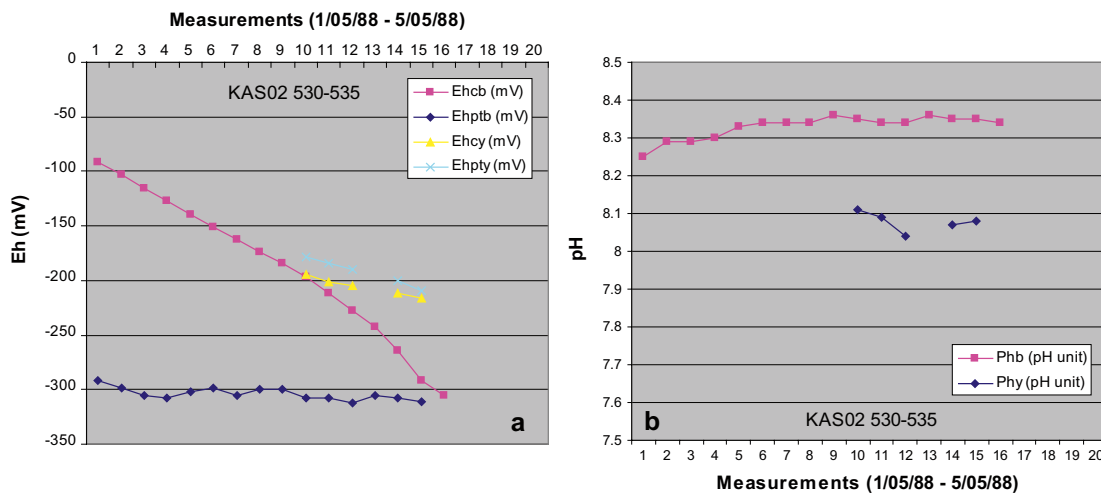

Figure A-12. *(a) Redox potential measurements (Eh) by glassy carbon and platinum electrodes in the borehole section and at the surface at KAS02 in section 530–535 m (borehole section). (b) Measurements of pH by one glass electrode in the borehole section (Phb) and one glass electrode at the surface (Phy).*

KAS02 at 860–924 m borehole length

For this section an Eh value of −150 mV was listed in Simpevarp 1.2 (SKB 2004) as representative. After applying the selection criteria, it was rejected and it was not reported in Laxemar 2.1 (SKB 2006b).

Chemmac Eh data for this section have only two working electrodes (Pt and Au, Figure A-13a) at the surface. While the Pt electrode shows a stable reading, the Au electrode does not. Moreover, over the whole period of measurement significant oxygen contents were measured (0.3–0.4 mg/L; Figure A-13b).

These rejection seems to be in agreement with the absence of Eh data for this section in the work by Smellie and Laaksoharju (1992, Table 5.1, page 87).

Besides, redox pair calculations performed by Gimeno *et al.* (2007) with the groundwater sample corresponding to this section (with Fe(II), S(–II) and CH_4 measured data) provides redox potential values between –256 to –386 mV. In fact, a redox potential of –150 mV would be identical to the value (–151 mV) provided by the redox pair Fe(OH)$_{3\text{ microcrystalline}}$/Fe^{2+} (solubility value proposed by Nordstrom *et al.* 1990), which would confirm the effect of an active intrusion of oxygen during logging.

The pH in this section is very stable and it has been selected for modelling (pH=8.5) (Figure A-13b).
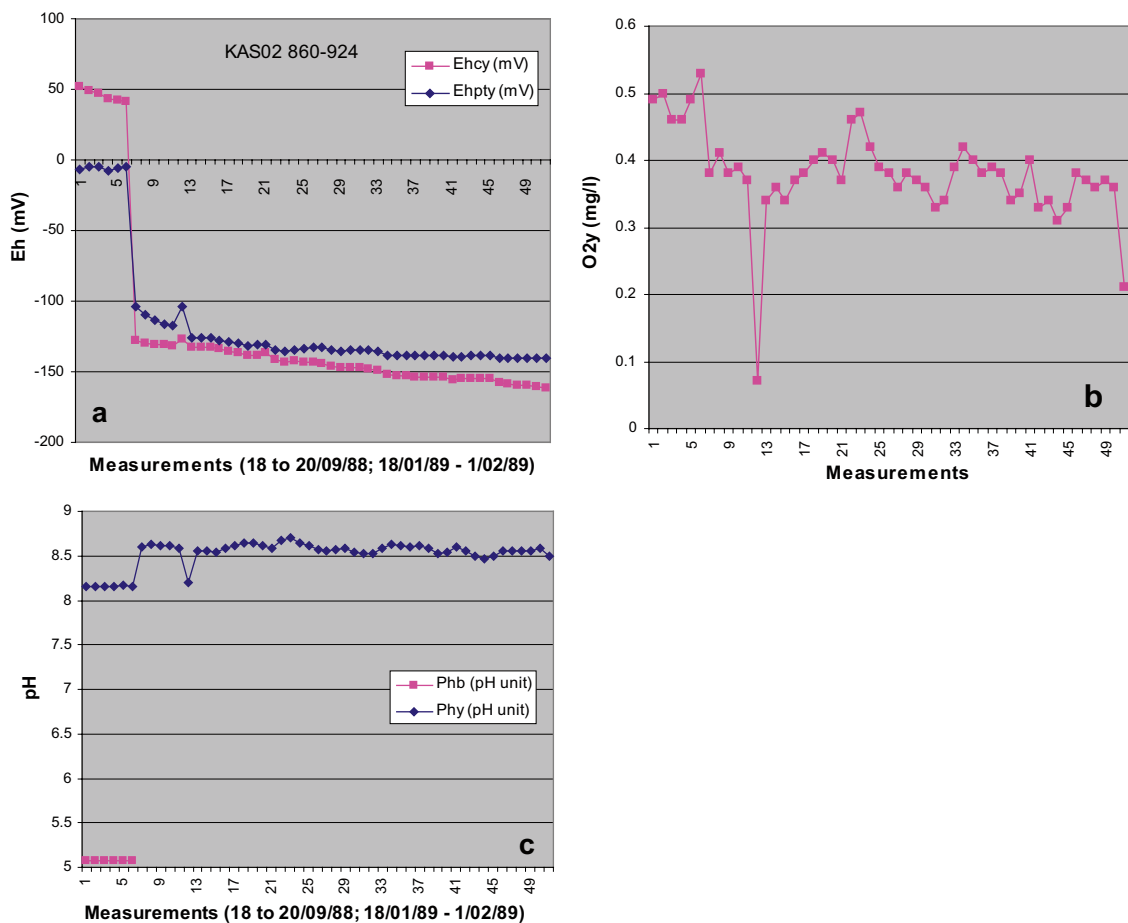
Figure A-13. *Redox potential measurements at surface with different electrodes (a), dissolved oxygen contents (b) and pH values in borehole and surface (c) at KAS02 in section 860–924 m (borehole section).*

KAS03

There are seven sections in this borehole, with Chemmac measurements, although only two of them have representative Eh values (129–134 m and 860–1,002, Section A.3.1). The values obtained for the rest of the sections (196–222 m, 248–251 m, 453–480 m, 609–623 m and 690–1,002 m borehole length) have been rejected in previous works and also here by the University of Zaragoza (see plots at the end of this appendix A). With respect to pH, in spite of the short periods of measurement the values have been selected when they were stable (see Table A-1 and A-3).

KAS04 at 440–480 m borehole length

The Eh values obtained for this section have been rejected in previous works and also here by the University of Zaragoza (see plots at the end of this appendix A). With respect to pH, a value of 8.04 ± 0.04 has been select due to the stable values shown in the logs.

KAV01 at 635–743 m borehole length

The Eh values obtained for this section have been rejected in previous works and also here by the University of Zaragoza (see plots at the end of this appendix A). The pH value selected here was very stable at around 8.15.

KLX01 at 272–277 m borehole length

The values obtained for this section have been rejected by the University of Zaragoza (see plots at the end of this appendix A).

KLX01 at 910–921 m borehole length

The Eh values obtained for this section have been rejected by the University of Zaragoza (see plots at the end of this appendix A). The pH value selected is 8.4.

KLX02

There are five sections in this borehole with Chemmac measurements but, as we already said, none of them have representative values (315–321 m, 335–340 m, 798–802 m, 1,090–1,096 m and 1,420–1,700 m borehole length; see plots at the end of this appendix A).

However we should point that for the section at 798–802 m the Eh value of –125 mV (measured in 2002) was reported in Laxemar 1.2 (SKB 2006a). It was rejected in Laxemar 2.1 because the review of Chemmac logs suggested the existence of important problems. There are loggings for the three electrodes at the surface, but only the Au electrode is roughly stable at the end of the measurement period (and only for a few days; Figure A-14). Considering all these defects, this value does not satisfy the criteria adopted by us for the modelling work in ChemNet for the SDM.
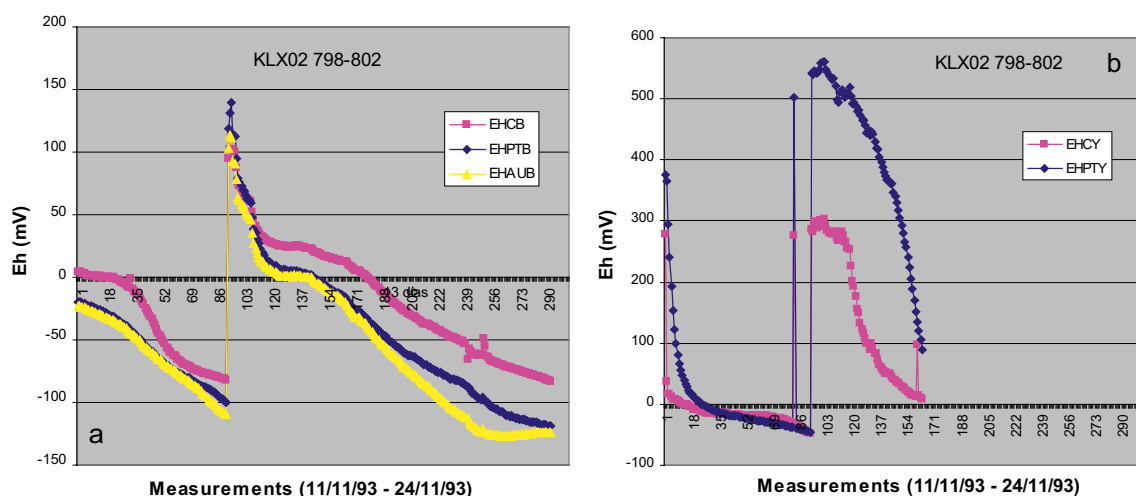
Figure A-14. *Redox potential measurements in KLX02 at 798–802 m depth (borehole section) in the borehole (a) and at the surface (b) with different electrodes.*

The pH value here were fairly stable and cover a wide period of time and therefore, a field pH value has been selected for modelling in Tables A-1 and A-3 for each section analysed. For this borehole, Laaksoharju *et al.* (1995) give no indications about the pH measurements.

A.4 Review of the Chemmac logs taken during the SDM phases after 2003 in KSH01, KLX03, KLX08, KLX13, KLX15 and KLX17 boreholes

Chemmac logs during the SDM phases are reviewed in this section. Some of them correspond to boreholes with available P-reports: KSH01 borehole (Simpevarp; Wacker *et al.* 2004), KLX03 and KLX08 boreholes (Laxemar; Bergelin *et al.* 2006, 2008a). But, except for borehole KLX13 (Bergelin *et al.* 2008b), the new data delivered in the 2.3 data freeze (from boreholes KLX15 and KLX17) do not have the corresponding p-report yet and the values are selected by the UZ group. The sections and the values analysed are shown in Table A-2.

A.4.1 Chemmac measurements in KSH01 (Simpevarp)

The available logs in KSH01 borehole correspond to sections at 156.5–167 m, 245–261.6 m and 548–565.4 m (borehole length).

The pH and Eh values indicated in the P-report (Wacker *et al.* 2004) for **section 156.5–167 m** (Eh = –257 mV and pH= 8.17) agree with those obtained in the evaluation performed by the UZ group (Eh = –250 mV and pH = 8.1). Therefore, these last values are kept (Table A-2 and A-3). The plots taken from the reports are shown in Figure A-15.

Table A-2. Sections analysed during the SDM work with the Eh values selected by the University of Zaragoza for geochemical modelling. When available, values reported in P-reports are shown as well. The pH values correspond to the values selected from down-hole or surface Chemmac logging, following the same criteria as for the Eh selection.

Subarea	Borehole	Sample represent.	Depth (elev. secmid)	Borehole section (m)	Eh value (mV) This work	Eh value (mV) P-reports	Reference	pH
Simpevarp	KSH01A	5263	–153	156–167	–250	–257	Wacker *et al.* 2004	8.17
		5268[1]	–242	245–261	–210	–160	Wacker *et al.* 2004	8.08
		5288[1]	–536	548–565	–240	–173	Wacker *et al.* 2004	8.15
Laxemar	KLX03	7952[2]	–171	193–198	–275	–285	Bergelin *et al.* 2006	8.17
		10091[3]	–380	408–415	–270	–271	Bergelin *et al.* 2006	8.1
		10242[1]	–701	735–748	–220	–210	Bergelin *et al.* 2006	7.5
		10076	–922	964–975		–118	Bergelin *et al.*2006	8.4
	KLX08	10649	–150	197–206	–266	–266	Bergelin *et al.* 2008a	8.1
		[4]	–320	396–400	–245	–245	Bergelin *et al.* 2008a	8.0
		11159	–391	476–485		–210	Bergelin *et al.* 2008a	7.6
		11228	–505	609–618		–239	Bergelin *et al.* 2008a	8.3
	KLX13			432–439	–287		Bergelin *et al.* 2008b	8.4
				499–506	–277		Bergelin *et al.* 2008b	8.2
	KLX15			623–634			Delivered by Sicada	7.6
	KLX17			416–437	–285	–297	Delivered by Sicada	7.92
				642–701	–303		Delivered by Sicada	8.36

[1] These samples are not representative, but there are no other samples highlighted as representative for these sections.

[2] The sample representative for this section is # 7953.

[3] The samples corresponding to this section have disappeared from 2.2 data freeze as they do not have chemical data.

[4] There are not selected samples as representative for this section.

Figure A-15. *Upper: Redox potential measurements (Eh) by platinum, gold and glassy carbon electrodes at surface (EHPTY, EHAUY and EHCY); Lower: pH measurements by two glass electrodes at the surface (PHY and PHIY) in KSH01 borehole at 156.5–167 m borehole length (directly taken from Wacker et al. 2004).*

For the section at **245–261.6 m** depth (borehole length), the UZ selected a pH value of 8.1 in agreement with the value indicated in the P-report (pH=8.17; Figure A-16). With respect to Eh, the value selected in the P-report (–160 mV, Table A-2) apparently corresponds to the mean value for the final measurements of the three Eh electrodes (Pt, Au and C) at the surface (down-hole Chemmac measurements were unsuccessful in all studied sections in KSH01 due to communication problems and borehole pump failure; Wacker *et al.* 2004). However, as it can be seen in Figure A-17, only the Pt and C electrodes provide stable measurements around –210 mV. The Au electrode (whose measurements were not even included in Sicada's compilation of Chemmac data) indicates an Eh value around –100 mV. As the difference with the other two readings is much higher than 50 mV, we selected the value indicated by the Pt and C electrodes (–210 mV), neglecting the Au electrode measurement.

For the section at **548–565.4 m** depth, the UZ selected a pH value of 8.05 in agreement with the value indicated in the P-report (pH=8.08; Figure A-18). The Eh value selected in the P-report was –173 mV. In this case, having a look at the readings of the three Eh electrodes (Pt, Au and C) at the surface (Figure A-19), the basis for this value is not clear at all. Pt and Au electrodes provide a stable and similar reading of −240 mV over more than a month, whereas the C electrode does not give a stable reading during this same time interval. Therefore, the value selected by the UZ as representative for this section is −240 mV.
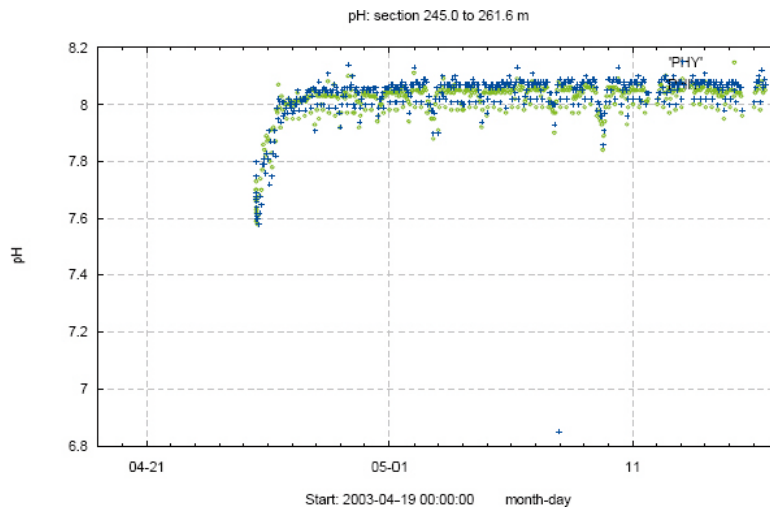
Figure A-16. *Measurements of pH two glass electrodes at surface (PHY and PHIY) at KSH01 borehole at 245–261.6 m, borehole length. The laboratory pH in each collected sample (PHL) is given for comparison. (from Wacker et al. 2004).*
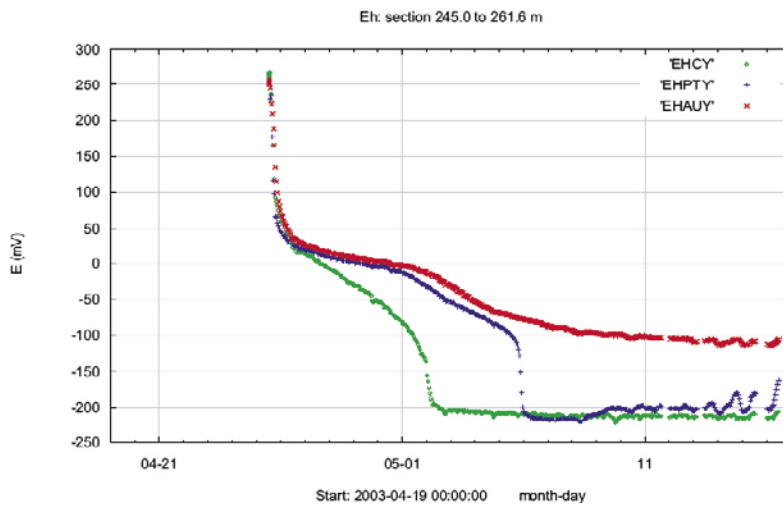
Figure A-17. *Redox potential measurements (Eh) by platinum, gold and glassy carbon electrodes at surface (EHPTY, EHAUY and EHCY) in KSH01 borehole at 245–261.6 m, borehole length (directly taken from Wacker et al. 2004).*
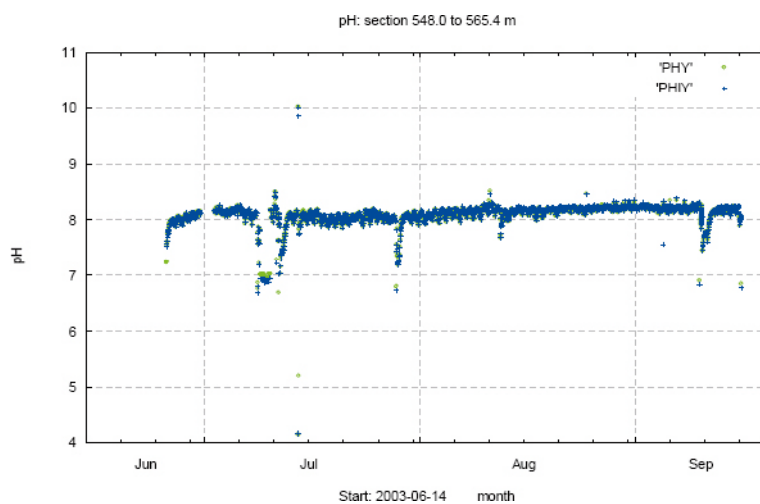
Figure A-18. *Measurements of pH two glass electrodes at surface (PHY and PHIY) at KSH01 in section 548–565 m, borehole length. (Directly copied from Wacker et al. 2004).*

253

The UZ selection of Eh for this last section (548–565.4 m depth) was based on the data reported in the corresponding P-report (Wacker *et al.* 2004) as the loggings provided by Sicada did not include the Au electrode measurements and the Eh values for the other two electrodes were wrong as they were reported as positive (stable values at +240 mV; Figure A-20, to be compared with Figure A-19).

So, this selection was done assuming that the correct values correspond to the ones presented in the P-report and that some kind of sign problem had happened during the transcription of the log data to Sicada.

A.4.2 Chemmac measurements in KLX03

The available loggings in KLX03 borehole correspond to sections at 193.5–198.4 m, 408.0–415.3 m, 735.5–748.0 m and 964.5–975.2 m. These values were delivered by Sicada in the 2.1 data freeze (July, 11th, 2005) but the corresponding P-report was not sent as a draft until February 2007. Therefore, representative Eh and pH values for this borehole were only based on the proposal of the UZ group in Laxemar 2.1. Now we can compare the selected values with the ones reported in the P-report and here we present this comparison and evaluation.

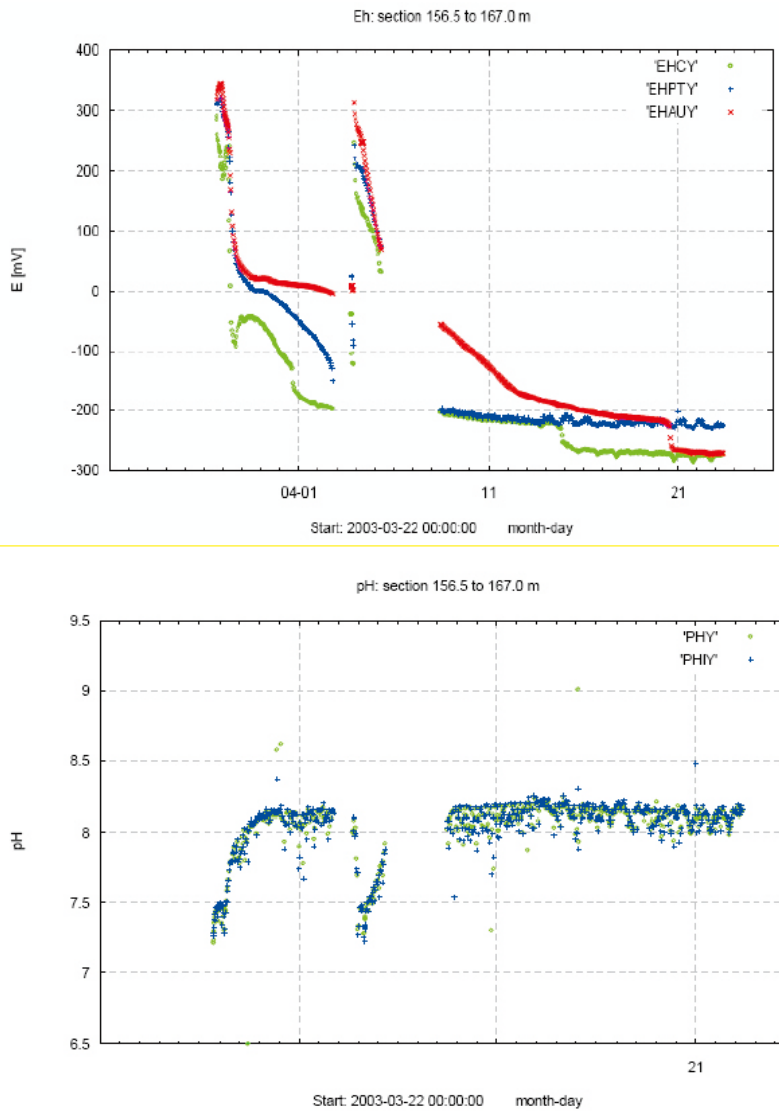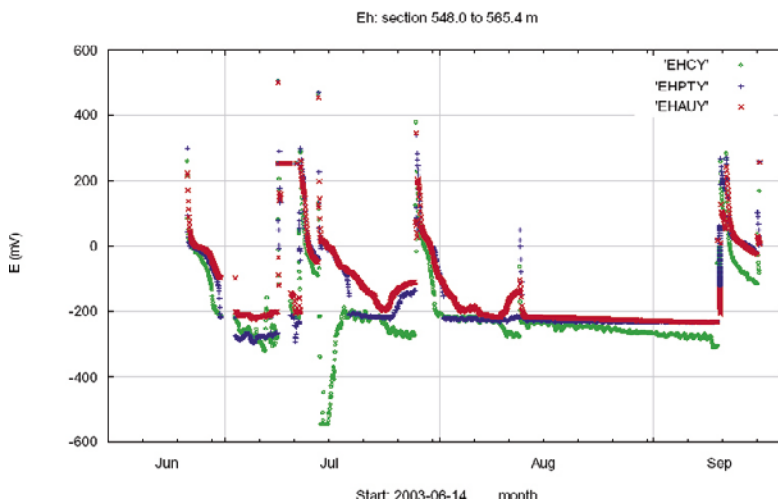***Figure A-19.*** *Redox potential measurements (Eh) by platinum, gold and glassy carbon electrodes at surface (EHPTY, EHAUY and EHCY) in KSH01 borehole at 548–565.4 m, borehole length (from Wacker et al. 2004).*
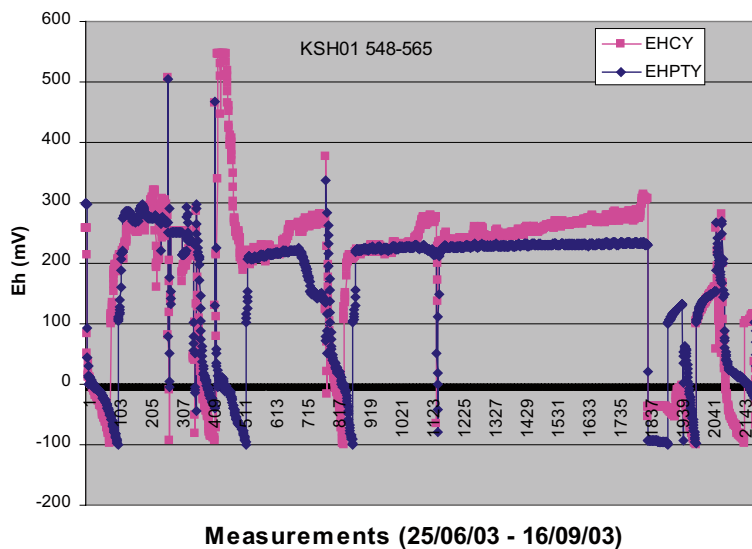
Figure A-20. *Values of redox potential measurements shown in Figure 19, as they were delivered from Sicada.*

For the section at **193.5–198.4 m** depth the selected values in the P-report are: Eh = −285 ± 19 mV from the down-hole electrodes and pH = 8.2 from the surface ones. In both cases the selection agrees very well with the representative values selected by the UZ for Laxemar 2.1 (Eh = −275 and pH = 8.17; Figure A-21) and therefore, these last values have been kept in order to be coherent with the data included in the table that ChemNet is using for modelling (Table A-3).

For the section at **408.0–415.3 m** depth the representative Eh value selected in the P-report (Eh = −271 ± 6 mV from surface electrodes; Figure A-22) agrees with the one selected by the UZ for Laxemar 2.1 (Eh = −270 mV). However, in the P-report a pH = 7.9 (both down hole and at the surface) is proposed from the final part of the log, whereas no value was selected by the UZ for Laxemar 2.1 due to stabilisation problems (Figure A-23).

Figure A-21. Upper: Redox potential measurements (Eh) by gold, glassy carbon and platinum electrodes in the borehole section (EHAUB, EHCB and EHPTB) and at the surface (EHAUY, EHCY and EHPTY) in boreholeKLX03, borehole section 193.5–198.4 m. The arrow shows the chosen representative Eh values for the borehole section. Lower: Measurements of pH by one glass electrodes in the borehole section (PHB) and two glass electrode at the surface (PHY and PHIY). The response from PHIB was not stable and was therefore rejected. The laboratory pH in each collected sample (PHL) is given for comparison. The arrow shows the chosen representative pH values for the borehole section. (The plots and the figure captions have been directly copied from Bergelin et al. 2006).

Figure A-22. *Upper: Redox potential measurements (Eh) by gold, glassy carbon and platinum electrodes in the borehole section (EHAUB, EHCB and EHPTB) and at the surface (EHAUY, EHCY and EHPTY) in borehole KLX03, borehole section 408–415.3 m. The arrow shows the chosen representative Eh values for the borehole section. Lower. Measurements of pH by one glass electrode in the borehole section (PHIB) and two glass electrodes at the surface (PHY and PHIY). The response from PHB was not stable and was therefore rejected. The laboratory pH in each collected sample (PHL) is given for comparison. The arrow shows the chosen representative pH values for the borehole section. (The plots and the figure captions have been directly copied from Bergelin et al. 2006).*
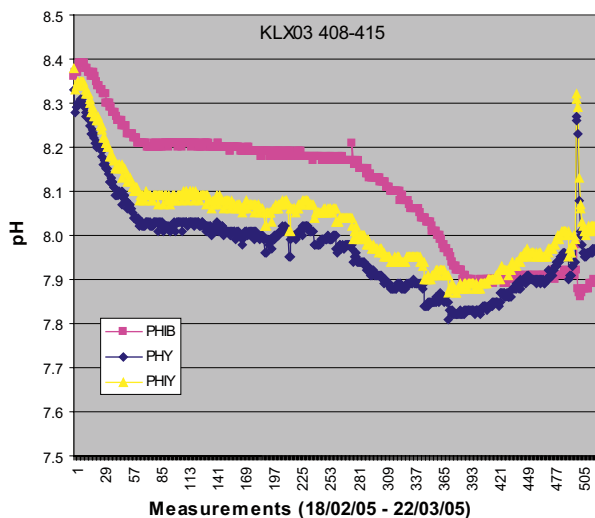
Figure A-23. *pH measurements in the borehole section KLX03 408–415 m (PHIB) and at the surface (PHY, PHIY). Data taken from Sicada database and plotted by the University of Zaragoza.*

256

For the section at **735.5–748.0 m** depth the representative Eh value selected in the P-report
(Eh = −210 ± 11 mV from surface electrodes) agrees with the one selected by the UZ for
Laxemar 2.1 (Eh = −220 mV; Figure A-24). At the beginning of the log, stable measurements
were recorded by the three pH electrodes but with different values: 8.0, 8.1 and 8.2. The laboratory
pH values during water sampling in this section (between 7.9 and 8.2), are in good agreement with
this range. Therefore a value of pH = 8.1 ± 0.1 has been suggested for this section in Laxemar 2.2,
although caution is recommended.

Two pH values are reported in the P-report: 7.1 at depth (borehole) and 7.5 at the surface. However,
the value at depth corresponds to a non-stable reading (Figure A-25, pink squares) and because of
that, for Laxemar 2.1 the UZ selected as representative the pH value measured at the surface simul-
taneously by two electrodes (also in agreement with the value indicated in the P-report, pH = 7.5).
Therefore, the Eh and pH values selected for Laxemar 2.1 have been kept.

Figure A-24. *Upper. Redox potential measurements (Eh) by gold, glassy carbon and platinum electrodes
in the borehole section (EHAUB, EHCB and EHPTB) and at the surface (EHAUY, EHCY and EHPTY) in
borehole KLX03, borehole section 735.5–748 m. The arrow shows the chosen representative Eh values for
the borehole section. Lower. Measurements of pH by one glass electrodes in the borehole section (PHIB)
and two glass electrodes at the surface (PHY and PHIY). The response from PHB was not stable and was
therefore rejected. The laboratory pH in each collected sample (PHL) is given for comparison. The arrow
shows the chosen representative pH values for the borehole section. (The plots and the figure captions have
been directly copied from Bergelin et al. 2006).*

257
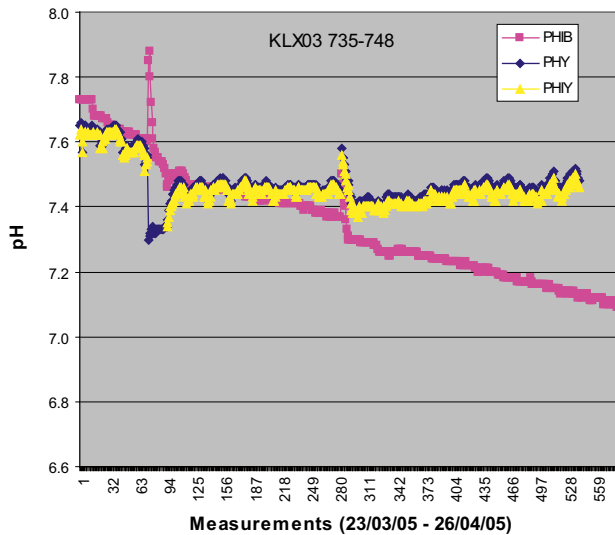
Figure A-25. pH measurements in the borehole section KLX03 735–748 m (PHIB) and at the surface (PHY, PHIY). Data taken from Sicada database and plotted by the University of Zaragoza.

For the section at **964.5–975.2 m** depth the down-hole pH value selected by the UZ for Laxemar 2.1 was 8.4. This value agrees with the value (pH = 8.3 ± 0.2) proposed in the P-report (Figure A-26). The Eh value selected in the P-report (−118 ± 35 mV) is the value that corresponds to the electrode with the most negative potential. No value was selected by the UZ in Laxemar 2.1 because readings, both down hole and at the surface, do not reach a perfect stable plateau (as it is recognised in the P-report) and differences between the Eh values recorded were higher than 200 mV (Figure A-27). The presence of oxygen (up to 0.5 mg/L over the logging time) seems to be the reason for these problems. Therefore the value of –118 ± 35 mV has been rejected.

Figure A-26. Measurements of pH by two glass electrodes in the borehole section (PHB and PHIB) and two glass electrodes at the surface (PHY and PHIY) in borehole KLX03, borehole section 735.5–748 m. The laboratory pH in each collected sample (PHL) is given for comparison. The arrow shows the chosen representative pH values for the borehole section. (The Plot and the Figure caption have been directly copied from Bergelin et al. 2006).
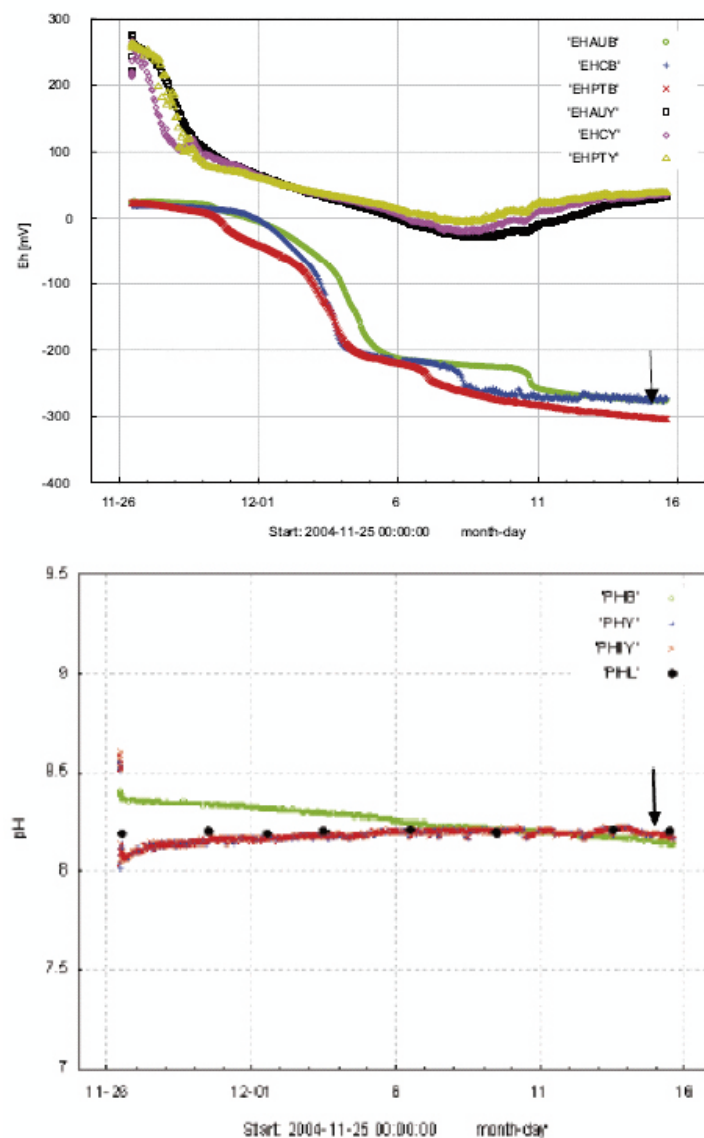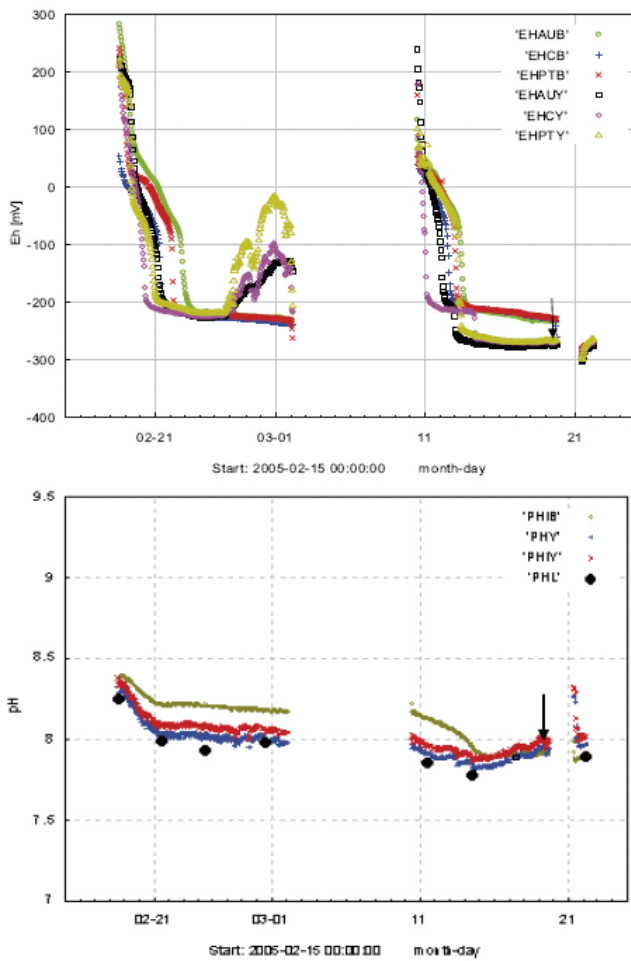
Figure A-27. *Redox potential measurements (Eh) by gold, glassy carbon and platinum electrodes in the borehole section (EHAUB, EHCB and EHPTB) and at the surface (EHAUY, EHCY and EHPTY) at KLX03 in section 964.5–975.2 m. The arrow shows the chosen representative Eh value for the borehole section in the P-Report (Bergelin et al. 2006; The plot and the figure caption have been directly copied from it).*

A.4.3 Chemmac measurements in KLX08

The available loggings in KLX08 borehole correspond to sections at 197.0–206.6 m, 396.0–400.9 m, 476.0–485.6 m and 609.0–618.5 m.

Pt, Au and C surface electrode readings at **197.0–206.6 m** indicate oxidant or not very reducing conditions. However, Pt and C down-hole electrodes provide stable and coincident readings (and at the end of logging also the Au electrode) around –260 mV although during Eh measurements oxygen was detected at levels of 0.1 mg/L. Two down-hole pH electrodes indicate stable and coincident readings of pH = 8.1. These values are in agreement with those indicated in the P-report, Eh = −266 ± 8 mV and pH = 8.1 ± 0.1 and are thus kept as representative (Figure A-28).

In the section at **396.0–400.9 m** Pt, Au and C surface electrodes do not reach stability. However, down hole the three electrodes provide stable and coincident readings at around –250 mV (also in this case oxygen was detected at levels of 0.06 mg/L). Two pH borehole electrodes indicate stable and coincident readings at pH = 8.0. These values are in agreement with those indicated in the P-report, Eh = −245 ± 24 mV and pH = 8.0 ± 0.1 and these last ones were selected as representative values (Figure A-29).

The Eh values indicated in the P-report for sections **476.0–485.6** and **609.0–618.5 m**, are −210 ± 52 and −239 ± 11 mV, respectively (Figure A-30). However it is also indicated there that the Eh electrodes did not reach stability within the measurement period. The review of the logs for these sections confirms this fact and thus the Eh values have been rejected.

The pH value selected by the UZ for the section at **476.0–485.6 m** is 7.6 (from two down-hole electrodes), in agreement with the value indicated in the P-report (7.6 ± 0.2). In the section at **609.0–618.5 m** the pH value proposed in the P-report is 8.4, both down hole and at the surface, but the down-hole log is too short and noisy and a more stable value around 8.2 is recorded in the surface electrodes (Figure A-31). Therefore, a pH value of 8.3 ± 0.1 has been selected.
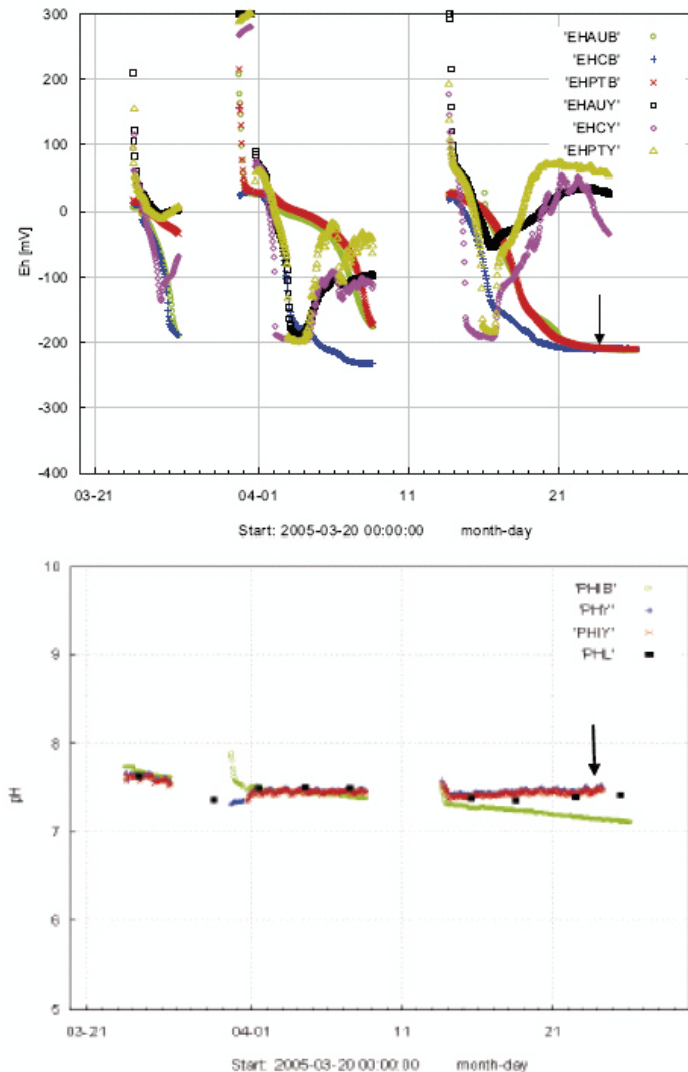
Figure A-28. *Upper: Redox potential measurements (Eh) by gold, glassy carbon and platinum electrodes in the borehole section (EHAUB, EHCB and EHPTB) and at the surface (EHAUY, EHCY and EHPTY) in borehole KLX08, borehole section 197–206.6 m. The arrow shows the chosen representative Eh values for the borehole section. Lower: Measurements of pH by two glass electrodes in the borehole section (PHB and PH1B) and two glass electrodes at the surface (PHY and PHIY). The laboratory pH in each collected sample (PHL) is given for comparison. The arrows show the chosen representative pH values for the borehole section. (The plots and the figure captions have been directly copied from Bergelin et al. 2008a).*
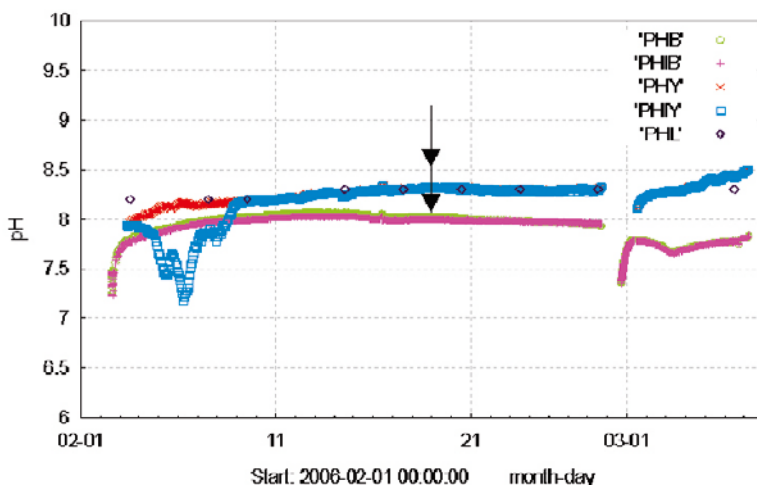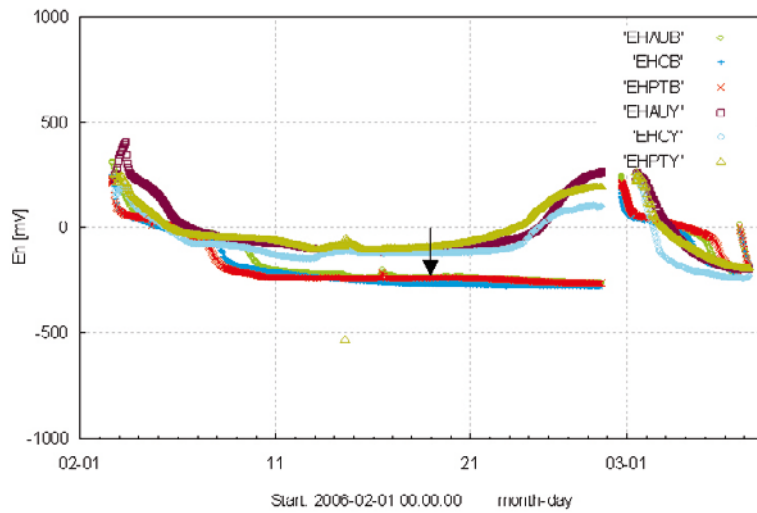
Figure A-29. *Upper: Redox potential measurements (Eh) by gold, glassy carbon and platinum electrodes in the borehole section (EHAUB, EHCB and EHPTB) and at the surface (EHAUY, EHCY and EHPTY) in borehole KLX08, borehole section 396–400.9 m. The arrow shows the chosen representative Eh values for the borehole section. Lower: Measurements of pH by two glass electrodes in the borehole section (PHB and PH1B) and two glass electrodes at the surface (PHY and PHIY). The laboratory pH in each collected sample (PHL) is given for comparison. The arrow shows the chosen representative pH values for the borehole section. (The plots and the figure captions have been directly copied from Bergelin et al. 2008a).*


Figure A-30. *Redox potential measurements (Eh) by gold, glassy carbon and platinum electrodes in the borehole section (EHAUB, EHCB and EHPTB) and at the surface (EHAUY, EHCY and EHPTY) in KLX08. The arrows show the chosen representative Eh values for the borehole section. Left: section 476–485. Right: section 609–618. (The plots and the figure captions have been directly copied from Bergelin et al. 2008a).*
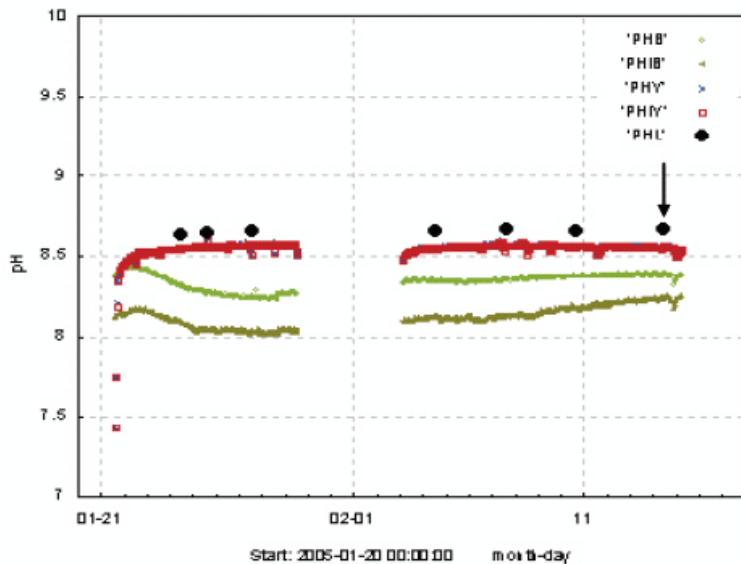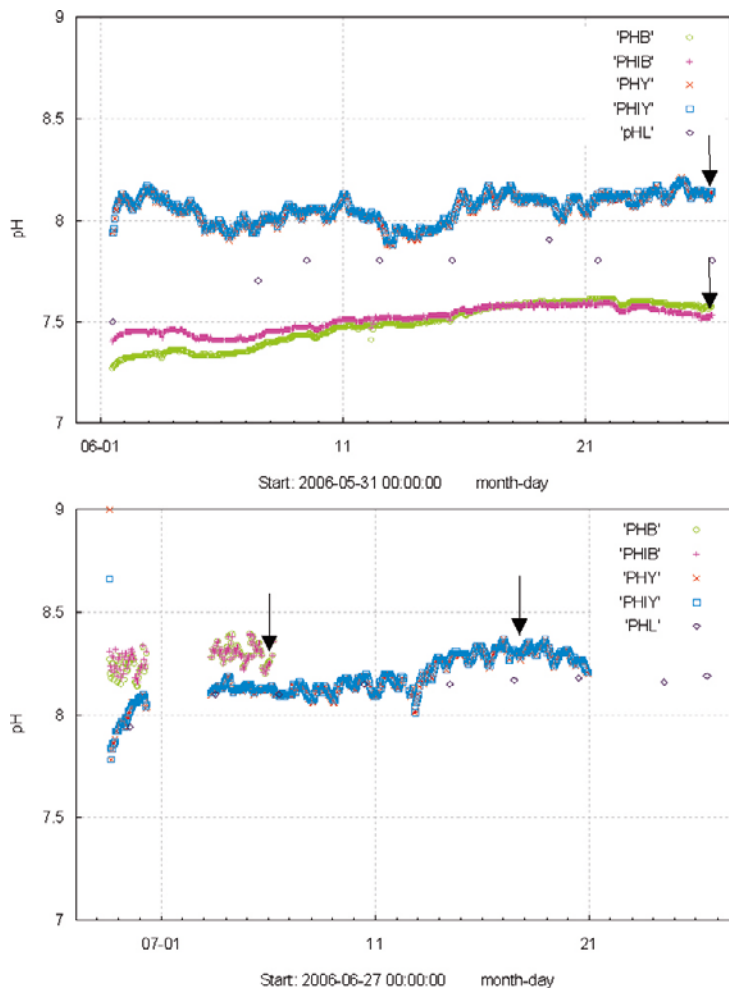
Figure A-31. *Measurements of pH by two glass electrodes in the borehole section (PHB and PH1B) and two glass electrodes at the surface (PHY and PHIY). The laboratory pH in each collected sample (PHL) is given for comparison. The arrows show the chosen representative pH values for the borehole section in the P-report (from Bergelin et al. 2008a). Upper. KLX08 in section 476–485 m. Lower: KLX08 in section 609–618 m.*

A.4.4 Chemmac measurements in KLX13

The available loggings in KLX13 borehole correspond to sections at 432–439 m and 499–506 m.

C and Pt surface electrode readings at **432–439 m** are not very stable and indicate oxidant conditions. However, C, Pt and Au down-hole electrodes provide stable and coincident readings about –287 mV. This value can be considered as Group 1 and it is in agreement with the value selected in the P-report. Two surface and one down-hole pH electrodes indicate stable and coincident readings of pH = 8.3. The other down-hole pH electrode indicates a stable reading about 8.55. Therefore, the final selected values are Eh = −287 mV and pH = 8.4 ± 0.1 (Figures A-32 and A-33).

In the section at **499–506 m** C and Pt surface electrodes do not reach stability. However, down-hole the three electrodes (C, Pt and Au) provide stable and coincident readings at around –277 mV. The two pH borehole electrodes indicate stable and coincident readings at pH = 8.2 and the two pH surface electrodes are very stable and with coincident readings at pH about 8. Therefore, the selected values are Eh = –277 mV (Group 1) and pH = 8.2 (Figures A-32 and A-33) in agreement with the selection indicated in the P-report. However, the water sample taken at this interval contained 16.6% of drilling water and therefore this sample has not been included in the modelling.
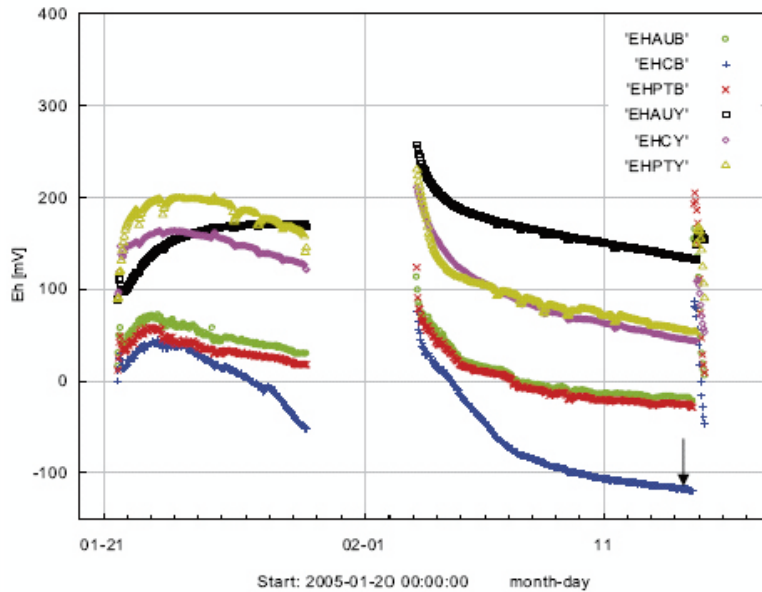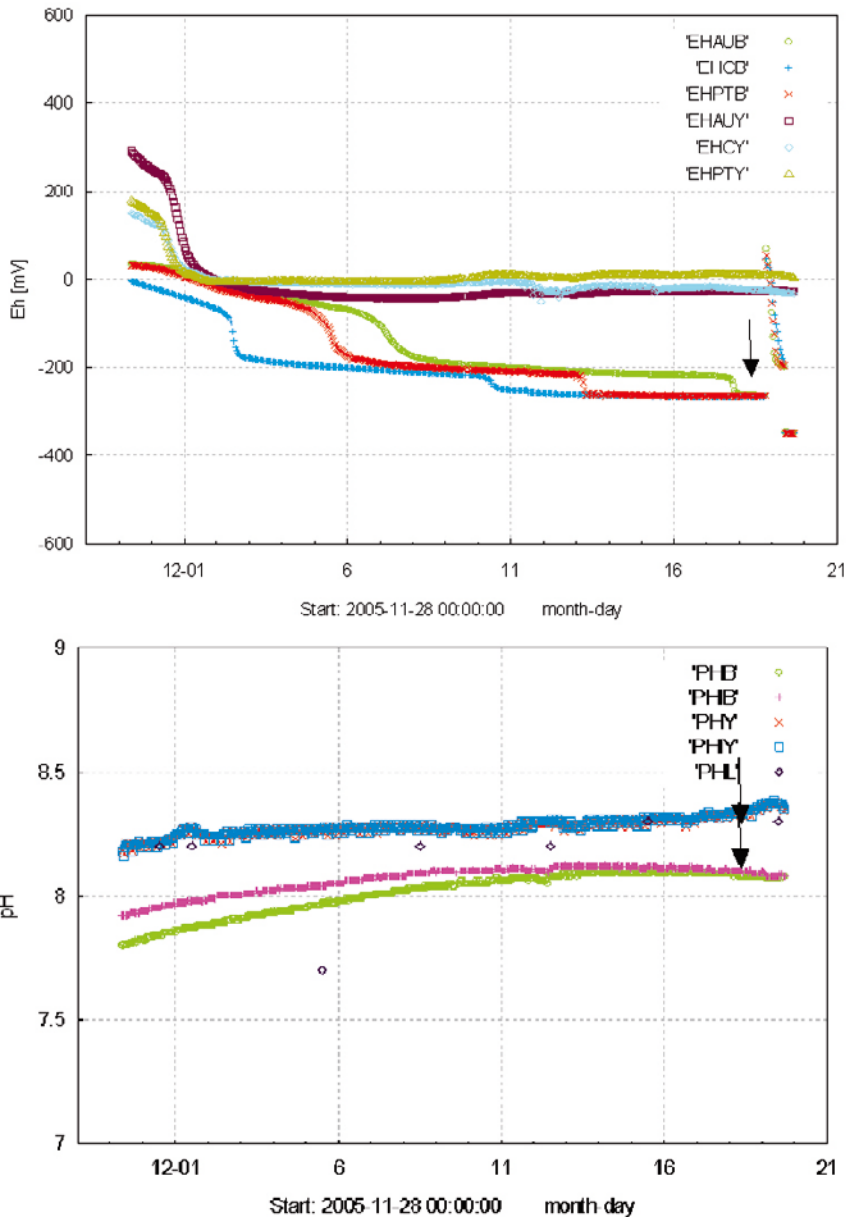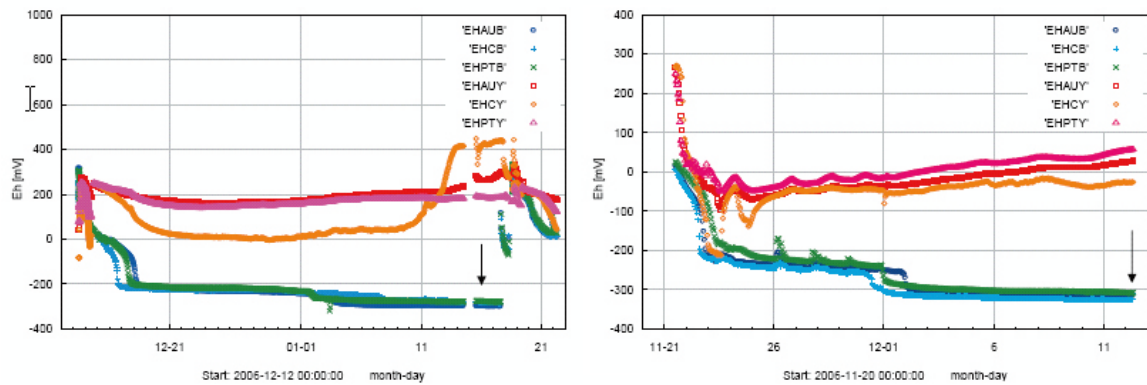
Figure A-32. *Redox potential measurements (Eh) by gold, glassy carbon and platinum electrodes in the borehole section (EHAUB, EHCB and EHPTB) and at the surface (EHAUY, EHCY and EHPTY). The arrows show the chosen representative Eh values for the borehole section. Left: KLX13A, section 432–439.2. Right: KLX13A, section 499.5–506.7 m. (The plots and the figure captions have been directly copied from Bergelin et al. 2008b).*
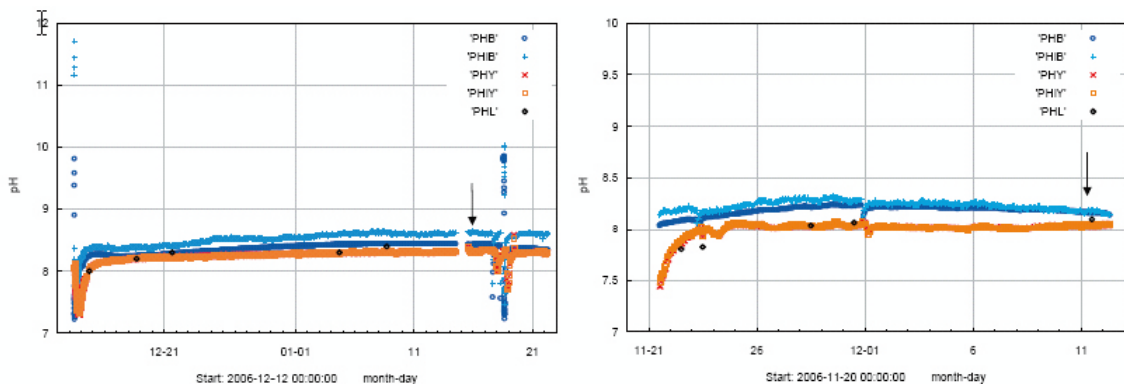
Figure A-33. *Measurements of pH by two glass electrodes in the borehole section (PHB and PH1B) and two glass electrodes at the surface (PHY and PHIY). The laboratory pH in each collected sample (PHL) is given for comparison. The arrows show the chosen representative pH values for the borehole section in the P-report (from Bergelin et al. 2008b). Upper. KLX13A, section 432–439.2 m. Lower: KLX13A, section 499.5–506.7 m. (The plots and the figure captions have been directly copied from Bergelin et al. 2008b).*

A.4.5 Chemmac measurements in KLX15

The only available logging in KLX15 borehole corresponds to section at 623–634 m.

C and Pt surface electrode readings are not very stable and indicate oxidant conditions. C, Pt and Au down-hole electrodes do not give stable readings and also indicate oxidant or slightly reducing conditions. Taken into account the criteria indicated in Section A-2, an Eh value cannot be selected. Groundwater samples taken at this section indicate the presence of dissolved Fe(II), CH_4 and even, in some moments, S(–II) above detection limit. Microbiological data indicate the presence of IRB, SRB, MRB, AA and HA. These characters indicate a clear reducing environment in absolute disagreement with the oxidant conditions qualitatively suggested by the Eh measurements. Therefore, some disturbances during Eh measurements must have occurred in this section.

Two surface pH electrodes indicate more or less stable and coincident readings of pH = 7.5. The two down-hole pH electrodes indicate a more or less stable reading about 7.7. Therefore, the Eh value is not representative and the final selected pH values is pH = 7.6 ± 0.1 (Figure A-34).

263
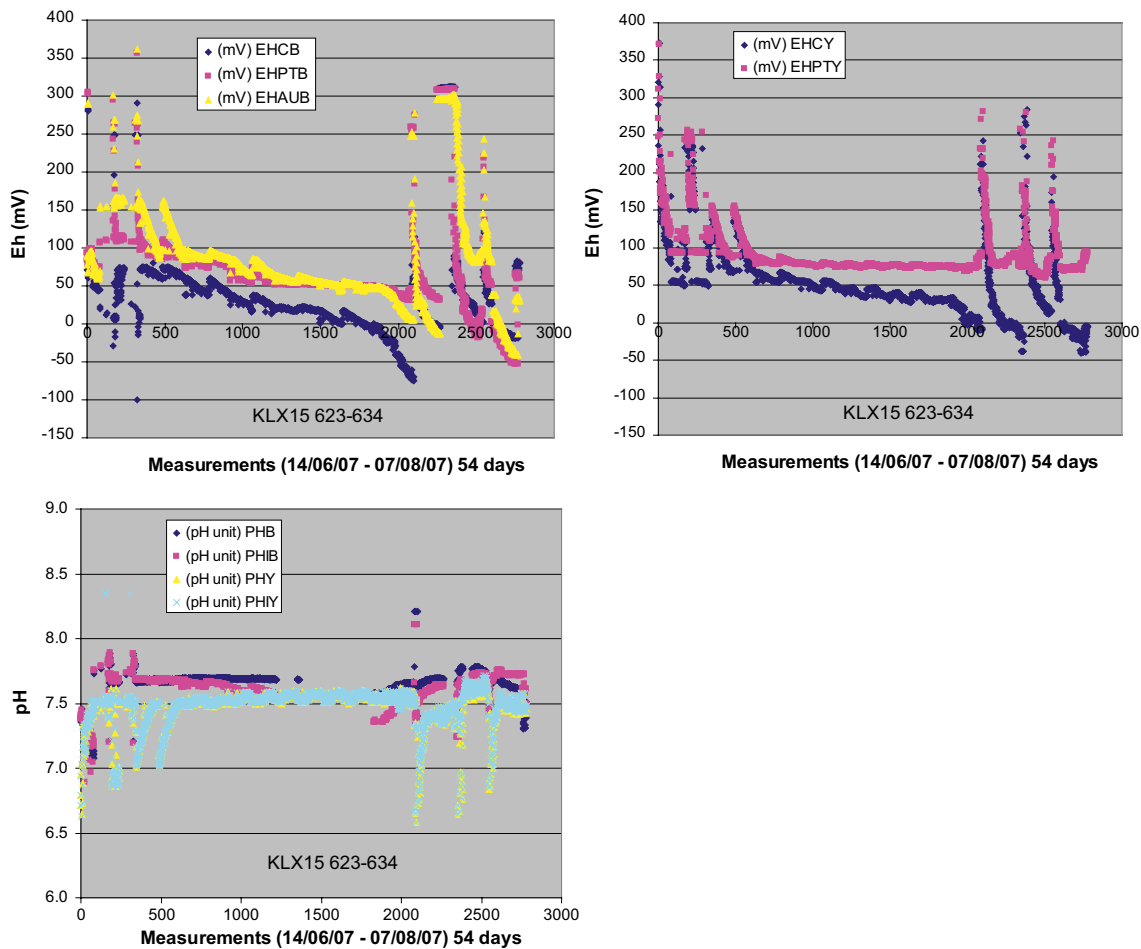
Figure A-34. *Redox potential measurements (Eh) by glassy carbon, platinum and gold electrodes in the borehole section (EHCB, EHPTB and EHAUB; upper left panel) and redox potential measurements by glassy carbon and platinum electrodes at the surface (EHCY and EHPTY; upper right). pH measurements in the borehole section (PHB, PHIB) and at the surface (PHY and PHIY; lower panel). Borehole KLX15, borehole section 623–634 m.*

A.4.5 Chemmac measurements in KLX17

The available loggings in KLX137 borehole correspond to sections at 416–437 m and 642–701 m.

C and Pt surface electrode readings at **416–437 m** are very stable and indicate reducing conditions with Eh values about −285 mV. Pt and Au down hole electrodes provide also stable and coincident readings about –285 mV. This value can be considered as Group1. Two surface and two down hole pH electrodes indicate stable and coincident readings of pH = 7.92. Therefore, the final selected values are Eh = −285 mV and pH = 7.92 (Figure A-35).

In the section at **642–701 m** there are not data from down-hole electrodes. C and Pt surface electrodes show initially more or less stable readings between −300 and −380 mV and finally both electrodes indicate a coincident reading of –303 mV. Therefore, the selected values are Eh = −303 mV (Group 2) and pH = 8.36 (Figure A-36).
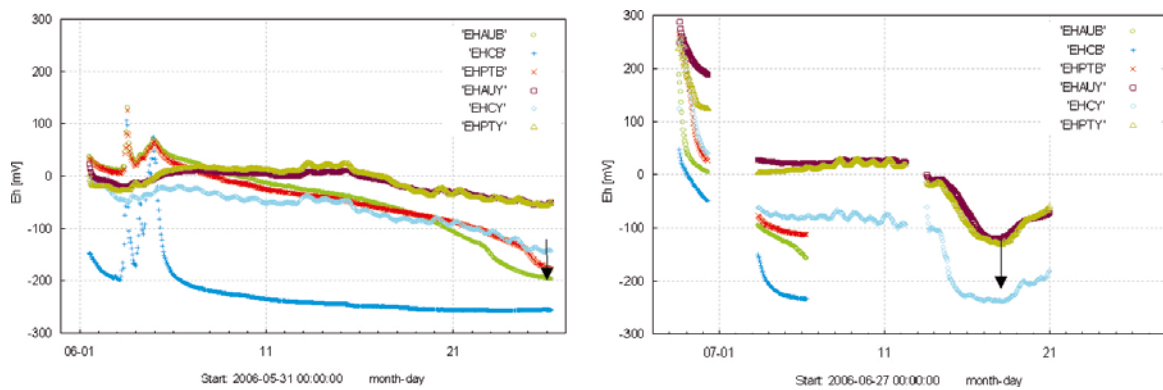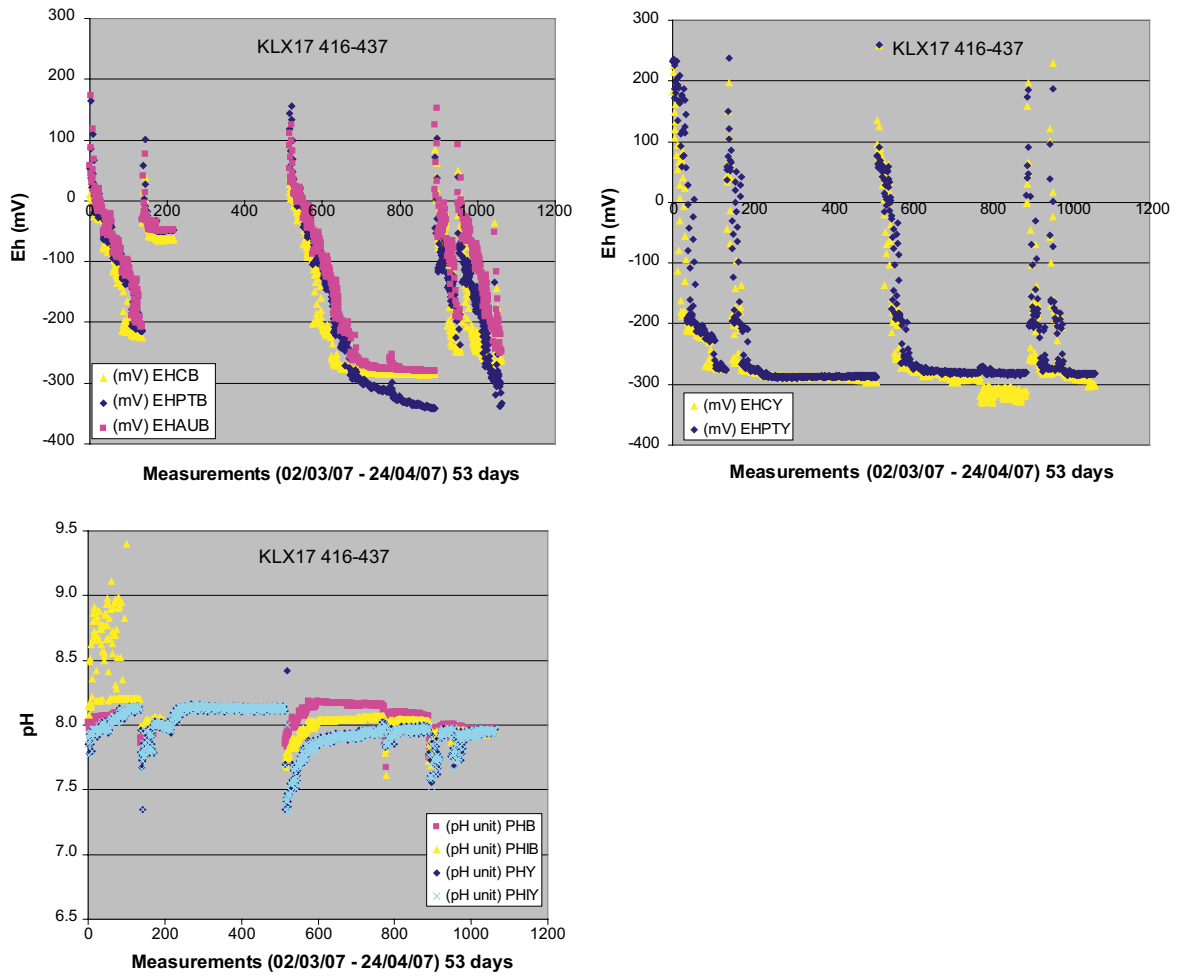
Figure A-35. *Redox potential measurements (Eh) by glassy carbon, platinum and gold electrodes in the borehole section (EHCB, EHPTB and EHAUB; upper left panel) and redox potential measurements by glassy carbon and platinum electrodes at the surface (EHCY and EHPTY; upper right). pH measurements in the borehole section (PHB, PHIB) and at the surface (PHY and PHIY; lower panel). Borehole KLX17, borehole section 416–437 m.*
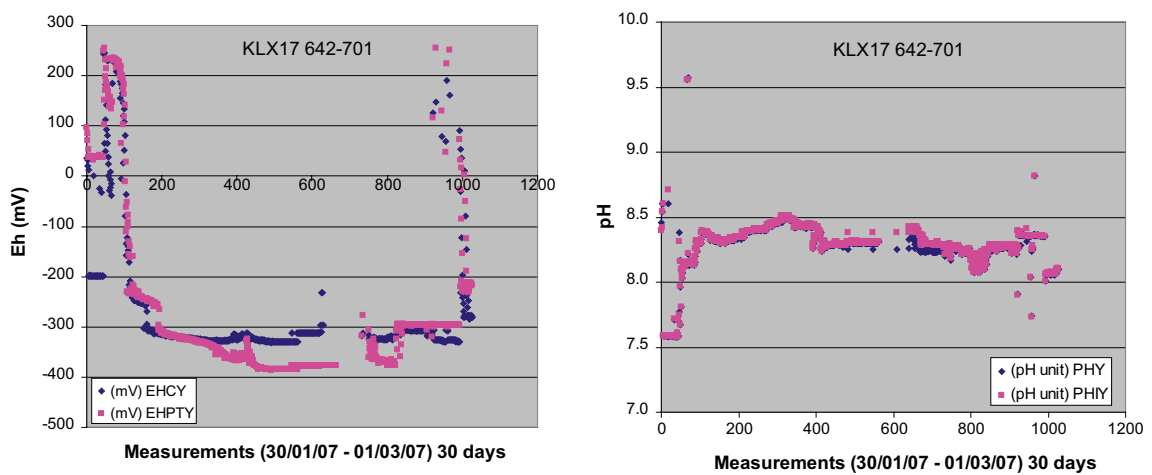
Figure A-36. *Redox potential measurements (Eh) by glassy carbon and platinum electrodes at the surface (EHCY and EHPTY; left). pH measurements at the surface (PHY and PHIY; right panel).*

A.5 Conclusions

The complete set of sections analysed with Chemmac is shown in Table A-3. In general, the sections with representative Eh values show two Eh data: one as reported by previous authors (when available) and the other as selected by the University of Zaragoza for ChemNet modelling tasks. When the values have been considered not representative, only the values reported in previous works (if they exist) are shown.

A.6 References
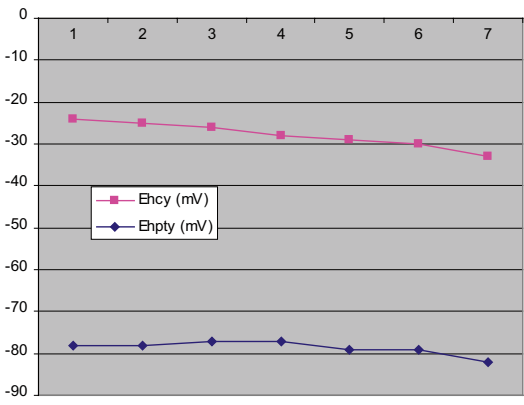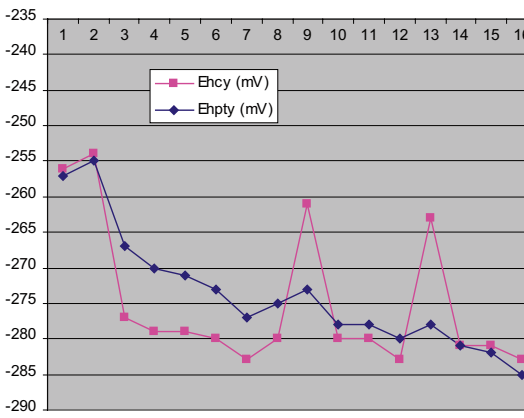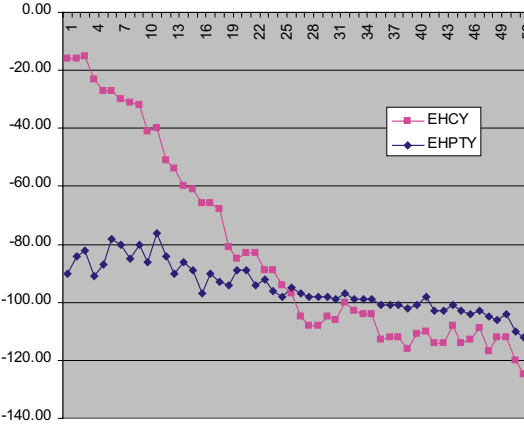
Auqué L, Gimeno M J, Gómez J and Nilsson A-C (2008). Potentiometrically measured Eh in groundwaters from the Scandinavian Shield. Appl. Geochem., 23, 1820–1833.

Bergelin A, Berg C and Wacker P (2006). Oskarshamn site investigation. Complete chemical characterisation in KLX03. Results from four investigated borehole sections: 193.5–198.4 m, 408.0–415.3 m, 735.5–748.0 m, 964.5–975.2 m. SKB P-06-08, 106 pp.

Bergelin A, Nilsson K, Lindquist A and Wacker P (2008a). Oskarshamn site investigation. Complete chemical characterisation in KLX08. Results from four investigated borehole sections: 197.0–206.6 m, 396.0–400.9 m, 476.0–485.6 m, 609.0–618.5 m. SKB P-06-308, 109 pp.

Bergelin A, Nilsson K, Lindquist A and Wacker P (2008b). Oskarshamn site investigation. Complete chemical characterisation in KLX13A. Results from two investigated borehole sections: 432.0–439.2 m, 499.5–506.7 m. SKB P-07-149, 92 pp.

Glynn P D and Voss C I (1999). SITE-94. Geochemical characterization of Simpevarp ground waters near the Äspö Hard Rock laboratory. SKI Report 96-29, SKI, Stockholm, Sweden, 210 p.

Gimeno M J, Auqué L F and Gómez J (2006). Mass balance modelling. In: SKB (2006), Hydrogeochemical evaluation. Preliminary site description. Laxemar subarea, version 2.1. SKB R-06-70, Appendix 3, pp. 175–210.

Gimeno M J, Auqué L F and Gómez J (2007). Water-rock interaction modelling issues. In: SKB (2007), Hydrogeochemical evaluation of the Forsmark site, modelling stage 2.1-issue report. SKB R-06-69, Appendix 3, pp. 131–187.

Grenthe I, Stumm W, Laaksoharju M, Nilsson A-C and Wikberg P (1992). Redox potentials and redox reactions in deep groundwater systems. Chem. Geol., 98, 131–150.

Laaksoharju M, Smellie J A T, Nilsson A-C and Skarman C (1995). Groundwater sampling and chemical characterisation of the Laxemar deep borehole KLX02. SKB TR 95-05.

Nordstrom D K, Plummer L N, Langmuir D, Busenberg E, May H M, Jones B F and Parkhurst D (1990). Revised chemical equilibrium data for major water-mineral reactions and their limitations. In: Melchior, D.C. and Basset, R.L. (Eds.) Chemical Modeling of Aqueous Systems II. ACS Symp. Ser. pp. 398–413.

Smellie J A T and Laaksoharju M (1992). The Äspö Hard Rock Laboratory: Final evaluation of the hydrogeochemical pre-investigations in relation to existing geologic and hydraulic conditions. SKB TR 92-31, 239 p.

SKB (2004). Hydrogeochemical evaluation for Simpevarp model version 1.2. Preliminary site description of the Simpevarp area. SKB R-04-74, 463 p.

SKB (2006a). Hydrogeochemical evaluation. Preliminary site description. Laxemar subarea, version 1.2. SKB R-06-12, 435 p.

SKB (2006b). Hydrogeochemical evaluation. Laxemar subarea version 2.1. SKB R-06-70.

Wacker P, Berg C and Bergelin A (2004). Oskarshamn site investigation. Complete hydrochemical characterisation in KSH01A.Results from four investigated sections, 156.5–167.0, 245.0–261.6, 586.0–596.7 and 548.0–565.4 metres. SKB P-04-12, 72 p.

Table A-3. Summary of all the sections analysed and the selected values for modelling in the different subareas of Laxemar-Simpevarp area. More information about the table is included in Table A-1 and Table A-2.

Subarea	Borehole	Sample No. #	Depth (elev. Secmid)	Borehole section (m)	Eh value (mV) For modelling	Eh value (mV) Previous works	Reference	pH value for model-ling	Group
Äspö	KAS02	1548	−199.8	202–214	−257	−260	Smellie & Laaksoharju (1992)	7.5	2
		1419	−308	314–319	−380	−400	Smellie & Laaksoharju (1992)	8.45	2
		1474	−317	308–344				7.6	
		1428	−456	463–468		−220	Delivered by Sicada	8.35±0.05	
		1433	−523	530–535		−310	Smellie & Laaksoharju (1992)	8.35	
		1560	−881.2	860–924		−150	Delivered by Sicada	8.5	
	KAS03	1569	−122	129–134	−260	−270	Smellie & Laaksoharju (1992)	8.0	1
		1437	−199	196–222				7.65	
		1448	−239	248–251				7.8	
		1445	−454	453–480					
		1452	−602	609–623				8.05	
		1455	−830	690–1002				8.05±0.05	
		1582	−914	860–1002	−270	−270	Smellie & Laaksoharju (1992)	7.3±0.1	2
	KAS04	1596	−185	226–235	−300	−300	Smellie & Laaksoharju (1992)	7.8	1
		1603	−276	334–343	−280	−280	Smellie & Laaksoharju (1992)	7.9	1
		1588	−377	440–480				8.04±0.04	
Ävrö	KAV01	1391	−408	420–425	−215		Grenthe *et al.* (1992)	7.35	1
		1383	−512	522–531	−310		Grenthe *et al.* (1992)	7.0±0.1	2
		1374	−546	558–563	−225		Grenthe *et al.* (1992)	7.4±0.2	2
		1354	−675	635–743				8.15	
Laxemar	KLX01	1537	−257	272–277					
		1528	−441	456–461	−280			8.6±0.1	2
		1516	−673	680–702	−265			7.8±0.2	2
		1773	−897	910–921				8.4	
	KLX02	2738	−299	315–321				8.1	
		2705	−318	335–340				8.05±0.05	
		2712	−778	798–802				7.75	
		3035	−1069	1090–1096				8.6	
		2731	−1531	1420–1700		−300	Delivered by Sicada	8.0±0.1	
	KLX03	7953	−171	193–198	−275	−285	Bergelin *et al.* 2006	8.17	2
		10091	−379.9	408–415	−270	−271	Bergelin *et al.* 2006	8.1	2
		10188	−706	735–748	−220	−210	Bergelin *et al.* 2006	7.5	1
		10076	−922.5	964–975		−118	Bergelin *et al.* 2006	8.4	
	KLX08	10649	−150.4	197–206	−266	−266	Bergelin *et al.* 2008a	8.1	2
		10747	−320	396–400	−245	−245	Bergelin *et al.*2008a	8.0	1
		11159	−390.7	476–485		−210	Bergelin *et al.* 2008a	7.6	
		11228	−504.5	609–618		−239	Bergelin *et al.* 2008a	8.3	
	13	11607	−408	432–439	−287		Bergelin *et al.* 2008b	8.4±0.1	1
		11544	−475	499–506	−277		Bergelin *et al.* 2008b	8.2	1
	15	15008	−467.2	623–634				7.6±0.1	
	17	11809	−342.3	416–437	−285	−297s	Delivered by Sicada	7.92	1
		11692	−548	642–701	−303		Delivered by Sicada	8.36	2
Simpevarp	KSH01A	5263	−152.7	156–167	−250	−257	Wacker *et al.* 2004	8.1	2
		5266	−241.7	245–261	−210	−160	Wacker *et al.* 2004	8.1	2
		5288	−536	548–565	−240	−173	Wacker *et al.* 2004	8.05	2

Eh values rejected for redox modelling (Section 3.2)

KAS02 (308-344)	
	All the logs from the sections in this page were rejected by short measurement periods.

KAS03 (196-222)	KAS03(248-251)

KAS03 (453-480)	KAS03 (609-623)
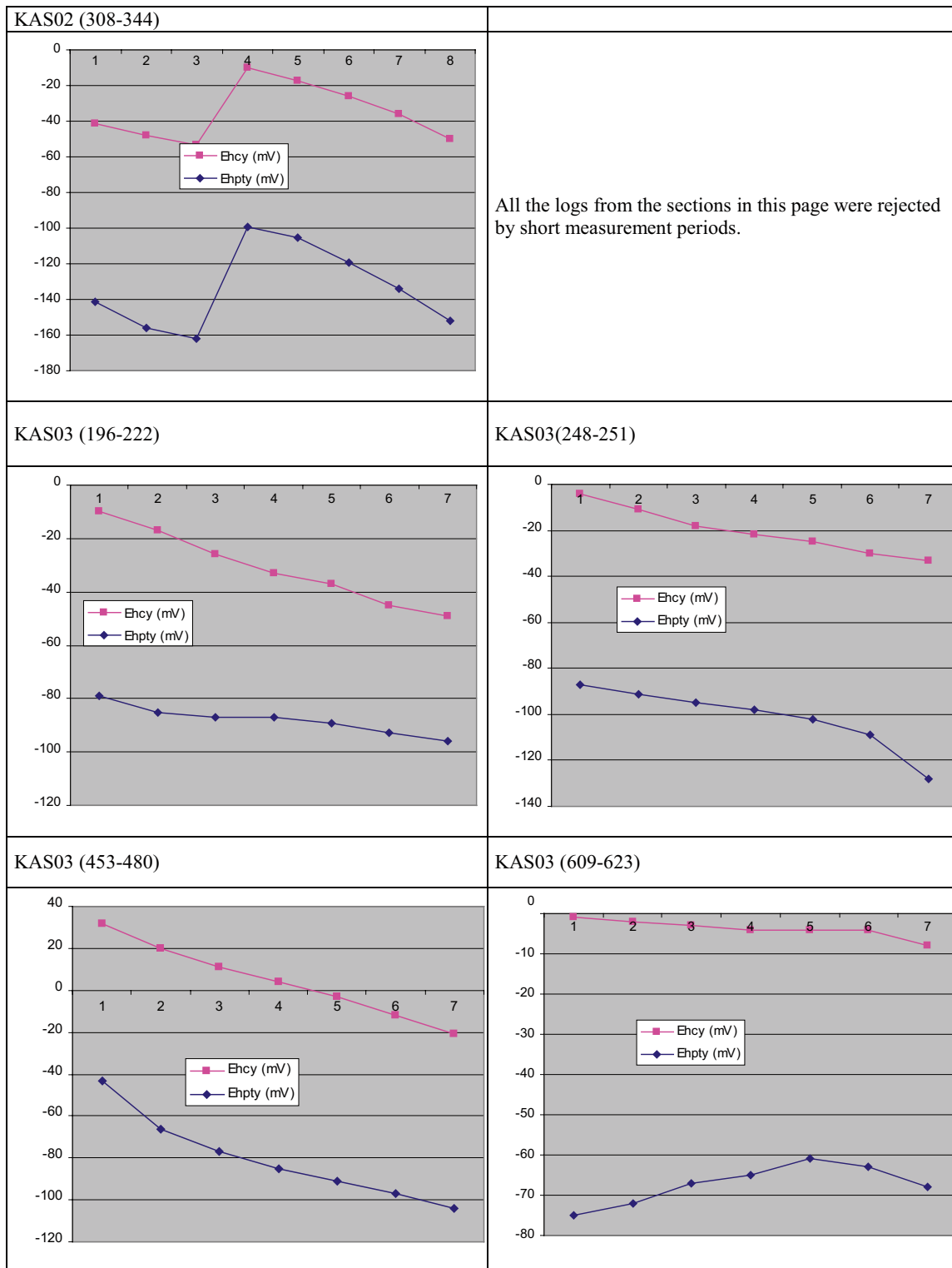
KAS03 (690-1002)	
	Value rejected by short measurement period.
KAS04 (440-480)	
	Value rejected by not stable readings.
KAV01 (635-743)	
	Value rejected by not stable readings.

KLX01 (272-277)
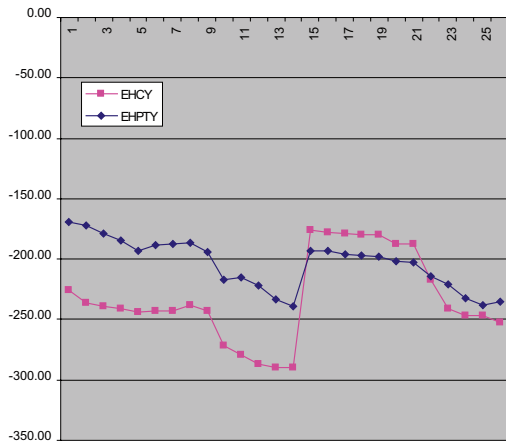
KLX01 (910-921)
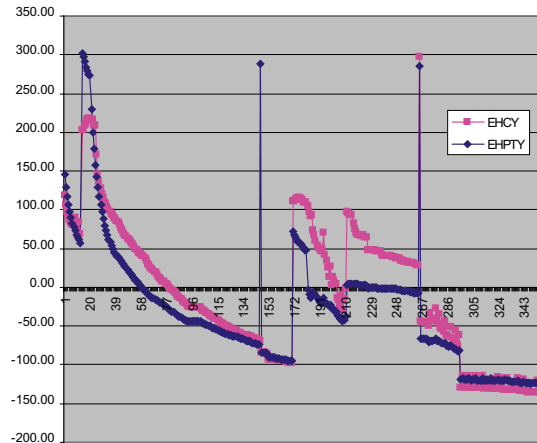
Values in these two sections from KLX01 were rejected by not stable readings.

KLX02 (315-321)
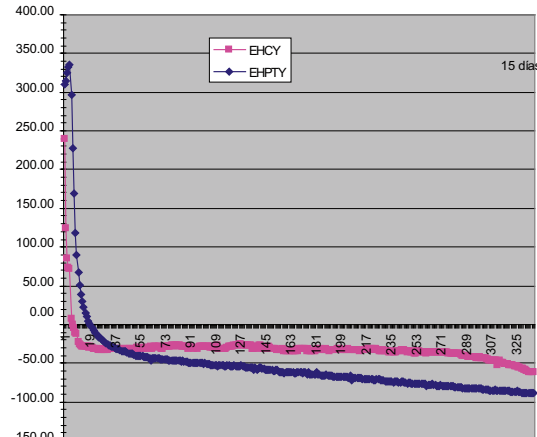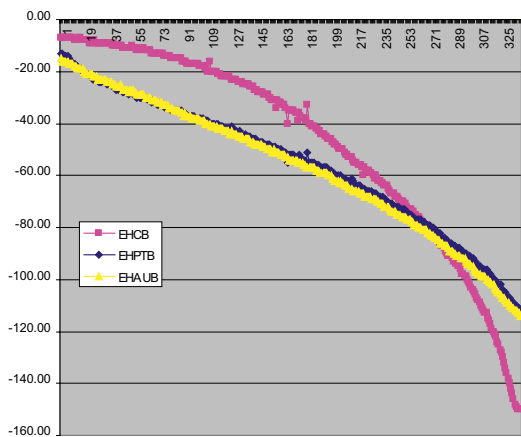
KLX02 (335-340)
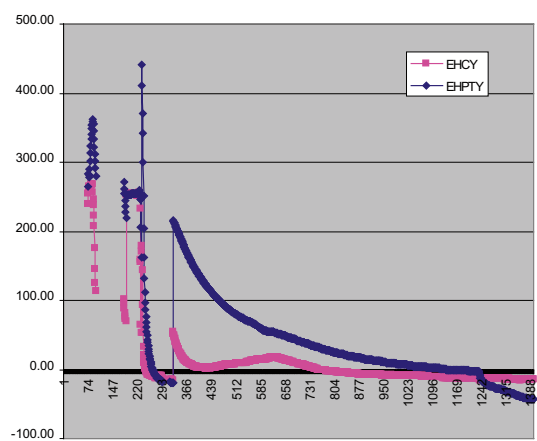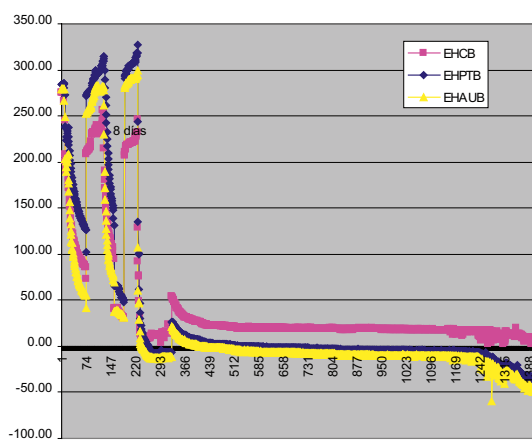
KLX02 (1090-1096)
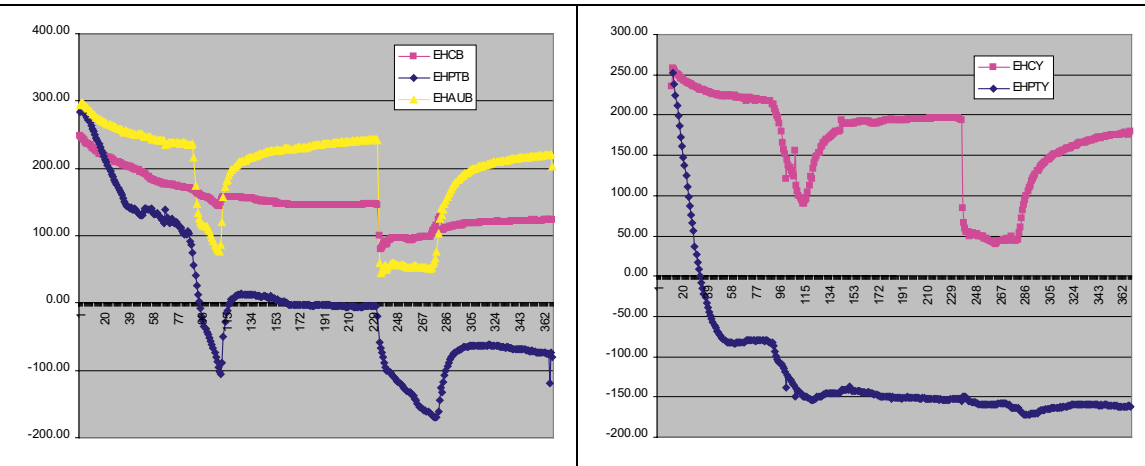
KLX02 (1420-1700)
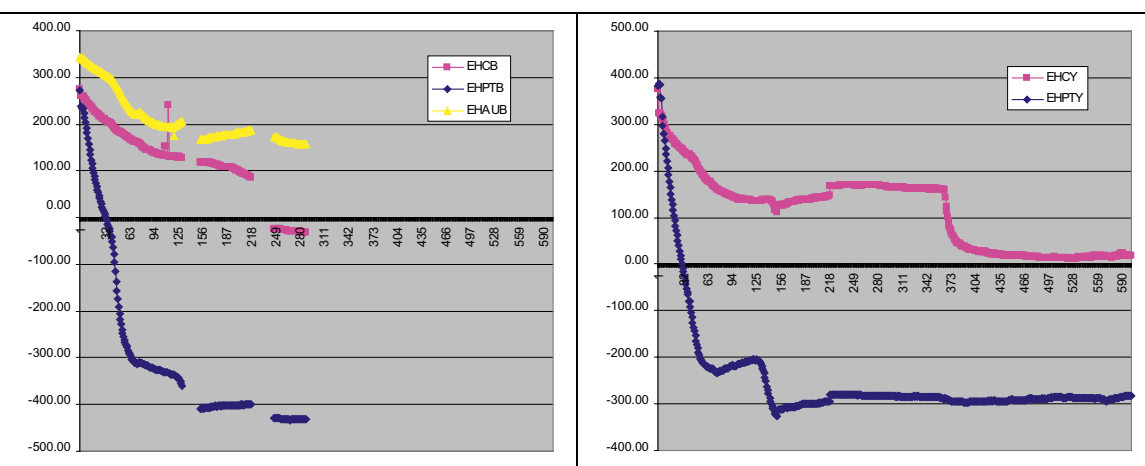
The values for all the sections in KLX02 were rejected in previous works (Laaksoharju *et al.*, 1995) and also by the University of Zaragoza.

271

Sensitivity analysis to the different approaches used for the activity coefficient calculations in the saline groundwaters of Laxemar subarea

B.1   Introduction

Groundwaters from Laxemar-Simpevarp area have a wide range of salinities from very dilute waters with very low TDS, to highly saline waters such as the water selected as the Deep Saline end-member from the Laxemar subarea (Cl = 47,200 mg/L, TDS = 75 g/L and ionic strength around 1.8 molal; for comparison, ionic strength of seawater is around 0.7 molal). Though they do not reach the extreme values found in some brines in the Canadian Shield or other areas in the Scandinavian Shield (Frape *et al.* 1984, Frape *et al.* 2005), the presence of these waters of high salinity can create problems when used in geochemical modelling.

First, density is not directly measured in most of the saline groundwater samples from Laxemar-Simpevarp and speciation-solubility calculations with PHREEQC (Parkhurst and Appelo 1999) have been performed using a value of 1 g/cm³. But, as geochemical codes work with molal units (per kg of solvent) and the available analytical data in Sicada are expressed in mg per litre of solution, density data would be necessary to properly transform the analytical data in molal units. Therefore, the absence of density data in these saline groundwaters is an uncertainty source in the results of speciation-solubility calculations that must be evaluated (sections B.2.1. and B.3.1).

The study of very saline waters in the framework of geochemical modelling is conditioned by the different approaches used to calculate the activity coefficients of the dissolved species. Most modern geochemical codes use the Ionic Association Model with different variants of the Debye-Hückel equation (e.g. the extended Debye-Hückel equation, the Davies equation, the B-dot equation, the Truesdell and Jones' equation, etc); these approaches are considered suitable, in the best of the cases, to model waters with ionic strengths (I) lower than 1 to 2 molal (Nordstrom and Munoz 1994, Bethke 1996, Drever 1997, Langmuir 1997, Zhu and Anderson 2002).

The approach used by the UZ group in the speciation-solubility calculations is the one implemented in the WATEQ4F database (Ball and Nordstrom 2001), i.e., the USGS approach based on the Truesdell and Jones' equation (see section B.2.2.), also incorporated in some Performance Assessment thermodynamic databases like the Nagra / PSI Chemical Thermodynamic Data Base 01/01 (Hummel *et al.* 2002) or SKB TDB (Duro *et al.* 2006). The suggested limit of application of this approach is I ≅ 2 molal (e.g. Langmuir 1997), just the value of the most saline groundwaters in the Laxemar-Simpevarp area.

Uncertainties associated with activity coefficient calculations in geochemical models are always a major concern and the degree of accuracy must be tested for specific (Zhu and Anderson 2002) or "limit" cases like that represented by the most saline groundwaters in Laxemar-Simpevarp. The influence of this uncertainty was already evaluated by Gimeno *et al.* (2004) using the most suitable approach for the activity coefficient calculations in this kind of saline solutions: the Specific Ion Interaction model based on the Pitzer equations (e.g. Pitzer 1973, 1979). Results of the sensitivity analysis indicated that the WATEQ4F database (and thus the USGS approach for activity coefficient calculations) provides similar results for the saturation states of some important minerals.

Uncertainties in geochemical modelling are a main issue in the framework of the hydrogeochemical site characterisation. Therefore, to make the traceability of the used methodology easy, a thorough sensitivity analysis for the geochemical modelling of the more saline waters in Laxemar-Simpevarp area is presented in this Appendix.

B.2   Methodology

Uncertainties in the density values or in the calculation approach used for the activity coefficients are higher in the more saline groundwaters. That is why the following analysis has been performed, mainly, on the more saline samples from the Laxemar-Simpevarp area including the Deep Saline end-member (from Laxemar subarea; composition indicated in Gimeno *et al.* 2008; Table B-1)

together with other samples from the Laxemar subarea such as #2731, #2931 and #2722 from the same borehole KLX02 with chloride contents from 45,500 mg/L to 15,800 mg/L (Table B-1). This wide range of salinities will allow seeing the different effects of the uncertainties as a function of this parameter. As sample #2722 has TDS and chloride values similar to those found in the most saline groundwaters from Forsmark, it can be used as a reference to indirectly evaluate these uncertainties in this area.

Additional groundwaters of similar salinity have also been used in this work as a comparative term for the speciation-solubility results obtained in Laxemar-Simpevarp: Olkiluoto (Finland) and batholith Lac du Bonnet (Canada). The most saline samples from these systems have also been included in this sensitivity analysis (Table B.1): samples KR4/860/1 and KR4/860/2 from Olkiluoto (Pitkänen *et al.* 2004) and samples WB1-7-7 and WB2-20-12 from Lac du Bonnet (Gascoyne 2004).

Finally, uncertainties associated with the activity coefficient calculations have also been explored in much more saline groundwaters from the Canadian Shield (Frape *et al.* 1984, Douglas *et al.* 2000), as a support to discuss some important results. Among them, real "brines", with TDS up to 325 g/L, are also included, allowing a more detailed analysis of the range of validity of the USGS approach for the calculation of activity coefficients.

B.2.1   Density calculations

As stated before, density was not directly measured in most of the available saline groundwater samples from Laxemar-Simpevarp and speciation-solubility calculations have been performed using a value of 1 g/cm³. Therefore, a density value must be obtained for the analysed samples to evaluate the effects of this first simplification. A computer code (SOLDEN, Sánchez Moral 1994) was used to calculate this intensive parameter for the selected samples.

This code uses the additive method for complex electrolyte solutions (e.g. Hovarth 1985, Millero 1985) to theoretically predict density values, between 0 and 50 °C, from analytical data. Density values are obtained from their relationship to the apparent partial molar volume of the solution which, in turn, is obtained by means of the Redlich and Meyer (1964) equation.

More refined methods for density calculations in brines, like that proposed by Monin (1989) based on Pitzer approach, are restricted to 25 °C and the model implemented in SOLDEN provides a very good approximation for waters with densities as high as 1.35 g/cm³ (Sanchez Moral 1994). The UZ group has verified this code by comparing its results with the measured densities in a wide range of groundwaters from the Canadian Shield (Frape *et al.* 1984), including "true" brines with densities up to 1.2 g/cm³ (Table B-2).

Table B-1. Main compositional characters of the saline groundwaters from Laxemar-Simpevarp area (Sweden), Olkiluoto (Finland; Pitkänen et al. 2004) and Lac du Bonnet (Canada; Gascoyne 2004) selected for the sensitivity analysis. Compositional data are expressed in mg/L. Density values, expressed in g/cm³, are calculated (see section B.2.1) except for the Olkiluoto samples, which correspond to measured data.

	Laxemar-Simpevarp				Olkiluoto (Finland)		Lac du Bonnet (Canada)	
	Deep saline end member	Sample #2731	Sample #2931	Sample #2722	Sample KR4/860/2	Sample KR4/860/1	Sample WB1-7-7	Sample WB2-20-12
Temp.	18.0	18.0	15.0	13.27	12.0	12.0	17.9	14.9
Density	1.052	1.050	1.033	1.021	1.051	1.050	1.033	1.026
pH	8.0	8.0	7.9	8.6	7.0	7.5	8.81	8.58
Alk.	14.1	9.0	9.0	8.0	8.2	9.2	10.0	20.0
Cl	47200.0	45500.0	31230.0	15800	45200	43000	30200.0	27900.0
SO_4^{2-}	906.0	832.0	1024.0	1,010	8.4	1.2	1040.0	835.0
Ca	19300.0	18600.0	11200.0	5620.0	18000	15100	8410.0	10540.0
Mg	2.12	2.7	2.7	2.1	130.0	108.0	51.0	34.2
Na	8500	8030	6210.0	3800.0	9540	9200	11000.0	4360.0
K	45.5	29.0	19.7	10.4	28.0	18.0	24.0	14.25
Si	2.9	4.8	4.94	5.2	2.62	1.96	0.56	3.4
Sr	337.0	275.0	191.0	80.7	190.0	160.1	105	96.0

Table B-2. Calculated density values for some "true" brines, saline and brackish ground-waters from the Canadian Shield. Analytical data from Table 1 in Frape et al. (1984).

	Temp (°C)	TDS (g/L)	Measured density (g/cm³)	Calculated density (g/cm³)
T-93	18.0	325.00	1.204	1.200 ± 0.015
S-139	21.5	240.00	1.185	1.174 ± 0.010
YK-17	22.5	237.11	1.172	1.160 ± 0.010
T-94	20.0	182.60	1.141	1.124 ± 0.007
YK-15	22.5	108.80	1.081	1.072 ± 0.003
YK-9	23.0	58.34	1.039	1.043 ± 0.001
S-154	19.5	18.81	1.014	1.012 ± 0.000
YK-73	12.5	8.83	1.006	1.005 ± 0.000

The appropriateness of the density values obtained with SOLDEN for the saline waters used in this appendix has been assessed using as a reference: (a) some saline groundwaters from Olkiluoto (with chemical characters very similar to the saline groundwaters in the Laxemar-Simpevarp area) for which the density has been measured; (b) the most saline sample from the Laxemar subarea with measured density; and (c) some theoretical estimations on the density of the Deep Saline end-member performed in the hydrogeological studies of the Laxemar subarea (Hartley *et al.* 2005, 2006).

Densities obtained previously by Gimeno *et al.* (2004) for some groundwaters in Olkiluoto have differences lower than 0.002 g/cm³ with respect to the measured ones. In the present study the calculated density for Olkiluoto sample KR4/860/2, with *in situ* temperature measurement at depth, is 1.051 ± 0.002 g/cm³, in perfect agreement with the measured one (Table B-1).

Sample #11145 from KLX02 borehole at section 1,145–1,164 m borehole length (Laxemar subarea) has a density of 1.016 g/cm³ and a chloride concentration of 15,000 mg/L. It is slightly more diluted than sample #2722 from the same borehole at a borehole length 1,090–1,096.2 m, but taken 13 years before (Table B-1). As temperature was not measured for sample #11145, its theoretical density has been calculated using the temperature value from sample #2722 (13.3 °C). The result is a density of 1.017 g/cm³, almost coincident with the measured one. The same calculation at 25 °C gives a density of 1.015 g/cm³ which indicates that the uncertainty in temperature does not have a significant effect on the result.

Finally, in the Laxemar subarea, the calculated density for the Deep Saline end-member at 18 °C is 1.052 ± 0.002 g/cm³. The groundwater sample used as the Deep Saline end-member in the Swedish site characterization program (a sample from borehole KLX02 in the Laxemar subarea at 1,631–1,681 m depth) lacks an *in situ* temperature datum and this parameter has been taken from the temperature measurement performed in a different section at a similar depth in the same borehole KLX02 (sample #2731 at 1,420–1,705 m depth).

Hartley *et al.* (2005, 2006) calculated the density of the Deep Saline end-member using an empirical correlation valid for NaCl brines at 30 °C and 25 MPa pressure, obtaining a value of 1.056 g/ cm³. Considering the different methodology and the different temperature and pressure conditions considered by these authors, the degree of accordance for the calculated density is noticeable.

Therefore, the method used here for density calculations can be considered a good approach. Table B-1 shows the calculated density for those samples lacking a density value (Laxemar-Simpevarp and Lac du Bonnet). It will be used in the following calculations. Only for Olkiluoto samples the measured density will be used (also shown in Table B-1).

B.2.2   Thermodynamic databases and codes

For the sensitivity analysis of the activity coefficients, the approach used in the WATEQ4F database (Ball and Nordstrom 2001) has been compared to the most suitable approach for this kind of solutions, Pitzer's formalism, implemented in the Pitzer database also distributed with PHREEQC, and in the code CHEMEQ (Clauser 2003, Kühn 2003).

In PHREEQC (Parkhurst and Appelo 1999) the approach used to calculate the activity coefficients depends on the database selected for the calculations. With the WATEQ4F database (Ball and Nordstrom 2001) the approach is the same implemented in all the USGS geochemical codes from WATEQ onwards (hereinafter USGS approach), that is:

a) for Ca^{2+}, Mg^{2+}, Na^+, K^+, Cl^-, SO_4^{2-}, HCO_3^-, CO_3^{2-}, $H_2CO_3^0$ and Sr^{2+}, Truesdell & Jones' activity coefficient equation (or WATEQ-type Debye-Hückel; Truesdell and Jones 1974); and

b) for the other charged species (for which the required data to implement the previous activity model are lacking) the extended Debye-Hückel or the Davies equation.

The Debye-Hückel-type equation developed by Truesdell and Jones (1974) is expressed as (T-J equation):

$$\log \gamma_i = -\frac{A z_i^2 \sqrt{I}}{1 + B a_i \sqrt{I}} + b_i I \tag{B-1}$$

where γ_i is the activity coefficient of ion i, A and B are well tabulated solvent parameters that depends on the density, the dielectric constant and the temperature of the pure solvent (e.g. Nordstrom and Munoz 1994), and I is the ionic strength of the solution. Truesdell and Jones (1974) fitted parameters a_i and b_i to individual ion activity coefficients obtained from experimental mean salt data up to ionic strengths of 5–6 molal. Therefore, it is not surprising that, for simple solutions (e.g. Na-Cl dominated solutions), the T-J equation has been found reliable up to $I = 3.5$ molal (Langmuir 1997, p. 142) or even up to 6 molal (Nordstrom and Munoz 1994, pp. 203–204, Finley and Nordstrom 1994, see also section B.3.2).

For complex solutions, when ion pairing increases, the USGS approach "mixes" the T-J equation for the main species with the Davies or the extended Debye-Hückel equation for the other species, and this "mixing" can decrease the validity of the approach as a whole. For these complex solutions, the suggested "conservative" limit of application of the USGS approach is 2 molal (Parkhurst 1990, Langmuir 1997). But this limit can vary depending on the considered ions or the particular composition of the solution. As this limit is near the maximum value in the Laxemar-Simpevarp groundwaters, the validity of the USGS approach for charged species must be verified in these groundwaters.

The USGS approach uses the empirical Setchenov equation for the activity coefficient of neutral species (e.g. $H_4SiO_4^\circ$):

$$\log \gamma_i = b_i I \tag{B-2}$$

where γ_i is the activity coefficient of neutral species i, I is the ionic strength and b_i takes a value between 0.02 and 0.23 at 25 °C depending on the neutral species i (Langmuir 1997). In the WATEQ4F database a value of $b = 0.1$ is considered for almost all the neutral species (Parkhurst and Appelo 1999). This approach is usually considered valid even at high ionic strengths (Chen and Marshall 1982, Langmuir 1997). However as it affects to an important species ($H_4SiO_4^\circ$) in Laxemar-Simpevarp groundwaters, it will be also included in the sensitivity analysis.

The results obtained with the USGS approach have been compared with the most suitable approach for this kind of concentrated solutions, the Pitzer's formalism for the activity coefficient calculations (Pitzer 1973, 1979). The USGS geochemical code PHRQPITZ (Plummer et al. 1988) implements Pitzer's formalism and it was used in the previous sensitivity analysis performed by Gimeno et al. (2004). However, since version 2.12 (September 2005) PHREEQC is distributed with the Pitzer.dat database, which includes the one developed by Plummer et al. (1988) for the PHRQPITZ code. Therefore, PHREEQC with the Pitzer.dat data base will be used here instead of PHRQPITZ.

Pitzer.dat database do not include updates or reviews to the values originally tabulated by Plummer et al. (1988) and therefore it does not include neither elements such as silica nor more recent data of the Pitzer interaction parameters for other elements or compositional systems. Because of this limitation, other code, CHEMEQ (geochemical module in the reactive transport program SHEMAT; Clauser and Villinger 1990, Clauser 2003) has been used for the sensitivity analysis. CHEMEQ was also developed using PHRQPITZ as a base but with a comprehensive review and update of the thermodynamic database (Kühn 2003) including: (a) the most recent data for Ba, Sr (Monin 1999) and especially the carbonate system (He and Morse 1993); (b) data for silica (Azaroual et al. 1997a, b); and (c) applicability to different temperatures (up to 200–250 °C).

This last improvement is not useful in this case as the saline waters in the studied systems are low temperature waters (12 to 18 °C; Table B-1). However, the first two points are very important as they involve elements and mineral phases relevant to the Laxemar-Simpevarp area (quartz, chalcedony, calcite, celestite, gypsum) and, in general, to the rest of the crystalline systems.

B.3 Sensitivity analysis results

The effects of the density and activity coefficient uncertainties have been evaluated mainly with respect to the saturation indices (S.I.) of the selected waters[61]. Saturation indices for each mineral phase are defined as:

$$S.I. = \log \frac{IAP}{K(T)} \tag{B-3}$$

where IAP is the ionic activity product and $K(T)$ is the equilibrium constant for the mineral phase at a given temperature. They are one of the main results of the speciation-solubility calculations. From these values water undersaturation (SI < 0), oversaturation (SI > 0) or equilibrium (SI ≈ 0) with respect to the mineral phase is defined and, therefore, the extension or importance of water-rock interaction in the studied system evaluated.

The studied mineral phases are those of especial interest in the Laxemar-Simpevarp area (and the rest of the systems included for comparison) because they are in or close to equilibrium in the most saline groundwaters: calcite, gypsum, celestite, chalcedony and quartz. Their solubility values are very similar in the different thermodynamic databases used here, including "new" data in CHEMEQ code (solubility values included in the Pitzer database in PHREEQC come from the ones included in the WATEQ4F database).

The largest difference in solubility values (log K) in the temperature range defined by the selected samples (12–18 °C; Table B.1) is 0.07 logarithmic units (for calcite and gypsum) while there are no differences at all for celestite, chalcedony and quartz (the solubility data for quartz proposed by Rimstidt 1997, has been included in the databases).

B.3.1 Sensitivity to density data

The sensitivity analysis with respect to density has been performed comparing the saturation indices obtained with the calculated density (section B.2.1) and with a density of 1 g/cm³ (Table B-3). The results have been obtained with PHREEQC and the WATEQ4F thermodynamic database.

As expected, molal concentrations obtained for the total elements in both cases are different and always higher when the density value is 1. The largest differences appear in the most saline waters (Deep Saline end-member or sample #2731) with almost 6% of variation for Cl or Ca. However, the differences produced on the saturation indices are lower than 0.04 SI units, which are negligible considering that the uncertainty values used in the SI calculations for these phases are between ±0.2 and ±0.4 SI units (e.g. Langmuir and Melchior 1985, Deutsch 1997).

For even more saline samples with chloride contents up to 30,000 mg/L (sample #2931; Table B-1) the uncertainty decreases to 0.02 SI units and to even lower values (0.01; Table B-3) in the sample with 16,000 mg/L of Cl (sample #2722), similar to the most saline waters found in Forsmark.

Results obtained with the CHEMEQ and the PITZER.dat databases are similar. The same happens when using groundwaters from Olkiluoto or Lac du Bonnet.

---

[61] Activity coefficient values by themselves are not meaningful when Specific Ion Interaction models (Pitzer approaches) and Ion Association Models (Debye-Hückel approaches) are compared. This is because ion association and complexation may be implicitly accounted for by activity coefficients (as typically done with Pitzer models, where most of the ion pairs and complexes are not evaluated) or explicitly computed with the use of secondary species (as done with Ion Association Models). Therefore, Specific Ion Interaction Models and Ion Association Models could predict quite different activity coefficients for a given primary aqueous species (e.g. Ca^{2+}, Cl^-) but quite similar activities or ion activity products (for further discussion see, e.g., Nordstrom and Munoz 1994).

Table B-3. Some results from speciation solubility calculations performed with the PHREEQC code and the WATEQ4F database using the calculated density or a value of 1 g/cm³ (dens.=1) for the samples. Total concentrations of Cl, Ca and SO₄²⁻ are expressed in molal units.

	Deep saline end-member		Sample 2731		Sample 2931		Sample 2722	
	dens.=1.052	dens.= 1	dens.=1.05	dens.= 1	dens.=1.033	dens.= 1	dens.=1.021	dens.=1
I.S.[1]	1.866	1.969	1.79	1.89	1.156	1.196	0.591	0.604
Cl	1.366	1.442	1.314	1.385	0.896	0.927	0.448	0.456
Ca	0.494	0.521	0.475	0.501	0.284	0.294	0.141	0.144
SO₄²⁻	$9.7 \cdot 10^{-3}$	$1.02 \cdot 10^{-2}$	$8.6 \cdot 10^{-3}$	$9.3 \cdot 10^{-3}$	$1.08 \cdot 10^{-2}$	$1.12 \cdot 10^{-2}$	$1.06 \cdot 10^{-2}$	$1.08 \cdot 10^{-2}$
SI calcite	+0.91	+0.95	+0.69	+0.73	+0.43	+0.45	+0.66	+0.67
SI gypsum	+0.25	+0.28	+0.20	+0.24	+0.20	+0.22	+0.09	+0.10
SI celestite	+0.17	+0.21	+0.06	+0.09	+0.13	+0.15	−0.05	−0.04
SI Chalced.	−0.13	−0.09	+0.08	+0.12	+0.06	+0.08	+0.01	+0.02
SI Quartz [2]	+0.07	+0.11	+0.28	+0.31	+0.26	+0.28	+0.21	+0.22

[1] Ionic Strength, molal

[2] Solubility data from Rimstidt (1997)

Therefore, as an important conclusion, the salinity (or density) of the most saline waters in Laxemar-Simpevarp and Forsmark is not high enough to produce significant errors in the calculated saturation indices when using a density of 1 g/cm³.

B.3.2 Sensitivity to activity coefficient calculations

This section is divided into two parts. The first one shows the results for the Laxemar-Simpevarp area and for the other comparison sites with similar salinity (Olkiluoto and Lac du Bonnet), all of them with ionic strengths lower to 2 molal. The second part shows the results for other groundwaters from the Canadian Shield (Frape *et al.* 1984, Douglas *et al.* 2000) with "true" brines and ionic strengths up to 9 molal. Though they are apparently far from the waters from Simpevarp, their study builds confidence on the sensitivity analysis.

Groundwaters from Laxemar-Simpevarp and other sites with similar salinities

Tables B-4 and B-5 summarise the results obtained with all the alternative approaches (WATEQ4F and PITZER databases, and PHREEQC and CHEMEQ codes). They present the saturation indices and also the ionic strengths and water activities which are especially important parameters in the calculation of activity coefficients (equations B-1 and B-2) and ionic activity products of some minerals (e.g. gypsum). The main conclusion is that the values calculated for these parameters (IS and water activity) are very consistent.

Calcite is slightly oversaturated in the Laxemar-Simpevarp and the Canadian Shield groundwaters (Tables B-4 and B-5, respectively) whereas it is in equilibrium in Olkiluoto (Table B-5) considering the uncertainty range of ±0.3 SI units. The more interesting outcome is that, independently of the approach used for the calculation of the activity coefficients, the results are very similar and, in most cases, the value obtained with WATEQ4F is in between the values obtained with the other two approaches (PITZER and CHEMEQ). Differences in the calcite saturation index are even smaller when the comparison involves the less saline waters (case of the sample #2722 from the Laxemar-Simpevarp area, with a maximum difference of 0.09 SI units).

Similar observations can be made with respect to sulphate phases, gypsum and celestite. The saturation index calculated with Pitzer´s approach for both minerals in samples from Laxemar-Simpevarp and Lac du Bonnet indicates a saturation state, in general, closer to equilibrium than the results from the WATEQ4F. However, even these differences are inside the precision range accepted for this kind of phases (around ± 0.2 SI units; Langmuir and Melchior 1985). These results strengthen the fact that sulphate minerals act as controlling phases in the deep saline waters from Laxemar-Simpevarp (and also from the Lac du Bonnet, as it was already suggested by Gascoyne 2004). Olkiluoto groundwaters show also negligible differences between the SI (calculated with the different approaches) for these two sulphate phases (Table B-5) but with a clear undersaturation state.

Table B-4. Calculated ionic strength, water activity and several saturation indices for the Deep Saline end member and three saline samples from Simpevarp area using the PHREEQC with the WATEQ4F and PITZER databases) and the CHEMEQ codes.

LAXEMAR-SIMPEVARP

	Deep Saline end member			Sample 2731			Sample 2931			Sample 2722		
	WATEQ4F	PITZER	CHEMEQ	WATEQ4F	PITZER	CHEMEQ	WATEQ4F	PITZER	CHEMEQ	WATEQ4F	PITZER	CHEMEQ
I.S.[1]	1.866	1.892	1.888	1.79	1.814	1.811	1.156	1.182	1.181	0.591	0.613	0.612
Cl (molal)	1.366	1.366	1.366	1.314	1.314	1.314	0.896	0.896	0.896	0.448	0.448	0.448
aH$_2$O	0.962	0.962	0.962	0.963	0.963	0.964	0.975	0.976	0.976	0.987	0.988	0.988
SI calcite	+0.91	+0.98	+0.77	+0.69	+0.77	+0.55	+0.43	+0.57	+0.34	+0.66	+0.69	+0.60
SI gypsum	+0.25	+0.07	+0.11	+0.20	+0.03	+0.07	+0.20	+0.07	+0.12	+0.09	+0.03	+0.07
SI celestite	+0.17	+0.02	+0.1	+0.06	–0.09	–0.013	+0.13	+0.01	+0.09	–0.05	–0.12	–0.03
SI chalced.	–0.13	–	–0.17	+0.08	–	+0.06	+0.06	–	+0.05	+0.01	–	+0.02
SI quartz [2]	+0.07	–	+0.03	+0.28	–	+0.26	+0.26	–	+0.25	+0.21	–	+0.22

[1] Ionic Strength, molal

[2] Solubility data from Rimstidt (1997)

Table B-5. Calculated ionic strength, water activity and several saturation indices for the most saline samples from Olkiluoto (Finland; samples KR4/860/1 and KR4/860/2; Pitkänen *et al.*2004)) and Lac du Bonnet Batholith (Canada; samples WB1-7-7 and WB2-20-12; Gascoyne, 2004) using the PHREEQC (with the WATEQ4F and PITZER databases) and the CHEMEQ codes.

	OLKILUOTO						LAC DU BONNET					
	KR4/860/2			KR4/860/1			WB1-7-7			WB2-20-12		
	WATEQ4F	PITZER	CHEMEQ	WATEQ4F	PITZER	CHEMEQ	WATEQ4F	PITZER	CHEMEQ	WATEQ4F	PITZER	CHEMEQ
I.S.[1]	1.802	1.801	1.800	1.605	1.604	1.601	1.111	1.135	1.134	1.056	1.057	1.056
Cl (molal)	1.305	1.304	1.304	1.236	1.235	1.235	0.867	0.867	0.867	0.801	0.801	0.801
aH$_2$O	0.962	0.963	0.963	0.965	0.966	0.966	0.973	0.974	0.974	0.978	0.979	0.979
SI calcite	–0.29	+0.01	–0.38	+0.14	+0.37	+0.08	+0.75	+0.67	+0.80	+1.19	+1.09	+1.10
SI gypsum	–1.78	–1.97	–1.93	–2.66	–2.84	–2.80	+0.11	0.00	+0.02	+0.11	0.00	+0.04
SI celestite	–2.07	–2.26	–2.16	–2.95	–3.12	–3.02	–0.10	–0.20	–0.13	–0.23	–0.34	–0.25
SI chalced.	–0.10	–	–0.12	–0.25	–	–0.27	–0.97	–	–0.93	–0.14	–	–0.136
SI quartz [2]	+0.10	–	+0.08	–0.05	–	–0.07	–0.77	–	–0.73	+0.06	–	–0.064

[1] Ionic Strength, molal

[2] Solubility data from Rimstidt (1997)

Silica phases (chalcedony and quartz[62]) have very similar saturation indices independently of the approach (WATEQ4F database or CHEMEQ code). This is an interesting result supporting the fact that the *a priori* simpler Setchenov approach (equation B-2) used by WATEQ4F for the activity coefficient calculation of the neutral species $H_4SiO_4^o$ gives results in very good agreement with the *a priori* much more precise Pitzer parameterization implemented in CHEMEQ. Even more, it also indicates that the discussion presented in section 3.5 (Chapter 3) on the possible mineral phase controlling dissolved silica in these systems is not affected by uncertainties coming from the calculation of the activity coefficients.

These results confirm the validity of the WATEQ4F database and the USGS approach to calculate the activity coefficients of the saline waters studied here. They are "simple" sodium-chloride waters with an ionic strength not high enough to produce important deviations in the calculation of activity coefficients (e.g. the T-J equation; equation B-1).

Groundwaters from the Canadian Shield with higher salinities

As already commented on, hydrogeochemical data reported by Frape *et al.* (1984) and Douglas *et al.* (2000) include "true" brines ($I \leq 9$ molal) and therefore, they allow a more comprehensive study of the T-J activity coefficient equation used by WATEQ4F and its application to waters much more saline that the ones sampled in the Laxemar-Simpevarp and Forsmark areas of Sweden.

All the Canadian Shield groundwaters from Frape *et al.* (1984), Douglas *et al.* (2000) and Gascoyne (2004) have been analysed. As before, the saturation indices for several interesting minerals obtained by different approaches (CHEMEQ code and WATEQ4F and Pitzer databases distributed with PHREEQC) have been compared.

Calcite saturation index is almost the same up to $I = 2$ molal with both databases, WATEQ4F and PITZER, and diverges for higher ionic strengths. However, these discrepancies do not indicate that the best values correspond to the Pitzer approach (more suitable for higher salinities) because of the important uncertainties that this approach has in this range of salinities when dealing with the carbonate system, related to problems with the measurement of pH in brines (Plummer *et al.* 1988, Knauss *et al.* 1990 and references therein).

First, the measured pH is not likely to be in the same activity-coefficient scale as the aqueous model because the buffers used to define pH are conventional. This problem of inconsistency between the measured pH and the adopted scale is less important at low ionic strengths but increases in brines. Plummer *et al.* (1988), using Pitzer's approach for a brine from the Canadian Shield (Sample T-93 from Frape *et al.*1984), calculated that this inconsistency can easily introduce uncertainties of $\pm$ 0.5 units in the saturation index of calcite (and even larger uncertainties for other carbonates)[63]. Moreover, there are specific "technical" problems in measuring pH in brines, like those associated with liquid-junction potentials (e.g. Knauss *et al.* 1990). These problems can promote even larger deviations in SI values for carbonates. Together, all the uncertainties associated with the carbonate system make it an unsuitable system to compare the different approaches for the activity coefficient calculation in brines[64].

Gypsum and celestite saturation indices are shown in Figures B-1a and b. The results obtained with the Pitzer and WATEQ4F databases are so similar that the symbols for both are almost superimposed. Figure B-1c shows the results for halite, which is in equilibrium in the most saline waters from the Canadian Shield. The agreement between the two approaches is also perfect for this phase. In detail, maximum differences in the gypsum saturation index in the most saline waters are 0.05 SI units for gypsum, 0.18 for celestite and 0.14 for halite.

---

[62] The solubility values for quartz used here are from Rimstidt (1997).

[63] For the most saline groundwater in the Laxemar-Simpevarp area (the Deep saline end-member, $I = 1.89$ molal) the effect of the problem of the activity-coefficient scale introduces an uncertainty of ± 0.06 units in the saturation index of calcite. Therefore, the uncertainty associated with the activity-coefficient scale is negligible (although other type of uncertainties can be affected the pH measurement in these groundwaters).

[64] This is also the reason of not including these brines in the discussion of calcite saturation indices in the Laxemar-Simpevarp groundwaters.
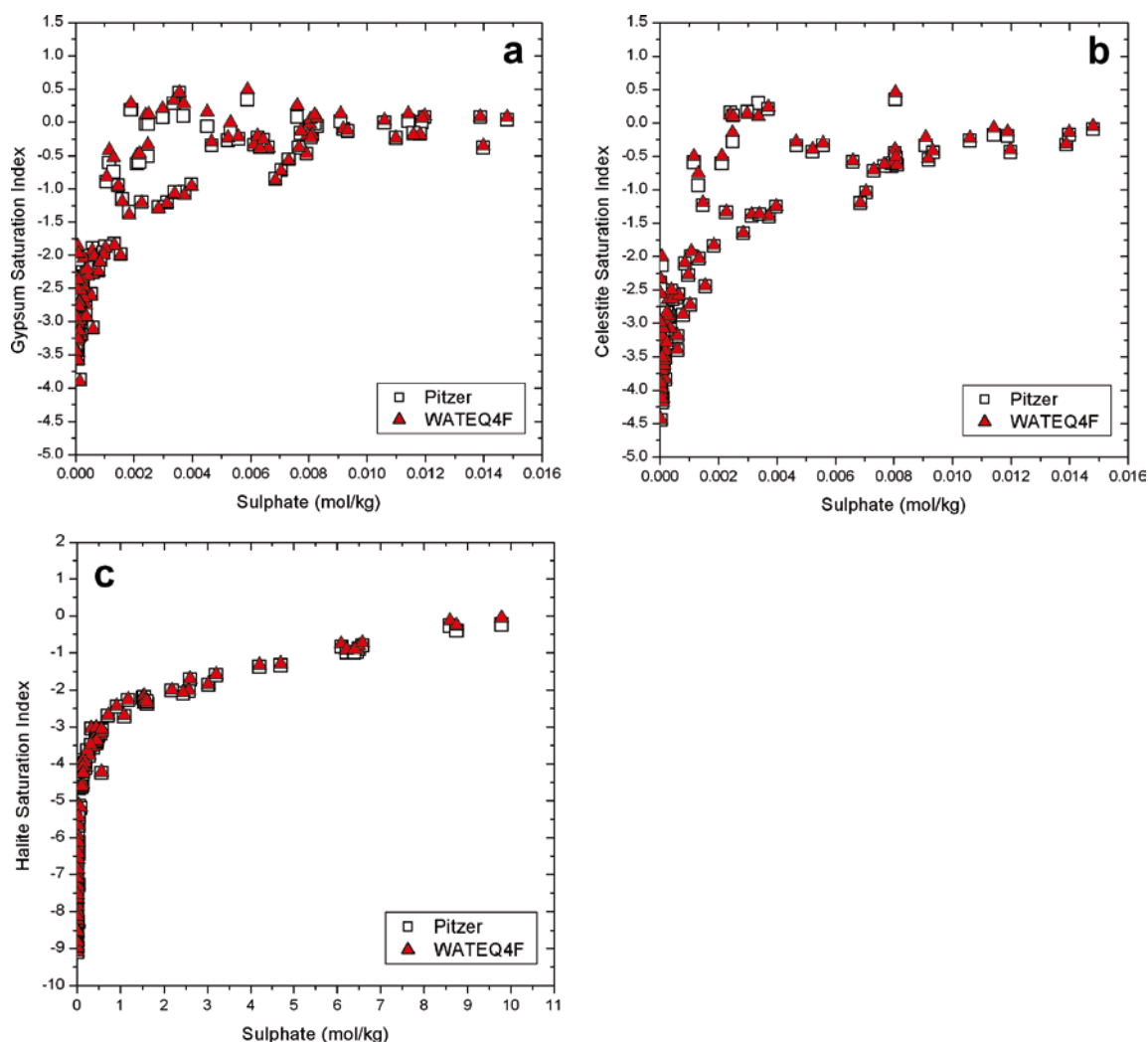
Figure B-1. *Gypsum, Celestite and halite saturation indexed for Canadian Shield groundwaters (Frape et al. 1984, Douglas et al. 2000, Gascoyne 2004) computed with the WATEQ4F and Pitzer databases distributed with PHREEQC.*

The results (not shown) obtained with the Pitzer approach included in CHEMEQ are almost identical to the results from PHREEQC and the PITZER database. Differences are less than 0.03 SI units for gypsum and halite and up to 0.1 SI units for celestite.

These results indicate that the equilibrium state with respect to gypsum and celestite in the most saline waters from the Canadian Shield is not affected by uncertainties in the activity coefficients. Moreover, they indicate that the USGS approach (T-J equation) is as good as other approaches based on the Pitzer equations for waters even more saline ($I \leq 8$ molal) than the ones present in Laxemar-Simpevarp and Forsmark.

Other authors had already indicated the suitability of the T-J equation in high ionic strength waters (section B.2.2), but under ideal conditions. Therefore, the wide range of applicability for this approach cannot be generalised to all brines. However, taken into account the confusion created in the bibliography with respect to the validity range of this approach, an important fact is worth highlighting: the T-J equation is "only" a fit to experimental data and, as long as the studied ions are those for which the fit was done and the compositional characteristics of the brine are similar to the experimental ones, it can give good results in high ionic strength conditions.

B.4   Conclusions

The occurrence of saline groundwaters in the Laxemar-Simpevarp area with ionic strength up to 1.8 molal (Deep Saline end-member, Laxemar subarea), can produce uncertainties in the speciation-solubility results coming from: (a) the absence of a measured density value; and (b) the type of approach used for the calculation of activity coefficients of the dissolved species.

Here, the effects of both uncertainties have been assessed and the results indicate that their impact in the calculated saturation indices is negligible, at least for the most important minerals in the hydrogeochemical conceptual model of the system.

When density data were not available, geochemical calculations on the most saline sample from Laxemar-Simpevarp area have been routinely performed using a default value of 1 g/cm³. Speciation-solubility calculations were repeated using a more realistic density value to verify the effects of the previous assumption. Comparison of the results indicate that the use of the default value (1 g/cm³) do not add uncertainties to those already attached to the saturation indices of the principal minerals. Moreover, the method used for the theoretical calculation of the density from the analytical data has been proved to be very precise in a wide range of salinities. Therefore, this approach could be used for other calculations that need a more precise knowledge of the density when this parameter has not been measured.

Sensitivity analysis performed using different types of approaches for the calculation of activity coefficients has confirmed that the USGS approach (mainly the T-J equation) incorporated in the WATEQ4F database delivers good results (for the elements and minerals considered here) in the whole range of salinity of the Laxemar-Simpevarp groundwaters. This conclusion simplifies the methodology to deal with these waters, making unnecessary the use of codes and/or databases incorporating Pitzer's approach to calculate the activity coefficients of the saline waters. Moreover, it supports the consistency of the equilibrium state defined for these waters in the geochemical model developed in this work.

B.5   References

Azaroual M, Fouillac C and Matray J M (1997a). Solubility of silica polymorphs in electrolyte solutions, I. Activity coefficient of aqueous silica from 25° to 250°C, Pitzer's parameterisation. Chem. Geol., 140, 155–165.

Azaroual M, Fouillac C and Matray J M (1997b). Solubility of silica polymorphs in electrolyte solutions. II. Activity of aqueous silica and solid silica polymorphs in deep solutions from the sedimentary Paris Basin. Chem. Geol., 140, 167–179.

Ball J W and Nordstrom D K (2001). User's manual for WATEQ4F, with revised thermodynamic data base and test cases for calculating speciation of major, trace, and redox elements in natural waters. U.S. Geological Survey Open-File Report 91-183, 188 p. (Revised and reprinted, April, 2001).

Bethke C M (1996). Geochemical reaction modelling. Concepts and applications. Oxford University Press, 397p.

Chen C-T A and Marshall W L (1982). Amorphous silica solubilities, IV. Behaviour in pure water and aqueous sodium chloride, sodium sulfate, magnesium chloride, and magnesium sulfate solutions up to 350° C. Geochim. Cosmochim. Acta, 46, 279–287.

Clauser C (ed) (2003). Numerical simulation of reactive flow in hot aquifers. SHEMAT and Processing SHEMAT. Springer, 332 p.

Clauser C and Villinger H (1990). Analysis of conductive and convective heat transfer in a sedimentary basin, demonstrated for the Rheingraben. Geophys. J. Int., 100, 393–414.

Deutsch W J (1997). Groundwater geochemistry. Fundamentals and applications to contamination. CRC Press, Boca Raton, 221 p.

Douglas M, Clark I D, Raven K and Bottomley D (2000). Groundwater mixing dynamics at a Canadian Shield mine. J. Hydrol., 235, 88–103.

Drever J I (1997). The Geochemistry of Natural Waters: Surface and Groundwater Environments. 3rd ed., Prentice Hall, New York, USA, 436 p.

Duro L, Grivé M, Cera E, Domènech C and Bruno J (2006). Update of a thermodynamic database for radionuclides to assist solubility limits calculation for performance assessment. SKB TR-06-17, 128 p.

Finley J B and Nordstrom D K (1994). Evaluation of the chemical model in WATEQ4F: 1. The major ion activity coefficients – Na, K, Ca, Mg, Cl. Miner. Mag., 58A, 270–271.

Frape S K, Blyth A, Blomqvist R, McNutt R H and Gascoyne M (2005). Deep fluids in the continents: II. Cryslalline Rocks. In: J.I. Drever (ed.). Surface and ground water, weathering, and solis. Treatise on Geochemistry, vol 5. pp. 541–580. Elsevier.

Frape S K, Fritz P and McNutt R H (1984). Water-rock interaction and chemistry of groundwaters from the Canadian Shield. Geochim. Cosmochim. Acta, 48, 1617–1627.

Gascoyne M (2004). Hydrogeochemistry, groundwater ages and sources of salts in a granitic batholith on the Canadian Shield, southeastern Manitoba. Applied Geochemistry, 19, 519–560.

Gimeno M J, Auqué L F and Gómez J (2004). Mass balance modelling. In: Hydrogeochemical evaluation of the Simpevarp area, model version 1.2. Preliminary site description of the Simpevarp area. SKB R-04-74, Appendix 4, pp. 289–352.

Gimeno M J, Auqué L F, Gómez J and Acero P (2008). Water-rock interaction modelling and uncertainties of mixing modelling. SDM-Site Forsmark. SKB R-08-86, 212 pp.

Hartley L, Hoch A, Hunter F, Jackson P and Marsic N (2005). Regional hydrogeological simulation. Numerical modelling using ConnectFlow. Preliminary site description. Simpevarp subarea, version 1.2. SKB R-05-12, 264 p.

Hartley L, Hunter F, Jackson P, McCarthy R, Gylling B and Marsic N (2006). Regional hydrogeological simulations using CONNECTFLOW. Preliminary site description. Laxemar subarea, version 1.2. SKB R-06-23, 312 p.

He S and Morse J W (1993). The carbonic acid system and calcite solubility in aqueous Na-K-Ca-Mg-Cl-SO$_4$ solutions from 0–90 °C. Geochim. Cosmochim. Acta, 57, 3533–3554.

Hovarth A L (1985). Handbook of aqueous electrolyte solutions. Physical properties, estimation and correlation methods. Part two. T.J. Kemp (ed.), Ellis Horwood, Wets Sussex, England, 347 p.

Hummel W, Berner U, Curti E, Pearson F J and Thoenen T (2002). Nagra/PSI Chemical Thermodynamic Data Base 01/01. Nagra Technical Report NTB 02-16, Nagra, Wettingen, Switzerland.

Knauss K G, Wolery T J, Jackson K J (1990). A new approach to measuring pH in brines and other concentrated electrolytes. Geochim. Cosmochim. Acta, 54, 1519–1523.

Langmuir D (1997). Aqueous environmental geochemistry. Prentice Hall, 600 p.

Langmuir D and Melchior D (1985). The geochemistry of Ca, Sr, Ba and Ra sulfates in some deep brines from the Palo Duro Basin, Texas. Geochim. Cosmochim. Acta, 49, 2423–2432.

Millero F J (1985). The physical chemistry of natural waters. Pure App. Chem., 57, 1015–1024.

Monin C (1989). An ion interaction model for the volumetric properties of natural waters: density of the solution and partial molal volumes of electrolytes to high concentrations at 25 °C. Geochim. Cosmochim. Acta, 53, 1177–1188.

Monin C (1999). A thermodynamic model for the solubility of barite and celestite in electrolyte solutions and seawater to 200 °C and to 1 kbar. Chem. Geol., 127, 141–159.

Norstrom D K and Munoz J L (1994). Geochemical Thermodynamics. 2nd Edition, 493 p.

Parkhurst D L (1990). Ion-Association models and mean activity coefficients of various salts. In: D.C. Melchior and R.L. basset (eds.), Chemical Modeling of Aqueous Systems. Am. Chem. Soc. Symp. Ser., 416, pp 30–43.

Parkhurst D L and Appelo C A J (1999). User's Guide to PHREEQC (Version 2), a computer program for speciation, batch-reaction, one-dimensional transport, and inverse geochemical calculations. Water Resources Research Investigations Report 99-4259, 312 p.

Pitkänen P, Partamies S and Luukkonen A (2004). Hydrogeochemical interpretation of baseline groundwater conditions at the Olkiluoto site. Posiva report 2003-07, 159 p.

Pitzer K S (1973). Thermodynamics of electrolytes. I: Theoretical basis and general equations. J. Phys. Chem., 77, 268–277.

Pitzer K S (1979). Activity coefficients in Electrolyte Solutions, Chap. 7. CRC Press, Boca Raton, FL.

Plummer L N, Parkhurst D L, Fleming G W and Dunkle S A (1988). A computer program incorporating Pitzer's equations for calculation of geochemical reactions in brines. U.S. Geological Survey Water-Resources Investigations Report 88-4153, 310 p.

Redlich O and Meyer D M (1964). The molal volumes of electrolytes. Chem. Rev., 64, 221–227.

Rimstidt D D (1997). Quartz solubility at low temperatures. Geochim. Cosmochim. Acta, 61, 2553–2558.

Sánchez Moral S (1994). Sedimentación salina actual en un lago continental (Laguna de Quero, Toledo). Aplicación de la modelización termodinámica al estudio de secuencias de precipitación salina. Tesis Doctoral, Universidad Complutense de Madrid. 391 p. (in Spanish).

Truesdell A H and Jones B F (1974). WATEQ, a computer program for calculating chemical equilibria of natural waters. Journal of Research, U.S. Geological Survey, v.2, pp. 233–274.

Zhu C and Anderson G (2002). Environmental applications of geochemical modelling. Cambridge University Press, 284 p.

Geochemical codes and thermodynamic databases

C.1   Introduction

Geochemical modelling calculations performed by the UZ group since the beginning of the site characterisation studies in Laxemar-Simpevarp and Forsmark areas have been performed with the PHREEQC code (Parkhurst and Appelo 1999) and one of the thermodynamic databases distributed with it, WATEQ4F (Ball and Nordstrom 2001).

The selection of the PHREEQC code and the WATEQ4F database as the reference "tools" for all the geochemical calculations was based on their wide use in the scientific literature and in Performance Assessment related studies (section C.2.1). A wide use of a thermodynamic database (in different environments and conditions) can be a confidence building criteria as the possible existing errors are either inconspicuous (Zhu and Anderson 2002) or more easily identified in the extensive bibliography on its use.

However, in the standard methodology of geochemical modelling it is always necessary to perform sensitivity or uncertainty analysis to determine the reliability of the obtained results (Nordstrom 2005). Sensitivity analysis can be performed from different points of views and at different levels of detail, but one of the most common is related to the thermodynamic data used in calculations. This sensitivity analysis is more necessary in the present case due to the fact that during the different SDM stages other modelling codes or thermodynamic databases have been used (section C.2.2.) and the WATEQ4F database has undergone additions, modifications and updates of some of its thermodynamic data (section C.3).

All the codes, databases and their modifications have been meticulously reported in the UZ contributions for the different SDM reports. This appendix compiles all this information to facilitate its traceability. It also enlarges the uncertainties analysis associated with the use of specific mineral phases as the iron oxyhydroxides, monosulphides and silica polymorphs in the studied systems.

C.2   Geochemical codes and databases

PHREEQC (Parkhurst and Appelo 1999) is the geochemical modelling tool used in the site characterisation work performed by UZ group. PHREEQC is a non commercial code available from the US Geological Survey web page http://wwwbrr.cr.usgs.gov/projects/GWC_coupled/phreeqc/ where it is maintained, updated, reviewed and refined[65].

PHREEQC has forward and inverse geochemical modelling capabilities (Plummer *et al.* 1983, Parkhurst and Plummer 1993, Glynn and Plummer 2005, Nordstrom 2005): it can perform speciation-solubility calculations, reaction-path calculations, 1D reactive transport simulations (forward modelling) and mass balance calculations (inverse modelling) and, therefore, it compiles the calculation capabilities distributed in different widely used USGS codes such as WATEQ4F (Ball and Nordstrom 2001), PHREEQE (Parkhurst *et al.* 1980, 1990), PHRQPITZ (Plummer *et al.* 1988) or NETPATH (Plummer *et al.* 1994).

In forward modelling calculations a thermodynamic database is needed. Nowadays, PHREEQC is distributed with six different thermodynamic databases that the user may easily select for calculations: WATEQ4F.dat, PHREEQC.dat, LLNL.dat, MINTEQ.dat, MINTEQV4.dat and PITZER.dat. Besides, other thermodynamic databases are available in PHREEQC format. For example, PA thermodynamic databases like Nagra/PSI TDB 01/01 (Hummel *et al.* 2002), JNC-TDB (Yui *et al.* 1999) and SKB-TDB (Duro *et al.* 2006a) are available for use with PHREEQC.

---

[65] The UZ group has been using the successively updated versions of the PHREEQC code since the beginning of its contributions to the site characterisation studies, starting with version 2.8 (April 15, 2003) up to the most recent one 2.15.0–2,697 (February 5, 2008). Through these versions the code abilities and the available thermodynamic databases have been not only enlarged or improved but also corrected for errors. None of the errors found in the successive versions used by the UZ group affect the results for the different SDM stages. All these improvements and corrected mistakes are reported in the "Release Notes" available from the web page http://wwwbrr.cr.usgs.gov/projects/GWC_coupled/phreeqc/.

This fact provides an important versatility to the code as some databases are more suitable for low temperature processes, some others for high temperature conditions and other for processes involving high salinity solutions.

The selection of the WATEQ4F thermodynamic database for the SDM geochemical modelling calculations in Forsmark and Laxemar-Simpevarp areas was based not only on its wide use in the scientific context but also on the wide experience of its use in different Performance Assessment related studies and, especially, in the Swedish Program.

C.2.1   The WATEQ4F database

The WATEQ4F database comes originally from the identically named WATEQ4F geochemical code. It is one of the most widely used in scientific literature and also in the Performance Assessment context. WATEQ4F is the latest version of the WATEQ series developed by the USGS in the seventies (Truesdell and Jones 1974). Since then it has been enlarged and improved in successive updates by researchers from this institution, including refinements to its thermodynamic data (e.g. Plummer *et al.* 1976, Ball *et al.* 1981, Nordstrom *et al.* 1984, etc). One of the main latest upgrades to the WATEQ4F database is that of Nordstrom *et al.* (1990).

This set of thermodynamic data has been included, in a reduced form, in other geochemical codes from the USGS such as NETPATH (WATEQFP; Plummer *et al.* 1994) and PHREEQE (Parkhurst *et al.* 1980, 1990). The latter code, the predecessor of the modern PHREEQC, was also extensively used in geochemical modelling activities and incorporates a thermodynamic database that is basically a reduced subset of WATEQ4F (less elements and minerals, now distributed as the phreeqc.dat database in PHREEQC).

As already mentioned, WATEQ4F is one of the databases distributed with the USGS code PHREEQC (Parkhurst and Appelo 1999). It is also distributed with other codes developed outside this institution. The codes CHESS (Van der Lee and De Windt 1999) and Geochemist's Workbench (GWB; Bethke 1994, 2002) enclose WATEQ4F database among others because of its wide use. Finally, WATEQ4F is frequently used as a source of thermodynamic data for geochemical studies and for the elaboration of other thermodynamic compilations.

Review of the use of the WATEQ4F database in Performance Assessment related studies

This section is a brief review of the use of the WATEQ4F database (or PHREEQE database) in the main geochemical modelling studies related to PA. These studies refer to natural analogues, underground research laboratories (and Test Sites) and the PA exercises themselves.

WATEQ4F database has been broadly used in *natural analogue studies* at different levels: hydrogeochemical modelling, Blind Predictive Modelling (BPM) exercises and also as a simple source of data. Some examples include: Cigar Lake (Cramer and Nesbitt 1994); Poços de Caldas (Nordstrom *et al.* 1992); El Berrocal (Gómez *et al.* 1996); Oklo (Gómez *et al.* 1998); Palmottu (Bruno *et al.* 1999, Gimeno *et al.* 2001); Tono Mine (Iwatsuki and Yoshida 1999); etc. The use of this database is also indicated in the BPM exercises review performed by Bruno *et al.* (2001, 2002).

The use of WATEQ4F (or PHREEQE) codes and databases in geochemical calculations related to *Underground Research Laboratories and Test Sites* is exemplified by the following: Bottomley *et al.* (1990) use WATEQF (Plummer *et al.* 1976) to study groundwater geochemical evolution at East Bull Lake (WRA, Canada); and Beaucaire *et al.* (2000) use PHREEQE to establish the geochemical groundwater evolution model at MOL (Belgium) in the context of the ARCHIMEDE project (Griffault *et al.* 1996).

However, this use is specially significant in the framework of the Swedish program: (a) Nordstrom and Puigdomènech (1986) used WATEQ3 for the analysis of redox states in deep groundwaters; (b) Nordstrom *et al.* (1989), in the context of the STRIPA project, used WATEQ4F, the code and the database; (c) Smellie and Laaksoharju (1992) used PHREEQE code and database in the Pre-investigation stage in Äspö; (d) Laaksoharju *et al.* (1995) used PHREEQE code and database for saturation index calculations to check colloid stability; (e). Düker and Ledin (1998) used PHREEQE code and database to check the colloid stability at Laxemar; and (f) Banwart (1999) used PHREEQE (with its own database, enlarged with Nordstrom *et al.* 1990) for geochemical calculations associated with the REDOX experiment at Äspö.

Finally, direct use of WATEQ4F or PHREEQE database in **PA exercises** can be considered at least as common as any other database. These codes and databases have been used in NRC-IPA phase II (Wescot *et al.* 1995), H3 (PNC 1992), H12 (JNC 1999), and the two last PA exercises in the Swedish Program: SITE-94 (SKI 1996) and SR-97 (SKB 1999). In SITE-94 Glynn and Voss (1999) used WATEQ4F for geochemical evolution of groundwaters and redox conditions. In SR-97 the authors used the results from WATEQFP (NETPATH) to characterise the geochemical evolution of the three considered sites. This use is specified in the main report. Moreover, WATEQ4F database has also been used indirectly in other exercises such as KRISTALLIN-I (NAGRA 1994), TILA-99 (Vieno and Nordman 1999) and SR-97 (SKB 1999) through the NAGRA-PSI database (see below).

WATEQ4F and other PA thermodynamic databases

It is clear that the WATEQ4F database has been repeatedly used in the kind of systems and studies that we are dealing with here. Moreover, it has been used as a main source of data in the development of PA-oriented thermodynamic databases like HATCHES NEA, NAGRA-PSI and SKB TDB.

One of the latest versions of this database (HATCHES NEA 13, Oct. 2000) includes most of the data from the PHREEQE database. This is explicitly indicated in the log K and ΔH values. The source of data is expressed as "USGS data" or "PHREEQC database", that is, data from Nordstrom *et al.* (1990).

The main references about the origin of the thermodynamic data contained in the *NAGRA-PSI* database are Pearson and Berner (1991), Pearson *et al.* (1992), and Hummel *et al.* (2002). These authors reported that they took almost all data from Nordstrom *et al.* (1990) for carbonate, sulphate, silica, aluminium, Fe and Mn inorganic systems (species and minerals). They even justify the use of these data by saying that their quality is guaranteed because they are included in WATEQ4F and PHREEQE.

NAGRA-PSI database has been used in PA exercises such as: (a) KRISTALLIN-I for the reference waters and solubility limit calculations (Berner 1995); (b) in SR-97 the authors created a specific thermodynamic database (SR-97 TDB, Bruno *et al.* 1997) based on this NAGRA-PSI (that is, Nordstrom *et al.* 1990) but modified for Np, Am, REE and Th; and (c) TILA-99 also used the SR-97 TDB and it was compared with data0.com 02 from EQ3/6 (Vuorinen *et al.* 1998).

SKB-TDB derives directly from the NAGRA database (Nagra/PSI TDB 01/01) with some modifications or extensions for elements of special interest (see section C.2.2.1) for Performance Assessment (Duro *et al.* 2006a).

Conclusions

PHREEQC code and WATEQ4F thermodynamic database have been used for the geochemical modelling in the SDM studies in Forsmark and Laxemar-Simpevarp. They have also been used by the UZ group in PA calculations for SR-Can and by other groups working in the Swedish or Finnish characterization program.

For example, Molinero *et al.* (2008) also use this code with the phreeqc.dat database in speciation-solubility and mixing calculations in their contribution to Forsmark 2.3; Tröjbom and Söderback (2006ab) use the WATEQ4F database in the study of the chemical characters of surface waters both in Forsmark and Simpevarp sites. Likewise, Pitkänen *et al.* (2004) use PHREEQC code with the phreeqc.dat thermodynamic database in geochemical calculations performed in Olkiluoto site (Finland).

In the SR-Can related modelling activities PHREEQC code and WATEQ4F database have also been used. Auqué *et al.* (2006) use them in simulations of the groundwater geochemical evolution during the initial period of temperate climate after repository closure. Duro *et al.* (2006b) use the WATEQ4F database, at least as a source of thermodynamic data, for the assessment of the concentration limits to be used in SR-Can. Also, Arcos *et al.* (2006) perform geochemical calculations with PHREEQC and PHAST (reactive transport code based on PHREEQC; Parkhurst *et al.* 2004) to study the evolution of the near field of a KBS-3 repository; and Guimerá *et al.* (2006) use PHREEQC in the study of deglaciation effects on groundwater composition. Unfortunately there is no indication of the thermodynamic database used in these two last works.

The main conclusion that can be drawn from the review of the use of the WATEQ4F database is that it has been widely used in PA-related works, and its thermodynamic data have also been frequently used in safety assessment as the source of data to create databases specifically developed for PA calculations. And this situation is especially true for the Swedish program. In this context, the use of the WATEQ4F database facilitates the comparison of results with previous and present studies in the Swedish sites and, at the same time, does not introduce significant discrepancies with respect to the common set of thermodynamic data from the PA-oriented thermodynamic databases used in more specific calculations.

However, although the selection of the WATEQ4F database seems to be an obvious choice, it does not mean that it is free of errors or that it can be used in all kind of conditions.

C.2.2 Other codes and databases

As already mentioned, some other codes and thermodynamic databases have also been used by the UZ group to perform different kinds of sensitivity analysis of speciation-solubility results. These analyses have dealt mainly with uranium species and high salinity waters (density and activity coefficient calculations). A brief summary of the peculiarities of uranium in geochemical modelling follows. The topic of high-salinity waters has been extensively treated in Appendix B, where the reader is referred to for details.

Uranium speciation-solubility calculations have been performed using three different thermo-dynamic databases: WATEQ4F (Ball and Nordstrom 2001), SKB-TDB (Duro *et al.* 2006a) and NAGRA[66] (Nagra/PSI TDB 01/01; Hummel *et al.* 2002).

SKB-TDB derives directly from the NAGRA database (Nagra/PSI TDB 01/01) with some modifica-tions or extensions for elements of special interest in Performance Assessment: Sm, Ho, Pa, Am, Np, Pu, Th, U, Cs, Sr, Ra, Sn, Se, Zr, Nb, Tc, Ni, Pd and Ag (Duro *et al.* 2006a).

Thermodynamic data for carbon, sulphur and silica species and minerals are identical to the ones included in NAGRA which, in turn, come basically from the review performed by Nordstrom *et al.* (1990) for these systems (Pearson and Berner 1991, Pearson *et al.* 1992, Hummel *et al.* 2002) and are the ones included in the WATEQ4F database (Ball and Nordstrom 2001). Therefore, differences in the speciation scheme and saturation states of the U system between the three databases will be mainly related to the different thermodynamic data considered for this compositional system.

These databases have been used in the geochemical calculations performed with the "high uranium groundwaters" found at Forsmark (Gimeno *et al.* 2008).

C.3 Review of some thermodynamic data and changes in the WATEQ4F database

To carry out the speciation-solubility and reaction-path calculations with PHREEQC (Parkhurst and Appelo 1999) during the site characterization program, a few modifications have been introduced to the WATEQ4F.dat database that is distributed with the code. The modifications affect the solubility (equilibrium constants) of several phases, quite problematical but very important in the groundwater systems under study. The modified phases are:

*   *Iron oxy-hydroxides and amorphous (nanocrystalline) and crystalline iron monosulphides*. Both groups of phases are involved in the redox processes and their solubility is highly dependent on the degree of crystallinity, specific surface area, and re-crystallization or ripening processes.

*   *Silica phases: quartz and chalcedony*. Quartz is present as a rock forming mineral and as a frac-ture filling mineral in most crystalline systems. Chalcedony is, basically, a more soluble fibrous-microcrystalline variety of quartz. Solubility control of dissolved silica by quartz or chalcedony in low temperature systems is, to say the least, controversial due to their sluggish kinetics, to the effect of particle size on solubility, and to the own solubility determination of these phases in low temperature conditions.

---

[66] WATEQ4F is distributed with the PHREEQC code. The other two databases have been formatted for their direct use with PHREEQC.

Modifications related to *iron* oxy-hydroxides and iron monosulphides have been discussed by the UZ group in previous SDM reports of Forsmark and Simpevarp (Gimeno *et al.* 2004, 2005, 2006, 2008) and in SR-Can (Auqué *et al.* 2006). Problems related to silica phases are specifically discussed in this report.

The next sections contain a brief discussion of the main difficulties encountered when working with this type of phases, the range of proposed solubility values, and the selected solubility values used in the granitic groundwater systems under study.

C.3.1 Iron oxy-hydroxides

The iron oxy-hydroxides is a group of minerals whose main specimens range from amorphous or poorly-crystalline (ferrihydrites or hydrous ferric oxides –HFO-, $Fe(OH)_3$; see Section 12.1 in Langmuir 1997), to intermediate phases like lepidocrocite ($FeOOH$), and more stable and crystalline phases like hematite (Fe_2O_3) or goethite ($FeOOH$). The stability, solubility and reactivity of this complex group of phases are controlled by their mineralogy, crystallinity, degree of hydration, impurities and particle size (see e.g. Langmuir and Whittemore 1971, Postma 1993).

From all the factors affecting the solubility, particle size and specific surface area are among the most important (Macalady *et al.* 1990, Nordstrom *et al.* 1990, Langmuir 1997). Both properties have a wide range of variation, complicated by temporal changes in each phase as the interaction time with groundwaters increases.

All the above ferric phases are thus linked by re-crystallization processes (ripening) by which less crystalline phases are converted with time into more crystalline ones (hematite and goethite), thus decreasing their solubility and increasing their particle size and decreasing specific surface area (Larsen and Postma 2001, Pedersen *et al.* 2005).

The fractured crystalline groundwater systems of the Scandinavian Shield have an ample variety of oxy-hydroxides, ranging in crystallinity from amorphous (ferrihydrites) in the near-surface groundwaters to fully crystalline (goethite and hematite) in fracture filling minerals in contact with deep, long-residence time reducing groundwaters (Grenthe *et al.* 1992). Besides, in groundwater systems with a variable redox potential iron oxy-hydroxides are not static phases of fixed composition, but dynamic entities that evolve as the surrounding groundwater changes (Pedersen *et al.* 2005).

Obviously, all these variable factors complicate the selection of the proper thermodynamic values and justify the revision of the WATEQ4F database. It is important to bear in mind that the inherent difficulty in selecting appropriate solubility values for the oxy-hydroxides sets a strict limit on the accuracy of the geochemical computations.

Solubility of oxy-hydroxides in the Swedish context: a literature review

Table C-1 and Figure C-1 summarise the solubility of the iron oxy-hydroxides found in the literature according to the following reaction:

$$Fe(OH)_{3(s)} \leftrightarrow Fe^{3+} + 3OH^- \tag{C-1}$$

From the lowest to the highest, solubility values span seven orders of magnitude, and those of individual phases have a spread of two to four orders of magnitude. The less crystalline phases ("ferrihydrites") show only a limited overlap in solubility with other iron oxy-hydroxides. Most authors agree on their solubility, but even so the range of values spans two orders of magnitude. This variability is a major concern when performing geochemical calculations (Majzlan *et al.* 2004).

The most stable phases, hematite and goethite, are affected by variations of solubility of four orders of magnitude. The solubility product of the low specific surface area varieties of these crystalline phases is around $pK = 44$ (44.15 for goethite and 44.0 for hematite; Macalady *et al.* 1990, Langmuir 1997), but it can vary with surface area.

For example, Bonneville *et al.* (2004) give for low-surface area (LSA) hematite ($12~m^2g^{-1}$) an experimentally derived pK of 42.8, whereas for nanocrystalline hematite (specific surface area of $125~m^2g^{-1}$) the value given is $pK = 41.5$.
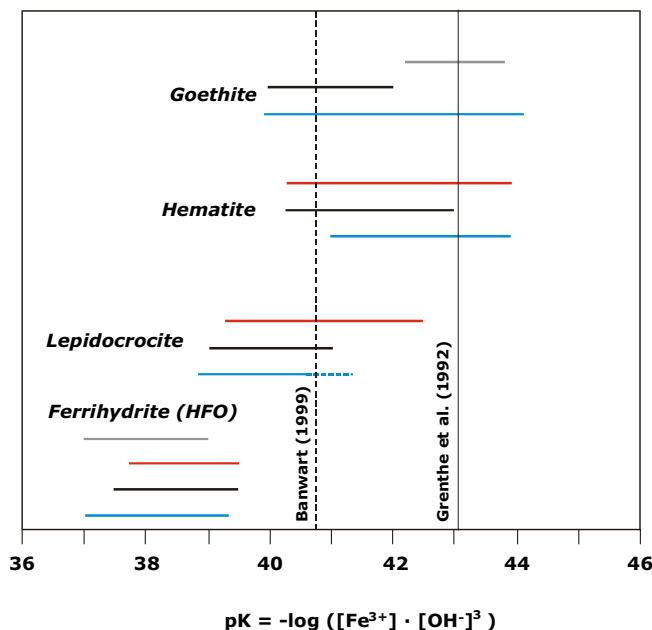
Figure C-1. *Reported solubility ranges at 25 °C for the main ferric oxyhydroxides. Blue lines represent the ranges obtained by Langmuir (1969; 1997); black lines correspond to the values suggested by Appelo and Postma (2005) from an analysis of Cornell and Schwertmann (2003) data; red lines represent the ranges reported in Bonneville et al. (2004); and, finally, grey lines represent the range of values proposed by Nordstrom et al. (1990). The most recent solubility ranges obtained by Majzlan et al. (2004) for 2-line and 6-line ferrihydrite (HFO: hydrous ferric oxyhydrides; values between 37.5 and 39.5) coincide with the ranges shown in the plot for this phase. The values reported by Macalady et al. (1990) for goethite (pK=44.15) and hematite (pK=44.0) are in agreement with the less soluble extreme of the range shown in the plot for these minerals. Empirical values deduced by Grenthe et al. (1992; pK=43.1) and Banwart (1999; pK = 40.8) for different Swedish groundwaters are also indicated.*

Table C-1. Solubility ranges for the main iron oxy-hydroxides. The solubility values is expressed as pK = −log K = −log([Fe3+]·[OH−]3) corresponding to reaction (C-1).

	(Langmuir, 1969; 1997)	(Cornell and Schwertmann 2003; Appelo and Postma 2005)	(Bonneville et al. 2004)	(Nordstrom et al. 1990)
Ferrihydrite [1]	37–39.4	37.5–39.5	37.7–39.5	37–39
Lepidocrocite	38.7–≥ 40.6	39–41	39.3–42.5	–
Hematite	41– 43.9	40.3–43	40.3–43.9	–
Goethite	39.9–44.1	40–42	–	42.2–43.8

[1] Hydrous ferric oxide (HFO), amorphous to microcrystalline, in the terminology of Nordstrom *et al.* (1990). For the other authors cited, "ferrihydrite" includes from 2-lines ferrihydrite to 6-lines ferrihydrite (e.g. Majzlan *et al.* 2004).

For the most crystalline phases, studies carried out in the Scandinavian Shield by Grenthe *et al.* (1992) can help narrowing the range of solubilities. This study of the factors controlling the reducing redox state of several Swedish groundwaters of long residence time allowed the indirect determination of the solubility of the iron oxy-hydroxides involved in the redox control. The deduced equilibrium constant for the reaction

$$Fe(OH)_{3(s)} + 3H^+ \leftrightarrow Fe^{3+} + 3H_2O \tag{C-2}$$

is log $K = -1.1 \pm 1.1$. Expressed in terms of reaction (C-1), that is, $pK = -\log K = -\log([Fe^{3+}]\cdot[OH^-]^3)$ this value is $pK = 43.1 \pm 1.1$, inside the range shown in Table C-1 and Figure C-1 for hematite and goethite, and also in agreement with the type of oxy-hydroxide found in these groundwater systems as fracture filling mineral (mostly hematite, with minor goethite). Furthermore, hematite (or goethite) is the expected iron oxy-hydroxide in long residence time groundwaters, where less stable phases have disappeared or re-crystallised to more stable varieties.

The re-crystallization is exceptionally fast, of the order of days to years, when the groundwaters are alkaline and reducing (Schwertmann and Murad 1983, Stipp *et al.* 2002, Pedersen *et al.* 2005). Thus, the solubility value found by Grenthe *et al.* (1992) is particularly important when dealing with long residence time waters. For this reason, the value has been incorporated into the WATEQ4F database.

The situation is much more complex when water-rock interaction occurs in the shallowest part of the groundwater system, where active circulation of oxic or sub-oxic meteoric waters is important. Here, several iron oxy-hydroxides can be present at the same time, with variable crystallinity and surface area, dynamically transforming into phases of higher stability as interaction time increases[67]. To deal with this situation a more detailed hydrochemical and mineralogical knowledge than presently available in the shallow parts of the systems is needed.

Moreover, a relevant scenario for the formation of a wide spectrum of iron oxy-hydroxides is the intrusion of oxygen in boreholes (e.g. Houben 2003). Oxygen intrusion in reducing media usually induces the precipitation of amorphous phases[68] (or ferrihydrites; Langmuir 1997), with a pK between 37 and 39 (Table C-1 and Figure C-1). As previously pointed out, these phases quickly re-crystallise to less soluble and more stable phases when reducing conditions return. These processes have been observed in field studies (e.g. in the Äspö large-scale redox experiment Banwart *et al.* 1994, Banwart 1999) and in laboratory experiments (Trotignon *et al.* 2002) from the Swedish Characterization Program.

In the Äspö large-scale redox experiment (Banwart *et al.* 1994, Banwart 1999), a vertical fracture zone exposed during the works at the tunnel entrance was used to study the ability of the geological system to buffer groundwater redox conditions against an intrusion of dissolved O_2. Eh (from -80 to −160 mV) seems to be controlled by the occurrence of iron oxyhydroxides and Banwart (1999) obtained a value of log K = 1.2 for reaction C.2 (pK= 40.9 in Table C-1 and Figure C-1) using the same methodology as Grenthe *et al.* (1992).

The presence of this "intermediate" iron oxyhydroxide with higher solubility than a crystalline phase was possible only if there is a brief oxidizing disturbance (Banwart *et al.* 1994). This disturbance promotes the precipitation of amorphous iron oxyhydroxides and, subsequently, they re-crystallise towards more crystalline ones when reducing conditions return.

Similar observations were indicated by Trotignon *et al.* (2002) in the replica experiment of the REX project. The Eh potential measured during different O_2 "pulses" of the experiment (spanning 6–12 days) are in agreement with a calculated log K of 4 for reaction C-2 (pK value of 38 for reaction C-1; Table C-1 and Figure C-1) for the controlling iron oxyhydroxide, that is, a typical amorphous one. However, during the long anoxic periods between pulses (up to three months) the system shifts towards equilibrium with goethite.

---

[67] For example, less crystalline Fe-oxyhidroxides like lepidocrocite or ferrihydrites (frequently described as "rust"; Tullborg 1989, Landström and Tullborg 1990) have been identified in the upper part of the bedrock in Klipperas and Äspö (usually in the upper tens of meters) together with goethite, hematite or very fine grained hematite (Tullborg, pers. com.). This variability in the mineralogy of Fe-oxyhydroxides is produced by the action of oxidising surface waters (Tullborg 1989, Puigdomènech 2001) that promote the precipitation of less crystalline phases and their subsequent recrystallization (aging). The depth of this zone affected by oxidation and with less crystalline iron oxyhydroxides can vary depending on the site (around 50 m at Klipperas, 10 m at Äspö and 15–20 m at Laxemar-Simpevarp; Puigdomènech 2001, Drake and Tullborg 2008). Moreover, crystalline low-temperature goethite is much more common in the upper 50 m than at depth, both, in Forsmark and Laxemar-Simpevarp areas (Drake *et al.* 2006, Drake and Tullborg 2008). The presence of crystalline goethite in this shallow -and nowadays reducing- environment suggests the existence of inputs of oxygenated waters in the past (Gimeno *et al.* 2008, Drake and Tullborg 2008). There are no detailed data on the characters of this mineral but the studied goethites in the work by Dideriksen *et al.* (2007), also associated with "old" oxygen inputs, show a very fine grained nature with particle sizes lower than 100 nm. All these observations support the wide range of Fe-oxyhydroxides, of varying crystallinity and surface area, that can be found in the overburden and at shallow depths in the bedrock of the sites.

[68] This is what happened in the Äspö underground laboratory when reducing groundwaters were put in contact with the oxygen-rich atmosphere of the tunnel. There, *bacteriogenic iron oxides* (BIOS) formed by ferrihydrite are precipitated (Ferris *et al.* 1999, Martínez *et al.* 2004).

The $Fe^{2+}/Fe(OH)_3$ heterogeneous redox pair is clearly electroactive and the platinum inert electrode can read the equilibrium potential involved in this pair when colloidal suspensions of ferric oxyhydroxides are present in the waters (Macalady *et al.* 1990) or when an amorphous or poorly-crystalline oxyhydroxide precipitates (Grenthe *et al.* 1992, Silvester *et al.* 2005). That is, when the surface area of the solid phase is high. Therefore, even very low amounts of oxygen can alter the Eh measurements through the induced precipitation of this type of less crystalline oxyhydroxides.

Oxygen intrusion can also be identified by comparing the potentiometrically measured Eh values with those coming from the $Fe^{2+}/Fe(OH)_3$ redox pair with different solubility values for the solid phase. That is, using the potentiometric Eh values to deduce the type of oxyhydroxide that may control these potentiometric values as it has been successfully done in previous studies both in the field (e.g. Grenthe *et al.* 1992, Banwart 1999) and in the laboratory (Macalady *et al.* 1990, Bonneville *et al.* 2004, Silvester *et al.* 2005).

This approach has been used in different SMD phases by the UZ group (e.g. Gimeno *et al.* 2006, 2007, 2008) expanding the WATEQ4F database with more solubility data for Fe- oxyhydroxides (see below).

Modifications to the WATEQ4F database

There are different iron oxy-hydroxide phases of interest in the WATEQ4F.dat database distributed with PHREEQC (Parkhurst and Appelo 1999).

Hematite and goethite. The log K values are –2 and –1, respectively, for reaction C-1; that is, pK values of 43 and 44 (these values plot in the low solubility tail of the range shown in Figure C1 for hematite and goethite)

Amorphous oxy-hydroxide, denoted as "Fe(OH)$_{(a)}$"in the database. For this less crystalline iron oxy-hydroxide a single log K value of 4.891 is included. This value is very close to the value usually assigned to the less crystalline ferrihydrite (2-lines ferrihydrite) of log K = 5 for reaction C.2 (or pK = 37 in Table C-1 or Figure C-1). This value is in the high solubility end of the range shown in Figure C-1 for ferrihydrite.

Therefore, the UZ group considered of interest the inclusion of some "intermediate" oxy-hydroxide in the database. The single entry "Fe(OH)$_{(a)}$", has been complemented with an entry for a less amorphous (microcrystalline) ferrihydrite, "Fe(OH) (micro)", following the terminology of Nordstrom *et al.* (1990). The corresponding entry in the database is:

```
Fe(OH)3(micro)

        Fe(OH)3 + 3 H+ = Fe+3 + 3 H2O

        log_k           3.00
```
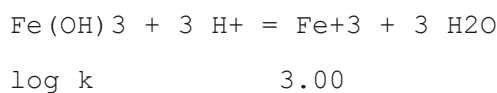
Another mineral phase has been included as well, called "Fe(OH)$_3$ (Banwart)" with the equilibrium constant deduced by Banwart (1999), an "intermediate" solubility iron oxyhydroxide for the whole range presented in Figure C-1 and representative of and "aged" oxyhydroxide after a brief oxidizing disturbance. The entry in the database is:

```
Fe(OH)3(Banwart)

        Fe(OH)3 + 3 H+ = Fe+3 + 3 H2O

        log_k           1.2
```
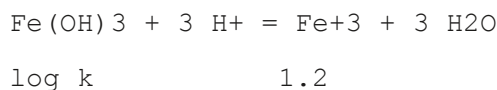
Finally, an additional mineral phase called "Fe(OH) (hematite_Grenthe)", with the equilibrium constant proposed by Grenthe *et al.* (1992), has also been included. This value is in the low solubility end of the range shown in Figure C-1 and Table C-1 and it can be considered representative of the solubility of stable iron oxyhydroxides (mainly hematite) under reducing conditions in the studied systems. The corresponding entry in the database is:
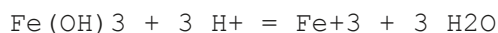
```
Fe(OH)3(hematite_grenthe)

        Fe(OH)3 + 3 H+ = Fe+3 + 3 H2O

        log_k          -1.1
```

As it has been stated before, the inclusion of these values helps the interpretation of the Eh measurements. Moreover, it facilitates the theoretical calculations of redox potentials (e.g. Auqué *et al.* 2006) according to the correlations observed in the Swedish sites and in different scenarios.

C.3.2. Ferrous iron monosulphides

Under this term the amorphous mono-sulphide ($FeS_{(am)}$ or $FeS_{(ppt)}$), more properly named disordered mackinawite (Wolthers *et al.* 2003, 2005) or nanocrystalline mackinawite (Rickard 2006, Rickard and Luther III 2007), the ordered or crystalline mackinawite (tetragonal FeS) and greigite (Fe_2S_4) are included. All of them can be involved in the transformation to pyrite (FeS_2). Although there are different reaction pathways that can explain this transformation (Wilkin and Barnes 1997, Benning *et al.* 2000), most of them start with the precipitation of an initially amorphous ferrous iron monosulphide which is transformed into pyrite via ordered mackinawite and greigite.

The amorphous monosulphide is the first phase that typically precipitates in most natural aqueous systems (Chen and Liu 2005, Rickard and Morse 2005, Rickard and Luther III 2007). It is the most soluble of the iron sulphides but, on the other hand, its precipitation kinetics is very fast (seconds; Rickard 1989, 1995): when waters reach the amorphous iron monosulphide saturation and, although they are already oversaturated with respect to other monosulphides, this amorphous phase precipitates first.

Mackinawite (the crystalline monosulphide) is slightly less soluble but its precipitation kinetics is also fast (days; Rickard 1989). It is also common to find this crystalline phase as a result of the re-crystallisation of amorphous monosulphides. Re-crystallization is also a fast process (Rickard 1995, Wilkin and Barnes 1997, Benning *et al.* 2000), and it can affect the composition of the surrounding solution, which would re-equilibrate to the activity product of crystalline mackinawite (Chen and Liu 2005).

From the identification of equilibrium states with respect to amorphous monosulphides in groundwaters some important conclusions can be drawn:

- Since the precipitation of amorphous monosulphides is kinetically very fast, a significant oversaturation is not expected to occur in natural groundwaters (Rickard and Lutther III 2007). This fact can provide some indirect evaluation on the quality of the analytical data used in geochemical calculations (oversaturation states will be very suspicious).

- As re-crystallisation to crystalline mackinawite is also usually fast, identification of this equilibrium situation will be indicative of an ongoing precipitation of monosulphides.

- This ongoing precipitation requires a continuous supply of H_2S to the system, enough to put waters over the solubility product of this phase and to produce its fast precipitation; therefore, it also indicates the presence of sulphate-reducing activity (produced by sulphate-reducing bacteria, SRB) taking place at present.

- The transformation (ripening) of these amorphous monosulphides can explain the presence of "recent" pyrite of biogenic origin identified in the most external and latest filling stage in conductive fractures (Drake and Tullborg 2004, Gimeno *et al.* 2008).

- When dissolved Fe(II) (or a source of this component) is also present in the system, precipitation of amorphous monosulphides can prevent the accumulation (high concentrations) of dissolved sulphides in the groundwaters.

- The precipitates of "amorphous" monosulphides actually correspond to nanoparticulate mackinawite (Wolthers *et al.* 2003, 2005, Rickard and Morse 2005, Rickard 2006, Rickard and Luther III 2007). This precipitation process can therefore induce the genesis of colloidal phases.

It is obvious from the above observations that monosulphide equilibrium situations can be related to several key processes in the hydrogeochemical conceptual model of the site (redox processes and bacterial activity, to name just a few) and to some important issues addressed in safety assessment studies (colloids, the corrosion of the copper canister by dissolved sulphides, etc).

The thermodynamic data used in geochemical calculations to identify these equilibrium situations are, therefore, of major concern. During the site investigation program problems related to the solubility of iron monosulphides were found and a review of the available values in the literature has been carried out (section C.3.2.1). Besides, sulphide speciation in alkaline conditions is nowadays under revision and the main uncertainties related to the speciation of iron and sulphur are also discussed (section C.3.2.2).

The solubility of iron monosulphides

The term *"amorphous" FeS* is used below, to simplify the terminology, as equivalent to the more accurate terms of disordered mackinawite or nanoparticulate mackinawite and the term *mackinawite* is used as equivalent to ordered mackinawite or crystalline mackinawite. Although in the recent studies of Rickard and Morse (2005), Rickard (2006) and Rickard and Luther III (2007) differences in solubility are discussed as belonging to the same mineral (mackinawite), it seems more convenient to keep the differentiation between these two terms.

Solubility measurements of "amorphous" FeS and mackinawite have been mostly performed in acidic conditions and they have been reviewed by Morse *et al.* (1987), Davison (1991), Rickard and Morse (2005) and Rickard and Luther III (2007). Solubility values of "amorphous" FeS and mackinawite are usually defined in the literature by the reaction:

$$FeS_{sol} + 2H^+ \leftrightarrow Fe^{2+} + H_2S \tag{C-3}$$

or:

$$FeS_{sol} + H^+ \leftrightarrow Fe^{2+} + HS^- \tag{C-4}$$

The transformation between the log K values of both reactions is straightforward through the dissociation reaction:

$$H_2S \leftrightarrow HS^- + H^+ \tag{C-5}$$

which has a log K value of −6.98 (Suleimonov and Seward 1997). Solubility values indicated in this work refer to reaction (C-4).

Solubility values in the WATEQ4F database

Several mistakes have been found in the solubility constants of amorphous iron monosulphides and mackinawite in the PHREEQC.dat and WATEQ4F.dat databases. The dissolution reaction for the two phases included in both databases correspond to reaction C-4, with an equilibrium constant value of log K = −3.91 for $FeS_{(am)}$ and log K = −4.648 for mackinawite.

The WATEQ4F user's manual (Ball and Nordstrom 2001) indicates that these values come from Berner (1967). However, Chen and Liu (2005) have shown that the value included in these databases is the consequence of a mistake during the conversion of the reactions and thermodynamic data from Berner (1967) to the format that the databases accept (reaction (C-4). The correct value, as deduced from Berner's data for $FeS_{(am)}$, should be log K = −2.98, i.e. almost one order of magnitude larger. A similar case affects the equilibrium constant of mackinawite (Gimeno *et al.* 2006). Manipulating the reactions and thermodynamic values proposed by Berner (1967) to obtain the equilibrium constant of reaction (C-4), the resulting value is log K = −3.6 for mackinawite.

This mistake is also found in the MINTEQ.dat database distributed with PHREEQC (Parkhurst and Appelo 1999). However, the newest version of this database, MINTEQ.v4.dat, has the correct values for $FeS_{(am)}$ and mackinawite (log K = −2.95 and log K = −3.6 respectively). Note, however, that together with MINTEQ.v4.dat, the older version of the database (MINTEQ.dat), including the mistakes mentioned above, is also distributed with PHREEQC.

Solubility values: a literature review

Besides the experimental solubility values of iron monosulphides obtained by Berner (1967), there are more recent studies based on experiments and natural systems.

Experimental studies by Davison *et al.* (1999) found a value of -3.00 ± 0.12 at 20 °C (with pH between 3 and 7.9 and under different H_2S partial pressures, 10^{-1} to 10^{-5} Mpa) and Theberge and Luther (1997) obtained a value of -2.95 (at 25 °C), all of them very similar to the value of log $K = -2.946 \pm 0.2$ (for reaction C-4) proposed in the review of Davison (1991).

For mackinawite, apart from Berner's (1967) experimental value (log $K = -3.55$), a very similar one (log $K = -3.6 \pm 0.2$.) was proposed in the review of Davison (1991) and a similar value was also recalculated by Davison *et al.* (1999) from Berner's data (log $K = -3.55 \pm 0.09$). In the ripening experiments of precipitated monosulphides performed by Benning *et al.* (2000) a value of log $= -3.77$ at 25 °C was obtained, slightly higher than the previous ones for "amorphous" FeS and similar to those of mackinawite. Benning *et al.* (2000) indicated that this effect was due to a longer ripening time in their experiments, which gave rise to a more crystalline phase (mackinawite).

Finally, Rickard (2006), using nanoparticulate mackinawite in acidic conditions, obtained a solubility value of log $K = -3.5$. Although nanoparticulate mackinawite ("amorphous" FeS) is used in the experiments, the solubility value is very close to that proposed for crystalline mackinawite. This author indicates that the difference between the measured solubility constants in his study and in that of Benning *et al.* (2000), with values of log $K = -3.5$ and -3.77, respectively, and those obtained by Berner (1967) and Davison *et al.* (1999), with values of log $K = -2.98$ and -3, seem to be related to the different experimental setup.

Benning *et al.* (2000) and Rickard (2006) measured the solubility of a FeS precipitated by adding OH^- to an acidic solution of Fe(II) and S($-$II). In the case of Berner (1967) and Davison *et al.* (1999), FeS was precipitated and its solubility was measured by acid dissolution. That is, dissolution methods give higher solubility constants than precipitation methods.

Nothing intrinsically wrong seems to be in any of the experimental approaches and therefore, Rickard (2006) suggested that the difference in solubilities may be due to different properties of the nanoparticulate material, with the FeS precipitated from acid solutions being more stable and less soluble than that precipitated from more alkaline solutions. Moreover, the nanoparticulate character of the precipitate and its very high specific surface area can easily promote aging processes (as it occurs in other putative "fine-grained" minerals like iron oxyhydroxides) of different intensity depending on time and experimental conditions (e.g. pH; Wolthers *et al.* 2003).

The effect of aging of the first precipitated FeS is well known and, after a period of days to months in aqueous solution, crystalline mackinawite develops (Rickard 1969, 1997). Even the first nanoparticulate mackinawite precipitated with a size of 2 nm changes to a 7 nm phase within a period of hours (Wolthers *et al.* 2003, Rickard and Morse 2005). This fast re-crystallisation kinetics can also affect the experimental solubility values of FeS (Wolthers *et al.* 2003).

Different authors have obtained solubility values for the amorphous monosulphides from ion-activity product (IAP) calculations ***in natural systems***. A value of log $K = -3.15$ was obtained for the amorphous FeS at temperatures from 12.8 to 18.8°C in a in situ study of sediments from the Baltic Sea by Bågander and Carman (1994). Chen and Liu (2005) reported a value of -3.07 ± 0.34 in a study of the groundwaters from the Chosui delta (Taiwan). These authors, using additional data of sulphidic waters in different bedrocks (limestones, coastal plain sediments, wetlands, fractured limestones, etc), obtained an average of log $K = -2.98$. Finally, a value of log $K = -2.98 \pm 0.36$ was obtained by Gimeno *et al.* (2006) for the sulphidic groundwaters in the Laxemar-Simpevarp area.

Solubility, pH dependence, and speciation

As stated before, solubility measurements of "amorphous" FeS and mackinawite has been mostly performed in acidic conditions and, until recently, data in solutions above pH=6 were very scarce (Rickard and Morse 2005). Alkaline conditions are even more problematical because the dominant species that control dissolved Fe(II) and dissolved S($-$II) in neutral-alkaline conditions is an actively investigated but still unsolved subject (Rickard and Morse 2005, Rickard and Luther III 2007).

"Amorphous" FeS and mackinawite solubilities are controlled by the pH-dependent reaction (C-3) under acidic conditions whereas works by Davison *et al.* (1999) and Wolthers *et al.* (2005) suggested the existence of a pH independent mechanism controlling the solubility in the pH range 6–8, possibly related to a change in the dominant dissolved species in neutral-alkaline conditions. Davison *et al.* (1999) indicated that a non-charged Fe bisulphide complex became the dominant dissolved species above pH=6 and Wolthers *et al.* (2005) or Rickard and Morse (2005) suggested that an aqueous FeS cluster[69] (see below) might provide the same result.

More recently, Rickard (2006) has measured the solubility of synthetic nanoparticulate mackinawite at 23 °C from pH 3 to 10 and total dissolved S(–II) concentrations from 10^{-1} to 10^{-5} M. Results indicate that no significant dependence of the solubility of the nanoparticulate FeS on S(–II) total concentration is observed in the neutral to alkaline pH range. Values of log Fe(II) tend to a constant value around 5.7 ± 0.27 over the whole range of S(–II) concentrations and pH values (5.5–9.7; Figure C-2) of the experiments.

The absence of a solubility dependence on total dissolved sulphide in neutral to alkaline pH values indicates that free H_2S or HS^- cannot be involved in the overall dissolution process in these conditions. As the experimental solutions showed the characteristic voltammetric signature of the aqueous FeS cluster, Rickard (2006) adjusted its solubility data in neutral-alkaline conditions using an uncharged species or cluster ($Fe_nS_{n(aq)}$)

$$n\text{FeS}_{sol} \leftrightarrow \text{Fe}_n S_{n(aq)} \tag{C-6}$$

with a Fe:S ratio of 1 and represented, in a simplified manner, by the monomer FeS^0 with a stability constant of $10^{2.2}$ for the acid dissociation reaction

$$\text{FeS}^0 + \text{H}^+ \leftrightarrow \text{Fe}^{2+} + \text{HS}^- \tag{C-7}$$

Therefore, this author indicates that the solubility of FeS can be represented by a pH-dependent reaction (reaction C-3) and a pH-independent reaction (reaction C-6). The measured solubility constant for the pH-dependent reaction (log $K = -3.5$ for reaction C-4) agrees with the solubility of "amorphous" FeS and mackinawite previously determined in acidic conditions by other authors (see section C.3.2.1). The intrinsic solubility of reaction (C-6) in alkaline conditions determined by Rickard (2006) is log $K = -5.7$.

These results are very important as they represent the first systematic measurements of the solubility of ferrous iron monosulphides in alkaline conditions. Nevertheless, the difference between the solubility in acidic and alkaline conditions is associated with difficulties in the identification of the dissolved species related to these solids in neutral-alkaline conditions[70].

This problem has cast some serious doubts (e.g. Rickard and Morse 2005) on the results of speciation-solubility calculations in neutral-alkaline waters because they extrapolate solubility values (equilibrium constants) experimentally obtained in acidic conditions (the only available ones until very recently and, therefore, included in the geochemical codes) to situations where the ionic activity product (speciation) is not well defined. Obviously, the same criticisms can be done in reaction-path (predictive) calculations performed in neutral-alkaline conditions.

---

[69] A cluster is essentially a multinuclear complex constituted by a system of bonds connecting each atom directly to its neighbours. Therefore, they do not show neither the typical structure of a complex with the atoms bound to a central atom (Rickard and Morse 2005), nor that of ion pairs with the atoms electrostatically bounded.

[70] For example, solubility of quartz (or any other silica polymorph) is low and pH-independent until pH values around 9 while the silica speciation is dominated by the neutral dissolved species $H_4SiO_4^0$. At higher pH values, solubility increases and it is dependent on pH as other dissolved silica species ($H_3SiO_4^-$, $H_2SiO_4^{2-}$) dominate in solution (Drever 1997, Langmuir 1997, etc). But in geochemical speciation-solubility calculations only a value of log K for quartz is necessary provided that dissolved silica speciation and the stability constants for the involved species are known.

Calculations with PHREEQC and the WATEQ4F database

After the above exposition, it seems that the only possible conclusion would be that the speciation-solubility calculations with respect to ferrous iron monosulphides in alkaline waters (like the groundwaters from Laxemar-Simpevarp and Forsmark) have important uncertainties, difficult to quantify. However, a fairly accurate evaluation of their suitability (or correction) can be obtained by trying and theoretically reproduce the experimental results available at present on the solubility of these phases for a wide range of pH, including alkaline conditions.

The idea is the following. Rickard (2006) experimentally determined the synthetic nanoparticulate mackinawite at 23 °C for a pH range between 3 and 10. Experimental determinations from Rickard (2006) were obtained in solutions with Fe, SO_4^{2-}, Cl and Na, keeping the H_2S gas content constant at 0.03, 0.3, 3 and 100% H_2S, that is, total dissolved sulphide contents (S_{tot}) between 10^{-1} and 10^{-5} M. Ionic strengths of the experimental solutions were between 0.106 and 0.649 M.

Following this, the calculations performed here use synthetic water with 0.1 mol/kg of Cl, Na, SO_4^{2-} and Ca (ionic strength around 0.32 molal). This initial water has been equilibrated with FeS at different pH values (between 5 and 9.5) and with constant S_{tot} contents (10^{-5} and 10^{-4} M or 0.32 and 3.2 mg/L; which is the range for most of the sulphidic waters sampled in Laxemar-Simpevarp and Forsmark areas).

The thermodynamic database used for the calculations is WATEQ4F (Ball and Nordstrom 2001) distributed with PHREEQC (Parkhurst and Appelo 1999). This database has a complete speciation scheme for dissolved iron and sulphur with almost all the species cited in the bibliography (even polysulphides, e.g. S_4^{2-}, S_5^{2-}, S_6^{2-}, etc; formation reaction and equilibrium constants are reported in Ball and Nordstrom 2001). The only thermodynamic value modified from the original data set is the equilibrium constant for the amorphous ferrous iron monosulphide; it has been included the solubility value experimentally obtained by Rickard (2006) in acidic conditions (log $K = -3.5$).

Figure C-2 shows the results of the simulation together with the experimental data from Rickard (2006). The agreement between the Fe(II) contents calculated and the ones experimentally measured is noticeably good for the range of S_{tot} content considered in the simulations. This good fit applies also to alkaline conditions where PHREEQC simulations even predict the stabilisation of the content of Fe(II) observed in experiments.
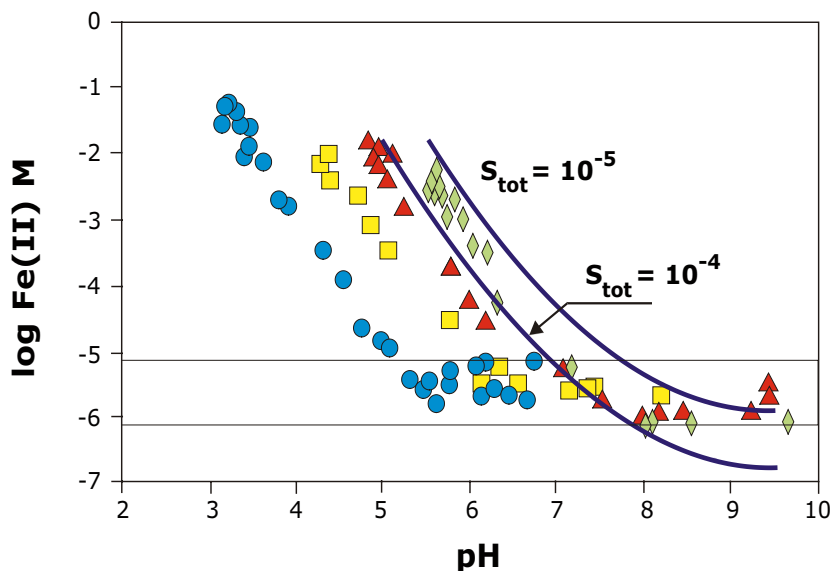
Figure C-2. Comparison of the results experimentally obtained by Rickard (2006) for the solubility of FeS (expressed as a function of the total content of Fe(II), log Fe (II) M) and the results calculated with PHREEQC. In both cases the S_{tot} contents have been kept constant at 10^{-4} and 10^{-5} M. Different symbols refer to the different H_2S_{gas} contents used by Rickard (2006) in his experiments (circles: 100% H_2S_{gas}; squares: 3%; triangles: 0.3%; and diamonds: 0.03%).

The reason for this behaviour is related to the changes in sulphur speciation as pH increases. For pH values lower than 7, the dominant species are H_2S and HS^-. For pH values higher than 8–8.5 polysulphide content (S_4^{2-}, S_5^{2-} and S_6^{2-}) increases and for pH > 9 they become dominant[71]. This change is the responsible of iron content stabilisation in this pH range (Figure C.2).

The main conclusion to be drawn is that iron and sulphur speciation must be reviewed in alkaline conditions, mainly for waters with higher total dissolved sulphur. However, it is clear from the performed calculations that the speciation scheme included in the WATEQ4F database allows a very good reproduction of the experimental results in the range of interest of dissolved sulphur. This fact strongly supports the results of monosulphide saturation states calculated by the UZ group in the different SDM stages for the Laxemar and Forsmark, and also the predictive calculations performed by Auqué *et al.*(2006) using these phases.

Modifications to the WATEQ4F database

The original solubility value of FeS(ppt) in the WATEQ4F.dat database has been changed from log K=−3.915 to −3.00:

```
FeS(ppt)                119

        FeS + H+ = Fe+2 + HS-

        log_k           -3.00
```

In the same manner, the original value of mackinawite has been changed from log K= −4.648 to −3.6:

```
Mackinawite            67

        FeS + H+ = Fe+2 + HS-

        log_k           -3.6
```

C.3.3 Silica phases: chalcedony and quartz

Control by equilibrium with quartz and chalcedony has been usually identified in thermal waters (higher than 80 °C) associated with crystalline rocks, and silica geothermometers based on the solubility of quartz and chalcedony have been successfully used to estimate in situ temperatures in geothermal aquifers (e.g. Fournier and Rowe 1962, Arnorsson *et al.* 1983, Michard *et al.* 1996).

Possible or apparent equilibrium with silica phases (e.g. chalcedony) has also been found or assumed in low-temperature systems including crystalline ones (Grimaud *et al.* 1990, Trotignon *et al.* 1999, Beaucaire *et al.* 1999, Neal *et al.* 2005, Banks and Frengstad 2006, Iwatsuki *et al.* 2005). Although the identification of this equilibrium can facilitate the geochemical modelling of the system, its detailed interpretation is much more complicated than it is usually assumed. In low-temperature systems different kinetically-controlled reactions with aluminosilicates can effectively participate in the control of dissolved silica, even in situations of apparent equilibrium with, for example, chalcedony (e.g. see the discussion of Banks and Frengstad 2006).

Long residence time groundwaters, like deep saline groundwaters in Laxemar-Simpevarp and Forsmark, could fulfil the ideal conditions to approach a real equilibrium with silica phases even in low temperature conditions. These groundwaters in contact with quartz during very long periods of time (at least 1.5 million years as estimated from [36]Cl data for groundwaters in Laxemar-Simpevarp and Forsmark; Louvat *et al.* 1999, Smellie *et al.* 2008) in near stagnant conditions, and unaffected by silica released from weathering reactions, can supersede the typical problems associated with the slow reaction rate of quartz and the effects of other reactions.

---

[71] This is in agreement with the recent results obtained by Kamyshny *et al.* (2004).

But, even neglecting the effects of alternative and/or concomitant reactions, solubility control of dissolved silica by quartz or chalcedony in low-temperature systems is hampered by problems related to the solubility of these phases, even considering that quartz is one of the minerals more exhaustively investigated (Heaney and Post 1992).

Moreover, the higher solubilities of microcrystalline quartz varieties, fibrous (e.g. chalcedony) or non-fibrous (simply, microcrystalline quartz; Knauth 1994), are primarily related to particle size effects, introducing new uncertainties, as a detailed mineralogical information on quartz crystal size is usually absent. These problems are discussed below.

Review of the solubility of quartz and chalcedony

Among the silica polymorphs, the solubility of quartz has been widely investigated (Kennedy 1950, Fournier 1960, Kitahara 1960, van Lier *et al.* 1960, Morey *et al.* 1962, Siever 1962, Fournier and Rowe 1962, Crerar and Anderson 1971, Mackenzie and Gees 1971, Walther and Helgeson 1977, Fournier and Potter 1982, Fournier 1983, Rimstidt 1997, Gunnarsson and Arnorsson 2000). In the temperature range between 100 and 250 °C results usually are in good agreement. However, below 100 °C some discrepancies exist between the reported results (Gunnarsson and Arnorsson 2000).

In Figure C-3 log *K* values for the dissolution reaction of quartz have been plotted:

$$SiO_{2(quartz)} + 2H_2O \leftrightarrow H_4SiO_4^0 . \tag{C.8}$$

These values are included in the WATEQ4F thermodynamic data base (Ball and Nordstrom 2001) and in SUPCRT 92 (Johnson *et al.* 1992), together with the values proposed by Rimstidt (1997). The solubility values for quartz in low-temperature conditions (21 to 96 °C; the duration of the solubility experiment at 21° C lasted for more than 13 years) presented by Rimstidt (1997) indicate a considerably higher solubility (log K = −3.746, equivalent to 11 ppm as SiO_2 at 25 °C) than previously reported and generally accepted (log K = −4, or 6 ppm of dissolved SiO_2).

These results for quartz solubility appear to be confirmed in later experiments by Gunnarsson and Arnorsson (2000) although this new solubility values have not been incorporated in most of the thermodynamic databases available at present and the consequences of this higher quartz solubility in natural systems remain highly unexplored.

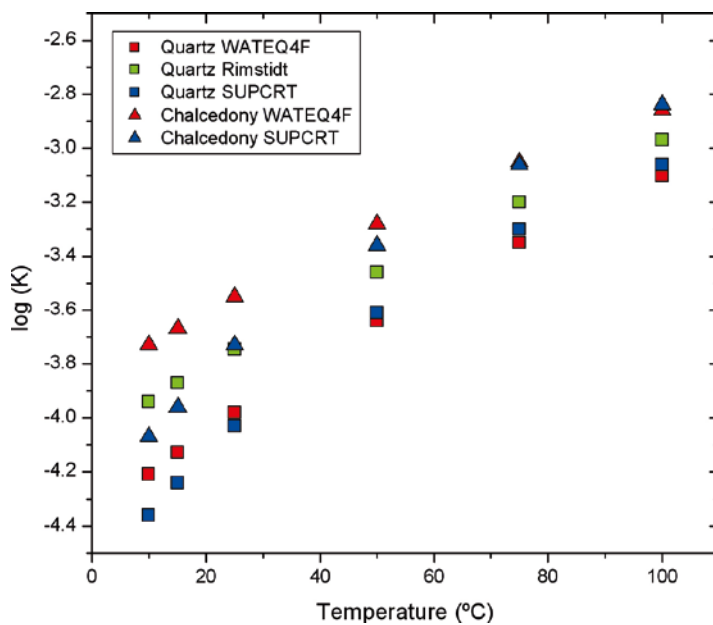**Figure C-3.** *Variations in log K with temperature for quartz and chalcedony considered in SUPCRT ( ) and WATEQ4F (Ball and Nordstrom 2001) thermodynamic databases. Experimental results for quartz obtained by Rimstidt (1997) are also included.*

Published data for the solubility of chalcedony are much less abundant. Fournier and Rowe (1962) and Fournier (1973) reported chalcedony solubility values from 92° C to 259°C. Later, based on those results, Fournier (1977) proposed the chalcedony geothermometer[72]. Using the same data, Walther and Helgeson (1977) calculated the standard state enthalpy and Gibbs free energy of formation for chalcedony at 25°C and 1 bar. Assuming that chalcedony is simply fine-grained quartz, they fitted the data of Fournier and Rowe (1962) and Fournier (1973) with Maier-Kelley heat capacity power function coefficients and the standard molal third law entropy of quartz.

The thermodynamic data obtained for chalcedony by Walther and Helgeson (1977), implemented in SUPCRT 92 (Johnson *et al.* 1992), have been included in some of the most popular thermodynamic databases and codes. The original dataset from Fournier (1985) was reviewed by Nordstrom *et al.* (1990) and included in the WATEQ4F database (Ball and Nordstrom 2001) and also in the MINTEQ database from the U.S. Environmental Protection Agency. These two proposals are compared in Figure C-3, where the progressive divergence for low temperatures (up to 0.4 logarithmic units at 10 °C) is clearly seen.

As both calibrations use exactly the same experimental data, differences indicate fitting uncertainties in the parameters, which is not strange considering the scatter in the experimental data as a function of temperature and the fact that there are no solubility data for temperatures lower than 90 °C. Uncertainties associated with the extrapolation to lower temperatures can be important.

Moreover, other authors (Hummel *et al.* 2002) indicate that these measurements were performed on few and ill-defined samples (only two chalcedony samples, one from a geode in Death Valley and other from a basalt in Montana; Fournier and Rowe 1962, Fournier 1973). In consequence, this phase was not included in the NAGRA-TDB (nor in the SKB-TDB; Duro *et al.* 2006a). Although this decision could be justified, it does not solve the problem associated with the solubility of chalcedony.

Solubility of chalcedony and particle size

Chalcedony is usually defined as the fibrous-microcrystalline variety of quartz. However, the solubility of chalcedony is apparently not defined by this fibrous character but by its microcrystallinity. In fact, the inherent assumption in the solubility function proposed by Walther and Helgeson (1977) is that chalcedony is simply fine-grained quartz.

This assumption was supported in later studies by Gislason *et al.* (1993a). They analysed by transmission electronic microscopy the distribution of crystal sizes in the chalcedony samples used by Fournier (1973) for his solubility experiments. Results indicate that crystal size (expressed as the radius of spherical crystals) is in the range of 0.01 to 0.1 μm with a maximum between 0.01 and 0.03 μm.

Minerals formed by crystals of small size, and therefore with a high specific surface area, have an excess Gibbs free energy associated with the solid-liquid interface that increase their solubility. The thermodynamic relation between solubility and crystal size, assuming spherical crystals with a smooth surface and radius *r*, is defined by the Freundlich-Ostwald (a.k.a. Gibbs-Kelvin) equation (Enüstün and Turkevich 1960, Williams *et al.* 1985, Stumm and Morgan 1996, Langmuir 1997):

$$\log\left(\frac{K_o}{K_s}\right) = \frac{2V\gamma}{2.303\,R\,T\,r} \tag{C-9}$$

where K_0 is the apparent equilibrium constant (solubility) of the solid of radius *r*, K_S is the solubility of an infinite plane surface (equilibrium constant independent of the particle size, that is, the conventional solubility) of the same solid, γ is the free energy of the solid interface, *R* the gas universal constant, *T* the absolute temperature and V the molar volume.

---

[72] In addition, Arnorsson *et al.* (1983) have reported a solubility function based on data from natural geothermal systems assuming to be in equilibrium with chalcedony.

Using equation (C-9) and solubility values for quartz and chalcedony, Gislason *et al.* (1993a) calculated the theoretical particle size of quartz and chalcedony. They obtained values between 0.011 and 0.02 μm, in good agreement with the measured ones. They concluded that the solubility of chalcedony can be adequately modelled by the solubility of quartz microcrystals with a size of 10–20 nm.

Although some other factors can influence the enhanced solubility of chalcedony (e.g. presence of small amounts of moganite in the samples, Gislason *et al.* 1993a, see below) this question is not a major concern.

Chalcedony, microcrystalline quartz and quartz

Non-fibrous microcrystalline quartz (or granular microcrystalline quartz, with particle sizes usually smaller than 20 μm; Blatt *et al.* 1972, Knauth 1994) also exists in nature (e.g. as fracture fillings in Simpevarp; Drake and Tullborg 2005, 2006ab) and possibly in higher proportions than the fibrous microcrystalline varieties, at least in sedimentary environments (Blatt 1992, Tucker 2001).

This non-fibrous microcrystalline quartz shows also a dependence of solubility on particle size (equation C-9) as it is widely recognized (e.g. Nordstrom *et al.* 1990, Gislason *et al.* 1997). This effect has been traditionally considered in the geochemical modelling of diagenetic evolution in sedimentary rocks (Williams *et al.* 1985, Williams and Crerar 1985, Maliva and Siever 1988ab) but, with some exceptions (Gislason *et al.* 1993b, Azaroual *et al.* 1997), it is not explicitly considered in the study of water-rock interaction processes in other contexts.

However, in most text books on Geochemistry, the microcrystalline character of chalcedony is highlighted when talking about its solubility (e.g. Drever 1977, Langmuir 1997) and saturation index calculations with respect to chalcedony are often interpreted in terms of microcrystalline quartz (.e.g. Banks and Frengstad 2006). Therefore, solubility calculations with respect to chalcedony are not necessarily related to the fibrous microcrystalline variety and, in most cases, they have been interpreted as a proxy of non-fibrous microcrystalline quartz. Much more detailed mineralogical analysis than usually available in groundwater systems would be needed to properly deal with this problem.

To make the situation even more complex, recent investigations indicate that the presence of a new silica polymorph, moganite, in microcrystalline quartz varieties may contribute to their enhanced solubility. Intergrowths of this polymorph have been found widely distributed in microcrystalline quartz varieties (both in fibrous and non-fibrous ones; Heaney and Post 1992, Heaney 1995) and moganite solubility is higher than that of quartz and chalcedony (Gislason *et al.* 1997).

However, this thermodynamic instability and the relative rapid dissolution rate of moganite compared to quartz (Gislason *et al.* 1997) is consistent with the depletion of moganite in weathered microcrystalline quartz varieties (Heaney and Post 1992) and with the scarcity of this polymorph in rocks older than 100 m.y. (Heaney 1995). These observations are important because the "moganite problem" can be neglected in the humid weathering environments of Sweden and thus in the groundwater evolution of Simpevarp and Forsmark, as quartz fracture fillings are much older than 100 m.y.

But uncertainties related to particle size or thermodynamic data still remain. For example, differences in log K values for quartz (from solubility data by Rimstidt 1997) and chalcedony (from WATEQ4F database) below 25 °C are lower than 0.2 units. Moreover, log K value for quartz proposed by Rimstidt (1997) at 25 °C is almost identical to the value obtained by Walther and Helgeson (1977) for chalcedony. Therefore, additional information to groundwater analysis (and saturation index calculations) or other types of evidences would be necessary to deal with this type of uncertainties (see Appendix D and section 3.5.4).

Modifications to the WATEQ4F database

To analyse the possible solubility control of dissolved silica by quartz or chalcedony (microcrystalline quartz) in long residence-time groundwaters from Simpevarp and Forsmark, the thermodynamic data proposed by Rimstidt (1997) for quartz have been included in the WATEQ4F database.

The experimental data for quartz solubility from 21° to 96°C obtained by Rimstidt (1997) was fitted by Hummel *et al.* (2002) to the log $K(T)$ equation used in PHREEQC databases,

$$\log K = A_1 + A_2 T + \frac{A_3}{T} + A_4 \log T + \frac{A_5}{T^2} \tag{C-10}$$

where T is absolute temperature (K), and A_1, A_2, A_3, A_4 and A_5 are fitting coefficients. The values indicated by Hummel *et al.* (2002) are: $A_1 = -13.25045$; $A_2 = 0.0$; $A_3 = -493.9341$; $A_4 = 4.510415$; and $A_5 = 0.0$. With these values a "new" mineral phase (Quartz_R) was added to the WATEQ4F database with the entry:

```
Quartz_R

       SiO2 + 2H2O = H4SiO4

       log_k      -3.7460

#    delta_h    20.6370

    -a_e   -1.325045E+01 -0.000000E+00 -4.939341E+02  4.510415E+00
0.000000E+00
```

C.4   References

Appelo C A J and Postma D (2005). Geochemistry, Groundwater & Pollution. Balkema, Rotterdam, The Netherlands, 2nd edition, 649 p.

Arcos D, Grandia F and Domènech C (2006). Geochemical evolution of the near field of a KBS-3 repository. SKB TR-06-16, 97 p.

Arnorsson S, Gunnlaugsson E and Svavarsson H (1983). The chemistry of geothermal waters in Iceland. III. Chemical geothermometry in geothermal investigations. Geochim. Cosmochim. Acta, 47, 567–577.

Auqué L F, Gimeno M J, Gómez J, Puigdomènech I, Smellie J and Tullborg E-L (2006). Groundwater chemistry around a repository for spent nuclear fuel over a glacial cycle. Evaluation for SR-Can. SKB TR-06-31, 123 p.

Azaroual M, Fouillac C and Matray J M (1997). Solubility of silica polymorphs in electrolyte solutions. II. Activity of aqueous silica and solid silica polymorphs in deep solutions from the sedimentary Paris Basin. Chem. Geol., 140, 167–179.

Bågander L E and Carman R (1994). In situ determination of the apparent solubility product of amorphous iron sulphide. Appl. Geochem., 4, 379–386.

Banwart S A (1999). Reduction of iron (III) minerals by natural organic matter in groundwater. Geochim. Cosmochim. Acta, 63, 2919–2928

Banwart S, Gustafsson E, Laaksoharju M, Nilsson A-C, Tullborg E-L and Wallin B (1994). Large-scale intrusion of shallow water into a vertical fracture zone in crystalline bedrock: initial hydrochemical perturbation during tunnel construction at the Äspö Hard Rock Laboratory, southeastern Sweden. Water Resour. Res., 30: 1747–1763.

Ball J W and Nordstrom D K (2001). User's manual for WATEQ4F, with revised thermodynamic data base and test cases for calculating speciation of major, trace, and redox elements in natural waters. U.S. Geological Survey Open-File Report 91-183, 188 p. Revised and reprinted, April, 2001.

Ball J W, Jenne E A and Cantrell M W (1981). WATEQ3. A geochemical model with uranium added. U.S. Geological Survey, Ope-File Report 81-1183, 81 p.

Banks D and Frengstad B (2006). Evolution of groundwater chemical composition by plagioclase hydrolysis in Norwegian anorthosites. Geochim. Cosmochim. Acta, 70, 1337–1355.

Beaucaire C, Gassama N, Tresonne N and Louvat D (1999). Saline groundwaters in the hercinian granites (Chardon Mine, France): geochemical evidence for the salinity origin. Appl. Geochem., 14, 67–84.

Beaucaire C, Pitsch H, Toulhoat P, Montellier S and Louvat D (2000). Regional fluid characterisation and modelling of water-rock equilibria in the Bloom clay Formation and in the Rypelian aquifer at Mol, Belgium. Appl. Geochem., 15, 667–686.

Benning L G, Wilkin R T and Barnes H L (2000). Reaction pathways in the Fe-S system below 100 °C. Chem. Geol., 167, 25–51.

Berner R A (1967). Thermodynamic stability of sedimentary iron sulfides. Am. J. Sci., 265, 773–785.

Berner U (1995). Kristallin-I: estimates of solubility limits for safety relevant radionuclides. Technical Report NTB 94-08, NAGRA, Wettingen, Switzerland, 60 p.

Bethke C (1994). The Geochemist's Workbench. A users guide to Rxn, Act2, React, Tact and Gtplot. University of Illinois, 213 p.

Bethke C (2002). The Geochemist's Workbench. A users guide to Rxn, Act2, React, Tact and Gtplot. Release 4.0. University of Illinois, 224 p

Blatt H (1992). Sedimentary Petrology. W.H. Freeman and Co., New york, 514 pp.

Blatt H, Middleton G and Murray R (1972). Origin of sedimentary rocks. Prentice-Hall, Inc., 634 pp. Chapter 16.

Bonneville S, Van Cappellen P and Behrends T (2004). Microbial reduction of iron(III) oxyhydroxides: effects of mineral solubility and availability. Chemical Geology, 212, 255–268.

Bottomley D J, Gascoyne M and Kamineni D C (1990). The geochemistry, age and origin of groundwater in a mafic pluton, East Bull Lake, Ontario, Canada. Geochim. Cosmochim. Acta, 54, 993–1008.

Bruno J, Cera E, de Pablo J, Duro L, Jordana S, and Savage D (1997). Determination of radionuclide solubility limits to be used in SR 97. Uncertainties associated to calculated solubilities. SKB TR 97-33, 184 p.

Brun, J, Cera E, Grivé M, Rollin C, Ahonen L, Kaija J, Blomqvist R, El Aamrani F Z, Casas I, de Pablo J. (1999). Redox Processes in the Palmottu Uranium Deposit. Redox measurements and redox controls in the Palmottu System. Technical Report, Quantisci, Barcelona, Spain, 76 p.

Bruno J, Duro L and Grivé M (2001). The applicability and limitations of the geochemical models and tools in simulating radionuclide behaviour in natural waters. Lessons learned from the Blind Predictive Modelling exercises performed in conjunction with Natural Analogue studies. SKB TR-01-20, 63 p.

Bruno J, Duro L and Grivé M (2002). The applicability and limitations of thermodynamic geohemical models to simulate trace element behaviour in natural waters. Lessons learned from natural analogue studies. Chem. Geol., 190, 371–393.

Chen W-F and Liu T-K (2005). Ion activity products of iron sulfides in groundwaters: implications from the Choshui fan-delta, Western Taiwan. Geochim. Cosmochim. Acta, 69, 3535–3544.

Cornell R M and Schwertmann U (2003). The iron oxides. Wiley-VCH, Weinheim, Germany. 2nd edition, p.

Cramer J J and Nesbitt W (1994). Groundwater evolution and redox geochemistry. In: J.J. Cramer and J.A.T. Smellie (Eds.), Final Report of the AECL/SKB Cigar Lake Analog Study. SKB TR 94-04.

Crerar D A and Anderson G M (1971). Solubility and salvation reactions of quartz in dilute hydrothermal solutions. Chem. Geol., 8, 107–122.

Davison W (1991). The solubility of iron sulfides in synthetic and natural waters at ambient temperatures. Aquat. Sci., 53, 309–329.

Davison W, Phillips N and Tabner B J (1999). Soluble iron sulfide species in natural waters: Reappraisal of their stoichiometry and stability constants. Aquat. Sci., 61, 23–43.

Dideriksen K, Christiansen B C, Baker J A, Frandsen C, Balic-Zunic T, Tullborg E-L, Mørup S and Stipp S L S (2007). Fe-oxide fracture fillings as a palæo-redox indicator: Structure, crystal form and Fe isotope composition. Chem. Geol., 244, 330–343.

Drake H and Tullborg E-L (2004). Oskarshamn site investigation. Fracture mineralogy and wall rock alteration Results from drill core KSH01A+B. SKB P-04-250, 120 p.

Drake H and Tullborg E-L (2005). Oskarshamn site investigation. Fracture mineralogy and wall rock alteration. Results from drill cores KAS04, KA1755A and KLX02. SKB P-05-174, 69 p.

Drake H and Tullborg E-L (2006a). Oskarshamn site investigation. Fracture mineralogy. Results from drill core KSH03A+B. SKB P-06-03, 65 p.

Drake H and Tullborg E-L (2006b). Oskarshamn site investigation. Fracture mineralogy of the Götemar granite. Results from drill cores KKR01, KKR02 and KKR03. SKB P-06-04, 61 p.

Drake H and Tullborg E-L (2008). Fracture mineralogy of the Laxemar site. Final report. SKB R-08-99.

Drake H, Sandström B and Tullborg E-L (2006). Mineralogy and geochemistry of rocks and fracture fillings from Forsmark and Oskarshamn: Compilation of data for SR-Can. SKB R-06-109, 105 p.

Drever J I (1997). The Geochemistry of Natural Waters: Surface and Groundwater Environments. 3rd ed., Prentice Hall, New York, USA, 436 p.

Düker A and Ledin A (1998). Properties of the particulate phase in deep saline groundwater in Laxemar, Sweden. Wat. Res, 32, 186–192.

Duro L, Grivé M, Cera E, Domènech C and Bruno J (2006a). Update of a thermodynamic database for radionuclides to assist solubility limits calculation for performance assessment. SKB TR-06-17, 128 p.

Duro L, Grivé M, Cera E, Gaona X, Domènech C and Bruno J (2006b). Determination and assessment of the concentration limits to be used in SR-Can. SKB TR-06-32. 143 pp.

Enüstün B and Turkevich J (1960). Solubility of fine particles of strontium sulphate. J. Am. Chem. Soc., 82, 4502–4509.

Ferris F G, Konhauser K O, Lyven B and Pedersen K (1999). Accumulation of metals by bacteriogenic iron oxides in a subterranean environment. Geomicrobiology J., 16(2),181–192 .

Fournier R O (1960). Solubility of quartz in water in the temperature interval from 25°C to 300°C. Geol. Soc. Amer. Bull., 71, 1867–1868.

Fournier R O (1973). Silica in thermal waters. Laboratory and field investigations. Proc. Symp. on Hydrogeochemistry and Biochemistry, Tokyo, Japan. Vol. I. Hydrogeochemistry. Clarke, Washington D.C., pp.122–138.

Fournier R O (1977). Chemical geothermometers and mixing models for geothermal systems. Geothermics, 5, 41–51.

Fournier R.O. (1983). A method of calculating quartz solubilities in aqueous sodium chloride solutions. Geochim. Cosmochim. Acta, 47, 579-586.

Fournier, R O (1985). In: B. R. Berger, P.M. Bethke (Eds.), Geology and Geochemistry of Epithermal Systems. Reviews in Economic Geology, vol. 2. Society of Economic Geologists. pp. 45–61.

Fournier R O and Potter R W (1982). An equation correlating the solubility of quartz in water from 25°C to 900°C at pressures up to 10,000 bars. Geochim. Cosmochim. Acta, 46, 1969–1973.

Fournier R O and Rowe J J (1962). The solubility of cristobalite along the three-phase curve, gas plus liquid plus cristobalite. Amer. Mineral., 47, 897–902.

Gimeno M J, Peña J and Pérez del Villar L (2001). Geochemical modelling of groundwater evolution in the Palmottu natural system. In H. von Maravic (Ed.), Book of Abstracts. 8th EC-Natural Analogue Working Group Meeting. Strasbourg, France, March 23-25, 1999. EC NST, Luxembourg, Luxembourg

Gimeno M J, Auqué L F and Gómez J (2004). Explorative analysis and Mass balance modelling. In: M. Laaksoharju (ed.), Hydrogeochemical evaluation of the Forsmark site, model version 1.1. SKB R-04-05, Appendix 2, pp. 113–160.

Gimeno M J, Auqué L F and Gómez J (2005). PHREEQC modelling. Contribution to the model version 1.2. In: SKB (2005), Hydrogeochemical evaluation. Preliminary site description. Forsmark area, version 1.2. SKB R-05-17, 403 p.

Gimeno M J, Auqué L F and Gómez J (2006). Mass balance modelling. In: Hydrogeochemical evaluation. Preliminary site description. Laxemar subarea, version 2.1. SKB R-06-70, Appendix 3, pp. 175–210.

Gimeno M J, Auqué L F and Gómez J (2007). Water-rock interaction modelling issues. In: SKB (2007), Hydrogeochemical evaluation of the Forsmark site, modelling stage 2.1-issue report. SKB R-06-69, Appendix 3, pp. 131–187.

Gimeno M J, Auqué L F, Gómez J and Acero P (2008). Water-rock interaction modelling and uncertainties of mixing modelling. SDM-Site Forsmark. SKB R-08-86. 212 pp.

Gislason S R, Heaney P J, Veblen D.R and Livi K J T (1993a). The difference between the solubility of quartz and chalcedony: the cause?. Chem. Geol., 107, 363–366.

Gislason S R, Veblen D R and Livi K J (1993b). Experimental water-basalt interactions. Characterization and interpretation of alteration products. Geochim. Cosmochim. Acta, 57, 1459–1471.

Gislason S R, Heaney P J, Oelkers E H and Schott J (1997). Kinetic and thermodynamic properties of moganite, a novel silica polymorph. Geochim. Cosmochim. Acta, 61, 1193–1204.

Gómez P, Turrero M J, Martínez B, Melón A, Mingarro M, Rodríguez V, Gordienko F, Hernández A, Crespo M T, Ivanovich M, Reyes E, Caballero E, Plata A and Fernández J M (1996). Hydrogeochemical and isotopic characterisation of the groundwater from El Berrocal site, Spain. Topical Report 4. In: ENRESA (Eds.) Characterisation and validation of natural radionuclide migration processes under real conditions of the fissured granitic environment. Topical Reports, Vol. II, Hydrogeochemistry. Publicación Técnica No Periódica PTNP 02/96, ENRESA, Madrid, Spain, pp. 7–358.

Gómez P, Turrero M J, Garralón A, Ortuño F and Valladares J (1998). Hydrogeochemical characterization of Bangombé groundwater. In: D. Louvat and C. Davies (Eds.), OKLO Working Group. Proceedings of the first joint EC-CEA workshop on the OKLO-natural analogue Phase II project. Sitges, Spain, June 18–20, 1997. CEE, Luxembourg, Luxembourg, pp. 215–225.

Guimerá J, Duro L and Delos A (2006). Changes in groundwater composition as a consequence of deglaciation . Implications for performance assessment. SKB R-06-105, 56 p.

Glynn P D and Plummer L N (2005). Geochemistry and the understanding of ground-water systems. Hydrogeology Journal, 13, 263–287.

Glynn P D and Voss C I (1999). SITE-94. Geochemical characterization of Simpevarp ground waters near the Äspö Hard Rock laboratory. SKI Report 96-29, SKI, Stockholm, Sweden, 210 p.

Grenthe I, Stumm W, Laaksoharju M, Nilsson A-C and Wikberg P (1992). Redox potentials and redox reactions in deep groundwater systems. Chem. Geol., 98, 131–150.

Griffault L, Merceron T, Mossmann J R, Neerdael B, De Canniére, Beaucaire C, Daumas S, Bianchi A and Christien R (1996). Acquisition et regulation de la chimie des eaux en milieux argileux pour le project de stockage de déchets radioactifs en formation géologique. Project Archimede argile. Report EUR 17454, 176 p.

Grimaud D, Beaucaire C and Michard G (1990). Modelling of the evolution of ground waters in a granite system at low temperature: the Stripa ground waters, Sweden. Appl. Geochem., 5, 515–525.

Gunnarsson I, Arnorsson S (2000). Amorphous silica solubility and the thermodynamic properties of H4SiO4° in the range of 0° to 350°C at Psat. Geochim. Cosmochim. Acta, 64, 2295–2307.

Heaney P J (1995). Moganite as an indicator for vanished evaporites: a testament reborn?. J. Sediment. Res., A65, 633–638.

Heaney P J and Post J E (1992). The widspread distribution of a novel silica polymorph in microcrystalline quartz varieties. Science, 255, 441–443.

Houben G J (2003). Iron oxide incrustations in wells. Part 1: genesis, mineralogy and geochemistry. Appl. Geochem. 18 (6), 927–939.

Hummel W, Berner U, Curti E, Pearson F J and Thoene, T (2002). Nagra/PSI Chemical Thermodynamic Data Base 01/01. Nagra Technical Report NTB 02-16, Nagra, Wettingen, Switzerland.

Iwatsuki T and Yoshida H (1999). Groundwater chemistry and fracture mineralogy in the basement granitic rock in the Tono uranium mine area, Gifu Prefecture, Japan – Groundwater composition, Eh evolution analysis by fracture filling minerals. Geochem. J., 33 (1); 19–32.

Iwatsuki T, Furue R, Mie H, Ioka S and Mizuno T (2005). Hydrochemical baseline condition of groundwater at the Mizunami underground research laboratory (MIU). Appl. Geochem., 20, 2283–2302.

JNC (1999). H-12. Project to establish the scientific and technical basis for HLW in Japan. Supporting Report JNC SR-3, JNC, Japan.

Johnson J W, Oelkers E H and Helgeson H C (1992). SUPCRT92: a software package for calculating the standard molal thermodynamic properties of minerals, gases, aqueous species and reactions from 1 to 5000 bars and 0 to 1000°C. Comp. Geosci., 18, 899–947.

Kamyshny A J, Goifman A, Gun J, Rizkov D and Lev O (2004). Equilibrium distribution of polysulfide ions in aqueous solutions at 25 °C: a new approach for the study of polysulfide equilibria. Environ. Sci. Technol., 38, 6633–6644.

Kennedy G C (1950). A portion of the system silica–water. Econ. Geol., 45, 629–653.

Kitahara S (1960). The solubility of quartz in the aqueous sodium chloride solutions at high temperatures and high pressures. Rev. Phys. Chem. Japan, 30, 115–121.

Knauth L P (1994). Petrogenesis of chert. In: (P.J. Heaney; C.T. Prewitt and G.V. Gibss, eds) Silica: physical behavior, geochemistry and materials applications. Reviews in Mineralogy, 29, Chapter 7, 233–258.

Laaksoharju M, Smellie J A T, Nilsson A-C and Skarman C (1995). Groundwater sampling and chemical characterisation of the Laxemar deep borehole KLX02. SKB 95-05, SKB, Stockholm, Sweden.

Landström O and Tullborg E-L (1990). The influence of fracture mineral/groundwater interaction on te mobility of U, Th, REE and other trace elements. SKB TR 90-37, 71 p.

Langmuir D (1969). The Gibbs free energies of substances in the system $Fe-O_2-H_2O-CO_2$ at 25 °C. Geological Survey Research, 1969. U.S.G.S. Prof. Paper, Vol. 650-B, pp. B180-B184.

Langmuir D (1997). Aqueous environmental geochemistry. Prentice Hall, 600 p.

Langmuir D and Whittemore D O (1971). Variations in the stability of precipitated ferric oxyhydroxides. In: J.D. Hem (Ed.), Nonequilibrium Systems in Natural Water Chemistry. Advances in Chemistry Series, 106. Amer. Chem. Soc., Washington, D.C. Chapter 8, pp. 209–234.

Larsen O and Postma D (2001). Kinetics of the reductive bulk dissolution of lepidocrocite, ferrihydrite, and goethite. Geochim. Cosmochim. Acta, 65, 1367–1379.

Louvat D, Michelot J L and Aranyossy J F (1999). Origin and residence time of salinity in the Äspö groundwater system. Appl. Geochem., 14, 917–925.

Macalady D L, Langmuir D, Grundl T and Elzerman A (1990). Use of model-generated Fe^{3+} ion activities to compute Eh and ferric oxyhydroxide solubilities in anaerobic systems. In: D.C. Melchior and R.L. Basett (Editors), Chemical Modelling of Aqueous Systems II. A.C.S. Symp. Ser. 416. Amer. Chem. Soc., Washington, D.C., pp. 350–367.

Mackenzie F T and Gees R (1971). Quartz: synthesis at earth surface conditions. Science, 173, 533–535.

Majzlan J, Navrotsky A and Schwertmann U (2004). Thermodynamics of iron oxides: Part III. Enthalpies of formation and stability of ferrihydrite ($\sim Fe(OH)_3$), schwertmannite ($\sim FeO(OH)_{3/4}(SO_4)_{1/8}$), and $\varepsilon-Fe_2O_3$. Geochim. Cosmochim. Acta, 68, 1049–1059.

Maliva R G and Siever R (1988a). Pre-Cenozoic nodular cherts: evidence for Opal-CT precursors and direct quartz replacement. Am. J. Sci., 288, 798–809.

Maliva R G and Siever R (1988b). Mechanism and controls of silicification of fossils in limestones. J. Geol., 96, 387–398.

Martinez R E, Pedersen K and Ferris F G (2004). Cadmium complexation by bacteriogenic iron oxides from a subterranean environment. J. Colloid and Interface Sci., 275 (1), 82–89.

Michard G, Pearson Jr, F J and Gautschi A (1996). Chemical evolution of waters during long term interaction with granitic rocks in northern Switzerland. Appl. Geochem., 11, 757–774.

Molinero J, Arcos D and Duro L (2008). Coupled hydrogeological and solute transport, visualisation and supportive detailed reaction modelling. In: Kalinowski, B. (Ed.) Background complementary hydrogeochemical studies. Forsmark 2.3. SKB R-08-87.

Morey G W, Fournier R O and Rowe J J (1962). The solubility of quartz in water in the temperature interval from 25 to 300°C. Geochim. Cosmochim. Acta, 26, 1029–1043.

Morse J W, Millero F J, Cornwell J C and Rickard D (1987). The chemistry of hydrogen sulfide and iron sulfide systems in natural waters. Earth Sci. Rev., 24, 1–42.

NAGRA (1994). Kristallin-I. Safety Assessment Report. Technical Report NTB TR 93-22, NAGRA, Wettingen, Switzerland, 396 p.

Neal C, Neal M, Reynolds B, Maberly S C, May L, Ferrier R C, Smith J and Parker J E (2005). Silicon concentrations in UK surface waters. J. Hydrol., 304, 75–93.

Nordstrom D K (2005). Modelling low-temperature geochemical processes. In: J.I. Drever (ed.), Surface and ground waters, weathering, and soils. Treatise on Geochemistry, 5. Elsevier, pp. 37–72.

Nordstrom D K and Puigdomènech I (1986). Redox chemistry of deep ground-waters in Sweden. SKB TR 86-03, 30 p.

Nordstrom D K, Valentine S D, Ball J W, Plummer L N and Jones B F (1984). Partial compilation and revision of basic data in the WATEQ programs. U.S.G.S. Water-Resources Investigation report 84-4186, 19 p.

Nordstrom D K, Ball J W, Donahoe R J and Whittemore D (1989). Groundwater chemistry and water-rock interactions at Stripa. Geochim. Cosmochim. Acta, 53, 1727–1740.

Nordstrom D K, Plummer L N, Langmuir D, Busenberg E, May H M, Jones,B F and Parkhurst D (1990). Revised chemical equilibrium data for major water-mineral reactions and their limitations. In: D.C. Melchior and R.L. Basett (Editors), Chemical Modeling of Aqueous Systems II. A.C.S. Symp. Ser. 416. Amer. Chem. Soc., Washington, D.C., pp. 398–413.

Nordstrom D K, McNutt R H, Puigdomènech I, Smellie J A T and Wolf M (1992). Groundwater chemistry and geochemical modelling of water-rock interactions at the Osamu Utsumi mine and the Morro do Ferro analogue study sites, Poços de Caldas, Minas Gerais, Brazil. J. Geochem. Explor., 45, 249–287.

Parkhurst D L and Appelo C A J (1999). User's Guide to PHREEQC (Version 2), a computer program for speciation, batch-reaction, one-dimensional transport, and inverse geochemical calculations. Water Resources Research Investigations Report 99-4259, 312 p.

Parkhurst D L and Plummer L N (1993). Geochemical Models. In: W.M. Alley (ed.), Regional ground-water quality. Van N ostrand Reinhold, New York. Chapter 9, pp. 199–226.

Parkhurst D L, Thorstenson D C and Plummer L N (1980). PHREEQE. A computer program for geochemical calculations. U.S. Geological Survey Water-Resources Investigations Report 80-96.

Parkhurst D L, Thorstenson D C and Plummer L N (1990). PHREEQE. A computer program for geochemical calculations. U.S. Geological Survey Water-Resources Investigations Report 80-96, 195 p. Revised and reprinted.

Parkhurst D L, Kipp K L, Engesgaard P and Charlton S R (2004). PHAST. A program for simulating ground-water flow, solute transport, and multicomponent geochemical reactions. U.S. Geological Survey, Techniques and Methods 6-A8, 154 pp.

Pearson F J Jr and Berner U (1991). Nagra thermochemical data base – I. Core data. Technical Report NTB 91-17, NAGRA, Wettingen, Switzerland, 70 p.

Pearson F J Jr Berner U and Hummel W (1992). Nagra thermochemical data base – II. Supplemental Data 05/92. Technical Report NTB 91-18, NAGRA, Wettingen, Switzerland, 250 p.

Pedersen H D, Postma D, Jakobsen R and Larsen O (2005). Fast transformation of iron oxyhydroxides by the catalytic action of aqueous Fe(II). Geochim. Cosmochim. Acta, 69, 3967–3977.

Pitkänen P, Partamies S and Luukkonen A (2004). Hydrogeochemical interpretation of baseline groundwater conditions at the Olkiluoto site. Posiva report 2003-07, 159 p.

Plummer L N, Jones B F and Truesdell A H (1976). WATEQF. A FORTRAN IV version of WATEQ, a computer program for calculating chemical equilibrium of natural waters. USGS Report 76-13, 61 p.

Plummer L N, Parkhurst D L and Thorstenson D C (1983). Development of reaction models for ground-water systems. Geochim. Cosmochim. Acta, 47, 665–686.

Plummer L N, Parkhurst D L, Fleming G W and Dunkle S A (1988). A computer program incorporating Pitzer's equations for calculation of geochemical reactions in brines. U.S. Geological Survey Water-Resources Investigations Report 88-4153, 310 p.

Plummer L N, Prestemon E C and Parkhurst D L (1994). An interactive code (NETPATH) for modeling NET geochemical reactions along a flow PATH. Version 2.0. U.S. Geological Survey Water-Resources Investigations Report 94-4169, 130 p.

PNC (1992). Research and development on geological waste disposal of high-level radioactive waste. First Progress Report. Progress Report PNC TN1410 93-059.

Postma D (1993). The reactivity of iron oxides in sediments: a kinetic approach. Geochim. Cosmochim. Acta, 57, 5027–5034.

Puigdomènech I (2001). Hydrochemical stability of groundwaters surrounding a spent nuclear fuel repository in a 100,000 year perspective. SKB Technical Report 01-28, 83 p.

Rickard D T (1989). Experimental concentration-time curves for the iron (II) sulphide precipitation process in aqueous solutions and their interpretation. Chem. Geol., 78, 315–324.

Rickard D T (1995). Kinetics of FeS precipitation. Part 1, competing reaction mechanisms. Geochim. Cosmochim. Acta, 59, 4367–4379.

Rickard D T (1997). Kinetics of pyrite formation by the H2S oxidation of iron(II) monosulfide in aqueous solutions between 25 and 125∞C: The rate equation. Geochim. Cosmochim. Acta, 61, 115–134.

Rickard D T (2006). The solubility of FeS. Geochim. Cosmochim. Acta, 70, 5779–5789.

Rickard D T and Luther III G W (2007). Chemistry of Iron Sulfides. Chem. Rev., 107, 514–562

Rickard D T and Morse J W (2005). Acid volatile sulfide (AVS). Marine Chemistry, 97, 141–197.

Rimstidt D D (1997). Quartz solubility at low temperatures. Geochim. Cosmochim. Acta, 61, 2553–2558.

Schwertmann U and Murad E (1983). Effect of pH on the formation of goethite and hematite from ferrihydrite. Clays Clay Min., 31, 277–284.

Siever R (1962). Silica solubility 0–200°C, and the diagenesis of siliceous sediments. J. Geol., 70, 127–150.

Silvester E, Charlet L, Tournassat C, Gehin A, Greneche J M and Liger E (2005). Redox potential measurements and Mossbauer spectrometry of Fe-II adsorbed onto Fe-III (oxyhy)droxides. Geochim. Cosmochim. Acta, 69(20), 4801–4815.

SKI (1996). SKI SITE-94. Deep repository performance assessment project. 2 vols. SKI R 96/36, SKI, Stockholm, Sweden, 305–660 p.

SKB (1999). SR 97. Processes in the repository evolution. Background report to SR 9. SKB TR 99-07.

Smellie J A T and Laaksoharju M (1992). The Äspö Hard Rock Laboratory: Final evaluation of the hydrogeochemical pre-investigations in relation to existing geologic and hydraulic conditions. SKB TR 92-31, SKB, Stockholm, Sweden, 239 p.

Smellie J, Tullborg E-L and Nilsson A-C (2008). Explorative analysis and expert judgement of major components and isotopes. SKB R-08-84.

Stipp S L S, Hansen M, Kristensen R, Hochella J MF, Bennedsen L, Dideriksen K, Balic-Zunic T, Léonard D and Mathieu H J (2002). Behaviour of Fe-oxides relevant to contaminant uptake in the environment. Chem. Geol., 190, 321–337.

Stumm W and Morgan J J (1996). Aquatic Chemistry. Chemical equilibria and rates in natural waters. 3rd ed., John Wiley & Sons, New York, USA, 1022 p.

Suleimonov O M and Seward T M (1997). A spectrophotometric study of hydrogen sulfide ionisation in aqueous solutions to 350°C. Geochim. Cosmochim. Acta, 61, 5187–5198.

Theberge S and Luther G W (1997). Determination of the electrochemical properties of a soluble aqueous FeS species present in sulfide solutions. Aquat. Geochem., 3, 191–211.

Tröjbom M and Söderbäck B (2006a). Chemical characteristics of surface systems in the Forsmark area. Visualization and statistical evaluation of data from surface waters, precipitation, shallow groundwater, and regolith. SKB R-06-18, 230 p.

Tröjbom M and Söderbäck B (2006b). Chemical characteristics of surface systems in the Simpevarp area. Visualization and statistical evaluation of data from surface waters, precipitation, shallow groundwater, and regolith. SKB R-06-19, 164 p.

Trotignon L, Beaucaire C, Louvat D and Aranyossy J F (1999). Equilibrium geochemical modelling of Äspö groundwaters: a sensitivity study of thermodynamic equilibrium constants. Appl. Geochem., 14, 907–916.

Trotignon L, Michaud V, Lartigue J-E, Ambrosi J-P, Eisenlohr L, Griffault L, de Combarieu M and Daumas S (2002). Laboratory simulation of an oxidizing perturbation in a deep granite environment. Geochim. Cosmochim. Acta, 66: 2583–2601.

Truesdell A H and Jones B F (1974). WATEQ, a computer program for calculating chemical equilibria of natural waters. Journal of Research, U.S. Geological Survey, v.2, pp. 233–274.

Tucker M E (2001). Sedimentary Petrology. Blackwell, 3rd edition, 262 p.

Tullborg E L (1989). The influence of recharge water on fissure-filling minerals. A study from Klipperas, southern Sweden. Chem. Geol., 76, 309–320.

Van der Lee J and De Windt L (1999). CHESS tutorial and Cookbook. Updated for version 2.4. Technical Report TR CIG/LHM/RD/99/05, EMP, Paris, France.

Van Lier J A, de Bruyn P L, and Overbeek J T G (1960). The solubility of quartz. J. Phys. Chem., 64, 1675–1682.

Vieno T and Nordman H (1999). Safety assessment of spent fuel disposal in Hästholmen, Kivetty, Olkiluoto and Romuvaara. TILA-99. Technical Report POSIVA 99/07, Posiva, 253 p.

Vuorinen U, Kulmala S, Hakanen M, Ahonen L and Carlsson T (1998). Solubility database for Tila-99. Technical Report Posiva 98-14, 117 p.

Walther J V and Helgeson H C (1977). Calculation of the thermodynamic properties of aqueous silica and the solubility of quartz and its polymorphs at high pressures and temperatures. Am. J. Sci., 277, 1315–1351.

Wescot R G, Lee M P, Eisenberg N A, McCartin T J and Baca R G (1995). NRC Iterative Performance Assessment Phase 2.Technical Report NRC IPA-2, NUREG, USA, 544 p.

Wilkin R T and Barnes H L (1997). Pyrite formation by reactions of iron monosulfides with dissolved inorganic and organic sulfur species. Geochim. Cosmochim. Acta, 60, 4167–4179.

Williams L A and Crerar D A (1985). Silica diagenesis. II. General mechanisms. J. Sedim. Petrol., 55, 312–321.

Williams L A, Parks G A and Crerar D A (1985). Silica diagenesis. I. Solubility controls. J. Sedim. Petrol., 55, 301–311.

Wolthers M, van der Gaast S J and Rickard D (2003). The structure of disordered mackinawite. American Mineralogist, 88, 2007–20015.

Wolthers M, Charlet L, van der Linde P R, Rickard D and van der Weidjen C H (2005). Surface chemistry of disordered mackinawite (FeS). Geochim. Cosmochim. Acta, 69: 3469–3481.

Yui M, Azuma J and Shibata M (1999). JNC thermodynamic database for performance assessment of high-level radioactive waste disposal system. JNC Tech. Rep., JNC TN8400 99-070.

Zhu C and Anderson G (2002). Environmental applications of geochemical modelling. Cambridge University Press, 284 p.

Solubility, particle size and specific surface area

D.1   Introduction

Some calculations related to the mineral solubility variations due to the particle size (or surface area) effects are presented in this Appendix. These calculations refer to silica phases (chalcedony, quartz) and Fe(III)-oxyhydroxides (goethite and hematite) as their particle size have important consequences in especially interesting processes taking place in the studied systems.

Solubility calculations for silica phases indicate that long residence time groundwaters can be in equilibrium with both chalcedony (as microcrystalline quartz variety) and quartz (using the solubility value from Rimstidt 1997), since they have very similar solubility values (see Appendix C). Mineralogical studies indicate the presence of both varieties, though without a clear determination of the microcrystalline quartz particle size. Therefore, some theoretical calculations have been performed to obtain, first, the estimation for the particle size from which the effects on the quartz solubility start to be important and, second, the particle size corresponding to the chalcedony solubility used in the speciation-solubility calculations. From these results, some judgement can be made on the silica variety involved in the aforementioned equilibrium situations.

For the Fe(III)-oxyhydroxides the size-driven thermodynamic differences among them must be taken into account to explain their stability, chemical reactivity and bioavailability (for iron reducing bacteria). These issues are especially important for the understanding of the redox processes in the groundwaters. Hematite (and much less frequently goethite) is widely distributed in the fracture fillings at all depths in the Laxemar-Simpevarp and Forsmark areas. Recently, some results on the particle size of the hematite and goethite in the fracture fillings have been presented (Dideriksen *et al.* 2007). In this Appendix these results are also completed with different theoretical calculations on the particle size and the equivalent surface areas and solubilities of hematite and goethite.

D.2   Equations

The thermodynamic relation between solubility and crystal size, assuming spherical crystals with smooth surface and radius *r*, is defined by the Freundlich-Ostwald – or Gibbs-Kelvin- equation (Enüstün and Turkevich 1960, Williams *et al.* 1985, Gislason *et al.* 1993ab):

$$\log\left(\frac{K_o}{K_s}\right) = \frac{2V\gamma}{2.303RTr} \tag{D-1}$$

where K_0 is the apparent equilibrium constant (solubility) for the target solid of radius *r*, K_S is the solubility of an infinite plane surface (equilibrium constant independent of the particle size, that is, the conventional solubility), γ the free energy of the solid interface, *R* the universal constant of gasses, *T* the absolute temperature and *V* the molar volume.

The value of $\log(K_0/K_S)$ gives an estimation of the solubility due to the excess of Gibbs free energy associated with the solid-liquid interface. It can be considered as a solubility excess index and is related to the particle or crystal size for the considered mineral phase (Maliva and Siever 1988ab). As the size increases, the free energy excess decreases and, therefore, the crystal solubility also decrease. When the crystal size reaches a specific value, the contribution of that energy excess from the interface becomes negligible and the crystal solubility becomes independent of the size ($K_0=K_S$).

The expression (D-1) assumes "ideal" spherical crystals but this assumption can be also relaxed including the surface roughness factor (η) in calculations. It is defined as the ratio between the real surface area and the hypothetic surface including the real one (Oelkers 1996). Keeping the assumption of spherical crystals, the roughness problem can be managed by multiplying the right member in equation (D-1) by the roughness factor (η) considered for the studied problem:

$$\log\left(\frac{K_o}{K_s}\right) = \left(\frac{2V\gamma}{2.303RTr}\right)\eta \tag{D-2}$$

The advantage of this equation is that the excess of solubility (log (K_0/K_S)) for spherical particles with the same radius but different surface area (two, three, four, etc times higher than the one of a smooth sphere) can be easily calculated by multiplying by roughness factors of 2, 3, 4, etc. (e.g. Maliva and Siever 1988a).

Alternatively, the Freundlich-Ostwald equation can be expressed as a function of the surface area A (average surface of the particles set per gram):

$$\log \frac{K_o}{K_s} = \frac{\frac{2}{3} M\gamma A}{2.303 RT} \tag{D-3}$$

where, apart from the variable already described above, M is the molecular weight.

The use of equations (D-2) and (D-3) allows calculating the range of the crystal sizes (or surface area) in with a mineral solubility is affected. Also, they allow calculating the particle size (or surface area) if solubilities (K_0 and K_s) of the minerals are known; or vice versa, to obtain their apparent equilibrium constant (K_0) if the particle size (or surface area) is known.

D.3   Calculations

D.3.1   Silica phases

Using equation (D-2) the minimum particle size from which the effects on the equilibrium constant of quartz start to be important can be calculated. The calculations are performed at 25 °C using a free energy of interface value of 3.5×10^{-5} J/cm^2 and a molar volume of 22.688 cm^3/mol for quartz (Parks 1984) and considering different roughness factors, 1, 2, 5 and 10, in order to include the effects associated with the own morphological complexity of the mineral or particle aggregates.

Figure D-1 shows that the effects of particle size on the solubility are negligible for values larger than 1 μm (10^{-4} cm). However, for particle sizes smaller than that value (at nanometrical scale, between 0.1 and 0.01 μm, for example) the effects might be really important and their magnitude is directly related to the particle roughness (surface area). Therefore, the crystal size becomes especially important in this range of sizes.
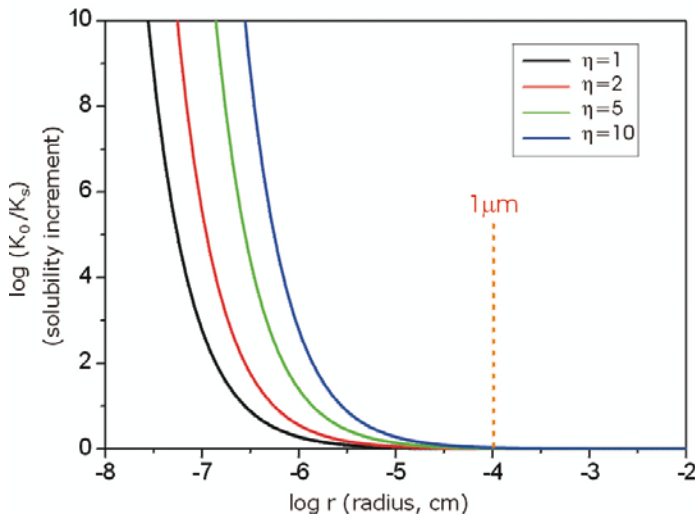

Figure D-1. *Solubility increment as a function of the radii of ideally spherical particles of quartz. The different curves represent different roughness factors (η). See text for details.*

Using equation (D-1) with the K_s (conventional solubility) value proposed by Rimstidt (1997) for quartz (log K = −3.746) and with the solubility from chalcedony in WATEQ4F (log K= −3.55) as K_o, it can be deduced that the microcrystalline quartz involved in the possible control of dissolved silica must be constituted by particle sizes of 15 nm. Therefore if chalcedony, as microcrystalline quartz, is the responsible for the dissolved silica control in the long residence groundwaters it should be constituted by this range of particle sizes. Although these values are much lower than those positively detected in the mineralogical analysis performed up to date in the fracture fillings their existence could not be definitively discarded.

However, microcrystalline quartz constituted by small particle sizes tends to re-crystallise, forming larger particles that minimise the excess of Gibbs free energy associated with the solid-water inter-face. Although these ripening processes can be very slow, most Palaeozoic microcrystalline quartz in sedimentary rocks has reached crystal sizes larger than 1 μm (Maliva and Siever 1988a, Blatt 1992). As fracture fillings in the Simpevarp and Forsmark areas are of that age or even older, it seems that the present existence of microcrystalline quartz with small particle sizes is not feasible.

D.3.2 Fe(III)-oxyhydroxides

Using equation (D-2) the minimum particle size from which the effects on the equilibrium constant of hematite (or goethite) start to be important can be estimated. The values considered for the calculations are the following: (1) free energy of interface: $0.184 \cdot 10^{-4}$ cal/cm^2 for hematite and $0.298 \cdot 10^{-4}$ cal/cm^2 for goethite; (2) density: 5.25 g/cm^3 for hematite and 4.3 gr/cm^3 for goethite (Langmuir and Whittermore 1971); and (3) the K_s (conventional solubility) values correspond to the minimal solubilities determined for both phases (e.g. Langmuir 1997), that is: $logK_{hematite}$= −44 and $logK_{goethite}$= −44.1 (see Appendix C, section C.2).

The calculations have been performed considering different roughness factors, 1, 2, 5 and 10, in order to include the effects associated with the own morphological complexity of the mineral (e.g. "porosity"; Cornell and Schwertmann 2003) or particle aggregates. Figure D-2 shows the results for hematite (goethite results are superimposed almost perfectly and are not plotted). As it is clearly seen, the effects of particle size on the solubility are negligible for values higher than 1μm (10^{-4} cm). At that point, the surface area loses its importance independently of the roughness.

However, for particle sizes smaller than that value, and mainly below 0.1 μm, the effects might be really important and their magnitude is directly related to the particle roughness (surface area). Therefore, the crystal morphology or the degree and shape of the particles-aggregates, become especially important in this range of sizes, whose presence in the system has been deduced (at least, below 1 micron) and recently confirmed (Dideriksen *et al.* 2007).
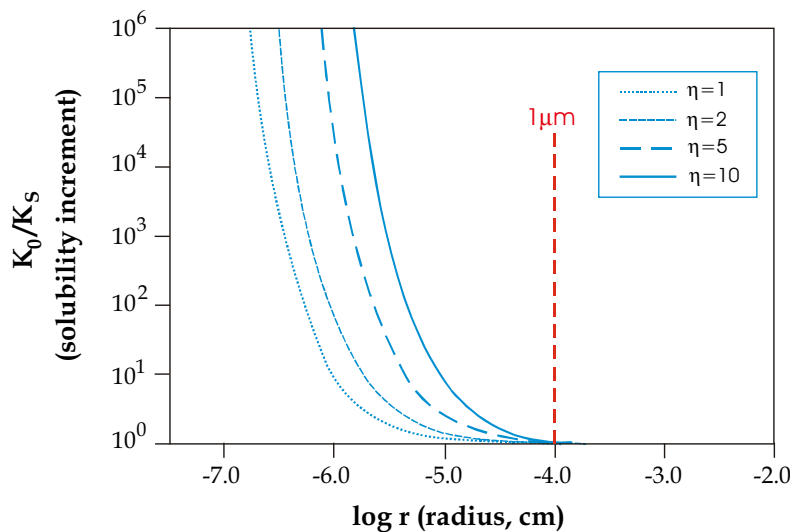

Figure D-2. Solubility excess as a function of the radii of ideally spherical particles of hematite. The different curves represent different roughness factors (η).

The estimation of the hematite (and goethite) surface area (A) in these systems could be made knowing their solubility value (equation D-3). If the value of pK = 43.1 deduced by Grenthe *et al.* (1992) for the solubility product of ferric oxyhydroxides in equilibrium with the deep groundwaters, is accepted as a representative value for the hematite solubility in the system the estimation can be made.

By using equation D-3 with the same data used above (free energy, density and conventional solubility) for hematite the surface area would be 62.7 m^2/gr and for goethite, 77.3 m^2/gr. These values would represent a significant surface taken into account the wide spread of hematite in the outermost part of fracture coatings. But, probably they represent a maximum estimation as crystals or aggregates of hematite in the micrometric range, and therefore with lower surface areas (possibly as low as 2 to 3 m^2/gr; Langmuir 1997), are also present in the fracture fillings (Drake and Tullborg 2008).

The results obtained from the calculation of the hematite particle size (ideally spherical) assuming the solubility value proposed by Grenthe *et al.* (1992) and using equation D-1, indicate that the oxyhydroxide would be constituted by nanometre particles of 0.01 μm. This size is in the lower limit of the particles sizes determined in typical soil hematite at low-temperatures, and at hydrothermal temperatures the expected sized would be higher (Cornell and Schwertmann 2003). Therefore this result may be affected by the simplification made considering spherical particles in the calculations.

All these results appear to be supported by the recent work of Dideriksen *et al.* (2007). They determined the particle size of hydrothermal hematite in samples from KOV01 and KAS02 boreholes and they found particle sizes as low as 0.08 μm and even lower for the old, low-temperature samples (mostly very fine-grained crystalline goethite but also hematite).

The theoretical solubility for the hematite with particle size of 0.08 μm would be of around pK= 43.9, near of the value determined by Grenthe *et al.* (1992) and clearly indicative of a crystalline hematite with low surface area. Unfortunately, they were not able to accurately determine the particle size for the old, low-temperature samples although probably they approach surface area values near the calculated above. However, this type of old, low-temperature crystalline oxyhydroxides is less abundant than the hydrothermal hematite and, therefore, the effects of its higher surface area much more localised.

Overall all these results appear to indicate the existence of crystalline (hydrothermal) hematite with variable but not exceedingly low particle size and, therefore, with surface areas not very high. Only locally, low temperature crystalline goethite and hematite can show significant surface areas with a rough estimate of 62–77 m^2/g. The calculated solubility from the particle size measured for hydrothermal hematite does not show important discrepancies with the value calculated by Grenthe *et al.* (1992) from potentiometrical Eh values in long residence time groundwaters.

D.4   References

Blatt H (1992). Sedimentary Petrology. W.H. Freeman and Co., New York, 514 pp.

Cornell R M and Schwertmann U (2003). The iron oxides. Wiley-VCH, Weinheim, Germany. 2nd edition, 664 p.

Dideriksen K, Christiansen B C, Baker J A, Frandsen C, Balic-Zunic T, Tullborg E-L, Mørup S and Stipp S L S (2007). Fe-oxide fracture fillings as a palæo-redox indicator: Structure, crystal form and Fe isotope composition. Chem. Geol., 244, 330–343.

Drake H and Tullborg E-L (2008). Fracture mineralogy of the Laxemar site. Final report. SKB-R-08-99.

Enüstün B and Turkevich J (1960). Solubility of fine particles of strontium sulphate. J. Am. Chem. Soc., 82, 4502–4509.

Gislason S R, Heaney P J, Veblen D R and Livi K J T (1993a). The difference between the solubility of quartz and chalcedony: the cause?. Chem. Geol., 107, 363–366.

Gislason S R, Veblen D R and Livi K J (1993b). Experimental water-basalt interactions. Characterization and interpretation of alteration products. Geochim. Cosmochim. Acta, 57, 1459–1471.

Grenthe I, Stumm W, Laaksoharju M, Nilsson A-C and Wikberg P (1992). Redox potentials and redox reactions in deep groundwater systems. Chem. Geol., 98, 131–150.

Langmuir D (1997). Aqueous environmental geochemistry. Prentice Hall, 600 p.

Langmuir D and Whittemore D O (1971). Variations in the stability of precipitated ferric oxyhydroxides. In: J.D. Hem (Ed.), Nonequilibrium Systems in Natural Water Chemistry. Advances in Chemistry Series, 106. Amer. Chem. Soc., Washington, D.C. Chapter 8, pp. 209–234.

Maliva R G and Siever R (1988a). Pre-Cenozoic nodular cherts: evidence for Opal-CT precursors and direct quartz replacement. Am. J. Sci., 288, 798–809.

Maliva R G and Siever R (1988b). Mechanism and controls of silicification of fossils in limestones. J. Geol., 96, 387–398.

Oelkers E H (1996). Physical and chemical properties of rocks and fluids for chemical mass transport calculations. In: P.C. Lichtner, C.I. Steefel and E.H. Oelkers (Eds.), Reactive transport in porous media. Reviews in Mineralogy, 34, 131–192.

Parks G A (1984). Surface and interfacial energy of quartz. Jour. Geophys. Res., 89, 3997–4008.

Rimstidt D D (1997). Quartz solubility at low temperatures. Geochim. Cosmochim. Acta, 61, 2553–2558.

Williams L A, Parks G A and Crerar D A (1985). Silica diagenesis. I. Solubility controls. J. Sedim. Petrol., 55, 301–311.

Groundwater composition at repository depth at Laxemar

E.1   Introduction

This section summarises (and extends) some of the SR-Can modelling results (Auqué *et al.* 2006) on the present three-dimensional distribution of the values of some important geochemical parameters at Laxemar-Simpevarp area. These results have been obtained using a novel procedure which combines CONNECTFLOW hydrogeological results obtained by Hartley *et al.* (2006ab) with PHREEQC mixing and reaction-path simulations. This coupling provides the theoretical composition of the groundwaters on a three dimensional rock volume constituted by a grid with around one million points that represents the whole regional area of Laxemar-Simpevarp down to 2.3 km depth.

The hydrological results (**based on SDM version 1.2**) contain the mixing proportions of four component waters (a deep saline groundwater, a glacial melt-water, old marine water, and Altered Meteoric water) at every node of the 3D regional model domain. The geochemical calculations include chemical mixing and equilibrium reactions with selected minerals: calcite, chalcedony and a Fe(III) oxyhydroxide (hematite with the equilibrium constant calculated by Grenthe *et al.* 1992). For most calculations the WATEQ4F thermodynamic database has been used as supplied with PHREEQC with the few modifications described in Auqué *et al.* (2006). In a few cases the "un-coupled" database (with suppressed redox equilibrium for the SO_4^{2-}/HS^- and HCO_3^-/CH_4 redox couples) has been used to test the effects on redox-sensitive elements (see Auqué *et al.* 2006 for more detailed information on the procedure and the calculations).

The composition obtained for 2020 AD (equivalent to present conditions) is generally in very good agreement with the data from the site[73] except for the most diluted samples from the upper 100 m of the rock volume (Auqué *et al.* 2006). The advantage of this approach is that the "samples" (i.e., the points of the 3D grid) fill the entire volume, in contrast with the sparseness of the real samples, located only in the available borehole sections within the repository candidate volume.

In this appendix the modelled distribution of key geochemical parameters at repository depth are presented in order to evaluate SKB's groundwater suitability criteria and to obtain a preliminary view on the spatial hydrochemical variability.

E.2   Modelled distribution of important geochemical parameters in groundwaters at repository depth

Considering the main Safety functions from SR-Can, results concerning the carbonate system (including Ca and alkalinity concentrations together with pH and calcite mass transfers), the potassium content, salinity (TDS) and the redox system (iron and sulphide concentrations, and Eh values) are presented here.

Results are shown following the same graphical scheme for all the geochemical parameters, with two different kinds of plots. The first type of plot consists of a 3D block with horizontal and vertical cross sections colour-coded with respect to the present-day values of each geochemical parameter as obtained from the SR-Can calculations. The vertical scale is exaggerated six times to display the system more clearly, from the surface to 1,500 m depth. The horizontal plane is at 500 m depth, the repository layout being also shown in that plane, and the vertical planes are drawn perpendicular and parallel to the coast. The top surface shows the topography with the land areas in shades of brown and the Baltic Sea in shades of blue (Figure E-1). The second type of plots consists of frequency histograms showing the variability of each geochemical parameter on the horizontal plane at repository depth (500 m).

Figures E-1 a to c show the 3D picture of the modelled system. In (a) and (b) plots, the point of view has been located in the SE part of the Laxemar-Simpevarp regional area, the first one from above the surface and the second from below. In plot (c) the point of view is located in the North part of the regional area from below the surface. Apart from the location of the boreholes and the categories

---

[73] The predicted results reproduce the main chemical trends defined by the present data in the full compositional space, covering the observed chemical variability (Auqué *et al.* 2006).
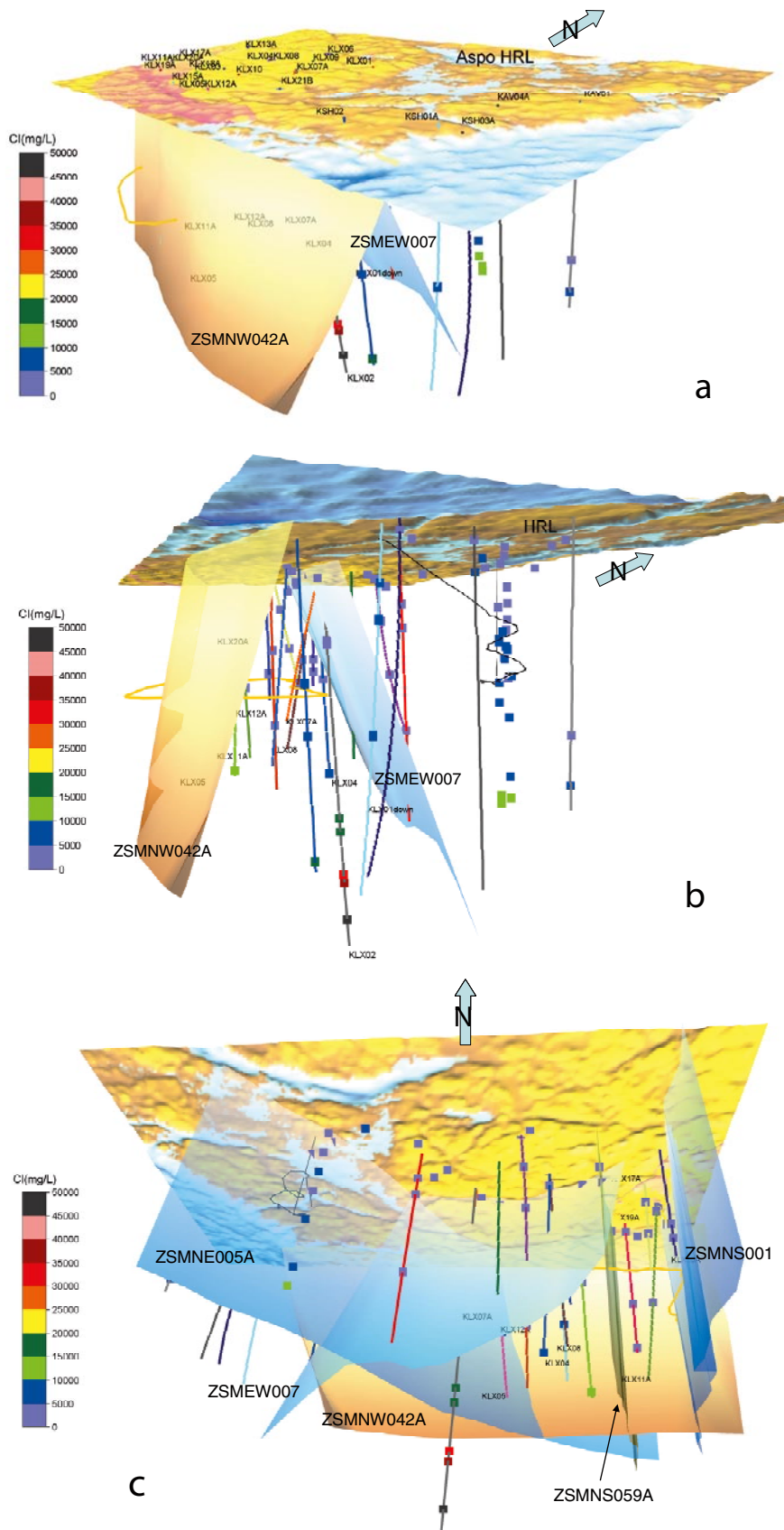
Figure E-1. *3D picture of the modelled volume. Apart from the location of the boreholes and the samples corresponding to categories 1 to 4 (with the chloride content indicated by colours), several of the main fracture zones have been represented: ZSMEW007, ZSMNW042, ZSMNS059A, ZSMNS001 and ZSMNE005A. (a) and (b): the point of view is located in the SE part of the Simpevarp regional area from above (a) and below the surface (b). (c) the point of view is located in the N part from below the surface.*

1 to 4 samples (with the chloride content indicated by a colour scale), two of the main fracture zones have been represented: ZSMEW007 (in light blue), and the ZSMNW042 (in tan) in plots (a) and (b), and the rest of the main fractures in plot (c).

E.2.1   Salinity (TDS)

The landscape in the Laxemar-Simpevarp area is characterised by small-scale topographic undulation (< 50 m.a.s.l.) and can be considered consisting of a large number of small catchments and mostly small water courses. Near surface recharge/discharge is largely determined by the local topography and is sensitive to seasonal fluctuations in precipitation. Lakes are considered to be permanent discharge locations, streams are sporadic discharge points during wet periods and wetlands/ marshes/bogs can be either typical discharge areas in contact with groundwaters, or represent closed surface systems with no underlying hydraulic contact (Smellie *et al.* 2006).

Since the last glaciation hydrological conditions have changed markedly due to shoreline displacement and changing salinity in the Baltic Sea region (fresh to brackish). This has resulted in the present spatial distribution of groundwater types (SKB 2004, 2006). In common with the surface environment, topography appears to control much of the groundwater flow pattern in the upper part of the rock volume, possibly down to 1,000 m depth. Increasing salinity with depth will reduce flow rates. Discharge areas are located at the extreme east of the Simpevarp area subarea along the Baltic Sea coastline and also onshore in conjunction with fracture zones.

Results from Simpevarp version 1.2 (SKB 2004) and Laxemar version 1.2 (SKB 2006) indicate that the Laxemar subarea is predominantly subjected to recharge conditions and that the Simpevarp subarea is an area of mainly groundwater discharge (Smellie *et al.* 2006).

In contrast with Forsmark, in the Laxemar-Simpevarp area there is a clear increase in the depth of the meteoric input (low TDS) when moving from the coast (Simpevarp subarea), where mixed waters can be found at shallow depth, towards the mainland (Laxemar local scale). However, in the western part of the system (Laxemar local scale) dilute groundwaters (< 500 mg/L) reach important depths, even below repository depth. Then, at depths between 800 and 1,000 m, salinity increases almost homogeneously in all the area toward higher values. Looking at the frequency histogram showing the variability at the repository depth, two main groups of values predominate, one dilute (200 mg/L, in Laxemar; Figure E-2) and the other brackish (11.5 g/L), clearly below the corresponding safety limit for the buffer, which is around 100 g/L (1.7 M).

E.2.2   Calcium

Calcium concentrations at Laxemar-Simpevarp (Figure E-3) increase with depth but quicker in the eastern part of the area. In fact the influence of meteoric waters is higher in the western part as it can be seen by the deeper input of dilute waters (already evident in the TDS plot). What is clear is the existence of a rock volume occupied by the most dilute waters (low calcium concentrations, around 1 mM, in blue in Figure E-4) which seems to be delimitated vertically by two of the main fracture zones (Figure E-4) and extending from the surface down to just below repository depth. The special hydrogeochemical features of this volume are also conspicuous when plotting other parameters.

Looking at the measured calcium concentrations (coloured squares along borehole lines in the upper part of Figure E-3), a very good agreement can be seen, which is a good support to the model used in the simulations. In general this plot shows a high variability on the plane located at repository depth, with a progressive increase in calcium towards the coast. But looking at the frequency histogram of Ca concentrations at repository depth (Figure E-3, lower panel) it is evident that all the values are higher than 1 mM, although most of them are very close to the safety limit.

This proximity to the safety limit calls for a more detailed study of the fate of calcium in the system. As the main reason for the low Ca values is the input of meteoric water, an assessment of the Ca content in the meteoric end member was carried out (Auqué *et al.* 2006).
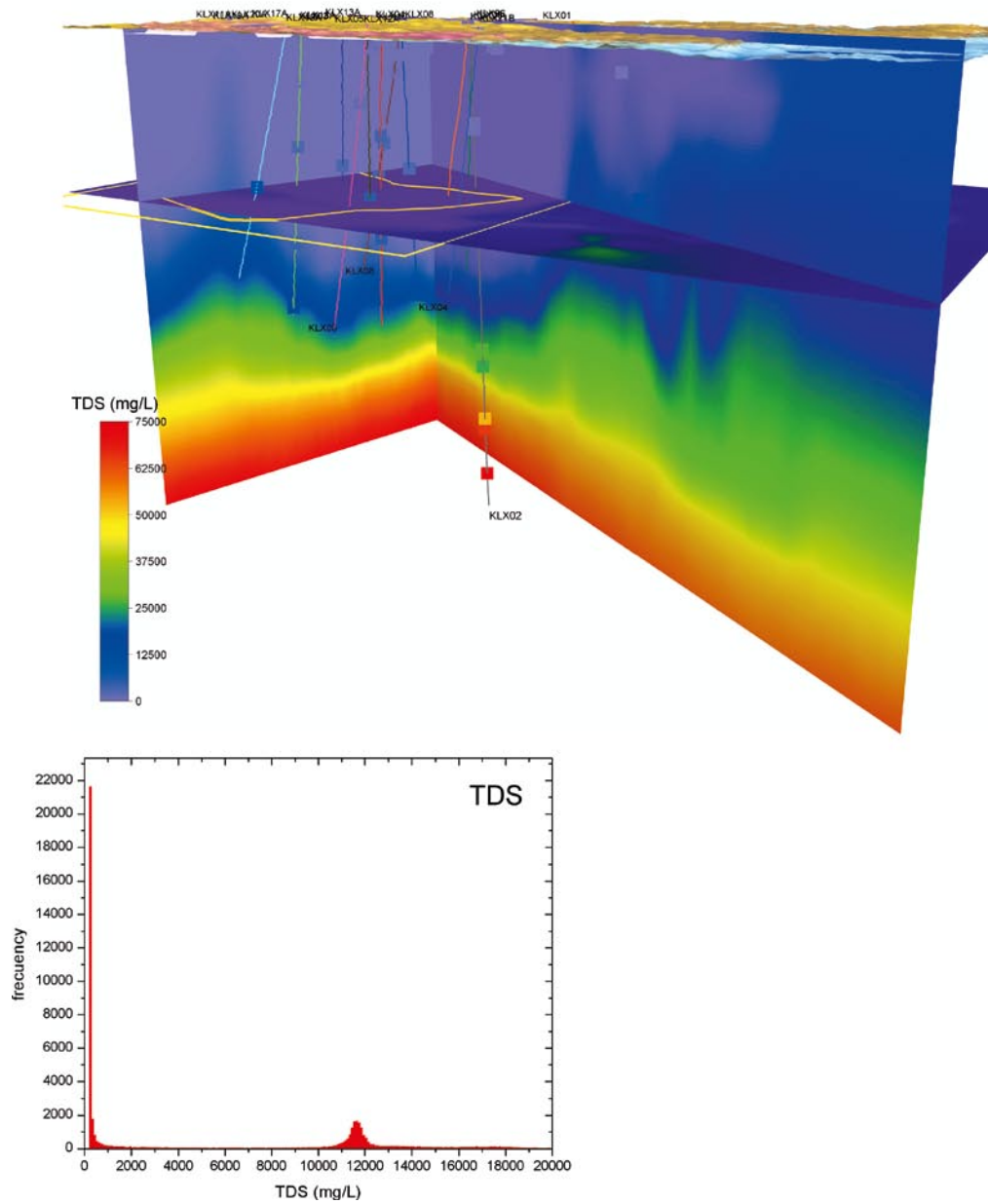
Figure E-2. *Calculated TDS at the Laxemar-Simpevarp site. Upper panel: Horizontal and vertical cross sections colour-coded with respect to the TDS content. Left panel: Frequency histogram showing TDS variability on a horizontal plane at repository depth (500 m) as shown in the figure above.*
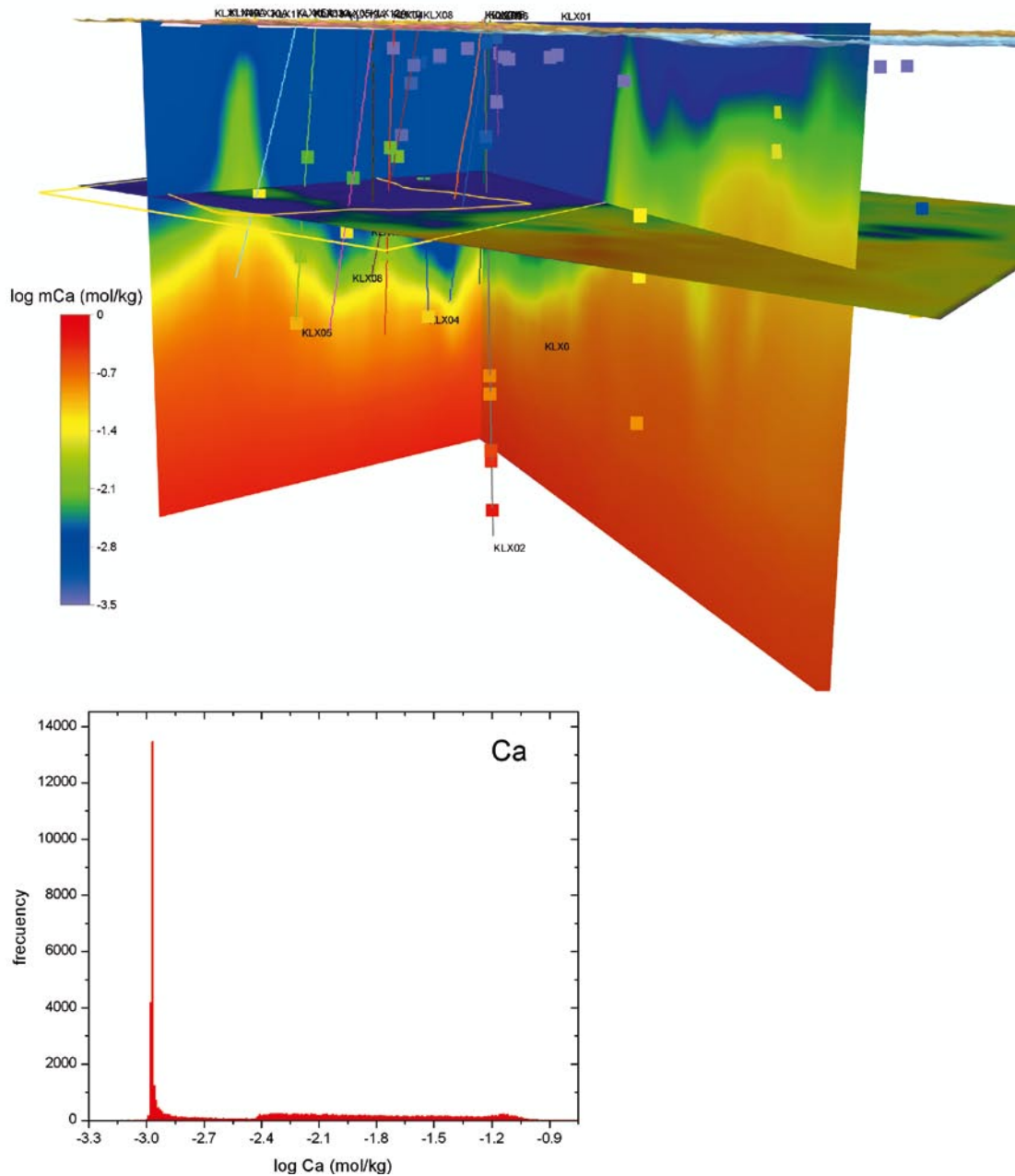
Figure E-3. *Calculated Ca contents at the Laxemar-Simpevarp site. Upper picture: Horizontal and vertical cross sections colour-coded with respect to the present-day concentration of calcium (in logarithmic scale). The real values measured in the system are also shown as coloured squares. Left panel: Frequency histogram showing calcium variability (in log scale) on a horizontal plane at repository depth (500 m) as shown in the figure above. See the text for details.*
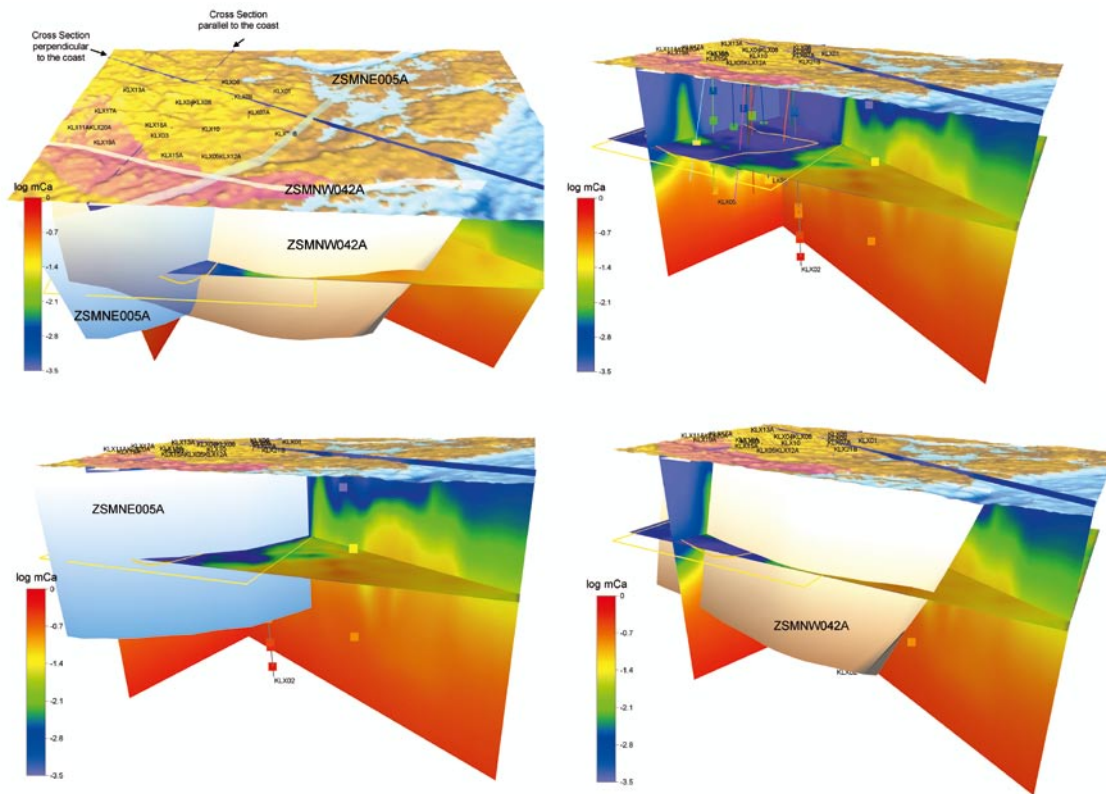
Figure E-4. *3D pictures of the system showing the location of two of the main fracture zone and their relation to the chemical distribution of calcium. Upper left: position of the fracture zones ZSMNE005 (in light blue), and the ZSMNW042 (in light orange) with respect to the surface. Upper right: distribution of calcium as it is shown in Figure D-4. Lower left and right: Position of ZSMNE005 and ZSMNW042 in depth and their effect on the calcium distribution.*

In Laxemar, with minor amounts of calcium carbonate in the overburden, recharge waters have very low calcium concentrations. Therefore, although the selected Altered Meteoric end-member for the Laxemar subarea (sample #2030, Table 5-5-2 in Auqué *et al.* 2006) has 38.4 mg/L of calcium, the same calculations were performed using a different sample as end member: sample #7345 (Table 5-5-2 in Auqué *et al.* 2006), with 18.8 mg/L of dissolved calcium. Results are shown in Figure E-5. The simulation confirms the possibility suggested by Auqué *et al.* (2006): very dilute groundwaters with calcium concentrations lower than the safety limit of 40 mg/L (10^{-3} mol/kg) may reach the repository zone with the related detrimental effects on the buffer and backfill materials.

E.2.3   pH and bicarbonate

For pH and bicarbonate, the mixing and reaction calculations are dominated by the (imposed) precipitation and the dissolution of calcite. Results are summarised in Figure E-6. The figure shows a distribution of bicarbonate very similar to the one shown by calcium (Figure E-4) but with the opposite depth-dependence: instead of increasing, it clearly decreases with depth. It also shows the isolated volume located in the Laxemar local scale subarea.

Bicarbonate values around 2.5 mM are common at repository depth in Laxemar, as the frequency histogram shows. However, towards the coast, values decrease to 0.5 mM.

pH also shows a slight increase with depth but with a narrower range of variability (around 7.8) from the surface to below the repository depth. In fact, the frequency histogram at repository depth points to 7.8 as the most frequent value at that depth. Only deeper groundwaters have pH higher than 8, corresponding to the pH of the Deep Saline end-member. Waters just below the isolated volume have the lowest pH values (around 7; blue colours). Toward the coast, this minimum-pH tongue reaches the repository depth.
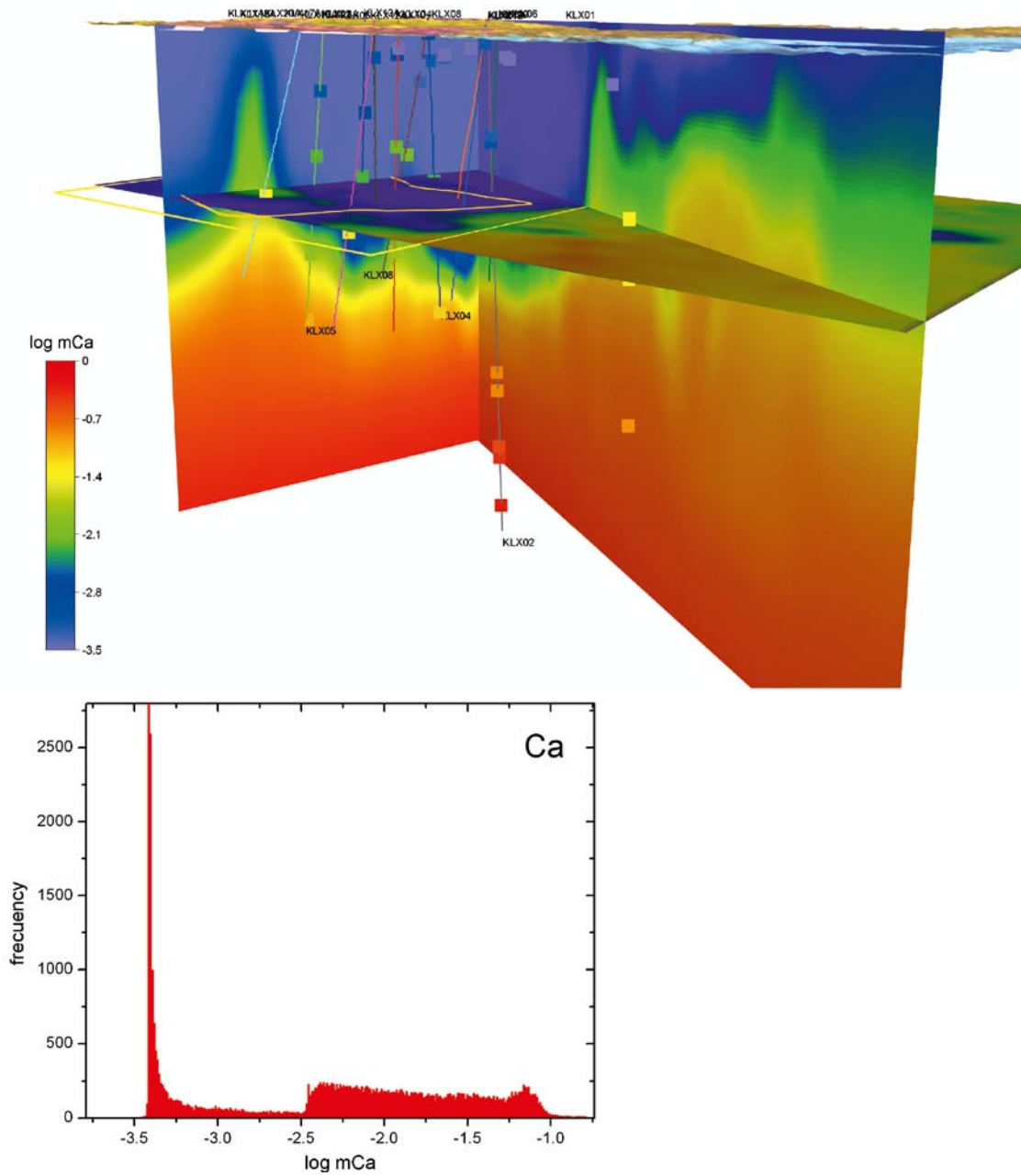
Figure E-5. *Calculated Ca contents at the Laxemar-Simpevarp site using a low calcium meteoric end member in the simulations. Upper picture: Horizontal and vertical cross sections colour-coded with respect to the present-day concentration of calcium (in logarithmic scale). The real values measured in the system are also shown as coloured squares. Left panel: Frequency histogram showing Ca variability (in log scale) on the horizontal plane at repository depth (500 m) showed in the figure above. See the text for details.*

323
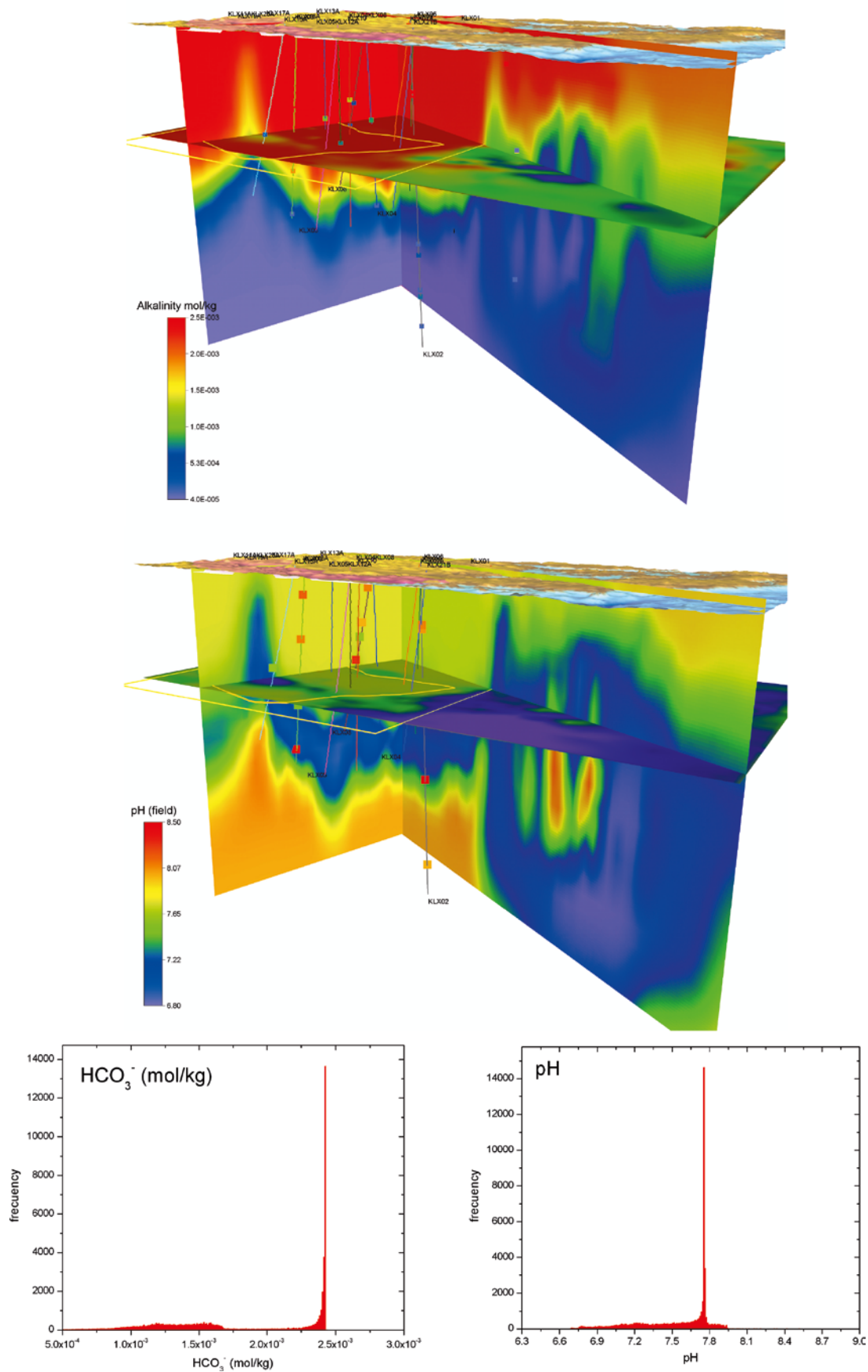
Figure E-6. *Calculated alkalinity (upper panel) and pH (medium panel) at the Laxemar-Simpevarp site. The frequency histograms for both parameters are also shown in the lower part of the plot.*

In the upper parts of the modelled domain meteoric waters dominate; they are relatively acidic (pH < 7.4) and have high bicarbonate and CO_2 contents (not displayed here). These meteoric waters are slightly undersaturated with respect to calcite (imposed on the model) and this mineral, present in fracture fillings, will therefore dissolve (Figure E-7; brown areas). As a result, pH and Ca increase. Deeper down, waters have already reached equilibrium with calcite (white colours in Figure E-7) and when they mix with deeper Ca-rich groundwaters calcite precipitates due to over-saturation (Figure E-7; blue areas).

The calculated amount of dissolved and precipitated calcite (mass transfer) for present-day conditions is shown in Figure E-7. Mass transfers are quite small, less than 1.5×10^{-4} mol per litre of groundwater (see the frequency histogram).[74]
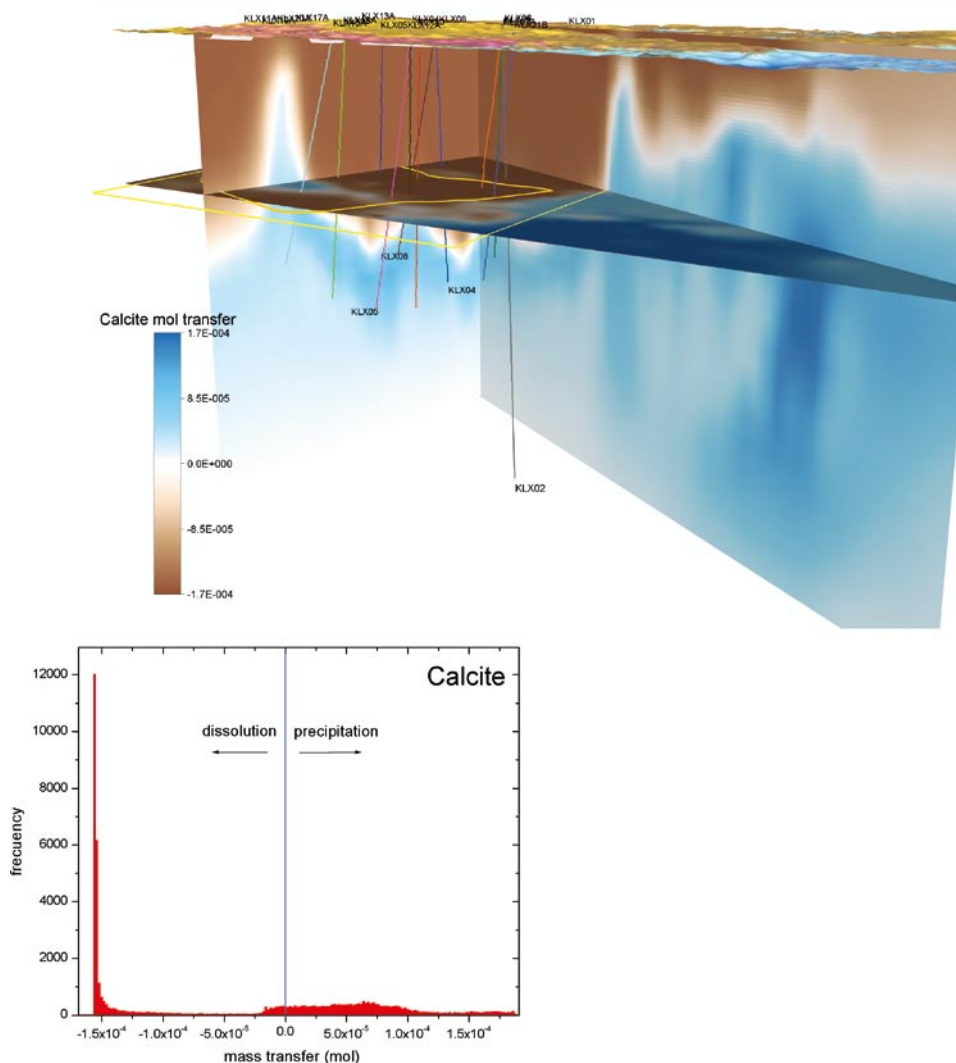
Figure E-7. *Calculated amounts of dissolved and precipitated calcite (mass transfer) for present-day conditions at Laxemar-Simpevarp site. Upper panel: Horizontal and vertical cross sections colour-coded. Left panel: Frequency histogram of the mass transfer variability on the horizontal plane at repository depth (500 m) showed in the figure above.*

---

[74] The mass transfer values must be treated with caution. They are calculated from the prescribed mixing proportions for the four end members and re-equilibrium with calcite. In the real system mixing events are developed in successive steps with re-equilibrium stages between them. The effects of these simultaneous or successive mixing processes over the non-lineal behaviour of calcite saturation index must be explored.

E.2.4 Potassium

Potassium concentrations are generally low in the groundwaters sampled at Laxemar-Simpevarp (Figure E-8) and two main processes have been proposed to explain these low values: solubility control by sericite (Nordstrom *et al.* 1989), and cation-exchange. None of them have been considered in SR-Can calculations; however, even if the exact mechanism is not known, all available groundwater data indicate that the increased infiltration of meteoric waters will not increase the present concentration of potassium (see Appendix C, in Gimeno *et al.* 2008).

Potassium concentrations calculated in "only mixing" simulations are below 4 mM for the whole 3D area and below 1 mM for the slice at the repository depth (see frequency histogram, Figure E-8) which fits the safety criterion "the lower the better" to avoid illitisation of the buffer.
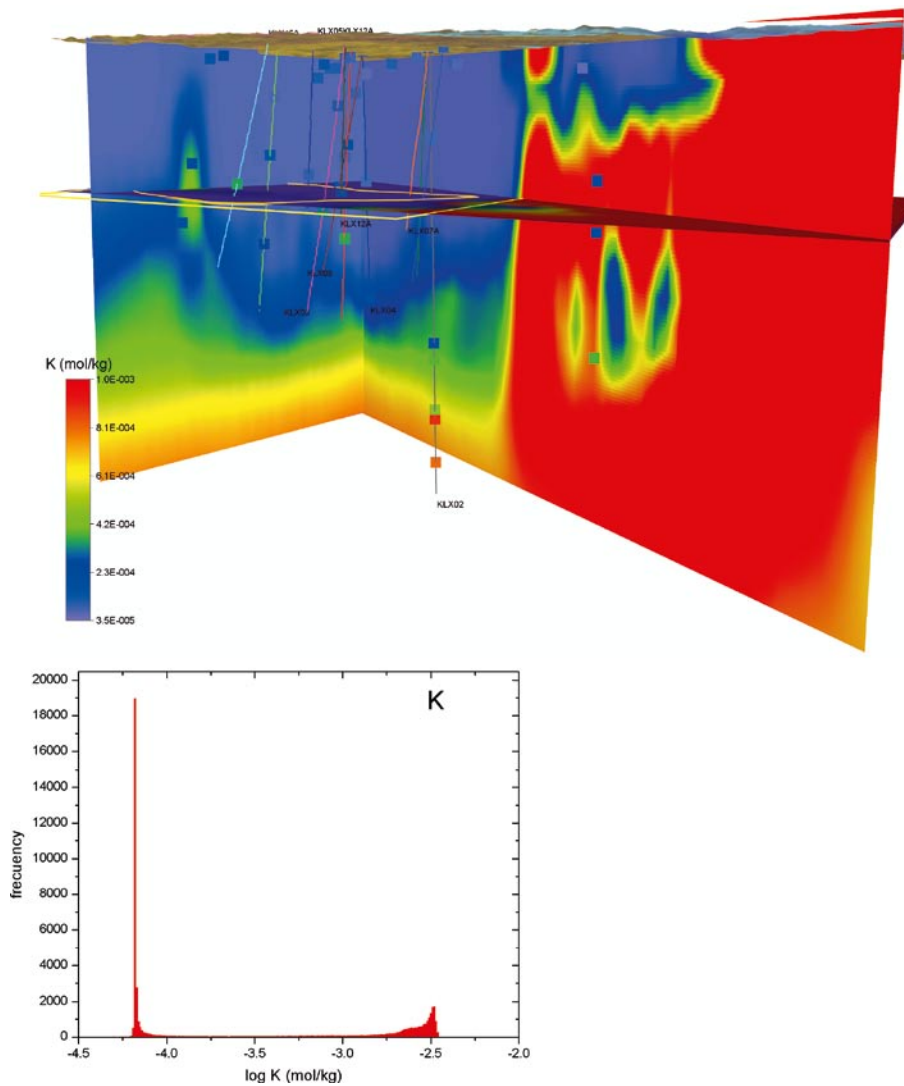
Figure E-8. *Calculate potassium concentration at the Laxemar-Simpevarp site. Upper panel: Horizontal and vertical cross sections colour-coded with respect to the concentration of potassium. Left panel: Frequency histogram showing the concentration variability on a horizontal plane at repository depth (500 m) as shown in the figure above.*

E.2.5 Redox system

A fundamental safety requirement is that of reducing conditions. A necessary condition is the absence of dissolved oxygen, because any evidence of it would indicate oxidising conditions. The presence of reducing agents that react quickly with O_2, such as Fe(II) and S(–II) is sufficient to indicate reducing conditions. SR-Can results with respect to three parameters, the redox potential (pe or Eh), and the contents of Fe(II) and S(–II) are summarised here. As it is the case for potassium, there are no quantitative requirements for these three parameters, only "the lower, the better".

SR-Can calculations include equilibrium with the Fe(III)-oxyhydroxide ($Fe(OH)_{3(hematite\_Grenthe)}$) proposed by Grenthe *et al.* (1992) and an alternative model including equilibrium with recently precipitated (amorphous) Fe(II)-sulphide $FeS_{(am)}$ instead. When imposing equilibrium with an iron oxyhydroxide, two alternative scenarios were also evaluated, allowing or not redox equilibrium between sulphate and sulphide (referred as "coupled" and "un-coupled" databases in Auqué *et al.* 2006, respectively). Results coming from the three different alternatives are shown here.

pe

The first interesting observation in Figure E-9 is that, in spite of a very similar distribution of values, the values themselves are quite different depending on the mineral phase considered to be in equilibrium (iron oxyhydroxides in the upper panels and FeS in the lower left panel) and, mainly, whether redox equilibrium between sulphate and sulphide is allowed or not (differences between left and right upper panels).

The highest calculated pe values are obtained assuming equilibrium with either $Fe(OH)_{3(hematite\_Grenthe)}$ or $FeS_{(ppt)}$ and using the "coupled" database. Both distributions are very similar although the highest pe values are found equilibrating with the iron oxyhydroxide (see also the red and blue frequency histograms in the lower left panel), mainly for the deepest and more saline waters in Laxemar.

The lowest pe values (and therefore most desirable from a safety point of view) are those obtained when the redox potential is controlled by the $Fe(OH)_3/Fe^{2+}$ couple, in particular at pH > 7.5 (see Figure D-5), for the "un-coupled" database (green frequency histogram).

Because of the correlation between calculated redox potentials and pH, the pe distribution pattern is very similar to the one observed for pH (Figure E-4), with the areas with lower pH (a consequence of calcite precipitation) corresponding to areas with the highest calculated Eh.

Iron and sulphide

Sulphur and the iron systems are the two main redox systems operating in Swedish groundwaters. The concentration of Fe(II) is regulated by a complicated set of reactions including the slow dissolution of Fe-silicates, the precipitation of Fe(II)-sulphides, and the redox reactions (including the activity of iron reducing bacteria). The concentrations of ferric iron are in general negligible in crystalline groundwaters, as the oxy-hydroxides of Fe(III) are quite insoluble and precipitate quickly. Moreover, the work by Grenthe *et al.* (1992) indicates that potentiometrically measured Eh in different Swedish groundwaters are controlled by equilibrium with a crystalline Fe(III) oxy-hydroxide. So, equilibrium with this phase was assumed for the reaction modelling.

Maximum sulphide concentrations measured in the Laxemar-Simpevarp groundwaters are lower than $10^{-4.1}$ mol/kg and usually below the reporting limit of 10^{-6} mol/kg. Under oxidising conditions sulphide is quickly oxidised to sulphate and, under reducing conditions, dissolved Fe(II) is normally present and the maximum sulphide concentrations are regulated by the precipitation of Fe(II)-sulphide. So, equilibrium with this phase was also considered for the reaction modelling.

Results for the two redox-sensitive groundwater components analysed here, total dissolved iron and sulphide, are illustrated in Figures E-10 and E-11. They show a range of variation of 10^{-6} to 5×10^{-5} mol/kg for ferrous iron, and 10^{-7} to 5×10^{-5} mol/kg for sulphide. This variation probably reflects the effect of several processes on components that have low concentrations: small changes have a large impact on the final concentration. Microbial processes in particular are expected to greatly influence the concentration of both.

Figure E-9. *Calculated redox potential (pe) at the Laxemar-Simpevarp site. Upper panels show the results using the iron oxyhydroxide for the mineral equilibrium calculations allowing (left) or not (right) the equilibrium between sulphate and sulphide. Lower left panel shows the results of equilibrating the waters with FeS with the same coupled data base as the plot just above. Lower right panel: Frequency histogram showing the pe variability on a horizontal plane at repository depth (500 m) as shown in the other panels.*

The lowest Fe(II) values are obtained when equilibrating with the iron phase when redox equilibrium between sulphate and sulphide is allowed (Figure E-10, upper left panel; see also the frequency histogram, red columns). These values are lower than the ones measured at the site, which is probably due to the fact that this model is the most conservative in giving the highest Eh values and the lowest reducing capacity, i.e. lowest Fe(II) content. Then, the highest ferrous iron values are found when equilibrating with the monosulphide (covering the maximum measured values of $10^{-4.6}$ mol/kg) and the intermediate values correspond to the equilibrium with the iron oxyhydroxide not allowing equilibrium between sulphate and sulphide (see frequency histogram). In the three cases the distribution of values is similar to the one observed for pe and pH.

With respect to sulphide, the lowest values are found when equilibrating with the iron phase and not allowing the equilibrium between sulphate and sulphide (Figure E-11, upper right panel; see also the frequency histogram, green columns). Equilibrium with FeS(ppt) gives the highest values, reaching almost the maximum concentrations analysed in the present-day groundwaters at Laxemar-Simpevarp (with a value of $10^{-4.1}$ mol/kg). The equilibrium with iron oxyhydroxides allowing the equilibrium between sulphate and sulphide gives intermediate values between the other two models.

Figure E-10. *Calculated Fe(II) contents at the Laxemar-Simpevarp site. Upper panels show the results using the iron oxyhydroxide for the mineral equilibrium calculations allowing (left) or not (right) the equilibrium between sulphate and sulphide. Lower left panel shows the results of equilibrating the waters with FeS with the same coupled data base as the plot just above. Lower right panel: Frequency histogram showing the Fe(II) variability on a horizontal plane at repository depth (400 m) as shown in the other panels.*

Discussion

Among all the variables required to define the geochemistry of groundwaters, the redox potential (Eh or pe) has been the most difficult to characterise and to model. Often disequilibrium between the different dissolved redox pairs is found in natural waters (Lindberg and Runnells 1984, Stefánsson *et al.* 2005) and an overall Eh value for a groundwater is often impossible to assign (Thorstenson 1984, Nordstrom and Munoz 1985, Langmuir 1997). On the other hand, concentrations of redox elements are mainly dependent on the microbiological and mineralogical reactions and less on the mixing processes occurring in the system. In modelling terms, these concentrations will be very sensible to the equilibrium assumptions used in the simulations.

The different "redox alternatives" used in the simulations essentially pretend to obtain "indicative" Eh values and a range of predicted Fe(II) and S(–II) concentrations to compare with the available data.

Assuming equilibrium with the crystalline $Fe(OH)_{3(hematite\_Grenthe)}$ and using the uncoupled database (redox equilibrium between sulphate and sulphide in solution is not allowed), the obtained redox potentials are more reducing than those potentiometrically measured in the system, up to −400 mV in the whole volume and between −142 and −350 at the repository level. Predicted iron concentrations range from 0.6 mg/L to 0.05 mg/L.
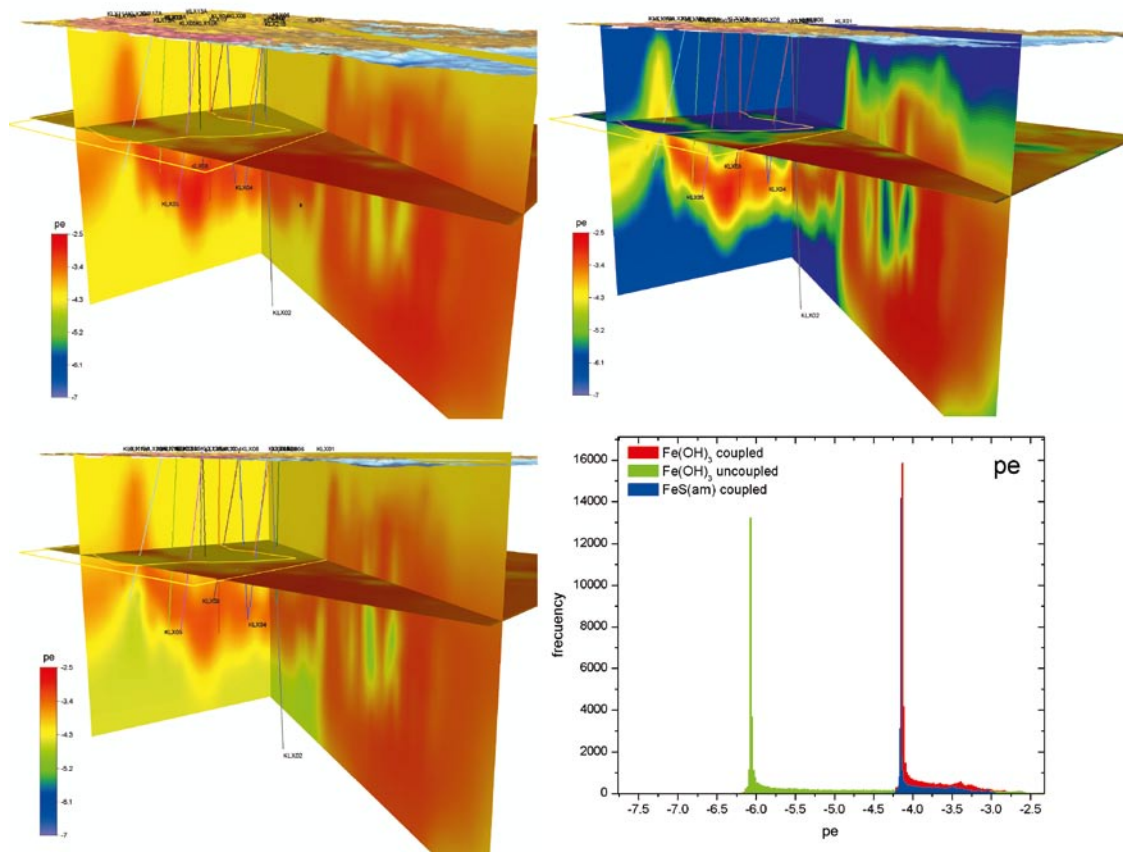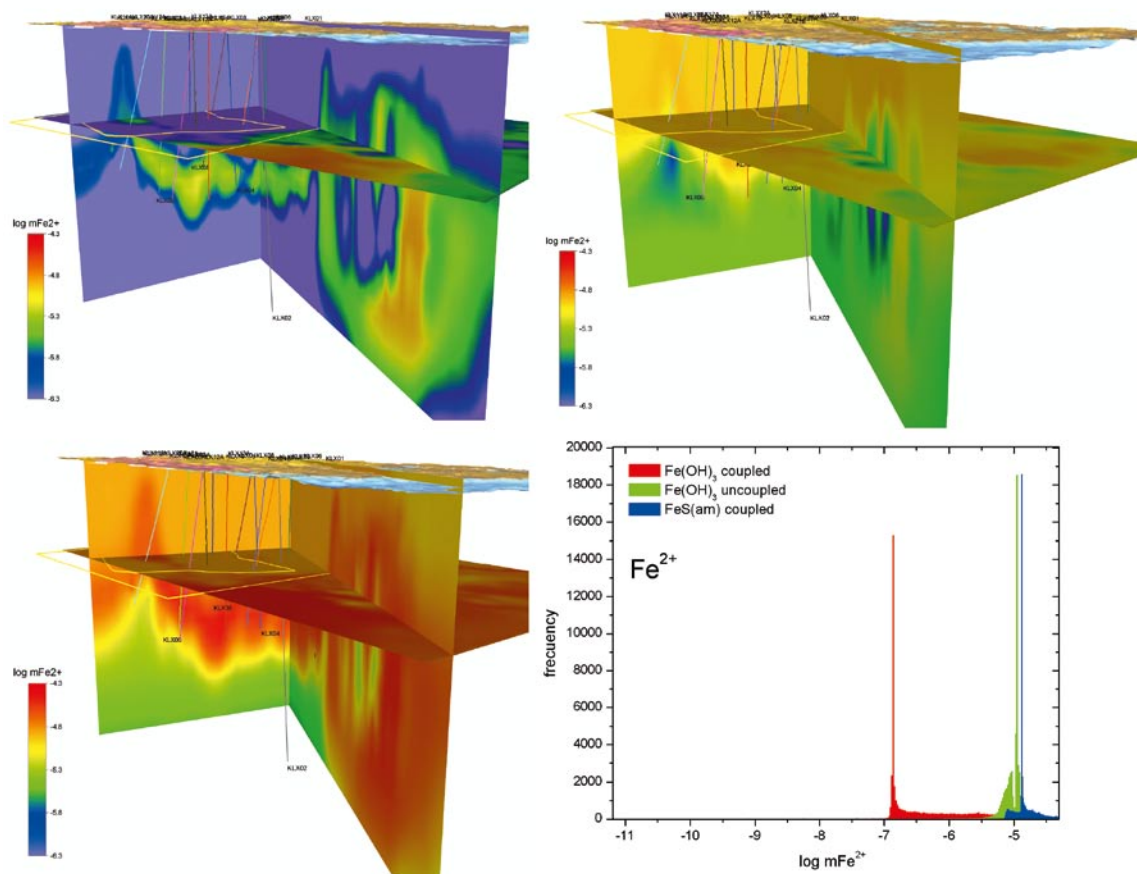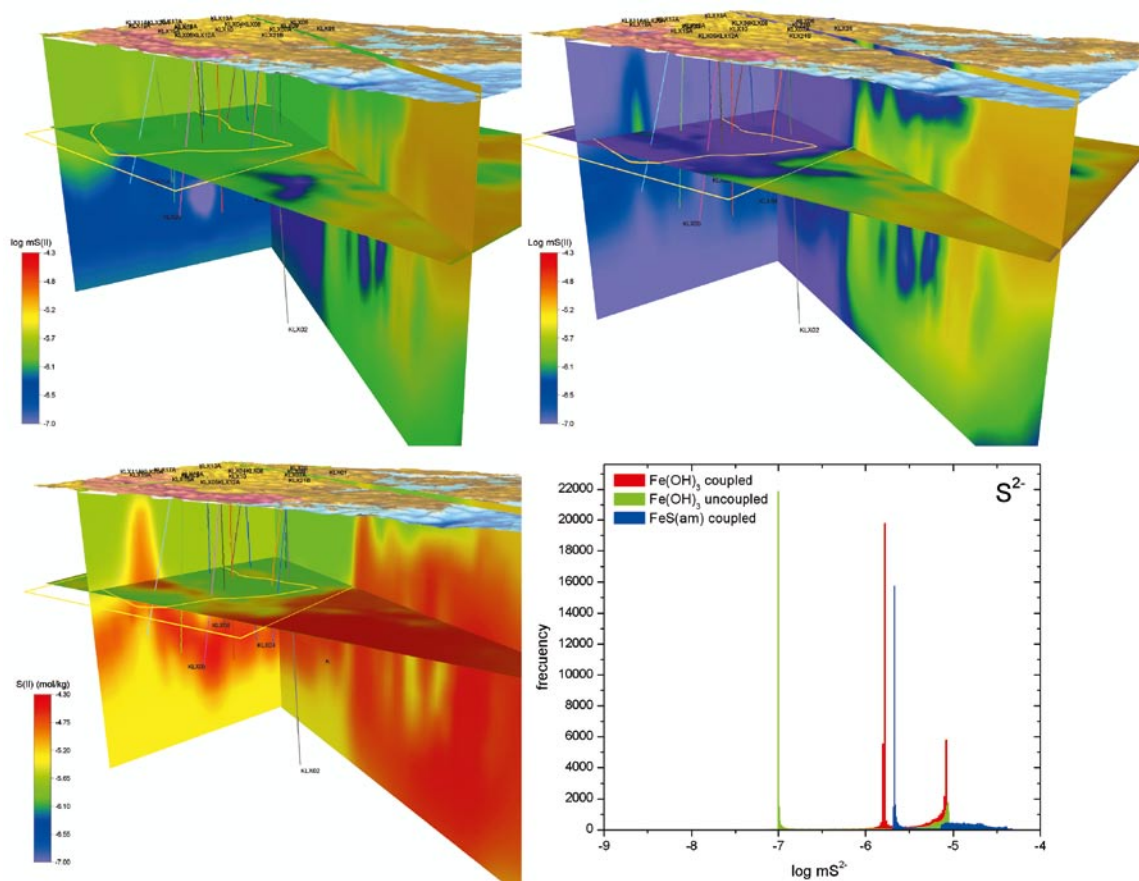
Figure E-11. *Calculated S(–II) contents at the Laxemar-Simpevarp site. Upper panels show the results using the iron oxyhydroxide for the mineral equilibrium calculations allowing (left) or not (right) the equilibrium between sulphate and sulphide. Lower left panel shows the results of equilibrating the waters with FeS with the same coupled data base as the plot just above. Lower right panel: Frequency histogram showing the Fe(II) variability on a horizontal plane at repository depth (500 m) as shown in the other panels.*

If redox equilibrium between sulphate and sulphide in solution is allowed, the predicted Eh values range from –142 and –230 mV, Fe(II) concentrations in the whole system are lower than 0.7 mg/L, but lower that 0.1 mg/L at the repository level. S(–II) concentrations are lower than 0.2 mg/L. If the redox system is controlled by the equilibrium with amorphous monosulphides (therefore, assuming the existence of SRB activity in the system) the predicted Eh values are between –142 to –285 mV in general, and −170 to −240 at the repository level. Fe(II) concentrations vary from 0.2 to 2 mg/L in the whole system, and they are around 0.9 mg/L at the repository level; and S(–II) concentrations range from 0.03 to 1.6 mg/L in the whole system and are around 0.1 mg/L at repository depth. From these results two main conclusions can be extracted:

- Allowing or not homogeneous redox equilibrium (e.g. equilibrium between dissolved sulphate and sulphide) has important consequences in the predicted Eh values. The importance of these effects in the potentiometric Eh values should be explored.

- The predicted ranges in Eh values and Fe(II) and S(–II) concentrations are in general agreement with those measured in the system. All calculated ranges include the measured ones except for the case of dissolved sulphide whose maximum measured values are slightly above the calculated ones.

Finally, it must be taken into account that all the results presented here correspond to simulations where a single redox equilibrium is imposed on the whole system. In the real system, all redox buffers can be working in different parts depending on mineralogical and microbiological peculiarities. But, even so, the total chemical variability in the redox parameters seems to be reasonably covered by the range of equilibrium assumptions considered here.

E.3   Conclusions

As part of the SR-Can assessment, CONNECTFLOW hydrogeological results obtained by Hartley *et al.* (2006ab) were coupled to PHREEQC mixing and reaction-path simulations on a rock volume that represent the whole regional area of Laxemar. Results of this coupling for the present situation can be used to address the conceptual 3-dimensional variability in the hydrochemical data derived from the present integrated knowledge on the system.

All the key chemical suitability parameters for groundwaters have been considered in this section, mainly at repository level. Modelled salinity, pH, Ca, HCO_3^- K and redox values are variable and heterogeneously distributed at repository depth, but all of them fulfil SKB's safety criteria even when results are extrapolated to unexplored volumes of the candidate area. The most problematical parameter is calcium, as its content is very close or even below the safety limit.

The total chemical variability observed in the system is covered by the predicted results and the 3D spatial distribution patterns of TDS, Ca, HCO_3^- and K concentrations are in qualitative agreement with the hydrochemical traits presently known in the system. This is not strange as the hydrogeological site model (Follin *et al.* 2006, Hartley *et al.* 2006b) was calibrated by comparing calculated mixing proportions, salinities and $\delta^{18}O$ values with the corresponding data measured at the site as well as with the mixing proportions calculated with the M3 code (Laaksoharju *et al.* 1999, Gómez *et al.* 2006).

But the model also shows the existence of a high degree of complexity in the detailed distribution patterns of these parameters, with lenses, fingers and tongues in the 3D domain. And, most important, some of these patterns (e.g. for pH and Eh) only arise from the coupling with geochemistry as they are essentially controlled by reactions and not by mixing.

Obviously, this modelled spatial variability must not be confused with the "field" variability, represented by the present, more limited available hydrochemical data, some of which were used to calibrate the hydrogeological model. Results presented here are only a model, but it is the first integrated hydrological and geochemical model for the state of the system at present.

The coupled approach used here integrates very different types of data, assumptions and uncertainties from different disciplines in a unique view that allows addressing their final consequences on the spatial hydrochemical variability. Moreover, they predict geochemical values in unexplored volumes of the system, providing the opportunity to empirically verify these predictions.

For the next site descriptive modelling (SDM version 2.2), an update of the groundwater flow modelling is expected. Using the same coupled approach with the updated hydrological model, it could be possible to verify which data, assumptions or extrapolations are more critical to the final results and re-evaluate them.

E.4   References

Auqué L F, Gimeno M J, Gómez J, Puigdomènech I, Smellie J and Tullborg E-L (2006). Groundwater chemistry around a repository for spent nuclear fuel over a glacial cycle Evaluation for SR-Can. SKB TR-06-31, 123 pp.

Follin S, Stigsson M and Svensson U (2006). Hydrogeological DFN modelling using structural and hydraulic data from KLX04. Preliminary site description. Laxemar subarea – version 1.2. SKB R-06-24.

Gimeno M J, Auqué L F, Gómez J and Acero P (2008). Water-rock interaction modelling and uncertainties of mixing modelling. SDM-Site Forsmark. SKB R-08-86, 212 pp.

Gómez J B, Laaksoharju M, Skårman E and Gurban I (2006). M3 version 3.0: Concepts, methods, and mathematical formulation. SKB TR-06-27.

Grenthe I, Stumm W, Laaksoharju M, Nilsson A-C and Wikberg P (1992). Redox potentials and redox reactions in deep groundwater systems. Chem. Geol., 98, 131–150.

Hartley L, Hoch A, Jackson P, Joyce S, McCarthy R, Swift B, Gylling B and Marsic N (2006a). Groundwater flow and transport modelling during the temperate period for the SR-Can assessment: Laxemar area – Version 1.2. SKB R-06-99.

Hartley L, Hunter F, Jackson P, McCarthy R, Gylling B and Marsic N (2006b). Regional hydrogeological simulations using CONNECTFLOW. Preliminary site description Laxemar subarea – version 1.2. SKB R-06-23.

Laaksoharju M, Tullborg E-L, Wikberg P, Wallin B and Smellie J (1999). Hydrogeochemical conditions and evolution at the Äspö HRL, Sweden. Appl. Geoch., 14, 835–859.

Langmuir D (1997). Aqueous environmental geochemistry. Prentice Hall, 600 p.

Lindberg R D and Runnells D D (1984). Ground water redox reactions: an analysis of equilibrium state applied to Eh measurements and geochemical modelling. Science, 22, 92–927.

Nordstrom D K and Munoz J L (1985). Geochemical Thermodynamics. 2nd Ed. The Benjamin/Cummings Publ. Co., Menlo Park, California, 477 pp.

Nordstrom D K, Ball J W, Donahoe R J and Whittemore D (1989). Groundwater chemistry and water-rock interactions at Stripa. Geochim. Cosmochim. Acta, 53, 1727–1740.

SKB (2004). Hydrogeochemical evaluation for Simpevarp model version 1.2. Preliminary site description of the Simpevarp area. SKB R-04-74, 463 p.

SKB (2006). Hydrogeochemical evaluation. Preliminary site description Laxemar subarea – version 1.2. SKB R-06-12, 435 pp.

Stefánsson A, Arnórsson S and Sveinbjörnsdóttir A E (2005). Redox reactions and potentials in natural waters at disequilibrium. Chem. Geol., 221, 289–11.

Smellie J, Tullborg E-L and Waber N (2006). Explorative analysis and expert judgement of major components and isotopes. Contribution to the model version 2.1. In: SKB(2006), Hydrogeochemical evaluation. Preliminary site description. Laxemar subarea, version 2.1. SKB R-06-70, 337 p.

Thorstenson D C (1984). The concept of electron activity and its relation to redox potentials in aqueous geochemical systems. USGS Open-File Report 84-072, U.S. Geol. Survey, Denver, Colorado, USA.

End members' composition

F.1 Introduction

The geochemical study of the Laxemar-Simpevarp and Forsmark groundwaters, using either simple conservative elements (Smellie *et al.* 1995, Laaksoharju and Wallin 1997, SKB 2005, 2006) or more refined isotopic techniques (Louvat *et al.* 1999, Wallin and Peterman 1999, Négrel and Casanova 2005) has confirmed the existence of at least four end member waters: an old deep saline water (Deep saline), an old marine water (ancient Littorina sea), a modern meteoric water (Altered Meteoric), and a glacial melt-water (Glacial). As a result, mixing can be considered the prime irreversible process responsible for the chemical evolution of the Laxemar-Simpevarp and Forsmark groundwater systems. The successive disequilibrium states resulting from mixing conditioned the subsequent water-rock interaction processes and, hence, the re-equilibration pathways of the mixed groundwaters.

The quantitative assessment of mixing and reaction in these groundwaters can be approached by inverse modelling (mixing and mass balance calculations) with standard geochemical codes like NETPATH (Plummer *et al.* 1994) or PHREEQC (Parkhurst and Appelo 1999) or with PCA-based codes like M3 (e.g., Laaksoharju *et al.* 1999, Gómez *et al.* 2006). A correct selection of the end-member waters is critical in both cases. The uncertainties associated with this selection procedure have already been discussed elsewhere (Luukkonen 2001, Bath and Jackson 2002, Laaksoharju *et al.* 2004).

Furthermore, the inclusion of water-rock chemical reactions on top of the first-order process of mixing represents an additional source of uncertainty that must be addressed when analysing the sensitivity of the computed mixing proportions to variable chemical reactions that could contribute to the evolution of the groundwater system. The uncertainties associated with the effects of water-rock chemical reactions in M3 calculations have been previously discussed in Gómez *et al.* (2008). A special section dealing with these uncertainties has been presented in this work (see section 3.7) as the effects of reactions are more important in the Laxemar-Simpevarp area than they were in Forsmark.

There are other evident sources of uncertainty when trying to apply mixing and mass balance calculations to real, complex groundwater systems. One of the most important sources of uncertainty is related to the chemical and physicochemical characteristics of each end-member and their possible spatial and/or temporal chemical variability. That was why the chemical and stable isotope characteristics ($\delta^{18}O$ and δ^2H) of the four end-member waters (Deep Saline, Glacial, Littorina and Altered Meteoric) used in the hydrochemical and hydrogeological characterization of Laxemar-Simpevarp and Forsmark areas were comprehensively analysed in the review presented in Gimeno *et al.* (2008).

During the Laxemar 2.2–2.3 SDM stage, the chemical composition of the selected end-member (and their uncertainties) has been further explored. In this Appendix the new results are presented together with a short summary of the review performed by Gimeno *et al.* (2008). The new results affect the Deep Saline, Glacial and Littorina end members.

F.2 Deep Saline end-member

The groundwater sample used as the Deep Saline end-member in the Swedish site characterization program corresponds to a 1,623 m depth sample from borehole KLX02 (Laxemar) which has the maximum salinity found in the area to date. Some of the compositional parameters not analysed in this sample (pH, Eh, Fe(II) and S(–II) concentrations) have been taken from a different sample, only slightly less saline, from the same borehole and at a similar depth (1,531 m depth, sample #2731, which could be used also as Deep Saline end-member since they are compositionally similar).

The absence of a proper deep saline sample in the Forsmark area to be used as an end-member constitutes one of the main uncertainties associated with this end-member and it casts a reasonable doubt on the real composition of the saline waters in the Forsmark area. However, the review and Monte Carlo simulations, performed in Gimeno *et al.* (2008), suggest the presence of a Deep Saline

end-member with an overall chemical (major elements) and isotopic ($\delta^{18}O$ and δ^2H) composition similar to the one defined and used in Laxemar-Simpevarp. The main difference should be a lower sulphate concentration. The precise sulphate concentration is not well constrained by any of the methods, therefore, a new saline end-member with a very low sulphate concentration (10 mg/L) was defined to be used in Forsmark (Deep Saline-Forsmark; Table F-1).

Therefore, the two end-members could be used for the sensitivity analysis of the computed mixing proportions in Forsmark. Additional, the sample KR4/860/1 from Olkiluoto (Finland; Pitkänen *et al.* 2004), was also suggested to be used as an alternative Deep Saline end-member in these sensitivity analyses as it introduces a higher variability in the concentration of Na, K, Ca, Mg, Cl, δ^2H and $\delta^{18}O$ (respect to the "Swedish" Deep Saline end-member) and also show very low dissolved sulphate concentrations in agreement with what has been observed in Forsmark.

In the Laxemar-Simpevarp area, the selection of the Deep Saline end-member is easier since the original composition given for this end member was determined from the more saline water sampled in Laxemar subarea. However, the dissolved sulphate in this end-member has values higher than 1,000 mg/L. These contents are the highest analysed up to now in any site studied within the framework of the Swedish and Finnish programs. Understanding the processes responsible for this peculiar character and their effects in the ulterior mixing processes with this end-member is, therefore, a key point in the construction of the conceptual model of the hydrogeochemical evolution of the site.

Geochemical simulations performed for the Laxemar-Simpevarp groundwaters (section 3.4.3) confirm that the more saline waters (Cl > 15,000 mg/L) are in equilibrium with gypsum and celestite through dissolution processes as the dilute waters mix with the Deep Saline end member (already in equilibrium with both phases).

Gypsum has been found in the fracture fillings at depths higher than 360 m, especially in the Laxemar subarea. According to Drake and Tullborg (2007, 2008), the paragenesis of gypsum, the relative temporal sequence of the different mineral associations and the stable isotopes suggest a hydrothermal origin (last crystallization stages) for this mineral and, therefore, an old age (Palaeozoic, several hundred million years ago). Therefore, gypsum has been available for reaction with groundwaters over a long time in the system, facilitating that long residence time waters (such as the Deep saline end member) reach equilibrium with this mineral phase. Once groundwaters reach equilibrium, the remaining gypsum would be stable in contact to the Deep saline end-member, which would justify the identification of this phase at depths where groundwaters have the highly saline character.

Table F-1. Final composition of the end-members selected for the mixing calculations in the Laxemar-Simpevarp and Forsmark areas. All the concentrations are in mg L^{-1}.

| | Deep Saline | | Littorina | Glacial | Glacial + Old meteoric | Altered Meteoric | |
	Laxemar	Forsmark				Forsmark #4919	Laxemar #10231
pH	8	8	7.6	–	–	7.12	8.17
Alkalinity	14.1	14.1	92.5	0.12	0.12	665.0	265.0
Cl	47,200	47,200	6,500	0.5	0.5	133	23.0
SO$_4$$^{2-}$	906.0	10	890	0.5	0.5	43.9	35.0
Br	323.66*	323.66*	22.2	–	–	0.529	b.d.l.
Ca	19300	19300	151	0.18	0.18	127	11.2
Mg	2.12	2.12	448	0.1	0.1	32.7	3.6
Na	8,500	8,500	3,674	0.17	0.17	156	110.0
K	45.5	45.5	134	0.4	0.4	12.5	2.97
Si	2.9	2.9	3.94	–	–	6.89	6.97
Fe(II)	–	–	0.002 (Fe tot)	–	–	–	–
δ^2H (‰)	–44.9	–44.9	–37.8	–158.0	–118	–78.6	–76.5
$\delta^{18}O$ (‰)	–8.9	–8.9	–4.7	–21.0	–16.0	–10.5	–10.9

* From a sampling 1994-Jan-17 at depth 1,392–1,670 m, in the same borehole, having C1 = 45.5 g/L. Bromide contents re-scaled (from 312 mg/L) to the higher salinity.

The behaviour of celestite is a bit more ambiguous. The obtained results (see section 3.4.4) indicate that celestite equilibrium during mixing between highly saline waters and old glacial meltwaters might be something apparent propagated from the equilibrium situation present in the Deep saline end member and favoured by the re-equilibrium with gypsum during mixing. However, this equilibrium situation in the end-member seems to be real although celestite has only been identified in a single fracture filling together with gypsum (KLX17A at 590 borehole length; Drake and Tullborg 2008).

Additional reasoning lines lead to this conclusion. **First**, analogue systems studied in the Canadian Shield (Gascoyne 2004 and Frape *et al.* 1984) display groundwaters in equilibrium with gypsum even for a range of salinity wider than that of Laxemar (subarea) groundwaters[75]. Figure F-1 shows celestite saturation indices (calculated using WATEQ4F[76] data base) for the two sets of groundwaters. Both reach clear equilibrium situations with respect to celestite although for different sulphate contents depending on their salinity. Some of these equilibrium situations with respect to celestite could also be apparent, but the truth is that the different Deep saline end members for these sets of waters are systematically in equilibrium with this mineral independently of their salinity.

Second, if the Deep saline end members are in simultaneous equilibrium with gypsum, calcite and celestite, the application of the Gibbs phase rule to the $CaCO_3$–$SrCO_3$–$CaSO_4$–$SrSO_4$ system (at constant T and P) indicates that these waters cannot be in equilibrium with strontianite ($SrCO_3$). At calcite, gypsum and celestite equilibrium, the strontianite saturation index is defined for a particular T and P by:

$$SI_{strontianite} = \log \frac{k_{calcite} \; k_{celestite}}{k_{gypsum} \; k_{strontianite}} \qquad \text{(F-1)}$$
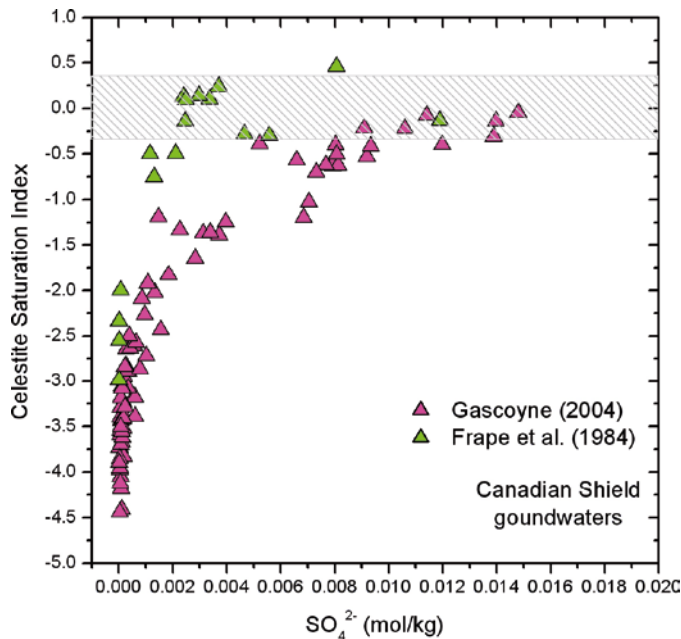
Figure F-1. *Celestite saturation indices with respect to celestite vs sulphate concentrations in some groundwaters from the Canadian Shield. Analytical data taken from Frape et al. (1984) and Gascoyne (2004).*

---

[75] The set of waters studied by Frape *et al.* (1984; Sudbury, Yellowknife, Thompson, etc) are, as a whole, more saline than the waters considered by Gascoyne (2004) including true brines with ionic strengths up to 9 molal.

[76] Sensitivity analysis to activity coefficient calculations has been performed using the Pitzer approach as the most suitable one for these very high saline groundwaters (see Appendix B). Saturation index results with the WATEQ4F database are in very good agreement with those obtained by the Pitzer approach.

Using thermodynamic data from WATEQ4F database (Ball and Nordstrom 2001), strontianite is expected to be undersaturated with values between –1.4 to –1.2 at temperatures from 25 to 15°C, respectively. Strontianite saturation index for the Deep saline end member in Laxemar-Simpevarp is –0.7 and for the most saline groundwaters from Lac du Bonnet (Canada, Gascoyne 2004) and the set of waters presented by Frape *et al.* (1984) is –0.68 and around –2.0, respectively. In spite of the uncertainties propagated by the problems associated with pH measurements (Appendix B), all these waters are clearly undersaturated with respect to strontianite, as expected from the simultaneous equilibrium with gypsum, calcite and celestite.

Therefore, the celestite equilibrium in the deep saline end member from Laxemar-Simpevarp (an in the other "similar "end members examined here) probably corresponds to a real situation. The implications of this fact should be considered in the study of the origin and evolution of these waters.

The calculations performed in previous sections lead to some considerations on the evolution of the Ca/Sr ratios in the saline groundwaters. In the case of the Laxemar-Simpevarp groundwaters, conservative mixing simulations and mixing with reaction simulations (sections 3.4.3 and 3.4.4) define an almost constant value all along the mixing path (Figure F-2) and they reproduce the observed situation in the real system for groundwaters with Cl > 0.1 mol/kg (Figure F-2, right).

Re-equilibrium with celestite during conservative mixing only varies the Ca/Sr relation from the original 104 value in the Deep saline end member to a maximum value of 111[77] which could be considered negligible. Therefore, one could say that the overall Ca/Sr relation is inherited, mainly, by mixing from the highly saline end member, in spite of the reaction processes affecting these elements. Only when the reequilibrium with gypsum is not effective and/or meteoric waters dominate the mixing proportion, the value for the ratio is considerably modified.

For Forsmark and, especially Olkiluoto, this ratio is locally modified at chloride concentrations from 3,500 to 5,500 mg/L due to the important Littorina contributions in these systems. But, again, the constant Ca/Sr value around 230 in the more saline groundwaters in Olkiluoto (Figure F-3) is apparently inherited from the deep saline end member in this area. In this case, the inheritance is mainly due to the mixing processes as the Olkiluoto groundwaters are clearly undersaturated with respect to gypsum and celestite.
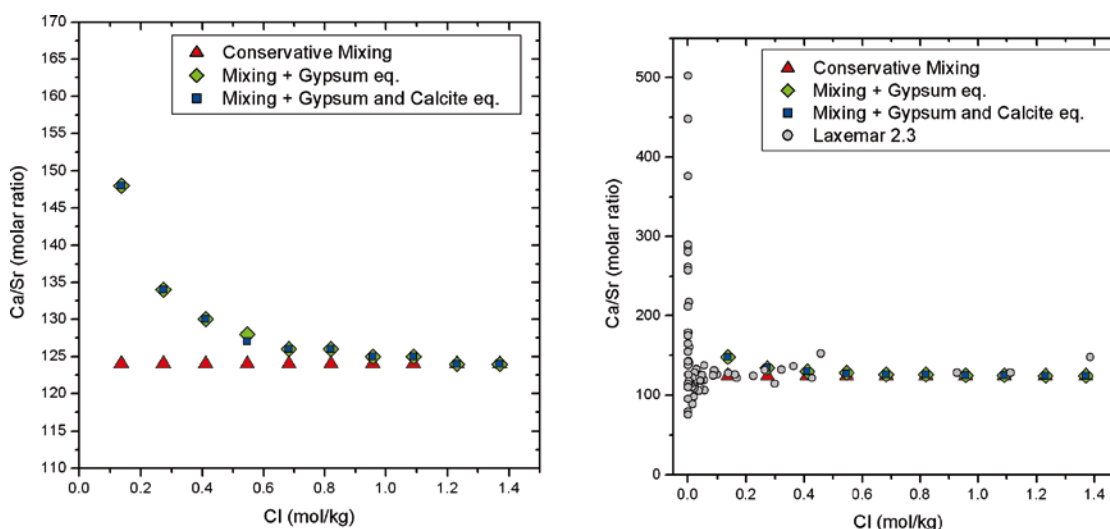
Figure F-2. *(left plot) Ca/Sr ratios with respect to chloride calculated for the different simulations: conservative mixing, mixing + gypsum equilibrium and mixing + gypsum and calcite equilibrium and (right plot) compared with the groundwater data for the Laxemar-Simpevarp area.*

---

[77] In the performed simulations the highly saline end member (sample #2731) has been previously equilibrated with calcite, gypsum and celestite; this is why the Ca/Sr relation is different from that observed in the groundwaters, around 120).
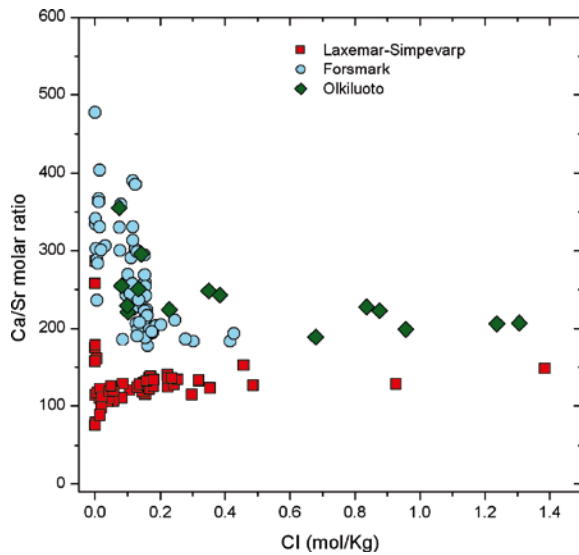
Figure F-3. *Ca/Sr ratios with respect to chloride for groundwaters from Forsmark and Olkiluoto compared with those from the Laxemar-Simpevarp area.*

A similar situation can be observed in the groundwaters from Lac du Bonnet Batholith (Canada) studied by Gascoyne (2004) and the brines studied by Frape *et al.* (1984). In these cases a relatively constant Ca/Sr value, around 160–240 and around 80–160, respectively is observed in the more saline groundwaters (Figure F-4) which are also in equilibrium with gypsum (see Appendix B, section B.3.2) and celestite (Figure F-1). These values are also inherited from the most saline groundwater found in their areas. Perhaps these results support the common origin suggested for these brines.

Another interesting observation comes from the comparison between the Ca/Sr in the fracture groundwaters with respect to the values found in the granite pore fluids. For instance, Ca/Sr values for the two pore fluid samples (with chloride contents around 55,000 mg/L) presented by Gascoyne (2004) ranges from 650–750, clearly different from the range in the more saline fracture groundwaters (around 160–240). However, speciation-solubility calculations performed with the pore fluids data presented by Gascoyne (2004) indicate that they are in equilibrium with gypsum, as it occurs with the saline end member, but clearly undersaturated with respect to celestite. If these pore fluids are equilibrated with celestite, the obtained Ca/Sr ratios are between 130 and 230, much closer to the one found in the saline groundwaters from fractures. More studies are needed to correctly interpret these results.
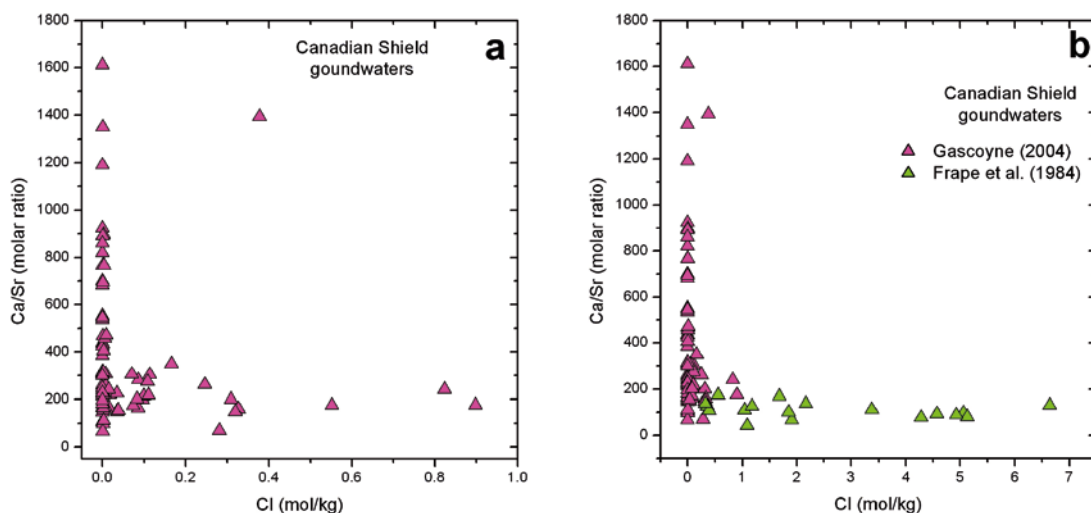
Figure F-4. *Ca/Sr ratios with respect to chloride in the groundwaters from Lac du Bonnet (a) studied by Gascoyne (2004) and from the different groundwater systems presented by Frape et al. (1984) in Canada (b).*

337

As a summary, apart from what was found in the previous review (Gimeno *et al.* 2008), thermodynamic calculations performed in Laxemar-Simpevarp area have provided interesting information on the geochemical characters of the Deep saline end member. This water seems to be in equilibrium with gypsum, celestite and calcite and it will have important consequences on the saturation state of these phases in groundwaters resultant of mixing with some percentage of this end member. These equilibrium situations are common to other deep saline waters in similar crystalline systems (e.g. Canadian Shield) but not in the Fennoscandian Shield. Therefore, these particularities must be taken into account when discussing the origin of the Laxemar-Simpevarp Deep saline groundwaters. Gypsum equilibrium appears to be one of the most distinctive characters of these groundwaters and, together with calcite and celestite equilibrium, may be used to constrain predictive mixing and reaction-path simulations.

Ca/Sr ratio in these very saline waters shows differences between the different examined groundwater systems. Therefore, compositional differences must exist in the end members of these systems (even between Laxemar-Simpevarp and Forsmark end members). However, these compositional differences are relatively constant over the mixing processes of these waters with other more dilute ones, remaining as a trace of the corresponding saline end member in spite of the reaction processes affecting both elements.

F.3   Glacial end member

The Glacial end-member represents the chemical composition of a melt-water from a previous glaciation (> 11000 BC). The composition adopted in the site investigation programme (Table F-1) corresponds to present melt-waters from one of the largest glaciers in Europe, the Josterdalsbreen in Norway, situated on a crystalline granitic bedrock (Laaksoharju and Wallin 1997). The major element composition of these waters is similar to that estimated by Pitkänen *et al.* (1999, 2004) in a model study of Olkiluoto (Finland).

Glacial melt-waters have a very low content of dissolved solids, even lower than present-day meteoric waters, and a very light isotopic signature, and they represent the chemical composition of surface melt-waters prior to water-rock interaction during infiltration in the basement.

The review presented in Gimeno *et al.* (2008) suggests the possibility of considering two different isotopic signatures for this Glacial end-member: (a) the one used up to now in the site characterisation studies ($\delta^{18}O = -21‰$ and $\delta^2H = -158‰$; Table F-1) and (b) a heavier isotopic signature ($\delta^{18}O = -16‰$ and $\delta^2H = -138‰$). With these two end-members part of the wide range of $\delta^{18}O$ values proposed by Kankainen (1986) for the glacial melt-waters is covered during uncertainty analysis. These two alternatives have also been considered in the Laxemar-Simpevarp mixing calculations.

The alternative "glacial" end-member with $\delta^{18}O = -16‰$ is not a pure end-member but a 50:50 mixture of a pure glacial melt-water with and an old meteoric water. This mixture corresponds to the groundwaters with the coldest isotopic composition found in the studied systems.

In the Laxemar-Simpevarp and Forsmark areas the composition of the groundwaters with a glacial component, is characterised by a relatively low salinity and a light isotopic signature (although not as light as the original Glacial end-member) but they have been extensively modified by mixing with waters of other origins. Therefore, there are no "undisturbed" glacial melt-water remnants that can be considered as a pure glacial mixing component modified only by water-rock interaction processes.

Nevertheless, the extent of the expected water-rock interaction processes during the infiltration of melt-waters may be inferred from the study of waters from other zones not affected by mixing. The review and compilation of data and studies carried out for the SKB site characterisation program, identifies groundwaters of glacial origin or of meteoric origin corresponding to climates colder than at present and high residence times (Table F-2).

Despite the fact that many of the sites studied in the Swedish program lack representative hydrochemical data (e.g. because of contamination with drilling water and/or other groundwaters), some indications of ancient glacial melt-water are apparent. For example, groundwaters below 500 m depth in Fjällveden seem to be residual melt-waters or alternatively meteoric waters from a colder climate (Wallin 1995, Tullborg 1997). A glacial origin for these groundwaters is suggested in the

Table F-2. Compositional data for different groundwaters from a glacial infiltration or simply cold waters in different zones in Sweden and Switzerland. pH and Eh data in the Swedish sites have been obtained from the continuous logging with Chemmac (only pH data in bold and italics correspond to values determined in laboratory). Chemical contents in mg/L.

	Fjallveden[1]		Gidea[2]	Lansjärv	Svartboberget		Switzerland	
	KFJ02 (#267)	KFJ07 (#372)	KGI04 (#194)	KLJ01 (#1410)	KSV04 (#116)	KSV04 (#122)	GTS [3]	Siblingen [4]
Depth (m)	605–607	542–544	404–406	237–500	430–436	630 –633	450	300–1500
Temp (°C)	–	–	–	–	–	–	12	up to 55
pH	8.9	9.2	9.3	9.2	9.1	9.1	9.6	7.6–8.1
Eh (mV)	–	–200	–200	–	–75	–150	–171	–30 to –250
Alk.	83.0	150.0	18	44.0	130.0	126.0	17.1	267–281
Cl	170.0	3.0	178	0.8	8.0	7.0	4.96	15–27
SO_4^{2-}	0.2	bdl.	0.1	4.4	1.2	0.8	5.8	128–146
Ca	12.0	10.0	21.0	7.7	17.0	17.0	6.61	9–12
Mg	0.8	2.0	1.1	1.2	2.0	1.9	0.05	0.4–1.4
Na	130.0	46	105.0	11.3	35.0	35.0	16.1	173–177
K	1.0	3.6	1.9	1.52	0.9	0.7	0.14	3.4–4.6
F	5.5	n.a	3.2	1.6	4.7	4.7	6.08	7.6–12
SiO_2	9.2	n.a.	10.05	7.9	9.2	15.7	11.9	–
Fe	0.34	0.51	0.07	0.01	0.25	0.27	0.06	bdl
δ^2H (‰)	–102.9	–	–99.4	–109.6	–95.0	–95.4	–	–85
$\delta^{18}O$ (‰)	–14.11	–	–13.63	–13.80	–13.0	–13.1	–	–11.9
Calcite SI	+0.24	+0.68	+0.14	+0.15	+0.80	+0.80	–0.13	
Fluorite SI	+0.14		–0.32	–1.27	–0.60	–0.60	+0.05	
Chalcedony SI	–0.18		–0.19	–0.28	–0.88	0.00	–0.13	
Quartz (R) SI	+0.20		+0.10	–0.08	–0.68	+0.20	+0.07	

(1) Wallin (1995), Tullborg (1997), Bath (2005).
(2) Wallin (1995).
(3) Grimsel Test Site (Switzerland; Degueldre, 1994).
(4) Sibinglen borehole in Switzerland (Thury *et al.*1994). It corresponds to the ranges used for the reference water in Kristallin-I (NAGRA, 1994).

work of Bath (2005) where "apparent" [14]C ages of around 12,000 to 14,000 years (i.e. late-glacial) are reported. At Gideå, there seems to be an indication of mixing between meteoric and post-glacial melt-waters (Wallin 1995). Finally, groundwaters in Lansjärv also show the isotopically light signature ($\delta^2H = -109.3$‰ and $\delta^{18}O = -13.8$‰) typical of glacial or old meteoric waters from colder climates.

Compared with the original composition of glacial melt-waters (see Glacial in Table F-1), all those Swedish waters have higher pH (≥ 9) and TDS values as a consequence of water-rock interaction. The differences are of orders of magnitude, especially for chloride, sodium and alkalinity. However, in spite of that, the final salt contents are still very low in absolute terms, even taking into account potential contamination. This means that, as expected, water-rock interaction modifies the compositional characteristics in a quite limited scale.

Similar conclusions have been obtained when analysing other cold meteoric and glacial waters in crystalline basements. For example, groundwaters from a recent meteoric origin at 450 m depth in the crystalline rocks of the Grimsel Test Site (Switzerland) are also very dilute (Degueldre 1994, Degueldre *et al.* 1996) similar to the ones observed in the Swedish groundwaters, Table F-2). Also in Switzerland, one of the waters selected as a reference water in the KRISTALLIN-I safety assessment, taken in the Siblingen borehole, represents an old water infiltrated during a cold climatic period 17,000 years ago and possibly during the last glaciation (Thury *et al.* 1994) and has exactly the same dilute characteristics as the Swedish groundwaters.

Therefore, these long residence time groundwaters still have very dilute characters. Compared with the dissolved concentrations of the Deep Saline and Littorina end-members the difference is huge. Thus, the lack of knowledge of the detailed composition of these glacial waters is not expected

to produce significant effects on the mixing and mass balance calculations with M3 and only the isotopic composition would be significant.

Although the identified groundwaters with glacial or cold meteoric origin in Table F-2 might have been affected by contamination with drilling water and/or with other groundwaters, speciation-solubility calculations allow obtaining some rough additional characters induced by the water-rock interaction processes.

Most of the groundwaters displayed in Table F-2 are in equilibrium with calcite but at extremely low pCO_2 values (log pCO_2 from -4.1 to -5.7). This character is in agreement with the theoretically deduced values in section 3.3.4 for the dilute groundwaters reaching higher depths and mixing with the already present saline groundwaters.

Except in one case, all the groundwaters are in equilibrium with fluorite and also with a silica phase like chalcedony or, especially, quartz with the solubility proposed by Rimstidt (1997). These equilibrium situations are reasonable considering the high residence time of these waters and they are common to those observed in the long residence time groundwaters from Laxemar-Simpevarp (or in the other crystalline systems presented in section 3.5).

These equilibrium situations may be assumed for the Glacial end-member in predictive mixing and reaction path calculations.

F.4 Littorina end member

The chemical composition of seawater during the Littorina stage has been selected as one of the end-members used in the hydrogeological and hydrogeochemical modelling of the Laxemar-Simpevarp and Forsmark sites, as well as in other Fennoscandian sites with a similar palaeogeographic evolution (for example, Olkiluoto in Finland; Pitkänen *et al.* 1999, 2004).

The Littorina stage in the postglacial evolution of the Baltic Sea started when the passage to the Atlantic Ocean opened through Öresund (in the southern part of the Baltic Sea) and seawater started to intrude at $\approx$ 6500 BC. The salinity increased until 4500–4000 BC, reaching estimated maximum values twice as high as modern Baltic Sea and this maximum prevailed at least from 4000 to 3000 BC. This period was followed by a stage where substantial dilution took place. During the last 2,000 years the salinity has remained almost constant to the present Baltic Sea values.

Based on shore displacement curves it is clear that the Forsmark area has been covered by the Littorina Sea for a long period of time (around 8,000 years). The low topography favoured that it reached several tens of kilometres further inland for a considerable part of that time and with maximum depths of around 60 m. The present meteoric recharge stage following uplift and emergence has only prevailed for the last 1,000 years.

The Laxemar-Simpevarp area, in contrast, was only partly covered by the Littorina Sea (with maxima depths around 15 m). Due to the topography of the area and the on-going isostatic land uplift, the Laxemar subarea was probably influenced only to a small degree, whereas the Simpevarp peninsula was covered for several thousands of years until its eventual emergence during uplift initiated a recharge of meteoric waters some 4,000 to 5,000 years ago (Smellie and Tullborg 2005). Therefore, groundwaters from most of these areas would have been affected by less saline marine intrusions over the time. This situation has important consequences when using the end-members for calculating the mixing proportions. In fact, one of the suggestions indicated in this work is to not use the Littorina end-member when dealing with conservative elements for the M3 calculations (see section 3.7), mainly for the Laxemar subarea groundwaters.

The Littorina Sea composition used in M3 calculations is shown in Table F-1. It is based on the maximum salinity estimation of 12‰ or 6,500 mg/L Cl (Kankainen 1986). The other main element concentrations were obtained by diluting the global mean ocean water (Pitkänen *et al.* 1999, 2004). Stable isotope composition assigned to the Littorina end member comes also from the $\delta^{18}O$ value ($-4.7‰$) proposed by Kankainen (1986) and from the δ^2H value considered by Pitkanen *et al.* (1999, 2004) for this end-member ($-37.8‰$).

Even though the use of an end-member representative of the maximum salinity stage is a simplification, it is reasonable since these waters would have the maximum capacity to penetrate the bedrock. Moreover, the contents of chloride, $\delta^{18}O$ and even sulphate, deduced from present groundwaters with high Littorina proportions in different sites are in reasonable agreement with the values proposed for the Littorina end member (Gimeno *et al.* 2008). Therefore, it seems that the Littorina end-member composition has been properly defined for the studied sites although different uncertainties are present.

The composition obtained using the above mentioned methodology corresponds to an old marine water prior to its infiltration into the groundwater system. Obviously, this compositional estimation presents uncertainties associated with the salinity variations with time (chloride contents, stable isotopes $-\delta^{18}O-$), and the compositional changes undergone by the marine water due to its reaction with the bottom sediments prior to its infiltration in the bedrock.

Uncertainties associated with the salinity variations were already assessed in Gimeno *et al.* (2008) where an alternative "Littorina end-member" was proposed to perform sensitivity analysis in hydrological or hydrochemical mixing calculations: the present composition of Baltic seawaters. Since the salinity and compositional characteristics of present Baltic waters are not homogeneous, the alternative end member proposed is the "average" Baltic seawater obtained by Pitkänen *et al.* (1999, 2004).

Here, a more detailed assessment of the uncertainties related to the compositional variations produced during infiltration of Littorina waters through the marine sediments is presented. In general, these changes do not seem to drastically decrease the most diagnostic elements for this end-member (SO_4^{2-} and Mg; Gimeno *et al.* 2008). However, these reactions may promote significant increases in other elements that may be used occasionally as Littorina indicators as well in the present groundwaters. This is the case of dissolved manganese, already identified in the previous work (Gimeno *et al.* 2008), and also alkalinity, dissolved SiO_2, potassium or NH_4^+. In groundwaters with Cl around 5,000 mg/L and a clear Littorina signature in the Laxemar-Simpevarp groundwaters and, specially, in Forsmark or Olkiluoto systems (with a much more important Littorina contribution) all these components show variable but high concentrations. This behaviour is clearly seen in their relations with Cl contents, as a vertical step defined by the waters with that chloride content, and all of them may be explained by diagenetic reactions with the marine sediments.

Variable and high dissolved ***manganese concentrations*** in brackish marine groundwaters from Laxemar-Simpevarp, Forsmark or Olkiluoto areas represent the inheritance of rhodochrosite formation during Littorina infiltration through the marine sediments (authigenesis of Mn-carbonates is an active process in the Baltic Sea since 7,000–8,000 year ago; Kulik *et al.* 2000, Neumann *et al.* 2002 and references therein) as it was discussed by Gimeno *et al.* (2008).

The high ***NH_4^+ concentrations*** found in some of these groundwaters with Littorina signature also represent an inherited character from their old marine signature. Seawater shows very low NH_4^+ concentrations, usually well below 0.05 mg/L in the available samples from the Baltic Sea. However, in marine sediments with organic matter, bacterial activity promotes the transformation of organic nitrogen compounds and the formation of NH_4^+, increasing ammonium concentrations with depth in the interstitial waters. It occurs as well in the present sediments of the Baltic Sea, where NH_4^+ concentrations from 4 to 16 mg/L are frequent (Carman and Rahm 1997).

The enrichment of ***potassium*** during infiltration of Littorina waters through marine sediments was already indicated by Gimeno *et al.* (2008) from a comparison between the composition of the Littorina end-member and interstitial waters found in Littorina sediments (data from Sjöberg *et al.* 1984).This enrichment is also found in the porewaters from sediments in the present Baltic Sea due to the breakdown of K-minerals such as K-feldspar or oligoclase, ubiquitous in the sediments of the Baltic proper (Carman and Rahm 1997 and references therein).

High ***silica concentrations*** can be acquired by marine waters when passing through bottom sediments with highly soluble diatom skeletons. The dissolution of these skeletons may lead to dissolved silica concentrations as high as 60 mg/L, as it occurs in sediment pore waters from the present Baltic Sea (e.g. Carman and Rahm 1997). Diatom ooze and diatomaceous muds are frequently present in the Littorina sediments (Burke and Kemp 2002 and references therein) and, therefore, variable

but high dissolved silica concentrations are expected in the Littorina marine waters recharging the groundwater system. These concentrations have been found in the aforementioned groundwaters with Cl around 5,000 mg/L in Forsmark and Laxemar-Simpevarp areas.

Finally, **alkalinity (HCO_3^-)** also shows "anomalously" high values in the groundwaters with Littorina signature. Average HCO_3^- contents in the present Baltic Sea are around 78.7 mg/L and the estimated value for Littorina waters is 92.5 mg/L (Table F-1), which is lower than the observed values in some of these groundwaters. However, during infiltration of the marine waters through sediments, biological activity promotes an important increase in HCO_3^- contents. For example, Carman and Rahn (1997) found HCO_3^- contents as high as 488 mg/L just 10 cm below the water-sediment interface in the present Baltic Sea.

As stated above, all these "indicators" are exclusively associated with groundwaters with a narrow range of chloride concentrations and with a clear Littorina contribution deduced by the classical diagnostic components (SO_4^{2-} and Mg). They are much more highlighted in the areas where Littorina contribution has been important (Forsmark, Olkiluoto) but there are still fingerprints in the Laxemar-Simpevarp area. Therefore, they can be considered as additional indicators of a marine component.

These components in the intruding Littorina groundwaters may have undergone different heterogeneous processes, or even mixing with the pre-existing waters, that might have decreased their high dissolved contents in greater or smaller extent, but not enough to completely mask their marine origin. Therefore, the typical diagenetic reactions in marine sediments provide additional diagnostic characters to identify Littorina contribution which can remain in the groundwaters in spite of their residence time.

The identification of these inherited characters has important consequences in the interpretation of the main geochemical processes in the groundwater systems, as additional microbial or water-rock interaction reactions in the bedrock are not needed to explain the high dissolved contents of these elements because the processes and mass transfers have happened mainly the initial evolution steps (marine sediments).

F.5   Altered Meteoric end-member

In previous modelling works with M3 a rain water sample called "Rain 60" or "Precipitation" has been used as the meteoric end-member (e.g. Laaksoharju and Wallin 1997, SKB 2004abc, 2006, Puigdomènech 2001). This water corresponds to a modern meteoric water with a modelled high tritium content that represents the rain water from 1960 (Laaksoharju and Wallin 1997). This end-member, with an extremely dilute character, presents the typical composition of rain water just before its interaction with the overburden. Therefore, it is not representative of the real recharge water after interaction with the shallower parts of the system.

To minimize this discrepancy, the ChemNet group has selected different samples representative of shallow groundwaters (less than 100 m depth) of recent meteoric origin after a short interaction with soils, overburden and granite in the studied areas. This is what has been finally called the "Altered Meteoric" (or sometimes "Dilute Granitic Groundwater") end-member.

The differences found between the hydrogeological systems and the possible recharge waters in Forsmark and Laxemar-Simpevarp support the decision of using two different Altered Meteoric end members for the modelling tasks (Table F-1).

For **M3 inverse calculations,** the performed sensitivity calculations indicate that the detailed composition of the selected Altered Meteoric end-member in each zone seems to be of little importance. Different dilute end-members with variable composition provide similar results and, therefore, any of the initially considered Altered Meteoric end-members could be used for M3 calculations. This can be attributed to the fact that the main effect of the Glacial and Altered Meteoric end-members in mixing is promoting dilution, independently of their detailed composition.

However, the detailed chemical composition of the selected Altered Meteoric end-member is much more important **in predictive (direct) calculations**, when transient periods -or local zones- without effective mixing are considered. The sensitivity analysis performed over calcium concentrations

(Gimeno *et al.* 2008, Auqué *et al.* 2006) indicates that the selection of a proper Altered Meteoric end-member is a critical issue in the dilution scenario predicted for the temperate period.

The results from the Monte Carlo method applied on the Forsmark set of groundwaters (Gimeno *et al.* 2008), indicate that all the elements except calcium are well constrained and most of them are compatible with the proposed composition of the Altered Meteoric end-member. Chlorine seems to be higher than the value presently used (< 181 mg/L) and the isotopes are again less negative than presently used, although the discrepancy is not large in any of the cases.

F.6   References

Auqué L F, Gimeno M J, Gómez J, Puigdomènech I, Smellie J and Tullborg E-L (2006). Groundwater chemistry around a repository for spent nuclear fuel over a glacial cycle Evaluation for SR-Can. SKB TR-06-31, 123 pp.

Ball J W and Nordstrom D K (2001). User's manual for WATEQ4F, with revised thermodynamic data base and test cases for calculating speciation of major, trace, and redox elements in natural waters. U.S. Geological Survey, Open File Report 91-183, USA.

Bath A H (2005). Geochemical Investigations of Groundwater Stability. SKI Report 2006: 12, 83 p.

Bath A H and Jackson C P (2002). Äspö Hard Rock Laboratory: Task Force on modelling of groundwater flow and transport of solutes. Review of Task 5. SKB IPR-03-10.

Burke I T and Kemp A E S (2002). Microfabric analysis of Mn-carbonate laminae deposition and Mn-sulfide formation in the Gotland Deep, Baltic Sea. Geochim Cosmochim. Acta, 66, 1589–1600.

Carman R and Rahm L (1997). Early diagenesis and chemical characteristics of interstitial waters and sediments in the deep deposition bottoms of the Baltic Proper. Journal of Sea Research, 37, 25–47.

Degueldre C (1994). Colloid properties in groundwaters from crystalline formations. NAGRA Technical Report 92-05. Nagra, Wettingen, Suiza, 96 p.

Degueldre C, Grauer R and Laube A (1996). Colloid properties in grantic groundwater systems. II. Stability and transport study. Appl. Geochem., 11, 697–710.

Drake H and Tullborg E-L (2007). Oskarshamn site investigation Fracture mineralogy Results from drill cores KLX03, KLX04, KLX06, KLX07A, KLX08 and KLX10A. SKB R-07-74, 132 p.

Drake H and Tullborg E-L (2008). Fracture mineralogy of the Laxemar site. Final report. SKB R-08-99.

Frape S K, Fritz P and McNutt R H (1984). Water – rock interaction and chemistry of ground-waters from the Canadian Shield. Geochim. Cosmochim. Acta, 48, 1617–1627.

Gascoyne M (2004). Hydrogeochemistry, groundwater ages and sources of salts in a granitic batholith on the Canadian Shield, southeastern Manitoba. Appl. Geochem., 19, 519–560.

Gimeno M J, Auqué L F, Gómez J B and Acero P (2008). Water-rock interaction modelling and uncertainties of mixing modelling. SKB R-08-86.

Gómez J B, Laaksoharju M, Skårman E and Gurban I (2006). M3 version 3.0: Concepts, methods, and mathematical formulation. SKB TR-06-27.

Gómez J B, Auqué L F and Gimeno M J (2008). Sensitivity and uncertainty analysis of mixing and mass balance calculations with standard and PCA-based geochemical codes. Appl. Geochem., 23 (7), 1941–1956.

Kankainen T (1986). Loviisa power station final disposal of reactor waste. On the age and origin of groundwater from the rapakivi granite on the island of Hästholmen. YJT-86-29, Nuclear Waste Commission of Finnish Power Companies, Finland.

Kulik D, Kersten M, Heiser U and Neumann T (2000). Application of Gibbs energy minimization to model early-diagenetic solid-solution aqueous-solution equilibria involving authigenic rhodo-chrosites in anoxic Baltic Sea sediments. Aquatic Geochemistry, 6, 147–199.

Laaksoharju M and Wallin B (Eds) (1997). Evolution of the groundwater chemistry at the Äspö Hard Rock Laboratory. Proceedings of the second Äspö International Geochemistry Workshop, Äspö, Sweden, June 6-7, 1995. SKB 97-04.

Laaksoharju M, Tullborg E-L, Wikberg P, Wallin B and Smellie J (1999). Hydrogeochemical conditions and evolution at the Äspö HRL, Sweden. Appl. Geochem., 14, 835–859.

Laaksoharju M, Gimeno M, Auqué L F, Gómez J, Smellie J, Tullborg E V and Gurban I (2004). Hydrogeochemical evaluation of the Forsmark site, model version 1.1. SKB R-04-05, 342 p.

Louvat D, Michelot J L and Aranyossy J F (1999). Origin and residence time of salinity in the Äspö groundwater system. Appl. Geochem., 14, 917–925.

Luukkonen (2001). Groundwater mixing and geochemical reactions. An inverse-modelling approach. In: A. Luukkonen and E. Kattilakoski (Eds.), Äspö Hard Rock Laboratory. Groundwater flow, mixing and geochemical reactions at Äspö HRL. Task 5. Äspö Task Force on groundwater flow and transport of solutes. Progress Report SKB IPR-02-41, SKB, Stockholm, Sweden.

NAGRA (1994). Kritallin-I safety assessment Report. Nagra Technical Report NTB 93-22E, Nagra, Wettingen, Switzerland.

Négrel P and Casanova J (2005). Comparison of the Sr isotopic signatures in brines of The Canadian and Fennoscandian shields. Appl. Geochem., 20, 749–766.

Neumann T, Heiser U, Leosson M A and Kersten M (2002). Early diagenetic processes during Mn-carbonate formation: evidence from the isotopic composition of authigenic Ca-rhodochrosites of the Baltic Sea. Geochim. Cosmochim. Acta, 66, 867–879.

Parkhurst D L and Appelo C A J (1999). User's Guide to PHREEQC (Version 2), a computer program for speciation, batch-reaction, one-dimensional transport, and inverse geochemical calculations. Water Resources Research Investigations Report 99-4259, 312 p.

Pitkänen P, Luukkonen A, Ruotsalainen P, Leino-Forsman H and Vuorinen U (1999). Geochemical modelling of groundwater evolution and residence time at the Olkiluoto site. Posiva report 98-10, 184 p.

Pitkänen P, Partamies S and Luukkonen A (2004). Hydrogeochemical interpretation of baseline groundwater conditions at the Olkiluoto site. Posiva report 2003-07, 159 p.

Plummer L N, Prestemon E C and Parkhurst D L (1994). An interactive code (NETPATH) for modelling NET geochemical reactions along a flow PATH-version 2.0. (Report USGS 95-4169), USGS, USA.

Puigdomènech I (2001). Hydrochemical stability of groundwaters surrounding a spent nuclear fuel repository in a 100,000 year perspective. SKB Technical Report 01-28, 83 p.

Rimstidt D D (1997). Quartz solubility at low temperatures. Geochim. Cosmochim. Acta, 61, 2553–2558.

Sjöberg E L, Georgala D and Rickard D T (1984). Origin of interstitial water compositions in postglacial clays (Northeastern Sweden). Chem. Geol., 42, 147–158.

SKB (2004a). Hydrogeochemical evaluation of the Simpevarp area, model version 1.1. SKB R-04-16, 398 p.

SKB (2004b). Hydrogeochemical evaluation of the Forsmark site, model version 1.1. SKB R-04-05, 342 p.

SKB (2004c). Hydrogeochemical evaluation for Simpevarp model version 1.2. Preliminary site description of the Simpevarp area. SKB-R-04-74, 463 p.

SKB (2005). Hydrogeochemical evaluation Preliminary site description. Forsmark area, version 1.2. SKB R-05-17, 403 p.

SKB (2006). Hydrogeochemical evaluation. Preliminary site description Laxemar subarea – version 1.2. SKB R-06-12, 435 pp.

Smellie J A T and Tullborg E-L (2005). Explorative analysis and expert judgement of major components and isotopes. Contribution to the model version 1.2 In: Hydrogeochemical evaluation. Preliminary site description. Forsmark area. Version 1.2. SKB R-05-17, 403 p.

Smellie J A T, Laaksoharju M, Wikberg P (1995). Äspö, SE Sweden: a natural groundwater flow model derived from hydrogeochemical observations. J. Hydrol., 172, 147–169.

Thury M, Gautschi A, Mazurek M, Müller W H, Naef H, Pearson F J, Vomvoris S and Wilson W (1994). Geology and Hydrology of the crystalline basement of Northern Switzerland. Synthesis of regional investigations 198-1993 within the Nagra Radioactive Waste Disposal Program. Nagra, Technical Report 93-01.

Tullborg E-L (1997). How do we recognize remnants of glacial water in bedrock?. In: L. King-Clayton, N. Chapman, L.O. Ericsson and F. Kautsky (eds.), Glaciation and hydrogeology. Workshop on the impact of climate change & glaciations on rock stresses, groundwater flow and hydrochemistry. Past, present and future. SKI Report 97:13.

Wallin B (1995). Paleohydrological implications in the Baltic area and its relation to the groundwater at Äspö, south-eastern Sweden. A literature study. SKB Technical Report 95-06, 68 p.

Wallin B and Peterman Z (1999). Calcite fracture fillings as indicators of paleohydrology at Laxemar at the Äspö Hard Rock Laboratory, southern Sweden. Appl. Geochem., 14, 953–962

Redox uncertainties

G.1   Introduction

Determination of the effective redox processes in an aquifer is usually an intensive task that needs the integration of very different type of data, including the analysis of some dissolved redox indicators and mineralogical and microbiological determinations.

The combined use of these data is intrinsically related to the classical redox zonation scheme (Champ *et al*. 1979, Thorstenson *et al*. 1979, Berner 1981, Stumm and Morgan 1996, Langmuir 1997, Kehew 2001, Appelo and Postma 2005). In this scheme, the sequential segregation of different terminal accepting processes (TEAPs) in separate zones during degradation of organic matter is thermodynamically explained in terms of Gibbs free energy yield. In the presence of multiple TEAPs, microorganisms are assumed to use the thermodynamically most favourable TEAP first until that species is exhausted and then other TEAPs are used sequentially in order of decreasing free energy yield for each reaction.

Organic matter reactivity is usually considered the ultimate engine that drives most redox reactions in aquatic systems (Appelo and Postma 2005) and, therefore, the microbial metabolisms (and the competition between metabolically distinct groups of microorganisms for metabolic intermediates; Lovley and Goodwin 1988) are at the base of these sequential successions of redox environments. In standard geochemical conditions (e.g. Stumm and Morgan 1996), the sequence of TEAP (or of metabolic groups) is assumed to be O_2 (aerobic bacteria) > NO_3^- (nitrate reducing bacteria, NRB) > Mn(IV)-oxides (manganese reducing bacteria, MRB) > Fe(III)-oxides (iron reducing bacteria, IRB) > SO_4^{2-} (sulphate reducing bacteria, SRB) > CO_2 (methanogenic microorganisms).

This sequence of metabolic reactions may change depending on the particular chemical environments (usually different from the standard conditions) in the studied system. However, the particular organization is assumed that can be determined by analysing:

- some dissolved redox indicators (those acting as terminal electron acceptors, TEA, and those produced in particular metabolic reactions: O_2, Mn(II), NO_3^-, Fe(II), SO_4^{2-}, S(–II), H_2 and CH_4),

- some key redox minerals (again, those acting as TEA like Fe(III) and Mn(IV) oxyhydroxides, or those formed as typical products of some metabolisms like iron sulphides), and their surface properties,

- or the *in situ* active metabolic groups.

These three approaches are tightly related and their results in each redox zone are usually integrated in the available classifications of redox environments, like the proposed by Berner (1981).

Although useful and widely used to identify and describe the redox evolution in a variety of aquatic systems (sediments, soils, aquifers), this sequential scheme of redox or biogeochemical zonation is not always observed to hold. There is substantial evidence from field studies suggesting that, under anoxic conditions, some TEAPs can be used simultaneously by distinct microorganisms, promoting different types of overlaps or the inexistence of a clear segregation between different redox zones (e.g. Postma and Jakobsen 1996, Jakobsen and Postma 1999, Thornton *et al*. 2001, Park *et al*. 2006, Jakobsen and Cold 2007).

This implies that the redox zonation scheme can be used as a "first" conceptual model but it must be verified in the systems under study. The simultaneous use of the aforementioned three basic methodologies to identify the active redox processes is especially important in this task. However, each approach shows its own uncertainties and some others arise when all the results are integrated. In this Appendix these uncertainties are discussed. Most of them are common to those found in other aquatic systems but some of them are more specific of the studied systems. The significance of the detected uncertainties are discussed inside the spatial frame provided by the redox zonation scheme from Berner (1981), usually employed in the hydrochemical and microbiological models for redox processes in the Finnish and Swedish programs (section G.4). As a result, some recommendations to avoid the detected problems and uncertainties have been made for future stages in the Site Descriptive Modelling (section G.5).

Hydrogen and methane data from the Laxemar-Simpevarp area are only sporadically commented in the main text as the available data are insufficient to properly use them in the evaluation of redox conditions and processes in the groundwater system. However, they are very important components as they are tightly related with different microbial metabolisms. Even, the hydrogen contents are at the base of the "Deep Biosphere" concept and they may also regulate the flow of carbon and electrons in virtually every step of the organic matter breakdown. Therefore, the available data for those gases, their uncertainties and their potential for the understanding of the overall redox conditions are also discussed in this Appendix (sections G.2.2 and G.2.3).

G.2   Dissolved redox indicators

Redox zonation in aquifer systems has frequently been identified in the same way as in classical works on marine sediments, i.e. by documenting the presence of redox sensitive parameters like O_2, $Mn(II)$, NO_3^-, $Fe(II)$, SO_4^{2-}, $S(-II)$ and CH_4 (Champ $et\ al$. 1979, Berner 1981, Thorstenson $et\ al$. 1979, Stumm and Morgan 1996, Langmuir 1997, Kehew 2001, Appelo and Postma 2005).

However, the study of aquifer systems usually presents technical difficulties associated to borehole and sampling activities, especially when reducing environments are investigated. These activities may result in the alteration of the pristine conditions at depth, as it is discussed below.

But, even assuming that these technical problems have been superseded, it is frequently difficult to delineate the dominant TEAP only by using hydrochemical data and this approach can drive to misleading interpretations, as it can occur in advective flow dominated systems (Chapelle 2001, Christensen $et\ al$. 2000, Appelo and Postma 2005). For example, dissolved methane is used to identify active methanogenesis; but methane produced in an active methanogenic zone can be transported over long distances by groundwater flow to non methanogenic zones. Therefore, the presence of dissolved methane might not mean that methanogenic activity is occurring in the sampled zone, but that it is taking place elsewhere (usually, upgradient) in the system (Chapelle 2001, Appelo and Postma 2005).

Under these circumstances, the most reliable method to identify the effective redox processes in aquifers is to analyse the consumption of electron acceptors (e.g. nitrate, sulphate, etc) and the production of reaction products (e.g. nitrite, sulphide, methane) along a segment of the flow path (Chapelle 2001, Kehew 2001).

However, specific flow paths can be very difficult to define in some hydrologic systems, especially if the scale of groundwater sampling is limited with respect to the spatial scale of the studied system. This situation is more complicated in the Swedish sites, with a long palaeohydrological history characterised by multiple mixing events, involving waters of contrasting features (end-members) that usually determine their own flow paths, resulting in the complex present situation: zones with active groundwater circulation, more or less isolated pockets of old mixing events, zones in apparent stagnant conditions, etc.

Transport or mixing processes, from natural or anthropogenic induced origin, may cause that the same groundwater sample contains, for example, ferrous iron, sulphide and methane, making the identification of the dominant redox processes more difficult: does the simultaneous presence of redox indicators reflect that different redox processes take place simultaneously in the same zone? or is it an artefact related to the transport of some of these indicators?.

But the question may be even more problematic, as other processes can promote the presence of dissolved redox indicators not directly related to microbial activities. These processes may exist independently (or overlapped) of the advective/mixing transport problems.

These processes may affect specifically to dissolved methane and hydrogen gases in the studied systems, as they may have an "unusual" (for other type of systems; e.g. soils, lake or sea sediments, shallow aquifers) inorganic origin (Figure G-1). Moreover, in common with which is observed in other systems, the rest of dissolved redox indicators ($Fe(II)$, $Mn(II)$) may also have a biogenic or inorganic origin, they may be affected by different overlaps between microbiological and inorganic reactions (e.g. $S(-II)$) or they may even show and inherited character from old diagenetic redox processes in marine sediments (e.g. $Mn(II)$ or NH_4^+ associated with Littorina contributions; see sections 4.4.4 and 4.5.2).
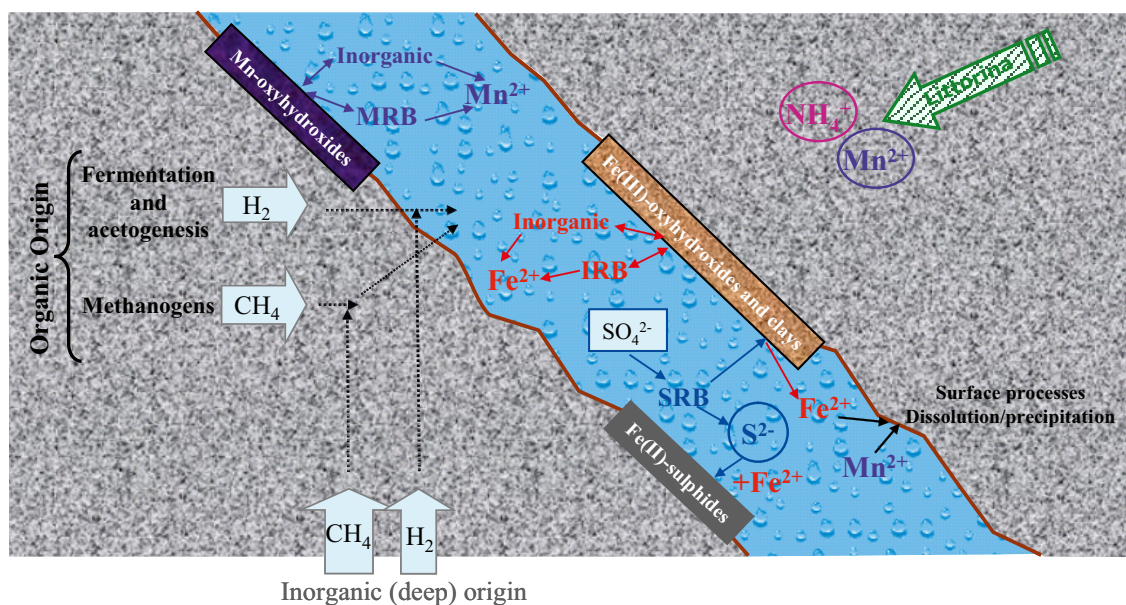
Figure G-1. *Simplified sketch on the origin and processes affecting the main dissolved redox indicators on a hypothetical fracture from the Laxemar-Simpevarp or Forsmark areas. Dissolved redox indicators in anoxic conditions, traditionally considered as by-products of on-going specified bacterial metabolisms, may really have both organic and inorganic origins. This is the case of CH_4 and H_2, important redox indicators and substrates for different metabolic activities. Additionally, Littorina inputs may contribute some dissolved redox indicators from "old" redox processes and, therefore, not active at present. Finally, inorganic reactions may affect some of the metabolic redox indicators (e.g. dissolved S(–II) may be eliminated by FeS precipitation or dissolved Fe(II) may be affected by surface processes).*

In this section, uncertainties associated to sampling disturbances, methane and hydrogen data, and overlapping between inorganic and organic processes for other dissolved indicators (Fe(II), Mn(II) and S(–II)) are presented.

G.2.1 Sampling disturbances: sulphide contents

Borehole and sampling activities in aquifers, especially when reducing environments are investigated, usually present different types of technical difficulties. The intrusion of oxygen, even in low amounts, can promote drastic decreases in the pristine concentrations of the reduced species that are diagnostic for redox zonation (e.g. Fe(II), S(–II), CH_4). Moreover, oxygen intrusion may alter the metabolic processes of strict anaerobes and, therefore, also the diagnostic products of their activities (see section G.3).

But even by ensuring the absence of oxygen input, pumping and sampling activities may promote disturbances in particularly redox-sensitive elements (e.g. dissolved sulphide) or induce more drastic effects by artificial mixing of different groundwaters with different redox indicators at the sampling point or by the total displacement of the existing groundwater at this point. Furthermore, the induced groundwater mixing may trigger different metabolic activities initially inactive.

A strict methodology, such as the one used in the Site Characterization Program, is needed to avoid or minimize these problems although it is very difficult to eliminate all of them. Therefore, much effort has been made to identify of, at least, some of these alterations of pristine conditions. For example, precipitation of poorly-crystalline iron oxyhydroxides, or their effects on the measured Eh, has been used to evaluate the existence of oxygen intrusion in some places at Forsmark (Gimeno *et al.* 2008).

On the other hand, special attention has been put on the evaluation of dissolved sulphide contents, as this component is of special concern in the performance assessment (it may promote corrosion processes in the canisters) but also, it is especially sensitive to the induced disturbances during drilling and sampling operations. With regard to dissolved sulphide concentrations, oxygen intrusion problems may promote:

a) Dissolved sulphide oxidation, decreasing or eliminating its presence.

b) SRB inactivation. These microbes are strict anaerobes that do not endure the presence of oxygen. Some SRB can survive in the presence of oxygen during a brief time interval but without metabolic activity (Konhauser 2007 and references therein). These effects will decrease the dissolved sulphide concentrations and affect the microbiological determinations.

c) Poorly-crystalline iron-oxyhydroxides precipitation. These phases may easily and quickly react with dissolved sulphide (Poulton *et al.* 2004) also decreasing or eliminating its presence. This effect can persist while the iron-oxyhydroxides are reactive, although the pristine SRB activity tends to recover.

Apart from the effects derived from oxidation, drilling waters may lead to a decrease in sulphide concentrations by dilution or by sulphide precipitation owing to the presence of dissolved Fe(II) in these drilling waters. Unfortunately, this last possibility cannot be evaluated as there are not Fe(II) analytical data for the drilling waters in the tables delivered by Sicada).

All these types of "theoretical" uncertainties appear to work in the same direction: detected dissolved sulphide concentrations would be minimized (or eliminated) from the studied sections. The analysis of data obtained in the monitoring program confirms this important subject. In the KLX15A borehole at 467 m depth, dissolved sulphide concentrations were well above detection limit (and even reaching 21.5 mg/L) during the monitoring program whereas, in the sample from this depth in the 2.3 data freeze, dissolved sulphide was below detection limit. In other boreholes sampled during the monitoring program, similar results were obtained. In KLX18A at 452 m depth with a dissolved sulphide concentration of 1.43 mg/L in the data freeze, values between 7.98 and 1.23 were measured during the monitoring period. In KLX019A at 414 m depth with an initial value of 0.027 mg/L S(–II), concentrations between 0.018 and 0.973 mg/L were measured during the monitoring. Furthermore, these observations are in agreement with the results obtained at the MICROBE site in the Äspö HRL experiments, where it was observed that the measured sulphide concentrations strongly depend on the flushing prior to sampling and on the time between consecutive samplings: frequent sampling and flushing lowered the sulphide concentrations (Hallbeck and Pedersen 2008a).

All these reasoning lines and empirical data indicate that the dissolved sulphide contents may be affected by different types of disturbances, lowering the measured concentration. Whereas this situation represents and obvious uncertainty, it also suggests that the number of groundwater samples with measurable dissolved sulphide concentrations in the Laxemar-Simpevarp area may be larger than available at present, which would reinforce even more the identified importance of the sulphur system and related processes.

In any case, the monitoring program developed in the last stages of the site investigations has been very useful to deal with the sulphide uncertainties related to borehole and sampling activities. Therefore, it is recommended to continue this methodology in future characterization works and enlarge the analysis to the rest of the dissolved redox indicators.

G.2.2 Methane contents

Methane contents are very low in the Laxemar-Simpevarp area. They are always below 1 ml/L and usually below 0.1 ml/L (the highest measured volume was 0.87 ml/L in the KLX03 borehole at 171 m depth; Figure G-2a) and they do not show any clear correlation with depth. The only exceptions are the four sections in KLX03, which show a decreasing trend with depth (Figure G-2a). Methane contents do not show either any correlation with the MPN (Most Probable Number) of methanogens (barely present in the Laxemar subarea; Hallbeck and Pedersen 2008b).

A similar situation can be observed for methane in the Forsmark area, also with very low contents (below 0.1 ml/L, except in the case of KFM01D borehole at 445 m depth where 4.2 ml/L was measured; Figure G-2b), without any evident correlation with depth or with the presence of methanogens (also detected in very low amounts, usually below 10 cell/mL; Hallbeck and Pedersen 2008c).

However, these observations in the Laxemar-Simpevarp and Forsmark areas contrast with those from other systems. For example, the available data in previous works performed in the Äspö groundwaters (Kotelnikova and Pedersen 1997ab) indicate the existence of higher methane contents (usually higher than 2 ml/L and reaching 20 ml/L), more or less homogeneously distributed in the range of 50–450 m depth. High MPN of autotrophic and heterotrophic methanogens were also found, with the numbers of autotrophic methanogens increased with depth (reaching $4.1 \cdot 10^4$ cells/mL) while heterotrophic methanogens decreased in number with depth (although still in significant levels, e.g. 100 cells/mL, at the maximum examined depth).

At Olkiluoto (Finland) methane contents (and also the total amount of dissolved gases) are much higher than in the Laxemar-Simpevarp and Forsmark areas. This is especially clear for the most saline and deepest Olkiluoto groundwaters, where methane represents the most abundant gas (Pitkänen and Partamies 2007) and its concentrations clearly increase with depth (Figure G-2c) from contents around 0.1 ml/L in the near-surface groundwaters to around 1,000 ml/L at 750 m depth (see also Figure 3-16 in Pedersen 2008). However, the detected amounts of methanogens in the Olkiluoto groundwaters were usually at or below the detection limits due to unclear causes (see the discussion by Pedersen 2008, pp. 102–103).

From this short review, it is clear that methane displays very different contents and trends in the compared systems and that the detected populations of methanogens appear to be also highly variable. Contrasting characters in the methane contents among different sites were also identified in the Finnish Shield by Pitkänen and Partamies (2007), who proposed a "lithological control" for the different contents found in the deeper groundwaters: strongly reducing nature of bedrock for systems with high methane contents and oxidising geological history, with abundant iron oxyhydroxides in fractures, for systems with low methane contents.

This hypothesis must be further explored as it is directly related to the different origins of methane in the studied systems, perhaps the main factor involved in the observed differences among the compared systems. Methane may be generated during organic processes (methanogenic microorganisms) but also during inorganic processes at depth in crystalline systems (Pitkänen and Partamies 2007; Hallbeck and Pedersen 2008bc and references therein). Inorganic methane may come from this deep source and move slowly by diffusion towards the surface, mixing with methane from biogenic origin.

The origin of this gas can be traced from its isotopic carbon signature (e.g. Pitkänen and Partamies 2007, and references therein) but there are no data available in Sicada. However, the available C1/(C2+C3) ratios in hydrocarbons can provide some insight on this subject. In the Laxemar-Simpevarp groundwaters, C1/(C2+C3) ratios indicative of a biogenic origin for methane are found in samples from KLX17A at 342 m depth and from KLX03 at 171 m and 380 m depth (these samples in KLX03 show the highest measured methane volumes; Figure G-2a). The ratios found in the other analysed sections indicate that most of the methane originates from an inorganic source, though some of the methane may have a biogenic origin (Hallbeck and Pedersen 2008b).

In the Forsmark area, C1/(C2+C3) ratios indicate that methane originates mostly from an inorganic source. The sample with the highest proportion of biogenic methane would correspond to KFM01D borehole at 445 m depth (Hallbeck and Pedersen 2008c), again the section with the highest volume of methane (Figure G-2b) measured in that area. In Olkiluoto, the use of isotopic data has allowed a more precise determination on the origin and distribution of methane. This gas seems to have two primary sources: a thermal origin from abiogenic hydrocarbons, predominant in the deepest groundwaters, and a bacterial origin, steadily increasing its importance towards the shallowest and CH_4-poored parts of the system (Pitkänen and Partamies 2007).

Figure G-2. *CH₄ contents vs depth in the Laxemar-Simpevarp area (a), Forsmark (b) and Olkiluoto (c) groundwaters. Data for Laxemar-Simpevarp and Forsmark have been taken from Hallbeck and Pedersen (2008bc, respectively) and for Olkiluoto from Pitkänen and Partamies (2007).*

Therefore, methane from biogenic and abiogenic sources is present and "mixed" in the Laxemar-Simpevarp and Forsmark groundwaters. However, the sparseness of data for the examined rock volume, especially in the Laxemar subarea, prevent from observing any clear variation trend. This represents a serious limitation in the understanding of the redox system as methane is a chemically active gas that may participate or control the redox state of the groundwater system at different depths, under different conditions and with variable rates or intensities depending on its origin.

Moreover, methane is a substrate for different metabolic activities (it may be used, for example, by methanotrophs in oxic conditions, or oxidised by sulphate reducing bacteria, in anoxic conditions; e.g. Kotelnikova 2002 Pitkänen *et al.* 2004) and the oxidation of methane has been considered a significant process for oxygen reduction in oxygen intrusion scenarios (Puigdomènech 2001).

All these circumstances highlight the need for more data of methane and hydrocarbons (including their stable isotope compositions) in order to clarify their origin and distribution in the studied systems and to fill these important gaps in the overall understanding of the redox processes. On top of that, methodological improvements for sampling procedures are also needed (see Hallbeck and Pedersen 2008bc).

G.2.3   Molecular hydrogen contents

The available data on the hydrogen contents in the Laxemar-Simpevarp groundwaters are very scarce. From the thirteen performed analysis, only five led to hydrogen concentrations above the detection limit of the used technique (a thermal conductivity detector; Hallbeck and Pedersen, 2008b). The detectable amounts of hydrogen, from 0.046 to 0.19 ml/L (1.8 to 8.48 μmol/L) were found between 242 and 700 m depth in KSH01A, KLX03 and KLX08 boreholes (Figure G-3a) without any trend with depth.

The available data are also very scarce in the Forsmark area (only six samples from the sixteen analysed were above the detection limit; Hallbeck and Pedersen 2008c). The detected values were in the range of 0.0054 to 0.22 ml/L (0.24 to 9.82 μmol/L) and the maximum amounts (at depths between 400 and 900 m depth; Figure G-3b) were similar to those found in the Laxemar and Simpevarp subareas.

Previous available data from Äspö (Kotelnikova and Pedersen 1997ab) indicate the presence of hydrogen in ten of the twelve examined sections (with contents from 0.045 μmol/L to 50 μmol/L) with the maximum amounts found near the deepest examined levels (around 400 m).
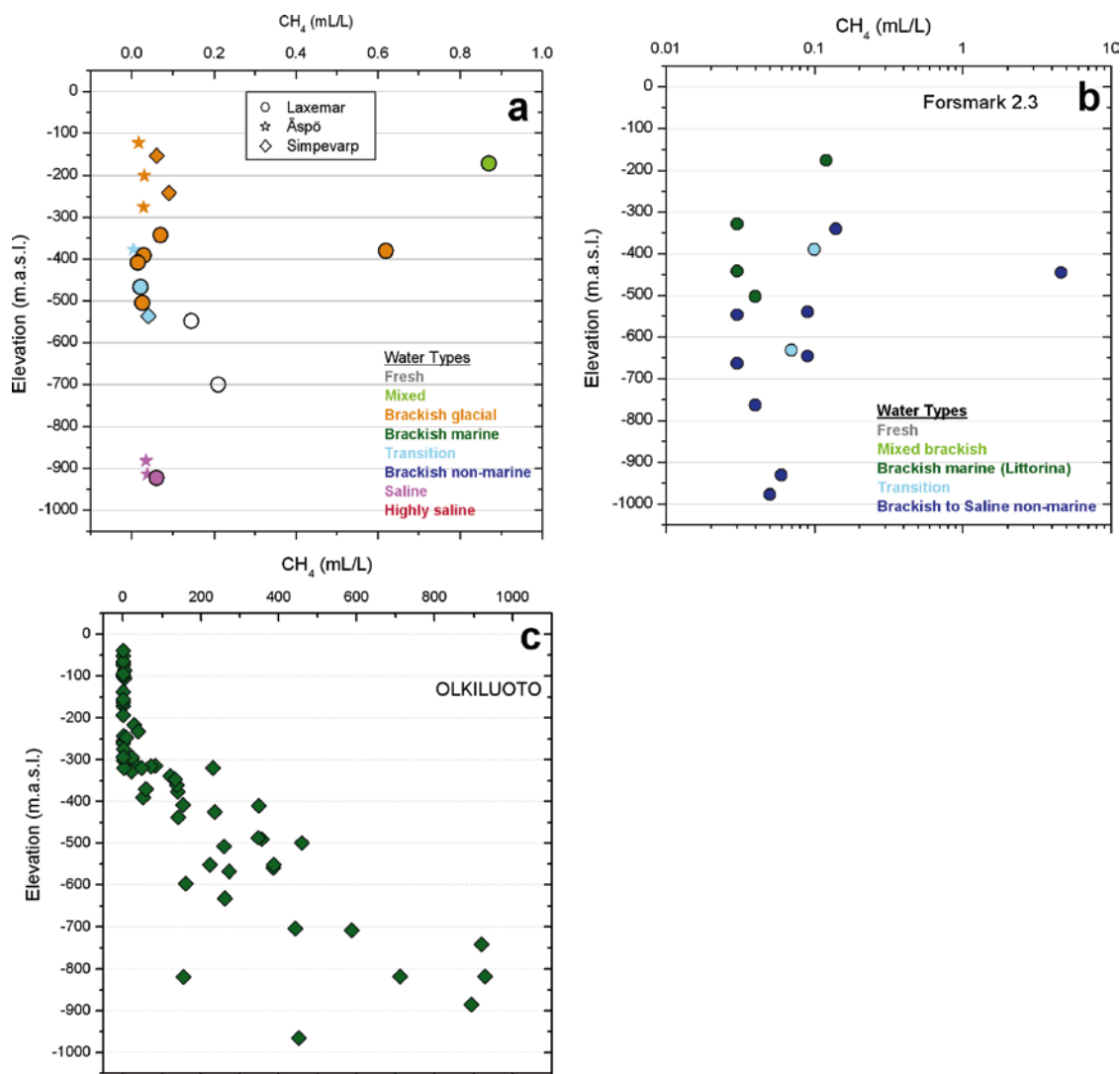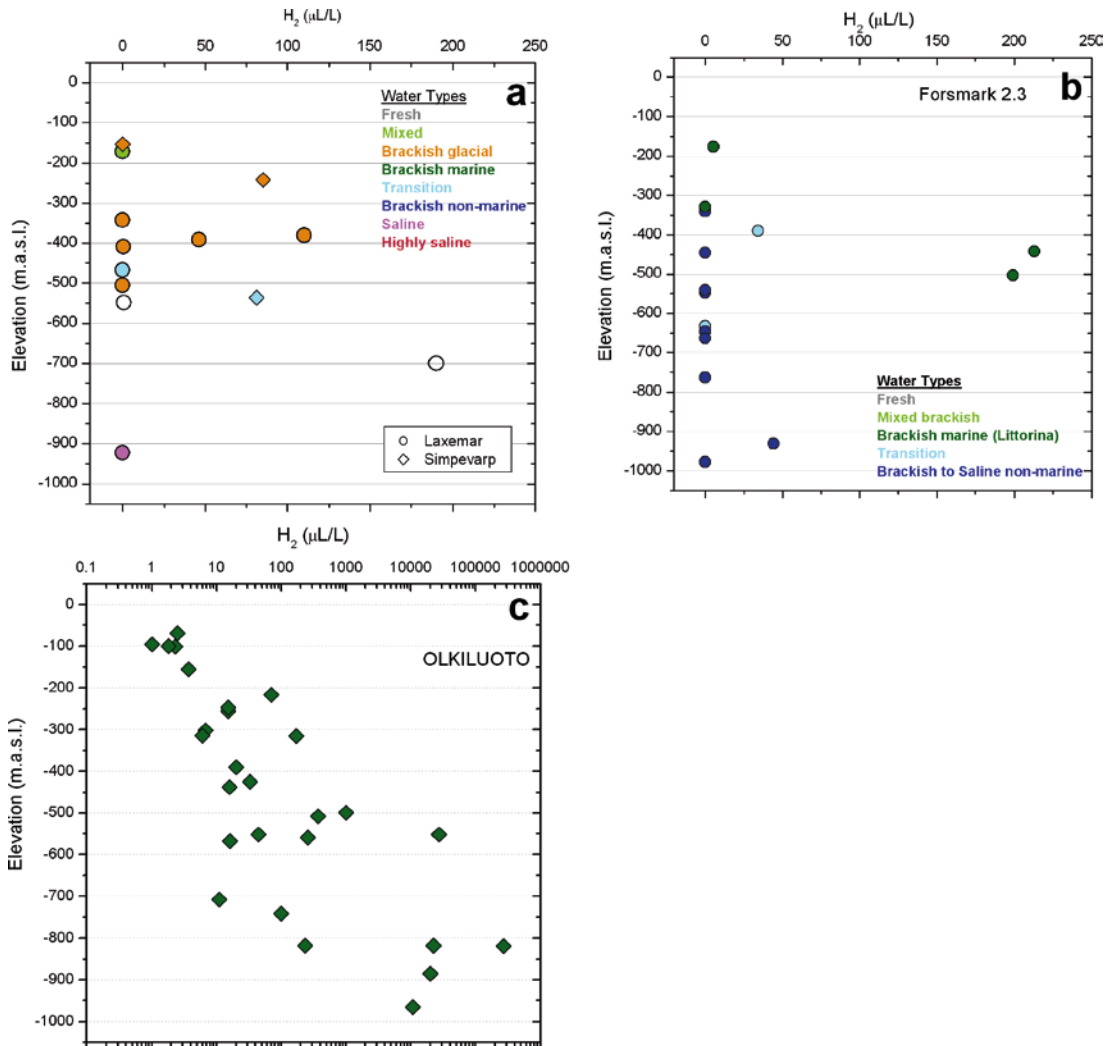

Figure G-3. *H2 contents vs depth in the Laxemar-Simpevarp area (a), Forsmark (b) and Olkiluoto (c) groundwaters. Data for Laxemar-Simpevarp and Forsmark have been taken from Hallbeck and Pedersen (2008b, c, respectively) and for Olkiluoto from Pitkänen and Partamies (2007).*

At Olkiluoto, the latest data presented by Pedersen (2008) show a rough increase of hydrogen contents with depth, reaching maximum values of 0.08 ml/L (around 3.5 µmol/L) in the examined depths (down to 742 m). Much higher contents were found at higher depths by Pitkänen and Partamies (2007), with concentrations from 10 to 22 ml/L (450 to 980 µm/L) at 800–1,000 m depth interval (Figure G-3c).

Overall, the detected amounts of hydrogen in all the above systems are usually several orders of magnitude higher than the maximum values (from biogenic origin) found in marine sediments, soils or shallow aquifers (usually, around 50 nM; Lovley and Goodwin 1988, Hoehler *et al*. 1998, Christensen *et al*. 2000, Lin *et al*. 2005), but in the range of the observed values in the groundwaters of crystalline shields (Lin *et al*. 2005 and references therein). The high values detected in these crystalline systems are related to the contribution of an abiogenic source of hydrogen (additional to that of biogenic origin) which may have been generated by, at least, six different inorganic processes (e.g. Hallbeck and Pedersen 2008bc).

The heterogeneity and variability in the distribution of hydrogen contents observed in the compared systems may be associated with the coexistence of both biogenic and abiogenic sources but also to the strong coupling of hydrogen with a very wide spectrum of interrelated microbial activities. It is well known, for example, that hydrogen is an excellent electron donor for a large number of microbial metabolisms, including methanogenesis, acetogenesis, sulphate reduction, iron reduction, manganese reduction, etc (Postma and Jakobsen 1996, Hoehler *et al*. 1998, Christensen *et al*. 2000, Appelo and Postma 2005).

Two main issues arise. First, hydrogen concentrations from pure biogenic origin in natural systems are usually much lower than the detection limit used in the Laxemar-Simpevarp and Forsmark areas. This situation affects most of the analysed samples for hydrogen in these areas and it may represent an important gap in the knowledge of metabolic-induced redox processes, as briefly discussed below (*Importance of low hydrogen contents*). Second, the existence of an additional (inorganic) source of hydrogen could affect the intensity and distribution of the metabolic activities in the system. This subject is also discussed below (*Importance of high hydrogen contents*).

Importance of low hydrogen contents

In the degradation sequence of organic matter, biogenic molecular H_2 and simple organic molecules (e.g. acetate) are continuously produced by fermentative bacteria (and also heterotrophic acetogens; see reaction G-8) from complex organic compounds that, in turn, are metabolised by other microorganisms using different TEAs, lowering the hydrogen concentrations. This way, for example, dissimilatory iron reducing bacteria can reduce iron oxyhydroxides using acetate (reaction G-1) or hydrogen (reaction G-2) as electron donors:

$$CH_3COO^- + 8FeOOH + 17H^+ \rightarrow 8Fe^{2+} + 2CO_2 + 14H_2O \tag{G-1}$$

$$4H_2 + 8FeOOH + 16H^+ \rightarrow 8Fe^{2+} + 16H_2O \tag{G-2}$$

Similarly, sulphate reducing bacteria can reduce the dissolved SO_4^{2-} through the reactions:

$$CH_3COO^- + SO_4^{2-} + 3H^+ \rightarrow H_2S + 2CO_2 + 2H_2O \tag{G-3}$$

$$4H_2 + SO_4^{2-} + 2H^+ \rightarrow H_2S + 4H_2O \tag{G-4}$$
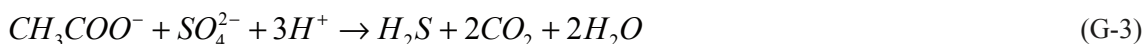
and methanogens can also use acetate or hydrogen through the reactions:

$$CH_3COO^- + H_2O \rightarrow CH_4 + HCO_3^- \tag{G-5}$$

$$4H_2 + CO_2 \rightarrow CH_4 + 2H_2O \tag{G-6}$$

The degradation of complex organic compounds by fermentative bacteria would become thermodynamically unfavourable unless fermentation products (e.g. H_2) are kept low. The concentration of these fermentation products are controlled by the microorganisms carrying out the TEAP (Postma and Jakobsen 1996, Christensen *et al.* 2000) and the relation between fermenters and consumers of fermentation products represent a mutually beneficial metabolic association. That's why the maximum hydrogen concentrations measured to date are very low (the aforementioned 50 nM).

But microorganisms mediating different TEAPs compete for the same "limited substrates" and for the energy supplied by the oxidation of H_2 or acetate. Reactions with a high-energy gain are able to bring down the electron donor concentrations, such as H_2, to a lower level than reactions with a lower energy gain. This way, for example, SRB may be metabolically active by using lower concentrations of H_2 than methanogenic bacteria and, therefore, SRB can exclude methanogens from being active by lowering the H_2 concentrations.

These effects were tabulated by Lovley and Goodwin (1988) for hydrogen as different TEAPs appear to have a characteristic H_2-utilisation efficiency, initially related to microbial physiology. This H_2-utilisation efficiency corresponds, in decreasing order to NO_3^--reduction, Fe(III)-reduction, SO_4-reduction and methanogenesis. The sequence of different electron accepting processes would proceed as predicted by equilibrium thermodynamics in the classical redox zonation scheme.

This approach is known as the *competitive exclusion* (CE) concept and it implies that, in steady-state redox systems[78] limited by the availability of organic matter, each anaerobic metabolism is characterised by a well-defined range of hydrogen concentrations. Therefore, hydrogen concentrations may be used as a diagnostic value to identify the dominant redox processes in a particular location of the system. Empirical steady-state H_2 concentration ranges for each TEAP have been obtained from field studies: NO_3^--reduction < 0.1 nM; Fe(III)- reduction, 0.2–0.8 nM; SO_4^{2-} reduction, 1–4 nM; methanogenesis, 5–30 nM.(e.g. Christensen *et al*. 2000, Chapelle 2001)

This approach is not a definite one and the simple relationship between hydrogen concentrations and the corresponding TEAPs is not always observed to hold (Jakobsen and Postma 1999, Park *et al*. 2006). However, hydrogen concentration is a very valuable tool in analysing the energetics of the microbial processes, enabling its integration in a thermodynamically based description (Hoehler *et al*. 1998, Christensen *et al*. 2000).

Since the initial work by Lovley and Goodwin (1988), this approach has became a classical one in text books (e.g. Chapelle 2001, Kehew 2001) and has been widely used to differentiate predominant TEAP in anaerobic aquifers (Christensen *et al*. 2000 and references therein). In the Laxemar-Simpevarp or Forsmark areas the UZ group has not used this method due to the unavailability of hydrogen analyses at the nanomolar scale. Taken into account the complexity of the redox processes, it would be advisable to improve the detection limits for hydrogen and to explore the nanomolar range of this component in the studied systems.

Importance of high hydrogen contents

The hydrogen contents from abiogenic sources in the Swedish and Finnish programs support the idea of a deep, hydrogen-driven biosphere in crystalline systems (Pedersen 1993, 1997ab). Hydrogen is the critical component to sustain the postulated autotrophic organisms in the base of the food chain in this deep biosphere (autotrophic acetogens and methanogens able to combine hydrogen with carbon dioxide to obtain energy and synthesize organic matter).

As discussed in the previous section, hydrogen may play a fundamental role in the regulation of many other microbial activities and, thus, of the redox conditions at shallower levels. For example, acetogens (heterotrophic and autotrophic) are the dominant microorganisms in all the studied sections in the Laxemar-Simpevarp and Forsmark areas (their MPN were often one or two orders of magnitude higher than the second most common organism type; Hallbeck and Pedersen 2008bc). As stated above, autotrophic acetogens produce acetate using hydrogen as electron donor:

$$4H_2 + CO_2 \rightarrow CH_3COO^- + H^+ + 2H_2O \qquad \text{(G-7)}$$

whereas heterotrophic acetogens may ferment sugars, fatty acids and aromatics to acetate and H_2 via a pyruvate intermediate (Konhauser 2007):

$$2C_3H_3O_3^- \, (pyruvate) + 2H_2O \rightarrow 2CH_3COO^- + 2CO_2 + 2H_2 \qquad \text{(G-8)}$$

---

[78] A steady-state redox situation implies that there is no net bacterial population growth. For example, a system shifting from Fe-oxide reduction to sulphate reduction as Fe-oxide reactivity decrease is in a non steady-state microbiological state (Jakobsen and Postma 1999). If the system changes as the reactivity of the minerals and the organic matter in the system change, but reaction rates are low compared to the flow rate, the system is in a steady-state or quasi-steady-state (Jakobsen and Cold 2007).

Therefore, acetogens may represent a source or a sink of hydrogen in the system, depending on the dominance or on the relative rates of their autotrophic and heterotrophic metabolisms. High hydrogen concentrations could inhibit fermentative activity (Chapelle 2001, Lin *et al.* 2005) and probably heterotrophic acetogenesis (reaction G-8), reducing then the availability of simple organic molecules for the respiratory activity of non-fermenting heterotrophs (e.g. reactions G-1, G-3 and G-5). On the other side, high hydrogen concentrations could favour autotrophic acetogenesis (reaction G-7), replacing the source of simple organic molecules and helping heterotrophic metabolisms to develop.

Moreover, if hydrogen is present in large concentrations, it may diminish the tendency of redox processes to segregate into different zones, as it occurs, for example, in petroleum-hydrocarbon aquifers (Chapelle 2001). Under these conditions, competition between heterotrophic organisms is very low due to the high amounts of electron donors (hydrogen or acetate produced by acetogens; see reaction G-1 to G-6). As a result, concomitant activity of different heterotrophic microorganisms, mediating different TEAPs, is possible (if the electron acceptors are available; Chapelle 2001).

Therefore, the effects of high hydrogen concentrations on the metabolic processes are very important and they must be further studied taken into account their effects on both autotrophic and heterotrophic microorganisms.

Implications

Abiogenic and biogenic sources of hydrogen in the studied systems are of major concern because hydrogen concentrations are determined by (and may determine) most of the proposed microbiological metabolic activities in the groundwaters. Hydrogen may not only couple oxidative and reductive processes, but also regulate the flow of carbon and electrons in virtually every step of the organic matter breakdown (Hoehler *et al.* 1998) and of the overall food chain emanated from the "Deep Biosphere" concept.

Autotrophic methanogens and, especially, acetogens, can metabolise abiogenic hydrogen gas to create a background level of suitable organic carbon, like acetate, in crystalline groundwater systems (Pedersen 2001, Lin *et al.* 2005). Since the produced acetate can be used by different heterotrophic organisms, the intensity of all these chained processes may depend on the inflow rate of hydrogen. High hydrogen concentrations may favour (indirectly, through acetate production by acetogens or, directly, as electron donor for a wide number of metabolic activities) the concomitant activity of different TEAPs, blurring the limits among different redox zones.

On the other hand, nanomolar concentrations of biogenic hydrogen, as an intermediate species of biodegradation pathways for organic matter, may be used as a diagnostic value to identify the dominant redox processes in a particular location of the system and to obtain the energy yield of the different TEAPs (Hoehler *et al.* 1998, Jakobsen and Postma 1999, Christensen *et al.* 2000). It would be necessary to analyse other intermediate species in the degradation of organic matter (like acetate, formate, etc) to extend this type of calculations.

The energy yield (Gibbs free energy, ΔG_r) of the TEAPs, using an adequate substrate (e.g. hydrogen, acetate, formate, etc) must be calculated explicitly from the concentrations and activities of the involved reactants and products in the studied systems (e.g. Jakobsen and Postma 1999, Park *et al.* 2006). The obtained energy for each TEAP is then compared with the respective thresholds of energy requirement for the reaction to proceed (a threshold energy level exists for the TEAPs, corresponding to the minimum energy necessary for microorganisms to store the gained energy as ATP; e.g. Hoehler *et al.* 1998, Jakobsen and Postma 1999). It is presumed that all TEAPs characterised by a free energy value lower than the threshold value may be active. Therefore, this may be a test to identify the potentially active TEAPs in each portion of the system and, ideally, a judgement of the possibility of a redox segregation (if only one redox process is predominant in each zone) or not (if different processes may occur concomitantly).

G.2.4 Overlaps between microbiological and inorganic reactions

Many biological and inorganic reactions occur in close proximity and even with mutually exclusive effects (e.g. elimination of dissolved sulphide by FeS precipitation). This situation makes very difficult the discrimination between the organic and inorganic reactions taking place and the identification of their effects on each type of reaction in the bulk chemical analysis (Canfield *et al.* 1993).

Many of the main redox indicators (Mn(II), Fe(II) and S(–II)) may be affected by inorganic surface processes, acting as sources or sinks depending on the geochemical conditions. Moreover, many important and fast inorganic reactions between some electron acceptors and metabolic reaction products are known, such as the reaction between iron oxyhydroxides and dissolved sulphides (Pyzik and Sommer 1981, Yao and Millero 1996, Poulton *et al.* 2004), according to

$$H_2S + 2FeOOH + 4H^+ \rightarrow S^0 + 2Fe^{2+} + 4H_2O \qquad \text{(G-9)}$$

the reactions between manganese oxides and dissolved sulphides (Yao and Millero 1993)

$$H_2S + MnO_2 \rightarrow S^0 + Mn^{2+} + 2OH^- \qquad \text{(G-10)}$$

$$H_2S + 4MnO_2 + 2H_2O \rightarrow SO_4^{2-} + 4Mn^{2+} + 4OH^- \qquad \text{(G-11)}$$
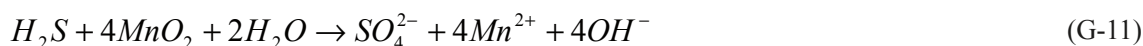
or between dissolved ferrous iron and manganese oxides (Postma 1985, 1993, Postma and Jakobsen 1996)

$$2Fe^{2+} + MnO_2 + 2OH^- \rightarrow 2FeOOH + Mn^{2+} \qquad \text{(G-12)}$$
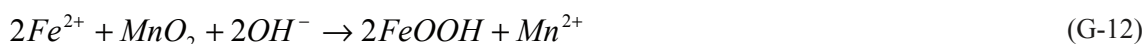
The existence of these fast abiotic reactions implies that microbes which use iron or manganese as terminal electron acceptors will often have to compete for the metals with those reactions. Besides, the existence of these abiotic reactions may have important implications in the interpretation of the dissolved redox indicators.

Mn(II) may be produced not only by direct dissimilatory manganese reduction carried out by MRB but also by the inorganic Mn(IV) reduction by the Fe(II) (reaction G-12) or by the H_2S (reactions G-10 and G-11) generated during Fe(III) reduction by IRB (Nealson *et al.* 1988) and sulphate reduction by SRB, respectively. Therefore, caution must be exercised when interpreting the presence of Mn(II) in the groundwaters, as the identification of dissolved Mn(II) does not necessarily indicate the existence of activity of MRB[79].

The identification of dissolved Fe(II), as indicative of an active dissimilatory iron reducing activity, must be also carefully evaluated. The inorganic reductive dissolution of iron oxyhydroxides by the dissolved sulphide generated by SRB (sulphidisation of iron minerals) is also a very usual process in some systems. Sulphidisation proceeds via the oxidation of dissolved sulphide at the mineral surface, followed by the release of the produced Fe(II) to solution and its subsequent reaction with additional dissolved sulphide to produce FeS (Pyzik and Sommer 1981, Yao and Millero 1996, Poulton *et al.* 2004):

$$Fe^{2+} + H_2S \rightarrow FeS + 2H^+ \qquad \text{(G-13)}$$

These processes would imply that the simultaneous identification of dissolved Fe(II) and S(–II) does not necessarily indicate the concomitant activity of IRB and SRB. Even more, reductive dissolution of ferric oxyhydroxides and precipitation of iron sulphides may consume all the dissolved sulphide, masking the most clear chemical effect of the sulphate reducing activity.

To deal with this type of problems, an integrated analysis (combining the evaluation of the relative amounts of dissolved redox indicators, the results of speciation-solubility calculations, the microbiological data and the mineralogical data on the solids acting as terminal electron acceptors) is needed. However, some of these data are still unavailable or they show different types of uncertainties as it is shown in the following sections.

G.2.5 Discussion

Analysing redox-sensitive species in groundwater samples is a simple and useful method for identifying the redox conditions and it has been successfully applied for characterisation of redox environments in aquifers. However, it has important limitations, some of them common to most aquifer systems and others more specific to the characters of the crystalline systems under study.

---

[79] Some dissolved organic components (e.g. siderophores) can also reduce MnO_2 inorganically at very fast rates (Stone and Morgan 1984). Moreover, in the studied systems, Mn(II) may show and inherited character from old diagenetic redox processes in Littorina marine sediments.

Modifications of the pristine redox dissolved indicators associated to borehole and sampling activities must be, at least, minimized to obtain reliable data. For the definition of the dominant redox processes or the assignment of redox zones (with their possible overlaps) a high spatial resolution in the sampling network, short screens, and small sample volumes are crucial in order to avoid mixing of groundwater from different redox zones (Christensen *et al.* 2000).

This need is especially critical in systems where horizontal and vertical variations may be significant, like the fractured crystalline systems studied in the Site Characterization Program. Their complex palaeohydrological history favours the existence of hydrogeochemical systems with local heterogeneities containing probably different redox environments. These characters preclude, at present, the use of the changes in concentration of redox-sensitive species along clear flow paths or the estimation of the dominant electron acceptor processes.

Some other uncertainties must be taken into account when using dissolved redox indicators. The major limitations of this approach in the studied systems are related to (a) the migration of the redox species away from active zones, (b) the presence (and migration) of redox indicators of inorganic origin and (c) the existence of inorganic geochemical processes representing an additional source or sink for these indicators.

These uncertainties critically affect the usual relationship established between the presence of dissolved indicators (e.g. Mn(II), Fe(II) or CH_4) and the existence of the corresponding microbiological processes (e.g. Mn(IV), Fe(III) reduction and methanogenesis, respectively; Thornton *et al.* 2001 and references therein). For example, products of specific TEAPs (e.g. Fe(II) and CH_4) may be transported into reduced zones where bacteria responsible for these reactions are not active.

Moreover, methane and hydrogen in the studied systems may have both organic and inorganic origin, making even more complicated the validity of the usual relationship considered between these gases and certain types of microbiological activities. However, these gases are chemically active species of redox couples that, independently of their origin, may participate or control the redox state of the groundwater system and/or act as substrates for different autotrophic and heterotrophic metabolisms. The available data of methane and hydrogen are still very scarce and merit further exploration, as this limitation even precludes the application of specific methodologies to identify the dominant redox processes.

Finally, many biological and inorganic reactions occur in close proximity and it is very difficult to discriminate between the organic and inorganic reactions taking place from the bulk chemical analysis. The reducers produced by the anaerobes (e.g. Mn(II), Fe(II), S(–II), etc) can inorganically reduce different TEAs: dissolved sulphide produced by the SRB may indirectly reduce available Fe(III)-oxyhydroxides to Fe(II), some of the Fe(II) may reduce MnO_2-oxides (if present) to Mn(II) and this Mn(II) may promote the reduction of NO_3^-. Thus, from a "simple" SRB activity, a chain of redox reactions can inorganically take place producing dissolved redox species that also can be indicative of other metabolic activities.

Therefore, the evaluation of redox conditions based on measurements of dissolved redox-sensitive species should only be taken as merely indicative, especially if the spatial scale of groundwater sampling is reduced compared with the whole studied system. Estimations based only in groundwater composition may be erroneous or, at least, incomplete, if the study of mineral phases (or related geochemical modelling calculations) or microbiological analyses are neglected. This type of integration has always been present in the work performed by the UZ group, but the use of these additional sources of information presents also some problems, which are discussed below.

G.3 Microbiological analysis

Direct identification of microbial communities or metabolisms in groundwater samples could be considered the clearest evidence of the ongoing biologically-mediated redox processes. But, unfortunately, this identification is not straightforward and different uncertainties are associated to it, mainly related to: biological contamination problems, disturbances during sampling and limitations of the MPN technique for determining the *in situ* metabolic groups (DNA techniques have not been used in the site characterization program).

G.3.1 Contamination and sampling disturbances

Perhaps the first and main problem is related to the possible biological contamination from surface induced during drilling and sampling operations (e.g. drilling waters). A strict methodology is used to perform microbiological analyses in the Swedish and Finish programs and different reasoning lines can support that this problem has been minimized (e.g. Pedersen 1997b, 2008)[80]. But even assuming the elimination of this uncertainty, some other important ones remain.

Disturbances during sampling may affect both dissolved redox indicators and microbiological determinations. Samples affected by short-circuit problems, such as those detected in the present data freeze (e.g. two of the samples in KLX17A; see section 4.2.1) may produce misleading microbiological results and interpretations at the section sampled. Oxygen intrusion problems and formation of low crystalline iron oxyhydroxides may also enhance the IRB activity (Gimeno *et al.* 2008) and artificial mixing is one of the reasons invoked to explain the puzzling high MPN of very diverse metabolic groups (including IRB and SRB) cultivated in some deep sections in Forsmark and Laxemar-Simpevarp areas; Hallbeck and Pedersen 2008bc).

Moreover, disturbances associated with flushing, prolonged pumping, etc can drastically decrease the pristine dissolved sulphide concentrations and also affect the MPN of SRB or IRB, as it has been documented in the MICROBE site in the Äspö hard rock laboratory (Hallbeck and Pedersen 2008a). Due to such disturbances, the values of SRB and sulphide have been considered by Hallbeck and Pedersen (2008b) not reliable for predictive modelling of microbial processes.

G.3.2 MPN technique and bacterial metabolic versatility

The MPN technique used in the microbiological investigations of the sites (e.g. Hallbeck and Pedersen 2008bc, Pedersen 2008) for the identification of microbial groups is based on the use of appropriate types of enriched cultures in the laboratory with the adequate TEA to support the metabolism of the searched metabolic group. However, microorganisms usually show a wide metabolic plasticity, being able, for example, to completely switch their TEAs as their preferable substrates are consumed or environmental conditions change. Therefore, the positive identification of a metabolic group in these laboratory cultures does not necessarily indicate that it is active in the groundwater conditions at depth.

For example, high values (MPN) of nitrate reducing bacteria (NRB) have been obtained in samples from Laxemar-Simpevarp or Forsmark groundwaters with extremely low values of dissolved nitrate (the TEA for NRB activity). NRB can use Fe(III)-oxyhydroxides as alternative TEA in absence of nitrate and, therefore, they may act as IRB in the groundwater system and as NRB in the laboratory cultures. Some of the sulphate reducing bacteria can switch to chemoheterotrophic NO_3^- reduction when this oxidant is available (Konhauser 2007). Furthermore, acetogens (the most abundant cultured microorganisms in Laxemar-Simpevarp and Forsmark areas) may also use nitrate as TEA (Drake *et al.* 2002). Therefore, the laboratory cultivation of NRB does not indicate that NRB activity is really active in the groundwater system.

This situation can be extended to other metabolic groups. Most of the known dissimilatory iron-reducing prokaryotes can reduce manganese as well, only switching to the reduction of MnO_2 when it becomes available (Nealson and Saffarini 1994). In this context, the correlation between MPN of IRB and MRB found in some studies on the microbiological populations in the Swedish sites (Hallbeck and Pedersen 2008bc) is not strange. But this fact represents an uncertainty in our knowledge of the microbiological activity at depth: are the detected MRB really active or are IRB switching to manganese reduction favoured by cultivation methods?

Other examples include some of the heterotrophic SRB, which are able of switching to Fe(III) reduction when this TEA is available (Konhauser 2007), or some few methanogens, which have shown the capacity for reducing iron minerals (Lovley *et al.* 2004).

---

[80] However, this type of contamination may still affect to some of the microbial data from the last data freeze in Forsmark (see the discussion by Hallbeck and Pedersen 2008c).

This problem especially affects the acetogens, the predominant microorganisms (both heterotrophic and autotrophic) in all the studied sections in the Laxemar-Simpevarp and Forsmark areas, with MPN often one or two orders of magnitude higher than the second most common organism type (Hallbeck and Pedersen 2008bc). Acetogens are known to be a diverse group of organisms that may switch between very different metabolic states, using a very wide range of diverse electron donors and acceptors (e.g. even many acetogens are both heterotrophic and autotrophic; Hallbeck and Pedersen 2008bc).

This capability represents an adaptative advantage, allowing to these microorganisms living under a wide range of redox conditions. However, it also represents a problem for assessing their *in situ* activities, as they may be very diverse and not restricted to acetogenesis (see Drake *et al*. 2002 for discussion). Moreover, this adaptability may cause that acetogens contribute to the MPN of different metabolic groups. To complicate the problem even more, acetogenic capabilities have been observed in some species of sulphate reducing bacteria (Drake *et al*. 2002).

This type of problems is not new in biogeochemistry. Although not necessarily active, viable bacteria of a particular functional group can be recovered from different environments using adequate types of enrichment cultures, even where those environments cannot support their growth (Falkowski *et al*. 2008 and references therein). Obviously, this situation represents an uncertainty when deciding if a zone is dominated by an individual functional group or if more than one group is concomitantly active.

Therefore, although the MPN technique may confirm the presence of a certain "microbial potential" for specific microbial redox processes (Christensen *et al*. 2000), which can help to identify redox processes in groundwater systems, the limitations detailed above indicate that their results should be used with caution.

G.3.3   Discussion

Microbiological analyses may be affected by sampling disturbances as it occurs with dissolved redox indicators. Moreover, the effects of these disturbances may be not obvious, since they affect the biological activities that can be favoured or limited depending on the metabolic group and/or the type of disturbance. On the other hand, since some organisms are able to use several electron-acceptors in their metabolic activities, they may contribute to the *apparent* number of bacteria belonging to other redox groups when determined by the MPN technique (Christensen *et al*. 2000).

The evaluation of the effects of these uncertainties on the microbiological results is presently a difficult task, as they could act in a superimposed manner and also combined with other uncertainty sources (e.g. those affecting to the dissolved redox indicators), complicating their interpretation.

In the last microbiological analyses performed in the Laxemar-Simpevarp and Forsmark areas it is frequent to cultivate a wide variety of metabolic groups in the same sections and at very different depths (Figure G-4). IRB, MRB, SRB, acetogens and, in some cases, even methanogens or high numbers of NRB (not show in Figure G-4) are obtained in the same sections and, therefore, almost the complete suite of microorganisms involved in the usual degradation of organic matter sequence has been cultivated.

These results could be attributed to the simultaneous presence of different metabolic activities widely distributed in the studied systems and, therefore, without a clear segregation in different redox zones. However, this wide distribution has not frequently been described in underground environments and, as previously discussed, the detection of a metabolic group by the MPN technique does not necessarily indicate its active presence at depth.

Moreover, as indicated by Hallbeck and Pedersen (2008bc) for the Laxemar-Simpevarp and Forsmark areas, there is no obvious explanation for this wide metabolic variability, especially in the sampled sections with the highest MPN values. Natural or induced mixing processes (during drilling and pumping activities) of different groundwaters are suggested, although possible contamination by flushing water is also possible, at least for some sections, in the Forsmark area.
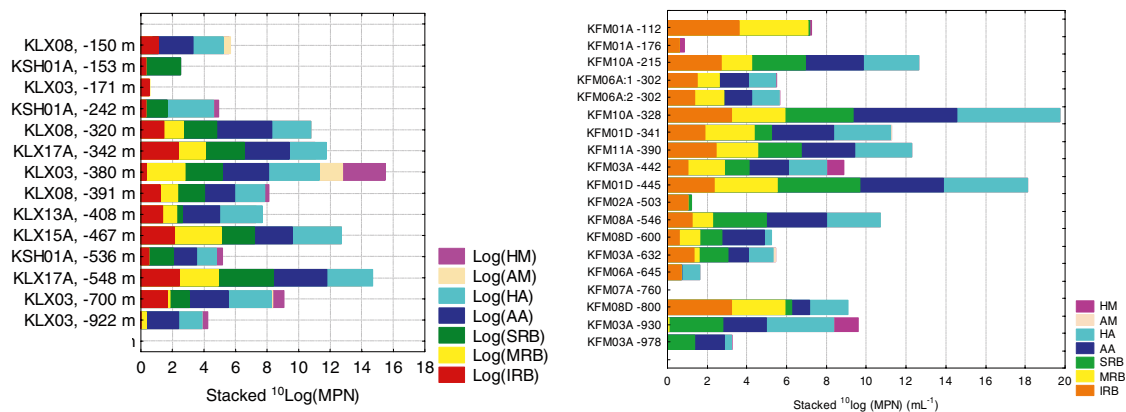
Figure G-4. Stacked MPN values (in logarithmic scale) for samples from Laxemar subarea (left) and Forsmark area (right) sorted by depth. From Hallbeck and Pedersen (2008b, c).

This situation represents a serious problem in the understanding of the biological control of redox processes because it precludes a clear determination of the metabolic processes actually active at the sampled depths. The described uncertainties prevent from knowing if the metabolic groups are segregated in zones (competitive exclusion), if some of them act concomitantly or if both situations are present in the studied systems depending on the distribution of local hydrochemical-hydrogeological characters or depth.

Again, only an integrated analysis, combining the microbiological analyses with other data and criteria, can provide some restrictions to this complex situation. In this sense, mineralogical data can be used as an important source of additional information, at least, for the assessment of the importance of some metabolic activities. These mineralogical aspects have been carefully evaluated in the present work (mainly referred to the iron and sulphur systems; see sections 4.3.2 and 4.3.5) and are further discussed in the next section.

G.4   Mineral indicators

From the classical works on redox zoning in marine sediments or rocks (e.g., Berner 1981), the use of diagnostic redox-related mineralogy to identify the present (or past) redox processes, has been established. For example, manganese and iron oxyhydroxides represent the TEA for manganese and iron reducing bacteria, respectively, and their presence is necessary to support these metabolisms. On the other hand, iron sulphides are the usual products of sulphate reducing activity that may remain as a clue of this type of bacterial activity over geological time periods.

These apparent strong relations between mineralogy and some microbiological metabolic groups have been applied in crystalline groundwater systems. Haveman *et al.* (1999) proposed that fracture-filling minerals are a better indicator of microbial metabolisms than groundwater chemistry. These authors studied four sites in Finland and found that SRB predominated in sites where iron sulphide fracture-filling minerals are common, whereas IRB dominate the systems with iron oxyhydroxides and without iron sulphides, in the fracture fillings. However these relations are not straightforward in many systems. For example, in systems like those studied in the Site Characterization Program, isotopic signatures must be used to differentiate between inorganic and biologically-mediated iron sulphide genesis (e.g. Drake and Tullborg 2008) as an important proportion of the pyrite found in fracture fillings may be of hydrothermal origin. Without this type of information, the deduced magnitude of SRB activity could be exaggerated.

On the other hand, the relationship between the occurrence of iron or manganese oxyhydroxides and iron or manganese reduction microbial activity in the studied systems is even much more diffuse and complex than previously thought, as it is discussed below.

361

G.4.1 Manganese oxyhydroxides and MRB activity

As described in many earlier works, MRB may use a wide number of Mn (IV) oxides as TEAs, including MnO_2 oxides (todorokite, vernardite, pyrolusite and birnessite) or mixed-valence and trivalent phases (hausmannite –Mn_3O_4– or manganite –MnOOH–). As it happens for iron oxyhydroxides and IRB (see section G.4.2), not all these manganese phases are equally susceptible to be reduced, being the amorphous phases (with high specific surface areas) more reactive than the crystalline oxides (with low surface areas; Burdige *et al.* 1992).

According to the mineralogical descriptions for Laxemar-Simpevarp and Forsmark, manganese is mainly associated with calcite and clay minerals (e.g. chlorite, corrensite) and chemical analyses of bulk fracture filling material show a positive correlation between manganese and iron, also supporting the presence of manganese in chlorite and clay minerals (Drake and Tullborg 2008). Mn-oxyhydroxides, which apparently are the main substrate for MRB activity, have only been found in fracture fillings at the shallowest levels in both Laxemar-Simpevarp and Forsmark (in the upper 10 m; Drake and Tullborg 2008). At greater depths, manganese concentrations in the bulk fracture filling material are low and relatively uniform (always below 0.4 wt. %) and, apparently, without the presence of "anomalous" contents associated with local accumulations of Mn-oxyhydroxides. That is, there is not a clear presence of the suitable TEAs for these microorganisms.

With regard to microbiological observations, the analyses indicate the presence of high MPN of MRB in some groundwaters at different depths in the Laxemar-Simpevarp and Forsmark areas (Figure G-4) although without correlation with the dissolved manganese contents. These results contrast with what has just presented above about the possible TEA for MRB activity in the deepest parts of the studied systems: there are not data on the presence of Mn-oxyhydroxides, necessary for MRB and, most important, the use of the structural Mn(IV) or Mn(III) in clays by MRB remains still undemonstrated. Therefore, the active presence of MRB at depths greater than 100 m and its effects on the groundwater composition must be considered with caution in the studied systems, more if the uncertainties associated with sampling disturbances or with the "ambiguous" results from the MPN technique (see section G.3.3) are taken into consideration.

This discussion highlights the importance of mineralogy to resolve the uncertainties related to the activity of this metabolic group and, also, the need of more detailed studies to confirm the absence of Mn-oxyhydroxides or the non bioavailability of Mn(IV) in clays. If these aspects are confirmed, a more simplified scheme arises for the redox processes at depth greater than 100 m; and the effects of MRB could be neglected.

G.4.2 Bioavailable Fe(III) and IRB activity

As regards mineral redox indicators of IRB activity, the presence of both Fe(III)-oxyhydroxides (mainly hematite with minor goethite) and abundant Fe(III)-rich chlorite, is widespread in the fracture fillings at Laxemar-Simpevarp and Forsmark areas (Drake and Tullborg 2008, Sandström *et al.* 2008). Many earlier studies have proven the ability of IRB to reduce Fe(III) present not only in oxyhydroxides but also in Fe(III)- phyllosilicates. Microbially-mediated reduction of octahedral Fe(III) in smectites is very well known for a long time (Stucki *et al.* 1987, Wu *et al.* 1988). More recent experiments confirm the possibility of microbially mediate reaction of structural Fe(III) bound in clay minerals (e.g. chlorites) as the sole electron acceptor (Kostka *et al.* 2002, Jaisi *et al.* 2007) and in the presence of Fe(III)-oxyhydroxides (Kukkadapu *et al.* 2006).

Despite the abundance of mineral substrate available as TEA for IRB activity, high numbers of IRB have only been detected very locally (Hallbeck and Pedersen 2008b). This apparent "paradox" has been examined with special attention in the present work and, although the data needed to solve it are still very scarce, a consistent explanation has been proposed (see section 4.3.5; Figure 4-21). Several important findings merit to be summarised:

- The use of ferric oxyhydroxides as TEA by IRB (and its ability to compete with other TEAPs like sulphate reduction) strongly depends on their crystallinity, particle size and surface area. These characters provide different thermodynamic stabilities that affect the energy that may be gained from iron reduction.

- The less crystalline phases (e.g. ferrihydrite and lepidocrocite) constitute usually the primary source (Roden 2003, Bonneville *et al.* 2004, Pedersen *et al.* 2005 and references therein) although, in some circumstances, more crystalline hematite or goethite can be used by IRB (e.g. when they show surface areas similar to those typical for amorphous Fe(III)-oxyhydroxides or under nutrient-rich conditions; see section 4.3.5). With the presently available data, and except at shallower levels, the identified Fe(III)-oxyhydroxides in the fracture fillings, correspond to crystalline phases (goethite and, mainly, hematite) with low surface areas. These characters have probably limited their use as TEA by iron reducing bacteria in the Laxemar-Simpevarp groundwater system.

- The overall extent of microbial reduction of both crystalline and poorly-crystalline iron oxyhydroxides is also limited by the inhibitory effects related to sorption processes (Figure 4-21) of dissolved Fe(II) on the mineral or cell surfaces (e.g. Roden and Urrutia 2002). In groundwaters with long periods in permanently reducing conditions, the accumulation of aqueous and surface-bound Fe(II) from biotically-induced or inorganic reactions may limit the enzymatic Fe(III)-reduction from ferric oxides. This inhibitory effect is particularly important in situations in which the removal of Fe(II) end-products is slow compared to the kinetics of Fe(III)-reduction or dissolution or in the cases in which bacterial growth is limited by the unavailability of nutrients, because cells would have little chance to remove sorbed Fe(II) by reproduction (Urrutia *et al.* 1999, Roden and Urrutia 2002). Therefore, in the long residence and reducing groundwaters from Laxemar-Simpevarp, these inhibitory effects may represent another limiting factor for IRB activity.

- The extent of microbially-mediated reduction of Fe(III) in clays is conditioned by the type or the relative proportions of clay minerals (and/or by the amounts of Fe(III) in their structures; Kukkadapu *et al.* 2006, Jaisi *et al.* 2007). Moreover, the reducibility of structural Fe(III) in clay minerals is known to decrease sharply when even small amounts of Fe(II) are sorbed on their surface, compromising IRB activity probably due to physical blockage of the electron transfer chain (Jaisi *et al.* 2007).

These limitations suggest that, under the pristine conditions of deep groundwaters with long residence time, IRB activity would be seriously disfavoured and may explain why IRB have not been frequently found in the microbiological analyses performed at Laxemar-Simpevarp. Under these conditions, sulphate reducing bacteria and methanogens would be favoured in the groundwater system in agreement with the results of geochemical calculations performed in section 4.3.5.

G.4.3 Discussion

Much effort has been done on the mineralogical evaluation of the reductive inorganic capacity of the studied systems, as it represent a key aspect for the stability of the repository in the long term. However, certain mineralogical aspects are of critical importance for the understanding of some microbial metabolisms at present, like metal (iron, manganese) reducing bacteria in the studied systems.

The existence of MRB activity in the deepest parts of the studied systems seems not to be supported by the observed fracture filling mineralogy. The presence of *Mn-oxyhydroxides,* which appear to be indispensable for sustaining MRB activity, has not been proven (or, at least, not in sufficient amounts) except at the shallowest levels in the Laxemar-Simpevarp and Forsmark areas. But, even at these shallow levels, MRB activity would not be particularly favoured, because it should probably compete with faster inorganic reductive dissolution reactions of Mn-oxyhydroxides, as it frequently occurs in marine sediments.

With regard to IRB activity, the analyses performed in the Laxemar-Simpevarp system indicate that the presence of active IRB appears feasible at shallow levels, where the available *Fe(III)-oxyhydroxides* with low crystallinity may be used as TEA. However, at higher depths, the active presence of this bacterial metabolic group seems to be disfavoured by the long residence time of these groundwaters under reducing conditions and by the actual data on the great crystallinity of Fe(III)-oxyhydroxides in the fracture fillings (goethite and, mainly, hematite). The great crystallinity and low surface areas of these ferric phases, as well as the inhibitory effects of dissolved Fe(II) (or secondary precipitates) have probably limited their use as TEA by iron reducing bacteria in the Laxemar-Simpevarp groundwater system.

All these findings have been summarised in a conceptual model for the IRB activity in the Laxemar-Simpevarp area consistent with the results obtained in field and laboratory experiments in the REX project (Banwart 1999, Trotignon *et al.* 2002). Even though this model is very preliminary, it identifies some key gaps in the knowledge of geochemical processes governing the relationships between the different metabolic groups and their influence on the redox processes in the studied system. Some of the remaining open questions are:

- Can dynamic flow conditions allow a dissimilatory reductive dissolution of Fe(III)-phyllosilicates or crystalline iron oxyhydroxides? The inhibitory effects by "passivation" of the Fe(III)-minerals and cell surfaces through Fe(II) sorption (Figure 4-21 and Figure G-1) are especially effective in more or less hydrologically static systems where the Fe(II) is not alleviated, or not totally alleviated, by advective transport (Roden and Urrutia 1999, 2002, Urrutia *et al.* 1999). But more dynamic-flow conditions, with active mobilisation of inhibiting agents (e.g. dissolved Fe(II)), may allow a dissimilatory reductive dissolution of Fe(III) phyllosilicates or, even, crystalline iron oxyhydroxides (Roden and Urrutia 1999, Roden *et al.* 2000). This point merits further studies as, in the investigated systems, contrasting hydrological and hydrochemical regimes (from old mixing processes and present recharge groundwaters) coexist.

- May IRB activity exist associated, for example, with the localised presence of crystalline Fe(III)-oxyhydroxides with higher surface areas than presently detected at depth? Overall, the extent and rates of reduction of more crystalline Fe(III) phases, including goethite, hematite, and Fe(III)-rich clays, are less than that of poorly-crystalline iron-oxyhydroxides (Roden and Zachara 1996, Liu *et al.* 2001, Zachara *et al.* 2002, Kostka *et al.* 1996, Roden 2003). But, even at lower rates and under some circumstances, the reduction of the most crystalline ferric oxyhydroxides by IRB has been described in the literature (see section 4.3.5).

These open questions are closely related to the existence of gaps in the knowledge of the complex surface-chemical and physiological interactions that control the rate and extent of reduction of Fe(III)-oxyhydroxides and Fe(III)-clay minerals and to the controls on the bacterial reducibility of these phases. Quantification of the IRB inhibitory effects is important for the understanding of the geochemical and microbiological relations and a prerequisite for the development of predictive (e.g. reactive transport) calculations including microbiological processes.

G.5 Redox zonation and redox conceptual model for the sites

The classification of redox environments proposed by Berner (1981) for the classical sequence of redox zones in marine sediments (Figure G-5) has been widely used to describe the redox evolution both in pristine and in contaminated aquifers (Langmuir 1997, Christensen *et al.* 2000, Appelo and Postma 2005). This redox zonation scheme has also been applied in the Finnish and Swedish programs in different ways.

In the Finnish program, the redox evolution with depth in Hästholmen or Olkilutoto (Snellman *et al.* 1998, Pitkänen *et al.* 1999, 2004, Pitkänen and Partamies 2007) has been described in terms of Berner's classification mainly from dissolved redox indicators. At Olkiluoto (Figure G-6) a post-oxic environment reaching 150 m depth is defined from dissolved Fe(II). The sulphidic zone, deduced from dissolved sulphide contents, would be restricted to the interval between 200–450 m depth. From this depth down, a methanic environment is proposed.

In the Laxemar-Simpevarp area the situation appears to be more complex, which can be partially attributed to the inclusion of different subareas in the depth profiles. To make the observation easier the redox depth distribution only in the Laxemar subarea will be discussed next.

The main redox zone that can be more clearly distinguished in the groundwater system of Laxemar subarea is a sulphidic zone. Even taking into account the uncertainties associated with the dissolved sulphide concentrations, which would generally tend to diminish them (see section G.2.1), the development of a wider sulphidic zone from 200 to 900 m depth (Figure G-7a) is apparent in the Laxemar subarea (as it also occurs from 100 to 900 m depth in the groundwaters from the Äspö subarea, see Figure 4-5). Moreover, the $\delta^{34}S$ values in dissolved sulphate and pyrites from the fracture fillings support the presence of past SRB activity, present in the studied systems for a long time and at least down to 800 m (see section 3.4.3).
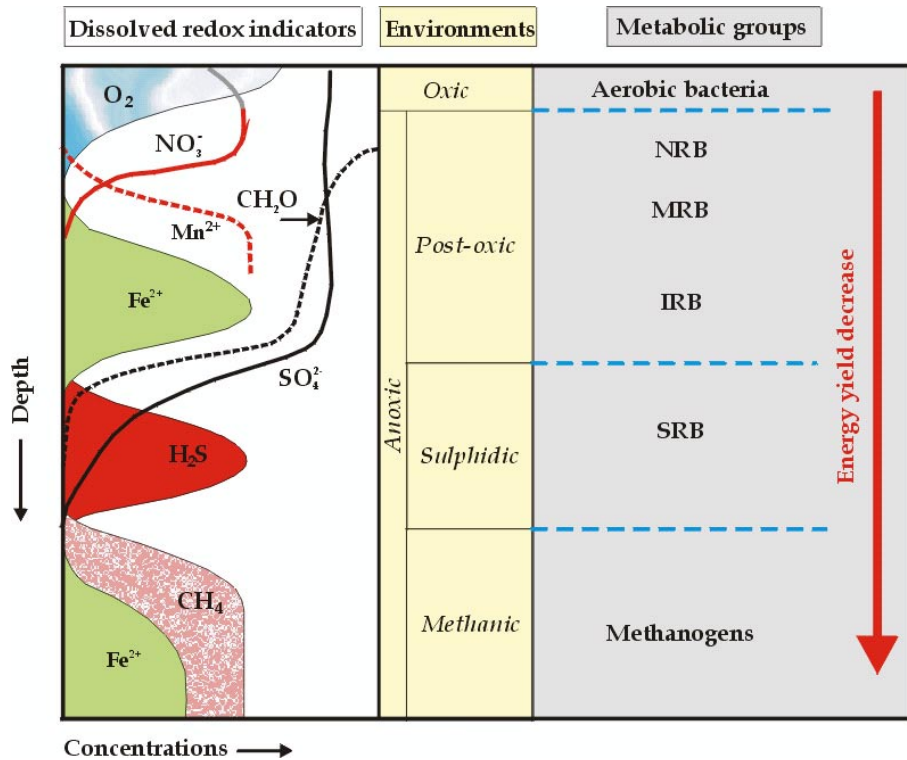
Figure G-5. *Sequence of redox environments proposed by Berner (1981) with the evolution of dissolved redox indicators and the theoretical sequence of the metabolic groups involved in the degradation of organic matter. Modified from Appelo and Postma (2005).*
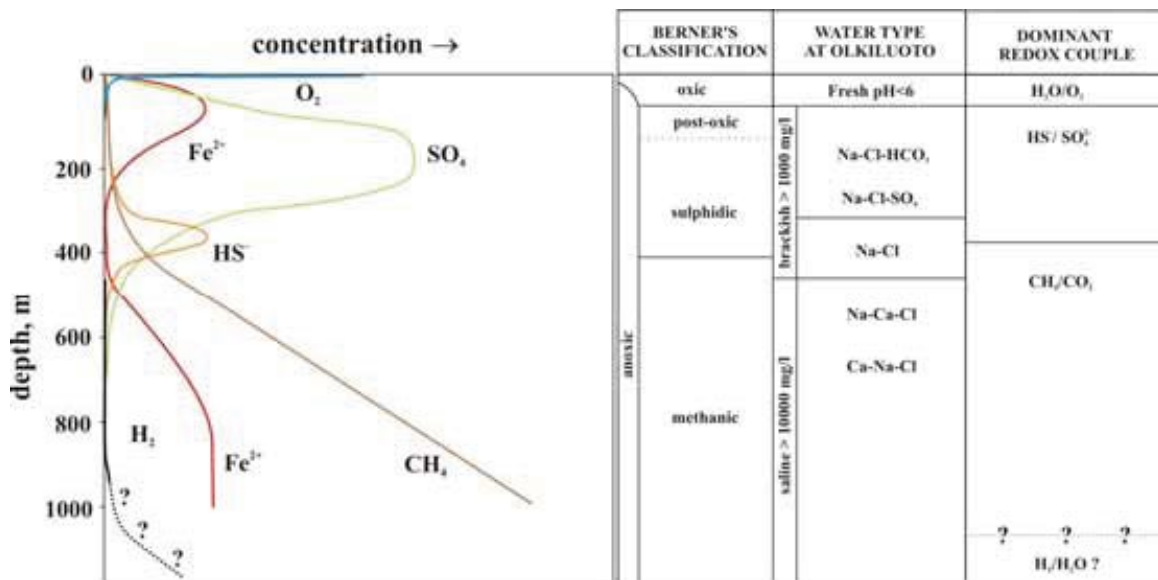
Figure G-6. *Sequential redox system with depth in the groundwater system at Olkiluoto. Relative concentrations of redox-sensitive dissolved species and redox couples correlating with Berner's (1981) classification are indicated. From Pitkänen and Partamies (2007).*

Figure G-7. *Dissolved redox indicators (Fe(II), Mn(II), S(–II) and CH₄) vs depth in the groundwaters from the Laxemar subarea*

The existence of a possible redox zone for manganese reduction remains uncertain. Manganese contents in groundwater samples from categories 1, 2 and 3 are generally below 0.2 mg/L, defining a relatively constant range with depth from the shallowest levels (Figure G-7b) as minor contribution from Littorina groundwaters occurs in the Laxemar subarea (compare with the values measured in Äspö and Si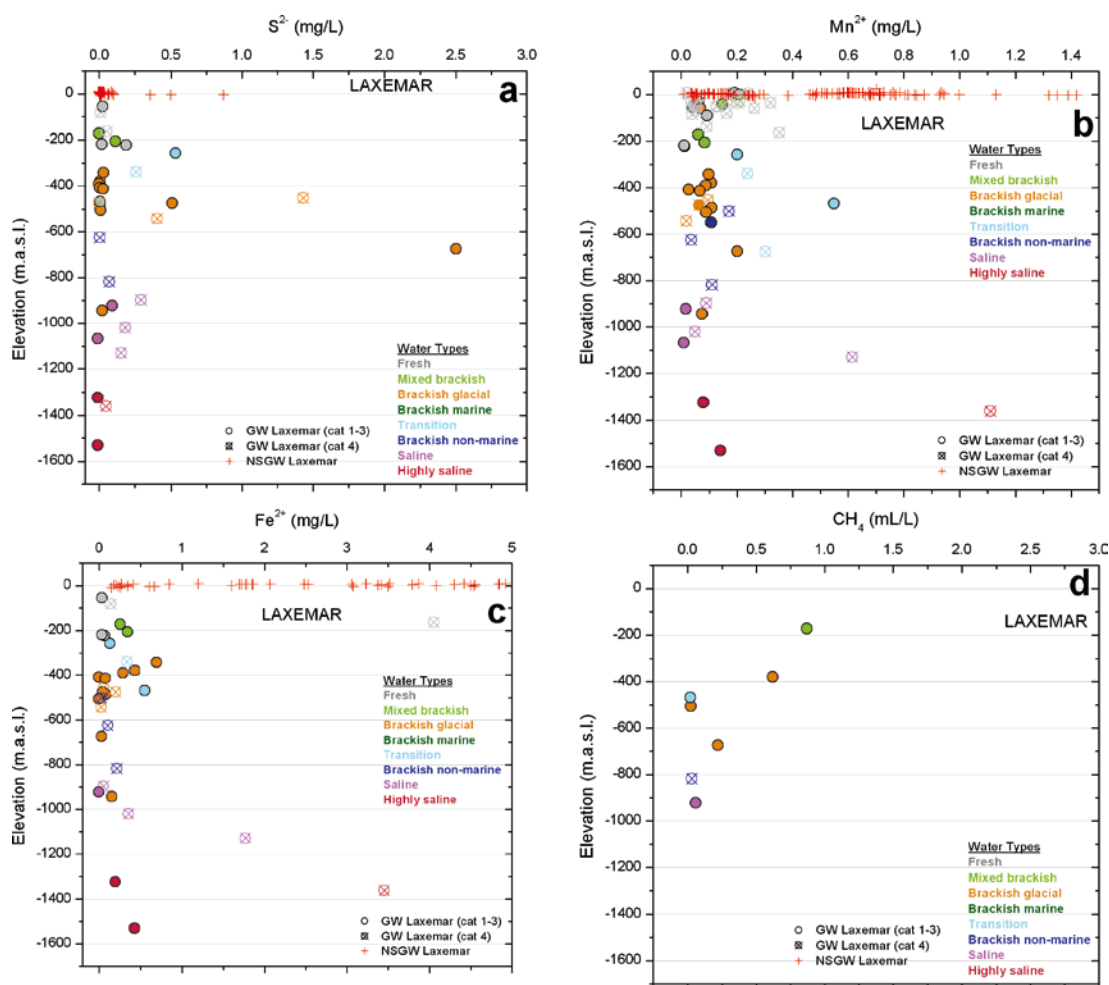mpevarp; Figure 4-22). The only exception to this general trend is the sample from KLX15 at 467 m depth (Mn concentration of 0.56 mg/L), which represent one of the scarce groundwaters in the Laxemar subarea with a certain Littorina contribution (around 10%) and, therefore, its dissolved manganese contents may represent an inherited diagenetic character. The low Mn concentrations, the absence of an identified TEA for MRB activity (Mn-oxyhydroxides) in the fracture fillings and the uncertainties associated with MPN technique to identify the *in situ* activity of this metabolic group (see section G.3) prevent from defining a clear manganese reduction redox zone.

With regard to the possible existence of an iron reduction redox zone, there are also many uncertainties associated. Iron concentration shows a peak at around 300–450 m depth, well inside in the depth range of the sulphidic zone (Figure G-7c). Roughly, in this depth range relatively high numbers of IRB (and SRB) has been found but most of the samples in this range show tritium and very low chloride contents and/or have been affected by short-circuit problems. Whether the increase of Fe(II) at those depths is related to *in situ* concomitant IRB activity, to abiotic reduction of Fe(III)-oxyhydroxides or to drilling induced modifications, must be further explored taken into account the problems with Fe(III) bioavailability indicated in section G.4.2.

Apparently, a methanic zone below the sulphidic one is developed neither in the whole Laxemar-Simpevarp area nor in the Laxemar subarea. Methane has been measured between 150 and near 700 m depth (Figure G-7d) and, therefore, mainly overlapped to the defined sulphidic zone. The highest methane concentrations (from biogenic origin; see section G.2.2) in the Laxemar subarea are found at around 200 m depth in fresh dilute groundwaters (Cl = 259 mg/L) and it may correspond to *in situ* methanogenic activity or to methane transported from shallower levels (e.g. produced in the wetlands).

From this careful examination of the redox zonation trends, the situation in the Laxemar subarea seems to be different from the one defined at Olkiluoto. The differences and their origin may have important consequences in the understanding of the redox processes in crystalline systems and, therefore, in their long-term evolution.

The extent and "intensity" of the sulphidic zone in the Laxemar subarea must be verified, since it could be affected by the sampling problems with dissolved sulphide. On the other hand, the apparent poorly developed and "patchy" methanic environment could be a sampling bias, as very scarce data are available for the Laxemar subarea, and it must be verified and explained. The remaining redox zones from the Berner`s (1981) scheme are not well constrained in the Laxemar subarea. Although post-oxic environments characterised by manganese and iron reduction processes may be developed in the overburden and shallowest groundwater system (until 100–150 m depth), their extent to greater depths is uncertain and, if present, they would be overlapped or "inserted" in the sulphidic zone.

In this situation at least three different possibilities should be further explored to clarify the redox scheme in the Laxemar subarea:

1. Poor development or inexistence of some of the redox zones defined by Berner's (1981) scheme. The presence or importance of a redox zone depends on the existence (and amounts) of the adequate TEA and, therefore, some of the redox zones may be poorly developed or inexistent (Berner 1981). The indicated limiting factors in TEA (Mn(IV)- and Fe(III)-oxyhydroxides or clays) bioavailability could support this type of situation in the Laxemar subarea.

2. Presence of concomitant metabolic activities (e.g. sulphate and iron reduction processes). The presence of concomitant metabolic activities (if the adequate TEAs are available) is possible in the redox zonation scheme, as redox zones may be dominated by one redox process and the others may also take place in subordinated conditions (Christensen *et al*. 2000). But also, if the rates of the concomitant metabolic activities are similar, different types of overlaps or not clear segregation at all between redox zones, may occur (Postma and Jakobsen 1996, Jakobsen and Postma 1999, Park *et al*. 2006).

3. Prevalence of both situations in different areas of the studied system. Due to the recharge character of the Laxemar subarea, groundwaters with different salinities, from fresh to brackish, occur in the same depth interval between 250 and 500 m. This situation would imply that groundwaters with a very different history are present at the same depths and that this heterogeneity could be translated to the detected redox environments (e.g. at a given depth, a post-oxic environment with active iron reduction processes is developed and in other point at the same depth, a sulphidic environment is present).

The overall microbiological results are extremely complex and do not help to constrain these possibilities. The microbiological model for the Laxemar-Simpevarp area (and also for the Forsmark area) proposes a classical depth-related segregation of the microbial populations comparable to that found in aquatic sediments. In the anaerobic subsurface zone (Figure G-8) the metabolic processes are organised with depth following Berner's scheme (Figure G-5) and extending to a depth of at least 1,000 m.(e.g. Hallbeck and Pedersen 2008bc).

However, as stated in section G.3, the last microbiological analyses performed for the Laxemar-Simpevarp and Forsmark areas show that almost the complete suite of microorganisms involved in the usual degradation of organic matter sequence (i.e. IRB, MRB, SRB, acetogens and, in some cases, even methanogens or high numbers of NRB) have been cultivated for the same sections and at very different depths (Figure G-4). If these microbiological results were attributed to the presence of simultaneous metabolic activities widely distributed with depth in the studied systems, this would be clearly inconsistent with the clear redox zone segregation proposed in the microbial model.
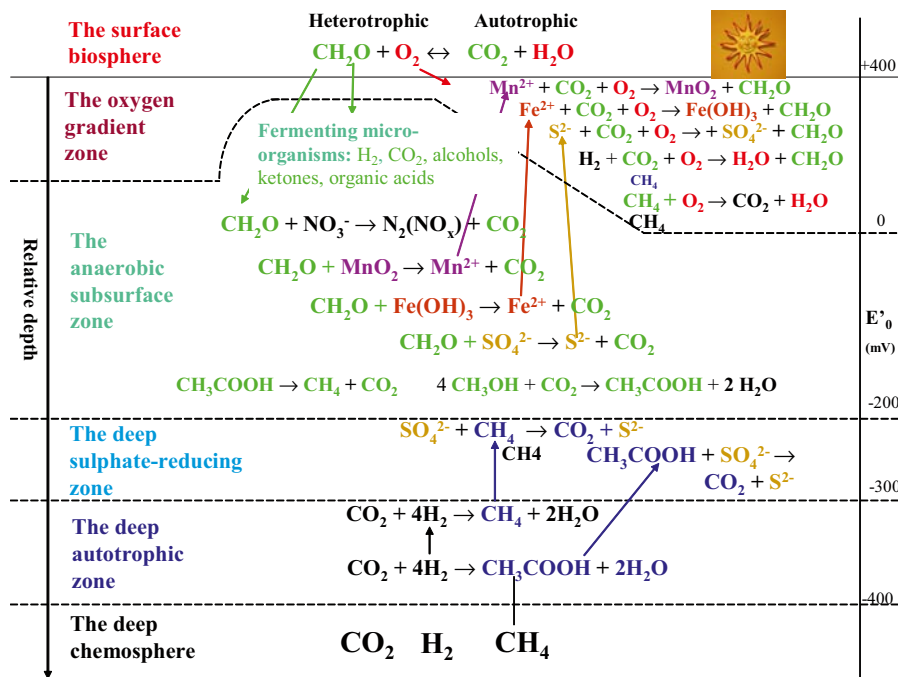
The surface biosphere

Heterotrophic   Autotrophic

$$CH_2O + O_2 \leftrightarrow CO_2 + H_2O$$

+400

The oxygen gradient zone

$$Mn^{2+} + CO_2 + O_2 \rightarrow MnO_2 + CH_2O$$
$$Fe^{2+} + CO_2 + O_2 \rightarrow Fe(OH)_3 + CH_2O$$
$$S^{2-} + CO_2 + O_2 \rightarrow SO_4^{2-} + CH_2O$$
$$H_2 + CO_2 + O_2 \rightarrow H_2O + CH_2O$$

Fermenting micro-organisms: H_2, CO_2, alcohols, ketones, organic acids

CH_4
$$CH_4 + O_2 \rightarrow CO_2 + H_2O$$
CH_4

0

The anaerobic subsurface zone

$$CH_2O + NO_3^- \rightarrow N_2(NO_x) + CO_2$$
$$CH_2O + MnO_2 \rightarrow Mn^{2+} + CO_2$$
$$CH_2O + Fe(OH)_3 \rightarrow Fe^{2+} + CO_2$$
$$CH_2O + SO_4^{2-} \rightarrow S^{2-} + CO_2$$
$$CH_3COOH \rightarrow CH_4 + CO_2 \qquad 4\,CH_3OH + CO_2 \rightarrow CH_3COOH + 2\,H_2O$$

E'_0 (mV)

-200

The deep sulphate-reducing zone

$$SO_4^{2-} + CH_4 \rightarrow CO_2 + S^{2-}$$
$CH4$
$$CH_3COOH + SO_4^{2-} \rightarrow CO_2 + S^{2-}$$

-300

The deep autotrophic zone

$$CO_2 + 4H_2 \rightarrow CH_4 + 2H_2O$$
$$CO_2 + 4H_2 \rightarrow CH_3COOH + 2H_2O$$

-400

The deep chemosphere

$$CO_2 \quad H_2 \quad CH_4$$

Relative depth

Figure G-8. *Theoretical model of microbial reactions in a crystalline groundwater environment proposed for the Laxemar-Simpevarp and Forsmark areas. From Hallbeck and Pedersen (2008b, c).*

In line with the three general hypotheses proposed above for the segregation and distribution of redox zones, the distribution of the *in situ* active metabolisms in the groundwater system should be clarified in order to answer some key questions:

- Are the redox zones segregated and dominated by mutually exclusive respirative functional groups of microbes or not?

- What are the limiting factors that control the rate of microbial respiration in the groundwater system? Is it the supply of electron donors, the availability of electron acceptors, the availability of chemical energy, or the kinetic properties of the microbes themselves?

- Do different limiting factors or processes dominate in different areas or depths depending on the particular structural, hydrological and hydrochemical characters?

Only with a clarification of these questions and also of the fluxes of metabolic substrates in the system (sections G.2.2 and G.2.3.) and of the interfacial properties of the available Fe and Mn oxy-hydroxides (section G.4.3), a more refined concept of redox buffering capacity including bacterial populations can be proposed (e.g. Trotignon *et al*. 2002).

G.6   Recommendations for the future

The identification of the dominant redox processes in the groundwater system is a basic step for the understanding of redox zone segregation and its spatial distribution. An integrated approach, using different criteria (chemical, microbiological and mineralogical data combined with different types of geochemical calculations) has been used in this report to accomplish this objective.

The results obtained have led to the identification of some important inorganic and biological processes in the control of the redox conditions of the studied groundwater systems and, also, of different types of uncertainties affecting the knowledge of the redox processes in the systems. Only a general awareness of these uncertainties and limitations will allow to put the interpretation and use of the identified redox processes into the correct perspective and to identify the main future research lines to fill the gaps in our current knowledge of the main processes determining the redox evolution of the Forsmark and Laxemar-Simpevarp groundwater systems.

The obtained results in the redox characterization critically depend on the number of sampling points (and suitable data) available from the studied system. This, in turn, depends on the desired spatial resolution and degree of detail in the knowledge of this type of processes in the research program. Some key points related to the spatial and the conceptual resolution should be carefully evaluated for the next characterisation stages:

- It would be desirable a higher spatial resolution in the sampling network in order to obtain a sample volume ideally smaller than the system heterogeneities. The studied fractured systems show a complex palaeohydrological history that favours the existence of hydrogeochemical heterogeneities. This large degree of heterogeneity may lead to the existence of local redox environments, which may be still poorly constrained at the present spatial discretisation and with the detected uncertainties (e.g. sampling disturbing effects). Therefore,

- It would be desirable to minimize the disturbing effects during sampling (e.g. flushing, mixing of groundwater from different redox environments) on the dissolved redox indicators and micro-biological data. Technical difficulties and possible solutions associated with the aforementioned uncertainties must be carefully evaluated by the experts prior to the development of a sampling program with higher resolution.

Superimposed to the points above, some other key issues must be further explored in order to enlarge the knowledge of the redox processes in the studied systems:

- More data and detailed studies on the methane contents and its isotopes are needed to better constraint the methanogenic activity vs. the "endogenous" origin of this component and to obtain a clear picture of the distribution of methane with depth.

- The apparently highly variable hydrogen contents need to be constrained with better detection limits to characterise the nanomolar range of this element and its influence on the different metabolic activities and/or in the development of different redox zones.

- Data on the concentrations of the different organic (acetate, formate, etc) and inorganic (H_2) substrates are needed to properly calculate the energy yield available for the different terminal electron acceptor reactions.

- The "in situ" active metabolic processes, their mutual or exclusive relations, the factors that control their spatial distribution and their corresponding rates must be clarified, as microbial metabolic activities are the ultimate engine that drives most redox reactions in aquatic systems. These aspects would also need a better knowledge on the fluxes of metabolic substrates in the system and on the interfacial properties of the available Fe and Mn oxyhydroxides.

G.7   References

Appelo C A J and Postma D (2005). Geochemistry, Groundwater & Pollution. Balkema, Rotterdam, The Netherlands, 2nd edition, 649 p.

Banwart S A (1999). Reduction of iron (III) minerals by natural organic matter in groundwater. Geochim. Cosmochim. Acta, 63, 2919–2928.

Berner R A (1981). A new geochemical classification of sedimentary environments. J. Sediment. Petrol., 51, 359–365.

Bonneville S, Van Cappellen P and Behrends T (2004). Microbial reduction of iron (III) oxyhydroxides: effects of mineral solubility and availability. Chem. Geol., 212, 255–268.

Burdige D J, Dhakar S P and Nealson K H (1992). Effects of manganese oxide mineralogy on microbial and chemical manganese reduction. Geomicrobiology Journal, 4, 361–387.

Canfield D E, Thamdrup B and Hansen J (1993). The anaerobic degradation of organic matter in Danish coastal sediments: iron reduction, manganese reduction, and sulphate reduction. Geochim. Cosmochim. Acta, 57, 3867–3883.

Champ D R, Gulens J, Jackson R E (1979). Oxidation–reduction sequences in ground water flow systems. Can. J. Earth Sci., 16, 12–23.

Chapelle F H (2001). Ground-water microbiology and geochemistry. John Wiley & Sons, Inc. 2nd edition, 477 p.

Christensen T H, Bjerg P L, Banwart S A, Jakobsen R, Heron G and Albrechtsen H-J (2000). Characterization of redox conditions in groundwater contaminant plumes. Journal of Contaminant Hydrology, 45, 165–241

Drake H and Tullborg E-L (2008). Fracture mineralogy of the Laxemar site. Final report. SKB-R-08-99.

Drake H L, Küsel K and Matthies C (2002). Ecological consequences of the phylogenetic and physiological diversities of acetogens, Antonie van Leeuwenhoek, 81, 1203–212,

Falkowski P G, Fenchel T and Delong E (2008). The microbial engines that drive Earths´s biogeochemical cycles. Science, 320, 1034–1039.

Gimeno M J, Auqué L F, Gómez J B and Acero P (2008). Water-rock interaction modelling and uncertainties of mixing modelling. SDM-Site Forsmak. SKB R-08-86, 212 p.

Hallbeck L and Pedersen K (2008a). Characterization of microbial processes in deep aquifers of the Fennoscandian Shield. Appl. Geochem., 23, 1796–1819.

Hallbeck L and Pedersen K (2008b). Explorative analysis of microbes, colloids and gases. SDM-Site Laxemar. SKB R-08-109.

Hallbeck L and Pedersen K (2008c). Explorative analysis of microbes, colloids and gases. SDM-Site Forsmark. SKB R-08-85.

Haveman S, Pedersen K and Ruotsalainen P (1999). Distribution and metabolic diversity of microorganisms in deep igneous rock aquifers of Finland. Geomicrobiology Journal, 16, 277–294.

Hoehler T M, Alperin M J, Albert D B and Martens C S (1998). Thermodynamic control on hydrogen concentrations in anoxic sediments. Geochim.Cosmochim. Acta, 62, 1745–1756.

Jaisi D P, Dong H and Liu C (2007). Influence of biogenic Fe(II) on the extent of microbial reduction of Fe(III) in clay minerals nontronite, illite, and chlorite. Geochim. Cosmochim. Acta, 71, 1145–1158.

Jakobsen R, and Postma D (1999). Redox zoning, rates of sulfate reduction and interactions with Fe-reduction and methanogenesis in a shallow sandy aquifer, Rømø, Denmark. Geochim. Cosmochim. Acta, 63, 137–151.

Jakobsen R and Cold L (2007). Geochemistry at the sulfate reduction–methanogenesis transition zone in an anoxic aquifer. A partial equilibrium interpretation using 2D reactive transport modelling. Geochim. Cosmochim. Acta, 71, 1949–1966

Kehew A E (2001). Applied chemical hydrogeology. Prentice Hall, 368 p.

Konhauser K (2007). Introduction to geomicrobiology. Blackwell Publishing, 424 p.

Kotelnikova S (2002). Microbial production and oxidation of methane in deep subsurface. Earth-Science reviews, 58, 367–396:5.

Kotelnikova S and Pedersen K (1997a). Evidence for methanogenic Archaea and homoacetogenic Bacteria in deep granitic rock aquifers. FEMS Microbiology Reviews, 20, 339–349.

Kotelnikova S and Pedersen K (1997b). Distribution and activity of methanogens and homoacetogens in deep granitic aquifers at Äspö Hard Rock Laboratory, Sweden. In: K. Pedersen (ed.), Investigations of subterranean microorganisms and their importance for performance assessment of radioactive waste disposal. Results and conclusions achieved during the period 1995 to 1997. SKB TR 97-22, pp.167–198.

Kostka J E, Stucki J W, Nealson K H and Wu J (1996). Reduction of structural Fe(III) in smectite by a pure culture of Shewanella putrefaciens strain MR-1. Clays Clay Miner., 44, 522–529.

Kostka J E, Dalton D D, Skelton H, Dollhopf, S. and Stucki, J.W. (2002). Growth of Iron(III)-reducing bacteria on clay minerals as the sole electron acceptor and comparison of growth yields on a variety of oxidised iron forms. Applied and Environmental Microbiology, 68, 6256–6262.

Kukkadapu R K, Zachara J M, Fredrickson J K, McKinley J P, Kennedy D W, Smith S C and Dong H (2006). Reductive biotransformation of Fe in shale–limestone saprolite containing Fe(III) oxides and Fe(II)/Fe(III) phyllosilicates. Geochim. Cosmochim. Acta, 70, 3662–3676.

Langmuir D (1997). Aqueous environmental geochemistry. Prentice Hall, 600 p.

Lin L H, Slater G F, Sherwood Lollar B, Lacrampe-Couloume G and Onstott T C (2005). The yield and isotopic composition of radiolytic H2, a potential source for deep subsurface biosphere. Geochim. Cosmochim. Acta, 69, 893–903.

Liu C, Kota S, Zachara J M, Fredrickson J K, and Brinkman C (2001). Kinetic analysis of the bacterial reduction of goethite. Environ. Sci. Technol., 35, 2482–2490.

Lovley D R and Goodwin S (1988). Hydrogen concentrations as an indicator of the predominant terminal electron-accepting reactions in aquatic sediments. Geochim. Cosmochim. Acta, 52, 2993–3003.

Lovley D R, Holmes D E and Nervin K-P (2004). Dissimilatory Fe(III) and Mn (IV) reduction. Advances in Microbial Physiology, 49, 219–286.

Nealson K H, Tebo B M and Rosson R A (1988). Occurrence and mechanisms of microbial oxidation of manganese. Advances in Applied Microbiology, 33, 270–318.

Nealson K H and Saffarini D (1994). Iron and manganese in anaerobic respiration: environmental significance, physiology and regulation. Annual Reviews of Microbiology, 48, 311–343.

Park J, Sanford R A, and Bethke C M (2006). Geochemical and microbiological zonation of the Middendorf aquifer, South Carolina. Chem. Geol., 230, 88–104.

Pedersen K (1993). The deep subterranean biosphere. Earth Science Reviews, 34, 243–260.

Pedersen K (1997a). Microbial life in deep granitic rock. FEMS Microbiology Reviews, 20, 399–414.

Pedersen K (1997b). Investigations of subterranean microorganisms and their importance for performance assessment of radioactive waste disposal. Results and conclusions achieved during the period 1995-1997. SKB TR-07-22, 284 p.

Pedersen K (2001). Diversity and activity of microorganisms in deep igneous rock aquifers of the Fennoscandian Shield. In: J.K Fredrickson and M. Fletcher (eds.), Subsurface microbiology and biogeochemistry.Wiley-Liss Inc., New York. pp. 97–139.

Pedersen K (2008). Microbiology of Olkiluoto Groundwater. 2004–2006. Posiva, 2008-02, 156 p.

Pedersen H, Postma D, Jakobsen R and Larsen O (2005). Fast transformation of iron oxyhydrosxides by the catalytic action of aqueous Fe(II). Geochim. Cosmochim. Acta, 16, 3967–3977.

Pitkänen P and Partamies S (2007). Origin and implications of dissolved gases in groundwater at Olkiluoto. Posiva 2007-04, 57 p.

Pitkänen P, Luukkonen A, Ruotsalainen P, Leino-Forsman H and Vuorinen U (1999). Geochemical modelling of groundwater evolution and residence time at the Olkiluoto site. Posiva 98-10, 184 p.

Pitkänen P, Partamies S and Luukkonen A (2004). Hydrogeochemical interpretation of baseline groundwater conditions at the Olkiluoto site. Posiva 2003-07,159 p.

Postma D (1985). Concentration of Mn and separation from Fe in sediments: I. Kinetics and stoichiometry of the reaction between birnessite and dissolved Fe(II) at 10 °C. Geochim. Cosmochim. Acta, 49, 1023–1033.

Postma D (1993). The reactivity of iron oxides in sediments: a kinetic approach. Geochim. Cosmochim. Acta, 57, 5027–5034.

Postma D and Jakobsen R (1996). Redox zonation: Equilibrium constraints on the Fe(III)/SO4-reduction interface. Geochim. Cosmochim. Acta, 60, 3169–3175.

Poulton S W, Krom M D and Raiswell R (2004). A revised scheme for the reactivity of iron (oxyhydr)oxide minerals towards dissolved sulfide. Geochim. Cosmochim. Acta, 68, 3703–3715.

Puigdomènech I (2001). Hydrochemical stability of groundwaters surrounding a spent nuclear fuel repository in a 100,000 year perspective. SKB Technical Report 01-28, 83 p.

Pyzik A J and Sommer S E (1981). Sedimentary iron monosulfides: kinetics and mechanism of formation. Geochim. Cosmochim. Acta, 45, 687–698.

Roden E E (2003). Fe(III) oxide reactivity toward biological vs. chemical reduction. Environ. Sci. Technol., 37, 1319–1324.

Roden E E and Urrutia M M (1999). Ferrous iron removal promotes microbial reduction of crystalline iron(III) oxides. Environ. Sci. Technol., 33, 1847–1853.

Roden E E and Urrutia M M (2002). Influence of biogenic Fe(II) on bacterial crystalline Fe(III) oxide reduction. Geomicrobiol. Jour., 19, 209–251.

Roden E E and Zachara J M (1996). Microbial reduction of crystalline iron (III) oxides: influence of oxide surface area and potential cell growth. Environ. Sci. Technol., 30, 1618–1628.

Roden E E, Urrutia M M, and Mann C J (2000). Bacterial reductive dissolution of crystalline Fe(III) oxide in continuous-flow column reactors. Appl. Environ. Microbiol., 66, 1062–1065.

Sandström B, Tullborg E-L, Smellie J, MacKenzie A B and Suksi J (2008). Fracture mineralogy of the Forsmark site. SDM-Site Forsmark. SKB R-08-102, 113 pp.

Snellman M, Pitkänen P, Luukkonen A, Ruotsalainen P, Leino-Forsman H and Vuorinen U (1998). Summary of recent observations from Hästholmen groundwater studies. POSIVA Working Report 98-44, Helsinki, Finland, 71 p.

Stone A T and Morgan J J (1984). Reduction and dissolution of manganese (III) and manganese (IV) oxides by organics. 2. Survey of reactivity of organics. Environmental Science and Technology, 18, 617–624.

Stucki J W, Komadel P, and Wilkinson H T (1987). Microbial reduction of structural iron(III) in smectites. Soil Sci. Soc. Am. J., 51, 1663–1665.

Stumm W and Morgan J J (1996). Aquatic Chemistry. Chemical equilibria and rates in natural waters. 3rd ed., John Wiley & Sons, New York, USA, 1022 p.

Thorstenson D C, Fisher D W and Croft M G (1979). The geochemistry of the Fox Hills-Basal Hell Creek aquifer in Southwestern North Dakota and Northwestern South Dakota. Water Resour. Res., 15, 1479–1498.

Thornton S F, Quigley S, Spence M J, Banwart S A, Bottrell S and Lerner D N (2001). Processes controlling the distribution and natural attenuation of dissolved phenolic compounds in a deep sandstone aquifer. Journal of Contaminant Hydrology, 53, 233–267.

Trotignon L, Michaud V, Lartigue J-E, Ambrosi J-P, Eisenlohr L, Griffault L, de Combarieu M and Daumas S (2002). Laboratory simulation of an oxidizing perturbation in a deep granite environment. Geochim. Cosmochim. Acta, 66, 2583–2601.

Urrutia M M, Roden E E, and Zachara J M (1999). Influence of aqueous and solid-phase Fe(II) complexants on microbial reduction of crystalline Fe(III) oxides. Environ. Sci. Technol., 33, 4022–4028.

Wu J, Roth C B, and Low P F (1988). Biological reduction of structural iron in sodium-nontronite. Soil Sci. Soc. Am. J., 52, 295–296.

Yao W and Millero F J (1993). The rate of sulfide oxidation by δMnO_2 in seawater. Geochim. Cosmochim. Acta, 57, 3359–3365.

Yao W and Millero F J (1996). Oxidation of hydrogen sulphide by hydrous Fe(III) oxides in seawater. Mar. Chem., 52, 1–16.

Zachara J M, Kukkadapu R K, Fredrickson J K, Gorby Y A, and Smith S C (2002). Biomineralization of poorly-crystalline Fe(III) oxides by dissimilatory metal reducing bacteria (DMRB). Geomicrobiol. Jour., 19, 179–207.